UNITED STATES
DEPARTMENT OF THE INTERIOR
GEOLOGICAL SURVEY

SUMMARIES OF TECHNICAL REPORTS, VOLUME XII

Prepared by Participants in

NATIONAL EARTHQUAKE HAZARDS REDUCTION PROGRAM

Compiled by

Barbara B. Charonnat
External Research Program

Thelma R. Rodriguez
Earthquake Prediction

Wanda H. Seiders
Earthquake Hazards and Risk Assessment
Global Seismology
and
Induced Seismicity

Open-File Report No. 81-833

The research results described in the following summaries were submitted by the investigators on May 15, 1981 and cover the 6-month period from October 1, 1980 through March 31, 1981. These reports include both work performed under contracts administered by the Geological Survey and work by members of the Geological Survey. The report summaries are grouped into the four major elements of the National Earthquake Hazards Reduction Program:

Earthquake Hazards and Risk Assessment (H)
Robert D. Brown, Jr., Coordinator
U.S. Geological Survey
345 Middlefield Road, MS-77
Menlo Park, California 94025

Earthquake Prediction (P)
C. Barry Raleigh, Coordinator
U.S. Geological Survey
345 Middlefield Road, MS-77
Menlo Park, California 94025

Global Seismology (G)
Eric R. Engdahl, Coordinator
U.S. Geological Survey
Denver Federal Center, MS-967
Denver, Colorado 80225

Induced Seismicity (IS)
Mark D. Zoback, Coordinator
U.S. Geological Survey
National Center, MS-905
12201 Sunrise Valley Drive
Reston, Virginia 22092

Open File Report No. 81-833

This report has not been reviewed for conformity with USGS editorial standards and stratigraphic nomenclature. Parts of it were prepared under contract to the U.S. Geological Survey and the opinions and conclusions expressed herein do not necessarily represent those of the USGS. Any use of trade names is for descriptive purposes only and does not imply endorsement by the USGS.

The data and interpretations in these progress reports may be reevaluated by the investigators upon completion of the research. Readers who wish to cite findings described herein should confirm their accuracy with the author.

CONTENTS

Earthquake Hazards Reduction Program

Page

I. Earthquake Hazards and Risk Assessment (H)

Objective 1. Establish an accurate and reliable national earthquake data base.---------------------------- 1

Objective 2. Delineate and evaluate earthquake hazards and risk in the United States on a national scale.--- 12

Objective 3. Delineate and evaluate earthquake hazards and risk in earthquake-prone urbanized regions in the western United States.------------------------ 26

Objective 4. Delineate and evaluate earthquake hazards and risk in earthquake-prone regions in the eastern United States.-------------------------------------- 78

Objective 5. Improve capability to evaluate earthquake potential and predict character of surface faulting.--- 114

Objective 6. Improve capability to predict character of damaging ground shaking.---------------------------- 192

Objective 7. Improve capability to predict incidence, nature and extent of earthquake-induced ground failures, particularly landsliding and liquefaction.--------- 242

Objective 8. Improve capability to predict earthquake losses.--- 260

II. Earthquake Prediction (P)

Objective 1. Obtain pertinent geophysical observations and attempt to predict great or very damaging earthquakes.-- 273

a. Operate seismic networks and analyze data to determine character of seismicity preceding major earthquakes.

b. Measure and interpret geodetic strain and elevation changes in regions of high seismic potential, especially in seismic gaps.

Page

Objective 2. Obtain definitive data that may reflect precursory changes near the source of moderately large earthquakes. Short term variations in the strain field prior to moderate or large earthquakes require careful documentation in association with other phenomena.---------------------------------- 357

a. Measure strain and tilt near-continuously to search for short term variations preceding large earthquakes. Complete development of system for stable, continuous monitoring of strain.

b. Monitor radon emanation water properties and level in wells, especially in close association with other monitoring systems. Monitor apparent resistivity, magnetic field to determine whether precursory variations in these fields occur. Monitor variations in seismic velocity and attenuation within the (San Andreas) fault zone.

Objective 3. Provide a physical basis for short-term earthquake predictions through understanding the mechanics of faulting.

Develop theoretical and experimental models to guide and be tested against observations of strain, seismicity, variations in properties of the seismic source, etc., prior to large earthquakes.------------------ 431

Objective 4. Determine the geometry, boundary conditions, and constitutive relations of seismically active regions to identify the physical conditions accompanying earthquakes.

Measure physical properties including stress, temperature, elastic and anelastic properties, pore pressure, and material properties of the seismogenic zone and the surrounding region.-------------------------- 466

III. Global Seismology (G)

Objective 1. Operate, maintain, and improve standard networks of seismographic stations.------------------------ 522

Objective 2. Provide seismological data and information services to the public and to the research community.------- 532

Objective 3. Improve seismological data services through basic and applied research and through application of advances in earthquake source specification and data analysis and management.---------------------- 537

Page

IV. Induced Seismicity Studies (IS)

Objective 1. Establish a physical basis for understanding the tectonic response to induced changes in pore pressure or loading in specific geologic and tectonic environments.---------------------------- 546

Index 1: Alphabetized by Principal Investigator---------------------- 567

Index 2: Alphabetized by Institution--------------------------------- 573

Seismicity and Related Data for Hazard Analysis

9950-02145

S. T. Algermissen
Branch of Earthquake Tectonics and Risk
U.S. Geological Survey
Denver Federal Center, MS 966
Denver, CO 80225
(303) 234-4014

Investigations

1. Work continues on review of the entire U.S. earthquake catalogue for larger events (I>V) and revision and (or) preparation of isoseismal maps. Work on this project has been coordinated with and supports a project in the Branch of Global Seismology aimed at the preparation of seismicity maps for all 50 states.

2. The intensity data for two significant and somewhat controversial earthquakes have been reviewed.

3. The liquifaction effects associated with two Puget Sound earthquakes, April 13, 1949 and April 29, 1965 have been reviewed making use of unpublished data collected by the University of Washington and previously published sources.

4. A field investigation of the Imperial Valley, California earthquake of April 25, 1981 was undertaken.

Results

1. Isoseismal maps of historical United States earthquakes reviewed and revised to date total 196: 26 in the Eastern U.S.; 63 in the Central U.S.; 41 in the Western Mountain region; 11 in the Pacific Northwest; and, 55 in California. Of these maps, 73 have been digitized. A computer programs to handle the digitized maps are operational on the VAX computer. Work is progressing on the statistical analysis of the intensity data.

2. A review of the intensity data for the November 8, 1882, Colorado earthquake has been completed for the Department of Energy at the request of the Regional Geologist, Central Region. A review of the intensity data for the December 14, 1872 Washington earthquake is nearly complete.

3. A study of ground effects, in particular liquefaction effects, resulting from earthquake shaking in the Puget Sound region is complete and is being reviewed prior to publication.

4. Building damage and geologic effects associated with the April 25, 1981, Imperial Valley earthquake was surveyed and a report is in preparation.

Reports

Hopper, Margaret G., and Reagor, B., G., 1980, Field survey of intensity for the earthquake of July 27, 1980, Sharpsburg, Kentucky: U.S.G.S. Open-file report 80-1242.

Reagor, B. G., Stover, C. W., and Hopper, M. G., 1981, Preliminary report of the distribution of intensities for the Kentucky earthquake of July 27, 1980: U.S.G.S. Open-file report 81-198.

Stover, C. W., Barnhard, L. M., Reagor, B. G., and Algermissen, S. T., 1980, Seismicity map of the state of New Jersey, MF-1260.

____, 1980, Seismicity map of the state of New Hampshire, MF-1261.

____, 1980, Seismicity map of the state of Vermont, MF-1262.

____, 1980, Seismicity map of the state of Massachusetts, MF-856.

____, 1980, Seismicity map of the state of New York, MF-1282.

____, 1980, Seismicity map of the state of Rhode Island and Connecticut, MF-1283.

____, 1980, Seismicity map of the state of Maine, MF-1284.

Stover, C. W., Reagor, B. G., and Algermissen, S. T., 1981, Seismicity maps of the states of Delaware and Maryland, U.S. Geological Survey, MF-1281.

Reanalysis of Instrumentally-Recorded U.S. Earthquakes

9920-01901

J. W. Dewey
Branch of Global Seismology
U. S. Geological Survey
Denver Federal Center, MS 967
Denver, Colorado 80225
(303) 234-4041

Investigations

1. Relocate instrumentally-recorded U.S. earthquakes using the method of joint hypocenter determination (JHD) or the master event method, using subsidiary phases (Pg, S, Lg) in addition to first-arriving P-waves, using regional travel-time tables, and expressing the uncertainty of the computed hypocenter in terms of confidence ellipsoids on the hypocentral coordinates.

2. Evaluate the implications of the revised hypocenters on regional tectonics and seismic risk.

Results

We have estimated the completeness of our catalog of instrumentally-recorded earthquakes that occurred in the eastern U.S. in 1925-1976. Comparison of magnitude-frequency plots for the periods 1925-1963 and 1964-1976 suggests that the earlier segment of the catalog is significantly incomplete below a magnitude (m_{bLg}) of about 4.5, and may be missing about five shocks of $m_{bLg}>4.2$. Shocks of m_{bLg} up to 5.2 were very sparsely recorded in the early years of 1925-1963, so the incompleteness of the instrumental catalog below $m_{bLg}=4.5$ is not surprising from that standpoint. However, on the basis of magnitudes computed from felt areas of earthquakes listed in Coffman and von Hake (Earthquake History of the United States, Publication 41-1, U.S. Department of Commerce), we are able to account for only two of the five or so "missing" shocks of $m_{bLg}>4.2$.

For the period 1964-1976, the catalog of instrumentally recorded eastern U.S. shocks is substantially incomplete below $m_{bLg}=3.5$.

Reports

Herrmann, R. B., Dewey, J. W., Park, S. K., 1980, The Dulce, New Mexico earthquake of January 23, 1966: Bull. Seism. Soc. Am., v. 70, pp. 2171-2183.

Dewey, J. W., and Gordon, D. W., 1980, Instrumental seismicity of the eastern United States and adjacent Canada (abstract): Earthquake Notes, v. 51, no. 3, p. 19.

Jones-Cecil, M., Wheeler, R. L., Dewey, J. W., 1980, Modified pattern recognition technique used to study southeastern United States seismicity (abstract): Earthquake Notes, v. 51, no. 3, p. 24.

Jones-Cecil, M. Wheeler, R. L., Dewey, J. W., Report on pattern recognition modified and applied to southeastern United States seismicity, in press as an Open-File report, 81-195.

Dewey, J. W., Relocation of instrumentaly recorded pre-1974 earthquakes from the South Carolina region, in press as a contribution to a new U.S.G.S. Professional Paper on the Charleston, S.C., earthquake region.

ANALYSIS OF OLD (1888 - 1950) DUPLEX-PENDULUM AND WIERCHERT SEISMOGRAMS OF LARGE AND MODERATE EARTHQUAKES IN WESTERN NEVADA

14-08-0001-18291

University of California, San Diego - La Jolla, CA 92093
Keith F. Priestley
Now at:
Department of Geology
University of Otago
Dunedin, New Zealand

Investigations

Several approaches are being followed in analyzing the pre-1900 seismicity of the Eastern Sierran front with special emphasis on the Reno/Carson City area. These are:

a) documentation of the pre-1900 earthquakes of damaging or potentially damaging intensities;

b) analysis of intensity data and recorded seismicity data to more accurately access the magnitude of pre-1930 events;

c) relocation of 1930-1960 earthquakes relative to recent events.

Results

a) Pre-1900 Seismicity:

Most potentially damaging events in the Reno/Carson City area for 1860 - 1900 are scattered through existing catalogues of California and Nevada earthquakes. A compilation of earthquakes with epicenters in Eastern Central California and Western Central Nevada with damaging or potentially damaging intensities in the Reno/Carson City area was made by a search of these catalogues.

b) Pre-1930 Magnitudes:

Magnitudes of early events are often estimated from analyses of intensity data. This can result in anomalously high magnitude estimates when high intensity or felt areas are used since a few possibly exaggerated or anomalous observations tend to dominate. Magnitude estimations based on moderate (IV-VI) intensities are likely to be more accurate since they tend to smooth out anomalous reports. The two largest reported earthquakes of the 1900 - 1930 period in the Reno/Carson City area occurred on February 18, 1914 and April 24, 1914. Slemmons *et al.*, (1965) have assigned magnitudes of 6 and 6.4 respectively based on felt areas. The intensity data were reexamined and local magnitudes of 4.5 (±0.1) and 6.0 (±0.1) respectively were assigned to these events based on the areas of moderate intensity. From intensities observed in the Reno/Carson City area, the two events were unrelated. The February 18 earthquake occurred west of Reno, probably in the same area as the 1948 and 1966 earthquakes, while the April 24 earthquake epicenter lay to the east of Reno. Seismoscope records of these events are among the few remaining recordings of the Reno duplex-pendulum. The method of Jennings and Kanamori (1979) was used to determine local magnitude of 5.0 (±0.2) and 6.0 (±0.1) respectively for these events.

REFERENCES

Jennings, P. C., and H. Kanamori (1979). Determination of local magnitude, M_4, from seismoscope records. *Bull. Seism. Soc. Am.*, *69*, p. 1267 - 1288.

Slemmons, D. B., A. E. Jones and J. I. Gimlett (1965). Catalog of Nevada earthquakes, 1852 - 1960. *Bull. Seism. Soc. Am.*, *55*, p. 537 - 583.

National Earthquake Catalog

9920-02648

J. N. Taggart
Branch of Global Seismology
U.S. Geological Survey
Denver Federal Center, MS 967
Denver, Colorado 80225

(303) 234-5079

Investigations

1. Coordinate the preparation of a national earthquake catalog.

2. Collect earthquake event lists for the catalog and check them against original sources.

3. Investigate the relation between the size of large shallow earthquakes and the duration of their signals recorded on long-period seismograms of the World-Wide Standardized Seismograph Network.

Results

1. No additional planning has been necessary during this reporting period. The collection and checking of event lists for the catalog has been given the highest priority because the research and data base development elements are dependent upon these data. The historical seismicity in the states east of the Mississippi River is nearly completely covered in a series of miscellaneous maps, quarterly seismicity reports (since 1975) and United States Earthquakes (annual), all published by Project 9920-01222, under the leadership of Carl Stover. The seismicity maps of the Mississippi Valley and Great Plains states are nearing completion under this project. D. W. Gordon has relocated many of the earthquakes in these latter two regions. J. W. Dewey and R. A. Page will soon begin relocation of well recorded earthquakes in the Rocky Mountains states and Alaska, respectively.

W. H. K. Lee and J. N. Taggart will design and develop an events list data base for operation on one or more computers during the summer, 1981. Relatively simple, transportable fortran software probably will serve best for the manipulation of the data base. B. G. Reagor will work with Lee and Taggart on the development of this software. Reagor currently is writing a program that adds or deletes events from existing files, or interactively replaces (corrects) event parameters through the use of keys. Existing edit routines are not suitable for this work because hard copies are needed before a new version of the file can be used.

2. Taggart, Carol Thomasson and Frank Baldwin have checked 14,000 event listings against original published sources during this reporting period. The regions covered by this work include five Rocky Mountains states, Alaska, Puerto Rico, Guam and American Samoa. The sources that have been checked include various U.S. Government publications, the International Seismological Summary, Gutenberg and Richter's Seismicity of the Earth, and several lists published in the Bulletin of the Seismological Society of America. The error rate continues to be less than one mistake per 100 earthquakes, but 6 to 10 percent of the pre-1963 earthquakes listed in the source references are missing from even the most accurate and complete event lists. After 1962, the omission of events is negligible because digital computers have been used to prepare the event lists. Karen Meagher is assembling event list data, phase data, and descriptive material on Northern California earthquakes for later processing by W. H. K. Lee.

3. Work on long-period codas has consisted only of preparing computer plots of observed durations vs. distance and azimuth. Analogous to short-period coda durations, the long-period durations are only weakly related to epicentral distance or epicenter-to-station azimuth.

Preparation of Isoseismal Maps and Summaries of Reported Effects for Pre-1900 California Earthquakes

14-08-0001-19200

Tousson R. Toppozada and Charles R. Real
California Division of Mines and Geology
2815 "O" Street, Sacramento, CA 95816
(916) 322-9309

Isoseismal maps are being prepared for the 110 earthquakes that caused the most damage in California during the nineteenth century. More than eleven thousand newspaper issues were searched and about one quarter of these reported earthquake effects at various locations. The effects of an earthquake reported at various locations are being used to construct the isoseismal maps. The isoseismal maps are being used to estimate magnitudes from the size of the areas shaken at or above various levels of intensity, and to locate epicenters within the zones of highest intensity. The annual report including the isoseismal maps, summaries of the reported effects, and a bibliography of the sources of data, should be available in September 1981.

A talk based on this research was presented at the 76th annual meeting of the Seismological Society of America, and the abstract was published in Earthquake Notes vol. 52, no. 1. The abstract discusses the eight earthquakes of M 6.5 or larger that occurred within 100 km of the rupture zone of the San Francisco earthquake during the 70 years preceding 1906. The isoseismal maps show that during each of these earthquakes, moderate damage to buildings ($I \gg$ VII MM) occurred over an area of at least 3,800 km^2. The abstract concludes that such a suite of earthquakes poses as great a hazard to the greater San Francisco Bay Area as does a repetition of the great 1906 earthquake.

Seismic Monitoring of the Hellenic Arc

14-08-0001-18226

Max Wyss
CIRES and Department of Geological Sciences
University of Colorado
Boulder, Colorado 80309
(303) 492-8020

In the western segment of the Hellenic island arc the potential for a large earthquake appears to be high. This assessment is based on the identification of seismic gaps and arc segments where seismicity quiescence exists at present (Wyss and Baer, 1981a, b). We therefore proposed to monitor the seismicity of the western Hellenic arc in an effort to record and possibly identify the expected foreshocks. The Greek national seismograph network (Figure 1) is at present not capable of monitoring seismicity in real time because none of the data are telemetered to the National Observatory at Athens. However, J. Drakopoulos is planning to transmit the data from four stations (dark circles in Figure 1) to Athens by telephone lines. With support from this contract we will install the three stations shown in Figure 2, and transmit their data by radio telemetry to Athens. This installation and the data analysis will be done by cooperation between the University of Colorado and the National Observatory, Athens.

Obstacles arose in obtaining radio frequencies for transmitting the data. This problem delayed progress of the work by about half a year. In February 1981 frequencies were assigned to J. Drakopoulos by the Greek government and we are now getting ready to install the small network.

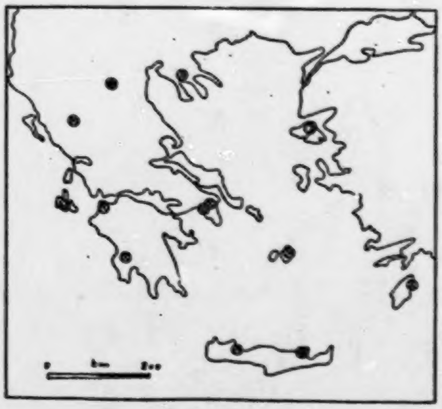

Figure 1: Greek seismograph network. Solid dots mark stations from which data will be transmitted by telephone line to the National Observatory, Athens. At present no data are telemetered.

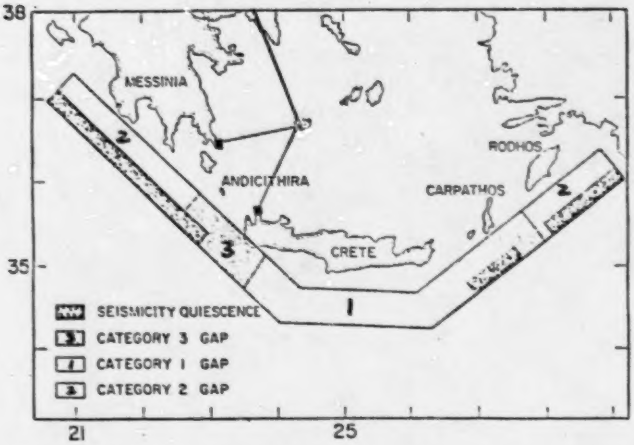
38
35
21
25
MESSINIA
ANDICITHIRA
CRETE
CARPATHOS
RODHOS
1
2
2
3
SEISMICITY QUIESCENCE
CATEGORY 3 GAP
CATEGORY 1 GAP
CATEGORY 2 GAP

Figure 2: Map of the Hellenic island arc showing the seismic gaps of categories 1 through 3, as well as segments which exhibit seismic quiescence. The planned tripartite seismograph network (squares) and its telemeter links will be operated in addition to the national Greek network shown in Figure 1.

Regional and National Seismic Hazard and Risk Assessment

9950-01207

S. T. Algermissen
Branch of Earthquake Tectonics and Risk
U.S. Geological Survey
Denver Federal Center, MS 966
Denver, CO 80225
(303) 234-4014

Investigations

1. Continued review of the seismotectonics and seismicity of various regions of the country.

2. Continued investigation of relationship between average return periods obtained from analysis of historical seismicity data and return periods developed from field investigations of fault slip.

3. Continued development and computation of revised probabilistic national acceleration and velocity maps.

4. Reassessed estimates of earthquake losses in the San Francisco Bay area and Los Angeles and Orange Counties, California.

Results

1. The results of a series of meetings with geologists and seismologists from within and outside the Survey on the seismotectonics of the United States as applied to hazard mapping is being synthesised and prepared for publication. The seismotectonic basis for the seismic source zones used in the new U.S. probabilistic hazards maps is also being compiled for publication.

2. The comparison of seismic activity derived from historical seismicity and that obtained from fault slip investigations is being extended from the Great Basin to coastal California.

3. The new probabilistic ground acceleration and velocity maps for the U.S. are complete. A text and maps will be ready for review about June 1. A technical paper on the computational scheme used for the maps is also in preparation.

4. Reassessed estimates of earthquake losses in the San Francisco Bay area and Los Angeles and Orange Counties, California which were incorporated, inpart, in a Federal Emergency Management Agency (FEMA) report to the National Security Council have been published as an Open File Report.

Reports

Steinbrugge, K. V., Algermissen, S. T., Lagorio, H. J., Cluff, L. S. and Degenkolb, H. J., 1981, Metropolitan San Francisco and Los Angeles Earthquake Loss Studies: 1980 Assessment, U.S. Geological Survey Open File Report 80-113, p. 44.

Seismic Wave Attenuation in Conterminous United States

9950-01205

A. F. Espinosa
Branch of Earthquake Tectonics and Risk
U.S. Geological Survey
Denver Federal Center, MS 966
Denver, CO 80225
(303) 234-5077

Investigations

1. Data reduction and analysis of 136 events in the magnitude range of 2.0 to 6.4, recorded on short period instruments throughout the United States, for the Pg, Pn, Sn and Sg (Lg) phases is in progress.

2. Data reduction and analysis of 29 NTS events recorded on strong motion instruments in the near-field (1 to 20 km) is in progress.

3. Data selection and tabulation of earthquakes recorded on Wood-Anderson instruments in the Western United States is in progress.

4. Data analysis of the October 10, 1980, El Asnam earthquake is near completion.

5. Data selection and tabulation obtained from the control explosion Early Rise recorded on short period instruments is in progress.

Results

1. Preliminary results of the mean γ-value distribution for Lg-waves, with a period of 1 second, have been derived from the recordings on short period seismograph systems throughout the U.S. (see Figure 1). The data base used in constructing the γ-distribution consists of 136 events with magnitudes from 2.0 to 6.4, and recorded in the distance range of 1° to 40°.

2. On a regional basis, for the Northeastern U.S., 50 events in the magnitude range of 1.8 to 3.2 have been used to derive a mean γ-value (see Figure 1). The distance range is between 30 to 400 km.

3. A full documentation has been done of the inconsistencies found in the Modified Mercalli intensity scale in Algeria. A map for the El Asnam-Beni Rached region, in Algeria, showing the intensity distribution in the areas that were affected by liquefaction, surface breakage, landsliding, also areas where bridges failed, rails bent appreciably, etc., have been completed.

4. The preliminary fault-plane solution for the October 10, 1980, El Asnam earthquake, indicates a dip-slip fault striking N40°E with a dip-angle of 62° to the west ($M_S = 7.3$). The main aftershock with a surface wave magnitude of 6.1 indicates a dip-slip fault plane solution striking N40°E with a dip-angle of 60° to the west. The strike of the thrust solution agrees with the mapped trace of

the surface faulting associated with the October 10, 1980, earthquake. The preliminary fault-plane solution of the major aftershock is also consistent with the main thrust and with the observations in the field. The combined field observations and teleseismic fault-plane solutions are indicative of a low-angle thrust at the surface with an increasing dip angle at depth. This earthquake was a low-stress-drop event ($\Delta\sigma$ = 26 bars).

Reports

Burford, R. O., Harsh, P. W., and Espinosa, A. F., 1981, 7.3 quake in Algeria reviewed: Geotimes, v. 26, May issue, p. 18-20.

Espinosa, A. F., 1981, The Algerian earthquake of October 10, 1980; A preliminary report: Earthquake Information Bulletin, v. 13, January February issue, p. 23-33.

Espinosa, A. F., 1981, M_L determination and horizontal ground acceleration from strong-motion accelerograms: in the forthcoming Imperial Valley, California, earthquake of October 15, 1979: U.S. Geological Survey Professional Paper (in press).

Espinosa, A. F., and Argeñal, R., 1981, Riesgo Sismico de Nicaragua (Seismic Risk of Nicaragua), An administrative oral report sponsored by U.S.A.I.D. presented to the Ministerio de Vivienda y Asentamientos Humanos, Managua, Nicaragua, April.

Espinosa, A. F., and Harding, S. T., 1981, The Algerian Earthquake of October 10, 1980; A field report: Seminar in Managua, Nicaragua (USAID), Ministry of Vivienda y Asentamiento Humano, April (Adm. report).

Espinosa, A. F., and Harding, S. T., 1981, The El Asnam Earthquake of October 10, 1980: A preliminary report: Proceedings of the III Venezuelan Earthquake Engineering and seismology Congress, Caracas, Venezuela, p. 2-5.

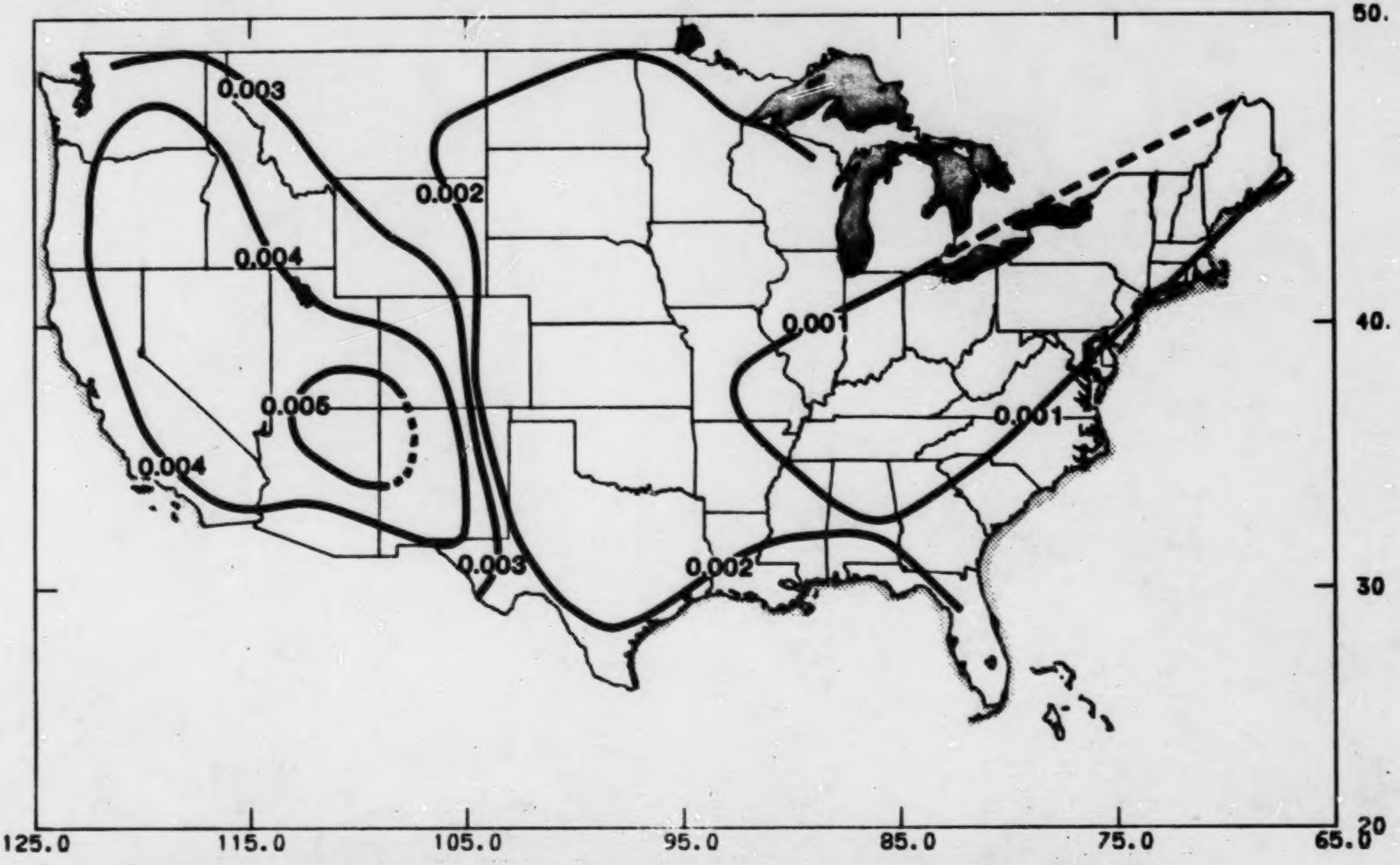
0.003
0.002
0.004
0.005
0.004
0.001
0.001
0.003
0.002
50.
40.
30
20
125.0
115.0
105.0
95.0
85.0
75.0
65.0

Figure 1.--Preliminary mean Lg-wave attenuation curves for conterminous United States. There is a definite correlation of the results shown in this figure with those obtained in crustal thickness determination by Pakiser and Steinhart. There is a good correlation of the γ-distribution in areas where high heat flow has been reported (Smith; Zoback and others). Furthermore, there is a good correlation for high γ-values with those Pg-wave attenuation values reported by Dave Hill . There is a remarkable change in attenuation between the Rocky Mountain region and the Great Plains.

H2

Investigation of Seismic Wave Propagation for Determination of Crustal Structure

9950-01896

S. T. Harding
Branch of Earthquake Tectonics and Risk
U.S. Geological Survey
Denver Federal Center, MS 966
Denver, CO 80225
(303) 234-5087

Investigations

1. A portion of a Seismic Reflection survey in southern Missouri which was done as part of the earthquake hazard reduction was reprocessed. The original data gave a hint of some reflection even below the strong reflection at .8 sec.

Results

It became apparent after the raw data was displayed that there was a problem in the field correlation of the vibroseis data. It is not known whether this developed as a result of non-linear interaction in the Mississippi mud or as a high noise level in the field instruments. This comparison is shown in figure 1. A synthetic vibroseis sweep was applied to the uncorrelated record. This is also shown in figure 1.

The record becomes much clearer in this process. Figure 2 is of a portion of the final stacked section. While there is some horizontal scale difference between the two sections, the use of the synthetic sweep measurably improved the section. This improvement permitted the making of a migrated record section (figure 3). A number of faults can be traced from 2.5 seconds almost to surface with some assurance. This exercise points out some of the pitfalls inherent in CDP data

Reports

Boore, D. M., Sims, J. D., Konamori, H., and Harding, S. T., 1981, The Montenegro, Yugoslavia earthquake of April 15, 1979 source orientation and strength: [Submitted] Physics of the Earth and Planetary Interior.

Harding, S. T., and Russ, D. P., 1980, Ray- and wave-theory modeling of seismic-reflection profiles to interpret geologic structure in the New Madrid seismic zone [abs.]: EOS, Transactions, American Geophysical Union, v. 61, no. 48, p. 1194.

Harmsen, S., and Harding, S. T., 1981, Surface motion on a sedimentary valley for plane P and SV waves, June: Bulletin of Seismological Society of America.

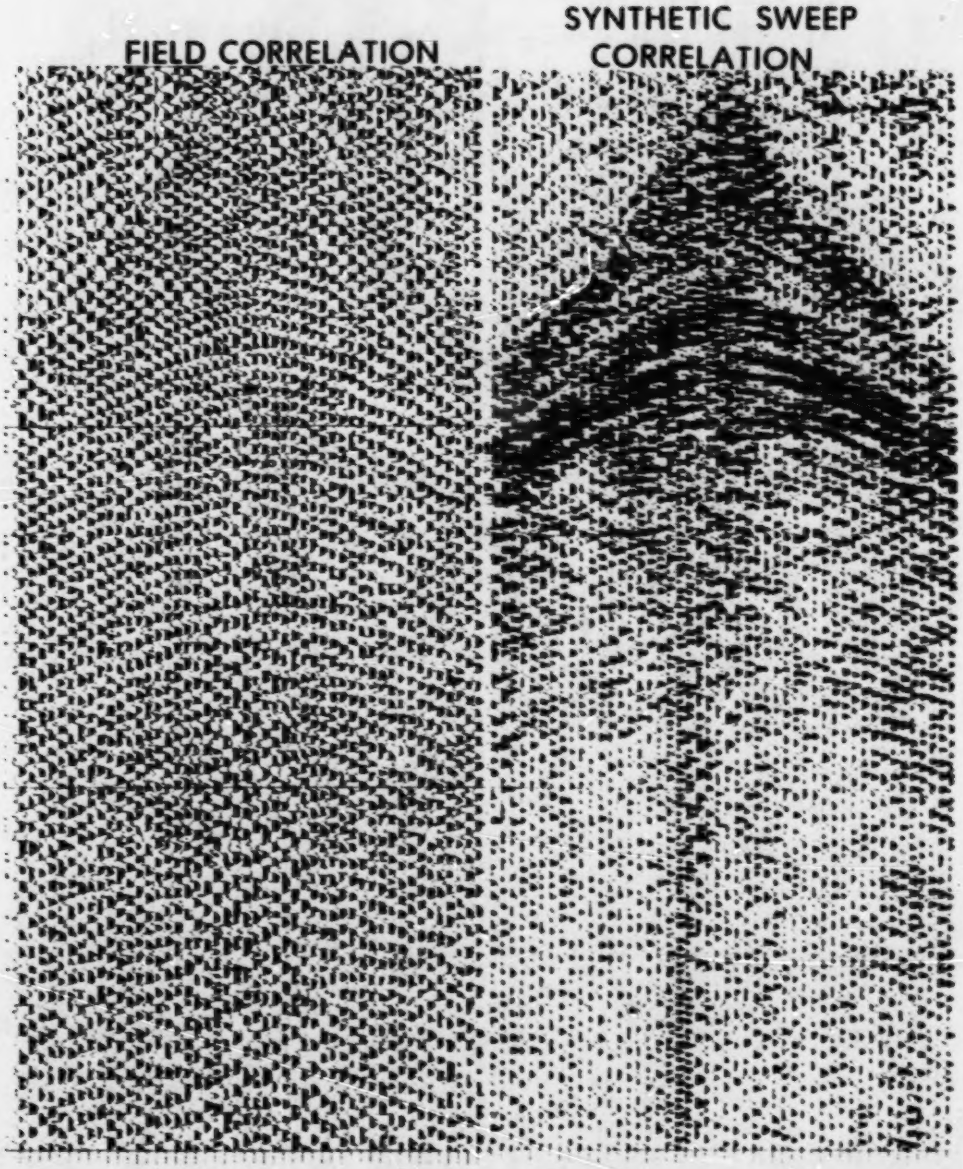

FIELD CORRELATION

SYNTHETIC SWEEP CORRELATION

Figure 1.--Comparison between the field vibroseis® sweep correlation and the correlation using a synthetic vibroseis sweep.

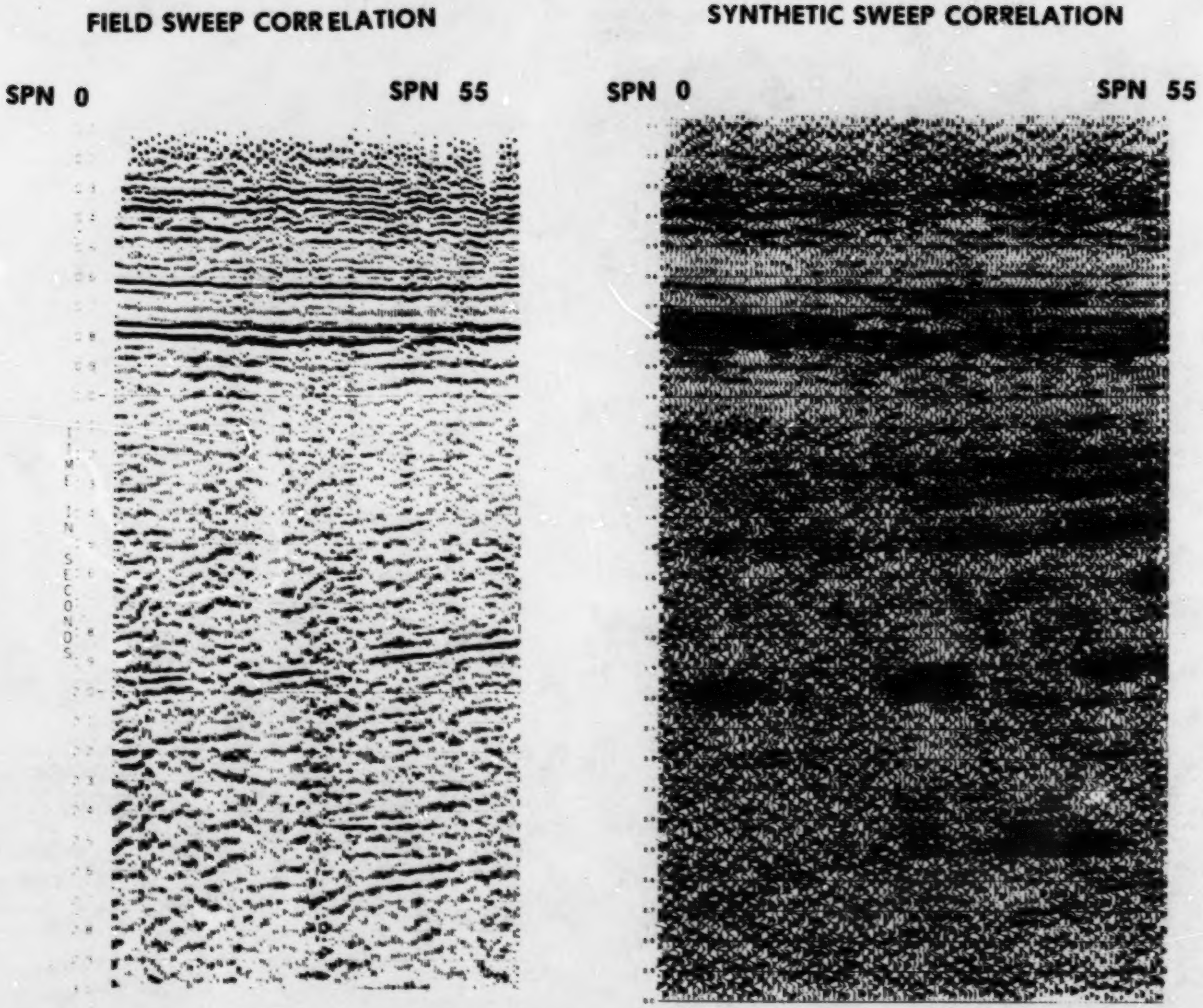

Figure 2.--These two record sections are the products of a common depth point (CDP) stack; the right is the original data received from contractor and the left is the reprocessed record section using a synthetic vibroseis sweep.

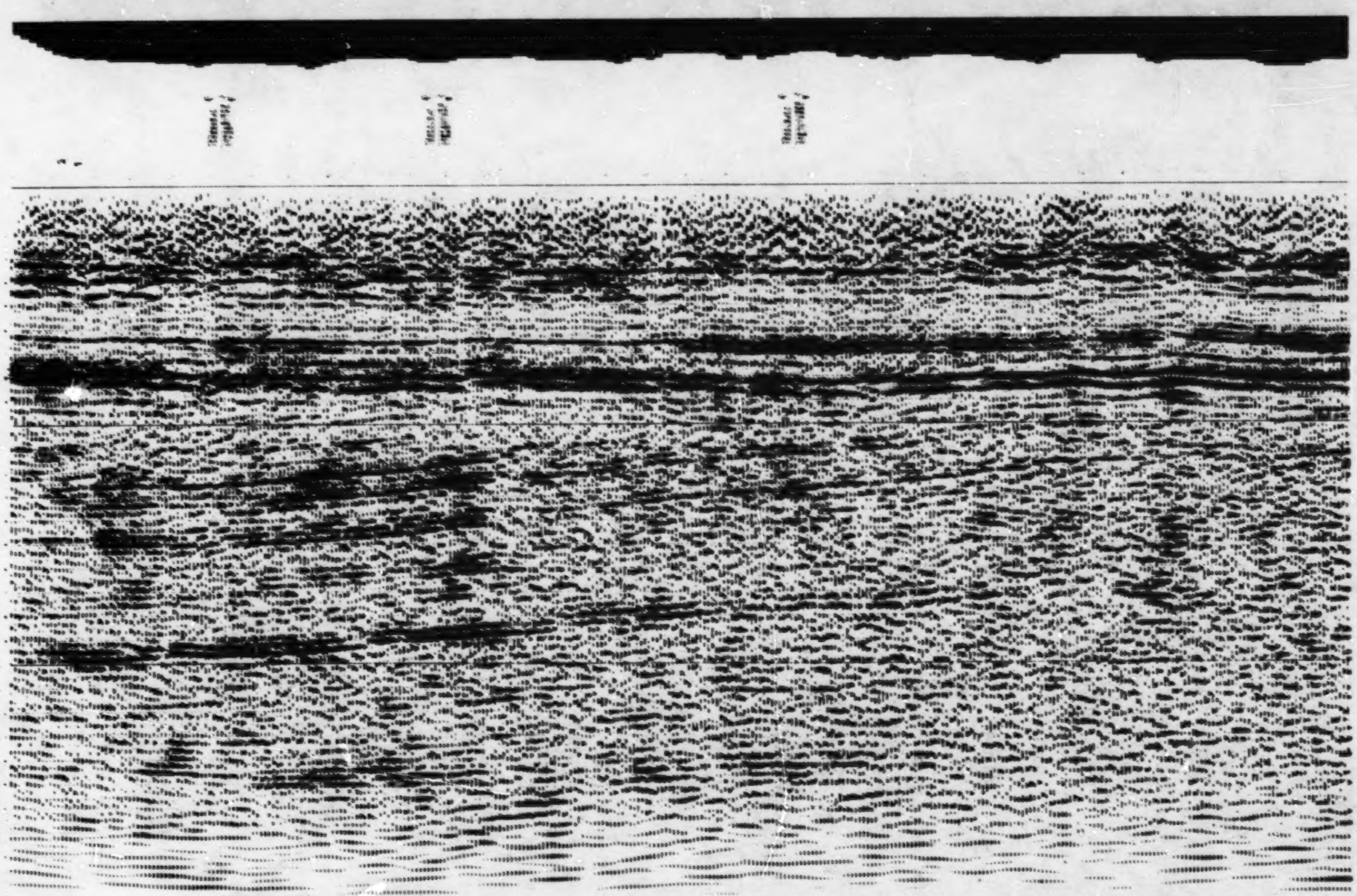

Figure 3.--Final migrated record section.

Research Applications

9900-90027

W. W. Hays
Office of Earthquake Studies
U.S. Geological Survey
905 National Center
Reston, VA 22092
(703) 860-6473

Investigations

1. The objective is to develop and to foster effective communication between producers of information in the USGS's Earthquake Hazards Reduction Program and users in Federal, State, and local governments, and the academic and private sectors.

Results

1. The Office of Earthquake Studies will join with FEMA and DOE to sponsor the 1981 Summer Institute on Multiprotection Design. The Institute will be held August 3-28, 1981, at Emmitsburg, Maryland. Earthquake protective designs will be discussed August 17-21. Applications to participate are being solicited.

2. U.S.G.S. prepared a special report entitled "Facing Geologic and Hydrologic Hazards - Earth Science Considerations." This report contains information about the hazards from earthquakes, floods, ground failures, and volcanic eruptions and their impact on the Nation. The report suggests actions based on earth science considerations which planners and decision makers may take to reduce losses.

3. USGS and FEMA are jointly sponsoring a workshop on "Preparing for and Responding to a Damaging Earthquake in the Eastern United States." The workshop will be held September 16-18 in Knoxville, Tennessee, immediately following the conference on "Earthquake and Earthquake Engineering in the Eastern U.S." The objective of the workshop is to involve easterners having a vested interest and a wide variety of disciplinary backgrounds to set goals and to define a 5-year action plan for improving the state-of-preparedness and the capability to respond to a damaging earthquake in the east. The plans will be published as an USGS Open-file report. About 50-60 selected participants will be invited to the workshop.

4. USGS participated in the annual meeting of the Western States Seismic Policy Council held in Salt Lake City, March 27-28.

Reports

1. Hays, W. W. (Editor), 1981, Evaluation of regional seismic hazards and risk: Proceeding of Conference XIII, August 25-27, 1980, Santa Fe, NM., U.S. Geological Survey Open-file Report 81-437, 220 p.

2. Hays, W. W. (Editor), 1981, Facing geologic and hydrologic hazards - earth science considerations: U.S. Geological Survey Professional Paper 1240-B., 116 p.

3. Hays, W. W., (in press), Construction of a zoning map of the earthquake ground-shaking hazard which shows the effects of geology on seismic waves: Proceedings of US-China Workshop on Seismic Zonation, September, 1981, 25 p.

Parameters for Seismic Risk Mapping

9910-03007

R.B. Matthiesen
Branch of Seismic Engineering
U.S. Geological Survey
345 Middlefield Road, MS-78
Menlo Park, CA 94025
(415) 323-8111 x2881

Investigations

The evaluation of parameters that are appropriate for use in the development of seismic risk maps requires an interdisiplinary team of seismologists and engineers. Such parameters must be determinable from the seismologists' standpoint and useful from the engineers' standpoint. A team is to be assembled both from within and without the Survey to evaluate what parameters will meet these criteria. The results should serve to guide future efforts in risk mapping.

Results

A contract with the Applied Technology Council (ATC) has been negotiated for ATC to assemble a team of engineers to develop background data on the relationship of ground motion parameters for use in seismic hazard and risk mapping to structural design procedures. The effective date of the contract is June 1, 1981, so no results have been obtained to date. Following the development of this background information, a workshop will be held to bring together this team of engineers, persons from within the Survey, and other interested persons.

Neotectonic Synthesis of U.S.

9540-02191

Carl M. Wentworth
Branch of Western Environmental Geology
U.S. Geological Survey
345 Middlefield Road, MS 75
Menlo Park, California 94025
(415) 323-8111, ext. 2474

Investigations

1. Reviewed historic record of surface faulting as a basis for selecting fault length, maximum displacement and average displacement for large earthquakes along the eastern seaboard, and reevaluated the frequency implications of the hypothesis that diffuse deformation on scattered northeast-trending reverse faults is responsible for large earthquakes along the eastern seaboard. Prepared a manuscript that develops the hypothesis for the whole eastern seaboard and addresses the frequency implications.

2. Explored the relation between the configuration of the basement surface along the Atlantic margin based on drill hole data and that generalized from the magnetic depth estimates of Klitgord and Behrendt (1979).

3. Pursued applications of the 1:250,000 digital terrain maps prepared for much of Southern California and the Coast Ranges.

4. Began an analysis of mountain fronts in the Basin and Range in Arizona and Southern California according to the degree of vertical tectonic activity. The classification, following the work of Bull, is based principally on quantitative determinations of mountain-front sinuosity and the ratio of valley-floor width to valley height.

5. Began a study of tectonic geomorphology and neotectonics north of the Grand Canyon, with particular attention to fault-scarp morphology and controls, escarpment morphology and genesis, significance of knickpoints in the Grand Canyon, and nonparametric classification in Quaternary mapping.

6. Through RFP 998W, established a contract with the State of Arizona to pursue neotectonic studies. Work will be directed principally at 1) refinement of the young fault map (being completed under a different contract) to include relevant older faults and kinds and ages of stratigraphic control, 2) analysis of scarp morphology along principal young faults, and 3) geomorphic study of representative topographic/tectonic elements in the State, including the transition from Colorado Plateau to Basin and Range.

Results

1. The eastern midcontinent has undergone broad warping in the past 70 m.y. that mimics Paleozoic structure. Average rates of subsidence in the Michigan Basin and Mississippi Enlargement are of the order of 1 m/m.y., similar to average rates of reverse faulting in the southeast.

2. The 120 m highland rim surrounding the 45,000 km^3 basin of Lake Superior can be wholly accounted for by isostatic uplift consequent to early Pleistocene glacial excavation of the basin, based on mathematical modeling using a crustal stiffness radius of 125 km.

3. Study of LANDSAT lineaments in the shield area between Lakes Superior and Michigan indicates a poor relation between lineaments and mapped faults. Both appear to form conjugate patterns, but the faults trend more easterly than the corresponding family of lineaments. There are few faults in the region that displace Paleozoic rocks, and apart from the Great Lakes tectonic zone, there appears to be no clear evidence for displacement of Pleistocene deposits or the Cretaceous rocks of Minnesota.

4. The northern Walker Lane in western Nevada is characterized by discontinuous evidence for right lateral faulting, including such geomorphic features as scarps, sag ponds, offset stream channels, and offset stone stripes. In the 110-km-long Walker Lake segment, at least 48 km of right slip has accumulated, involving a maximum slip rate of about 0.5 mm/yr for individual faults. In the 160-km-long Pyramid Lake segment, post-Miocene offset amounts to between 1.6 and 16 km, and 20-m stream offsets in Pleistocene deposits suggest a minimum offset rate of 0.2 mm/yr.

5. A stratigraphic horizon about 1 m.y. old in the Ventura Basin records vertical displacements as great as -3.5 km and more than + 5 km. Horizontal displacements are as great as 10.8 km. (See separate report on Regional Tectonic Analysis of the Ventura Basin, Transverse Ranges, California by R. S. Yeats.)

6. The frequency of damaging earthquakes (M about 7) along the eastern U.S. seaboard, assuming scattered reverse-fault sources (Wentworth and Mergner-Keefer, 1981), is probably about 1x10^{-3} per year. This conclusion depends on relatively small source dimensions--based on smaller values from the world-wide record of historic reverse fault events--of a 20-km fault length and 0.8-m maximum displacement, and a ratio of average to maximum displacement of 0.3. This 1x10^{-3} annual rate determined from geologic parameters is strikingly similar to that calculated by Perkins and others (1979) from the historic earthquake record for the region.

7. The digital terrain maps in which average altitudes for quarter-minute quadrangles are contoured produce a model of the terrain in which only the smallest topographic variations are filtered out. The resultant topographic surface is immediately determinable by eye, in contrast to 2-degree sheet topography, and reflects the main features of the terrain. Most features correlate well with geologic units, boundaries, and faults as represented on 1:250,000-scale maps.

8. Subtraction of super- and subenvelope surfaces is an effective method of defining and determining topographic relief. In the ideal case, the profiles of ridge lines and drainages would be used to establish these surfaces, and the resultant relief would be the depth of the valleys so defined. For the digital terrain relief map, a cell size of 1 minute was selected to generously bridge typical Coast and Transverse Range valleys.

9. Initial mountain-front analysis in northwestern Arizona yields high

mountain-front sinuosity and valley height /width ratios, values that are indicative of inactive fronts. This result is consistent with the typical presence in this region of broad pediments flanking the ranges. The work has emphasized the sensitivity of the method to delineation of the mountain front, the position of which directly influences both geomorphic measures. As yet unresolved problems are posed in areas where external drainage has resulted in entrenchment or widespread removal of alluvial basin fill.

Reports

Wentworth, C. M., and Mergner-Keefer, Marcia, 1981, Regenerate faults of small Cenozoic offset as probable earthquake sources in the Southeastern United States: U.S. Geological Survey Open-File Report 81-356, map scale 1:250,000.

Heller, P. L., Wentworth, C. M., and Poag, C. W., 1981, Episodic post-rift subsidence of the U.S. Atlantic continental margin: Geological Society of America Bulletin, in press.

Mayer, Larry, Mergner-Keefer, Marcia, and Wentworth, Carl M., 1981, Probablilty models and computer simulation of landscape evolution: U.S. Geological Survey Open-File Report 81-656.

Wentworth, C. M., and Mergner-Keefer, Marcia, 1981, Reverse faulting along the eastern seaboard and the potential for large earthquakes: Proceedings of the Conference on Earthquakes and Earthquake Engineering, the Eastern U.S., September 1981, in press.

Southern California Seismic Arrays

Contract No. 14-08-0001-19268

Clarence R. Allen
Seismological Laboratory, California Institute of Technology
Pasadena, California 91125 (213-356-6904)

Investigations

This semi-annual report summary covers the six-month period from 1 October 1980 to 31 March 1981. The contract's purpose is the partial support of the seismological arrays on the joint USGS-Caltech SCARLET (Southern California Array for Research on Local Earthquakes and Teleseisms), which is also supported by other groups, as well as by direct USGS funding through its employees at Caltech. According to the contract, the primary visible product will be a joint USGS-Caltech catalog of earthquakes in the southern California region, to be issued on a yearly basis, although quarterly epicenter maps and preliminary catalogs are also required.

Results

Figure 1 shows the epicenters of all shocks that were located during the reporting period; coverage above M = 3.0 is felt to be complete. Some of the seismic highlights in the southern California region during the six-month period are as follows:

Number of earthquakes located: 3,048
Number of earthquakes of M = 3.0 and greater: 196
Number of earthquakes of M = 4.0 and greater: 18
Number of earthquakes of M = 5.0 and greater: 0
Number of earthquakes for which systematic telephone notification made: 5
Largest earthquake: M = 4.7 (12-24-80, near Mammoth)
Smallest earthquake reported felt: M = 2.0 (10-10-80, 3 km NW Canoga Park)

This was a period of activity much closer to the long-term normal than was the previous period, which was marked by 4 earthquakes of M = 6.0 and greater. As can be seen from Figure 1, swarm activity continued in the Mammoth area, as well as in the Huntoon Valley (Nevada) area some 50 km to the north. No conspicuous swarms occurred in the Imperial Valley. A marked seismic gap continued to develop in the Anza area (Figure 2), accentuated by a "hot spot" of intense activity to the south of the gap. The largest event in the "hot spot" was of M = 3.7, and activity continues to the time of this writing.

During most of the reporting period, the CEDAR (Caltech Earthquake Detection and Recording) system was only partially operative, owing to a changeover to the more sophisticated CUSP (Caltech-USGS Seismic Processor) system that has been under development by Dr. Carl Johnson of the USGS.

Nevertheless, we feel that no significant earthquakes have been missed during this period, and there should not be significant degradation of the catalog quality. The new system went into routine operation on 27 March and uses the PDP 11/34 on-line and the 11/70 off-line. Not only is it far more efficient in its operation, but it will also permit analysis of the increased number of stations that will presently be recorded here.

New seismograph stations added to the network during the reporting period, with telemetry to Pasadena, include BAT CAVE BUTTE [BAT] (12-17-80), BORREGO MOUNTAIN [BRG] (3-31-81), SALTON SEA NAVAL STATION [SLT] 3-31-81, and YAQUI MEADOWS [YAQ] (3-31-81).

Publications

Allen, C. R., 1981, The modern San Andreas fault, Ch. 15 (p. 511-534) *in* Ernst, W. G., *ed.*, The Geotectonics development of California, Rubey Vol. 1: Engelwood Cliffs, Prentice-Hall, 706 p.

Hutton, L. K., and others, 1981, Caltech-USGS monthly preliminary epicenters for January 1980 through December 1980; Pasadena, California Institute of Technology, 61 p.

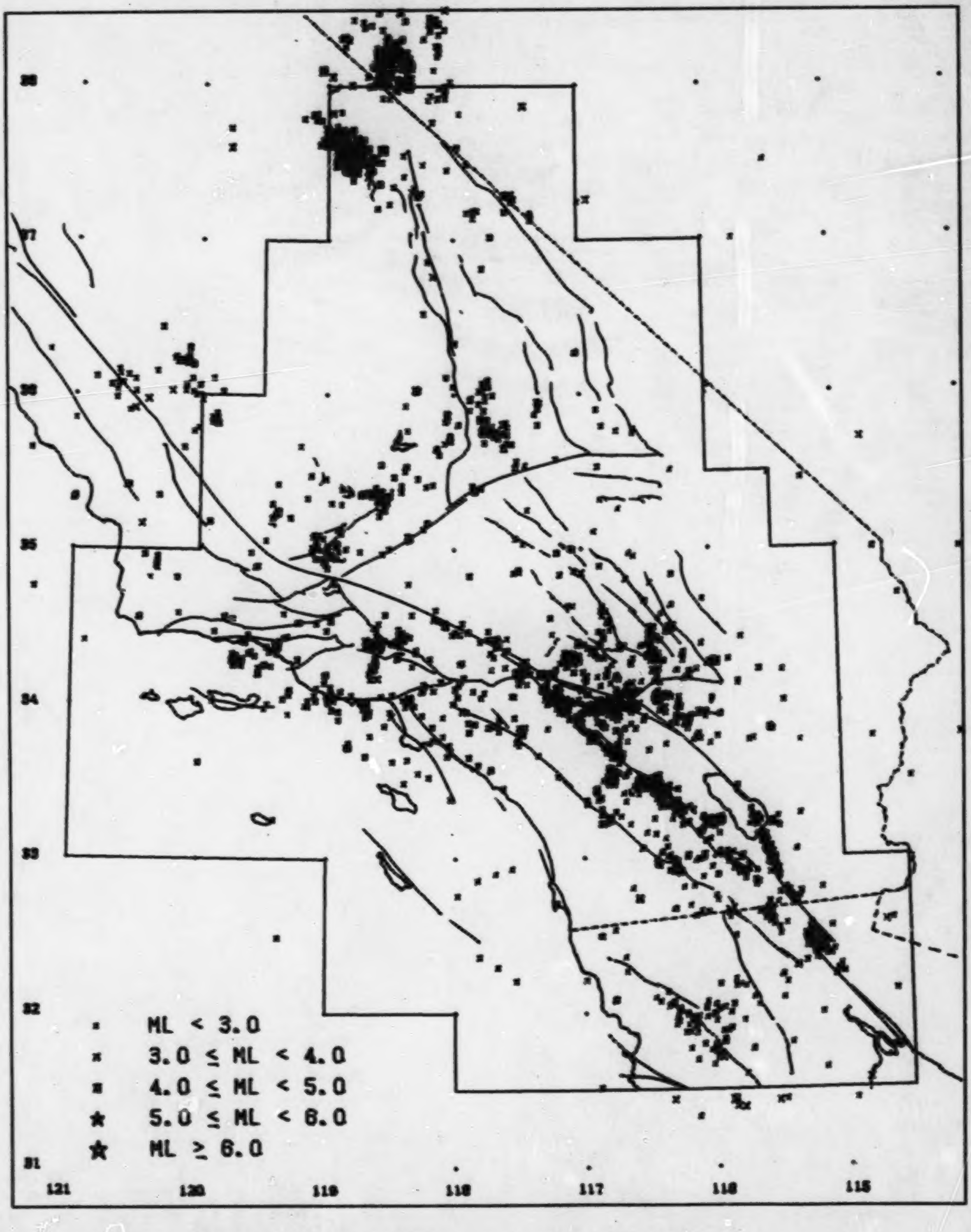
38
37
36
35
34
33
32
31
121
120
119
118
117
116
115
ML < 3.0
3.0 ≤ ML < 4.0
4.0 ≤ ML < 5.0
5.0 ≤ ML < 6.0
ML ≥ 6.0

Figure 1.--Epicenters of earthquakes in the southern California region, 1 October 1980 to 31 March 1981. Data should be complete for M = 3.0 and larger events.

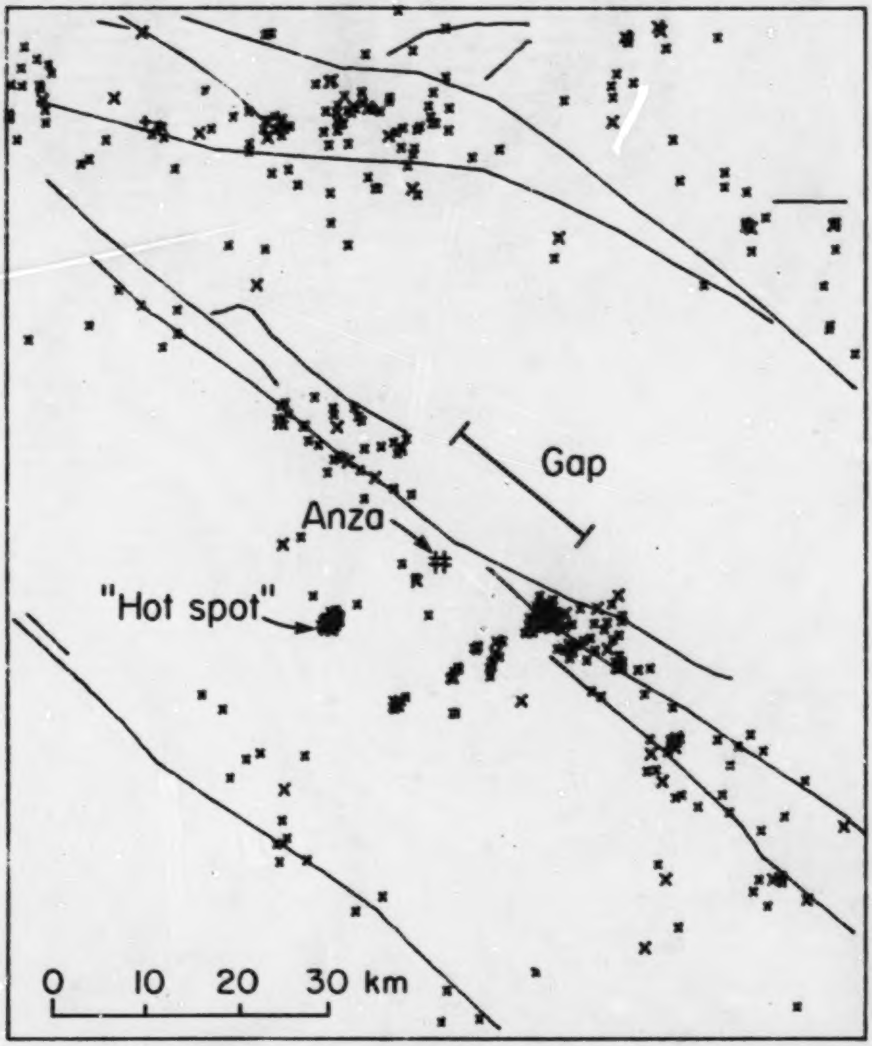

Figure 2.--Earthquakes of magnitudes greater than 2.2 in the Anza area, Riverside County, between 1 January 1978 and 31 March 1981. Note 18-km-long seismic gap along San Jacinto fault opposite Anza. "Hot spot" has been particularly active during the current reporting period.

Tectonic Framework San Francisco Bay Region

9540-01618

Earl E. Brabb
Branch of Western Environmental Geology
U.S. Geological Survey
345 Middlefield Road, MS 75
Menlo Park, CA 94025
(415) 323-8111, ext. 2203

Investigations

1. Continued work on map of fault potential for San Mateo County seismic zonation (I-1257 series).

2. Continued evaluation of different kinds of slope maps for San Mateo County.

3. Continued work on map showing general direction and amount of dip of bedrock units in San Mateo County.

4. Finished map of geologic, scenic, and historic points of interest in San Mateo County.

5. Conferred with Morton Markowitz, U. S. Army Corps of Engineers, about tsunami map for San Mateo County.

6. Conferred with Andy Spieker about map of flood-prone areas for San Mateo County.

7. Attended meeting at U. C. Davis to discuss need for and content of legislation to cope with landslide hazards in California.

8. Gave talk on earthquake hazards to 300 public health officials in Oakland.

9. Gave talk to Seismological Society of America on effects of next great San Francisco earthquake.

10. Continued compilation, editing and drafting of geologic maps by T. W. Dibblee, Jr.

Results

1. The text for the fault potential map is nearly finished. Conferred with Earl Hart, CDMG, and learned that Alquist-Priolo zones, which form part of the San Mateo map, are being revised and will be available by July 1. Need to meet with Jean Olson to discuss joint geology-seismology text.

2. We are having problems comparing ground profiles with several types of slope maps that have been produced by computer methods. The problems involve location of information on the slope maps relative to the ground profiles, and how to generalize the slope intervals on the ground profiles so that they can be compared with the computer-generated maps.

3. The map showing dip direction has been delayed for several months by the company preparing the digital tape.

4. The map of geologic, scenic and historic points of interest for San Mateo County has been approved by the Director and is being prepared for publication in the I257 series.

5. The Corps of Engineers had intended to prepare 7-1/2' maps of the San Francisco Bay region showing which areas might be inundated by a tsunami, but the project has been recessed. The main difficulty is obtaining adequate elevation data.

6. Andy Spieker will insure that the WRD flood-prone maps for San Mateo County are reduced to 1:62,500 and put on the standard base map for the county as part of the I-1257 series.

7. The meeting at Davis was attended by representatives from the California Department of Conservation, the California Division of Mines and Geology, a state senator's office, several counties, 3 universities, and the U.S.G.S. The group concluded that legislation and funding for landslide hazard mapping is needed but that chances are slim for such legislation at this time.

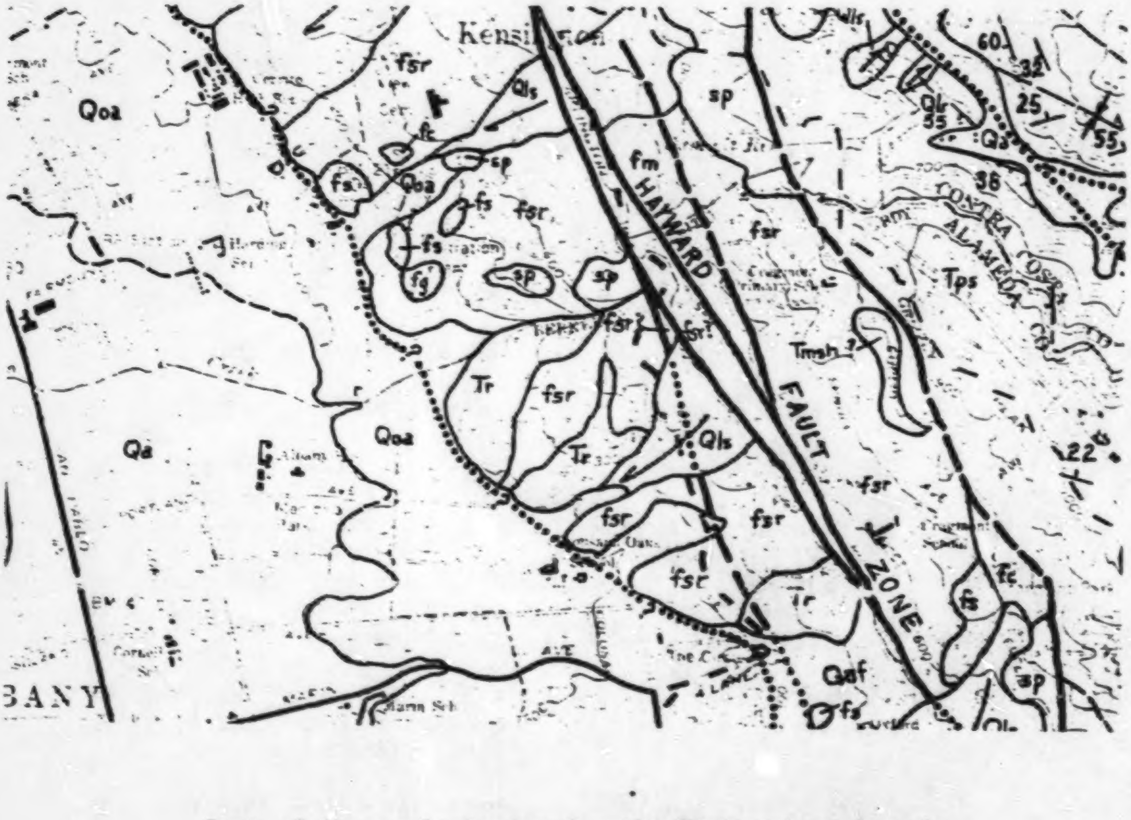

Part of the geologic map for the Richmond quadrangle

Status of Seismic Zonation Maps for San Mateo County
Miscellaneous Field Investigations I-1257 Series

	Authors	Maps	Comments
Brabb, Pampeyan	Geology I-1257A	In press	
Wieczorek, et al.	Earthquake induced landslides	Map finished, text being written.	
Mark Newman Brabb	Slope	Elevation data in digital form. Need to compare with ground data.	
Brabb, Taylor	Geologic, scenic and historic sites	Finished, in BTI	
Brabb	Dip direction and amount	Map in preparation	
Youd	Liquefaction potential	Almost ready for branch review.	
Brabb	Fault potential	Map finished. Text nearly finished	
Olson	Epicenters	Map nearly finished. Need text. Will probably combine with fault map.	
Brabb, Pampeyan	Landslide inventory	Will be done when time availabe.	
Brabb, et al.	Landslide susceptibility	Will be done by computer when landslide inventory and slope map finished.	
Perkins (ABAG)	Building risk	In branch review.	
Uncertain	Dam inundation	Available in digital form.	
Fumal, Gibbs	Seismic units	Nearly ready for branch review.	
Joyner, Gibbs	Ground response	In preparation.	
Uncertain	Tsunami	Data available in digitial form.	
Uncertain	Flood prone areas	From WRD maps.	
Uncertain	Land use	Data available in digital form.	
Wentworth, Ellen	Hillside materials	In TRU review.	
Uncertain	Vegetation	Available in digital form. May be used to make landslide susceptibility map.	
Brabb	Composite hazards	Will begin when all other maps are finished	

Reports

Brabb, E.E., and Herd, D.G., 1981, Seismic zonation: anticipating the consequences of future San Francisco Bay area earthquakes: Earthquake Notes,. v. 52, p. 5

Dibblee, Thomas W., Jr., 1980, Preliminary geologic map of the Hayward quadrangle, Alameda and Contra Costa Counties, California: U.S. Geological Survey Open File Report 80-540, scale 1:24,000

Dibblee, Thomas W., Jr., 1980, Preliminary geologic map of the Port Chicago quadrangle, Solano and Contra Costa Counties, California: U.S. Geological Survey Open File Report 81-108, scale 1:24,000.

Dibblee, T. W., Jr., 1981, Preliminary geologic map of the Mare Island quadrangle, Solano and Contra Costa Counties, California: U.S. Geological Survey Open File Report 81-234, scale 1:24,000.

Dibblee, Thomas W., Jr., 1980, Geologic map of the Honker Bay quadrangle, Solano and Contra Costa Counties, California: U.S. Geological Survey Open File Report 80-2009, scale 1:24,000.

Dibblee, Thomas W., Jr., 1980, Preliminary geologic map of the Richmond quadrangle, Alameda and Contra Costa Counties, California: U S. Geological Survey Open-File Report 80-1100, scale 1:24,000.

Dibblee, Thomas W., Jr., 1981, Preliminary geologic map of the Mendenhall Springs quadrangle, Alameda County, California: U.S. Geological Survey Open-File Report 81-235, scale 1:24,000.

Dibblee, Thomas W., Jr., and Brabb, E. E., 1980, Preliminary geologic map of the Loma Prieta quadrangle, Santa Cruz and Santa Clara Counties, California: U.S. Geological Survey Open File Report 80-944, scale 1:24,000.

Seismic Hazards of the Hilo 7 1/2' Quadrangle

9550-02430
Jane M. Buchanan-Banks
Engineering Geology Branch
U.S. Geological Survey
Hawaiian Volcano Observatory
Hawaii Volcanoes National Park
Hawaii, 96718
(808) 967-7328

Investigations

Geologic mapping of the Hilo quadrangle and especially of the Wailuku River were emphasized during the drought conditions that have prevailed since last summer. Field checking of the thicknesses of the ash, the underlying clay bed and saprolite deposits in the Hilo, Papaikou, Akaka Falls and Pi'ihonua quadrangles was completed.

Results

Mapping in the Wailuku River indicates that about 10,500 C14 years before present a voluminous aa flow, the Anu'enu'e aa, of Mauna Loa origin used the present and ancestral Wailuku River channel as a flow path. From the western quadrangle boundary eastward to Rainbow Falls, a local scenic viewpoint, the Anu'enu'e aa lies almost exclusively on Mauna Kea eruptive products. Below the falls, however, the aa has blocked the ancestral river channel and forced the present river northward, where it eroded and exposed older Mauna Loa rocks. No interfingering of the deposits from the two volcanoes was observed in the mapped portions of the river. A first draft of a map showing ash thickness/clay bed thickness/ and type of underlying deposits has been prepared. Not all factors are known for every locality; in some cases, the clay bed does not exist and in others, the clay bed and/or the bedrock are not exposed. Where the basal saprolite is exposed, it has not been possible to determine its thickness at enough localities to attempt to make an isopach map. The text which will accompany the map is presently being written. A copy of this preliminary map has been sent to the Engineering Geology Branch in Menlo Park for their use in preparing a slope stability map of the same area.

Reports

Wieczorek, G. F., Wilson, R. C., Jibson, R. W., and Buchanan-Banks, J. M., 1981, Seismic slope instability in Hawaii--a consequence of sensitive volcanic ash abs. : (Seismol. Soc. America meeting, Berkeley, California, March 1981).

Characteristics of Active Faults in the Great Basin

9950-01538

R. C. Bucknam
Branch of Earthquake Tectonics and Risk
U.S. Geological Survey
Denver Federal Center, MS 966
Denver, CO 80225
(303) 234-5089

Investigations

1. Continued study of Great Basin active faults, including (1) mapping fault scarps in unconsolidated sediments, relative dating of faulted sediments, and profiling fault scarps in the Tooele 2° sheet, Utah, and (2) reconnaissance field mapping and profiling in the Elko 2° sheet, Nevada.

Results

1. Geomorphic and geologic evidence collected by R. L. Dodge and Ted Barnhard in the Tooele 2° sheet indicates that the most recent scarp-forming earthquake events on the nine fault zones investigated predate formation of the Bonneville shoreline scarp (age about 15,000 years B.P.). Many of the faults are marked only by vegetation lineaments or very eroded scarps. Bonneville and post-Bonneville sediments are not offset; offset sediments are mainly pre-Bonneville alluvial gravels. Shoreline-fault scarp relationships, such as scarps truncated by shorelines or shorelines developed on scarp faces, also indicate a pre-Bonneville age for faulting. The locations of fault scarps in nine zones have been compiled at a scale of 1:250,000 preparatory to publication of a final map of the Tooele 2° sheet. Several minor fault zones remain to be field checked; photointerpretation indicates the last movement on these faults also predates the Bonneville shoreline scarp.

Where profile data were sufficient (four fault zones) statistical analysis defined regression lines for the scarp height-scarp-slope angle relationship defined by Bucknam and Anderson (1979). For relative dating, Tooele fault zone regression lines were compared to those of the wave-cut scarp at the high stand of Lake Bonneville, and to those of other scarps in western Utah for which Bucknam and Anderson (1979) estimated the age of last movement (fig. 1). Although the northern Oquirrh-Bonneville shoreline relative age relationship appears ambiguous on figure 1, shoreline-fault scarp relationships along scarps in the zone indicate a pre-Bonneville age for faulting. The last movement on the Stansbury, Mercur, and Sheeprock faults also pre-date the Bonneville shoreline scarp. Profile data on the remaining five fault zones, although inadequate for statistical analysis, also plot below the Bonneville regression line suggesting a pre-Bonneville age for faulting.

Reconnaissance field-checking of photogeologic mapping in the Elko 2° sheet, Nevada, involved identifying fault scarps in unconsolidated sediments and collecting general geologic-geomorphic data for relative dating. Additionally, five sites were selected for scarp profiling. Statistically defined regression lines for scarpheight-scarp-slope angle on the five Elko fault zones fall below the regression line for the Bonneville shoreline scarp, indicating that the latest fault movement is older than about 15,000 years B.P.

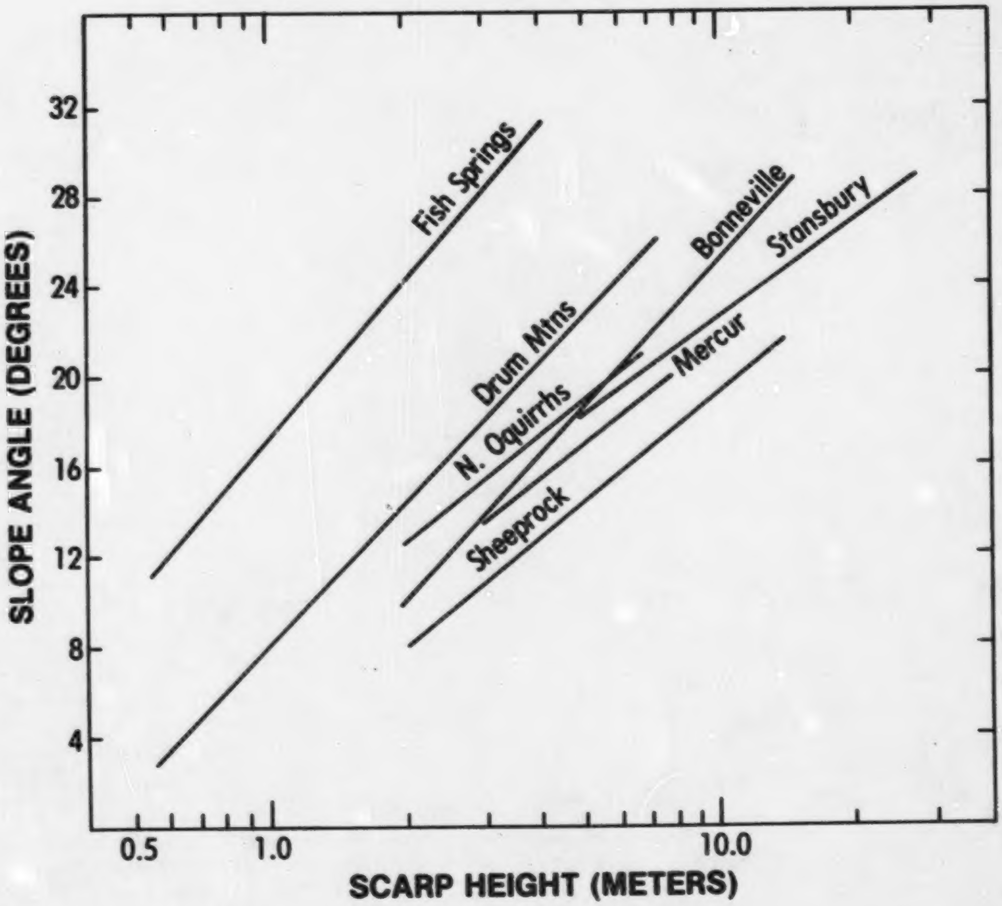
SLOPE ANGLE (DEGREES)
32
28
24
20
16
12
8
4
0.5
1.0
10.0
SCARP HEIGHT (METERS)
Fish Springs
Drum Mtns
N. Oquirrhs
Bonneville
Stansbury
Mercur
Sheeprock

Vertical Tectonics

9950-01484

Robert O. Castle
Branch of Earthquake Tectonics and Risk
345 Middlefield Road, M/S 77
Menlo Park, CA 94025
(415) 323-8111, ext. 2482

Investigations

1. Continued studies of historic crustal deformation based on the results of repeated levelings and both continuous and discontinuous sea-level measurements and how this deformation may be related to the late Cenozoic tectonics in selected parts of California.

2. Began investigations designed to explain the maintenance of the divide between the Gulf of California and the Salton Sea.

Results

1. Completed report on the evolution of the southern California uplift, 1955-76.

2. Completed report on historic surface deformation near Oildale, California.

Reports

Burford, R. O., Harsh, P. W., and Espinosa, A. F., 1981, 7.3 quake in Algeria reviewed: Geotimes, v. 26, p. 18-20.

Anchorage-Susitna Lowlands Earthquake Hazards Mapping

9310-02078

O. J. Ferrians, Jr.
Branch of Alaskan Geology
U.S. Geological Survey
345 Middlefield Road
Menlo Park, CA 94025
(415) 323-8111, ext. 4108

Investigations

1. Continued office compilation of surficial/engineering geologic mapping and Quaternary stratigraphic studies.

2. Continued collection and synthesis of subsurface engineering soils data.

Results

1. Completed preliminary surficial/engineering geologic maps of part of the study area.

2. Obtained logs and soils analyses from boreholes. These data, obtained from private, state, and federal organizations, have been catalogued in a card file and currently are being synthesized.

Reports

Schmoll, H. R., Dobrovolny, Ernest, and Gardner, C. A., 1980, Preliminary geologic map of middle part of the Eagle River valley, Municipality of Anchorage, Alaska: U.S. Geological Survey Open File Report 80-890, 1 plate, 11 p.

Schmoll, H. R., Dobrovolny, Ernest, and Gardner, C. A., 1981, Preliminary geologic map of Fire Island, Municipality of Anchorage, Alaska: U.S. Geological Survey Open File Report 81-552, 1 plate, 5 p.

Ground Response Along the Wasatch Front

9940-01919

W. W. Hays
Office of Earthquake Studies
905 National Center
Reston, VA 22092
(703) 860-6473

Investigations

1. The objective is to improve fundamental knowledge about how the local geology along the Wasatch front affects ground response. The activities during the past 6 months mainly focused on the preparation of data reports and journal manuscripts for publication. These forthcoming publications will document the ground motion data as well as the analysis of ground response in the Salt Lake City, Ogden, Provo, Logan, and Cedar City areas. Analysis consisted of correlating the characteristics of the time histories, response spectra, and site transfer functions with the local and regional geology, utilizing the available drillers logs and other subsurface information to augment surficial geology maps.

Results

1. The ground response information derived from simultaneous recordings of nuclear-explosion ground-motion data at sites underlain by unconsolidated material and rock provides a basis for seismic zoning decisions along the Wasatch front. For example, the horizontal ground response increases as distance from the Wasatch front increases. The ground response, relative to a rock site on the Wasatch front, varies in some period bands by about a factor of 10 throughout the corporate city limits of Salt Lake City; it is greatest when the fine grained soil is the thickest and wettest.

2. The ground response in the Logan area varies by as much as a factor of 10 in some period bands, relative to the site that recorded the accelerogram during the 1962 Cache Valley earthquake. The spatial variation correlates fairly well with the laterally varying properties of the subsurface geology. The characteristics of ground response also correlate with the intensity distribution for the 1962 earthquake.

Reports

1. Hays, W. W. , Miller, R. D., and King, K. W., 1981, Correlation of geology and ground response along the Wasatch front, Utah (abstract): Earthquake Notes (abstract), v. 52., mo. 1., p. 77.

2. King, K. W. and Hays, W. W., An estimate of the ground rsponse in the Logan, Utah, area during the 1962 Cache Valley earthquakes: Earthquake Notes (abstract): Earthquake Notes, v. 52., mo.1., p. 76.

H3

Sonoran Earthquake of 1887: Earthquake Tectonics of Southern Arizona, Sonora, and Chihuahua

9540-02685

Darrell G. Herd
Branch of Western Environmental Geology
U. S. Geological Survey
345 Middlefield Road, MS 75
Menlo Park, CA 94025
(415) 323-8111, ext. 2951

Investigations

1. A second reconnaissance field investigation of the 1887 Sonoran earthquake fault near Agua Prieta, Sonora, was made during February 1971 with Robert C. Bucknam (Proj. #9950-01538, Physical and Mathematical Description of Active Faults) and William B. Bull, University of Arizona. The field work was directed at determining whether the 1887 rupture extended south of the San Bernardino Valley into the Sierra Pilares de Teras. Measurements of scarp height and slope angle were made, and evidence of pre-1887 fault displacements was examined.

2. Mapping (scale 1:50,000) of the 1887 fault rupture was completed. Work was begun on an interpretative report on surface faulting and ground failure during the Sonoran earthquake of 1887.

Results

1. The Sonoran earthquake rupture was traced southward into the Sierra Pilares de Teras, beyond the southern end of the San Bernardino Valley. The rupture, which was previously thought to end near Colonia Morelos (a rupture length of only about 50 km), continues an additional 26 km, ending opposite the north end of Presa Angostura. With the discovery of the additional fault length, the 1887 fault break becomes the longest documented rupture of any normal fault in the world.

2. The fault displacement on the main break was found to average about 2.00 m (vertical surface offset) and 4.07 m (apparent net slip), but it exceeds a maximum of 5.14 m north of Arroyo Pitaycachi.

3. The main rupture is paralleled about 4 to 6 km to the west by a zone of secondary fractures and low (<0.5 m), predominantly west-facing scarps that extend nearly 30 km southward along the axis of San Bernardino Valley, from the confluence of Arroyos Cajón Bonito and Los Embudos, toward Colonia Morelos.

4. The numerous fissures and sand volcanoes that were reported by Aguilera (1888) and Goodfellow (1888) to have opened near streams up to 160 km away from the main fault rupture were undoubtedly ground failure in Holocene floodplain alluvium.

5. Reconstructions of seismic moment from fault length, average fault offset, and intensity, reveal that the Sonoran earthquake of 1887 was one of the

greatest earthquakes in intermontane North America, perhaps even larger than the San Francisco earthquake of 1906. The seismic moment of the earthquake can be estimated between 7.30 x 10^{26} and 1.48 x 10^{27} dyn cm, and may have been as large as about 5 x 10^{27} dyn cm. These seismic moments would equal a moment magnitude (M) range of 7.2 to 7.8 (the San Francisco earthquake had a moment magnitude of 7.7.

6. There is evidence of at least 2, and possibly 3 pre-1887 fault displacements along the main rupture in the San Bernardino Valley. At several sites two successively higher erosional bevels can be seen above the 1887 break. The first above the 1887 break dips between 15 and 22°; the second and higher bevel dips at only about 4 to 7°. Compared to prehistoric fault scarps in the Great Basin, these erosional bevels appear to represent a fault displacement that occurred about 10,000-15,000 years ago, and a much older fault offset that may have occurred several hundreds of thousands of years ago. Exposures of the 1887 break in stream canyons and gullies reveal similar multiple pre-1887 fault offsets.

Neotectonics of the San Francisco Bay Region, California

9540-01950

Darrell G. Herd
Branch of Western Environmental Geology
U. S. Geological Survey
345 Middlefield Road, MS 75
Menlo Park, CA 94025
(415) 323-8111, ext. 2951

Investigations

1. A cooperative investigation of the seismologic and geologic record of large earthquakes in the San Francisco Bay area was continued with W. L. Ellsworth (Proj. #9930-02103, Seismic Studies of Fault Mechanics), A. G. Lindh (Proj. #9930-02098, Parkfield Prediction Experiment), W. L. Prescott (Proj. #9960-01187, Crustal Strain), and Kaye M. Shedlock (Proj. #9950-01207, Regional and National Seismic Hazard and Risk Assessment). An assessment of the probability of large earthquakes in this century was attempted through a comparison of the historic record of large earthquakes in the Bay area during the last two centures with geologic reconstructions of the frequency of large earthquakes during the last several thousand years.

2. Work on the preparation of map syntheses (scale 1:250,000) and interpretative reports on active faults and earthquakes in the San Francisco Bay area was continued with W. L. Ellsworth.

3. An international investigation of the December 12, 1979 Tumaco, Colombia earthquake (magnitude 8) was concluded.

Results

1. The San Francisco Bay area appears to be at the threshold of the return of large earthquakes. In 1906, San Francisco was struck by a great M_s 8¼ earthquake on the San Andreas fault. The great earthquake ended nearly a century of large (M 6 to 7), frequent (about 1 per decade) earthquakes in the Bay area. For nearly 50 years following 1906, there were no $\geq$M 5 shocks in the entire San Andreas fault system north of San Jose. Since 1955, M 5 earthquakes have resumed north of San Jose. The size of the largest shocks has been steadily increasing; the last in 1980 was nearly of M 6.

2. Future large earthquakes could occur on any of a number of recently active faults in the northern California Coast Ranges (almost all of the recently active faults in northern California are of sufficient length or area to generate earthquakes of $M>6$). They are most likely on the San Andreas, Hayward, Calaveras-Sunol, Calaveras-Paicines, Rodgers Creek, Maacama, and Green Valley faults, which produced M 6 to 7 earthquakes in the last century. The San Gregorio fault, although practically aseismic throughout recorded history, might equally as well be the locus of future large shocks.

3. Although a M 8 earthquake is not impossible today, the next 1906-size tremor in the San Francisco Bay area seems distant, likely decades away. Geologic slip rates and geodetic strain rates suggest that the interval between 1906-size earthquakes on the San Andreas fault north of San Juan Bautista is about 130 to 190 years.

Reports

Published:

Brabb, E. E., and Herd, D. G., 1981, Seismic zonation: Anticipating the consequences of future San Francisco Bay area earthquakes (abst.): Seismological Society of America Earthquake Notes, v. 52, no. 1, p. 5.

Herd, D. G., Ellsworth, W. L., Lindh, A. G., Prescott, W. H., and Shedlock, K. M., 1981, The next large San Francisco Bay area earthquake (abst.): Seismological Society of America Earthquake Notes, v. 52, no. 1, p. 4-5.

Herd, D. G., Youd, T. L., Meyer, Hansjurgen, Arango C., J. L., Person, W. J., and Mendoza, Carlos, 1981, The great Tumaco, Colombia earthquake of 12 December 1979: Science, v. 211, no. 4481, p. 441-445.

Accepted for publication:

Ellsworth, W. L., Lindh, A. G., Prescott, W. H., and Herd, D. G., 1981, The 1906 San Francisco earthquake and the seismic cycle, in Proceedings, Third Maurice Ewing Symposium, Earthquake Prediction, May 12-16, 1980: American Geophysical Union, in press.

Sharp, R. V., Lienkaemper, J. J., Bonilla, M. G., Burke, D. B., Cox, B. F., Herd, D. G., Miller, D. M., Morton, D. M., Ponti, D. J., Rymer, M. J., Tinsley, J. C., Yount, J. C., Kahle, J. E., Hart, E. W., and Sieh, K. E., 1981, Surface faulting in the central Imperial Valley, in The Imperial Valley, California, earthquake of October 15, 1979: U. S. Geological Survey Professional Paper, in press.

Director's Approval:

Herd, D. G., Ellsworth, W. L., Lindh, A. G., and Shedlock, K. M., 1981, Future large earthquakes in the San Francisco Bay area, California: to be submitted to Science.

Puget Sound Lowland Focused Geophysical Studies

9830-71110

Mark L. Holmes
Branch of Pacific-Arctic Marine Geology
U.S. Geological Survey
1107 Northeast 45 Street, Suite 110
Seattle, Washington 98105
(206) 442-1995

Investigations

1. Land and marine field work for this project was conducted during February, March, and April 1981, aboard the USGS research vessel DON J. MILLER. A total of 675 km of marine gravity and 550 km of single channel reflection lines were obtained in Lake Washington and central and southern Puget Sound. Twenty-four air gun sonobuoy refraction profiles were shot using a 148 cubic inch air gun. These data supplement and extend the coverage obtained during the 1980 field season. Land gravity measurements were made at 15 stations; samples were collected from a deep (3600 m) well and several Tertiary outcrops for laboratory density and velocity measurements.

Results

1. The data obtained during the 1981 field operations were of much higher quality than the 1980 data; this improvement was due mostly to several significant changes in instrumentation. Commercial sonobuoys were extensively modified to make them more rugged and to permit reuse. A new sonobuoy receiver was employed which eliminated television interference from the strong local stations and permitted all of the geophysical measurements to be conducted from a single vessel. A larger air compressor was installed on DON J. MILLER in order to double the air gun firing rate and data density. These changes also enabled us to collect almost three times as many data during the same amount of ship time as in 1980.

2. The results of the 1980 work were presented at a Puget Sound Workshop in Seattle in October 1980. The refraction and gravity data suggest the existence of an 8-km deep basin beneath the Seattle gravity minimum filled mostly with Tertiary sedimentary rocks having densities of 2.48 to 2.58 gm/cc. The uppermost 2 km of the basin probably consists of Tertiary and Quaternary deposits with densities of 1.6 to 3.1 km/sec.

3. South of the Seattle gravity minimum the upper crustal section contains higher density rocks with correspondingly higher seismic velocities. The section consists mostly of extrusive volcanics (Crescent Formation?) overlain by Tertiary and Quaternary sedimentary rocks up to 2 km thick. Tertiary intrusive and extrusive volcanics crop out in places along a west-trending belt which seems to be directly associated with the steep gravity gradient.

4. The cause of the gravity gradient itself could be a steep fault or faulted flexure forming the southern boundary of the Tertiary basin lying beneath Seattle and Lake Washington. The gravity model suggests that much of the steepness of the gravity gradient over this feature is due to a near-surface density contrast between high density Tertiary volcanic rocks to the south and low density tuffs or pyroclastic volcanics and sedimentary rocks in the deep basin to the north.

5. The single channel seismic reflection records collected in 1980 and 1981 show that the Puget Sound basin contains up to 500 m of postglacial sediment consisting of three major acoustic units. The buried Pleistocene-Holocene surface upon which these units rest exhibits the classical U-shaped cross-section associated with glacially eroded valleys. The basal unit, about 75 m thick, shows coherent horizontal acoustic stratification and probably represents outwash deposits which were laid down during the northward retreat of the Puget lobe about 13,500 yBP. The middle unit is acoustically transparent to frequencies of 30-120 Hz, suggesting deposition in large proglacial lakes which might have formed in front of the retreating ice. Average thickness of this unit is about 125 m. The thickest (300 m) and uppermost unit shows broadly "folded" reflectors which can be interpreted as indicating deposition under marine estuarine conditions where tidal currents have greatly influenced sediment transport and deposition. The unconformity between the middle and upper units appears to mark the time at which the Puget lobe had retreated far enough to the north to allow a fairly rapid incursion of marine waters from the Strait of Juan de Fuca.

Alaska Seismic Studies

9940-01162

John C. Lahr
Branch of Ground Motion and Faulting
U.S. Geological Survey
345 Middlefield Road, Mail Stop 77
Menlo Park, CA 94025
415 323-8111, Ext. 2510

Investigations

1. Seismic data are collected and analyzed from a network of stations extending across southern Alaska and as far north as the Talkeetna Mountains. These data establish an important base of information for the study of the tectonic deformation, the potential for moderate-to-large earthquakes, and the nature of strong ground motion in southern Alaska.

2. The coastal stations east of Kayak Island are funded by NOAA's Outer Continental Shelf Environmental Assessment Program (OCSEAP). Data obtained from this network are particularly important for establishing criterion for safe oil development on the shelf.

3. A network consisting of one three-component and four vertical-component seismic stations began operation in November 1980 with Army Corps of Engineers funding to monitor the seismicity around the proposed Bradley Lake Hydroelectric project. Data from this network are being analyzed to determine the distribution and nature of the seismicity both within the crust and within underlying Aleutian megathrust.

4. A network of 24 kinemetrics SMA-1 strong motion instruments is being operated in southern Alaska from Kodiak to Juneau. Sixteen of these instruments are located in or around the Yakataga seismic gap in order to insure that a high-quality suite of accelerograms will be obtained from the major earthquake(s) expected within the next two or three decades. The chance for a magnitude 7 or larger earthquake to occur within this region during the next several years is judged to be equal to or greater than that for any other seismic zone in the United States. Strong motion data from within 25 km of a magnitude 7 or 100 km of a magnitude 8 earthquake would make an important contribution to studies of the acceleration to be expected near large earthquakes.

Results

1. During the past 6 months, data processing has remained on schedule, and preliminary earthquake locations have been obtained for August 1980 through February 1981. Currently, an average of over 450 events are being located each month. Catalogs of earthquakes in southern Alaska for October-December 1979 and January-March 1980 have been released as U.S. Geological Survey Open-File reports. The catalog for April-June 1980 has received Director's approval, and the catalog for July-September 1980 is in preparation.

2. Seismicity in the region of the Bradley Lake Hydroelectric project has been reviewed and a comparison made between events located during the first month of operation of the Bradley Lake network with those located with the regional network during the previous 8 years. In both data sets the predominate source of earthquakes is the Benioff zone, and the depths of these events suggest that the Aleutian megathrust is about 35 km deep below Bradley Lake. The distribution of earthquakes above the Benioff zone is diffuse, and although over half of the epicenters are located within 10 km of mapped fault traces, the correlation is insufficient at this time to be certain that any of the mapped faults are seismogenic.

3. During the period October 1979 to February 1981 several interesting features were observed in the seismicity that occurred between the longitudes of eastern Prince William Sound and Icy Bay, an area that includes the Yakataga seismic gap. The most notable observation was an increase in the the rate of seismicity in the offshore area that began in June 1980 and continued until October 1980. During this 5-month period the monthly average of events with coda-duration magnitudes of 2 and larger was 8 per month, as compared to an average of about 1 1/2 per month for the previous 8-month period. Most of the activity was localized in two areas, one about 50 km southwest of Kayak Island and the other about 20 km northwest of Middleton Island. The largest earthquake to occur during this time, an event of coda-duration magnitude 5 on September 4, 1980, was located about 60 km southeast of Kayak Island and did not have any locatable aftershocks. This was also the largest earthquake to occur in this offshore area in almost 10 years.

About one month after the rate of offshore activity decreased, an apparent increase was observed in the average rate of onshore seismicity near Waxell Ridge, relative to the previous 14-month period for which the data analysis is completed. Waxell Ridge is located about 75 km northeast of Kayak Island near the center of the Yakataga seismic gap. This area has been continually active since at least September 1974 when the seismic network east of Prince William Sound was expanded to near its present configuration. The seismicity in the Waxell Ridge area is being closely monitored for unusual patterns that may prove to be premonitory to the gap-filling rupture(s) expected in this area. Although the analysis of seismic data since 1974 is incomplete, the available seismic record indicates that the local rate of activity does vary with time over periods of several months to years. It is not clear how significant these apparent rate changes are because the magnitude range in which they occur is at or below the estimated magnitude threshold for completeness.

4. Seismicity north of the eastern portion of the network forms two separate trends offset from but parallel to two of the major faults mapped in the area, the Denali and Duke River faults. Considering the possible bias of hypocenters from this area, the earthquakes may be closely related to these faults. Thus, the Denali fault east of its juncture with the Totschunda fault may be seismically active, contrary to the lack of geologic evidence to support Holocene displacements on this portion of the fault.

References

Hasegawa, H. S., Lahr, J. C., and Stephens, C. D., 1980, Fault parameters of the St. Elias, Alaska, earthquake of February 28, 1979, Bulletin of the Seismological Society of America, v. 70, no. 5, p. 1651-1660.

Lahr, J. C., and Stephens, C. D., 1980, Eastern Gulf of Alaska seismicity: Quarterly report to the National Oceanic and Atmospheric Administration for April 1, 1980, through June 30, 1980, U.S. Geological Survey Open-File Report 80-943, 8 p.

Lahr, J. C., and Stephens, C. D., 1981, Review of earthquake activity and current status of seismic monitoring in the region of the Bradley Lake Hydroelectric Project, Alaska. Prepared for the Alaska District Corps of Engineers, 33 p.

Lahr, J. C., Stephens, C. D., Hasegawa, Henry, and Boatwright, John, 1980, Alaska seismic gap only partially filled by 28 February 1979 earthquake, Science, v. 207, p. 1351-1353.

Moore, G. W., Page, R. A., and Lahr, J. C., Earthquake potential and ground motions for the Pillar Mountain landslide, Kodiak, Alaska, U.S. Geological Survey Open-File Report 80-1129, 18p.

Stephens, C. D., Fogleman, K. A., Lahr, J. C., Helton, S. M., Cancilla, R. S., Tam, Roy, and Freiberg, J. A., 1980, Catalog of earthquakes in southern Alaska, January-March 1980, U.S. Geological Survey Open-File Report 80-1253, 55 p.

Stephens, C. D., Lahr, J. C., Fogleman, K. A., Helton, S. M., Cancilla, R. S., Tam, Roy, and Baldonado, K. A., 1980, Catalog of earthquakes in southern Alaska, October-December 1979, U.S. Geological Survey Open-File Report 80-2002, 53 p.

Earthquake Hazards Studies
Upper Santa Ana Valley and Adjacent Areas, Southern California

9540-01616

Douglas M. Morton and Jonathan C. Matti
Branch of Western Environmental Geology
US. Geological Survey
345 Middlefield Road
Menlo Park, CA 94025
(415) 323-8111, ext. 2353, 2358

Investigations

1. Studies of the Quaternary history of the upper Santa Ana Valley. Emphasis is currently on: (a) the three-dimensional distribution of the valley fill and its lithologic, lithofacies, and pedogenic character; and (b) generation of liquefaction susceptibility and liequefaction opportunity maps.

2. Studies of the Banning Faiult zone. The study has focused on: (a) mapping fault strands that deform crystalline basement rocks, Tertiary sedimentary rocks, and Quaternary surficial units; (b) evaluating the sedimentary and tectonic evolution of Tertiary sedimentary units within the fault zone; and (c) identification of Quaternary units to establish Quaternary depositional patterns and the relative ages of faults strands within the Banning fault system.

3. Studies of fault zones of the southeastern San Bernardino Mountains and the eastern San Gabriel Mountains. The emphasis focuses on identifying the relative ages and activity along various fault strands within the San Andreas-San Jacinto system. current emphasis is on: (a) geometry and kinematics of interactions between San Andreas-type right-lateral faults and Transverse Range-type reverse and thrust faults; and (b) further refinement of ground-rupture recurrence intervals, based on fault scarp morphology.

4. Studies of Quaternary surficial materials within the Perris block. The emphasis focuses on delineation of surficial materials in terms of their ground response characteristics.

Results

Reexamination of the alluvial deposits along the south side of the eastern San Gabriel Mountains has led to the recognition of four Pleistocene and five Holocene mappable units. Displacement of these units by strands of the Cucamonga fault indicates an involved ground displacement history. Generalization of the Pleistocene-Holocene fault history suggests vertical displacement of about two meters. The available data further suggest a recurrence of about 700 years for ground rupture over the past 13,000 years. Fault scarp morphology indicates the last ground displacement was about 800 years B.P.

Seismicity and Earthquake Source Properties in the Yakataga Seismic Gap, Alaska

9940-03005

R. A. Page and J. R. Pelton
Branch of Ground Motion and Faulting
U.S. Geological Survey
345 Middlefield Road, Mail Stop 77
Menlo Park, California 94025
415 323-8111, Ext. 2567

Investigations

1. Completed development and testing a new semi-automated system for routine scaling of earthquake data recorded on Develocorder films. The system features simultaneous projection of four film images onto digitizing table and on-line location of earthquakes by a mini-computer. Began routine scaling of unprocessed data from the southern Alaska seismic network from the second quarter of 1978 to fill in recent seismic history of the Yakataga seismic gap.

2. Obtained computer programs from J. Dewey for the determination of hypocenters by master-event and joint-hypocenter techniques and began experiments to test the resolution of teleseismic relocations of historic earthquakes in the Yakataga gap and neighboring regions.

3. Began timing of P-wave arrivals from teleseisms recorded by the USGS Alaska network. Data to be used in 3-D inversion for crust and upper mantle velocity structure beneath southern Alaska (between 139°W and 152°W) in cooperation with George Zandt at the University of Utah.

Results

1. Experience to date suggests that an increase of as much as a factor of two in the rate of data processing using the new four-film scaling system can be realized relative to standard processing practices of scaling events sequentially on different films and locating the events off-line.

2. Results from items 1 and 2 above are not yet available.

Reports

None

Geologic Earthquake Hazards in Alaska
9310-01026

George Plafker
Branch of Alaskan Geology
345 Middlefield Road, MS 908
Menlo Park, CA 94025
(415) 323-8111
ext. 4103

Investigations

1. Completed reconnaissance of regional uplift along shorelines in southeastern Alaska.

2. Completed study of the offset history of the Chatham Strait segment of the Denali fault system.

3. Completed evaluation of marine terraces in the Yakataga seismic gap near Icy Bay.

Results

1. Comparison of 1959-1960 tidal bench mark data as determined by Hicks and Shofnos (1965) (figure 1) with data obtained by Travis Hudson, Kirk Dixon, and George Plafker in 1979-1980 (figure 2) indicates that uplift at rates as high as 3 cm/yr continues to affect an area at least 500 km long by 150 km wide. The uplift data summarized in figures 1 and 2 suggest the following tentative interpretations: a) The localized zone of most rapid uplift in Glacier Bay is due mainly to isostatic rebound related to ice unloading as suggested by Hicks and Shofnos (1965). The northward migration of the locus of maximum uplift between the 1959-60 and 1979-80 studies seems to reflect rapid historic retreat of the major tidewater glaciers. It is not at all clear, however, why this zone of maximum uplift should extend eastward to the vicinity of the Chilkat Peninsula between the 1959-60 and 1979-80 studies. b) The localized uplift noted in the 1979-80 study at Taku Inlet does not seem to be attributable to unloading of ice as the Taku Glacier at the head of the inlet has been advancing slowly. The cause of this apparent anomaly is unknown and it may simply be due to measurement errors in the 1980 reconnaissance study. c) The localized uplift indicated by the 1979-80 data that extends from Admiralty to Chichagof Island is in a topographically low nonglacial area and cannot be related to ice unloading. Assuming that the data are not systematically in error, this feature is best interpreted as a transient bulge of tectonic origin. Additional closely-spaced tide series measurements are required in this area to determined the configuration and uplift rate of this feature. d) The cause of the broad regional uplift remains enigmatic. Its distribution relative to mountain areas with extensive Holocene glaciers and icefields suggests that it cannot be solely attributed to unloading of ice as suggested by Hicks and Shofnos (1965). However, shrinkage of glaciers certainly could be a factor in the northern part of the region. The alternative is that the uplift is tectonic in origin and is somehow related to compression along the active boundary that is defined by the Queen Charlotte-Fairweather transform fault system which lies roughly along the western margin of the uplifted region.

2. Geological and marine geophysical studies along the Chatham Strait fault in southeastern Alaska together with mapping along its onshore continuation northwestward into British Columbia by Travis Hudson, Kirk Dixon, Paul Carlson, and George Plafker indicate that a) the fault has undergone a total dextral slip on the order of 150 km, b) all of this slip is post-middle to Late Cretaceous, c) as much as 100 km of the total slip may postdate emplacement of middle to late Oligocene volcanics (28-32 m.y. B.P.) along the fault, d) there is no indication of Holocene deformation along the fault either onshore or offshore, and e) vertical offsets along the fault, if any, are relatively minor.

3. Additional studies of marine terraces near Icy Bay by Travis Hudson, Meyer Rubin, and George Plafker confirm the presence of three surfaces with average beach angle elevations above mean higher high water of 52±3 m, 24±2 m, and 16±1 m with minimum radiocarbon ages of about 5,000 years B.P. (stage I), 2,500 years B.P. (stage II), and 1,300 years B.P. (stage III), respectively. Our data lead to the following tentative conclusions: a) Indicated average uplift rate has been about 1.05 cm/yr during the past 5,000 years. Approximately the same uplift rate would be indicated for two data samples from benches above the terraces if their elevations are corrected for the post-glacial eustatic sea level rise (about 57 m in the last 12,000 years). This rate is remarkably close to that of the Middleton Island and Lituya Bay terrace sequences (Plafker and Rubin, 1978; Hudson and others, 1976) and is an order of magnitude less than the uplift rate in the Icy Cape area as deduced from a tree ring study by Beavan and others (1979). b) The time between uplift of the stage II and III terraces is about 1,150 years and the uplift step is roughly 8 m. c) The 26 m interval between the stage I and II terraces probably represents more than one uplift step but the corresponding terraces either have not been recognized or have been removed by erosion. d) There is no evidence of measurable post-stage III uplift that could be associated with the 1899 earthquake as was reported by Beavan and others (1979). e) The last uplift step of 16 m that formed the stage III terrace occurred about 1,300 years ago. Thus, if the 1,150 years between the stage II and III terraces represents an approximate recurrence interval for major tectonic uplift steps--and presumably large earthquakes--the data suggest that another uplift event may be anticipated in the area in a time interval that is short relative to the interval between major uplift events.

Reports

Bruns, T. R., Carlson, P. E., and Plafker, George, 1981, Structure of the northern Gulf of Alaska: A transform to convergent margin transition [abs.]: American Association of Petroleum Geologists Annual Meeting.

Carlson, Paul, Plafker, George, and Bruns, T. R., 1981, Seaward extension of the Fairweather fault on the southeastern Alaska shelf [abs.]: EOS, v. 62, no. 6, p. 60.

Plafker, George, Hudson, Travis, and Rubin, Meyer, 1980, Holocene marine terraces and uplift history in the Yakataga seismic gap, Alaska: Transactions, American Geophysical Union, v. 61, no. 46, p. 1110.

Winkler, G. R., and Plafker, George, 1981, Tectonic implications of framework grain mineralogy of sandstone from the Yakutat Group, in Albert, N. R. D., Travis, eds., The United States Geological Survey in Alaska: Accomplishments during 1979: U.S. Geological Survey Circular 823-B, p. B68-B70.

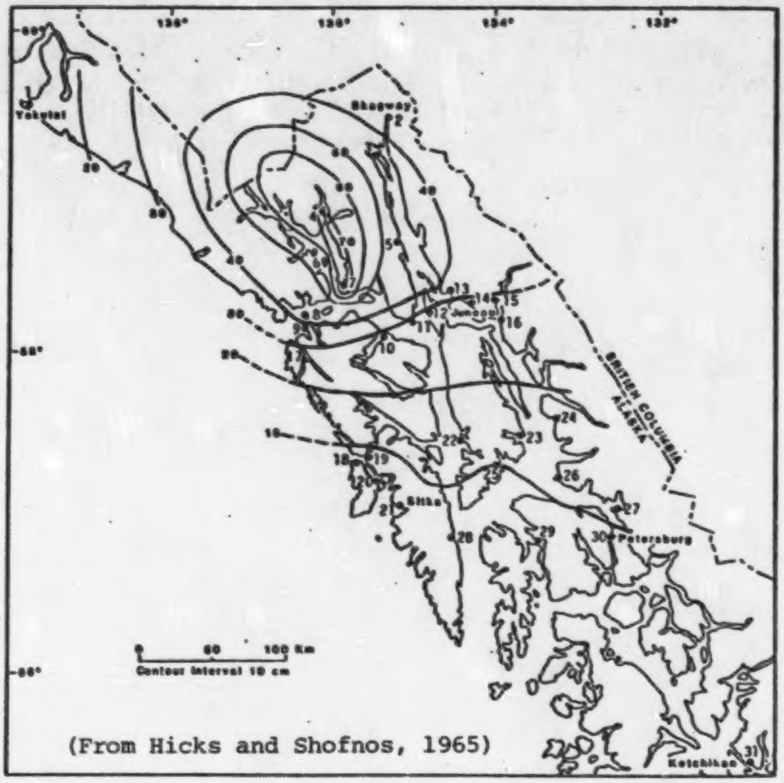

60°
136°
134°
132°
58°
56°
Yakutat
Skagway
Juneau
Sitka
Petersburg
Ketchikan
BRITISH COLUMBIA
ALASKA
0 50 100 Km
Contour interval 10 cm

(From Hicks and Shofnos, 1965)

Figure 1.

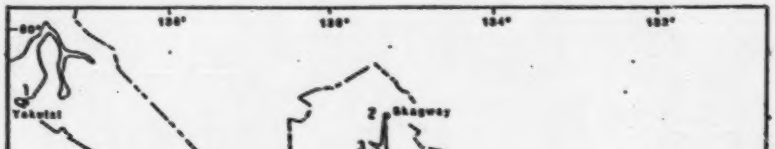

60°
136°
134°
132°
58°
56°
Yakutat
Skagway
Juneau
Sitka
Petersburg
Ketchikan
BRITISH COLUMBIA
ALASKA
0 50 100 Km
Contour interval 10 cm

Figure 2.

Maps showing uplift contours in cm for the periods 1939-1959 (fig. 1) and 1959-1979/1980 (fig.2).

SEISMIC ZONATION STUDIES IN LOS ANGELES BASIN

9940-01730

A. M. Rogers
Branch of Ground Motion and Faulting
US Geological Survey
Denver Federal Center, MS 966
Denver. CO 80225
(303) 234 3131

Investigations

1. A large data matrix has now been completed for the 100 recording sites in the Los Angeles region that includes mean site response in ten separate period bands, mean void ratios, mean % silt-clay in three depth ranges, depth-to-basement, thickness of Quaternary, mean % saturation, age of surfacial deposits, soil or rock type, and depth-to-water table.

2. Regressions were computed using mean site response in two period bands for the dependent variables and the geologic parameters as independent variables.

3. Cluster analysis was performed on the independent variables to estimate intervariable dependence. The correlation matrix on the independent variables served as the similarity matrix.

4. Cluster analysis was also run between stations to determine if the size of the data matrix could be reduced by grouping stations and, thus, also reducing data scatter. The similarity matrix in this case was computed by first normalizing the independent variables $[(X_o-\bar{X})/\sigma]$ transposing the data matrix and computing a correlation matrix between stations.

5. Mean site shear velocities are being incorporated into the data matrix.

Results

1. Regressions on the raw data matrix using subsets of independent variables with mean site response as the independent variable are generally not significant. Part of the problem with this approach is that linear models are not appropriate for some of the variables. Secondly, the scatter in some of the geological variables is undoubtedly high.

2. Subjective clustering of sites based on the range of variable values leads to regressions on the clustered data that are significant and that explain a high percentage of the variation in site response (40-80% depending on variables used). The principal variables are void ratio, depth-to-basement, age, and thickness-of-Quarternary. Regressions on clusters objectively determined from the formal cluster analysis have not yet been performed, but are expected to lead to improved regression fits. The final regressions will be run with appropriate models determined either theoretically or based on examination of regression residuals.

Reports

Rogers, A. M., Covington, P. A., Park, R. B. Borcherdt, R. D., and Perkins, D. M., 1980, Nuclear event time histories and computed site transfer functions for locations in the Los Angeles region, U.S. Geol. Survey Open-File Report 80-1173, 207 p.

Rogers, A. M., Tinsley, J. C., Hays, W. W., and King, K. W., 1981, Reply to H. R. Shifflett's "Comments on 'Evaluation of the relation between near-surface Geologic Units and ground response in the vicinity of Long Beach, California'", Bull. Seism. Soc. Am. 71, p. 571-572.

H3

Earthquake Prediction and Earthquake Hazard Along the Eastern Front of the Sierra Nevada

Contract 14-08-0001-19299

Alan Ryall
Seismological Laboratory
University of Nevada, Reno
Reno, NV 89557
(702) 784-4975

Investigations

Investigate the seismic potential and state of activity of large known or suspected faults along the Sierra Nevada-Great Basin boundary fault zone; search for changes in seismicity or earthquake mechanisms that may indicate an impending major earthquake; analyze the distribution, magnitude and mechanism of earthquakes in the area of interest; continue analysis of western Great Basin earthquakes recorded by the University of Nevada seismic network.

Results

1. Anomalous temporal vatiations in the southern part of the Sierra Nevada-Great Basin boundary zone (SNGBZ) from 1977 to 1980 followed a pattern that several authors have identified as precur- to strong earthquakes. From January 1977 to September 1978 a general decrease in seismicity was observed in the southern part of the zone, followed by a burst of moderate earthquakes from Doyle in the northern part of the SNGBZ to Bishop in the south. The 1977-1979 variations are particularly noteworthy because they occurred over the entire SNGBZ, indicating a regional rather than local cause. In the southern part of the zone, a magnitude 5.7 shock 25 km northwest of Bishop on October 4, 1978 was followed by an earthquake swarm in the Mammoth Lakes area, with peaks in activity during late 1979 and the spring of 1980. The Mammoth Lakes activity spread gradually to the west during the first year of this sequence, apparently involving several northerly-trending fracture zones in an area of about 900 km^2. Bursts of activity from December 1979 to April 1980 had increasingly dense spatial clustering. Temporal clustering showed monthly peaks in the spring of 1980, and intense swarming occurred in mid-May, about ten days before the largest (M_L 6.0-6.3) events in the series. Activity in the southern SNGBZ still remains relatively high, and a number of earthquakes with M_L about 5 have occurred in that area. This suggests that the potential for major earthquake activity in the Bishop-Mono Lake-Bridgeport area is still relatively high.

2. Shallow earthquakes around the southwest boundary of Long Valley caldera, west of the Hilton Creek fault, are characterized by lack of S-waves at regional seismic stations to the northwest, north and northeast, and P-waves for these same station-event combinations are deficient in frequencies higher than about 2-3 Hz. Earthquakes east of the Hilton Creek fault and southeast of the caldera have normal P- and S-wave signatures at the same stations. These effects are explained by propagation through a zone of melting in the south-central part of Long Valley caldera, at depth greater than 7-8 km. A tendency for earthquakes along the southwest caldera boundary to occur as intensive swarms suggests that tectonic stress within the cauldron block may still be at least partly relieved by movement of magma.

3. Pn data collected by the University of Nevada have been reanalyzed to determine crustal thickness in the northern Great Basin. Sources used in this study included explosions at the Nevada Test Site and Central Nevada Test Site, as well as earthquakes in the northern and southern Sierra Nevada and the Black Rock Desert. Analysis of apparent velocities for profiles in different directions indicates that if Pn velocity anisotropy exists in the western Great Basin it is a small effect. Pn traveltimes in the Adobe Hills area east of Mono Lake are late by about 0.5 second, in agreement with teleseismic delays observed by VanWormer and Ryall (1980). A broad region of relatively thin crust is found in the northwest Great Basin, and in general the location of this area of thin crust is in excellent with an area of high Bouguer gravity found by Eaton (1979). The crust is thinnest (20 km or less) in three areas (Reno, Carson Sink, Buena Vista Valley) along a zone trending NW from Reno and correlating generally with the location of the Midas trough. The lineup of areas with very thin crust also correlates with a zone of high velocity in the upper mantle, suggesting that it represents a structural discontinuity of major proportions.

Reports

Priestley, K. F. and A. S. Ryall (1981). Crustal structure in the northern Great Basin, Earthquake Notes, 52, 51 (abstract).

Ryall, Alan and Floriana Ryall (1981). Spatial-temporal variations in seismicity preceding the May 1980 Mammoth Lakes, California, earthquakes, Bull. Seism. Soc. Am., 71, 747-760.

Ryall, Floriana and Alan Ryall (1981). Attenuation of P and S waves in a magma chamber in Long Valley caldera, California, Geophys. Res. Letters, in press.

Earthquake Hazard and Prediction Research in the Wasatch Front--Southern Intermountain Seismic Belt

14-08-00001-19257

R.B. Smith, W.J. Arabasz, G. Zandt, and W.D. Richins*

Department of Geology and Geophysics
University of Utah
Salt Lake City, Utah 84112
(801)581-6274

Investigations

1. Analyses of earthquakes recorded by University of Utah seismic network.

2. Implementation of varied software on USGS-supplied PDP-11/70 computer system--both for earthquake-related research and routine analysis.

3. Seismicity and elastic deformation associated with Basin and Range fault blocks in northern Utah.

4. Subsurface geometry of the Wasatch fault zone from seismic reflection and refraction data.

5. Coda studies for estimates of Q, M_o, and M_L in the Utah region.

6. Critical evaluation of hypocentral resolution of shallow earthquakes located with USGS earthquake-location programs.

7. Reduction of microearthquake data from target studies with portable seismographs near the southern end of the Wasatch fault and in an area of mining-related seismicity in the SE part of our Wasatch Front study area.

Results

1. During the 6-month report period, 441 earthquakes were located in the Utah region, including eight felt shocks. The largest (M_L=3.9, MMI=V) occurred near Orem, Utah, on February 20, 1981. The Orem earthquake displayed a normal-faulting mechanism typical for the Wasatch Front area and apparently was associated with the Wasatch fault zone. Significantly, (1) it was the first shock of such size to occur since 1955 within a 70-km-long microseismic gap along the fault, and (2) not a single microaftershock followed. A new seismicity catalog for the Utah region for the period July 1978-December 1980--extending that in our recent volume "Earthquake Studies in Utah, 1850 to 1978"--has been completed and will soon be released. The new catalog includes 2300 earthquakes, of which 33 were reported felt.

---

*Semi-Annual Technical Report also includes contributions from W. Bashore, H. Benz, S. Clawson, G. M. Hathaway, M. E. McKee, and G. E. Randall.

2. On-line detection and recording of seismic events became fully operational on the PDP-11/34 during the reporting period. Noise and crosstalk problems with the LPA's were isolated and significantly improved. System trigger parameters were refined for our network geometry. A number of seismological research programs were implemented on the PDP-11/70 including: (1) a reflection seismology package, (2) a series of programs useful in the study of hypocentral location problems, (3) a storage-efficient program which simultaneously locates earthquakes and determines a three-dimensional velocity structure, (4) a ridge-regression inversion program used in studying the lateral variation in crustal Q structure, (5) a package of programs to compute theoretical displacement and strain fields of finite rectangular dislocations in an elastic half-space, and (6) a package of programs to pick and catalog teleseismic events.

3. Recent seismicity in northern Utah has been characterized by generally diffuse, yet locally clustered epicentral patterns (Figure 1a). Also, the Wasatch fault with geological evidence of repeated Holocene displacement appears currently to be unusually aseismic except for small, isolated clusters of miroearthquakes near Brigham City, Fielding, and just north of the Idaho-Utah border (42°N). In cross-sections perpendicular to the structural grain, the seismicity remains diffuse with no hint of significant planar clustering (Figure 1b). Four new focal mechanisms for earthquakes in the study area were determined and combined with previously published results (Figure 1c) to summarize the available information on the current state of strain in the northern Wasatch Front. Both geodetic data (Prescott et al., 1979) and the focal mechanisms indicate that areas of "reversed strain" occur locally within the generally extensional strain regime of the study area. One possible mechanism for such strain reversals is the variation in strain associated with aseismic movement on buried faults. This mechanism was modeled by computing the displacement and strain fields surrounding a rectangular dislocation in an elastic half-space. The horizontal components of surface displacement and strain along the right bisector of the fault trace are shown in Figure 1d. The strain curves show that a zone of horizontal compression can occur as a result of normal movement on a buried dip-slip fault. The compressional zone is localized at the surface to an area almost directly above the fault surface, regardless of whether the fault is dipping at a high-angle or a low-angle. A simple calculation, assuming the geodetic data from Ogden averaged the strain over an area equivalent to the shaded areas in Figure 1d showed that ∿2-3 cm/yr of slip is necessary to cause the observation of ∿0.2 μstrain/yr near Ogden. Although such a slip rate is certainly too large for the Basin and Range province for a geologically long term, it may be within the realm of possibility during periods of rapid strain release for short periods of time, i.e. tens of years.

4. The PDP-11/70 LPA system was temporarily converted for use in digitizing cassette-tape recorded refraction data. The necessary software were implemented to retrieve the data, add header information, and produce record sections. Programs are being implemented to study both the refraction and reflection phases generated from both earthquake and synthetic sources through forward two-dimensional ray-tracing and synthetic seismogram modeling.

5. Techniques and theory developed by Aki, Chouet, and others for the extraction of propagation and source information from coda waves of local earthquakes can enhance effective use of digital network data. We are assembling software for

our PDP-11/70 to implement a bank of zero-phase, finite-impulse-response, bandpass digital filters that duplicate the frequency responses specified by Aki and Chouet (1975) for their spectral analyzing seismograph in the 1-16 Hz passband. Attempts to use coda amplitudes from Benioff SPZ seismographs--following Aki (1969) and Herrmann (1980)--for estimates of M_o face the obstacle of unusually low corner frequencies for Utah earthquakes. For $M\sim4$ to 5½, local earthquakes appear to follow a scaling path of constant corner frequency of about 0.2 Hz with increasing M_o of 10^{23} to 10^{24} dyne-cm.

6. In an investigation of the convergence properties of hypocentral location programs, we computed the RMS error surface of the hypocentral mislocation. Both synthetically generated data and the actual observed phase data have been used to map the error surface in a two-dimensional cross-section in the solution space. In test cases with multiple local RMS error minima, initial results indicate that HYPO80 is unstable in regions of multiple local minima, and HYPOELLIPSE will converge to the local minimum nearest to the initial location. Further work should allow careful testing of the convergence properties of hypocentral programs, and detailed investigation of troublesome events may provide clues on how to improve convergence in location programs.

7. Episodic bursts of microseismicity have been detected in Goshen Valley at the southern end of Utah Lake since 1974. All clusters have occurred in either the April-May period or the December-January period. Despite detailed studies of spatial resolution and focal mechanisms, the correlation with geologic structure remains unclear. Microearthquake field studies along the eastern margin of the Wasatch Plateau, an area of active underground coal mining, have allowed improved resolution of intense mining-related seismicity, the discrimination of seismicity 6-15 km *beneath* the levels of mining, and compressional focal mechanisms that spatially identify a transition in stress orientation from the Great Basin to the Colorado Plateau.

Reports and Publications

Doser, D. I. (1980). Source parameters of Utah earthquakes (abstract), *EOS*, *Trans. Am. Geophys. Union* *61*, 1028.

Owens, T. J. (1980). Flexure and normal faulting in an elastic-perfectly plastic plate (abstract), *EOS*, *Trans. Am. Geophys. Union* *61*, 1123.

Richins, W. D. and G. Zandt (1981). Seismicity and elastic deformation associated with Basin and Range fault blocks in northern Utah (abstract), *Earthquake Notes* *52* (1), 63.

Carver, D. and W. D. Richins (1981). Fine details of the aftershock process following the September 30, 1977, Uinta Basin, Utah, earthquake (abstract), *Earthquake Notes* *52* (1), 62.

Arabasz, W. J., W. D. Richins, and C. J. Langer (1981). The Pocatello Valley (Idaho-Utah Border) earthquake sequence of March to April 1975, *Bull. Seism. Soc. Am.* *71*, 803-826.

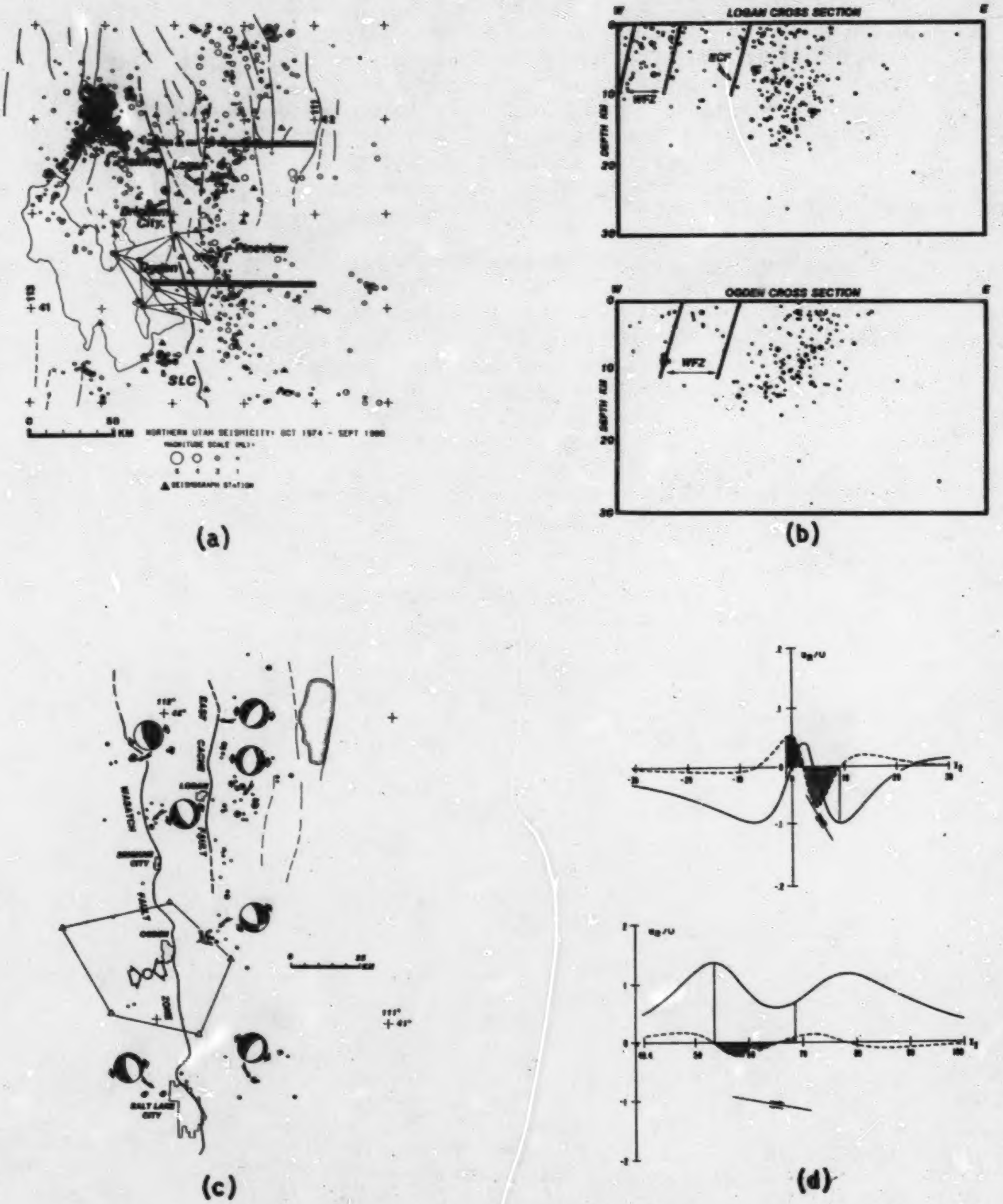
LOGAN CROSS SECTION
W
E
ECF
WFZ
DEPTH KM
0
10
20
30
OGDEN CROSS SECTION
SLC
Logan
Brigham City
Pineview
Ogden
0
50
KM
NORTHERN UTAH SEISMICITY: OCT 1974 - SEPT 1980
MAGNITUDE SCALE (ML)
SEISMOGRAPH STATION
WASATCH
FAULT
ZONE
EAST CACHE FAULT
LOGAN
BRIGHAM CITY
OGDEN
SALT LAKE CITY
0
25
KM
112°
41°
2
1
-1
-2

(a)

(b)

(c)

(d)

Figure 1. (a) Seismicity of northern Utah: October 1974-September 1980. (b) Cross-section of seismicity in northern Utah. (c) Summary of strain data for northern Utah. (d) Surface horizontal displacement and strain along the right angle bisector of a dislocation buried in an elastic half-space.

H3

Quaternary Framework for Earthquake Studies
Los Angeles, California

9540-01611

John C. Tinsley
Branch of Western Environmental Geology
U. S. Geological Survey
345 Middlefield Road, MS 75
Menlo Park, California 94025
(415) 323-8111, x 2037

Investigations

1. Continued analyzing and interpreting chemical and physical characteristics of pedogenic soils based on 5 chronosequences along a transect across southern California from the Los Angeles Basin and San Gorgonio Pass across the Mojave Desert to the Vidal area (L. D. McFadden and J. Tinsley).

2. Continued installation on the U.S.G.S. computer the geotechnical data base for the western portion of the San Fernando Valley (J. Tinsley, M. Vivrette, D. Ponti).

3. Completed reconnaissance soils-geomorphic study of the Cucamonga Fault Zone (with J. Matti and D. Morton).

4. Continued 1/24,000 geomorphic/photogeologic/soil stratigraphic mapping of surficial geology in the Los Angeles area.

5. Assigned to separate investigations 15% of this report period.

Results

1. Holocene rates of accummulation of $CaCO_3$ in arid soils have been modeled successfully based on solution kinetics of CO_3, CO_2, and H_2O. The model predicts the amount of $CaCO_3$ and the profile depth at which the $CaCO_3$ accumulates as a function of time in arid, semi-arid and xeric moisture regimes during the past 13,000 years. The predicted values match closely actual amounts of CO_3 and profile depths of calcic horizons measured in the field and in the laboratory.

2. Installation on the computer of The San Fernando Valley geotechnical data base is 60% completely installed on the Multics computer.

3. U.S.G.S. professional paper manuscript and strip map (1/24,000) is now in technical review.

4. Surficial geologic mapping is 75% complete.

Reports

Hastorf, Christine A., and Tinsley, John C., 1981, Maps and index of radiocarbon dated samples from southern California. U.S. Geological Survey Miscellaneous Field Studies Map MF-1294. (in press).

Mark, R. H., Tinsley, J. C., Newman, E. B., Gilmore, T. D., and Castle, R. O., 1981, An assessment of the accuracy of the geodetic measurements that define the southern California uplift: Journal of Geophysical Research, v. 86, no. B4, p. 2783-2808.

McFadden, L. D., Hendricks, D. M., and Tinsley, J. C., 1981, Changes in pedogenic iron oxyhydroxide with time in soils formed on lithic arkosic alluvium, southern California: Geological Society of America, Cordilleran Section, Abstracts with Programs, v. 13, no. 2, p. 96.

Geothermal Seismotectonic Studies - Olympic Peninsula

9930-02097

Craig S. Weaver
Branch of Seismology
U.S. Geological Survey
at Geophysics Program AK-50
University of Washington
Seattle, Washington 98195
(206) 545-1730

Investigations

1. Earthquakes with magnitudes greater than 3.0 that have occurred south of Olympia (approximately 47 degrees north) are being analyzed in an effort to determine fault plane solutions and to establish the existence of crustal seismic zones. The Elk Lake earthquake on February 13, 1981 and the aftershock sequence are being incorporated into this study. Following the Elk Lake mainshock (M_L = 5.5), a five-day tape recorder was deployed 6 km north of the mainshock epicenter to help control the hypocenter depths calculated for the aftershocks. Field investigations in the area were undertaken in an effort to find possible surface features resulting from the earthquake, but were hampered by heavy rain and very poor visibility.

2. A study of the focal mechanisms of deep earthquakes along the Olympic Peninsula-Puget Sound interface has been initiated. Earthquakes with magnitudes greater than 3.0 are being reread on all available seismographic stations operating in Washington.

3. Crustal structure studies on the Olympic Peninsula have advanced to the stage of ray-tracing and the development of velocity models. Analysis is focused on the Canadian refraction data recorded last summer and on data acquired from an on-shore/offshore refraction profile shot across the Washington margin south of the Olympic Mountains.

Results

1. A crustal strike-slip seismic zone has been delineated from Mount St. Helens north-northwest approximately 70 km to the area west of Alder Reservoir. This zone continues south of Mount St. Helens about 20 km to the vicinity of Swift reservoir. The February 13, 1981 M_L = 5.5 Elk Lake earthquake was located at 46°21', 122°16' at a depth of 7 km along this seismic zone. The aftershocks define a north-northwest striking zone approximately 6 km long, and focal mechanisms for the main shock and two of the largest aftershocks (M_{coda} = 3.7 and 3.9) show strike-slip faulting with fault planes striking a few degrees west of north and the auxiliary plane striking a few degrees north of east. These mechanisms are consistent with the focal mechanisms calculated for earthquakes that occurred near the Elk Lake mainshock in the weeks following the May 18, 1980 eruption of Mount St. Helens.

2. Record sections from the Olympic Peninsula have P_n arrivals with apparent velocities of 7.3 km/sec which have been interpreted as the result of a 7.9 km/sec oceanic slab dipping 7 degrees beneath the Washington coast. Offshore, the apparent velocity under the oceanic crust implies a fairly flat Moho with a velocity of 7.8 km/sec. The boundary between Puget Sound and the Olympics is sharp in the upper crust (above 12 km), and this boundary continues into the lower crust. Along a profile south of the Olympic Mountains that is perpendicular to the continental margin and the crustal boundary between the Olympics and Puget Sound, only P_n arrivals are recorded from oceanic shots, implying that the downgoing slab is continuous beneath the crustal boundary between the Puget Sound and the Olympics.

Reports

Taber, J. J., and Smith, S. W., 1981, Seismic structure of the Olympic Peninsula from refraction data (abs): Earthquake Notes, v. 52, no. 1, p. 52.

Grant, G. C., Weaver, C. S., and Malone, S. D., 1981, Post-eruption earthquake swarms at Mount St. Helens, Washington (abs.): Earthquake Notes, v. 52, no. 1, p. 65.

Weaver, C. S., Endo, E. T., and Malone, S. D., 1981, Seismic evidence for fault dominated magma transport at Mount St. Helens, Washington (abs.): Earthquake Notes, v. 52, no. 1, p. 65.

Weaver, C. S., Grant, W. C. Malone, S. D., and Endo, E. T., 1981, Post-May 18 seismicity - Volcanic and tectonic implications: U.S. Geological Survey Professional Paper 1250 (in press).

Endo, E. T., Malone, S. D., Noson, L. J., and Weaver, C. S., 1981, Locations, magnitudes, and statistics of the March 20-May 18 earthquake sequence: U.S. Geological Survey Professional Paper 1250 (in press).

Malone, S. D., Endo, E. T., Weaver, C. S., and Ramey, J. W., 1981, Seismic monitoring for eruption prediction: U.S. Geological Survey Professional Paper 1250 (in press).

Tectonic Tilt Measurements Using Lake Levels

9950-02396

Spencer H. Wood
Branch of Earthquake Tectonics and Risk
U. S. Geological Survey
Boise State University
Boise, ID 83702
(208) 385-1631

Investigations

The surfaces of large lakes are used as a level reference surface to detect elevation changes of shoreline benchmarks. Measurements are made by simultaneous operation of water-level recorders for several days at stations around a lake. The records are twice referenced to nearby benchmarks by precise leveling. Noise level of repeated annual measurements of elevation change between two points is conservatively estimated at ± 30mm.

Results

Twelve large lakes in southern Alaska are occasionally measured in order to detect and monitor tectonic tilt. A pair of stations 25 km apart on Kenai Lake measured in the summer of 1964,1966, 1979, and 1980 show a 200 mm ± 30mm component of down-to-southeast tilt (9 ± 1 micro-radians) occurred between 1966 and 1979.

Reports

Wood, S. H., 1981, Tectonic tilt derived from lake levels:southern Alaska, (abs.), Earthquake Notes, Seismological Society of America, Berkeley, California.

Regional Neotectonic Analysis of the Ventura Basin, Transverse Ranges, California

Final Summary Report for contract 14-08-0001-18283
under Neotectonic Synthesis of U.S., 9540-02191

Robert S. Yeats
Department of Geology
Oregon State University
Corvallis, Oregon 97331
(503) 754-2484

Investigations

1. Net displacements of a horizon about 1 million years old were calculated for the Ventura basin from the central Santa Barbara Channel east to the San Gabriel fault and from Santa Cruz Island and the northern edge of the Santa Monica Mountains north to the Santa Ynez and Topa Topa Mountains. The Los Angeles 2^o topographic sheet was enlarged to a scale of 1:100,000 for a base map.

2. The section on the south flank of the Ventura Avenue anticline was used for calibration. Amino-acid racemization dates by K. Lajoie and associates from the Saugus (San Pedro) Formation range from 400 to 100 ka, and a marine terrace which overlies Saugus strata dipping 40^{o}S and which is itself tilted 10^{o}S is dated as 85 ka. Ash beds in the sequence were correlated by A. Sarna-Wojcicki and associates by trace-element geochemistry to radiometrically-dated ash beds; these range in age from 600 ka to 1 Ma. G. Izett and associates dated the Bailey ash, just below the contoured horizon, as 1.2 ± 0.2 MA. J. Liddicott found the Brunhes-Matuyama paleomagnetic boundary in the sequence, and R. Yeats and G. Blackie found the Jaramillo and Olduvai events in a nearby oil field in such a position that their position at the Ventura Avenue anticline section could be calculated. On the basis of these data, the age of the contoured horizon was estimated as 1 Ma.

3. Microfaunal markers and physical stratigraphy permitted the correlation of the 1 Ma horizon to the Santa Clara syncline, South Mountain, Oxnard Plain, and the Santa Barbara Channel. Less precise correlations extended the contours to Santa Cruz Island shelf, Carpinteria basin, upper Ojai Valley, the area between South Mountain and the Santa Susana fault, and the east Ventura basin. Throughout much of the basin, the horizon was deposited in several hundred meters of water; this had to be taken into account before calculating the net vertical displacement of the horizon by subsidence or uplift.

4. It was possible in a general way to determine the amount of tectonic shortening or convergence across the Ventura basin for the last million years. This was done through the construction of north-south cross sections through the central Santa Barbara Channel, the coastal Ventura basin from Oxnard Plain to the Ojai Valley, and the central Ventura basin between the Santa Monica Mountains and Topa Topa Mountains.

5. The age-calibration control at Ventura Avenue anticline permitted a resolution of horizontal and vertical displacements to show a more complex picture than was possible elsewhere where control is lacking.

Results

1. The vertical displacements and displacement rates of the 1 Ma marker are among the largest recorded in the world. The marker subsided more than 3.5 km east of Fillmore in the Santa Clara Valley, and it was uplifted more than 5 km on the south flank of Sulphur Mountain where it is controlled by data. Uplift at the crest of Sulphur Mountain is undoubtedly much greater. Differential displacement of this marker across the Oak Ridge fault is greater than 3.5 km east of Santa Paula. In the Santa Barbara Channel the Dos Cuadras anticline and the Mid-Channel anticline are locally uplifted more than 1 km, even though the eroded tops of these structures ae today below sea level. Differential displacment documented across the Red Mountain fault is greater than 1 km; it is far greater than this onshore where there is no control on the hanging-wall block. The Mid-Channel fault and the offshore Oak Ridge fault also show documented displacements of the 1 Ma marker greater than 1 km.

2. Horizontal displacements are reported as convergence of points on the three cross sections toward the southern edge of the Ventura basin. South of the Oak Ridge fault, these displacements are relatively small, but in the zone between the Santa Clara syncline and the mountains to the north, these displacements are large. Displacements increase eastward from 1.8 km in the Santa Barbara Channel to 5.5 km at Ventura to 10.8 km in the central Ventura basin east of Fillmore. In the east Ventura basin, displacements are lower than those east of Fillmore and are concentrated on the Sierra Madre fault system at the southern edge of the San Gabriel Mountains.

3. The more extensive age calibration of the Ventura section allows the determination of displacements in greater detail, and shows that displacements are not monotonic over the last million years. The rate of separation across the Oak Ridge-Montalvo fault system accelerated from 0.2 mm/y in the period 3 to 1.5 Ma to 1.4 mm/y for the next million years, then decelerated to zero about 0.2 Ma ago. Differential subsidence between the Santa Clara syncline and the Ventura Avenue anticline began to occur about 1.5 Ma ago and accelerated to 1.4 mm/y for the next million years. About 0.2 Ma ago, deposition ceased, probably due to the initiation of folding on the Ventura anticline. The crest of the anticline uplifted at a rate of 11 mm/y as the flanks of the fold were rotated at a rate of 3.4 microradians/y. On the crest of the Ventura Avenue anticline, Horizon 5 was at -250 m when deposited and is now at +850 m; the detailed age calibration shows that the change of altitude was not monotonic, and there was an excursion of the horizon to -1300 m at 0.2 Ma.

4. If it is assumed that convergence across the Ventura basin was monotonic for the past million years, the convergence at Ventura would be at a rate of 5.5 mm/y, and the convergence east of Fillmore would be 11 mm/y. But the major part of the shortening may not have begun until 0.2 Ma. As an extreme, if all the convergence east of Fillmore occurred since 0.2 Ma, the convergence rate would be 54 mm/y, a higher rate than the north-south component of San Andreas displacement of 37 mm/y NW-SE. If convergence across other thrust faults related to the San Andreas fault at this longitude, mainly the Frazier Mountain and Pleito faults, is added to this, the convergence rate would considerably exceed the north-south component of San Andreas motion, and even exceed the north-south component of Pacific-American plate motion. This, together with the great variability in convergence rates from west to east,

suggests that part of the convergence may be due to gravity tectonics, possibly involving the entire Cenozoic sedimentary section, although most of it undoubtedly relates to the big bend of the San Andreas fault.

Reports

Yeats, R. S., 1981, Quaternary detachment structures in Ventura basin, southern California (abs.): EOS: Trans. Am. Geophys. Union, v. 62, no. 17, p. 398.

Earthquake Hazards Studies, Metropolitan Los Angeles-Western Transverse Ranges Region

9540-02907

R. F. Yerkes
Branch of Western Environmental Geology
U.S. Geological Survey
345 Middlefield Road
Menlo Park, CA 94025
(415) 323-8111 ext. 2350

Investigations and results (Yerkes)[1]

1. Completed acquisition and began processing microfilmed phase-data cards for 1931-69, southern California network.

2. Continued evaluating data and compiling fault map of region.

3. Continued collecting and evaluating data for seismic velocity model of region.

4. Evaluated several dozen fault-plane solutions, derived by USGS cooperators, for small earthquakes in study area.

Investigations (Sarna-Wojcicki)[2]

5. Continued chemical analyses and identification of late Cenozoic ashes and tuffs in the Transverse Ranges (Ventura, South Mountain, and Ridge basins), and the Los Angeles basin.

6. Helped lead I.G.C.P. Field Conference and field trip for Projects 41 and 128 (late Cenozoic magnetostratiraphy and Neogene/Quaternary boundary, respectively). Purpose of the field conference was to examine late Cenozoic continental and marine stratigraphic sections in the Southwest United States for selection as Quaternary stratotypes, and for the identification of the Plio-Pleistocene boundary.

Results

A core sample of tuff obtained from a depth of about 1200 m at Santa Fe Springs in the Los Angeles basin (work in cooperation with T.H. McCulloh), has been identified as the Nomlaki Tuff. The tuff is within the Repettian forminiferal zone. The identification is based on emergy-dispersive X-ray fluorescence analysis for several major and minor elements in volcanic glass separated from the tuff (table 1). The potassium values in this sample are low compared to analyses of this tuff from surface outcrops. This may be due to leaching of alkali cations from the glass under the higher temperature- and hydrostatic-pressure storage conditions for the core sample.

This tuff, a widespread Pliocene marker bed, was erupted in the southern Cascade Range in northeastern California. It is found in the continental Tuscan Fm. east of the Sacramento Valley, where it has been dated at 3.4 m.y. by the K-Ar method (Evernden and others, 1964), and in the continental Tehama

Formation, east of Sacramento Valley. We confirm its presence in the subsurface in the Sacramento Valley from a core-hole sample obtained near Orland at a depth of 430 m (table 1). Previously, we have identified this tuff in the Kettleman Hills of San Joaquin Valley, where it is present in the middle section of the San Joaquin Formation (Sarna-Wojcicki and others, 1979), and in the "Repetto" beds in the Malaga Cove area west of the Palos Verdes fault, where the tuff is exposed a few tens of meters above sea level. (see Vol. IX, p. 117-118, Dec. 1979).

Sedimentation rates in depositional basins are indirect indicators of uplift in adjoining or tributuary land areas, and/or indicators of basin subsidence. Long-term sedimentation rates for the part of the Los Angeles basin near Santa Fe Springs calculated from the age and depth of this tuff are 0.35 m/1000 years. The sedimentation rates are rapid compared to many late Cenozoic basins--for instance, the sedimentation rate calculated from the depth and age of the Nomelaki Tuff near Orland in the Sacramento Valley is only 0.12 m/1000 years--but low compared to such active basins as the Ventura, where a long-term rate of about 2.4 m/1000 years has been calculated for the period 0.2 to 1.8 m.y. B.P., followed by rapid uplift rates of as much as 10-15 m/1000 years over the last 0.2 m.y.

Reports

Yerkes, R. F., and Campbell, R. H., 1980, Geologic map of the east-central Santa Monica Mountains, Los Angeles County, California: U. S. Geological Survey map MI 1146, 1 sht. at 1:24,000, with sections and explanation.

Yerkes, R. F., Greene, H. G., Tinsley, J. C., and Lajoie, K. R., 1981, Seismotectonic setting of the Santa Barbara Channel area, southern California: U. S. Geological Survey map MF 1169, 27 pp incl. 2 tables, 16 figs., 2 pls.

Wehmiller, J. F., Sarna-Wojcicki, A. M., Yerkes, R. F., and Lajoie, K. R., 1981, anomalously high uplift rates along the Ventura-Santa Barbara coast, California (abs): Tectonophysics, v. 52, p. 380.

Sarna-Wojcicki, A. M., Hillhouse, J. W, Meyer, C. E., Woodward, M. J., Liddicoat, J. C., and Yerkes, R. F., 1981, Progress in teprochronological correlation, magnetostratigraphy, and isotopic age determination of Pliocene and Pleistocene strata in California, in Abstracts, International Field Conference, Neogene/Quaternary Boundary, Project 41 and 128, I.G.C.P.-I.U.G.S., U.N.E.S.C.O.

Liddecoat, J. C., Lajoie, K. R., Bailey, R. A., Sarna-Wojcicki, A. M., Russell, P. C., and Woodward, M. J., 1980, Reversal of the paleomagnetic field in Bruhnes-age lacustrine sediments in Long Valley and Mono Basin, California: Abs. in American Geophysical Union, Abstracts with Program, EOS, v. 61, no. 17, p. 215.

Sarna-Wojcicki, A. M., Waitt, R. B., Jr., Woodward, M. J., Shipley, Susan, and Rivera, Jose, 1981, Premagmatic ash erupted from March 27 through May 14, 1980--extent, mass, volume and composition, in Lipman, P. W., and Mullineaux, D. R., eds., the 1980 eruptions of Mount St. Helens, Washington: U.S. Geol. Survey Prof. Paper 1250 (in press) (11 MS pages, 5 figs., 1 table).

Sarna-Wojcicki, A. M., Shipley, Susan, Waitt, R. B., Jr., Dzurisin, Daniel and Wood, S. H., 1981, Areal distribution, thickness, mass, volume and grain size of airfall ash from the six major eruptions of 1980, in Lipman, P. W., and Mullineaux, D. R., eds., (etc., as above reference) (25 MS pages, 24 figs., 2 tables).

Sarna-Wojcicki, A. M., Meyer, C. E, Woodward, M. J., and Lamothe, P. J., 1981, Composition of air-fall ash erupted on May 18, May 25, June 12, July 22, and August 7, in Lipman, P. W., and Mullineaux, D. R., eds., (etc., as above reference) (25 MS pages, 9 figs., 6 tables).

Waitt, R. B., Jr., Hansen, V. L., Sarna-Wojcicki, A. M., and Wood, S. H., 1981, Stratigraphy and field sedimentology of proximal airfall deposits from 24 May through 7 August, 1980, in Lipman, P. W., and Mullineaux, D. R., eds., (etc., as above references).

1/ Assigned to other investigations 55% of reporting period.
2/ assigned to other investigations 80% of reporting period

Table 1. - Energy-dispersive X-ray fluorescence spectrometric analyses of volcanic glass from tuff samples. Normalized, integrated peak intensity counts for each of two spectral regions (K through Zn, and Rb through Nb, respectively), expressed as ratios to total counts within each spectral region (peak plus background), X 10^4. M. J. Woodward, analyst.

Sample	K	Ca	Ti	Mn	Fe	Cu	Zn	Rb	Sr	Y	Zr	Nb
1	405	73	239	191	925	62	129	1225	1485	619	2685	481
2	778	71	230	183	889	60	124	1225	1485	619	2685	481
3	798	67	219	176	861	59	121	1237	1487	606	2669	459
4	808	66	222	168	861	57	123	1225	1442	638	2748	482

1. Bell-60: Core sample from Santa Fe Springs, Union Oil Co. Sampled interval depth is 3941-3943.5 feet.
2. Same sample. Values for K adjusted for probable post-depositional leaching, and values for Ca through Zn recalculated accordingly.
3. Nomlaki tuff from Bidwell Park, east of Sacramento valley, near base of Tuscan Fm.
4. 264-I-6: Core sample from near Orland, Orland Syndicate Well, Central Sacramento Valley. Sampled from a depth of about 1435 feet.

Earthquake Hazards Puget Sound, Washington

9540-02197

J. C. Yount
Branch of Western Environmental Geology
U. S. Geological Survey
345 Middlefield Road
Menlo Park, CA 94025
(415) 323-8111 x 2905

Investigations:

1. Determine the nature and distribution of subsurface geologic materials that likely control seismic ground shaking in the Port Townsend 1:100,000 map area of Puget Sound.

2. Compile and map the distribution of surficial geologic materials in the west half of the Seattle 1:100,000 map area, with emphasis on grouping deposits according to their potential for seismic ground shaking and liquifaction.

Results

1. Seismic reflection profiles in the eastern Strait of Juan de Fuca show a number of faults in the Quaternary section west of Whidbey Island. It is not known whether the faulting is the result of glacial loading and/or basal glacial shear, or alternatively, whether the faulting reflects tectonism along some of the deep-seated structural features, defined by major west and northwest trending gravity and aeromagnetic gradients cutting across central Puget Sound.

2. As much as 1100 m of Quaternary sediment exists in the Port Townsend 1:100,000 map area. Compilation of depth to bedrock data, from water wells, geotechnical wells and seismic reflection profiles, has been done in cooperation with F. Pessl, Jr. and S. Safioles, Puget Sound Earth Science Applications Project. The resulting distribution shows a trough with 600 to 1100 m of Quaternary sediment trending easterly along the axis of the Strait of Juan de Fuca to central Whidbey Island, then turning southeasterly down the east shore of Whidbey Island toward Seattle. The northeast quadrant of the Port Townsend 1:100,000 map area is underlain by a relatively thin (less than 30 m) Quaternary cover, as is the San Juan Island region along the north border of the map area. The Quaternary section also thins rapidly from the Strait of Juan de Fuca, south toward the Quimper and Miller Peninsulas.

3. Preliminary compilation of the thickness of post-Vashon alluvium in the east half of the Port Townsend 1:100,000 map area indicates that maximum thicknesses of 30 m, 70 m, and 90 m of alluvium exist at the mouths of the Snohomish, Stillaguamish, and Skagit Rivers, respectively. Geotechnical wells, drilled for highway and building projects have encountered some fine-grained sand units within these aluviums whose resistances to penetration are anomalously low and may, as a result, be susceptible to liquifaction.

Relative Hazards of Southern California Faults

9940-03012

Joseph I. Ziony
Branch of Ground Motion and Faulting
U.S. Geological Survey
345 Middlefield Road, Mail Stop 77
Menlo Park, California 94025
(415) 323-8111, Ext. 2214

New project; no report.

Geophysical and Tectonic Investigations of the Intermountain Seismic Belt

9950-02669

Mary Lou Zoback
Branch of Earthquake Tectonics and Risk
U.S. Geological Survey
National Center, MS 935
Reston, VA 22092
(703) 860-7233

Investigations

1. Basin and Range fault slip data were analyzed to infer principal stress orientations. The slip data comes from measurements in Nevada and Utah on bedrock scarps along fault zones with Holocene and/or Late Quaternary movement.

2. Hydraulic fracturing stress measurements were made in a ~0.6 km deep well located 21 km east of the Wasatch fault at about the latitude of Spanish Fork, Utah. The well site lies within a 50 km wide zone of normal faulting and high heat flow that extends eastward from the Wasatch fault zone into the Colorado Plateau.

Results

1. To obtain information on the orientation and relative magnitudes of principal stress in the northern Basin and Range, fault-slip data from faults with late Quaternary movement along the Wasatch fault zone in central Utah and in north-central Nevada have been analyzed. The technique used was described by Angelier (1980, Tectonophysics, v. 56, p. 17-26) and utilizes a least-squares minimization of the component of shear stress perpendicular to the measured slickensides. By assuming that the observed slip direction represents the direction of maximum resolved shear stress on the fault, the analysis provides a mean deviatoric stress tensor for slip on a given family of faults. The patterns of slip and stress in the northern Basin and Range province suggest a 30°-40° difference in principal stress/strain orientation between north-central Nevada and the Wasatch fault zone in Utah. Least-principal-stress orientations inferred from the Wasatch fault zone slip data range from E-W to N70°W in contrast to a roughly N60°W-S60°E least-principal-stress orientation determination for the north-central Nevada slip data. The Wasatch stress orientation is consistent with a moment tensor analysis of Utah earthquakes (primarily along the Wasatch fault zone) that indicated a regional strain tensor having an extensional minimum principal strain component oriented N79°E - S79°W (Doser, 1980, EOS, v. 61, p. 1028) and with a recent hydrofrac test 21 km east of the Wasatch fault zone that indicated a mean least-principal-stress orientation of N73°E - S73°W (see below).

2. Hydraulic fracturing stress measurements were made at depths of 575-610 m in a well-indurated calcareous siltstone of the Tertiary North Horn Formation. The average direction of maximum horizontal compression was found to be N17°W ($\pm 15^\circ$). The tests indicated a large difference between the two horizontal principal stresses and between the least horizontal principal stress and the vertical stress. In one test, the magnitudes of the horizontal principal stresses were found to be S_h=55 bars and S_H=150 bars, where S_h and S_H are the minimum and maximum horizontal principal stress, respectively. S_v, the vertical stress, was computed from sample densities and found to be approximately equal to S_H. The difference between S_v (or S_H) and S_h is approximately that required to cause frictional sliding on optimally-oriented planes (for a coefficient of friction of 0.8). The orientation of the maximum horizontal compressive stress is sub-parallel to Quaternary normal faults in the region, and is consistent with the maximum horizontal compressional strain direction determined from focal mechanisms of regional earthquakes (Doser, EOS. V. 61, No. 46, 1980) and is also consistent with the horizontal compressive stress direction yielded by analysis of fault slip data on the Wasatch fault (see 1 above). The hydraulic-fracturing tests were somewhat unique due to effects caused by the large difference in the magnitudes of the horizontal principal stresses and the extremely anisotropic tensile strength of the formation.

Reports

Zoback, M. L., 1981, State of stress inferred from fault slip data in the northern Basin and Range: abstract for American Geophys. Union, Spring 1981.

Zoback, M. D., Zoback, M. L., Svitek, J. and Liechti, R., 1981, Hydraulic-fracturing stress measurements near the Wasatch fault, central Utah: abstract for American Geophys. Union, Spring 1981 meeting.

Zoback, M. D. and Zoback, M. L., 1981, State of stress and intraplate earthquakes in the central and eastern United States, accepted for publication in Science.

TITLE:	Earthquake Hazard Studies in Northeastern United States
PRINCIPAL INVESTIGATORS:	Y. P. Aggarwal, Lynn R. Sykes
CONTRACTOR:	The Trustees of Columbia University in the City of New York
CONTRACT NUMBER:	USGS-14-08-0001-18387

The Lamont-Doherty seismic network presently consists of 38 short period stations located in New York, New Jersey, and Vermont. Of these 38 stations, 37 have single-component vertical seismometers and one (RAMA - Ramapo Mountain, New Jersey) is a three component site. In addition to these 38 stations three SMA-1 strong motion accelerographs are currently deployed in the field. Sites for these instruments have been chosen in each of the three seismically active regions in New York State -- southeastern New York, the northern New York Adirondacks, and western New York. Data for local events recorded by this network as well as other stations in New England and adjacent Canada are analyzed to study the earthquake hazard, the relationship of earthquakes to known geologic faults, the state of stress, and the crustal and upper mantle velocity structure in the northeastern United States and adjacent Canada.

During 1979 and 1980 we recorded 131 local earthquakes ranging in magnitude from 1 to 5, and three earthquakes occurred within the area covered by our network which were well enough recorded that their focal mechanisms could be constrained by P-wave first motions. In general, the region covered by the network was much more seismically active in 1980 than in 1979. Whereas in 1979 only 48 events were recorded, 83 events were recorded in 1980.

On June 6, 1980 an event of $m_b = 3.8$ was located by our network near Boonville, New York close to the contact between the Adirondacks and the Paleozoic structures of western New York. The fault plane solution for this event indicates thrusting on NW striking planes similar to results for other events in the Adirondack region.

An earthquake of $m_b = 3.0$ was recorded on December 30, 1979 near Mt. Kisco, New York within the Manhattan Prong. The fault plane solution we obtained for this event is predominatly thrust faulting with NE striking nodal planes. P-wave first motion data for another event which occurred in the Manhattan Prong (September 4, 1980, $m_b = 3.2$) are also consistent with faulting on a NE striking plane. The NE strikes of the earthquake fault planes for the Mt. Kisco and Thornwood events, as well as other earthquakes in the Manhattan Prong, correlates well with the general NE trends of the geologic structures and the seismicity in that region.

Geophysical Studies in the Charleston Earthquake Area

9730-02083

J. C. Behrendt
Branch of Regional Geophysics
U.S. Geological Survey
Denver Federal Center, MS 964
Denver, CO 80225
(303) 234-5917

Investigations

1. Multichannel seismic data were collected and are being processed in the area of the Charleston 1886 Earthquake.

Results

1. The new data are not processed to the point where any results can be interpreted.

2. The data collected in 1979 under this program in conjunction with studies funded by the Nuclear Regulatory Commission showed the existence of several northeast-trending high angle reverse faults, of small displacement (10-50 m) offsetting sediments as young as Miocene or Pliocene age. One fault is in the area of recent epicenters in the meizoseismal area of the 1886 earthquake but no causal relation of this structure to seismicity has been demonstrated.

Reports

Behrendt, J. C., Hamilton, R. M., Ackermann, H. D., and Henry, V. J., 1981, Cenozoic faulting in the vicinity of the Charleston, South Carolina 1886 Earthquake: Geology 9, p. 117-122.

Behrendt, J. C., Hamilton, R. M., Ackermann, H. D., Henry, V. J., and Bayer, K. C., 1981, Marine multichannel seismic reflection evidence for Cenozoic faulting and deep crustal structure, in Gohn, G. S., ed., Studies related to the Charleston, South Carolina earthquake of 1886--Second Report: U.S. Geological Survey Professional Paper (in press).

Hamilton, R. M., Behrendt, J. C., and Ackermann, H. D., 1981, Land multichannel seismic-reflection evidence for tectonic features near Charleston, South Carolina, in Gohn, G. S., ed., Studies related to the Charleston, South Carolina earthquake of 1886--Second Report: U.S. Geological Survey Professional Paper (in press).

Seismotectonics of Northeastern United States

9950-02093

W. H. Diment
Branch of Earthquake Tectonics and Risk
U.S. Geological Survey
National Center, MS 935
Reston, VA 22092
(703) 860-6520

Investigations

1. Compilation and interpretation of regional earth science information relevant to the seismicity of the eastern United States continued.

2. An attempt was begun to define seismic source zones for the northeastern United States.

Results

1. A preliminary version of the gravity map of Pensylvania was exhibited. A final version at a scale of 1:250,000 with a contour interval of two milligals is being prepared. Progress has been slowed by the necessity of making terrain corrections for some stations.

2. An average elevation map of the conterminous United States was produced at a scale of 1:2,500,000; 20 m contours in the east, 100 m in the west. This map has now been printed and distributed, as GP-933.

3. Several regional cross-trending gravity features were identified from a new regional gravity map of New York and Pennsylvania and their relationship to seismicity explored. Additional geophysical information regarding these features is being evaluated.

4. It was noted that some of the aseismic regions of the eastern United States exhibit geologic conditions which tend to suppress shallow earthquake activity (e.g. soft sediments, geopressured zones, bedded salt, pre-existing bedding-plane thrusts, and the like). Cautions are expressed that the historical seismicity, based largely on felt reports, may not adequately reflect the stress regime at depth because of decoupling or aseismic slip near the surface. This study has continued using more recent data.

5. A continuing study of thermal convection in water-filed holes has begun to reveal some information on the nature of the fluid motions. This information may be useful in interpreting temperature-time data in terms of crustal strain. It may also be useful in assessing the accuracy of other in-hole measurements that are sensitive to small fluid motions.

Reports

Diment, W. H., and Urban, T. C., 1981, An average elevation map of the conterminous United States (Gilluly averaging method): U.S. Geological Survey Map, GP-933.

Diment, W. H., Urban, T. C., Nathenson M., Nehring, N. L., Shaeffer, M. H., 1981, Thermal convection in cased water-filled drill holes: effects of small quantities of gas: EOS, American Geophysical Union Transactions, v. 62 (accepted).

Urban, T. C., and Diment, W. H., 1980, Thermal convection in cased, water- filled drill holes: observations over a wide range in conditions, EOS, American Geophysical Union Transactions, p. 1130.

Robertson, E. C. (chm.), Diment, W. H., Hemingway, B. S., Johnson, C. B., Shankland, T. J., Stottlemyre, J. A., and Rov, R. F., 1981, Thermophysical, thermomechanical, and thermochemical properties, chapter 8, in Rock-mechanics research requirements for resource recovery, construction, and earthquake hazard reduction: National Academy of Sciences, National Technical Information Service, Report No. NRC/AMPS/RM-80-1, Springfield, VA 22161, p. 246-296. (In press).

Eastern U.S. Seismicity and Tectonic Studies

9950-02303

R. M. Hamilton
Branch of Earthquake Tectonics and Risk
U.S. Geological Survey
National Center 935
Reston, VA 22092
(703) 860-6529

Investigations

1. Research on the nature of faulting in the New Madrid region and the tectonic evolution of the mid-continent area.

2. Completion of chapters for the new New Madrid and Charleston USGS Professional Papers, and preparation of other papers on seismicity in these areas.

3. Preliminary analysis of land seismic-reflection profiles obtained in the Charleston, South Carolina, area by Virginia Polytechnic Institute and State University during the 1980-81 winter, and by Seisdata Services Inc. during the Spring of 1981.

4. Preliminary analysis of seismic-refraction data obtained in the New Madrid area in the Fall of 1980.

5. Chairman of the Science Advisory Committee.

Results

1. The origin of New Madrid seismicity is seen as follows:

The Mississippi Embayment was the site of continental rifting before the late Cambrian. Uplift, major faulting, igneous intrusive activity, and mineralization in the northern embayment region during the late Paleozoic indicate reactivation of rifting, perhaps caused by the Ouachita and Allegheny orogenies. Alkalic igneous intrusive activity and minor normal faulting in the Late Cretaceous, possibly indicating yet another episode of rift reactivation, evolved to reverse faulting after the middle Eocene. The hypothesis that earthquakes in the northern Mississippi Embayment region, including activity in the New Madrid seismic zone, are caused by reactivation of ancient faults in a stress regime of east-west compression is supported by the characteristics of modern seismicity, although some areas where activity might be expected have not experienced historical earthquakes.

2. Analysis of the various new data sets from New Madrid and Charleston is at such an early stage that reporting of results will be deferred until next time.

Reports

Hamilton, R. M., 1980, Tectonic evolution of the northern Mississippi Embayment — implications for New Madrid seismicity (abs.): EOS, v. 61, p. 1026.

Wegener, S. S., Hamilton, R. M., and Healy, J. H., 1980, Seismic refraction study in the New Madrid, Missouri, seismic zone (abs.): EOS, v. 61, p. 1026.

Behrendt, J. C., Hamilton, R. M., and Ackermann, H. D., 1980, Deep crustal seismic reflection study offshore in the area of Charleston, S.C., 1886 earthquake (abs.): EOS, v. 61, p. 1040.

Ackermann, H. D., Behrendt, J. C., and Hamilton, R. M., 1980, Marine multichannel seismic reflection sections in the vicinity of the 1886 Charleston, South Carolina, earthquake (abs.): EOS, v. 61, p. 1040.

Behrendt, J. C., Hamilton, R. M., Ackermann, H. D., and Henry, V. J., 1981, Cenozoic faulting in the vicinity of the Charleston, South Carolina, 1886 earthquake: Geology, v. 9, p. 117-122.

Hamilton, R. M., and Zoback, M. D., in press, Tectonic features of the New Madrid seismic zone from seismic reflection profiles, *in* McKeown, F. A., and Pakiser, L. C., Investigations of the New Madrid, Missouri, Earthquake Region: U.S. Geological Survey Professional Paper 1236-F.

Hamilton, R. M., and Russ, D. P., in press, Seismotectonics of the New Madrid region, *in* Hays, W. W., ed., Proceedings of Conference on Evaluation of Regional Seismic Hazards and Risk, Santa Fe, New Mexico, August 25-27, 1980: U.S. Geological Survey Open File Report.

Tectonic Framework of the New Madrid Seismic Zone from Geophysical Studies

9730-01035

Thomas G. Hildenbrand
Branch of Regional Geophysics
U.S. Geological Survey
Denver Federal Center, MS 964
Denver, CO 80225

Investigations

1. Analyses of aeromagnetic and gravity data to delineate the termini of the Mississippi Valley graben.

2. Compiled a map of digital magnetic data of central United States.

Results

The northeast-trending Mississippi Valley graben probably formed during early stages of rifting in late Precambrian or early Paleozoic time and presently contains the area of principal seismicity in the northern Mississippi Embayment region. The delineation of its termini, consequently, plays an important role in determining seismic risk in the midcontinent. A recently compiled aeromagnetic map of central and northeastern Arkansas and gravity map of Arkansas provide some insight to the southwestward extension of the Mississippi Valley graben. The geophysical expression of the graben is abruptly terminated by a steep, northwest-trending gradient in eastern Arkansas. In this structural-complex region four intense geophysical highs reflect mafic or ultramafic igneous bodies, such as the Magnet Cove ring-dike complex and the syenite bodies near Little Rock. Extension along structures associated with the northwest-trending gradient may have resulted in the emplacement of these large igneous bodies. An east-northeast-trending zone of geophysical highs, related to structures of the Ouachita Mountains, also intersects the graben feature in this region. More detailed analyses will be performed to determine if the graben terminates in eastern Arkansas, at its intersection with the northwest-trending gradient and the east-northeast-trending magnetic highs, or if its trend changes to a more westerly direction paralleling geophysical features associated with the Ouachita Mountains.

The location of the northern terminus of the Mississippi Valley graben is also ambiguous. A recently compiled map of digital aeromagnetic data of central United States expresses a prominent megalineament trending northwest from southeastern Tennessee to southeastern Nebraska. This megalineament may represent a major crustal flaw conceivably formed during a period of Archean time when the crust was thin and susceptible to internal stresses. The Mississippi Valley graben, defined as a 70 km wide depression with a series of plutonic masses along its margins, terminates in western Kentucky at its intersection with the megalineament. Derivative and trend maps, however, suggest a magnetic lineament continues northeastward into Indiana and Illinois, possibly representing a crustal flaw along which the graben developed. It is interesting to note that this interpreted magnetic feature parallels two other midcontinent mega-lineaments, the midcontinent geophysical high and the New York to Alabama lineament. Apparently, the midcontinent is underlain by major crustal flaws trending northeast and northwest. Future studies of these crustal flaws will be very helpful in understanding intra-cratonic tectonics and therefore, structures responsible for the control or release of seismic energy.

Reports

Hendricks, J. D., Keller, G. R., and Hildenbrand, T. G., 1981, Simple Bouguer gravity map of Arkansas: U.S. Geological Survey Geophysical Investigations GP-944, scale 1:500,000.

Hildenbrand, T. G., Kucks, R. P., and Johnson, R. W., 1981, Aeromagnetic map of east-central United States: U.S. Geological Survey Geophysical Investigations Map GP-948, scale 1:1,000,000.

Central and Eastern U.S. Earthquake Study

9730-02176A

M. F. Kane
Branch of Regional Geophysics
U.S. Geological Survey
Denver Federal Center, MS 964
Denver, CO 80225

Investigations

1. Analyses of gravity, digital terrain and aeromagnetic data covering extensive regions of the central and eastern United States are being used to delineate crust and mantle structure and to investigate the relation of such structure to tectonism and seismicity.

2. Wavelength filtering, an apparent effective method of separating the residual and regional parts of continental-scale gravity fields is being studied to establish the parameters of the separation process.

Results

1. Wavelength filtering has been used to prepare a series of maps which are separated to a first approximation according to the depth interval of anomaly sources. A map composed of wavelengths greater than 250 km shows a gravity gradient with 40 to 100 Mgal displacement, positive to the southeast, that extends from Maine to Alabama. The underlying terrane is made up for the most part of crystalline rock. Clusters of seismicity tend to concentrate along the gradient and notably along offsets which displace the gradient progressively westward along its southwest trend. The most simple explanation of the gradient is that it marks a substantial change in crustal thickness (3 to 5 km); it may indicate the principal zone of continental convergence in middle to upper Paleozoic time. A possible explanation of the relation of the gradient to seismicity is that the change in crustal thickness causes a concentration of deviatoric stress along the boundary. The offsets probably indicate the location of transform faults; one of the largest of the offsets projects into the vicinity of the Charleston earthquake zone.

A map composed of wavelengths less than 250 km shows a series of major gravity highs, flanked by lows, that strike along the general northeast trend of the Appalachians in the region underlain by sedimentary strata. The highs and their flanking lows are offset one from another in a direction transverse to the Appalachians trend. The pattern of the anomalies is analogous to that of a rift system where the highs are caused by mafic rocks of the central rift and the offsets are transform faults. This interpretation is compatible with recent models of sedimentary basins which postulate that initial downwarping is caused by crustal thinning including subjacent mantle upwarp and injection. The previously reported gravity cross-trend extending from western Virginia to southeast Tennessee causes a major disruption of the rift pattern described above. Orientation of major gravity anomalies southeast of the trend is distinctly more easterly than that of anomalies to the northwest indicating that the cross-trend marks a major crustal boundary. An apparent offset in long wavelength magnetic anomalies indicates that there may be right-lateral displacement of the order of 100 km. As noted in the last report, the Virginia-Alabama seismicity belt is concentrated along and southwest of the cross-trend.

2. Wavelength filtering appears to be a remarkably effective method of separating gravity anomalies according to the depth-interval of sources, at least for continental-scale gravity fields and for depth intervals of ten km or more. In general it may be stated that anomalies composed of short wavelength must have shallow sources because short wavelengths are damped out exponentially with depth. Long wavelength anomalies of substantial amplitude (tens of Mgals) may be caused by deep sources or by broad shallow sources. Calculations using ideal sources suggest that the ratio of wavelength to source-depth may vary from 6 to 12 depending on the source shape. A specific test of a line source located at 40 km depth showed that a low-pass filter of 250 km retained an accurate horizontal anomaly configuration and 65% of the anomaly amplitude; similar results were obtained for a line source at 20 km using a low-pass filter of 100 km. These initial tests indicate that our preliminary estimates of effective depth-interval separation are approximately correct, that is, that a 100 km high-pass filter restricts anomalies to sources in the upper 10-15 km of crust (except shallow broad sources) that a 250 km high-pass filter gives the gravity field of crustal sources (except broad crustal sources) and that a 250 low-pass filter gives the gravity field of mantle sources and broad shallow sources. A notable type of broad shallow source is a sequence of laterally extensive sedimentary strata like those of the Appalachian region. Thus the map composed by means of a 250 km high-pass filter may be further restricted to crustal sources in crystalline rock (unless there is a broad region of the crystalline crust with a singular contrasting density). Further tests with ideal sources need to be done to refine depth-interval estimates and to examine effects like the leakage of long wavelength components of shallow anomalies into the fields of lo-pass maps. Ultimately constraints on depth of anomaly sources may be determined more uniquely by means of other methods such as deep-sounding seismic surveys.

Report

Kane, M. F., Simpson, R. W., and Osberg, P. H., New gravity evidence of crust-mantle structure and seismicity in the Appalachians (abs.): approved by Director; accepted for presentation at 1981 Spring Meeting of the American Geophysical Union.

Quaternary Stratigraphy and Bedrock Structural Framework of Giles County, Virginia

9510-02463

Robert C. McDowell
Branch of Eastern Environmental Geology
U.S.Geological Survey
National Center, MS 928
Reston, VA 22092
(703) 860-6503

Investigations

1. Surficial quaternary deposits are being studied by Hugh Mills in a search for possible effects of local seismicity. These studies include mapping and mineralogical analysis of New River terrace and flood plain deposits, mapping and sedimentological analysis of colluvium on mountain slopes, and trenching of selected surficial deposits.

2. Paleozoic bedrock structures are under study to determine possible relationships to present seismicity, and to provide a framework for evaluating seismic effects.

Results

1. Detailed mapping and study of colluvial deposits on steep slopes near Mountain Lake, Virginia has made it possible to identify five depositional environments on the basis of color, texture, fabric, and degree of weathering. Age estimates based on the latter suggest the oldest deposits are pre-Illinoian, while the youngest are no older than late Wisconsinan. Transport mechanisms include gelifluction, during Pleistocene glacial conditions, and debris flow, during catastrophic rainstorms; the effect of seismic shaking is under study.

2. Samples of sediments from Mountain Lake have recently been obtained with the help of George Simmons, VPI Biology Department. These will be examined for deformation features induced by the nearby earthquake of 1897 (intensity VIII). The possibility of tracing the local seismic history is not good because of an apparently very low rate of deposition.

3. Bedrock studies have as yet shown no effects that can be ascribed to current seismicity or to a deep basement fault postulated by Bollinger and Wheeler. Paleozoic structures are consistant with the "thin-skinned" model of Appalachian deformation, and current studies will bear an unresolved problems of sequence and chronology during Paleozoic tectonism.

Reports

McDowell, R. C., 1981, The Hurricane Ridge, Glen Lyn, and Caldwell synclines of southeastern West Virginia and southwestern Virginia: a reinterpretation: submitted to Southeastern Geology.

Mills, H. H., 1981, Boulder deposits and the retreat of mountain slopes, or "gully gravure" revisited: Journal of Geology (in press).

The Determination of the Magnitude and Date of Dip-Slip Faulting by Discordance in Sets of Sea Level Curves.

14-08-0001-17729

W.S. Newman, R.R. Pardi, L.F. Marcus, L.J. Cinquemani and J.A. Sperling
Queens College of the City University of New York
Flushing, NY 11367
(212) 520-7651

Investigations

We have now dated 121 basal peat samples from twelve tidal marshes along a 135 kilometer transect striking north from Cheesequake State Park on the New Jersey Coast of Raritan Bay up the Hudson Estuary to Marlboro, New York. The transect crosses the Ramapo Fault Zone between kilometers 32 through 38 south of Marlboro. Our purpose is to determine the practicality of discerning Holocene movement of the fault zone block segments by comparing marine transgression curves across and within the fault zone.

Results

Ratcliffe's (1980, 1981) recent work in the vicinity of the Ramapo Fault Zone proves to be the catalyst that has dissipated our previous confusion concerning our results. Ratcliffe's Timp Pass Fault passes through four of our sampling sites: the tidal marshes at Constitution Island, Con Hook, Manitou, and Ring Meadow-adjacent to Iona Island. Although we were unable to locate any basal peat at Con Hook and only one at Manitou, our data from Constitution Island and Iona Island clearly demonstrate the divergence of sea level curves we had been seeking. The southeast shore of the Constitution Island Marsh has subsided at least one meter relative to Constitution Island over the past 6000 years while the southeast bedrock basement of Ring Meadow had dropped at least 4 meters within the past 2000 years. Furthermore, our data suggests several differentially dropped fault splinters are involved in the Ramapo Fault Zone Graben which strikes southwest across the Hudson Estuary south of the Bear Mountain Bridge. Cedar Pond Brook Marsh, 1.5 kilometers south of Stony Point and at the north edge of Haverstraw, yields a sea level curve similar to the western edges of both Constitution Island and Ring Meadow indicating that this station is located south of the Ramapo Fault Zone Graben. Although still evaluating our data, we now firmly believe that we have in hand a method that can aid in the determination of fault throw and recurrence interval in littoral environments.

References Cited

Ratcliffe, N.M., 1980, Brittle fault (Ramapo fault) and phyllonitic ductile shear zones in the basement rocks of the Ramapo seismic zone, New York and New Jersey, and their relationship to current seismicity, in Field Studies of New Jersey Geology and Guide to Field Trips, 52nd Ann. Mtg. N.Y. Geol. Assoc., Rutgers Newark, p. 278-311.

Ratcliffe, N.M., 1981, Northeastern U.S. Seismicity and Tectonics, in Summaries of Technical Reports, v. XI, National Earthquake Hazzards Reduction Program, U.S. Geol. Survey Open-File Report 81-167, p. 124-126.

Northeastern Seismicity and Tectonics

9510-02388

N. M. Ratcliffe
Branch of Eastern Regional Geology
U.S. Geological Survey
Reston, VA 22092

Investigations

1. Tectonic framework of the Ramapo Seismic zone New York - New Jersey

Results

1. A conceptual model of the crustal structure and tectonic framework of the Ramapo seismic zone has been developed based on epicentral data and the preliminary tectonic map illustrated in the previous report.

2. Cross sections across aseismic areas (north of 41° 5N and west of the Green Pond syncline) suggest that Proterozoic Y basement forms thin sheets that occupy several different structural levels from 15 km to near the surface. These areas may be effectively separated from the crustal stress field as they are highly segmented or broken by Mesozoic faults, or form thin slivers cushioned in Paleozoic metasedimentary rocks.

3. Current seismicity to depths of 12 km occurs in areas where steep basement faults occur in the Proterozoic Y gneisses of the Reading Prong and the Manhattan Prong.

4. Although reactivation of faults appears to be the cause of current seismicity, fault plane solutions and hypocenter data indicate that subhorizontal faulting on hypothetical Mesozoic listric faults or on deep decollements is unlikely.

Reports

Ratcliffe, N.M., 1980, Brittle fault (Ramapo fault) and phyllonitic ductile shear zones in the basement rocks of the Ramapo seismic zone, New York and New Jersey, and their relationship to current seismicity, in Field Studies of New Jersey Geology and Guide to Field Trips, 52nd Ann. Mtg. N.Y. Geol. Assoc., Rutgers Newark, p. 278-311.

Ratcliffe, N.M., Armstrong, R.L., Mose, D.G., Seneschal, Ronald, Williams, Neil, and Baiamonte, Matthew, in press, Emplacement history and tectonic significance of the Cortlandt complex, related plutons and dike swarms in the Taconide zone of southeastern New York based on K-Ar and Rb-Sr investigations: Amer. Journal Science (in press).

Ratcliffe, N.M., 1981, The Cortlandt-Beemerville magmatic belt: a late Taconic alkalic crosstrend in the central Appalachians: Geology.

_____Results of core drilling of the Ramapo Fault at Sky Meadow Road, Rockland County, N.Y., U.S. Geological Survey, M.I. Map ____, in press.

_____1981, Reassessment of the Ramapo fault system as control for current seismicity in the Ramapo seismic zone and the New York recess, Geol. Soc. Amer., Abstracts with Programs, vol. 13, no. 3, p. 171.

Mississippi Valley Seismotectonics

9950-01504

D. P. Russ
Branch of Earthquake Tectonics and Risk
U.S. Geological Survey
Denver Federal Center, MS 966
Denver, CO 80225
(303) 234-5065

Investigations

1. A seismic reflection program was conducted on the Mississippi River between Osceola, Ark., and Wickliffe, Ken., a distance of about 245 km. Data was recorded by the USGS research vessel, Neecho, with geophysical supervision provided by S. Harding (Br. Earthquake Tectonics and Risk) and boat operations supervision under the direction of D. O'Leary (Br. Atlantic-Gulf of Mexico Geology). The survey was undertaken to detect subsurface structure in and adjacent to zones of seismicity in the northern Mississippi Embayment and to tie together land-based Vibroseis® reflection profiles recorded 2 years earlier. K. Shedlock, in close association with S. Harding and D. Russ, has begun processing the data.

2. Continued field and office investigations of Cenozoic faults and terraces in the northern Mississippi Embayment to establish structural framework and to determine nature of Quaternary tectonism.

3. A geologic and geomorphic analysis of the evolution of the stress field in the Mississippi Embayment was begun.

4. An intensive study of subsurface information in extreme northeastern Arkansas and adjacent parts of Tennessee and Missouri was undertaken to document the history of movement along a northeast-trending fault in Crittenden County, Ark.

5. Historic intensity data for the New Madrid region was studied to determine the threshold for eruptive liquefaction in the northern Mississippi Embayment.

6. Work continued on radiometric age-dating, petrologic, and geochemical studies of igneous rock cuttings from wells in the Mississippi Embayment. This study is a cooperative effort with R. Zartman and B. Doe of the Branch of Isotope Geology. It is being done to characterize the igneous history of the Mississippi Embayment and to determine its relationship to tectonics and seismicity.

7. Began cooperative investigation to look for evidence that Quaternary tectonism may influence the morphology and channel characteristics of the Mississippi River. The study is being led by Dr. S. Schumm of Colorado State University and personnel of the U.S. Army Corps of Engineers, Vicksburg, Miss., District.

Results

1. The Mississippi River reflection survey recorded 12 channels of 1 second (2-way travel time) CDP digitized data. Preliminary processing of the data is currently being done to determine the most efficient and useful parameters and equipment to use in order to obtain the highest-quality seismic profiles possible. Results to date indicate that the expected reflectors in the area (top of Paleozoic, Cretaceous, and Paleocene surfaces) are clearly resolvable. One section at the northernmost end of the survey in Kentucky, reveals a fault or zone of faults in Paleozoic sediments near the location where the northwest border of the Reelfoot Rift crosses the Mississippi River (Figure 1). Processing and interpretation of the data is continuing.

2. Subsurface faults interpreted from seismic reflection profiles are providing a clearer picture of the nature and inter-relationship of seismic source zones in the New Madrid seismic zone. Within the Reelfoot Rift, the majority of the detected faults occur along the rift axis and borders. They are spatially coincident with linear patterns of microearthquakes recorded by the St. Louis University seismic network. In the area between Dyersburg, Tenn., and New Madrid, Mo., discontinuous en echelon fault segments suggest an important association between seismicity, Holocene uplift, and the discontinuous fault pattern.

3. Examination of a northeast-trending fault in Crittenden County, Ark., shows that the fault lies very close to the southeast border of the Reelfoot Rift, about 30 km northwest of Memphis, Tenn. Stratigraphic interpretations from geophysical well logs indicate that the fault has a sense of movement opposite to that associated with formation of the rift. Study of this fault and others in the area provides evidence that some of the faults in the Mississippi Embayment have experienced reversals of movement.

4. A study of intensity data for New Madrid area earthquakes that occurred between 1838 and the present suggests that the threshold for eruptive liquefaction (primarily sand blows) is $MM_I = 8$ ($m_b = 6.2$). In this time interval 6 $MM_I = 7$ and two minimal $MM_I = 8$ earthquakes failed to produce any sand blows. The only earthquake since the 1811-12 New Madrid series to have sand blows associated with it was the October 31, 1895, Charleston, Mo., shock of $MM_I = 8$, $m_b = 6.2$. It is thus suggested that $MM_I = 8$ ($m_b = 6.2$) represents the probable threshold for eruptive liquefaction in the New Madrid seismic zone.

Reports

Crone, A. J., 1980, Deformation of the Paleozoic bedrock surface in the New Madrid seismic zone, northern Mississippi Embayment [abs.]: Geological Society of America Abstracts with Programs, 1980 Annual Meetings, v. 12, no. 7, p. 408.

Crone, A. J., 1981, Sample description and stratigraphic correlation of the New Madrid test well 1-X, New Madrid County, Missouri: U.S. Geological Survey Open-File Report 81-479, 25 p.

Hamilton, R. M., and Russ, D. P., Seismotectonics of the New Madrid region, in Proceedings of Conference, Evaluation of regional seismic hazards and risk: U.S. Geological Survey Open-File Report, in press.

Harding, S. T., and Russ, D. P., 1980, Ray- and wave-theory modeling of seismic-reflection profiles to interpret geologic structure in the New Madrid seismic zone [abs.]: EOS, Transactions, American Geophysical Union, v. 61, no. 48, p. 1194.

McKeown, F. A., and Russ, D. P., 1980, Possible significance of rifts and alkalic rocks to the location of earthquakes in the New Madrid, Missouri, region [abs.]: EOS, Transactions, American Geophysical Union, v. 61, no. 48, p. 1194.

Russ, D. P., 1980, Holocene deformation and earthquake recurrence in the northern Mississippi Embayment [abs.]: Geological Society of America, Abstracts with Programs, 1980 Annual Meetings, v. 12, no. 7, p. 513.

Russ, D. P., 1981, Model for assessing earthquake potential and fault activity in the New Madrid seismic zone [abs.]: Conference on Earthquakes and Earthquake Engineering: The Eastern United States, Knoxville, Tennessee, in press.

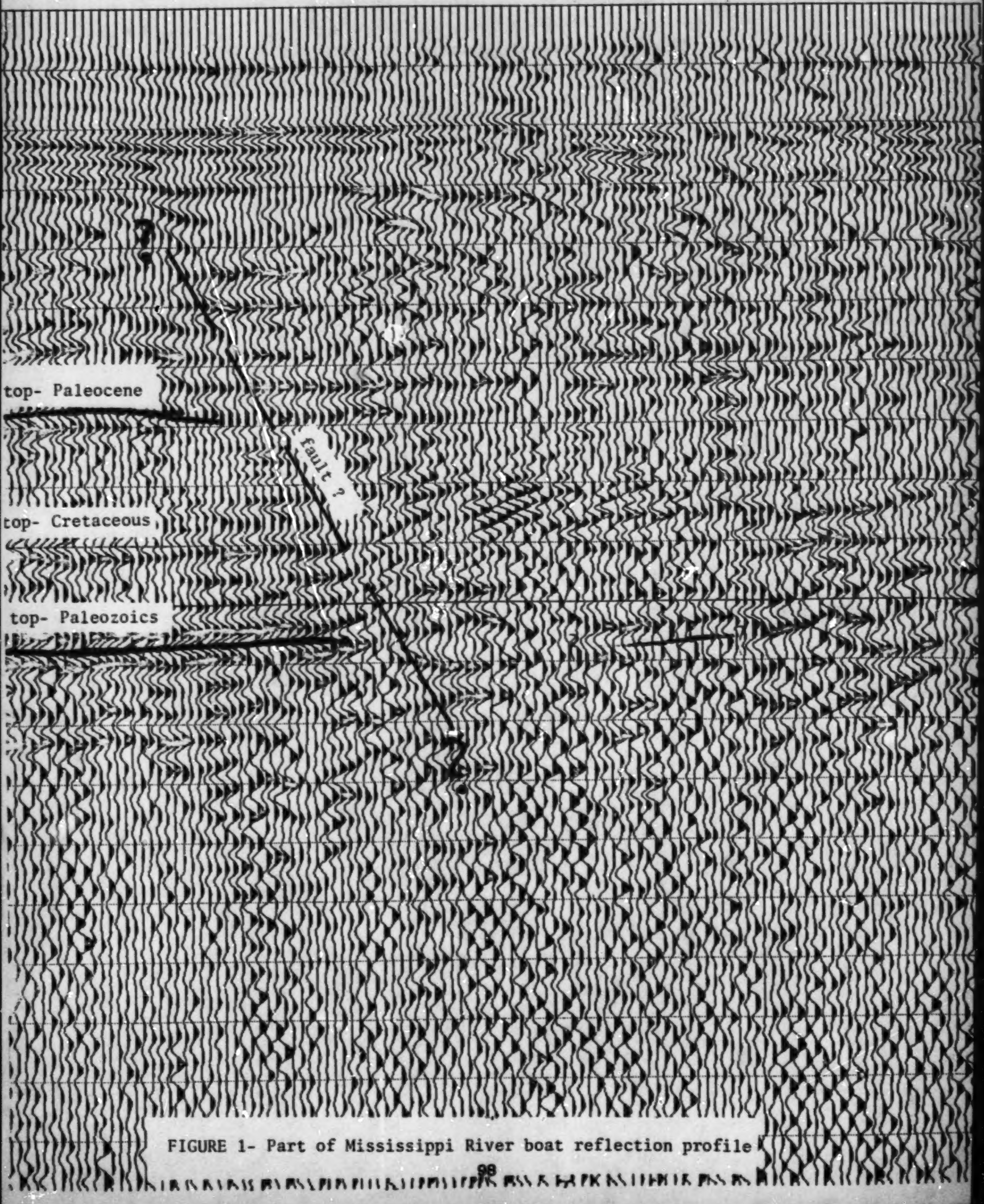

FIGURE 1- Part of Mississippi River boat reflection profile

Northeast Tectonics and Geophysics

9730-00364

Robert Simpson
Branch of Regional Geophysics
U.S. Geological Survey, MS/89
345 Middlefield Road
Menlo Park, CA
(415) 323-8111, X 2249

Investigations

1. Compilation of available gravity data for the Northeast. Publication of contoured gravity maps at various scales suitable for regional and local studies.

2. Compilation and digitization of available aeromagnetic data from the Northeast, and collection of additional data from areas of interest. Publication of contoured maps and digitized data sets.

3. Collection of gravity, magnetic and other geophysical data in areas of tectonic or seismic significance.

4. Interpretation of regional geophysical anomalies and their relation to tectonic features and the plate tectonic history of the region.

5. Modelling and interpretation of local geophysical anomalies to test specific hypotheses for the origin of seismicity.

Results

1. Colored gravity and terrain maps of the Northeastern U.S. are now on open-file in the form of color slides. The maps include Bouguer gravity, free-air gravity, gradient maps, and wavelength filtered residual maps.

2. New gravity compilations of the Eastern U.S. (from 109°W) have been plotted as color maps at a scale of 1:5,000,000. The geologic information contained in these maps is quite impressive. Especially in the midcontinent area the maps reveal structures and provinces in the buried Precambrian basement with unparalleled clarity. It may be possible to relate much of the seismicity in the Eastern U.S. to a fabric of ancient structures which are being reactivated by a regional E-W to NE-SW compressive stress regime.

Reports

Simpson, R. W., Bothner, W. A., and Godson, R. H., 1981, Colored gravity anomaly and terrain maps of the Northeastern U.S. and Adjacent Canada: U.S. Geological Survey Open-File Report 81-560.

Earthquake Hazard Studies in Southeast Missouri

14-08-0001-16708

William Stauder
Robert B. Herrmann
Brian J. Mitchell
Department of Earth and Atmospheric Sciences
Saint Louis University
P.O. Box 8099 Laclede Station
St. Louis, MO 63156
(314) 658-3120

Goals

Monitor seismicity in the New Madrid Seismic Zone, using data from a twenty-five station seismic array.

Conduct research on eastern United States seismic sources by using array data and data from other stations.

Investigations

The project consists of the operation of a 25 station microearthquake array (to be augmented to 32 stations) in the central Mississippi Valley, near New Madrid, MO. Since the installation of the array of 1 July 1974, a total of 1330 earthquakes have been located through December 31, 1980. The locations of these earthquakes are shown in Figure 1. The operation and analysis of array data is an ongoing effort. Quarterly bulletins of microearthquake locations and readings are published.

The earthquake data file has been upgraded by recomputing all magnitudes since July 1, 1974, using revised magnitude formulas and by placing all phase cards in the same format. The same data file format has been used for Nuttli's catalog of historical earthquakes. For the first time a comparison of historical and microearthquake recurrence rates is possible.

Larger eastern United States earthquakes are investigated with techniques that examine surface wave amplitude and phase spectra and that attempt to model the entire waveform.

In addition, considerable effort has gone into improving the quality and reliability of the FM telemetry used for seismic data acquisition.

Results

The Kentucky earthquake of July 27, 1980 was characterized by right lateral strike-slip motion on a plane dipping 50° SE and striking N 30° E. The seismic moment of 4.0×10^{23} dyne-cm makes this earthquake the second largest east of the Rocky Mountains since 1960. Studies on matching Lg amplitudes continue.

A crustal Q regionalization map is being constructed for the entire U.S. (Figure 2) by S. Singh. The map utilized Q data contained in the coda of local earthquakes. The application of this technique to microearthquake data from regional networks looks promising.

Publications

Herrmann, R.B., J.W. Dewey, and S.K. Park (1980). The Dulce, New Mexico earthquakes of January 23, 1966, Bull. Seism. Soc. Am. 70, 2171-2183.

Herrmann, R.B., S.K. Park, and C.Y. Wang (1981). The Denver earthquakes of 1967-1968, Bull. Seism. Soc. Am. (in press).

Singh, S., and R.B. Herrmann (1981). Regionalization of Crustal Q values in conterminous United States (Abstract, 1981 Meeting, SSA), Earthquake Notes 52, 34.

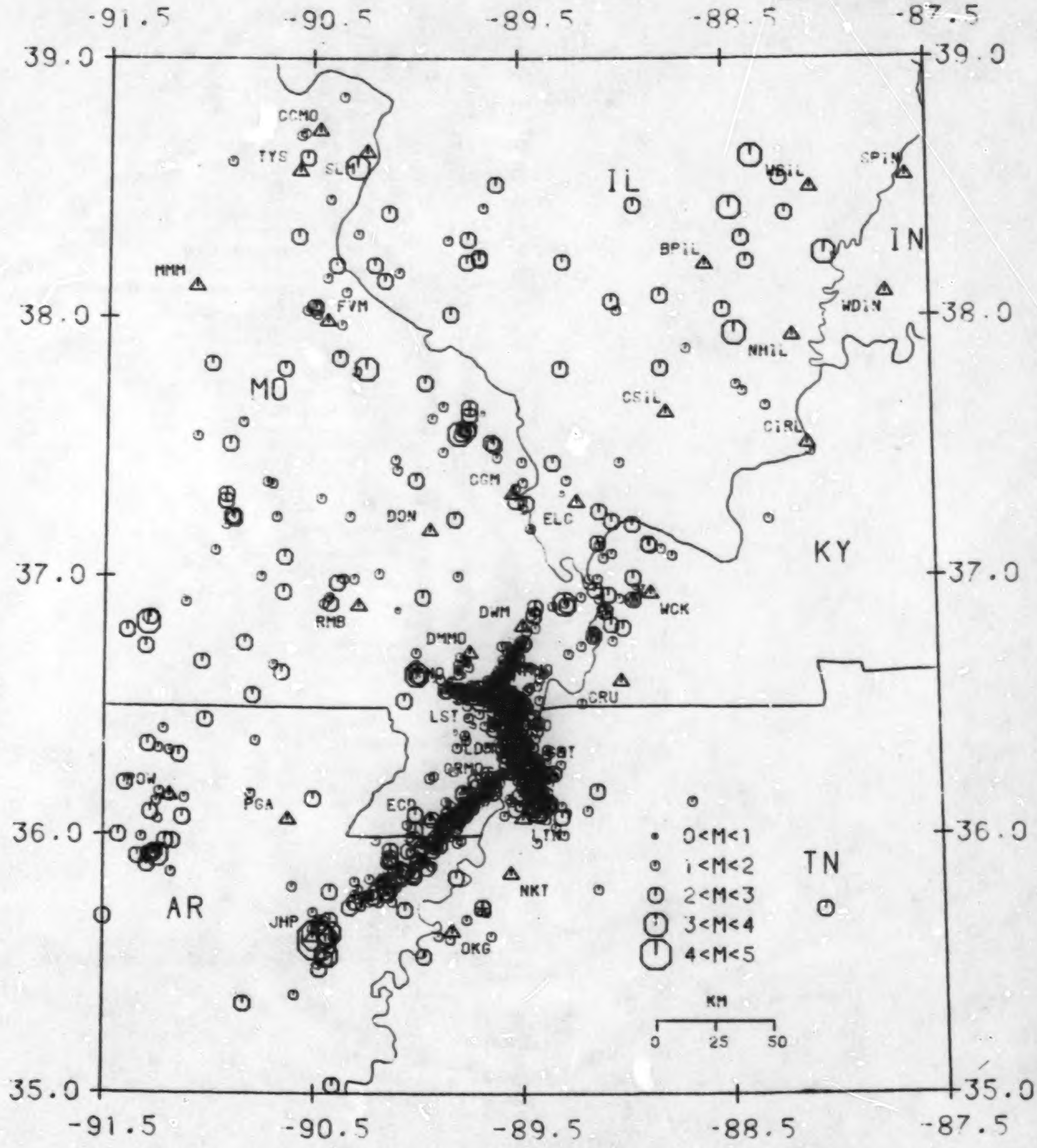
-91.5
-90.5
-89.5
-88.5
-87.5
39.0
38.0
37.0
36.0
35.0
MO
IL
IN
KY
TN
AR
CCMO
TYS
SLM
MMM
FVM
BPIL
WSIL
SPIN
WDIN
NMIL
CSIL
CIRL
CGM
ELC
DON
RMB
DWM
WCK
DMMO
CRU
LST
LDM
GBT
GRMO
HOW
PGA
ECD
LTN
NKT
JHP
OKG
0<M<1
1<M<2
2<M<3
3<M<4
4<M<5
KM
0
25
50

FIGURE 1
CUMULATIVE EVENTS 01 JUL 1974 TO 31 DEC 1980
LEGEND . ▲ STATION ⊙ EPICENTER

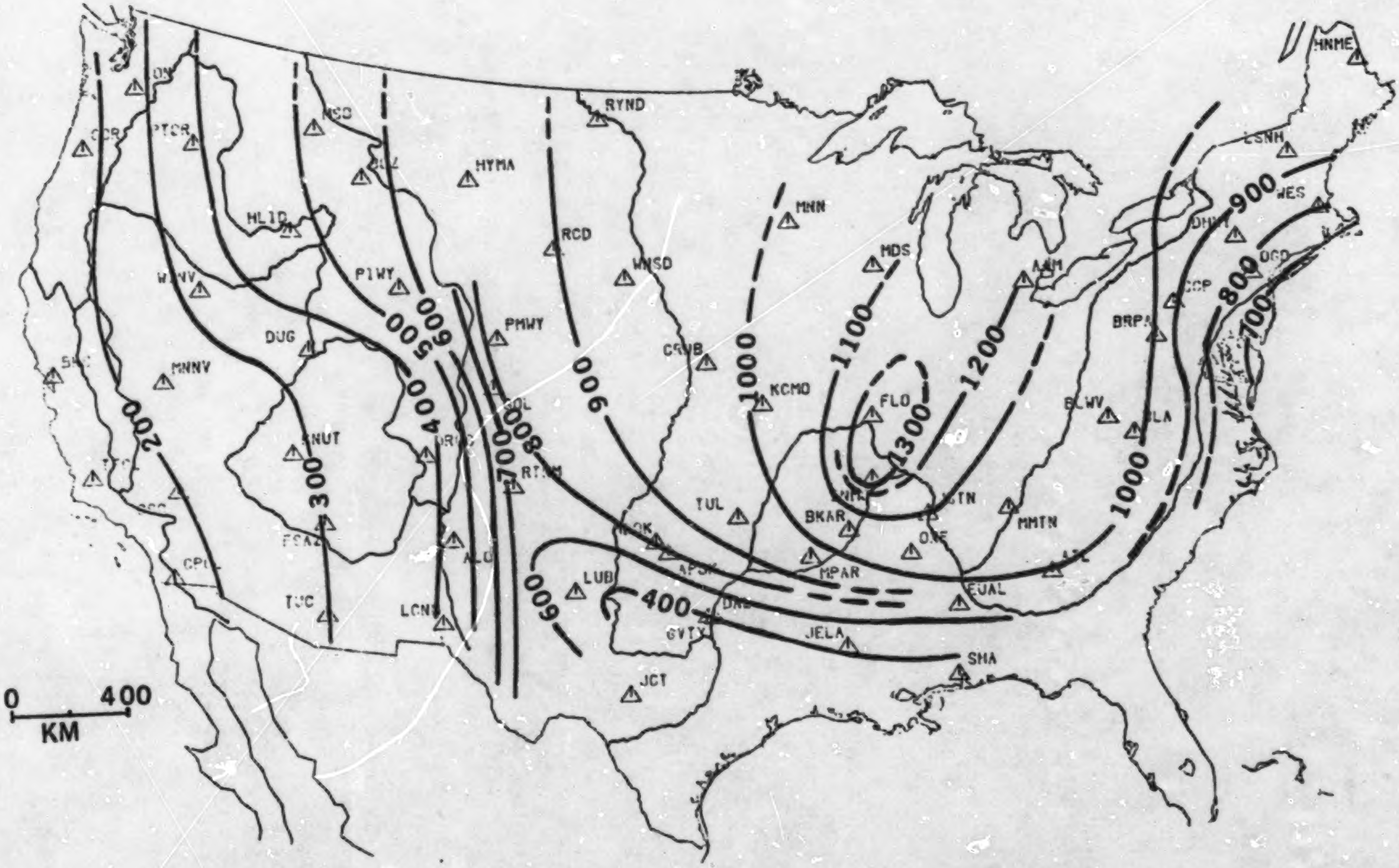
200
300
400
500
600
700
800
900
1000
1100
1200
1300
1000
900
800
700
600
400
0
400
KM
HNME
LSNH
WES
OGD
DHN
CCP
BRPA
BLWV
BLA
AAM
MDS
MNN
FLO
MMTN
ATL
EUAL
SHA
JELA
MPAR
BKAR
OXF
TUL
KCMO
CRNB
WNSD
RCD
RYND
HYMA
PMWY
PIWY
MSO
HLID
DUG
MNNV
GOL
RTNM
ALQ
LCNM
TUC
FSAZ
CPL
SNUT
PTOR
CCR
LUB
JCT
GVTX
DNB
APSK
TOK

Figure 2. Contours of 1 Hz crustal Q estimated from coda of WWSSN SP seismograms.

Glacial Lake Passaic

9510-02724

Byron D. Stone
Branch of Eastern Environmental Geology
U.S. Geological Survey
National Center, MS 928
Reston, VA 22092
(703)860-6503

Investigations

1. Analysis of two cores which sampled lacustrine and fluvial sediments of late Wisconsinan to early Holocene(?) age in the glacial Lake Passaic basin, northern New Jersey, included study of sedimentologic features and preliminary study of palynology and paleomagnetism.

Results

1. The middle portion of a core from the Great Swamp, 8 km south of the late Wisconsinan terminal moraine, sampled 18.9 m of uninterrupted, rhythmically layered clay (mean grainsize class 11.80) and silt (mean grainsize class 7.70) couplets which average 3.1 cm thick. The coarser layers of many of the couplets are composed of microlaminations of silt, probably derived from density currents which originated from meltwater entering the lake at the terminal moraine. As many as 700 couplets, interpreted to be varves, may be present. This count, interpolated over unsampled parts of the varve sequence, extends our estimate of the duration of the Moggy Hollow stage of Lake Passaic, which was dammed by the ice sheet during the late Wisconsinan glacial maximum. The upper 6 m of the core contain thinner and more irregular rhythmites; some of these may also be annual couplets, and may have been deposited during initial retreat of the ice from the terminal moraine. The upper rhythmites show soft-sediment deformation, folds and faults, in several horizons. Oriented paleomagnetic samples from 11 horizons record normal paleomagnetic polarity. Agreement of paleomagnetic directions is good (deviation of directions for samples within a horizon $\pm 5^{o}$) to excellent (deviation $<2^{o}$).

No buried weathering zones or abrupt changes in the stratigraphic record were sampled; thus, we believe that all sediments are of late Wisconsinan age. Samples from a very fine sand below the varves contain spruce and pine, birch, fir, a variety of hardwood trees, shrubs, and boreal herbs, which are representative of a spruce pollen zone similar to the late-glacial spruce pollen zone of northeastern U.S. The varves contain only a few scattered pollen grains. One sample, from a silt bed in the upper part of the varve sequence, contains oak, chestnut, older birch and willow.

2. A core from Fairfield, 14 km north of the terminal moraine, sampled 5.8 m of coarse, oxidized fluvial sand in the upper part. The sand comprises a post-lake terrace which may be of the same age as parts of the extensive peat and local lacustrine deposits which overlie the glacial lake sediments. Below the fluvial sand, a sequence of 3.4 m of irregularly laminated silt and clay which overlies 4 m of corse, dirty gravel (till?), confirms a complex, near-surface, glacial/lacustrine history of the northern part of the basin, as indicated by previous subsurface sampling.

Reports

Reimer, G. E., Ashley, G. M., Liddicoat, J. C., Pavich, M. J., and Stone, B. D., 1981, Glacial Lake Passaic: preliminary coring, paleomagnetic and stratigraphic analysis [abs.]: Geol. Soc. America, Abstracts with Programs, v. 13, no. 3, p. 171.

The major part of FY'81 activities are planned for the summer field season.

FY'81 target activities, Earthquake Hazards Program, summer, 1981:

1. Detailed mapping of surficial geology will be initiated in Chatham, Bernardsville, and Morristown quadrangle.

2. Reconnaissance of surficial deposits in Morristown, Pompton Plains, Mendham, and Bernardsville quadrangles will assess extent and age of Quartenary sediments which overlie and/or extend across the Ramapo fault system. We plan to collaborate with Nick Ratcliffe in trenching some of these deposits.

3. Extent and altitude of beaches and lake deltas will be assessed in reconnaissance of the southern lake basin.

4. Preliminary synthesis of existing subsurface data will be completed for the entire basin.

5. Complete vertical sequences of lake clays will be sampled, probably distally to proximally, with Swedish foil sampler. Samples will be processed for pollen, ^{14}C, and paleomagnetism analysis in FY'82.

H4

STUDY OF EARTHQUAKE RECURRENCE INTERVALS ON THE WASATCH FAULT ZONE, UTAH

14-08-0001-19115

F. H. Swan, Principal Investigator
Kathryn L. Hanson
David P. Schwartz

Woodward-Clyde Consultants
Three Embarcadero Center, Suite 700
San Francisco, California 94111
(415) 956-7070

Investigations

1. A research age-dating program is being conducted with Dr. Allen Tucker at San Jose State University, in conjunction with Stanford University, to evaluate the feasibility of using an accelerator to measure carbon radioisotope concentrations in very small (approximately 3 mg) samples of charcoal and other organic material.

2. Ground reconnaissance has been conducted along the northern and southern portions of the Wasatch fault zone to assess variations in fault behavior along different segments of the fault.

3. Detailed geologic studies, which include mapping of the late Quaternary deposits, topographic profiling of displaced geomorphic surfaces, and exploratory trenching across the main fault scarp, have been completed at a site located at the mouth of North Creek, 16 km north of Nephi, Utah.

Results

1. Preliminary age-dates for three samples of detrital charcoal from the scarp-derived colluvium and graben deposits at Little Cottonwood Canyon site (Swan and others, 1980b), which were not sufficiently large enough to date using conventional radiocarbon methods, have been obtained by Dr. Tucker using an accelerator at the Swiss Federal Institute of Technology in Zurich. The age-dates are 7,800 (+400, -600) for sample LC 1-1; 8,600 (+500, -400) for samples LC 1-2, and 9,000 (+400, -600) for samples LC 3-1. A fourth samples, LC 2-1, consisting of carbonized wood or burned root collected from an organic-rich infilling that fills a fissure in the graben deposits yielded a modern age. The preliminary dates, which were calibrated using samples of known age, appeared to be stratigraphically consistent within the assigned error values. Continued studies are being conducted to assess the reliability of these dates and to date additional small samples

collected at the North Creek site and other locations along the fault zone.

2.a. Observations along the 90-km long northern part of the Wasatch fault zone between the Kaysville site, which is 32 km north of Salt Lake City, and the northern part of the Wellsville Range suggest that there is a decrease in Holocene activity from south to north. 1) At the Kaysville site an alluvial fan surface, estimated to be 6,000 ± 2,000 years old, is displaced 10 to 11 m. Data from trenches excavated across the main fault and graben at this site indicate that the cumulative displacement was produced by at least three surface faulting events (Swan and others, 1979; 1980a). 2) From the Kaysville site north to North Ogden, a distance of approximately 35 km, the fault zone is generally characterized by a single, prominent, main fault scarp and associated local graben; geomorphic evidence indicates there have been repeated Holocene displacements along this part of the fault zone. 3) The fault scarps between North Ogden and Nerva, where a prominent embayment in the range front occurs, are more subdued and appear to be older, with the exception of a complex zone of scarps in the Pole Patch area. The patterns and complexity in this area suggest that landsliding and/or liquefaction may have played important roles in the origin of these scarps. 4) Evidence of repeated Holocene displacement is also apparent along the front east of Nerva and extending 10 km northward to Threemile Creek north of Willard. The geomorphic expression of faulting north of the Threemile Creek has been modified by shoreline erosion and is discontinuous. With the exception of a prominent 2 km-long fault scarp in the northeastern part of Brigham City that displaces Holocene alluvial fans, and scarps across older alluvial fans at Antimony and Dry canyons 6.5 km north of Brigham City, there is little evidence for Holocene activity. 5) The most northerly location where fault scarps are clearly recognizable is aproximately 16 km north of Brigham City near the mouth of Jim May canyon. Alluvial fan deposits displaced across these fault scarps are probably pre-Bonneville in age. Although Bonneville lake sediments may be faulted in places north of Brigham City, the faulting is less continuous, more subdued and commonly masked by shoreline features. The decrease in the amount of Holocene faulting along the Wasatch fault at about latitude 41.5°N appears to coincide with southern end of the Cache Valley fault to the east and of the Pocatello fault to the west.

b. Along a 45 km long portion of the fault south of Santaquin, the Wasatch fault zone has had late Quaternary displacement along at least six distinct traces. The recently active traces are defined by nearly continuous, fresh-looking scarps and they range in length from 1.5 to 24 km. These traces are separated by gaps up to 27 km long that do not appear to have experienced Holocene and/or late Pleistocene displacement.

3. The following observations are based on geologic studies at the North Creek site:

   a. Cumulative net vertical tectonic displacement of an alluvial fan at the mouth of North Creek is 7.0 ± 0.5 m down to the west across the main fault scarp. Detrital charcoal from the upper section of the faulted alluvial fan is dated by Buckman (1978) at 4,580 ^{14}C yr B.P. (3,525 to 3,270 B.C.; calibration based on Clark, 1975). The late Holocene slip rate at this location is approximately 1.3 ± 0.1 mm/year.

   b. Estimates of the amount of displacement during the most recent surface faulting event range from 1.0 m to less than 4.5 m, with a preferred value of approximately 2 m.

   c. Two or three surface faulting events have occurred along this trace of the fault since deposition of the dated fan deposits. At least one and possibly two events occurred post 4,580 ^{14}C yr B.P. (3,525 to 3,270 B.C.). The most recent surface faulting event occurred post 1,110 ± 60 ^{14}C yr B.P. (770 to 965 A.D.). The interval between the two most recent events was greater than 2,900 years and probably less than 4,500 years. If there have been three events post deposition of the North Creek fan, the interval between the second and third most recent events was less than 1,600 years.

References Cited/Selected Reports

Bucknam, R. C., 1978, Northwestern Utah seismotectonic studies: U.S. Geologic Survey, National Earthquake Hazards Reduction Program, Summaries of Technical Reports, v. VII, p. 64.

Clark, R. M., 1975, A calibration curve for radiocarbon dates: Antiquity, v. XLIX, p. 251-266.

Schwartz, D. P., Coppersmith, K. J., Swan, F. H., III, Somerville, P., and Savage, W. U., 1981, Characteristic earthquakes on normal faults: Earthquake Notes, v. 52, no. 1, p. 71.

Swan, F. H., III, Schwartz, D. P., and Cluff, L. S., 1979, Recurrence of surface faulting and moderate to large magnitude earthquakes on the Wasatch fault zone at the Kaysville and Hobble Creek sites, Utah, in Proceedings of Conference, Earthquake Hazards along the Wasatch and Sierra-Nevada Frontal Zones: U.S. Geological Survey Open-File Report 80-801, p. 227-275.

Swan, F. H., III, Schwartz, D. P., and Cluff, L. S., 1980a, Recurrence of moderate to large magnitude earthquakes produced by surface faulting on the Wasatch fault, Utah: Bulletin of the Seimological Society of America, v. 70, no. 5, p. 1431-1462.

Swan, F. H., III, Hanson, K. L., Schwartz, D. P., and Knuepfer, P. L., 1980b, Study of earthquake recurrence intervals on the Wasatch fault zone, Utah: U.S. Geological Survey, National Earthquake Hazards Reduction Program, Summaries of Technical Reports, v. x, p. 166-168.

Structural Framework of Eastern United States Seismic Zones

9950-02653

R. L. Wheeler
Branch of Earthquake Tectonics and Risk
U.S. Geological Survey
Denver Federal Center, MS 966
Denver, CO 80225
(303) 234-5087

Investigations

1. Work continued to use new and existing data and understanding of Appalachian structures and tectonics, to identify and map the most likely types of faults responsible for seismicity in and near Giles County, southwestern Virginia. Efforts were coordinated with faculty at Virginia Polytechnic Institute and State University (especially G. A. Bollinger), other USGS projects, and other pertinent investigators. See Results 2 and 3, Reports 1, 3, 5, 6, and 7.

a. M. Jones-Cecil and R. L. Wheeler spent 4 weeks in the field in and near Giles County, mostly mapping intensity of joints to locate and trace a seismogenic zone discovered by Bollinger.

b. Bollinger and Wheeler gave 2 talks at the eastern SSA meeting and 1 at the national GSA meeting (abstracts cited in last technical report), and are working on a manuscript describing and interpreting seismicity in and near Giles County.

2. Jones-Cecil continued work on modification of a pattern recognition program by incorporating a statistical test and increasing the flexibility of the classification method. The modified program has been applied to the Southeastern U.S. to seek associations of geological, geophysical, and topographic variables with presence or absence of seismicity. Additional minor modifications to the program are underway. Jones-Cecil gave a talk at the eastern SSA meeting (abstract cited in last technical report). Planning has begun to test the technique in a Western U.S. area with a larger seismic data base than available in the Southeast. See Result 1.

3. Mathematical and statistical collaboration was provided to other projects, through work of K. M. Shedlock. See Result 4, Reports 2 and 4.

a. Shedlock continued work on a manuscript (Director's approval, Feb. 1981) with D. G. Herd and others on "The next great San Francisco Bay area earthquake", intended for Science. Travel and computer work supported by project 9540-01950 (D. G. Herd) and project 9930-02103 (W. L. Ellsworth).

b. Shedlock completed work on evaluating sensitivity of risk calculations to various parameters used in the calculations, with D. M. Perkins. Computer work supported by project 9950-01207 (S. T. Algermissen).

c. Shedlock began processing and interpreting data from refraction and small-boat reflection surveys in the Mississippi embayment. Travel and computer work supported by project 9950-01504 (D. P. Russ).

Results

1. Jones-Cecil has completed a test application of the modified pattern recognition program to the Southeast U.S. The modifications enable the use of statistical rather than operator-defined criteria for the selection of associations of geology, geophysics, and topography with seismicity. In addition, the modifications make it possible to apply the program in areas that do not have a uniform cause of seismicity. However, identification of associations for a subset of earthquakes is dependent on sample size. Preliminary results of the application to the Southeastern U.S. show associations characterizing two broad areas of moderate seismicity, and other associations characterizing much of the intervening non-seismic or less seismic area. Absence of most of these associations in four areas having had large or moderate earthquakes, including around Charleston, S.C., and Giles County, Va., implies that these areas may have different causes of seismicity than does most of the Southeast. However, positive associations characterizing these seismic areas cannot be identified because of the small sample of moderate and large earthquakes in the Southeast. The positive associations from the preliminary results are intriguing, but not easily interpretable. For example, two variables contributing to positive associations with seismicity are the presence of anticlinal structures and the absence of high topographic relief. Final interpretation of the positive associations should be accompanied by reevaluation of the original data sets and of the choice of variables. Though still in press at the end of the report period and so not cited below, a 137 page open-file report (OFR 81-195) has been published as of this writing. It describes the modifications to the pattern recognition technique and the test application of the technique to the Southeast.

2. The gravity gradient that runs the length of the Appalachians is regarded as overlying the eastern edge of relatively intact North American continental crust, inherited from the early opening of the Iapetus Ocean. Several observations suggest that that boundary may separate large crustal blocks of different seismic hazard, to which may be added local hazards accentuated by smaller structures. (1) Others have recently recognized remains of Paleozoic island arcs, marginal or back-arc basins, and other microplates east of the gravity gradient in various parts of the Appalachians. (2) This has suggested to several of us the applicability to the Appalachians of the concept of tectono-stratigraphic terranes as developed for western North America. A commonly cited modern example is the complex of small plates and plate boundaries caught between Australia and Southeast Asia.

To the extent that such a model applies to the Appalachians east of the gravity gradient, the lithosphere there could consist of small, heterogeneous blocks separated by sheared zones of crustal dimensions. (3) Such a fabric may not show in near-surface geology above the COCORP sole thrust: interpretation of maps of wavelength-filtered Bouguer gravity values produced by R. Simpson (project 9730-00364) and coworkers indicates that the gravity gradient has sources throughout the crust and the upper mantle. (4) Mesozoic basins south of New York City lie mostly or entirely east of the gravity gradient. That is consistent with the hypothesis that the crust has different mechanical properties on opposite sides of the gradient. Consequently the gradient may provide a western boundary for the applicability of such suggested bases for zoning as the domain of young reverse faults, proposed by C. Wentworth and M. Mergner-Keefer (project 9540-02191).

3. At the suggestion of S. T. Algermissen and F. A. McKeown, Wheeler consulted various USGS personnel to investigate the feasibility of a systematic search of large areas of the East for sand blows. Such a search seems feasible and practical. It has the potential to aid estimation of recurrence rates, to place a lower limit on maximum likely earthquake size, and perhaps to help define boundaries of some zones of seismic hazard. It was decided that preliminary investigation will start in the next reporting period, as time allows.

4. Results obtained by Shedlock in collaborative work with other projects will be reported by projects listed above under investigation 3.

Reports

Berger, P. S., and Wheeler, R. L., 1980, Western limit of extension fracturing in West Virginia, in Wheeler, R. L., and Dean, C. S., eds.: Western Limits of Detachment and Related Structures in the Appalachian Foreland, Chattanooga, Tennessee, April 6, 1978, Proceedings, DOE/METC/SP-80/23, p. 34-40; available from National Technical Information Service, Springfield, Va. 22161.

Herd, D. G., Ellsworth, W. L., Lindh, A. G., Prescott, W. H., and Shedlock, K. M., 1981, The next large San Francisco Bay area earthquake (abs.): Earthquake Notes, v. 52, no. 1, p. 4-5.

LaCaze, J. A., Jr., and Wheeler, R. L., 1980, Expression of a cross-strike structural discontinuity in Pennsylvanian rocks of the eastern Plateau province: Southeastern Geology, v. 21, p. 287-297.

Perkins, D., Bender, B., and Shedlock, K., 1980, Rules of thumb relating to issues in probabilistic ground motion mapping: Conference on Evaluation of Regional Seismic Hazards and Risk, Santa Fe, N.M.

Wheeler, R. L., 1980, Cross-strike structural discontinuities: possible Exploration tool for natural gas in detached Appalachian foreland, in Wheeler, R. L., and Dean, C. S., eds.: Western limits of detachment and related structures in the Appalachian foreland, Chattanooga, Tennessee, April 6, 1978, Proceedings, DOE/METC/SP-80/23, p. 41-55; available from National Technical Information Service, Springfield, Va. 22161.

Wheeler, R. L., and Dean, C. S., eds., 1980, Western limits of detachment and related structures in the Appalachian foreland, Chattanooga, Tennessee, April 6, 1978, Proceedings, DOE/METC/SP-80/23, 177 p.; available from National Technical Information Service, Springfield, Va. 22161.

Wilson, T. H., Dixon, J. M., Shumaker, R. C., and Wheeler, R. L., 1980, Fracture patterns observed in cores from the Devonian shale of the Appalachian Basin, in Wheeler, R. L., and Dean, C. S., eds.: Western limits of detachment and related structures in the Appalachian foreland, Chattanooga, Tennessee, April 6, 1978, Proceedings, DOE/METC/SP-80/23, p. 100-123; available from National Technical Information Service, Springfield, Va. 22161.

Late Tertiary and Quaternary Shoreline Datum Planes and Tectonic Deformation in the Southeastern United States

9590-02744

Thomas A. Ager
Branch of Paleontology and Stratigraphy
U.S. Geological Survey
12201 Sunrise Valley Drive
Mail Stop 970
Reston, Virginia 22092
(703) 860-7745

Investigations

1. Biostratigraphic research on Atlantic Coastal Plain deposits of Pliocene and Quaternary age continues, involving in particular samples from the southern Virginia-northern North Carolina segment of the coastal plain. Final project-related fieldwork is planned for May, 1981 to that region.

2. Project participants are all involved in preparation of manuscripts that discuss various aspects of the research generated by this project. The project is scheduled to terminate officially at the end of FY 81. Therefore we are attempting to wind up sample analysis and report and manuscript preparation in anticipation of that deadline.

Results

1. All project participants, both official and non-official, have contributed to scientific papers (generated by this project) published since the last semi-annual report was submitted. These publications are listed below in the Reports section. Some of the major findings in these new publications include:

a. Uranium-series dating of Atlantic Coastal Plain high sea level stands at 72,000 (7 ± 3 meters), 94,000 (6.5 ± 3.5 m), 120,000 (7.5 ± 1.5 m) and 188,000 years ago (7 ± 5 m) (Cronin et al., 1981 in Science).

b. Studies of calcareous nannofossils and planktic foraminifera from Atlantic Coastal Plain sedimentary units of Pliocene and Quaternary age revealed 3 discrepancies between the nannofossil and foram biostratigraphic assignments of certain formations and the sea level curve of Vail. The Croatan, Bear Bluff, upper Yorktown formations (all Pliocene) and the Waccamaw Formation (Pleistocene) were deposited at times when sea level stood relatively higher than at present. According to Vail, however, sea level was supposedly lower than at present during the times when these formations were deposited. Either Vail's curve is incorrect, or significant tectonic uplift has occurred in the Atlantic Coastal Plain during Pliocene and Quaternary time (Bybell and Poore, 1980).

c. According to Blackwelder (1980 in Geology), evidence from deposits along the middle Atlantic Coast between New York City and South Carolina suggest tectonic stability in the region during the past ca. 12,000 years. In addition, he presents evidence that suggests that sea level stood at about -30 m 12,000 years ago, whereas previous estimates suggested a sea level position at -60 m at that time. Previous suggestions of significant post-glacial uplift along the coast were based in part on the erroneous estimate of sea level position 12,000 years ago.

Reports

Blackwelder, Blake W., 1980, Late Wisconsin and Holocene tectonic stability of the United States mid-Atlantic coastal region: Geology, v. 8, p. 534-537, 2 figs., 1 table.

Blackwelder, Blake W., 1981, Stratigraphy of upper Pliocene and lower Pleistocene marine and estuarine deposits of northeastern North Carolina and southeastern Virginia: U.S. Geol. Survey Bull. 1502-B, 16 p., 1 pl., 6 figs.

Blackwelder, B.W., Late Cenozoic Marine deposition in the United States Atlantic Coastal Plain related to tectonism and global climate: Palaeogeography, Palaeoclimatology, Palaeoecology, 60 p., 3 figs.
9-12-80 - Accepted for publication.

Blackwelder, B.W., Late Cenozoic stages of the U.S. Middle Atlantic Coastal Plain: Jour. Paleontology, 65 p., 9 figs., 1 table, 10 pls.
10-23-80 - Accepted for publication.

Blackwelder, B.W., and Cronin, T.M., Atlantic Coastal Plain geomorphology illustrated by computer generated block diagrams; U.S. Geol. Survey Misc. Field Invest. Map 1242: 19 ms p., 2 maps.
10-8-80 - Approved for the Director

Bybell, Laurel M., and Poore, R.Z., 1980, Calcareous nannofossil and planktic foraminiferal biostratigraphy of Pliocene and Pleistocene Atlantic Coastal Plain deposits: Geological Society of America Abstracts with Programs, v. 13, no. 1, p. 3.

Cronin, T.M., Szabo, B.J., Ager, T.A., Hazel, J.E., and Owens, J.P., 1981, Quaternary climates and sea levels, U.S. Atlantic Coastal Plain: Science, vo. 211, p. 233-240.

Cronin, T.M., in press, Eustacy, hydroisostasy and lithospheric flexure: the rates and causes of neotectonic vertical crustal movements of the emerged southeastern Atlantic Coastal Plain: Geological Society of America Bulletin.

DuBar, J.R., DuBar, S.S., Ward, Lauck W., and Blackwelder, Blake W., 1980, Cenozoic biostratigrpahy, Carolina outer coastal plain. Field trip 9, in Frey, R.W., ed., Excursions in southeastern geology, v. 1: Geol. Soc., America, Ann. Mtg., (93rd), Atlanta 1980, Field Trip Guidebooks, p. 211-236, 18 figs., 8 tables.

Pilkey, O.H., Blackwelder, Blake W., Knebel, H.,J. and Ayers, M.W., 1981, The Georgia Embayment continental shelf: Stratigraphy of a submergence: Geol. Soc. America Bull., Pt. I, v. 92, no. 1, p. 52-63, 8 figs., 2 tables.

Ward, Lauck W. and Blackwelder, Blake W., 1980, Stratigraphy of Eocene, Oligocene and lower Miocene formations - coastal plain of the Carolinas, in Dubar, J.R., DuBars S.S., Ward, L.W., and Blackwelder, B.W., Cenozoic biostratigraphy of the Carolina outer coastal plain, in Frey, R.W., ed., Excursions in southeastern geology, v. 1: Geol. Soc. America, Ann. Mtg., (93rd), Atlanta 1980, Field Trip Guidebooks, p. 190-208, 27 figs.

Neotectonics of the North Frontal Fault System of the San Bernardino Mountains, Southern California

Contract No. 14-08-0001-19754

Clarence R. Allen and Kristian E. Meisling
Seismological Laboratory, California Institute of Technology
Pasadena, California 91125 (213-356-6904)

Investigations

1. We are engaged in geologic mapping of the north frontal fault system of the San Bernardino Mountains between Silverwood Lake and Cushenbury Canyon. Emphasis is currently on (a) establishing a better constrained uplift history for the San Bernardino Mountains, and (b) elucidating the nature and modes of deformation acting on the northern range front. Our longer term goals are to (c) estimate Holocene rates of deformation along the northern range front and (d) estimate, if possible, recurrence intervals and vertical/lateral offsets for the frontal fault system. We have finished detailed mapping of the range front from Silverwood Lake to Deep Creek Flood Control Basin. This work is considerably augmented by the results of a detailed neotectonic investigation recently completed between Cajon Pass and Silverwood Lake by Ray Weldon and Kristian Meisling, under contract with the California Department of Water Resources (Weldon et al; in preparation). The USGS and California DWR studies are inseparable insofar as they share the same goals and cover adjoining areas. Hence, credit for the results below goes partially to Ray Weldon and the California DWR.

Results

1. Bedrock in the study area consists of an extremely complex igneous/metamorphic terrane composed primarily of Cretaceous(?) foliated quartz-monzonites and granodiorites (Miller and Morton, 1980; R.E. Powell, pers. comm.). A deeply weathered erosion surface, developed on the bedrock complex, is tentatively correlated with the extensive late Tertiary surface developed atop most of the San Bernardino Mountains (Oberlander, 1972).

The late-Tertiary Crowder Formation once overlay much of the bedrock erosion surface as evidenced by numerous remnants, protected from erosion by faulting, throughout the western San Bernardino Mountains. The Crowder Fm, widely exposed in Summit Valley, is dominantly lithic arkose with local conglomeratic beds. Although the age of the Crowder Fm is only firmly constrained between 15 and 0.6 my, it is estimated to be 2-4 my old based on structural and stratigraphic arguments (Foster, 1980). East of Grass Valley the lower Crowder Fm contains a 150-meter-thick section of heretofore undescribed interbedded tuffs and volcanogenic siltstones, sandstones, and swelling claystones. Ray Weldon is currently preparing a sample of tuff from this section for dating.

Younger Pleistocene alluvial fan and terrace deposits, well developed in Summit Valley, Cleghorn Canyon and Miller Canyon, are graded to levels that postdate the original downcutting of Summit Valley. Well-graded alluvial fan and terrace deposits in Summit Valley, generally less than 10 m thick, are underlain by an extensive pediment surface developed on the Crowder Formation. Correlation of terrace sequences in Summit Valley and Cajon Pass suggests that the initial downcutting of Summit Valley may have occured more than 500,000 years ago rather than since 100,000 years ago as recently suggested by Foster (1980). Two distinct terrace levels in Cleghorn Canyon are tentatively classified as >>100,000 and <100,000 years in age. Poorly-graded alluvial fan/colluvial mantle deposits in Miller Canyon can also be assigned to these two age groups. Correlation of these terrace levels with terraces being studied by Ray Weldon in Cajon Pass promises to yield much better age constraints.

2. Four distinct Plio-Pleistocene(?) structural episodes postdate deposition of the late-Pliocene(?) Crowder Formation in the western San Bernardino Mountains. In sequential order they are: (A) Folding of the basal Crowder Fm into N-trending, N-plunging asymmetric anticline/syncline pairs (N-plunging monoclines; E-down), probably reflecting sediment "draped" over basement steps. (B) Minor displacement on a pervasive set of WNW- to W-trending, high-angle reverse faults. Preservation of the late Tertiary erosion surface throughout the area and minimal offset of plunging monoclines rules out more than 350 meters of total vertical and lateral displacements on high-angle reverse faults. Furthermore, throw on the high-angle reverse faults is SW-block-down, clearly the wrong sense for uplift of the range to the south. (C) Uplift of the western San Bernardino Mountains by tilting. Both the bedrock erosion surface and overlying Crowder Fm consistently dip 30° N over a broad area of the range front, suggesting that tilting was the dominant mode of mountain uplift. The Pleistocene Harold Fm, which buries at least one high-angle reverse fault in Cajon Pass, dips about 25° NE , suggesting that tilting largely postdates high-angle reverse faulting. Ray Weldon's work on alluvial units in Cajon pass shows that northward tilting is still going on. (D) Development of the left-lateral strike-slip Cleghorn system partly through "piracy" of pre-existing high-angle reverse faults. The Cleghorn fault splits into two traces just west of Silverwood Lake; one branch occupies Miller Canyon, the other crosses to the NE-trending range front. In both Miller and Cleghorn Canyons, kinks are evident where the Cleghorn fault jumps from one pre-existing zone of weakness to another. The Cleghorn system clearly offsets plunging monoclines and high-angle reverse faults

Low-angle, SE-dipping range-front thrusts first appear to the east of Grass Valley. The relationship between this range-front thrusting and the high-angle reverse or strike-slip faulting is unclear at this time.

3. Both strands of the Cleghorn fault show evidence of Quaternary activity. Terraces in Cleghorn and Miller Canyons are disrupted by the Cleghorn fault. Relatively undegraded scarps in Cleghorn Canyon suggest Holocene activity. Pediment surfaces along the NE-trending branch of the Cleghorn system at Silverwood Lake are clearly truncated; trench logs made by the California Department of Water Resources also show this strand cutting terrace materials (California Department of Water Resources, 1968).

Several lines of evidence support significant left-lateral motion on the Cleghorn fault. Streams cut into the younger terrace level in Cleghorn

Canyon are offset up to 200 meters left-laterally. Both older alluvial fan deposits in Miller Canyon and the older terrace level in Cleghorn Canyon also appear to be offset left-laterally about 1.3 km. A consistent 3 to 4 km left-lateral offset of plunging monoclines, distinctive high-angle reverse faults and bedrock structure along the Cleghorn fault indicate that this cumulative left-lateral displacement has taken place entirely since the cessation of high-angle reverse faulting.

The most conservative interpretation of these findings yields a minimum rate of left-lateral displacement on the Cleghorn fault of roughly 0.8 mm/yr (3.3 km since Crowder deposition ~4 mya). This calculation allows no time whatsoever for the complex series of structural events that clearly postdate the deposition of the Crowder Fm and predate the onset of left-lateral strike-slip faulting. Offset of older terraces in Cleghorn and Miller Canyons (1.3 km since 0.5 to 0.7 mya) suggest a higher left-lateral rate of about 2 mm/yr on the Cleghorn fault. Offset of ~100,000 year old terraces up to 200 m also yields an average slip-rate of 2 mm/yr.

References Cited

California Department of Water Resources, 1968, Geology and construction materials data, Cedar Springs Dam: Cal. Dept. Water Res., Southern District Design and Construction Branch, Project Geology Report D-102

Foster, J.H., 1980, Late Cenozoic tectonic evolution of Cajon Valley, southern California: Ph.D. thesis, Univ. of Cal., Riverside, 235 pp.

Miller, F.K., and Morton, D.M., 1980, Potassium-argon geochronology of the eastern Transverse ranges and southern Mojave Desert, southern California: U.S.G.S. Professional Paper 1152, 30 pp.

Oberlander, T.M., 1972, Morphogenesis of granitic boulder slopes in the Mojave Desert, California: Jour. Geol., v. 80, p. 1-20

Weldon, R.J., Meisling, K.E., Sieh, K.E., and Allen, C.R., in preparation, Neotectonics of the Silverwood Lake area: Report to the California Department of Water Resources.

Southwestern Utah Seismotectonic Studies

9950-01738

R. Ernest Anderson
Branch of Earthquake Tectonics and Risk
U.S. Geological Survey
Denver Federal Center, MS 966
Denver, CO 80225
(303) 234-5109

Investigations

1. A study was made of the Tanlu fault in eastern China with R. V. Sharp during October 1980.

2. As part of a continuing effort to better understand the tectonic framework of the eastern Great Basin area, geologic mapping was done in the Gunlock, Motoqua, Dodge Spring, and Goldstrike 7.5° quadrangles and in parts of the Maple Ridge, Docs Pass, and Jacks Mountain 7.5° quadrangles, southwest Utah and adjacent Nevada.

Results

1. The Tanlu fault extends about 2,400 km north-northeast from the Yangtse River across the north China plain, Bo Hai (Gulf), and northeastern China to the Russian frontier--truly one of the great faults of the world in terms of its length. Our geoscientist hosts from the Peoples Republic of China regard the Tanlu as an intraplate strike-slip fault that locally consists of several subparallel strands. For China, the Tanlu fault is possibly one of the most important structures to understand in terms of its history of activity. It is most active in its central part where there have been 27 historic earthquakes of magnitude greater than 6. The Tanlu fault is known from the historic record to be capable of generating M>8 earthquakes (last one in 1668), and the fault traverses the country's principal region of agricultural production and the greatest concentration of population in China. For example, Shandong, Jiangsu, and Anhue Provinces are crossed by the fault and have populations estimated to be about 70, 50, and 45 million respectively; and Hefei, the capitol of Anhue Province, is a "small" city with a population larger than that of the Denver metropolitan area.

We were guided by our hosts on a 9-day field trip along the south part of the Tanlu fault. The landscape through most of this part of China consists of broad flat plains broken by widely spaced hills and flanked, locally, by mountains. The plains are underlain by unconsolidated to weakly consolidated Quaternary sediments that range in thickness from a thin veneer to more than 100 m. These sediments have supported an intense agricultural industry for thousands of years. The volume of surficial material that has been relocated to construct terraces, irrigation systems, dams, and canals is staggering. The flatness of the terrain and its disturbance by man essentially preclude on-the-ground identification of fault traces in the plains.

The exposures of the fault to which we were conducted are widely spaced and typically only a few meters to several hundred meters long. They are located in areas of exposed bedrock or at bedrock-alluvium contacts on the flanks of hills. Most of these exposures are of very good quality as a result of either youthful erosional downcutting by transverse drainages that head in adjacent highlands or by excavations of fault gouge for pottery and/or building materials. The Chinese geologists have done a very credible job of interpreting the fault relationships that were shown to us. In general, stratigraphic relationships, including assignment of Quaternary materials to a fourfold stratigraphic grouping, appear to be well established locally and regionally.

At several localities that we visited, Quaternary materials that include alluvium, colluvium and loess are involved in the faulting. At all but one of those localities, field relationships document a vertical component of slip and at most of them, a high-angle reverse mode of failure is indicated. This is not surprising because field studies of faulted bedrock by the Chinese geologists show high-angle reverse faulting is to be common at the present level of exposure on the flanks of uplifted basement blocks. Whether the reverse mode of faulting represents mushrooming of the uplifted blocks under shallow conditions of low confining pressure or a response to first-order tectonic stress is not known. At one locality, about 10 km southeast of Tancheng, Quaternary stream channel deposits appear to be offset several meters in a right-lateral sense. This sense of slip agrees with that of offset and dragged mafic dikes of late Tertiary(?) age at the same locality. At none of the localities is the age of faulted Quaternary materials well enough known to provide reliable estimates of slip rates.

Geomorphic expression of faulting as it can be judged by what we saw, is only locally evident. Although we did see some prominent scarps, one is probably a fault-line feature produced by differential erosion of contrasting materials on opposite sides of the fault rather than reflecting young vertical offset along the fault. Only a few unambiguous fault scarps that could be ascribed at least partly to young displacement along fault strands of the zone were seen. Probably the best example is located along a minor strand in the zone northeast of Tancheng; it consists of a low scarp and convincing evidence that a vertical component of slip has added to the height of the scarp in relatively recent time (possibly Holocene). Possible geomorphic evidence of very young (possibly Holocene) right-slip displacement was seen about 20 km northeast of Tancheng where small east-flowing transverse drainages are constrained to abut and flow southward around the ends of short ridges composed of fractured and relatively nonresistant bedrock.

Our study of the Tanlu fault provides an adequate basis for planning future cooperative investigations of the fault.

2. Geologic mapping in southwestern Utah and adjacent Nevada has provided a basis for evaluating genetic and temporal structural relationships between the Great Basin (GB) and Sonoran Desert (SD) sections of the Basin and Range province. A 100-km-wide corridor that was relatively amagmatic during late Cenozoic time separates the southern limit of late Cenozoic magmatism in the GB section from the northern limit of late Cenozoic magmatism in the SD section (figs. 1, 2).

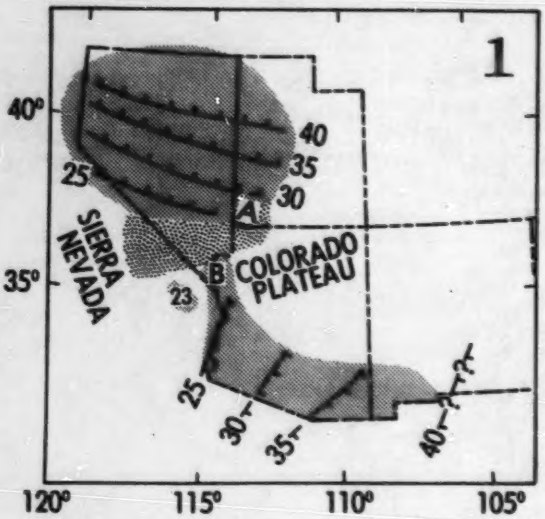

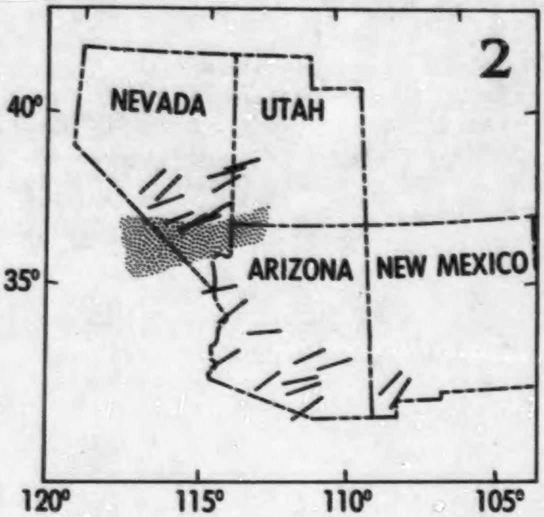

Figure 1.--Map showing patterns of migration of Cenozoic magmatism with calc-alkaline affinities (hachured heavy lines with ages in mega years) modified from Dickinson and Snyder, 1978. The two main areas of magmatism (fine stipple) are separated by an amagmatic corridor that extends from the Colorado Plateau in the Arizona-Nevada border area west to the Sierra Nevada (coarse stipple). A and B mark localities where magmatism began 21-20 m.y. ago.

Figure 2.--Map showing variously derived least principal stress directions within Cenozoic magmatic terrains, from Zoback and others, 1981.

Recent mapping (unpublished) within and north of the eastern part of the corridor in the Beaver Dam and Bull Valley Mountains of southwesternmost Utah and in the Clover Mountains of adjacent Lincoln Co., Nevada, reveals a major episode of southerly to southwesterly directed pre Basin-Range thin-skinned extensional tectonic transport. In its early stages, this deformation was active as listric growth faults associated with 15-14-m.y.-old volcanic activity, but it continued and reached major proportions between about 14 and 11 m.y. ago. During extensional deformation volcanic rocks were structurally transported away from the magmatic axis toward, and, in some places, into the adjacent amagmatic corridor on complex systems of listric and transverse faults. Available data suggest that Precambrian crystalline rocks and Paleozoic and Mesozoic sedimentary rocks within the amagmatic corridor were transported on faults that are similar to, and, in some places, coextensive with those that displace Cenozoic rocks. Locally, Cenozoic volcanic rocks are decoupled from subjacent pre Cenozoic rocks along low-angle fault zones at which there is generally evidence of stratigraphic attenuation. Such decoupling zones are not unique to the base of Cenozoic volcanic rocks, but are also found within the volcanic sequence and in adjacent areas of pre Cenozoic rock. All exposed rocks about 14 m.y. old and older appear to have participated in the episode of south to southwest tectonic transport, the magnitude of which is more dependent on geographic than stratigraphic position.

Available data, including slip lineations from fault systems within and adjacent to the eastern part of the amagmatic corridor suggest that complex coeval extensional structures entered the corridor from the north, passed through it, and splayed southward across its south margin thus providing structural ties between the GB and SD sections of the Basin and Range province.

Reports

Anderson, R. E., 1981, Structural ties between the Great Basin and Sonoran Desert sections of the Basin-Range province: U.S. Geological Survey Open-File Report (in press).

Earthquake Hazards and Tectonic History of the San Andreas Fault Zone, Los Angeles County, California

14-08-0001-19193

Allan G. Barrows,[1] James E. Kahle,[2] and David J. Beeby[3]

California Division of Mines and Geology
1416 Ninth Street, Room 1341
Sacramento, California 95814
[1](213) 825-3787 [2](213) 620-3560 [3](916) 445-0515

Investigations

It is the purpose of the current project, which is the final phase of the Division's program involving a 100-km stretch of the San Andreas fault zone in Los Angeles County, to produce an analysis of the geologic history of the fault. Data collected during earlier phases of this program, along with new data from minor gaps that remained along this stretch of the fault are being brought together into a summary paper and strip maps. A better understanding of how fault behavior may be changing through time in offset history, recurrence interval, or in the physical location of ground rupture is the primary goal of this project.

Results

Geologic maps have been prepared for the east-half Three Points and Pine Canyon segments, a 15-km stretch of the fault that was the final gap in geologic coverage.

Topographic base maps, at 1:12,000 scale, have been prepared for the entire 100 km that has been mapped. These maps cover the fault zone in eight contiguous sheets, each representing 12.5 km, to form a detailed geological strip map. Compilation of the geology is in progress. A composite geologic column derived from six existing explanation sheets is being prepared through review, revision, and simplification of the original nomenclature.

Revision of annotated fault activity maps, on orthophoto bases at 1:12,000 scale, and preparation of maps for the previously unmapped Juniper Hills segment is underway.

Quaternary Fault Map of the Reno 1x2° Quadrangle

Contract No. 14-08-0001-18375

John W. Bell
Nevada Bureau of Mines and Geology
University of Nevada-Reno
Reno, Nevada 89557
[702] 784-6691

Goals

1. To compile all existing published and unpublished maps showing young faulting within the Reno 1x2° quadrangle.
2. To cross-check existing data and map young faults in unstudied portions of the quadrangle.
3. To assess recency and recurrence of movement on all major fault zones in the quadrangle.

Approach

Low sun-angle, black and white aerial photography (1:40,000-scale) was flown for the entire 1x2° area and provided complete, uniform coverage for the study. It was supplemented with existing 1:60,000-scale AMS photography and large-scale (1:12,000) low sun-angle photography in certain portions of the quadrangle. Fault scarps, suspected fault scarps, and fresh-appearing bedrock alluvial lineaments were mapped on the new photography. The mapped features were cross-checked against existing literature, and all major fault scarps were investigated by field reconnaissance. Interpretations of recency of movement have been made based upon an evaluation of the alluvial-, fluvio-lacustrine-, and soil-stratigraphic record at each site. Selected faults and suspected faults have been trenched.

Fault scarps are delineated on a 1:250,000-scale map on the basis of age of most recent movement:

1. Historic surface rupture
2. Post-high Lahontan shoreline scarp (less than 12,000-18,000 years old)
3. Pre-high Lahontan shoreline scarp (late Pleistocene and older)
4. Youthful-looking bedrock/alluvial contact of probable tectonic origin, but of uncertain age

Results

The results of this study show that much of the Holocene-age fault activity is concentrated along the major structural features in the quadrangle: the Sierra Nevada Frontal Fault Zone, the Walker Lane, the Carson Lineament, and the Olinghouse Fault Zone. In particular, the junctures of these structural features show evidence of repeated Holocene activity. Most other areas of recognized Holocene movement appear related to north-northeast-trending conjugate structures of the right-lateral

Walker Lane.

Six areas of historic surface rupture are known to have occurred within the quadrangle:

1869	Olinghouse Fault Zone
1903	Gold King Fault
1954	Rainbow Mountain Fault (July)
1954	Rainbow Mountain Fault (August)
1954	Dixie Valley Fault Zone
1954	Fairview Peak Fault Zone

A seventh area of surface rupturing may have occurred in the Pyramid Lake-Carson Desert area around 1850.

Major areas of prehistoric Holocene faulting include:

1. Sierra Nevada Frontal Fault Zone from Steamboat Hills south to Genoa
2. Walker Lane from Pyramid Lake south to Fernley
3. Walker Lane at Weber Dam/Reservoir
4. Carson Lineament at Lahontan Dam/Reservoir
5. Hot Springs Mountains
6. Carson Sink/Carson Lake area
7. East flank of Stillwater and Sand Springs Ranges

Analysis of faulting along the right-lateral Walker Lane suggests that Quaternary-age movement in the quadrangle changes style of deformation along this structure from northwest to southeast. In the Pyramid Lake segment of the zone, prominent northwest-trending scarps, pressure-ridges, and sag ponds characterize the movement. To the southeast, however, the northwest-trending structures appear to be truncated by the east-northeast-trending Carson Lineament. In the Desert Mountains/Carson Lake area, the zone is characterized by broad, arcuate faults concave to the north-northwest. The northwest-trending scarps resume farther south in the Weber Dam/Reservoir area.

Recurrence (re-rupture) data is presently based upon age control derived from the soil- and lacustrine-stratigraphic record. Re-rupture intervals on the major structures in the quadrangle appear to be thousands of years, but less than 10,000 years. Intervals on other structures may be an order of magnitude longer.

Surface Faulting Studies

9940-02677

M. G. Bonilla
Branch of Ground Motion and Faulting
U.S. Geological Survey
345 Middlefield Road, MS-77
Menlo Park, CA 94025
(415) 323-8111, Ext. 2245

Investigations

1. Study of rupture fraction

2. Statistical studies of surface faulting

3. Preparation of reports

Results

1. Work on the rupture fraction (surface rupture length/total fault length) consisted primarily of bibliographic research on total length of selected faults that have had surface faulting. The bibliographic search is largely completed for eight faults in the U.S. and has been started for six faults in other countries. Large to intermediate scale topographic maps, and geologic literature has been ordered for several faults. Various geologic maps were examined for the manner in which geologic faults are shown to terminate. The maps examined show faults terminating in about 10 different geometric and/or structural patterns. A start was made in a) examining the literature dealing with theoretical analyses of the terminations of faults, and b) reviewing how the total lengths of faults have been established in actual practice during evaluation of seismic risk for particular projects.

2. Work continued on the empirical relation between maximum fault displacement at the surface and magnitude of the associated earthquake, and between surface displacement and surface rupture length. Estimates were made of the probable errors in reported displacement for selected historic events. Earthquake magnitude, and errors in magnitude, were determined for 7 earthquakes using the same standardized method that was used for the 30± events in the magnitude vs. rupture length data set. Statistical correlations are now being made between surface displacement and earthquake magnitude for 28 events and between surface displacement and surface rupture length for 26 events, including consideration of errors in both earthquake magnitude and surface displacement. (Coinvestigators J. J. Lienkaemper and R. K. Mark.)

3. The report on the Pleasant Valley, Nevada, exploratory trench was completed and released on open file. It has been revised and submitted for a U.S. Geological Survey Professional Paper. A report "Evaluation of surface faulting and other tectonic deformation" was prepared for the Interagency Committee on Seismic Safety in Construction, and is being revised after technical review. A checklist for geologic study of earthquake effects was revised and submitted for publication.

Reports

Bonilla, M. G., Villalobos, H. A., and Wallace, R. E., 1980, Exploratory trench across the Pleasant Valley fault, Nevada: U.S. Geological Survey Open-File Report 80-1245, 35 p.

Bonilla, M. G., and Bailey, E. H., in press, Check list for geologic study of earthquake effects: American Geological Institute Data Sheet.

Quaternary Deposits and Tectonics of the Antelope Valley-Western Mojave Region, California

9940-02090

Dennis B. Burke
Branch of Ground Motion and Faulting
345 Middlefield Road, MS-77
Menlo Park, California 94025
(415) 323-8111, ext. 2048

Investigations and Results

The map showing the Quaternary geology and tectonic features of the central portion of the Antelope Valley is now completed, in review, and should be released shortly. Other investigations planned for this summer's field season include:

1) Completion of the Quaternary mapping in the western portion of the Mojave wedge in the vicinity of the Garlock-San Andreas Fault intersection. Preliminary reconnaissance in this region suggests that late Pleistocene alluvial terraces in this region may have experienced extensive and rapid uplift;

2) Continued drilling and shear wave velocity measurements of the various Quaternary units (in cooperation with J. Gibbs and T. Fumal of USGS);

3) Preparation of a Quaternary deformation map for the entire Antelope Valley region. The deformation study will include paleomagnetic and paleontological examinations of several cores taken from a distinctive, deformed, 100 m thick lacustrine(?) unit that apparently underlies much of the lower region of the central and eastern Antelope Valley basin;

4) Preparation of depth-to-basement and particle size distribution maps for the entire Antelope Valley region. These maps will incorporate data from over 1000 test borings that have been encoded into the MAT_DISPLAY computer system.

Continued streamlining of the MAT_DISPLAY system's data structure has greatly increased its efficiency. This subsurface geotechnical data base display system is now being utilized by J. Tinsley for data in the San Fernando Valley. Several thousand drill holes are now stored in the system (refer to Summaries of Technical Reports, Volume XI, Open-File Report 81-167, for details of this system's capabilities).

RECURRENCE INTERVALS ON THE PLEITO THRUST FAULT, TRANSVERSE RANGES, CALIFORNIA

Prepared by
N. Timothy Hall, William R. Cotton and Edward A. Hay

Foothill-De Anza Community College District
12345 El Monte Road
Los Altos Hills, California 94022

14-08-0001-19164

INTRODUCTION

The intention of this research program is to evaluate the potential seismic hazards associated with the Pleito thrust fault and to document its late Quaternary geomorphic and tectonic evolution. The Pleito fault is a 50 kilometer-long, southward dipping, range-front thrust belt located at the southern end of the San Joaquin Valley (Figure 1) that coincides with the northern limits of the Southern California uplift (Castle and others, 1976).

The Pleito fault is a likely candidate for near-future activity since it lies within the same N-S regional system of compressive stress genetically associated with the "big bend" of the San Andreas fault as do the recently active San Fernando and White Wolf faults. All of these faults have similar structural relationships to the San Andreas fault system; indeed, the recent activity of the White Wolf and the San Fernando faults may have resulted from the release of strain across the southern locked segment of the San Andreas fault which has not experienced surface rupture since 1857. This locked segment appears to be characterized by slip events of 10-11 meters that occur every 200-300 years at Wallace Creek in the nearby Carrizo Plain (Hall and Sieh, 1977) and every 160 to 225 years at Pallet Creek (Sieh 1978a). It is possible that episodes of movement on the Pleito fault might have a similar recurrence interval since the 1857 displacement where the San Andreas fault enters the Transverse Ranges was approximately 2 meters less than the maximum displacement recorded further north in the Carrizo Plain (Sieh, 1978b). Due to the variable strike of the surface expression of the plate boundary within the Transverse Ranges, both the thrusting on the Pleito fault and the strike-slip movement on the San Andreas fault are logical crustal responses to the inferred direction of plate movement.

INVESTIGATIONS

Sites along the topographically best expressed segment of the Pleito fault were selected for detailed geologic mapping and subsurface analysis (Figure 2). The primary objectives of our research is to determine such factors as: 1) the width of ground disturbances along the fault traces, 2) the kinds of disturbances (surface offset, lurch cracks or fissures, ground settlement, compression features, etc.) preserved along these traces, 3) the amount of

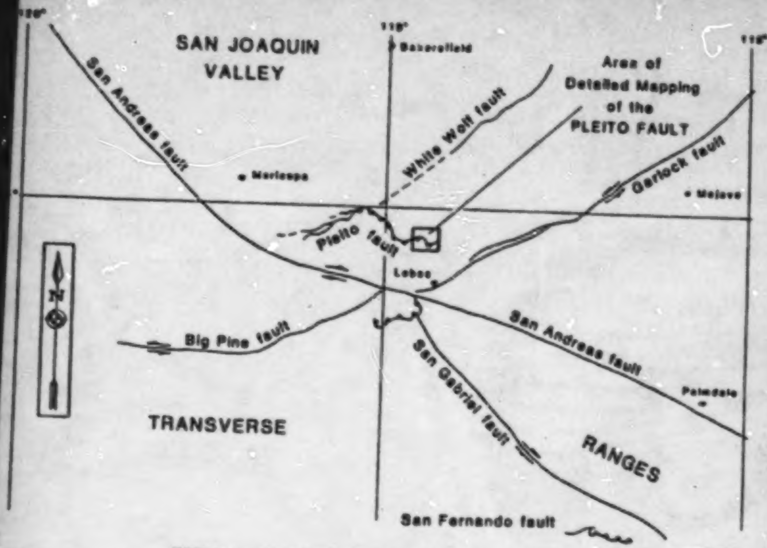
SAN JOAQUIN VALLEY
119°
Bakersfield
118°
Area of Detailed Mapping of the PLEITO FAULT
San Andreas fault
White Wolf fault
Garlock fault
Maricopa
Mojave
Pleito fault
Lebec
N
Big Pine fault
San Andreas fault
San Gabriel fault
Palmdale
TRANSVERSE
RANGES
San Fernando fault

FIGURE 1 - Map of major faults in California (Modified from Jennings, 1975)

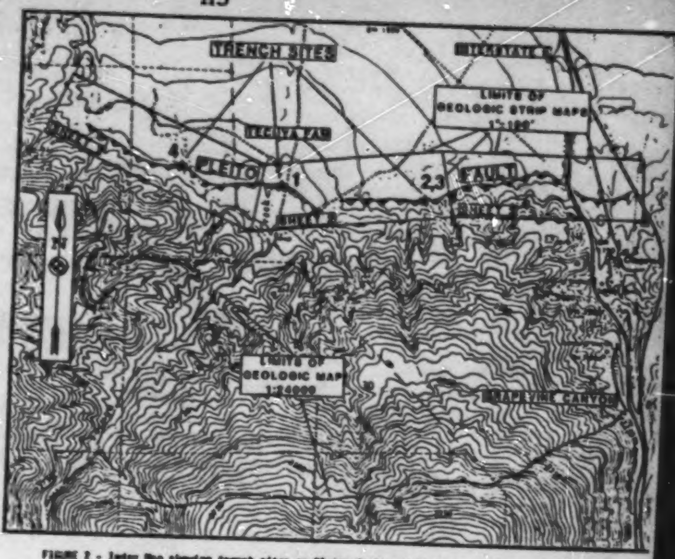
TRENCH SITES
INTERSTATE 5
LIMITS OF GEOLOGIC STRIP MAPS 1"=100'
TECUYA FAN
4
PLEITO
1
2,3
FAULT
SHEET 2
N
LIMITS OF GEOLOGIC MAP 1:24000
GRAPEVINE CANYON

FIGURE 2 - Index Map showing trench sites on Pleito fault and limits of geologic mapping. Topographic Base U.S.G.S. Grapevine 7.5 minute Quadrangle.

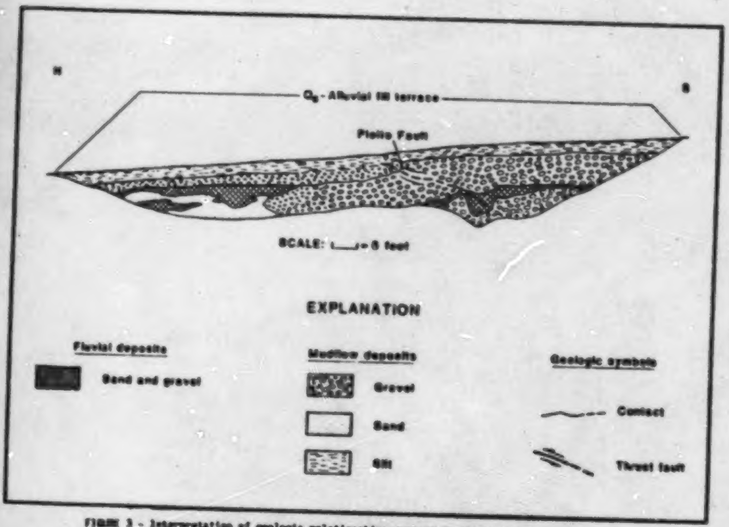
N
S
Q_3 - Alluvial fill terrace
Pleito Fault
SCALE: = 5 feet
EXPLANATION
Fluvial deposits
Sand and gravel
Mudflow deposits
Gravel
Sand
Silt
Geologic symbols
Contact
Thrust fault

FIGURE 3 - Interpretation of geologic relationships exposed in the east wall of Pleito fault trench "Fumarole 1".

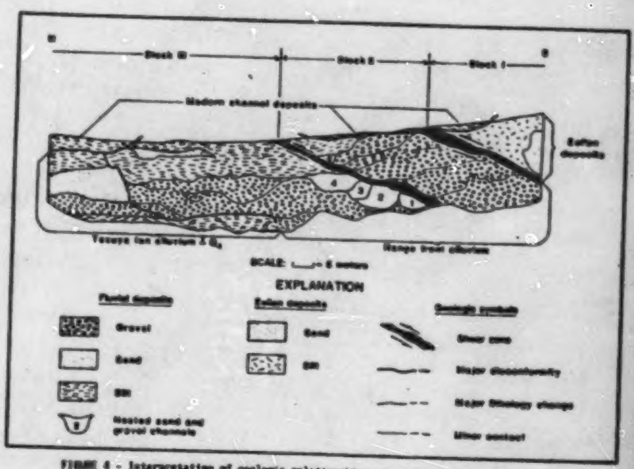
N
S
Block III
Block II
Block I
Modern channel deposits
Eolian deposits
4
3
2
1
Tecuya fan alluvium Q_3
Range front alluvium
SCALE: = 5 meters
EXPLANATION
Fluvial deposits
Gravel
Sand
Silt
Nested sand and gravel channels
Eolian deposits
Sand
Silt
Geologic symbols
Shear zone
Major disconformity
Major lithology change
Minor contact

FIGURE 4 - Interpretation of geologic relationships exposed in the east wall of Pleito fault trench "Fumarole 2".

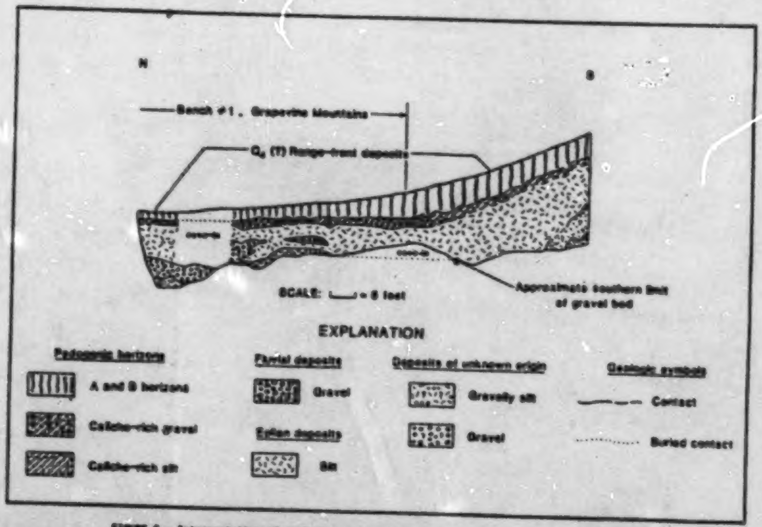
N
S
Bench #1, Grapevine Mountains
Q_4 (?) Range-front deposits
SCALE: = 5 feet
Approximate southern limit of gravel bed
EXPLANATION
Pedogenic horizons
A and B horizons
Caliche-rich gravel
Caliche-rich silt
Fluvial deposits
Gravel
Eolian deposits
Silt
Deposits of unknown origin
Gravelly silt
Gravel
Geologic symbols
Contact
Buried contact

FIGURE 5 - Interpretation of geologic relationships exposed in east wall of Pleito fault trench "Fumarole 3".

displacement that has occurred during past seismic events, 4) the timing of fault movements, 5) the geomorphic evolution of thrust fault scarps, and 6) the nature of the more regional deformation recorded by the sedimentary rocks of Tertiary age in the hanging wall block. We anticipate that a synthesis of these factors will yield a recognition of the geologic controls governing the variable effects of thrust fault movement. To obtain this information, a detailed surface and subsurface program is currently in progress.

RESULTS

To date, our analysis of the Pleito thrust fault has been progressing successfully as follows:

Surface Analysis of the Pleito Fault

- Bedrock mapping of the hanging wall block at a scale of 1:24,000 is 75% complete.
- Preparation of a detailed geologic strip map along the Pleito fault at a scale of 1"=100' is 60% complete.
- Logging of existing natural exposures has not been initiated pending analysis of the trench logs. However, a canyon wall that exposes the Pleito fault has been scraped of colluvial cover by a bulldozer and a backhoe and will be logged during the Spring of 1981.

Subsurface Investigations of the Pleito Fault

- Four backhoe trenches for a total length of approximately 110 meters were excavated during September 1980. Three crossed the most recently active trace of the Pleito fault; two were logged in detail and materials collected for radiocarbon dating (see Figures 3 and 4). One trench lacked datable material and was, therefore, not logged. The fourth trench was cut in an escarpment of unknown origin higher in the range (see Figure 5). To date five radiocarbon dates have been generated and several more charcoal samples are currently being processed.

  The subsurface investigation of the Pleito fault is 80% accomplished. Several bucket auger holes and backhoe test pits will be dug next spring to complete this portion of the project.

Determination of Recurrence Intervals

- Analysis of a vast amount of data gathered during both the surface and subsurface investigations of the Pleito fault is now well underway.

CONCLUSIONS

The major preliminary conclusions we are able to draw at this time are:

- The Pleito fault has experienced repeated movements during late Quaternary time, the most recent of which occurred between 345 and 475 to 1465 years ago.
- Locally the Pleito fault consists of at least two strands which dip southward into the San Emigdio Mountains at angles averaging 20-30°.
- The characteristic net slip per event on the Pleito fault appears to be approximately 1 meter.

Tectonics of Central and Northern California

9950-01290

William P. Irwin
Branch of Earthquake Tectonics and Risk
U.S. Geological Survey
345 Middlefield Road, M/S 77
Menlo Park, CA 94025
(415) 323-8111, ext. 2065

Investigations

1. Paleomagnetic orientation of the Klamath Mountains province; in collaboration with E. A. Mankinen and S. C. Gromme. First draft completed for a report on the paleomagnetism of some Cretaceous and Tertiary sandstones of the Klamath Mountains province.

2. Age dating of ancient oceanic terranes and timing of their accretion to western North America; in collaboration with D. L. Jones and B. R. Wardlaw. First drafts completed for reports on (1) the tectonic significance of ophiolitic terranes of western North America, and (2) conodonts of the western Paleozoic and Triassic belt of the Klamath Mountains.

3. Tectonic relations of carbon dioxide discharges and seismicity; in collaboration with Ivan Barnes.

Results

1. Study shows that most Cretaceous and Tertiary sandstones that lie unconformably on Jurassic (Nevadan) and older rocks of the Klamath Mountains are strongly remagnetized. The sampled sandstones include Great Valley sequence (Lower and middle Cretaceous), Hornbrook Formation (Upper Cretaceous), Montgomery Creek Formation (Eocene), and Weaverville Formation (Oligocene). However, some of the Cretaceous sandstones survived remagnetization and have a mean remnance direction close to the average Cretaceous magnetic field that would be expected of the Klamath Mountains. Sparse data obtained on the Tertiary sandstones also are compatible with the idea that little or no post-Cretaceous rotation of the Klamath Mountains province has occurred. Other workers have measure substantial amounts of clockwise rotation of Tertiary rocks at many localities in the western Cascades of Oregon and Washington, but this rotation must have occurred independently of the Klamath Mountains. Although rotation of the Cretaceous and Tertiary rocks of the Klamath Mountains appears negligible, preliminary measurements suggest that some of the Paleozoic rocks of the province have rotated clockwise through a large angle.

2. The original subdivision of the Klamath Mountains into various tectonic terranes was based partly on differences in sparse shelly fossil faunas.

Recently we extracted conodonts, a phosphatic microfossil, from limestones and radiolarian cherts of three of the terranes, and these fossils also show faunal differences. Late Paleozoic conodonts occur in both the North Fork and Hayfork terranes. The Hayfork terrane also contains Early, Middle, and Late Triassic conodonts, mostly *Neogondolella*. The Rattlesnake Creek terrane yielded only Late Triassic conodonts, mostly *Epigondolella*. Color alteration of the conodonts indicates that the rocks of all three terranes were heated to temperatures between 300° and 500°C during regional tectonism.

Reports

Irwin, W. P., 1981, Tectonic accretion of the Klamath Mountains, *in* The geotectonic development of California, W. G. Ernst (ed.): Prentice-Hall, Inc., Rubey Volume 1, p. 29-49.

Tephrochronology of the Central Region

9530-02169

Glen A. Izett
Branch of Central Environmental Geology
U.S. Geological Survey
National Center MS-908
Reston VA 22092
(703)860-6411

No report received

Correlating and Dating Quaternary Sediments by Amino Acids

9830-01996

Keith A. Kvenvolden
Pacific-Arctic Branch of Marine Geology
U.S. Geological Survey
345 Middlefield Road
Menlo Park, CA 94025
(415) 856-7150

Investigations

1. A survey was conducted of the amino acid geochemistry of five species of fossil mollusks from localities in the Puget Lowland, Washington. We evaluated two parameters considered useful for correlation and age estimation: (1) relative amino acid composition (mole percent) and (2) degree of amino acid racemization (D/L ratio). The amino acid age of one locality on Whidbey Island, previously estimated to be ∿ 80,000 years, has been reassessed to be ∿ 120,000 years old.

2. Completed a preliminary study using amino acid gechronologic techniques to estimate the age of marine sediments recovered from the Navarin Basin province of the Bering Sea.

3. To evaluate the potential of wood for amino acid geochronology we initiated a preliminary survey of the geochemistry of amino acids in wood samples recovered from estuarine deposits at Willapa Bay, Washington.

Results

1. Specimens of *Saxidomus giganteus*, *Nuculana fossa*, *Macoma nasuta*, *Clinocardium ciliatum*, and *Hiatella arctica* were sampled from radiocarbon-dated glacial marine sediments (11,000 - 13,000 yr BP) at five localities throughout the Puget Lowland. These specimens were analyzed for amino acid composition and stereochemistry. The mole-percent of different amino acids are similar for samples of the same species but are dissimilar for samples from different species. For example, the mole-percent of aspartic acid in *Macoma nasuta* is ∿ 13.6, but is ∿ 31.1 in *Clinocardium ciliatum*. On the other hand, there is no significant differences between ratios of amino acid enantiomers (D/L ratios) between various species. This result is likely due to the low extent of amino acid racemization that has occurred in these relatively young specimens. For example, the average D/L ratio for leucine is ∿ 0.12 and for aspartic acid is ∿ 0.35.

Analyses of newly-collected samples of *Saxidomus* from the Admiralty Inlet locality on Whidbey Island in Puget Sound yielded higher D/L ratios than measured previously. The earlier D/L leucine values of ∿ 0.29 were measured on the shells, and an age of ∿ 80,000 yr was estimated. Newly-collected specimens of *Saxidomus* were more robust and the average D/L leucine ratios obtained were ∿ 0.36 yielding an age of ∿ 120,000 yr. Comparisons of D/L ratios of amino acids in thin and thick specimens of *Macoma nasuta* also show similar differences. Localized post-depositional leaching of the shell deposit likely accounts for the variations in shell thickness and the differences in D/L ratios. Thus, the age of this shell deposit is estimated to be early rather than late Sangemon age.

2. Amino acids were extracted from specimens of fossil mollusks collected from gravity cores during the 1980 cruises of the R/V Discoverer in the Navarin Basin province, Bering Sea. Specimens analyzed include *Nuculana fossa, Nuculana radiata, Macoma obliqua, Macoma brota, Mya truncata, Cyclocardia crebricostata, Clinocardium nuttallii,* and *Yoldia myalis*. Samples from the Puget Lowland (having an integrated temperature of ∿ 10°C) were used for calibration in order to calculate leucine racemization rate constants applicable to Navarin Basin sediments (temperatures estimated to be ∿ 2°C from bottom waters). Ages calculated for Bering Sea sediment range from about 6,000 to 50,000 yr BP. Age estimates based on amino acid and micropaleontologic considerations indicate a complex sedimentation history involving erosion or non-deposition, sediment reworking during glaciation, and submarine slumping. Radiocarbon dating is planned to provide in situ calibration samples, to verify age estimations and to test paleotemperature assumptions.

3. A preliminary study was conducted of the organic geochemistry of amino acids in wood. Samples of fossil wood were collected from exposures of estuarine sediments at Willapa Bay, Washington. The study was designed to determine if amino acids in wood can be used for age estimations. Surprisingly high concentrations of amino acids were found in all samples. Comparisons were made between two stratigraphic units having ages of ∿ 120,000 and ∿ 200,000 years (determined previously by amino geochronologic methods applied to fossil mollusks). The total amino acid concentration of wood in the younger unit (IV) is ∿ 10 micromole/g, whereas in the wood of the older unit (I) the concentration is ∿ 40 micromoles/g. The observation of higher concentrations of amino acids in older specimens of wood is contrary to previous results using fossil mollusks. The results suggest that the younger wood specimens may have been preferentially leached of their amino acids. The D/L ratios of the amino acids in both units are variable with few systematic relationships. Proline D/L ratios, however, provide reasonably consistent results. Wood in IV has an average proline D/L ratio of 0.06; in I the wood average ratio is 0.09. The difference is significant and in the direction expected for stratigraphic units of increasing age. Further work is required to test the validity of these preliminary results.

Reports

Kvenvolden, K. A., Blunt, D. J., and Clifton, H. E., 1981, Age estimations based on amino acid racemization: reply to comments of J. F. Wehmiller: Geochim. Cosmochim. Acta, v. 45, p. 265-267.

Kvenvolden, K. A., Blunt, D. J., McMenamin, M. A., and Strahan, S. E., 1980, Geochemistry of amino acids in shells of the clam *Saxidomus*: In Douglas, A. G., and Maxwell, J. R., eds., Advances in Organic Geochemistry 1979, Pergamon Press, Oxford, p. 321-332.

Kvenvolden, K. A., and Blunt, D. J., 1981, Amino acids in sediment from Leg 68 Site 502: In Prell, W. L., Gardner, J. V. et al., Initial Reports Deep Sea Drilling Project, v. 68, Washington (U.S. Govt. Printing Office) (in press).

Coastal Tectonics, Western U.S.

9940-01623

Kenneth R. Lajoie
Branch of Ground Motion and Faulting
U.S. Geological Survey
345 Middlefield Road, M/S 77
Menlo Park, California 94025
(415) 323-8111, ext. 2642

Investigations

1. Continuation of mapping and dating late Quaternary marine terraces and deposits in numerous coastal sites in western U.S. with emphasis on San Mateo, Santa Barbara, Ventura, Los Angeles, San Luis Obispo and San Diego Counties, California. Project personnel are George Kennedy, paleontologist/geologist; Scott Mathieson, geologist; Dan Ponti, geologist; and Pat McCrory, PST. Cooperative projects are with Andrei Sarna-Wojcicki and Robert Yerkes (OEG) in the Ventura area; Gerald Weber in San Mateo County; Phil Kern (San Diego State University) in San Diego County; Preston Cloud (U.C. Santa Barbara, retired); Joseph Liddicoat (Lamont-Doherty) and Steve Robinson (USGS) in Mono County. With Dave Keefer conducted postearthquake investigation of November 8, 1980 Humboldt, CA earthquake.

2. Participated in investigative hearing conducted by California PUC to obtain data on tectonic setting of proposed site of liquid natural gas facility near Point Conception, CA.

Results

1. Collected three new fossil localities in San Luis Obispo County at Mallagh Landing and south of Shell Beach. The cool-water aspect of the molluscan fauna from each indicates they are younger than 120 kA. ^{14}C analysis on the lowest (3-4 m) yields an age of $\geq$ 36 kA. The two low faunas and associated terraces may correlate in age to similar faunas 15-20 km north near Diablo Canyon, indicating relatively low tectonic uplift rates ($\leq$ 0.3 m/kA) for this section of coast. If the highest (20 m) fauna correlates to the low faunas local crustal deformation is indicated. The highest fauna contain corals so uranium-series analyses will provide absolute dates to calibrate amino-acid data in this area. This date will be the first absolute age for an isotope stage 5a or 5c fauna on the entire west coast.

2. Collected paleomagnetic samples from the same stratigraphic horizon at different localities in Mono Basin to verify part of secular variation curve for Wilson Creek beds (age 36-12 kA). Results from all localities consistent.

3. Fourteen ^{14}C dates on tufa plates and nodules and ostracodes from the Wilson Creek beds (lacustrine deposits) in Mono Basin plot along a straight line (r = 0.004) over a 7 m stratigraphic interval and range from 34.9 kA at the bottom to 12.8 kA at the top. These dates provide calibration for other dating techniques used in tectonic studies of the basin.

4. Collected fossil molluscs from two localities (one outcrop, one bore hole) on the Half Moon Bay terrace in San Mateo County, CA. These are the first molluscan fossils ever found on this intensely deformed marine terrace. Amino-acid analyses of fossil molluscs should provide correlation to other independently dated localities. The resultant age assignment will provide a check on previously calculated rates of tectonic deformation based on unsupported age estimates.

5. Damage caused by the November 8, 1980 Humboldt County earthquake was minor, considering the size of the tremor (M_L = 7.0). The damage was minor, probably because the focus was about 14 km deep and 50 km offshore. Most damage occurred south of Eureka where two spans of a freeway overpass collapsed (design failure) and a few old houses were shaken from their foundations (poor construction). Two smaller earthquakes in 1954 (M_L = 6.2) and 1975 (M_L = 5.2) caused more damage than the 1980 earthquake, probably because their foci were closer to developed areas.

6. Three remnants of emergent marine terrace north of the mouth of San Mateo County originally mapped as three separate terraces at different elevations are actually one terrace displaced across two high angle reverse faults. The age of the terrace is not precisely known (100-300 kA?) so rates of displacement cannot be accurately determined.

Reports

Weber, G. and Lajoie, K. R., 1980, Map of Quaternary faulting along the San Gregorio fault zone, San Mateo and Santa Cruz Counties, California: U.S. Geol. Survey Open-File Report 80-907, scale 1:24,000.

Cloud, Preston and Lajoie, K. R., 1980, Calcite-impregnated defluidization structures in littoral sands of Mono Lake, California: Science, Vol. 210, No. 4473, p. 1009-1012.

STUDY OF SEISMIC ACTIVITY BY SELECTIVE TRENCHING ALONG THE ELSINORE FAULT ZONE, SOUTHERN CALIFORNIA

Contract No. 14-08-0001-19144

D. L. Lamar and S. C. Swanson
Lamar-Merifield, Geologists
1318 Second Street, Suite 27
Santa Monica, California 90401
Telephone: (213) 395-4528

Investigations

Published literature and engineering geology reports bearing on potential seismicity of the Elsinore fault zone were reviewed. A field reconnaissance was accomplished to locate promising sites where trenches might reveal datable Holocene fault displacement history, and possibly times between major seismic events. Nine sites which have the potential of revealing ruptured Holocene sediments across strands of the Elsinore fault zone have been identified. Permission to trench three sites has been obtained and a site (S-6, Fig. 1) on the south branch of the Wildomar fault, a strand of the Elsinore fault zone southeast of Lake Elsinore, has been trenched.

Results

Radiocarbon dating of sediments disrupted by the south branch of the Wildomar fault indicates activity within the past 4120 ± 260 years (Fig. 2). The relationship between the dated sediment and two distinct sets of secondary faults which were active before and after the deposition of a gravel layer indicates that one or possibly two seismic events occurred since deposition of the dated sediments. The lack of correlation of sediments on opposite sides of the main fault, the orientation of a sub-parallel drag fold and slickensides in a silty clay layer suggest an important but unknown component of right-slip.

References

Envicom, 1976, Riverside County Seismic Safety Element.

Kennedy, M. P., 1977, Recency and character of faulting along the Elsinore fault zone in southern Riverside County, California: Calif. Div. Mines and Geol., Spec. Report 131, 12 p.

Rogers, T. H., 1965, Geologic map of California, Santa Ana sheet: Calif. Div. Mines and Geology.

Weber, F. H., Jr., 1977, Seismic hazards related to geologic factors, Elsinore and Chino fault zones, northwestern Riverside County, California: Calif. Div. Mines and Geol., Open-file Report 77-4 LA, 96 p.

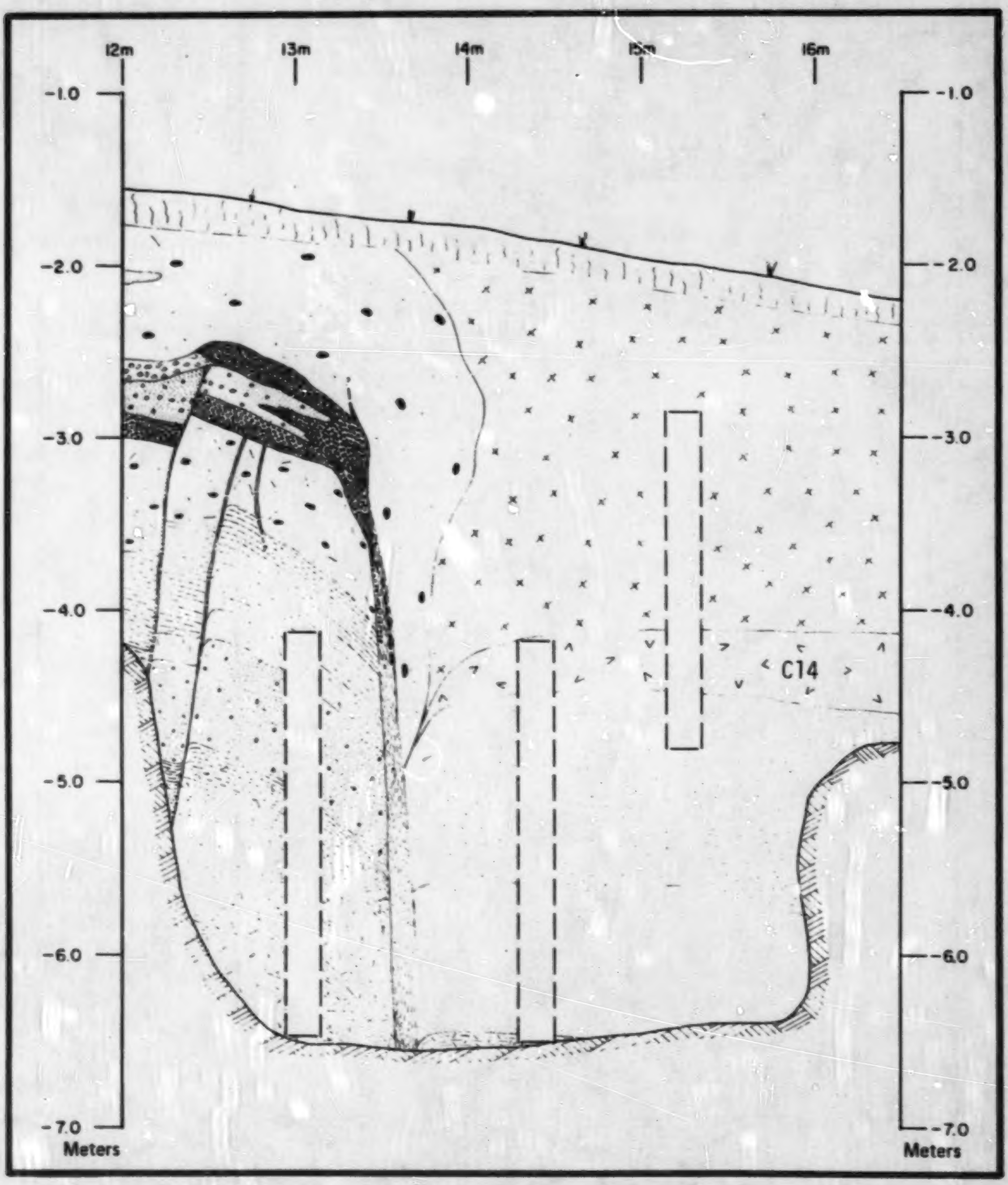
12m
13m
14m
15m
16m
-1.0
-2.0
-3.0
-4.0
-5.0
-6.0
-7.0
Meters
C14

Fig. 2 - Detailed trench log across main trace of south branch of Wildomar fault. See Fig. 1 for location. C14: layer dated by radiocarbon method.

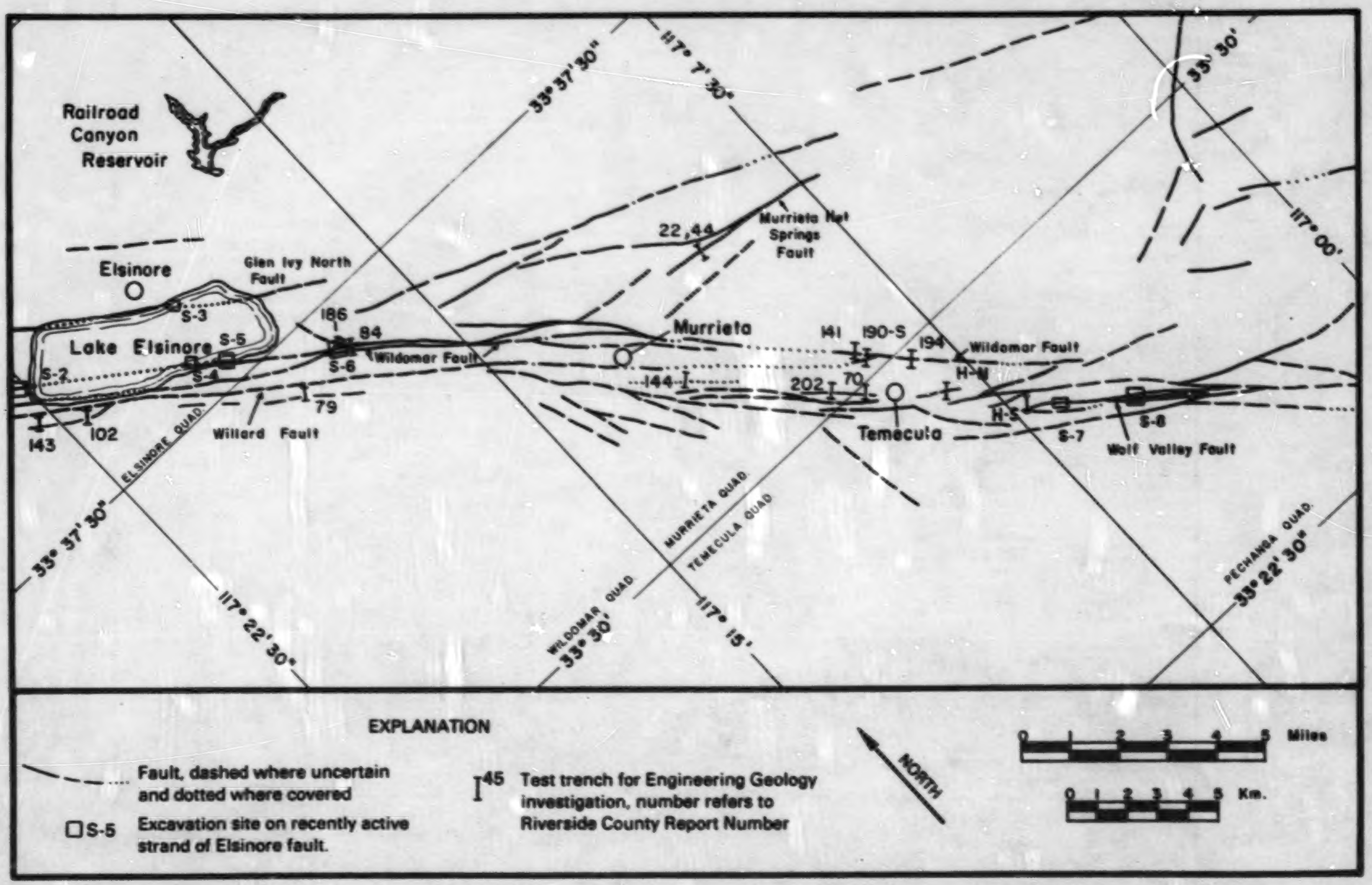
Railroad Canyon Reservoir
Elsinore
Lake Elsinore
Glen Ivy North Fault
Murrieta Hot Springs Fault
Murrieta
Temecula
Wildomar Fault
Willard Fault
Wolf Valley Fault
S-2
S-3
S-4
S-5
S-6
S-7
S-8
H-N
H-S
143
102
79
186
84
22,44
144
141
190-S
194
202
70
33° 37' 30"
117° 7' 30"
33° 30'
117° 00'
117° 22' 30"
117° 15'
33° 22' 30"
ELSINORE QUAD.
MURRIETA QUAD.
TEMECULA QUAD.
WILDOMAR QUAD.
PECHANGA QUAD.
EXPLANATION
Fault, dashed where uncertain and dotted where covered
S-5 Excavation site on recently active strand of Elsinore fault.
45 Test trench for Engineering Geology investigation, number refers to Riverside County Report Number
NORTH
0 1 2 3 4 5 Miles
0 1 2 3 4 5 Km.

Fig. 1 - Map showing Elsinore fault zone between Lake Elsinore and Temecula area and excavation sites. From Rogers (1965) with modifications based on Weber (1977), Kennedy (1977) and Envicom (1976).

Menlo Park Geochronology Laboratory

9740-00377

Marvin A. Lanphere
Branch of Isotope Geology
U.S. Geological Survey
345 Middlefield Road, MS 18
Menlo Park, CA 94025
(415) 323-8111, EXT. 2649

Investigations

The Geochronology (Menlo Park) Project is not involved in any formal investigations for the Earthquake Hazards Reduction Program. Funding received from the Program is used to cover part of the expenses of guest scientists working in the geochronology laboratory and part of the costs of small K-Ar dating projects carried out for the Program.

Magnetostratigraphy of Sediments in the Atlantic Coastal Plain and Pacific Coast of the United States as an Aid for Dating Tectonic Deformation

14-08-0001-18377

Joseph C. Liddicoat
Neil D. Opdyke

Lamont-Doherty Geological Observatory
of Columbia University
Palisades, New York 10964
(914) 359-2900, Ext. 521

Investigations

1. Using the paleomagnetic polarity time scale, improve the chronology of Quaternary sediments in the Delmarva Peninsula and northern Tidewater Virginia.

2. Distinguish sedimentary units and formations in the Atlantic Coastal Plain of South Carolina using the paleomagnetic polarity time scale.

3. Augment the record of paleosecular variation for the late Pleistocene and Holocene in the northeastern United States for application to dating tectonic deformation.

4. Establish the magnetostratigraphy of Quaternary deposits in the Ventura Basin of southern California to improve the dating of four important tephra units.

Results

1. To improve the chronology of Quaternary sediments in the northern Atlantic Coastal Plain, we used paleomagnetic samples from fully oriented cores (Shelby tube) and outcrops. In the Delmarva Peninsula (Delaware, Maryland, Virginia), the samples are from the informal Accomack Formation near Chincoteague, Virginia. Following alternating field (core samples) or thermal (outcrop samples) demagnetization, the samples record normal paleomagnetic polarity exclusively. On the basis of those data, coupled with biostratigraphic and radiometric (uranium series on corals) information, we believe the Accomack Formation was deposited during the Brunhes Normal Chron (0.73 myBP-Present). The Pliocene Yorktown Formation in Tidewater Virginia near Warsaw, Virginia, records reversed polarity when sampled in outcrop and subjected to alternating field demagnetization. The most plausible interpretation is that the Yorktown Formation was deposited during the Matuyama Reversed Chron (2.48-0.73 myBP).

2. Outcrop samples of the Canepatch and Waccamaw formations near Myrtle Beach, South Carolina, record normal and reversed paleomagnetic polarity, respectively, after alternating field demagnetization. The data confirm the polarity of the Waccamaw Formation at the type locality on the Waccamaw River near Nixonville, South Carolina, and of the Canepatch Formation at several localities nearby. The new data for the Canepatch Formation are for the type

locality on the Intracoastal Waterway. The paleomagnetic data are being used in the evaluation of amino acid enantiomeric ratios as a means for dating Quaternary sediments in South Carolina and elsewhere in the Atlantic Coastal Plain.

3. A fully oriented, 30-meter Shelby tube core from glacial Lake Passaic (New Jersey) is being used to determine the age and stratigraphic relationship of Quaternary sediments between the New Jersey Highlands and the Watchung Mountains. One objective is to document late Pleistocene and Holocene tectonic deformation in the northern Atlantic Coastal Plain, with attention focused on behavior of the Ramapo Fault. Our paleomagnetic work involves paired samples from 11 depths. Agreement of paleomagnetic directions (declination, inclination) within depths 4.6, 16.9, and 23.0 meters is excellent following alternating field demagnetization. Elsewhere in the core, the directional difference between samples at each depth is approximately 5°. The opportunity thus exists for a reliable and detailed record of secular variation that will augment curves of declination for upstate New York and Lake Ontario (Brennan, et al., 1980) should additional and carefully oriented cores be obtained from New Jersey and the surrounding region.

4. Our investigation addresses the relationship between four tephra units that are being mapped by A. Sarna-Wojcicki (USGS) in the Ventura Basin (California) and several boundaries of the paleomagnetic polarity time scale. The tephra units from young to old and the radiometric or otherwise assigned age are the Bishop Ash (0.7 myBP), the "ash of Mono Glass Mountain" (0.9 myBP), the "Ventura Gray Ash" (1.0 myBP), and the Bailey Ash (1.2 myBP). The pertinent polarity boundaries are the Brunhes/Matuyama (0.73 myBP), the young (0.9 myBP) and old (0.97 myBP) limits of the Jaramillo Normal Subchron, and the Cobb Mountain Normal Subchron (1.12 myBP). Improved dating of the tephra units using the paleomagnetic method is important because the units are diagnostic stratigraphic markers in the Ventura Basin and beyond.

We took paleomagnetic samples from exposures of fine-grained marine sediment (Santa Barbara and Pico formations) in the Ventura Avenue Anticline. Alternating field and thermal demagnetization and a fold test have been used to determine the polarity of the sediment. Much of the work has focused on locating the Jaramillo Normal Subchron (0.97-0.9 myBP), which should occur near, possibly between, the "ash of Mono Glass Mountain" and the "Ventura Gray Ash." So far, we have been unsuccessful in identifying the Jaramillo Normal Subchron. However, we have demagnetized paleomagnetic data that indicate the Santa Barbara Formation 100 meters below the Bishop Ash in Hall Canyon north of Ventura changes from normal to reversed paleomagnetic polarity, giving us an approximate position for the Brunhes/Matuyama boundary.

References

Brennan, W. J., D. R. Hutchinson, M. J. Hamilton, and R. K. Kilbury, 1980, Holocene and late Pleistocene secular variation in the eastern Great Lakes region: Abstracts with Programs, 1980 Ann. Meetings, Geol. Soc. Am., v. 12, no. 7, p. 391.

Reports

Liddicoat, J. C., and R. B. Mixon, 1980, Paleomagnetic investigation of Pleistocene sediments in the Delmarva Peninsula, Central Atlantic Coastal Plain: Abstracts with Programs, 1980 Northeastern Section Meeting, Geol. Soc. Am., v. 12, no. 2, p. 70.

Liddicoat, J. C., L. McCartan, R.E. Weems, and E. M. Lemon, 1981, Paleomagnetic investigation of Pliocene and Pleistocene sediments in the Charleston, South Carolina, area: Abstracts with Programs, 1981 Southeastern Section Meeting, Geol. Soc. Am. (submitted).

Liddicoat, J. C., and W. Newell, 1981, Paleomagnetic investigations of late Neogene deposits in northern Tidewater Virginia: Abstracts with Programs, 1981 Northeastern Section Meeting, Geol. Soc. Am. (submitted).

Reimer, G. E., G. M. Ashley, J. C. Liddicoat, M. J. Pavich, and B. D. Stone, 1981, Glacial Lake Passaic: preliminary coring, paleomagnetic and stratigraphic analysis: Abstracts with Programs, 1981 Northeastern Section Meeting, Geol. Soc. Am. (submitted).

Soil Correlation and Dating, Western Region

9540-02192

Denis E. Marchand (By Jennifer W. Harden)
Branch of Western Environmental Geology
U.S. Geological Survey
345 Middlefield Road, MS 75
Menlo Park, CA 94025
(415) 323-8111 x 2009

Investigations

Radiometrically dated soil chronosequences in varied climatic and geologic environments are sampled and analyzed to determine which soil properties are most useful as age indicators and how rates of soil development vary in the different environments. Analyses for each soil profile and its horizon samples include more than 100 physical, chemical, and mineralogical properties: 39 elements are determined by bulk chemistry, 25 properties by extractive chemistry, 25 properties by field descriptions, bulk density, particle size and mineralogical analysis by x-ray diffraction, thin section and grain mounts. Investigations of the past six months include:

1. Continuation of lab analysis of the samples.

2. Interpretation of completed data sets.

3. Coordination of results with other projects conducting research in Quaternary dating methods and projects in need of soil correlation tools.

Results

Preliminary results substantiate the importance of many laboratory analyses, which are currently being conducted at University of California at Davis, under the direction of Michael Singer and Alan Busacca. Within the past six months, about 330 soil analyses have been completed, which concludes sample analysis of the soil chronosequences in Merced, CA., Arapaho Glacier, CO., and Dry Creek, CA. Analyses of soil chronosequences of Ventura, Honcut Creek and Ano Nuevo in California and Cowlitz River in Washington are progressing.

Alan Busacca and Peter Janitzky conducted a study on the effectiveness of ultrasonic techniques to disperse soil samples for particle size and bulk chemical analysis. They found that sonic dispersion of soil samples can be as effective as conventional chemical dispersive treatments such as sodium dispersal and iron oxide removal. The advantage of the sonic technique is that no chemical contamination occurs and coarse soils containing sands and gravels are rapidly cleaned of clay coatings.

A comprehensive data storage system using the Multics computer was recently devised by Emily Taylor. Raw data, including replicate analyses of samples, is stored and eventually archived. Software routines now can calculate the analytical mean and standard deviation of replicate lab analyses for samples. Programs were also written to assemble or to composite data in any combination: for example, data can be grouped by chronosequence, by analysis, by soil horizon or soil age. New data can be added at any time.

Field work of Cowlitz River, Wa., was completed by David P. Dethier, U.S.G.S. and John Bethel, University of Washington. A report entitled "Surficial deposits along the Cowlitz River near Toledo, Lewis County, Washington" was submitted for open-file in April. The report summarizes the geologic investigations and mapping conducted for the chronosequence study. Analysis of the soils is near completion in the labs at University of Washington under the direction of F. C. Ugolini.

Field work of Honcut Creek, Ca., was completed by Alan Busacca, U. C. Davis. Busacca consulted with E. J. Helley and D. S. Harwood of the Sacramento Valley Project in order to correlate Honcut mapping units to those of Helley and Harwood. An Open-File map of the Honcut Creek alluvial stratigraphy will be published by Busacca as the basis for the Honcut Creek chronosequence study. The map will also contribute to a compilation of the Sacramento Valley geology.

Mapping and preliminary soil analyses on a chronosequnce in the Bighorn Basin, Wyoming, was completed by Marith Cady Reheis and presented at the International Conference on Aridic Soils, Israel in March, 1981 (see Reheis, 1981). In a cold, arid environment, Reheis found that gypsum, derived from eolian deposition, has been accumulating in the soil for 600,000 years (fig. 1). Continuous gypsum accumulation suggests that no major change in effective precipitation occurred within the past 600,000 years. Prior to that period, leaching of gypsum may have been more effective (fig. 1), indicating a climate of higher leaching in the early Pleistocene. Reheis also studied soils in a climatic transect in the Bighorn Basin in order to determine which soil properties are indicative of climatic change. Data analysis and additional sampling is continuing.

Peter W. Birkeland, University of Colorado, led seminars on interpreting paleoclimatic records from soil data at the Bet Shiva Seminar in Israel in October 1980 (see Birkeland, 1980). Applying data of soil chronosequences from various climatic settings, he found that dithionite and oxalate-extractable iron and aluminum are useful indices of soil age in many regions. Phosphate fractions are useful indicators of high leaching regimes. In a regional framework, his preliminary conclusions were that soil formation rates are highest in:

New Zealand > Rocky Mountains > Sierra Nevada Range > Arctic Region

Harden devised a soil development index from soil field descriptions of Merced, Ca., in order to quantitatively measure a soil's degree of development (see Harden, 1981). Eight soil field properties, including soil texture, soil structure, color hue and chroma (named rubification), color value, moist consistence, dry consistence, pH and clay films, can be quantified according to their development relative to the parent material. Most of the properties showed significant correlation with time (figs. 2, 3) and an index, combining the properties with horizon thickness, was used to express soil development in one value. Based on only field descriptions, the index provides a convenient tool for soil comparisons. Reproducibility of time plots of chronosequences is good enough to allow calibration for age control of soils of unknown age.

Harden and Taylor (1981) applied the soil development index above to three other chronosequences of similar parent material but different soil moisture regimes in Coastal California, Southern New Mexico and Central Pennsylvania. When profile sums of individual properties ((property x horizon thickness)) are compared, a striking similarity is found among soils of variable climates (figs. 2, 3). These results suggest that: 1) although basic soil differences are found in different climates, the amount of development in the profile relative to parent material is very similar for a given age of soil, and 2) correlation of Quaternary deposits using the soil development index may be possible on a regional basis. The present objective is to gather more data for statistical testing and to include soils having other types of parent material. The preliminary results were presented at the International Conference on Aridic Soils in Israel, March, 1981.

Results of this project were applied to and coordinated with several U.S.G.S. projects. Denis Marchand and Emily Taylor assisted Quaternary geologists of the Central Valley Project in using soils to differentiate and correlate deposits (see Lettis, Marchand, and May, 1981). D. Marchand and J. Harden supplied Rosholt of U.S.G.S. Denver with radiometrically dated soils of the San Joaquin Valley in order to coordinate Uranium-Trend and Soil Chronology dating techniques. Since the death of D. Marchand, Harden is completing Marchand's contributions to a report entitled "Uranium-Trend Dating of Quaternary Alluvial Deposits in the San Joaquin and Sacramento Valleys, California" by J. N. Rosholt, J. W. Harden, D. E. Marchand and G. M. Huestis. Data analysis undertaken by Marchand will be completed by Harden and other project members.

Publications

Birkeland, Peter W., 1980, On approaches and methods in paleoclimatic records with emphasis on aridic areas, in Programs and abstracts for the Bet Shiva seminar, pub. Hebrew Univ., Jerusalem and Weizmann Institute of Science.

Birkeland, Peter W., and Meierding, T. C., 1980, Quaternary glaciation of Colorado: Colorado Geology, ed. H. C. Kent and K. W. Porter, Pub. Rocky Mt. Assoc. Geologists, p. 155-173.

Harden, Jennifer W., 1981, A quantitative index of soil development from field descriptions; submitted to Geoderma April 10, 1981.

Harden, Jennifer W., and Taylor, Emily M. 1981, Response of soil development to moisture regimes: International Conference on Aridic Soils, Jerusalem, Israel, March 29-April 4, 1981, Abstracts, p. 48-49.

Lettis, W., Marchand, D. E., and May, Rodd, 1981, Climatic implications of a regional Quaternary stratigraphy in the west-central San Joaquin Valley, California, Cordilleran section, International Meeting, the Geological Society of America 77th annual meeting, March 25-27, 1981, Abstracts with Programs; p. 66.

Reheis, Marith Cady, 1981, Gypsic soil chronosequence in a cold arid region, Bighorn Basin, Wyoming, USA;: International Conference on Aridic Soils, Jerusualem, Israel, March 29-April 4, 1981, Abstracts, p. 22.

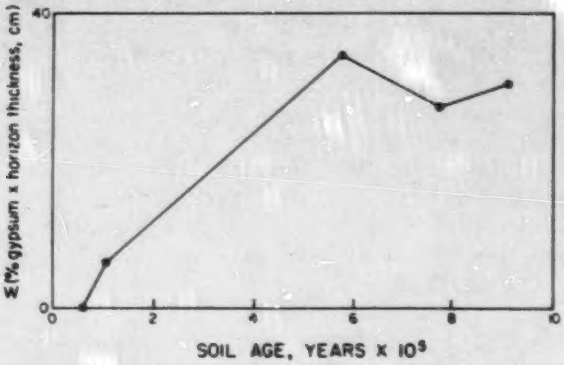

Fig. 1. Gypsum accumulation rates in Bighorn Basin, Wyoming. Percent gypsum is multiplied by horizon thickness in cm. The products are summed through the profile and plotted against soil age in years x 10^5.

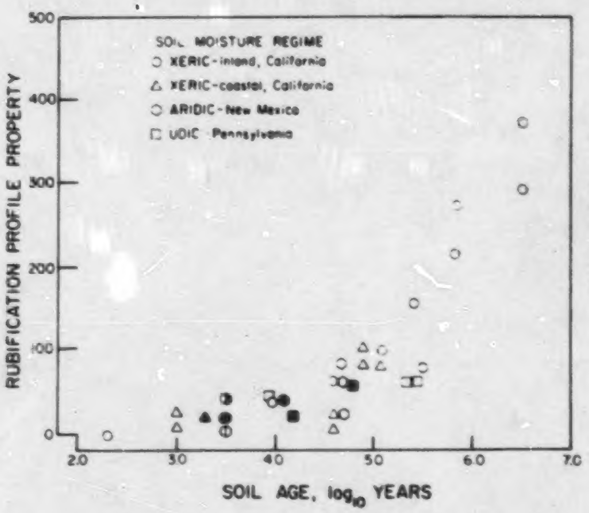

Fig. 2. Profile rubification versus soil age. Rubification development (increase in hue + chroma from parent material) is multiplied by horizon thickness in cm. The products are summed through the profile and plotted against soil age in $\log_{10}$ years. Solid symbols indicate more than 1 sample.

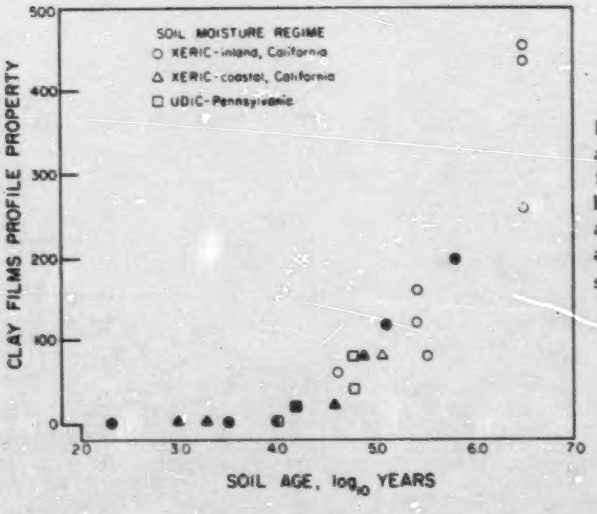

Fig. 3. Profile clay films versus soil age. Clay film development (development from parent material) is multiplied by horizon thickness in cm. The products are summed through the profile and plotted against soil age in $\log_{10}$ years. Solid symbols indicate more than 1 sample.

Fault Scarp Morphology: Indicator of Paleoseismic Chronology

Contract Number 14-08-0001-19109

David B. Nash
Department of Geology
University of Cincinnati
Cincinnati, Ohio 45221
(513) 475-3732

Investigations:

1. Map and profile fault scarps and Madison River terraces in the West Yellowstone Obsidian Sand Plain south of Hebgen Lake, Montana.
2. Collect datable materials to determine the ages of the fault scarps and Madison River terraces.
3. Test the accuracy and utility of the morphologic dating technique outline by Nash (1980).
4. Investigate the distribution and mode of formation of the conical depressions in the West Yellowstone Obsidian Sand Plain.

Results:

1. The studied fault scarps, Madison River terraces, and conical depressions are shown on the accompanying figure along with the positions, lengths, and orientations of the surveyed fault and terrace profiles.
2. Buried volcanic ash and wood were collected from a conical depression at the foot of a Madison River terrace (see accompanying figure). The characteristics of the ash are similar to those of the Mazama ash (formed 6,600 to 6.700 B.P.), providing a minimum age for the associated terrace. A sample of the log buried with the ash has been sent off for radiocarbon dating.
3. The inverse relationship between scarp height and rate of degradation discussed by Wallace (1977), Bucknam and Anderson (1979), and Nash (1980) is seen in the profiles of the Madison River terraces. The relationship is not as clear for the collected profiles of the fault scarps, probably because of complications resulting from displacements along the fault during the 1959 earthquake.

4. Myers and Hamilton (1964) ascribe the origin of the conical depressions in the West Yellowstone Obsidian Sand Plain to collapse into giant sand boils. I believe the depressions were formed, and are still forming, by seepage of the obsidian sand into underlying dilated fractures associated with the fault scarps. They may cause the runway of the West Yellowstone Airport to subside.

5. Analysis of the collected data is in progress. Field work will be continued during the summer of 1981.

References:

Bucknam, R. C., and Anderson, R. E., 1979, Estimation of fault-scarp ages from a scarp-height-slope-angle relationship: Geology, v. 7, p. 11-14.

Myers, W. B., and Hamilton, W., 1964, Deformation accompanying the Hebgen Lake earthquake of August 17, 1959, in the Hebgen Lake, Montana earthquake of August 17, 1959: U. S. Geological Survey Professional Paper 435-I, p. 55-98.

Nash, D. B., 1980, Morphologic dating of degraded normal fault scarps: Journal of Geology, v. 88, p. 353-360.

Nash, D. B., 1981, FAULT: A FORTRAN program for modeling the degradation of active normal fault scarps: Computers and Geoscience, in press.

Wallace, R. E., 1977, Profiles and ages of young fault scarps, north-central Nevada, Geological Society of America Bulletin, v. 88, 1267-1281.

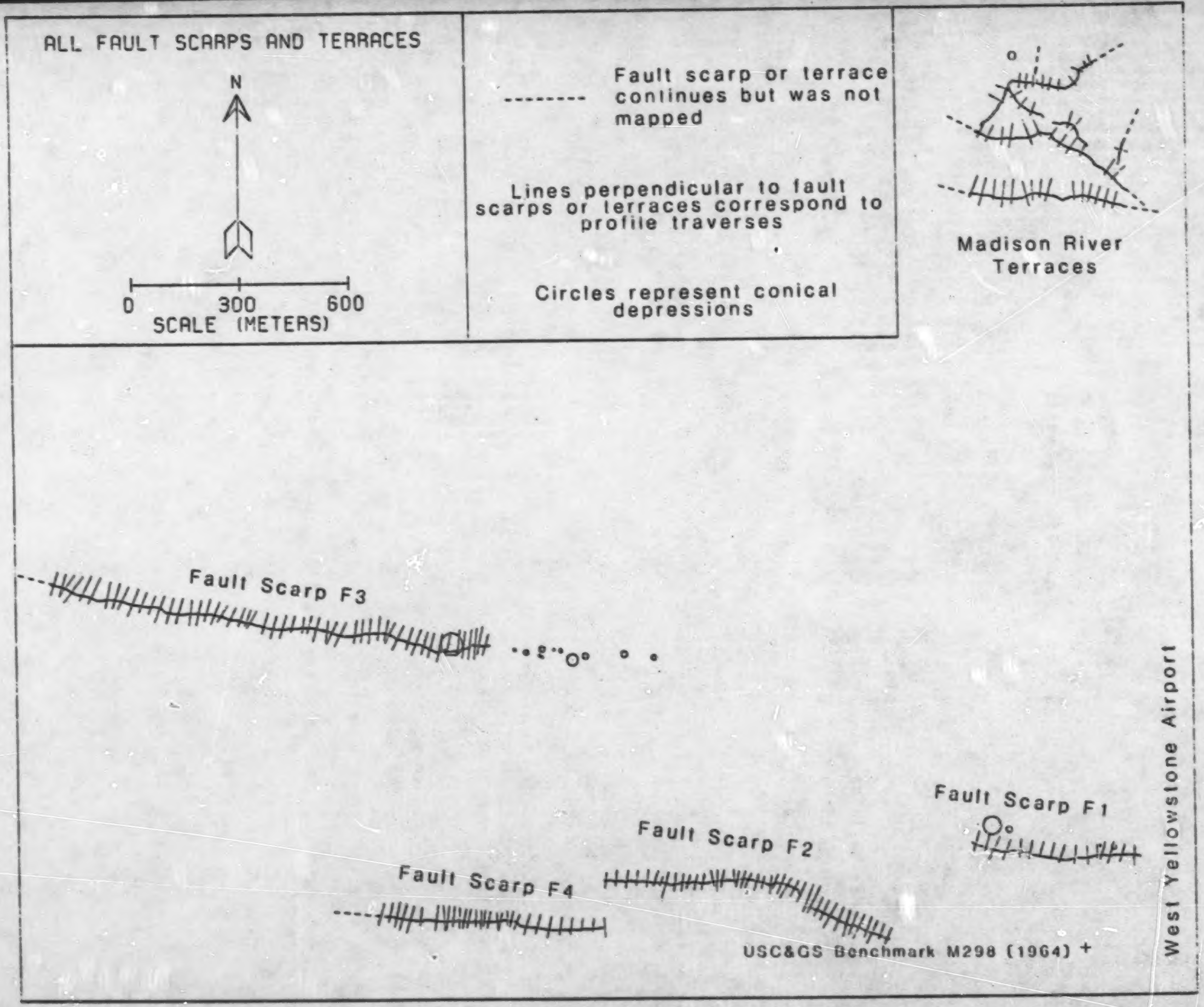
ALL FAULT SCARPS AND TERRACES
N
0
300
600
SCALE (METERS)
Fault scarp or terrace continues but was not mapped
Lines perpendicular to fault scarps or terraces correspond to profile traverses
Circles represent conical depressions
Madison River Terraces
Fault Scarp F3
Fault Scarp F1
Fault Scarp F2
Fault Scarp F4
USC&GS Benchmark M298 (1964) +
West Yellowstone Airport

Quaternary Dating and Neotectonics

9530-01559

K. L. Pierce
Branch of Central Environmental Geology
U.S. Geological Survey
Box 25046, MS 913
Denver, CO 80225
(303) 234-2737

Investigations

1. Synthesize available data on age of last (Pinedale) glaciation in the Rocky Mountain region (K. L. Pierce).

2. Determine age and correlation of upper two loess units in southeastern Idaho (K. L. Pierce).

3. Continued compilation of map of Miocene and younger tectonic features in Colorado. Analyzed morphometric field data for multiple-event fault scarps in the Rio Grande Rift of Colorado. Modified the theoretical degradation model for single-event scarps for application to multiple-event scarps (S. M. Colman).

4. The morphologies of fault scarps produced by ground rupture along discrete segments of the La Jencia Fault in central New Mexico during the last 33,000 yr were compared to their ages of displacement to observe possible temporal changes in scarp degradation rates. Previous investigators using models of scarp degradation have made estimates of scarp ages assuming constant scarp degradation rates (M. N. Machette).

5. Analyzed age-related properties of soil B horizons formed in surficial deposits cut by range-front faults along the Wasatch Mountains between Kaysville and Springville, Utah (R. R. Shroba).

6. Summarized data on soil properties useful for helping to date Quaternary deposits in the Western United States. The findings are discussed in two manuscripts currently in preparation on soil development with time in the Rocky Mountains and trends in late Quaternary soil development in the mountains of the Western United States (R. R. Shroba).

Results

1. The last (Pinedale) glaciation has traditionally been considered to be restricted to the late Wisconsin (25,000-10,000 yr ago). Recent numerical and relative-age studies suggest it includes much more time than this. Some Pinedale end moraines are probably 30,000-40,000 yr old, and others may be even older. Such glacial deposits and associated outwash are widely used to date range-front faulting (K. L. Pierce, investigation No. 1).

2. The stratigraphy of the upper two loess units in southeastern Idaho is consistent over distances of 350 km. Loess unit A accumulated between 10,000 and perhaps as early as 70,000 yr ago. Loess unit B accumulated during a similar time interval centering on about 150,000 yr ago. These loess units are used directly to date faulting, and to date faulted alluvial deposits (K. L. Pierce, investigation No. 2).

3. Both the theoretical model of scarp degradation based on the diffusion equation and empirical morphometric data for scarps in the Rio Grande Rift of Colorado indicate that the relations among height, slope, and age are valid for multiple-event scarps as well as for single-event scarps. However, multiple-event scarps have lower slope angles than single-event scarps for similar heights and ages. On the basis of these relations, the morphologies of many scarps in the study area are consistent with their estimated ages, but in some locations, a strong lithologic effect was also apparent (S. M. Colman, investigation No. 3).

4. The La Jencia Fault has a history of at least four to as many as seven surface rupture events during the past 33,000 yr along discrete segments of the fault; earlier Quaternary faulting occurred about 150,000 yr ago along the northern part of the fault. The net result is a nearly continuous, 35-km-long fault scarp of up to 7 m in height. This history was determined from exploratory trenching, detailed laboratory analyses of soil stratigraphic units, and morphometric analysis of scarp profiles (M. N. Machette, investigation No. 4).

5a. The youngest segments of the La Jencia Fault (segments A, C, and E) are less degraded than older segments (B and D). The morphometric relationship between scarp height (H) and maximum scarp-slope angle (θ) for three of the fault segments are as follows:

Segment	Age	Relationship
C	5,000	$\theta = 7.8 + 20.2 \log H$
B	15,000	$\theta = 0.9 + 26.0 \log H$
D	33,000	$\theta = 1.1 + 22.2 \log H$

b. Scarp ages can be estimated from Nash's (1980) model using segment B (5,000 yr) for control. Assuming the three segments were degraded at the same rate, then the estimated ages for segments B and D are 11,000 and 17,000 yr, respectively. These ages are clearly incompatible with those generated from detailed analyses of soils developed in fault-scarp derived colluvium along each segment.

c. To reconcile the disparity between the two sets of scarp ages, the effect of temporal changes in scarp degradation rate were analyzed with a step-function equation modeled in accordance with suspected changes in climate between the latest Pleistocene and Holocene. The necessary change in degradation rate varies from a maximum of 10.2×10^{-4} m^2/yr in the Holocene to a minimum rate of 2.4×10^{-4} m^2/yr in the late Wisconsin (about 15,000 yr B.P.).

d. The magnitude of change in scarp degradation rates (4x) is such that direct morphometric comparisons of Holocene and late Pleistocene scarps is probably not justifiable in most areas, unless it can be shown that possible climatic changes had no effect on scarp degradation rates (M. N. Machete, investigation No. 4).

6a. Along the Wasatch Front, B-horizon properties that correspond with the age of underlying surficial deposits are (1) increase in clay content, (2) frequency, thickness, and morphology of clay films, (3) grade and type of structure, (4) color (hue and chroma), and (5) horizon thickness.

b. Soils formed in deposits about 10,000-15,000 yr old along the Wasatch Front commonly have weak Bt horizons, although some are slightly better developed. The amount of textural development in these soils is influenced to a considerable extent by the original grain size of the surficial deposits, especially the clay content. Bt horizons are best expressed where formed in loess, silty eolian sand, or gravel overlain by loess, but are weakest where formed in sandy overbank sediment or the underlying gravel (R. R. Shroba, investigation No. 5).

Reports

Colman, S. M., McAlpin, J., and Ostenaa, D. A., 1981, Morphology of fault scarps in the Rio Grande Rift, Colorado, as an indicator of age of faulting [abs.]: Association of Engineering Geologists Symposium on Seismic Hazards in Colorado, 1981, Proceedings [in press].

Kirkham, R. M., and Colman, S. M., 1981, An overview of the tectonic history of Colorado, with emphasis on the Cenozoic [abs.]: Association of Engineering Geologists Symposium on Seismic Hazards in Colorado, 1981, Proceedings [in press].

Machette, M. N., 1980, Preliminary geologic map of the southwest quarter of the Beaver Quadrangle, Beaver County, Utah: U.S. Geological Survey Open-File Report 80-1670.

Machette, M. N., and Steven, T. A., 1980, Preliminary geologic map of the northwest quarter of the Beaver Quadrangle, Beaver County, Utah: U.S. Geological Survey Open-File Report 80-1669.

Shroba, R. R., 1981, Physical properties and performance characteristics of surficial deposits and rock units in the Greater Denver area, a chapter in Hansen, W. R., and Crosby, E. J., Environmental geology of the Front Range Urban Corridor and vicinity, Colorado: U.S. Geological Survey Professional Paper 1230 [in press].

Post-Earthquake Shaking Effects and Fault Creep

9940-02675

Christopher Rojahn and Robert Nason
Branch of Ground Motion and Faulting
U.S. Geological Survey
345 Middlefield Road, MS 77
Menlo Park, California, 94025
(415) 323-8111 x2760

Investigations

1. An earthquake of magnitude 7.0 occurred offshore of northern California on 8 November 1980, and was recorded on nearby strong-motion instruments. The shaking area was investigated to determine the disturbance and building damage near the strong motion instruments and in the general area.

2. The compilation of eye-witness and other reports of the earthquake damage (pre-fire) to ordinary buildings in San Francisco in the great April 1906 earthquake has increased to more than 200 buildings, of which 137 were brick buildings. The listing shows the amount of hazard that might occur again with brick buildings in any future great earthquake.

Results

1. The 8 November 1980 earthquake caused a shaking disturbance of seismic intensity MM VI-VII in a region of 120 km north-south along the coast of northern California near Eureka, California. The MM VI-VII intensity occurred uniformly over the region.

2. The compilation of 1906 earthquake damage to brick buildings in San Francisco shows that 13 buildings had full or partial collapse internally, while 90% of the buildings described did not have internal collapse. However, more than half the described buildings had significant fall of bricks off of outer walls, sometimes causing fatalities.

3. The 1906 shaking damage to brick buildings in areas of major ground failure was less than the reported damage to brick buildings on firmer ground. This suggests that the type of shaking which damages brick buildings was less severe in areas of ground failure than elsewhere, perhaps because of absorbtion of seismic energy in the ground failure process.

Reports

Nason, Robert, 1981, Damage of brick buildings in San Francisco in the April 1906 earthquake (abs): Seismological Society of America meeting, Earthquake Notes, Vol. 52, no. 1, p. 10.

Uranium Series Dating

9740-00378

J. N. Rosholt
Branch of Isotope Geology
U.S. Geological Survey
Denver Federal Center
Denver, CO. 80225
(303) 234-6941

Investigations

1. Uranium-trend dating has been used to estimate the time of deposition of alluvium and eolian deposits over the time range of 3,000 years to about 800,000 years ago. The dating technique consists of determining an isochron from analyses of several samples covering the various soil horizons in a given alluvium unit; approximately 4 to 9 samples of each alluvium unit are analyzed. The results of these analyses are plotted where $(^{238}U-^{230}Th)/^{238}U$ vs. $(^{234}U-^{238}U)/^{238}U$ ideally yield a linear relationship where the measured slope changes in a predictable way with increasing age of alluvium for a given half period of the flux controlling the migration of uranium in the alluvium environment. An empirical model compensates for different climatic and environmental regimes and the model has primary time calibrations at 11,000 years, 140,000 years (Bull Lake), 600,000 years (Pearlette Ash) and 720,000 years (Bishop Tuff). Calibrations have been made based on correlations with similar material that has been dated by radiocarbon and K-Ar.

2. Uranium-trend dating of marine terraces is being tested on several sites collected in California, Virginia, North Carolina, and South Carolina. It appears that separate calibration points, provided by marine deposits of known age, will be required before final uranium-trend ages can be calculated from analyses of the $^{238}U-^{234}U-^{230}Th$ system in these type deposits.

Results

1. Radioisotope analyses have been completed on seven marine terrace deposits from California and one section from the North Myrtle Beach area, South Carolina. Only two of these deposits have known ages determined by U-series dating of coral; the Nestor Terrace, San Diego, CA (120,000 ± 10,000 years) and the Canepatch Formation, SC (440,000 + 140,000 years). Three younger terraces from Ventura, CA that have been dated by ^{14}C are being prepared for chemical analyses. Additional sections from Virginia and North Carolina contain deposits that have been dated at 190,000 + 20,000 years using U-series techniques on coral. These sections are being collected to obtain additional time-calibration points for uranium-trend dating of marine terraces.

Reports

Cronin, T. M., Szabo, B. J., Ager, T. A., Hazel, J. E., and Owens, J. P., 1981, Quaternary climates and sea levels of the U.S. Atlantic Coastal Plain: Science, v. 211, p. 233-240.

Rosholt, J. N., 1980, Uranium and thorium disequilibrium in zeolitically altered rock: Nuclear Technology, v. 51, p. 143-146.

Rosholt, J. N., Uranium-trend dating of Quaternary sediments: (Approved by the Director, Submitted to Bull. Geol. Soc. America).

Basement Tectonic Framework Studies
San Andreas Fault System

9950-01291

Donald C. Ross
Branch of Earthquake Tectonics and Risk
U.S. Geological Survey
345 Middlefield Road, MS-77
Menlo Park, CA 94025
(415) 323-8111, ext. 2341

Investigations

1. Geologic mapping and sampling of basement rock units on both sides of the Kern Canyon-Breckenridge fault continued in October.

2. Thin sections were studied from about 200 samples of metasedimentary and metavolcanic rocks from both sides of the Kern Canyon-Breckenridge fault zone, and from cataclastically deformed basement rocks within the fault zone.

3. More than 200 samples of granitic rocks from both sides of the Kern Canyon-Breckenridge fault zone were slabbed, stained, and modally analyzed by point counting by Deborah Goaldman (San Jose State University).

4. A re-examination of basement outcrops west of Grapevine Canyon in the San Emigdio Mountains was made to confirm the presence of a maverick fault sliver of Rand Schist (see Results).

Results

Within the west-trending tail of the southernmost Sierra Nevada (San Emigdio mountains) a distinctive belt of schist and quartzite has been mapped between Grapevine and San Emigdio Canyons (figure 1) that is of lower metamorphic grade than the surrounding rocks, and is separated from the surrounding terrane by faults wherever the contact relations have been observed.

The schist and quartzite belt is characterized by coarse, dark biotite-rich layers alternating with impure quartzite layers, which are also quite dark colored. In thin section the most striking feature of these rocks is the abundance of large "dirty", poikilitic masses of virtually untwined sodic plagioclase strongly dusted with graphite or other carbonaceous matter. Also distinctive in the schist and quartzite belt are prominent, thick white "bull quartz" veins or sills. The physical appearance and metamorphic grade of these rocks is strikingly reminiscent of rocks in the Rand Schist in the western part of the Rand Mountains and also to some of the rocks in Rand Schist slivers along the Garlock fault between the San Andreas fault and the Rand Mountains. I therefore suggest that the schist and quartzite belt in the San Emigdio Mountains is a correlative of the Rand Schist, which has long been considered to be related to the Pelona-Orocopia Schist terrane. The general setting and shape of the probable Rand Schist in the Sierra Nevada tail suggests it is a sliver along a transcurrent fault, but at its east end the north contact appears to plunge under the adjacent dark amphibolitic gneiss unit. The south contact appears to be an abrupt, steeply dipping fault contact against granodiorite and metasedimentary rocks of strikingly different character from the schist and quartzite belt.

It is probably no more coincidence that the faulted south contact of the Rand Schist sliver in the San Emigdio Mountains essentially lines up with the Pastoria fault zone of Crowell (1952). I suggest that both these features are part of a fundamental break in the basement rocks of the Sierran tail. West from the Garlock fault on a somewhat crinkled but generally east-west trend to the end of the basement outcrop at the west end of the San Emigdio Mountains metasedimentary rocks of continental affinity and associated granodiorite on the south are in abrupt contact with hornblende-rich plutonic and metamorphic rocks of possible oceanic affinity on the north.

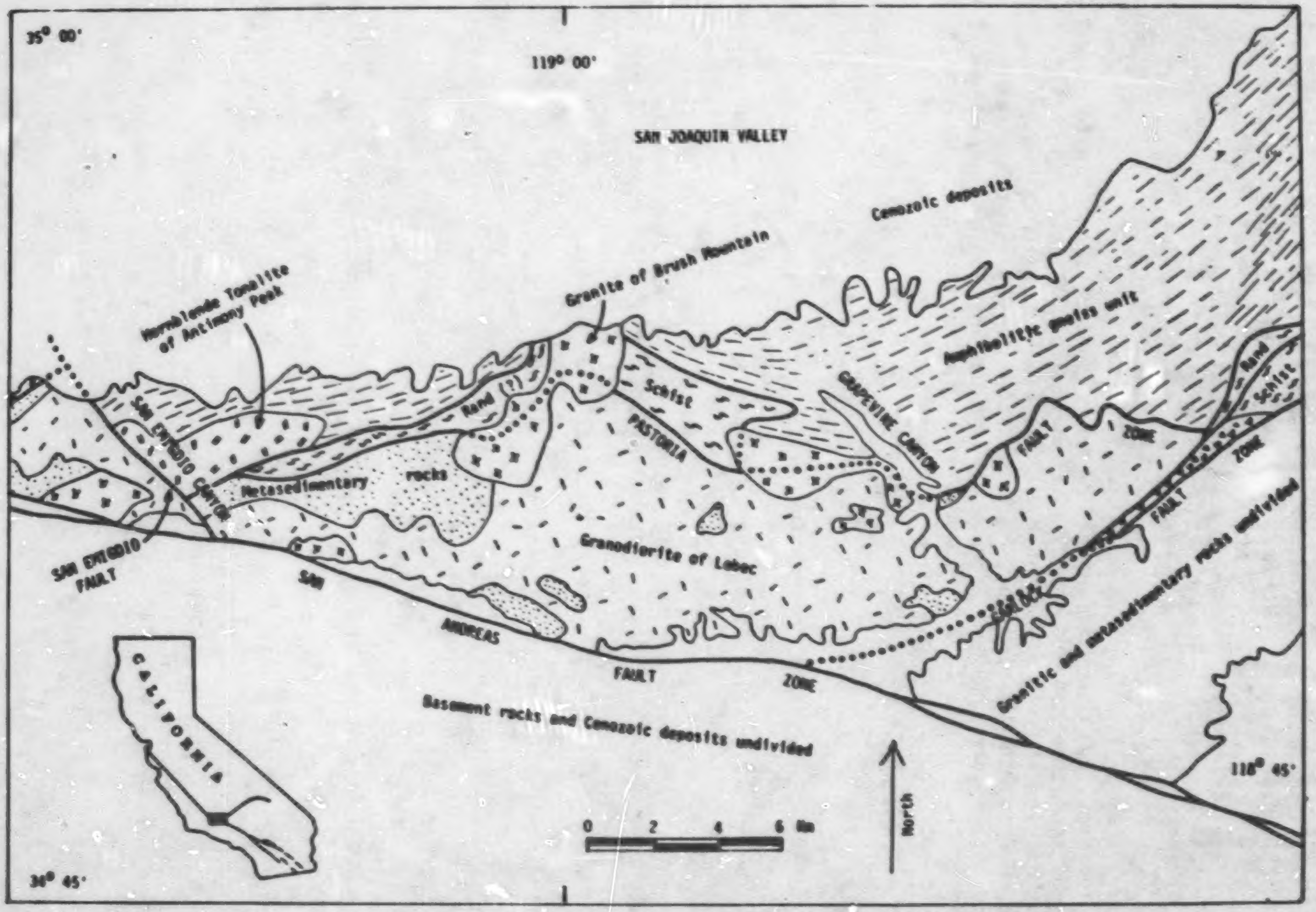
35° 00'
119° 00'
SAN JOAQUIN VALLEY
Cenozoic deposits
Granite of Brush Mountain
Hornblende Tonalite of Antimony Peak
Amphibolitic gneiss unit
Schist
Rand
(?)
Rand Schist
SAN EMIGDIO CANYON
PASTORIA
GRAPEVINE CANYON
FAULT ZONE
Metasedimentary rocks
Granodiorite of Lebec
SAN EMIGDIO FAULT
SAN ANDREAS FAULT ZONE
GARLOCK FAULT ZONE
Granitic and metasedimentary rocks undivided
Basement rocks and Cenozoic deposits undivided
CALIFORNIA
0 2 4 6 km
North
118° 45'
34° 45'

Figure 1. Generalized geologic map of the Sierra Nevada tail showing the probable Rand Schist sliver in the San Emigdio Mountains, California

Teprochronology of the Western Region

9540-01947

Andrei M. Sarna-Wojcicki
U. S. Geological Survey
345 Middlefield Road, MS 75
Menlo Park, CA 94025
(415) 323-8111 ext. 2745

Summary

Continued sampling, chemical and petrographic analysis, and fission-track age dating of tephra (ashes and tuffs) of young geological age in order to provide age control for studies of recent tectonism and volcanism in California, Nevada, Oregon, and Washington. Neutron activation, X-ray fluorescence and electron microprobe analyses of separated volcanic glass and crystals are used to identify widespread tephra units of known radiometric age. New tephra units identified by chemical and petrographic analysis are dated by appropriate radiometric age dating methods.

Investigations

1) Continued analyses of areal distribution, thickness, mass-per area, and stratigraphy of downwind ashes from 1980 eruptions of Mount St. Helens, as models for interpretation of dispersal patterns and stratigraphic features in pre-historic ashes and tuffs.

2) Began study to evaluate hazards to planned and existing nuclear reactor sites from downwind airfall ash erupted in the Pacific Northwest of the U. S.

3) Continued to completion report on areal extent, mass, volume and composition of premagmatic ash erupted from Mount St. Helens, March 27 through May 14, 1980 (U.S.G.S. Prof. Paper 1250 chapter).

4) Continued to completion report on areal distribution, thickness, mass, volume, and grain size of airfall ash from the six major eruptions of Mount St. Helens in 1980 (U.S.G.S. Prof. Paper 1250 chapter).

5) Continued to completion report on composition of air-fall ash from four magmatic eruptions of Mount St. Helens in 1980 (U.S.G.S. Prof. Paper 1250 Chapter).

6) Continued sample collection, analysis, and identification in the following areas:

- a) Southern California (Ventura, Ridge, Los Angeles, Anza-Borrego, and Lake Tecopa basins)
- b) Northern California (Humboldt basin)
- c) Central Valley (Sacramento and San Joaquin Valleys)
- d) California borderland, cores from Deep Sea Drilling Programs.

Results

1) Electron microprobe analyses of glass and pumice shards obtained from a core (D.S.D.P. site 173) drilled approximately 100 km SW of Cape Mendocino, northern California, match well with those of an ash in the marine Rio Dell Formation (Wildcat Group) exposed in the Centerville Beach section north of the cape and with an ash exposed inland, near Scotia Bluffs, in the Carlotta Fm. The ages assigned to the Rio Dell ash by others on the basis of K-Ar analyses, magnetostratigraphy, and biostratigraphy range widely from about 1.2 to 2.3 m.y. The correlation, at present still tentative because more diagnostic trace-and minor-element data are lacking, would correlate the on-land marine section and associated magnetostratigraphy-biostratigraphy with the world-wide deep-ocean chronology, and support an age closer to about 1.2 m.y. (with S. Morrison and K. R. Lajoie).

2) Results of energy-dispersive X-ray fluorescence and elctron microprobe analysis indicate that an ash in the marine Eel River Fm. (Wildcat Group), in the Centerville section, underlying the Rio Dell Formation, is correlative with the Putah Tuff member of the continental Tehama Fm., in southwestern Sacramento Valley, previously dated at 3.4 m.y. by the K-Ar method.

Reports

Sarna-Wojcicki, A. M., Hillhouse, J. W., Meyer, C. E., Woodward, M. J., Liddicoat, J. C., and Yerkes, R. F., 1981, Progress in tephrochronological correlation, magnetostratigraphy, and isotopic age determination of Pliocene and Pleistocene strata in California, in Abstracts, International Field Conference, Neogene/Quaternary Boundary, Projects 41 and 128, I.G.C.P.-I.U.G.S.,U.N.E.S.C.O.

Liddicoat, J. C., Lajoie, K. R., Bailey, R. A., Sarna-Wojcicki, A. M., Russell, P. C., and Woodward, M. J., 1980, Reversal of the paleomagnetic field in Bruhnes-age lacustrine sediments in Long Valley and Mono Basin, California: Abs. in American Geophysical Unio, Abstracts with Program, EOS, v. 61, no. 17 p. 215.

Sarna-Wojcicki, A. M., Waitt, R. B., Jr., Woodward, M. J., Shipley, Susan, and Rivera, Jose, 1981, Premagmatic ash erupted from March 27 through May 14, 1980--extent, mass, volume, and composition, in Lipman, P. W., and Mullineaux, D. R., eds., the 1980 eruptions of Mount St. Helens, Washington: U.S. Geol. Survey Prof. Paper 1250 (in press).

Sarna-Wojcicki, A. M., Shipley, Susan, Waitt, R. B., Jr., Dzurisin, Daniel and Wood, S. H., 1981, Areal distribution, thickness, mass, volume,and grain size of airfall ash from the six major eruptions of 1980, in Lipman, P. W., and Mullineaux, D. R., eds., (etc., as above reference).

Sarna-Wojcicki, A. M., Meyer C. E., Woodward, M. J., and Lamothe, P. J., 1981, Composition of air-fall ash erupted on May 18, May 25, June 12, July 22, and August 7, in Lipman, P. W., and Mullineaux, D. R., eds., (etc., as above reference).

Waitt, R. B., Jr., Hansen V. L., Sarna-Wojcicki, A. M., and Wood, S. H., 1981, Stratigraphy and field sedimentology of proximal airfall deposits from 24 May through 7 August, 1980, in Lipman, P. W., and Mullineaux, D. R., eds., (etc., as above references).

Quaternary Stratigraphy of the Wasach Front

9530-02174

W. E. Scott
Branch of Central Environmental Geology
U.S. Geological Survey
Box 25046, MS 913
Denver, CO 80225
(303) 234-5215

Investigations

1. Reports on Lake Bonneville stratigraphy and chronology are being prepared in cooperation with W. D. McCoy, University of Colorado, and R. R. Shroba, U.S. Geological Survey.

2. Compilation of field data and photogeologic mapping are in progress for strip maps of faults and surficial deposits in the Salt Lake and Utah Valleys. A map of the Salt Lake Valley will be completed following the 1981 field season.

Results

1. Additional radiocarbon analyses provided by Meyer Rubin (USGS) on wood from Lake Bonneville deposits are in accord with our previous interpretations of the history of the last lake cycle. The available dates that are considered reliable define the chronology of the last lake cycle shown in the following figure. The altitudes of the samples have been adjusted to compensate for isostatic deformation. The rise and fall of lake level are shown as straight lines; however, the scatter in ages and local stratigraphic relations suggest that minor fluctuations of lake level occurred during transgression and regression. The wood dates are considered to provide maximum ages as the wood was growing above the lake and sometime after death was deposited in nearshore lagoons. Also, some of the dated wood occurs in alluvial deposits related to a rising lake, which were subsequently covered by the lake. Dates on gastropod shells obtained by previous workers are regarded as minimum ages because of the susceptibility of shells to contamination with young carbon. Dates close to the Bonneville shoreline are not available; however, the highest dates from transgressive deposits and dates from below the Provo shoreline suggest that the abandonment of the Bonneville shoreline and rapid fall to the Provo shoreline during the Bonneville Flood occurred sometime between 14,000 and 15,000 years ago.

H5

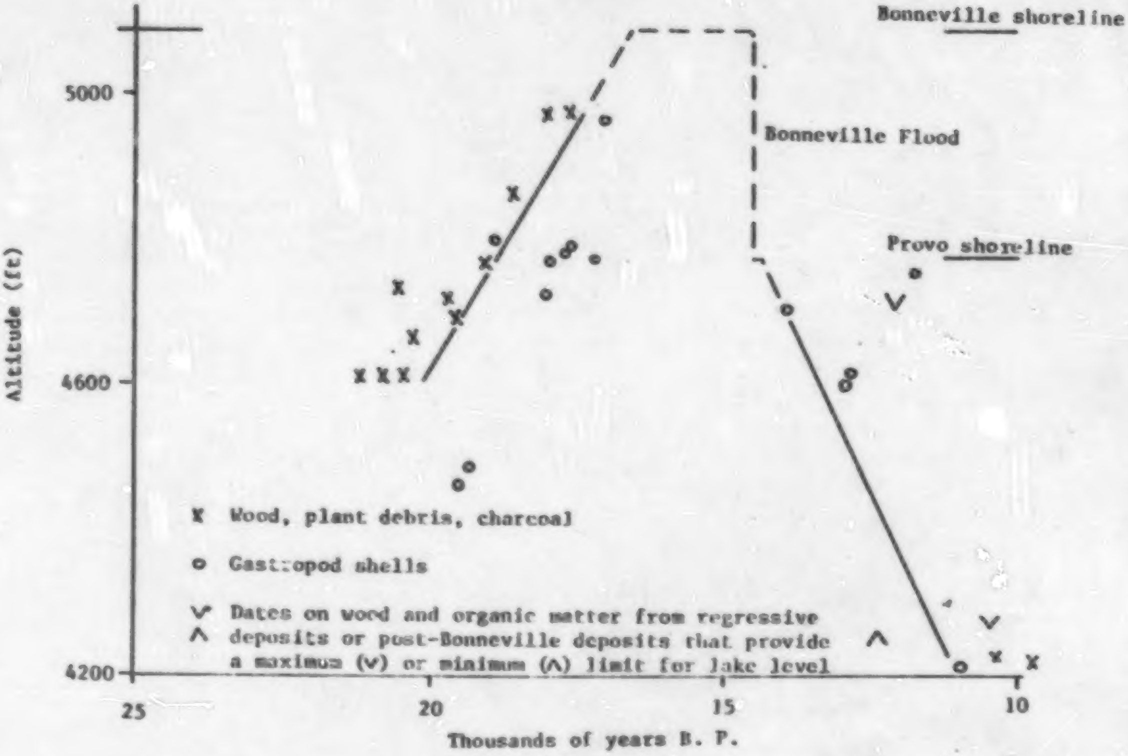
Bonneville shoreline
Bonneville Flood
Provo shoreline
Altitude (ft)
5000
4600
4200
25
20
15
10
Thousands of years B. P.
X Wood, plant debris, charcoal
o Gastropod shells
V Dates on wood and organic matter from regressive
Λ deposits or post-Bonneville deposits that provide
a maximum (V) or minimum (Λ) limit for lake level

High Resolution Seismic Reflection Surveying in Northwestern Tennessee

14-08-0001-19117

John L. Sexton
Department of Geosciences
Purdue University
West Lafayette, IN 47907
(317) 494-6841

Investigations

A high resolution seismic reflection survey has been conducted in northwestern Tennessee on Reelfoot scarp and at Cottonwood Grove. The purpose of the study is to help determine nature, near surface extent and age of faulting observed on vibroseis (Conoco trademark) reflection records. Data collected include three lines on Reelfoot scarp and two lines in the Cottonwood Grove area. Lines on Reelfoot scarp include one line about 1500 meters long, a second line 750 meters long and located about 600 meters to the south of the first line and a third line about 500 meters long and about 600 meters south of the second line. In the Cottonwood Grove area, two lines were run, one 4000 meters long and one short line 650 meters long. All lines utilized the Mini-Sosie (trademark Societe Nationale Elf Aquitane) source except the 650 meter long line at Cottonwood Grove. A shotgun source was used for this line.

Results

Processing of the seismic reflection data is not yet complete and only preliminary results are presented here.

The Minie-Sosie records are generally lower in frequency content than records obtained from a previous survey which utilized a small explosive source. However, the Minie-Sosie records have higher frequency content than the vibroseis records. The overall quality of the Minie-Sosie records is comparable to that of the explosive records and in certain portions of the record, the Minie-Sosie records are superior. Continutiy of reflections on the Minie Sosie records is excellent. Good quality reflections are observed from shallow beds corresponding to two way travel times of 150 milliseconds and from deeper beds corresponding to two way travel times of 700 milliseconds.

The seismic reflection data from the three lines on Reelfoot scarp reveals a localized zone about 300 meters wide in which reflections are offset by 40 milliseconds two way time (approximately 40 meters). This distrubed zone appears to be folding or faulting and possibly a small graben-like structure associated with a laterally larger fault with east side down by only 20 milliseconds two way time. From the west end of the line to the east end, the Paleozoic and Cretaceous reflection times are different by about 20 milliseconds two way time (east side down) except with the localized zone. Effects of this disturbed zone appear to extend upward to reflection times of about 200 milliseconds and possibly shallower. Further data processing will aid in the final interpretation of the near surface extent and effects of this feature.

Interpretation of vibroseis records from Cottonwood Grove area by USGS personnel indicates that a fault of approximately 80 meters offset (west side down) exists in Paleozoic, Cretaceous and Eocene rocks. A data gap resulted in some uncertainty of the near surface extent of that fault. A Minie-Sosie survey has been conducted along the same line as the vibroseis survey. The data gap has been filled in and near surface reflections obtained in the critical area. The data clearly show the deep structural feature observed on the vibroseis data. This fault appears to have some affect on the reflection in the shallow section, at least to 300 milliseconds and possibly shallower. The offset appears to decrease toward the surface and does not appear to offset the reflections at 200 milliseconds.

The short shotgun line at Cottonwood Grove was located along the Minie-Sosie line and was located to coincide with an USGS trench used to determine if the fault observed on the vibroseis line actually came to the surface. No faulting was observed in the trench. Preliminary results show reflections as shallow on 80 milliseconds. No large offsets are observed on the reflection records in agreement with Minie-Sosie records and observations in the trench.

Salton Trough Tectonics and Quaternary Faulting

9940-01292

Robert V. Sharp and Malcolm M. Clark
Branch of Ground Motion and Faulting
U.S. Geological Survey
345 Middlefield Road, MS-77
Menlo Park, CA 94025
(415) 323-8111, Exts. 2596, 2591

Investigations

1. Continuation of monitoring horizontal and vertical components of afterslip of the 15 October 1979 earthquake on the Imperial fault.

2. Installation of leveling arrays on the Clark and Coyote Creek faults of the San Jacinto fault zone, on the San Andreas fault, and across the basin of former Mesquite Lake between the Imperial fault and the Brawley fault zone.

3. Continuation of mapping of Quaternary faults on the west side of Imperial Valley.

4. Continuation of investigations of Mammoth Lakes earthquakes of May, 1980.

5. Investigate the Yosemite Falls rockfall of November 16, 1980.

Results

1. By the end of 1980 the rate of horizontal afterslip on the Imperial fault had decreased so much that further movement could no longer be resolved with the techniques that were used in measuring offset of canals shortly after the earthquake. Data on future horizontal afterslip will be obtained only from alinement arrays, geodetic networks, and creepmeters, which are sparsely distributed along the length of the 1979 rupture.

Releveling to determine vertical afterslip has been done along the length of the fault only twice since the earthquake. The last period of measured vertical movement, March 1980 to January 1981, showed no further increase in uplift of the southwest side of the fault from Barbara Worth Road southeastward to the limit of rupture 6.5 km away. Northwest of Barbara Worth Road, however, vertical afterslip was recorded at 12 of the 14 leveling sites for this period and reached a maximum of about 3 cm at a canal about 0.8 km north of Carey Road and 0.8 km from the northern terminus of 1979 movement on the Imperial fault. The amount of vertical afterslip was erratic along the length of the active segment of the fault; no simple relation of total vertical afterslip or slip rate to the coseismic vertical slip component is evident.

2. New arrays for monitoring tilt and possible displacement have been built across the Coyote Creek fault at Middle Willows and Coyote

Mountain. Two arrays across the Clark fault, at Jackass Flat and southeastern Clark Valley, have also been established. All of these lines are located within the southern part of the San Jacinto fault zone identified as a seismic gap by Thatcher and others, 1975.

A new array has been constructed across the San Andreas fault at North Shore for the same purpose. The two preexisting leveling arrays on Harris Road in Imperial Valley, one across the Imperial fault and the other across three known strands of the Brawley fault zone, have been connected with a leveling line more than 5 km in length. This line will provide better control on the scale and depth of deformation associated with each fault structure.

3. A complex pattern of Quaternary normal faults in and north of the Superstition Hills, as well as the historically active Superstition Hills fault that at places forms the southwestern boundary of the hills, have been mapped at 1:24,000 scale. Structural evidence discovered in the mapping shows that the Superstition Hills fault existed and was active at the time of deposition of continental sediments now exposed at the surface. The range of age of the sediments is not known exactly, but from regional stratigraphic relations their age is probably late Pleistocene. The distribution of the normal faults shows that they have been influenced by the Superstition Hills fault and are not older features, at least at the surface. Some of the normal faults form scarps and cut young alluvial materials. Although the ages of last movement on these faults are now unknown, seismicity that is presently scattered under the region of the Superstition Hills suggests that all of these structures are potentially active at the surface.

4. Releveling in October 1980 of a first-order level line along U.S. 395 in the epicentral region of the May, 1980 Mammoth Lakes earthquakes shows abrupt vertical displacement of 120 mm (0.40 feet), west side relatively up, between 1975 and October, 1980 at the Hilton Creek fault. The leveling also shows about 100 mm of additional vertical displacement between 1975 and October 1980 westward from the Hilton Creek fault for about 10 km. The line was established in 1932. Re-surveys in 1957 and 1975 showed total vertical changes of less than 25 mm along this route since 1932.

This vertical fault displacement of 120 mm, combined with field evidence of surface rupture and comparable offset along adjacent parts of the Hilton Creek fault, plus Savage's finding of 60-80 mm of regional extension roughly perpendicular to the strike of the Hilton Creek fault between 1979 and September 1980, strongly supports the possibility of significant normal tectonic slip on Hilton Creek fault at the time of the earthquake.

The level line crosses Hilton Creek fault at a prominent scarp that offsets outwash of late Pleistocene glaciers of Convict Creek. Outwash of the maximum Tioga glaciation (about 15,000 y b.p.) is offset about 25 m, and outwash of the Tahoe glaciation (ca. 50,000 to 130,000 y b.p.) is offset about 110 m. The present 25-m scarp in Tioga outwash at the level line could have been built in 15,000 y b.p. by about 200 1980-type events, with an average recurrence interval of 75 years.

The brief historic record of earthquakes (since about 1870) does not support such a short recurrence interval. However, the historic record certainly cannot eliminate it as a possible average recurrence interval over the last 15,000 y. Whether the 25-m-high scarps at the level line at U.S. 395 and at McGee Creek were built by hundreds of 1980-type events is thus still unknown.

5. On November 16, 1980 a rockfall destroyed part of the Yosemite Falls trail, killing 3 hikers and seriously injuring several others. I (Clark) witnessed the rockfall from Sierra Point, 5 km away, the site of the largest of several rockfalls in Yosemite Valley triggered by the Mammoth Lakes earthquakes of May 1980, about 65 km away. Gerald Wieczorek of Engineering Geology and I briefly inspected the rockfall 5 days later.

Because the slab that failed survived shaking from the Mammoth Lakes earthquakes, it is apparent that those earthquakes did not "harvest" all the susceptible rocks in Yosemite. It is likely that the earthquakes both triggered rockfalls and moved some other potential rockfalls closer to failure. Observations of the large number of rockfalls triggered elsewhere in the Sierra Nevada by the Mammoth Lakes earthquakes, and consideration of the high seismicity along the eastern base of the Sierra Nevada suggests that earthquake-triggered rockfalls may be a significant, if not dominant, cause of Sierran rockfalls. The rockfall record of the Sierra may contain much information about past earthquakes.

Reports

Sharp, Robert V., 1981, Variable rates of late Quaternary strike slip on the San Jacinto fault zone, southern California: Jour. Geophys. Research, v. 86, p. 1754-1762.

Sharp, Robert V., 1981, Surface faulting in the Colorado River delta region in Mexico associated with the $M_S = 6.3$ earthquake of June 9, 1980 (abstract): Earthquake Notes, v. 52, p. 48.

Lubetkin, Lester, and Clark, M. M., 1980, Late Quaternary activity along the Lone Pine fault, eastern California (abs.): Trans. American Geophys. Union, v. 61, p. 1042.

Clark, M. M. and Yount, J. C., 1981, Surface faulting along the Hilton Creek fault associated with the Mammoth Lakes, California earthquakes of May, 1980 (abs.): Earthquake Notes, v. 52, p. 45.

Clark, M. M., and Gillespie, A. R., 1981, Record of late Quaternary faulting along the Hilton Creek fault in the Sierra Nevada, California (abs.): Earthquake Notes, Eastern Section, v. 52, p. 46.

Title of Study - Aspects of the Late Holocene Behavior
of the San Andreas Fault System

Contract No. - 14-08-0001-18385

Principal Investigator - Kerry E. Sieh

Institution - California Institute of Technology
1201 E. California Blvd.
Pasadena, CA 91125
(213) 356-6115

This contract supported continuing investigations of the late Holocene behavior of the faults of the San Andreas fault system. The purpose of these studies has been to determine the long-term fault slip rates and the frequencies and spatial relationships of large earthquakes along the faults. Such information may lead to forecasts of the location, time, and size of future large earthquakes along the fault.

During 1980, work progressed as outlined below:

1) A new series of radiocarbon dates from Pallett Creek (locality 2, Fig. 1) is enabling a more accurate determination of the dates of the 9 to 13 prehistoric earthquakes recorded in the late Holocene sediments there. The average recurrence interval is somewhere between 125 and 225 years. Variations among actual intervals are difficult to assess, in part because of imprecisions of the ^{14}C dates.

2) A program of three-dimensional excavations begun last summer at Pallett Creek (see 1979 Final Technical Report) has resulted in documentation of right-lateral offsets that increase with with age. Also, a complex pattern of evolution of faulting and other deformation is emerging.

3) New analyses of radiocarbon dates from Wallace Creek (locality 3, Fig. 1) suggest that 64 mm/yr is an upper limit on the Holocene slip rate for the San Andreas fault there. Analysis of this and older data reported at the end of 1979 indicate that the slip rate is between 34 and 64 mm/yr. These rates lead to the conclusion that great earthquakes occur on the average every 140 to 270 years at Wallace Creek. One implication of this fast slip rate is that plate motions are accumulating more rapidly than they are being relieved along the creeping segment of the fault to the north. We may therefore expect the creeping segment to generate large earthquakes as well as creep. This also raises the possibility of continuous seismic rupture of the northern, central and south-central segments of the fault (see Fig. 1).

4) Surficial and subsurficial geologic mapping along the San Andreas fault near Indio (locality 1 on Fig. 1) began to reveal the prehistoric behavior of the historically dormant segment of the fault. Apparently, no large slip events have occurred at the site for at least the past 480 and perhaps the past 680 years. About 1 m of strike-slip has occurred during this time period, however. It may be associated with one or more moderate earthquakes or aseismic creep.

5) Howard Shifflett's studies of offset cultural features along the creeping segment of the fault (locality 4, Fig. 1) aimed at discovering variation in slip rate(s) during the past 100 years are progressing, but we have no conclusive results to report yet.

6) Ray Weldon has continued his studies of the Lost Lake terraces along the fault near Cajon Pass (locality 6, Fig. 1). Last year's final report, which described Weldon's work there during 1979, outlined his tentative evidence for a Holocene slip rate of 2 to 2-1/2 cm/yr at this site. Subsurface work this year provided additional samples that will confirm or modify this range of values. He has also identified several late Holocene colluvial deposits, each of which may represent one seismic event. ^{14}C dates of samples related to these deposits are not yet determined.

7) Surficial and subsurficial studies of earthquake recurrence at my site along the San Jacinto fault zone in San Bernardino (locality 7, Fig. 1) were partially successful. Flooding of the site forced termination of the work in late January. Resumption of work may be permanently prevented by construction of a housing development at the site. Data in hand indicates an average recurrence interval of $\lesssim$800 years.

8) My work with Kristian Meisling on the effect of the 1857 earthquake on trees was published in the Journal of Geophysical Research (June, 1980). Now that it is clear that tree rings do record a known, historical seismic event, Don Piepgras and I have collected many cores and slabs from very old trees near the fault in an attempt to discover the exact year of the youngest large prehistoric event.

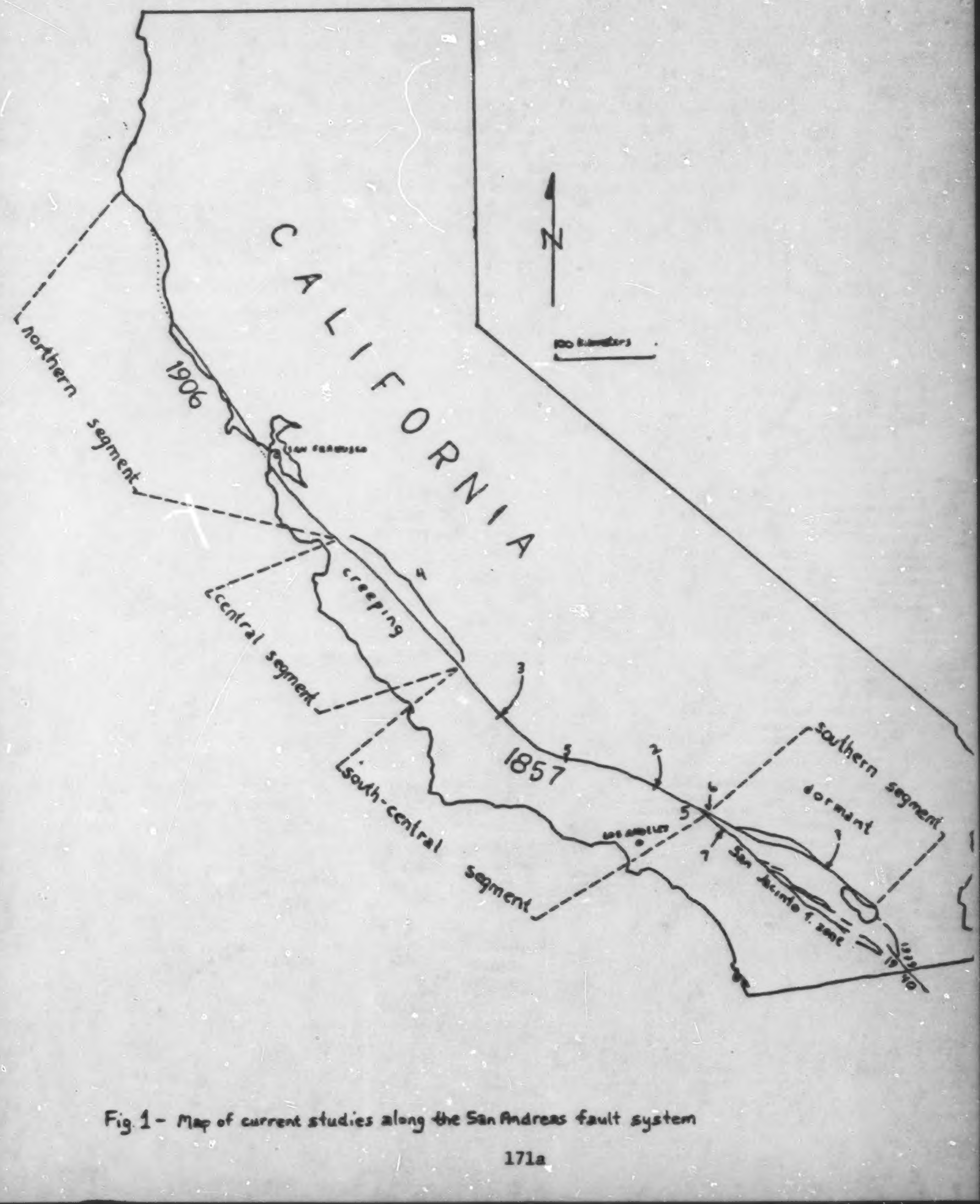
CALIFORNIA
N
100 kilometers
SAN FRANCISCO
LOS ANGELES
1906
1857
northern segment
creeping
central segment
south-central segment
southern segment
dormant
San Jacinto f. zone
1
2
3
4
5
6
7
19
40

Fig. 1 - Map of current studies along the San Andreas fault system

Quarternary Reference Core, Clear Lake, California

9950-02394

John D. Sims
Branch of Earthquake Tectonics and Risk Analysis
U.S. Geological Survey
345 Middlefield Road
Menlo Park, California 94025
(415) 323-8111, ext. 2252 or 2159

Investigations

1. Sedimentological and stratigraphic studies of core CL-80-1 from Clear Lake taken in July and August 1980.

2. Distribution of samples for initiation of geochemical and paleontological studies on core CL-80-1.

3. Completion of subsampling and preliminary sedimentological and stratigraphic studies on core CL-80-2 from Clear Lake taken in August 1980.

Results

1. The sediments cored at site CL-80-1 have been characterized by determining bulk density and weight loss on drying and ignition. Stratigraphic studies have yielded a preliminary tephra distribution in the section as well as a preliminalry palynological zonation of the core. Volumetric samples taken at about 2 m intervals were weighed, dried at 105°C for 8 hrs, and ashed at 550°C and 950°C for 4 hr each for analysis of bulk density, water content, and organic and inorganic carbon content.

Sample density increases with depth in core CL-80-1 from about 1.3 to 2.99 gm cm in the upper 90 m of the core. Below 90 m, however, density values have no clearcut trend but appear to generally decrease linearly from the about 2.0 gm cm at 90 m to a minimum of 1.24 gm cm at 129.5 m. Density values again increase in a generally linear trend between about 140 and 168 m (fig. 1).

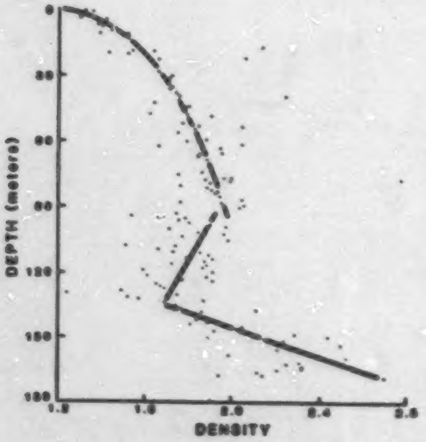

Figure 1. Density versus depth plot for core CL-80-1. Line segments are visual estimates of trends in the data. The curved line segment suggests the trend for the upper 90 m and is defined by the logarithmic function $Y = -91.96 + 262.04 \ln X$. The straight line segment that suggests the trend for the interval between 95 and 135 m is defined by the function $Y = 489.85 - 205.27X$. The straight line segment that suggests the trend for the interval between 140 and 165 m is defined by the function $Y = 90.19 + 28.95X$.

Weight loss on drying at 105°C records water content of the sediment. These values are highest in the upper 10 m of the core where they average about 76 percent. Between 10 and 28 m the water content decreases rapidly to about 56 percent. Below 28 m there is a gradual linear decline in the water content to about 17 percent at 168.5 m. The local extreme variations in water content in figure 5 are due to local differences in lithology. Such differences are usually the contrast between silt and clay lamina and the resulting pore volume changes.

Organic and inorganic carbon contents are generally constant throughout the core, ranging from 2 to 12 percent for organic carbon and from a trace to about 4 percent for inorganic carbon. Extreme values are due to samples taken in localized slightly organic-rich horizons such as at 76.14 m, which is a concentration of ostracod tests in a cemented zone. One series of samples between 125 and 130 m shows a consistently high organic carbon content with values ranging between 5 and 7 percent and an inorganic carbon content with values ranging from 2 to 4 percent.

Stratigraphic studies show the variation in oak and pine pollen through time (fig. 2) and allow a preliminary biostratigraphic zonation. The zonation is proposed by Adam, Sims, and Throckmorton (in press) and is correlated to ^{18}O stages determined in cores from ocean basins.

The pollen record from cores CL-80-1 and CL-73-4 are the longest continuous pollen records yet reported from the North American continent. Clear Lake is near the windward edge of the continent, several hundred kilometers south of the maximum extent of continental ice sheets, thus the cores do not reflect local climatic effects produced by nearby ice fields. The core sites are presently about 3 km from land and have apparently been so throughout the deposition of the sediments. Thus the influence of local vegetation on the pollen rain is minimal.

The pollen curves show good agreement with the deep-sea oxygen isotope record, the long pollen record from Grande Pile in France, and a composite vegetational sequence for the Netherlands (Adam, Sims and Throckmorton, in press). Because the sedimentation rate is higher at Clear Lake than at either Grande Pile or the deep-sea sites that have been studied, many details are preserved in the Clear Lake records that are obscure or absent at sites with lower sedimentation rates.

Evidence for major climatic fluctuations early in the last glacial cycle has been available for many years, but the available pollen sections generally cover only a small part of the interval between the last interglacial and the full development of continental glaciation. Because the time period involved is at or beyond the limits of radiocarbon dating, the correlations between the various sections studied were not clear. Only with the availability of continuous pollen records spanning the time from the last interglacial to the present, such as those from Grande Pile and Clear Lake, can the correlation of the shorter pollen records be firmly placed in broader context.

Age assignments for core CL-80-1 are based on previous studies (Sims, 1976; Sims, Adam and Rymer 1981, and Adam, Sims, and Throckmorton, 1981) allow the age of the bottom of the core to be estimated at about 175,000 to 200,000 years (fig. 3). The deeper penetration of cores CL-80-1 and CL-80-2 as well as their correlations with earlier cores also allow preliminary paleographic reconstructions of the phases of ancient Clear Lake (fig. 4).

The success of both the Clear Lake and Grande Pile cores demonstrates that it is both possible and desirable to obtain long, continuous pollen records from continental deposits and that such records can be correlated over long distances. Once a few long records from near-glaciated regions can be related to the available glacial chronologies, the interpretation of long records from unglaciated regions will be simplified. Although the study of relatively short pollen records in old deposits will remain important, the development of long, continuous pollen records is now of critical significance for understanding both climatic history and climatic change.

2. Subsamples, taken from core CL-80-1 at the field laboratory for diatom and ostracod analyses have been distributed to J. Plat Bradbury and Rick Forester (both U.S.G.S.), respectively. Subsamples for organic geochemistry, plant pigments and inorganic major-element geochemistry have been distributed to John Sanger (Ohio Wesleyan University) and Walter Dean (U.S.G.S.) for the individual studies. Size and clay mineralogy analyses are in progress.

3. Core CL-80-2 has been split, described radiographed and subsampled. Bulk density determinations and weight loss on drying and ignition studies are complete. The radiographs have been interpreted and the report describing the preliminary physical stratigraphy and sedimentology with a catalog of subsamples is in preparation.

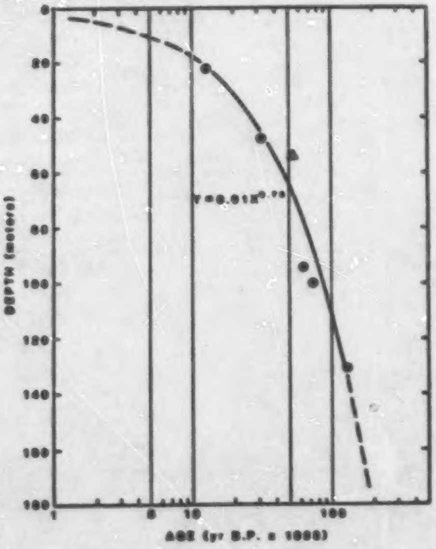

Figure 3. Preliminary age-depth relationships in core CL-80-1. Points A through E are determined from palynological analysis of core CL-80-1 and represent major changes in oak pollen frequency that also occur in core CL-73-4 and which are correlated with the ^{18}O-stage boundaries in deep sea cores (Hayes and others, 1976). (A) ^{18}O-stage 1-2 boundary, (B) ^{18}O-stage 2-3 boundary, (C) ^{18}O-stage 3-4 boundary, (D) ^{18}O-stage 4-5 boundary. (E) ^{18}O-stage 5-6 boundary (L. E. Heusser, written commun., 1980). Triangle is from correlation with a distinctive ash bed present in both cores and dated by amino acid racemization ratios at 59,000 ± 13,000 yr B.P. (Blunt and others, in press).

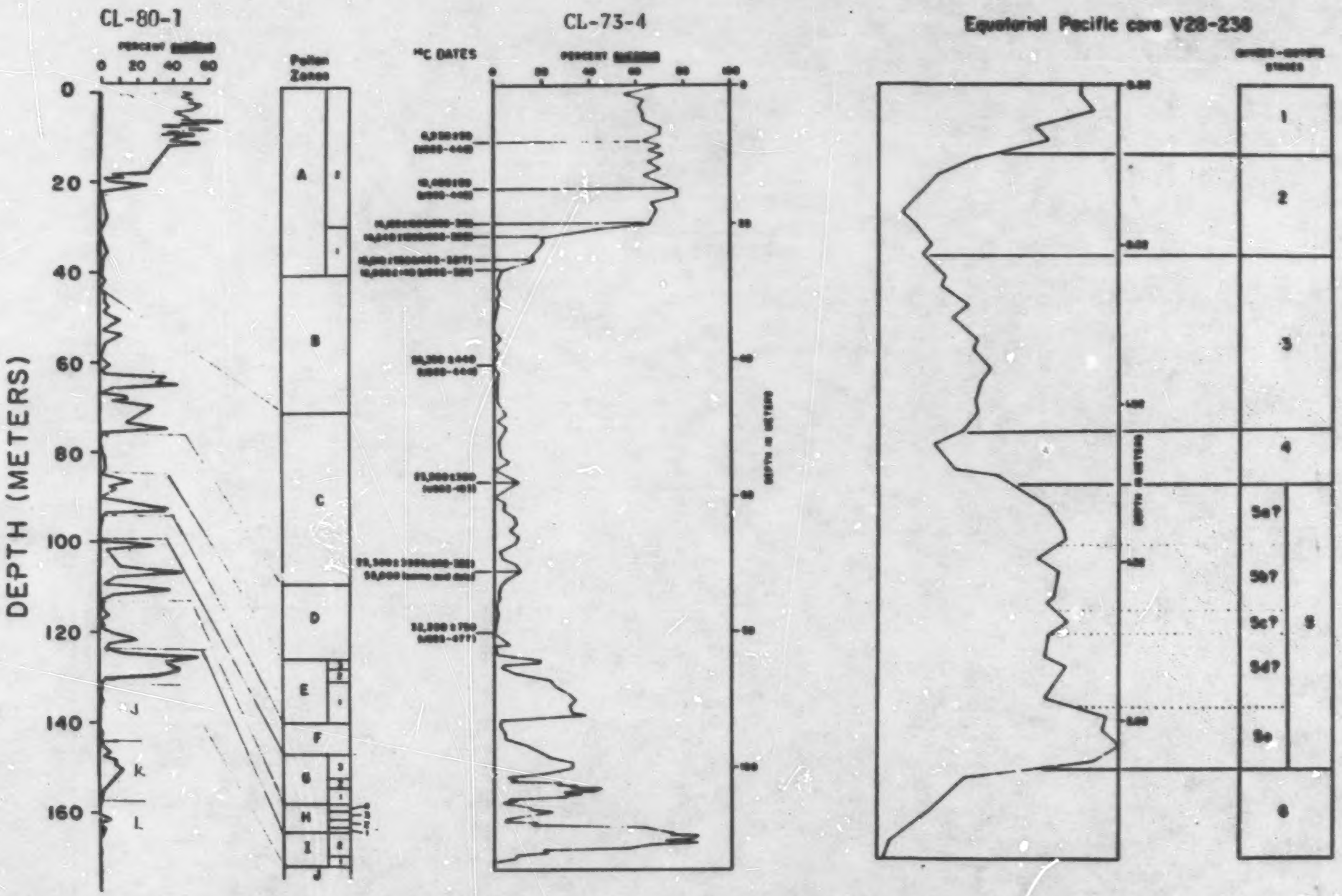

Figure 2. Tentative correlation of core CL-80-1 with pollen zones determined for core CL-73-4 in Clear Lake (Adam, Sims, and Throckmorton, in press). Equatorial Pacific core V28-238 with ^{18}O-stage boundaries is plotted at the same scale as core CL-73-4 for comparison of the oak-pollen curve with the ^{18}O curve.

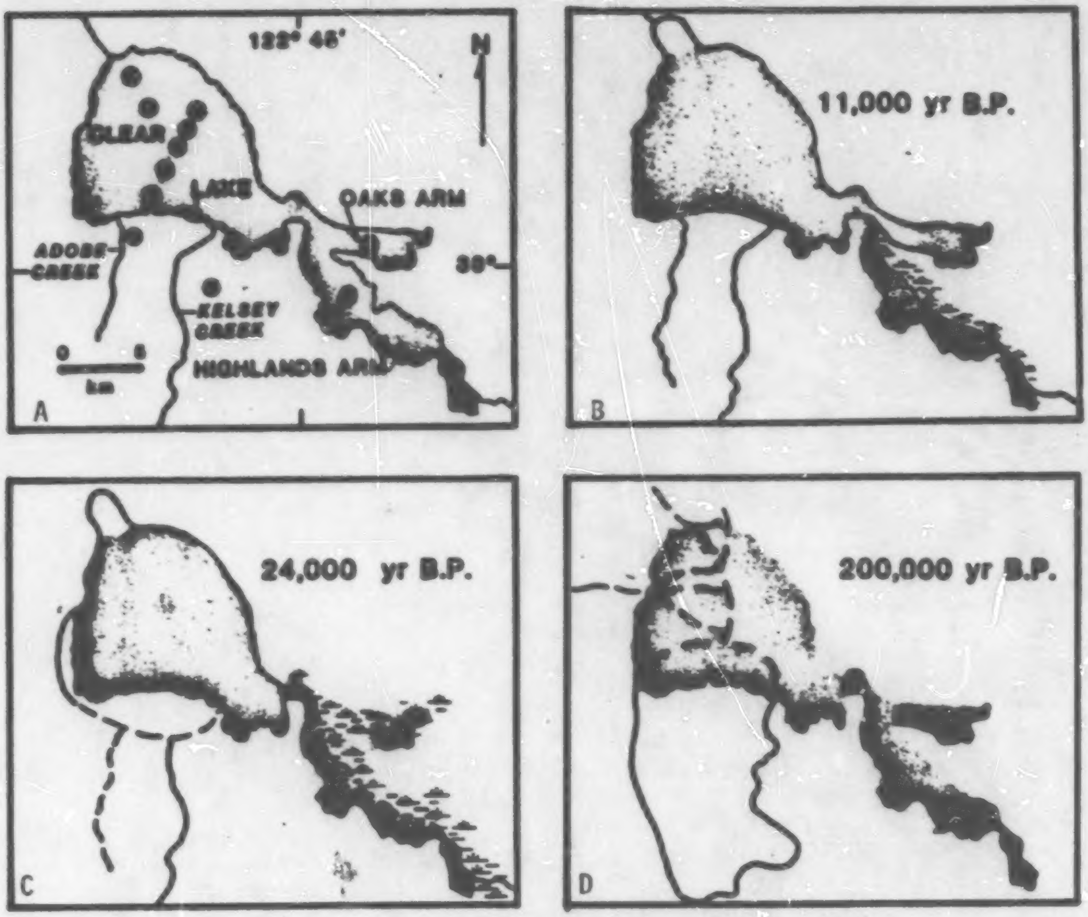
122° 45'
N
CLEAR
LAKE
OAKS ARM
ADOBE CREEK
39°
KELSEY CREEK
0 5
km
HIGHLANDS ARM
A
11,000 yr B.P.
B
24,000 yr B.P.
C
200,000 yr B.P.
D

Figure 4. Paleogeographic reconstruction of Clear Lake for the late Pleistocene. A) Present day lake ans location of cores taken in the lake in 1973 and 1980, and two deep water wells on land south of the lake. B) Clear Lake paleogeography about 11,000 yr B.P., with the Highlands Arm a swamp (water depth <2 m). C) Clear Lake about 24,000 yr B.P., with both the Highlands and Oaks arms swamp areas. D) Clear Lake about 200,000 yr B.P., with westerly derived alluvial fans dominating the area of the present day lake basin. Lacustrine deposition is centered in the outcrop area of the Kelseyville Formation(Rymer, 1981).

Reports

Adam, D. P., Sims, J. D., and Throckmorton, C. K., in press, A 130,000-year continuous pollen record from Clear Lake, Lake County, California: Geology, v. , p. .

Ager, T. A., and Sims, J. D., 1981, Holocene pollen and sediment record from Tangle Lakes area, central Alaska: Palynology, v. 5, p. 85-98.

Blunt, D. J., Kvenvolden, K. A., and Sims, J. D., in press, Amino acid dating of sediments from Clear Lake, California: Geology, v. , p. .

Heuser, L. E., and Sims, J. D., 1981, Palynology of core CL-80-1, Clear Lake, California: Geological Society of America Abstracts with Programs, v. 13, p. 61.

Liddicoat, J. C., Sims, J. D., and Bridge, W. D., 1981, Paleomagnetism of a 177-m-long core from Clear Lake, California: Geological Society of America Abstracts with Programs, v. 13, p. 67.

Rymer, M. J., Sims, J. D., Hedel, C. W., Bridge, W. D., Makdisi, R. S., and Mannshardt, G. A., 1981, Sample Catalog for core CL-80-1, Clear Lake, California: U.S. Geological Survey Open-File Report 81-245, 53 p.

Sims, J. D., Adam, D. P., and Rymer, M. J., 1981, Late Pleistocene stratigraphy and palynology of Clear Lake, Lake County, California in McLaughlin, R. J., and Donnelly-Nolan, J. M., Research in the Geysers-Clear Lake Geothermal Area: U.S. Geological Survey Prof. Paper 1141.

Sims, J. D., and Rymer, M. J., 1981, Deep coring of Quaternary Sediment in Clear Lake, California: Geological Society of America Abstracts with Programs, v. 13, p. 106.

Sims, J. D., Rymer, M. J., Flora, L. A., and Perkins, J. A., 1981, Description and preliminary interpretations o core CL-80-2, Clear Lake, Lake County, California: U.S. Geological Survey Open-File Report 81- , p.

Sims, Rymer, M. J., and Perkins, J. A., 1981, Description and preliminary interpretations of core CL-80-1, Clear Lake, Lake County, California: U.S. Geological Survey Open-File Report 81- , p. .

H5

Detailed Geologic Studies: San Andreas Fault Zone

9950-01294

John D. Sims
Branch of Earthquake Tectonics and Risk Analysis
U.S. Geological Survey
345 Middlefield Road, M/S 77
Menlo Park, California 94025
(415) 323-8111, ext. 2252 or 2159

Investigations

1. Detailed mapping of structure and surficial and bedrock deposits in the Bickmore Canyon Quadrangle (Perkins).

2. Detailed mapping of structure and surficial and bedrock deposits in the Monarch Peak, Hepsadam Peak and Priest Valley quadrangles (Rymer).

3. Detailed mapping of structure and surficial and bedrock deposits in the Cholame Valley quadrangle (Sims).

Results

1. Geologic mapping of the San Andreas fault zone in the Bickmore Canyon quadrangle at a scale of 1:24,000 reveals the San Andreas fault zone has an average width of approximately 1-1.5 km. A single main trace is found throughout the area mapped, and its shear zone varies in width from a few meters to many tens of meters. The main trace offsets all three Holocene terrace deposits mapped along the San Benito River. Numerous subparallel subsidiary faults are found within the fault zone. Most of the subsidiary faults occur in the Plio-Pleistocene(?) unconsolidated gravels present southwest of the fault zone. Geomorphic expression of these subsidiary faults suggests recent activity. Rock units found along the southwest portion of the fault zone consist of: unconsolidated granitic and volcanic gravels, Paso Robles Formation, and Monterey Shale. Rock units found along the northeast portion of the fault zone consist of: San Benito Gravels, Etchegoin Formation, Santa Margarita Formation, and a thin band of serpentinite. Marble breccia and chert, possibly derived from the Franciscan Assemblage, are found locally within the shear zone of the main trace. Landslide deposits cover approximately 10 percent of the area mapped.

2. Mapping at a scale of 1:12,000 the San Andreas fault zone along Mustang Ridge, San Benito and Monterey Counties, suggests that the main trace is located in a wedge-shaped diapir of Franciscan assemblage lithologies and serpentinite. The diapir is delineated by boundary faults subparallel to parallel to the San Andreas Fault and is assymetrical, with steeper dips on the southwest side. Dips of the boundary fault on the northeast side of the diapir range from 20° to 40° and dips on the southeast side range from 45° to 80°. The Franciscan assemblage in the area mapped is a melange of greywacke,

chert, greenstone, shale, blueschist and limestone. Locally, serpentinite and diabase are thoroughly mixed with rocks of the Franciscan assemblage, suggesting that both serpentinite and the Franciscan assemblage have been in close proximity for a long time. This latter relationship suggests that the presence of the serpentinite is not the result of recent thrusting from the east.

3. Geologic mapping of the San Andreas fault zone in the Cholame Hills, Cholame Valley, and Cholame 7-1/2 minute quadrangles has been limited to photogeologic studies with fieldwork to begin in May on the Cholame Valley quadrangle. The photogeology has been used for inventory of and familiarization with recent breaks and their associated geomorphic features as mapped by Brown (1970). The photogeology has been extended to Holocene terrace identification and mapping in the drainage of Cholame Creek and its tributaries in and near the fault zone.

Reports

None.

Tectonic Analysis of Active Faults

9900-01270

Robert E. Wallace
Office of Earthquake Studies
345 Middlefield Road, MS 77
Menlo Park, California 94025
(415) 323-8111, ext. 2751

Investigations

1. Analysis of fault scarp data in northcentral Nevada and overview analysis of paleoseismicity and tectonics of the Basin and Range province.

2. Evaluation of fault scarps in the Stillwater "Gap" to see if the gap is characterized by different recurrence intervals than the adjacent fault zones that broke in 1915 and 1954. Faults in the gap may be more permanently locked, or they may be nearing a rupture point.

3. Repeated measurements of erosion nets established on selected fault scarps to determine rate, pattern, and processes of erosion of scarps.

4. Evaluation of lichenometery techniques for dating prehistoric events along fault scarps.

Results

1. Iron spikes and metal fence posts were placed in various patterns across and along several fault scarps in 1979 to establish the position of the ground surface at that time. The effects of erosion were measured in 1980 and will be remeasured at least annually. The crest of the 1915 fault scarp in Pleasant Valley, Nevada had retreated 21 cm in the one-year period from 1979 to 1980. The rate of 21 cm/yr is high compared to a rate of retreat of 9-10 cm/yr estimated for the period since 1915 when the scarp was formed.

The surface on a scarp of Holocene age near Imlay, Nevada had lowered by between 0.8 and 2 cm at 6 spikes in the one year, 1979 to 1980. At one spike the ground surface had built up by 0.5 cm. The average rate of erosion seems high compared to slope-decline rates estimated during Holocene (10,000± yrs) time. The one-year interval is undoubtedly too short as a basis for extrapolating back thousands of years.

2. Observations in the field during thaws in winter time and during summer rain storms suggest that one of the most important agents of erosion is a mudflow process triggered by freeze-thaw cycles which number more than 120 per year in this part of Nevada. Patches of ground from a few m^2 to 100^2 m liquefy and flow when the morning sun hits them after a night of freezing temperatures.

3. Janet Hoare and Harry Thiers of the Department of Botany, San Francisco State University are evaluating the use of lichenometry for dating relatively recent, but prehistoric, events. For example, three distinct sets of boulders have rolled from the range front at a site along the 1915 scarp, presumably triggered by earthquake shaking. One set of boulders apparently relates to the 1915 earthquake. On the basis of growth rates of Lecidea atrobrunnea, which grow on the boulders, the next older set of boulders may have been thrown down 300-500 years ago. The oldest set of boulders has not been dated yet.

No other earthquake as young as 300-500 years has been indicated by other data along the fault that produced the 1915 scarp, but scarps along the northwest flanks of both the Shoshone Range and the Cortez Mts (only the northernmost 11 km of range front) may be that young. Possibly ground shaking generated by earthquakes along those fault segments could have triggered the boulder fall along the Tobin Range.

Reports

Wallace, R. E., Davis, J. F., and McNally, K. C., 1981, Suggested terminology for expressing earthquake potential and probability [abs.]: Seismological Socity of America Annual Meeting, Berkeley, CA, March 1981

Wallace, R. E., 1981, G. K. Gilbert's studies of faults, scarps and earthquakes: in Geological Society of America Special Paper 183,, E. L. Yochelson, ed., p. 35-44.

Wallace, R. E., 1981, Active faults, paleoseismology and earthquake hazards in the western United States: in Proceedings Volume, Fourth Ewing Symposium, Earthquake Prediction (in press).

EARTHQUAKE HAZARDS ASSOCIATED WITH THE VERDUGO-EAGLE ROCK AND BENEDICT CANYON FAULT ZONES, LOS ANGELES COUNTY, CALIFORNIA

14-08-0001-18245

F. Harold Weber, Jr.

California Division of Mines and Geology
1416 Ninth Street, Room 1341
Sacramento, California 95814
(213) 620-3560

The Verdugo, Eagle Rock and San Rafael fault zones compose a system of faults about 32 km in length that extends southeasterly from the south edge of the Pacoima Hills at the north edge of the San Fernando Valley to Pasadena where the San Rafael fault apparently terminates against the Raymond fault zone. Faults of the system generally separate pre-Late Cretaceous igneous and metamorphic rocks of the Verdugo Mountains and San Rafael Hills on the northeast side from Cenozoic sedimentary rocks and sediments of the San Fernando Valley and other lowlands on the southwest. At the northwest end of the system, the Verdugo fault probably bends westward and joins the Mission Hills fault zone, although it may be truncated by an east-trending fault (not recognized at the ground surface) which lies between the Mission Hills and Northridge Hills faults.

Faults of the Verdugo - Eagle Rock - San Rafael system dip gently to steeply northward, but only along the west part of the Eagle Rock fault are dips well-defined (15-30° north). The most active segment of the system may be the Verdugo fault between Verdugo Wash on the southeast and Big Tujunga Wash on the northwest, a distance of 20 km. Along this segment of the Verdugo fault, well-defined south-facing breaks in slope in the uppermost part of alluvial fans of late Quaternary (including Holocene) age in the Burbank - west Glendale area bordering the Verdugo Mountains apparently are relatively youthful fault scarps. These scarps are 2 or slightly more meters in height but the details of their morphology have been obliterated by development in this area. These scarps not only lie at the base of the steepest and highest part of the Verdugo Mountains but they also coincide with a steep gravity gradient. Northwest of these scarps, in the Sun Valley area, a sand and gravel pit along the zone once exposed minor faults cutting very late Quaternary sand and gravel deposits of Big Tujunga Wash at a depth of nearly 45 m beneath the ground surface. These faults are now covered by fill.

The Benedict Canyon fault zone trends diagonally eastward through the Santa Monica Mountains and along the north edge of the easternmost part of the mountains, at the south edge of the easternmost part of the San Fernando Valley, and extends eastward toward the Eagle Rock fault zone. The fault is part of the Hollywood - Santa Monica - Raymond system. No surface evidence was found during this study for evaluating the recency of activity of the Benedict Canyon fault zone. The only evidence for relatively recent movement along it occurs in the subsurface slightly east of the Santa Monica Mountains where the very gently north-sloping base of apparently youthful ground water-bearing sediments is offset downward relatively to the north about 125 m, based on differences in total depth of alluvial deposits in two nearby water wells. The fault in this vicinity coincides with a steep north-dipping gravity gradient. No remnants of scarps or other surface features of faulting are preserved in this part of the Los Angeles River drainage which has been in a state of rapid aggradation during Holocene time.

This system of east-trending faults made up by the Hollywood, Santa Monica and Raymond faults in the study area contains many surface features which indicate that it has been active during latest Quaternary (probably Holocene) time. Especially noteworthy are east-trending, south-facing breaks in slope as high as 2-3 m that occur along the Hollywood fault in the Atwater - Glassell Park area, which is underlain by Holocene floodplain deposits adjacent to the Los Angeles River Channel. These apparent scarps occur approximately above alluvial beds that are depicted in a cross section by Williams and Wilder (1971) to be offset downward relatively on the south side of a subsurface fault about 35 m.

Based on offset alluvial sediments and other geologic evidence, both the Verdugo and Hollywood fault zones are judged to have been active during very late Quaternary (including Holocene) time. The fact that scarps 2-3 meters high are preserved in youthful alluvial sediments in a relatively humid climate with rapid alluviation caused by voluminous sediment runoff from the nearby mountains during heavy rains at least one winter in every 10 or 15 years is considered to be ample proof that the faults have been active in latest Quaternary time. Also apparent is that geomorphic features indicating very late Quaternary movement are more abundant, more pronounced and better preserved along the eastern Hollywood and western Raymond fault zone than they are along the Verdugo, Eagle Rock and San Rafael fault zones. Accordingly, it appears that, overall, the features along the former fautls are the result of large and/or more frequent earthquakes than those of the latter faults.

In addition, relatively recent tectonic activity in the study area is suggested by localized changes in elevation disclosed by the precision survey net of the City of Los Angeles. For example, repeated surveys by the City of Los Angeles disclose that a subsidence trough extends eastward through the North Hollywood area of the San Fernando Valley. This trough occurs over a gravity low and may be the result of tectonic downdropping between two concealed fauts or along a syncline, perhaps accentuated by the withdrawal of ground water. Also, additional tectonic features, possibly active in latest Quaternary time, are inferred from geologic, gravity, ground water and elevation change data to lie beneath the alluvial surface of the eastern San Fernando Valley.

More precise zones of possible fault rupture during future earthquakes than is known by the present mapping could be delineated by very detailed field mapping along faults of the study area. Such mapping would consist of a very careful amalgamation at large scale of geologic, elevation change, ground water and geophysical data, augmented by trenching. Targets especially important for such future projects are the Verdugo fault zone in the Glendale-Burbank area and the eastern Hollywood - western Raymond fault zones in the Hollywood - Glassell Park - Highland Park areas. Features of surface faulting in these areas are well-developed; and the areas are especially populous and contain many high-rise buildings, schools, hospitals and older, especially earthquake-prone buildings. New buildings will continue to be constructed as older areas are redeveloped. Additional targets of such analysis of surface features of faulting could be the Northridge Hills and other known and possible faults of the San Fernando Valley.

Reference:

Williams, D. E., and Wilder, D.G., 1971, Gasoline pollution of a ground-water reservoir - case history: Groundwater, v. 9, no. 6, p. 50-56.

H5

Geologic Consultants
Weber and Associates

GEOLOGIC INVESTIGATION OF THE MARINE TERRACES OF THE SAN SIMEON REGION AND PLEISTOCENE ACTIVITY ON THE SAN SIMEON FAULT ZONE, SAN LUIS OBISPO COUNTY, CALIFORNIA

14-08-0001-18230

GERALD E. WEBER
WEBER AND ASSOCIATES
1729 SEABRIGHT AVENUE
SANTA CRUZ, CALIFORNIA 95062
(408) 426-9255

INVESTIGATIONS:

The object of this study is to determine the late Pleistocene history of movement along the San Simeon fault zone. This includes determination of rates of movement, style of deformation, recurrence intervals for faulting, and the most recent episode of fault movement on both the fault zone as a whole, and on individual faults within the zone.

We hope to achieve these goals through detailed field mapping of the marine terrace sequence and the fault zone from the Cape San Martin area south to Cayucos. If terraces in the terrace sequence can be correlated between the major fault blocks and across the fault zone, we can estimate the magnitude of the vertical and horizontal components of motion along the fault and the rates of motion.

RESULTS:

1) The complexity of the fault zone is greater than previously recognized. Between six and ten complexly anastamosing fault strands transect the coastline between the mouth of Carpoforo Creek and San Simeon Point. The fault zone is widest to the northwest (approximately 2 miles wide) with the faults converging to the southeast into a zone less than 1000 feet wide near San Simeon Cove.

2) The movement along apparent principal displacement faults (San Simeon, Arroyo Laguna, and Arroyo del Oso) appears to be a combination of right lateral and normal, with the southwest side upthrown. Reverse faulting is locally present along the Arroyo del Oso fault where fault strands are oriented in a more east-west direction. The dominant southwest side up movement has formed a 250 foot high, erosionally modified northeast facing fault scarp along the Arroyo Laguna and San Simeon faults.

3) Northeast of the fault zone are four well developed marine terraces and possibly a fifth, ranging in shoreline angle elevation from 80 feet to 650 feet above sea level. The lowest terrace consists of two seperate abrasional platforms, the older and higher of which correlates with the dated terrace at Cayucos. These terraces are relatively undeformed, exhibiting only a few broad warps between San Simeon and Cayucos.

4) Numerous terraces are present in the intensely faulted area within the fault zone. However, it has been impossible to correlate with confidence these terrace remnants with those either to the northeast or southwest of the fault zone.

5) Three terraces, including a broad lower terrace with two abrasional platforms, are present southwest of the San Simeon fault zone. The lowest terrace can be confidently correlated with the lowest terrace northeast of the fault, but the higher terraces cannot be correlated simply.

6) Although correlations are uncertain, we would suggest an average right lateral movement rate of 0.5 to 1.0 cm per year for the San Simeon fault zone during middle and late Pleistocene time.

7) In the seacliffs at San Simeon Cove, a strand of either the Arroyo Laguna or San Simeon fault offsets weakly cemented aeolian deposits of probable Holocene age. Other faults in the fault zone appear to have smaller amounts of total offset and have not moved as recently as the Arroyo Laguna and San Simeon faults.

Subsurface Geology of the San Gabriel, Holser, and Simi-Santa Rosa Faults, Transverse Ranges, California

14-08-0001-19138

Robert S. Yeats, Principal Investigator
Leonard T. Stitt
David Hanson
Department of Geology
Oregon State University
Corvallis, Oregon 97331
(503) 754-2484

Investigations

1. Completed surface geologic map, structural cross-sections, and structure contour maps of the eastern half of the Simi fault. Report now being reviewed.

2. Continued construction of cross sections on the Holser fault and across the San Gabriel fault north of its intersection with the Holser fault.

3. Acquired two trench logs by Geotechnical Consultants across the Camarillo fault, near the western end of the Simi fault system in the city of Camarillo.

Results

1. Several authors have proposed large-scale lateral motion on the Simi fault system, either by right-lateral or by left-lateral strike slip. Electric-log markers in the Sespe Formation may be correlated directly across the Simi fault, indicating that lateral displacement, if present at all, is no more than a few kilometers. The Llajas Formation of Eocene age grades westward from shallow-marine strata to proximal turbidites near the western end of the Simi Hills outcrop belt south of the Simi fault. A similar westward gradation to proximal turbidites is documented north of the Simi fault between the Strathearn oil field and the Marathon Vail 1 well, where the turbidites occur. Eocene facies boundaries do not show major lateral displacement.

2. Much of the displacement on the Simi fault in the Simi Valley is pre-Quaternary (pre-Saugus) in age. This can be determined because near the eastern edge of the Simi Valley, the fault divides into pre-Quaternary and late Quaternary splays. The late Quaternary fault, marked by a well-defined although moderately eroded scarp at

the northern edge of the Simi Valley, ends near the eastern edge of the valley. The older faults include both south-dipping faults of the Brugher and Frew types and north-dipping faults of the Torrey type. Farther west, the C.D.L.B. fault is unconformably overlain by the Saugus Formation, and the Strathearn fault may also be pre-Saugus.

3. There is no evidence for Holocene displacement on the Simi fault. In the Tierra Rejada Valley, surface mapping suggests that uplifted, dissected older alluvium overlies and is not displaced by the Simi fault. However, the Simi fault does appear to cut older alluvium just east of Tapo Canyon.

4. The Camarillo fault marks the south side of a narrow, west-trending ridge south of downtown Camarillo. M.C. Jakes, in an earlier semi-annual report, showed that the fault displaces aquifers within the Saugus by 150 feet and uplifts and apparently warps older alluvium on the west-trending ridge. Two trenches were dug by Geotechnical Consultants, Inc. across the southern edge of this ridge to determine the effect of the Camarillo fault on Pleistocene deposits. At the north end of the trenches, on the south side of the hill, Saugus Formation dipping 40° to 43°S is overlain concordantly by older alluvium which dips up to 36°S. Dip in the older alluvium decreases southward away from the hill front, and the older alluvium is overlain concordantly in one of the trenches by deltaic sediments of the Oxnard Plain which dips 22°S near the contact and 2°S near the south end of the longest trench. Except for the 2° dips, the dips are steeper than the slope of the ground surface. The Saugus is cut by north- and south-dipping shear zones, and south-dipping reverse faults cut the older alluvium and the overlying deltaic sediments. The older alluvium is also cut by relatively uncommon north-dipping low-angle reverse faults. These are interpreted by us not as the surface trace of the Camarillo fault, but as minor faults associated with the monoclinal bending of these sediments across the subjacent Camarillo fault which does not reach the surface.

5. The Holser reverse fault dips south, and the dip of the fault appears to decrease with increasing depth. Possibly it becomes a bedding fault at depth. If so, it may pose only a minor seismic shaking hazard, even if it is shown to cut late Quaternary deposits.

Reports

Yeats, R.S., in press, Late Cenozoic structure of the Santa Susana fault zone, California: U.S. Geol. Survey Prof. Paper, Transverse Ranges.

Subsurface Geology of Potentially Active Faults in the Coastal Region between Goleta and Ventura, California

14-08-0001-19173

Robert S. Yeats, Principal Investigator
Patrick A. Jackson
Daniel Olson
Department of Geology
Oregon State University
Corvallis, Oregon 97331
(503) 754-2484

Investigations

1. Completed work on the Carpinteria basin and submitted it to U.S.G.S. for an open-file report.

2. Continued data collection and construction of cross sections in the Santa Barbara and Goleta basins.

Results

Faults in the coastal region can be classified according to their potential for seismic shaking hazard (Yeats and others, 1981). Faults which extend downward into rocks of high strength such as crystalline basement rocks are capable of generating large earthquakes because the rocks through which the fault passes are capable of storing a significant amount of elastic strain energy. In contrast, faults which flatten at depth and involve only low-strength sedimentary rocks would be expected to move aseismically or to produce smaller earthquakes because such faults are capable of storing much less elastic strain energy.

Seismically active faults such as the Red Mountain fault (Yeats and others, in press), 1971 San Fernando fault, and Newport-Inglewood fault show little or no seismicity near the surface, even though the San Fernando fault, for example, ruptured the ground surface in 1971. Seismicity is concentrated at depth, where rocks have high strength. If the major seismogenic thrust faults of the Transverse Ranges (Santa Susana, San Cayetano, Red Mountain) flatten with depth, as suggested by Yeats (1981), such faults may be divided into three domains according to their seismicity: (1) a near-surface domain, where the fault passes through low-strength sedimentary rocks, and strain release would be aseismic or by small earthquakes, (2) an intermediate domain, where the fault passes through high-strength rocks, and strain release would be by large, destructive earthquakes, and (3) a deep domain, where the fault passes through ductile basement rocks of low strength, and strain release would be aseismic.

The Carpinteria, Holloway, Rincon Creek, and Shepard Mesa reverse faults are south-dipping and probably become bedding faults at depth, similar to faults in the Ojai-Oakview and Timber-Orcutt Canyon areas to the east characterized by Yeats and others (1981) as having low ground-shaking potential. All four faults displace late Pleistocene alluvial fan material which overlies the Pleistocene Casitas Formation with angular unconformity. A marine terrace cut by the Carpinteria fault may be a western extension of the Punta Gorda terrace dated by amino-acid racemization as 45,000 ka. The Rincon Creek fault produces a north-facing scarp 2-3 m high on the sea floor south of Summerland.

Even though the Rincon Creek fault cuts late Quaternary deposits, it shows evidence of being folded in association with the Summerland Offshore anticline and the Red Mountain fault. The fault appears to be drag-folded as an accompaniment to motion on the subjacent Red Mountain fault. Folding by the Red Mountain fault and the degree of asymmetry of the Carpinteria basin increase eastward as separation on the Red Mountain fault increases. This implies that the Rincon Creek is a secondary fault, controlled by motion on the dominant Red Mountain fault.

The Arroyo Parida fault, like the Rincon Creek fault to the south, has the south side up, but unlike the Rincon Creek fault, it has normal separation and dips 60°-74°N. Relations in the Shell-Fithian 1 well, which cuts the fault in one and possibly two places, suggest that the fault steepens and may become a reverse fault at depth. One possibility is that the fault originally dipped south, like the Rincon Creek fault, but it was deformed during folding of the Carpinteria basin such that it now dips north near the surface. Trench logs indicate that in the town of Montecito, the fault cuts fanglomerate or older alluvium. Suggestions by others of lef-lateral separation on the Arroyo Parida fault are not supported by subsurface data: the subcrop of the Vaqueros Formation against the Pleistocene Casitas Formation shows no lateral separation along the fault.

The onshore Red Mountain fault dips 55° to 63°N, but offshore, the dip steepens to at least 85°N as separation diminishes. Because this is the only seismogenic north-dipping fault with subsurface control this far west, the 1978 Santa Barbara earthquake sequence should be re-examined to consider a fault with a very steep dip. If the earthquake fault dips 80°N, it may be Fault Y of Lee and others (1978) rather than a fault with surface trace farther south.

Reports

1. Yeats, R.S., 1981, Quaternary flake tectonics of the California Transverse Ranges: Geology, v. 9, p. 16-20.

2. Yeats, R.S., Clark, M.N., Keller, E.A., and Rockwell, T.K., 1981, Active fault hazard in southern California: Ground rupture versus seismic shaking: Geol. Soc. America Bulletin, v. 92.

3. Yeats, R.S., Lee, W.H.K., and Yerkes, R.F., in press, Geology and seismicity of the eastern Red Mountain fault, Ventura County, California. U.S. Geol. Survey Prof. Paper, Transverse Ranges.

Physical Constraints on Source of Ground Motion

9940-01915

D. J. Andrews
Branch of Ground Motion and Faulting
U.S. Geological Survey
345 Middlefield Road
Menlo Park, CA 94025
(415) 323 8111, ext. 2752

Investigations

1. Dynamic stochastic fault modeling.
2. Source spectra from coda waves of Mammoth Lakes sequence.

Results

Work has started to examine source spectra of events from the Mammoth Lakes earthquake sequence of 1980 using spectra of coda waves.

Report

Andrews, D. J., 1981, A stochastic fault model, 2. Time-dependent case: Submitted to Jour. Geophys. Research.

3-D Near-field Modeling and Strong Motion Predictions in a Layered Medium

9940-02674

Ralph J. Archuleta
Branch of Ground Motion and Faulting
U.S. Geological Survey
345 Middlefield Road, MS-77
Menlo Park, CA 94025
(415) 323-8111, Ext 2062

Results

As the final checks on our explanation for the large amplitude vertical accelerations recorded at some stations during the 1979 Imperial Valley earthquake, we have computed travel time curves for S-P conversions and synthetic vertical accelerations, S-P conversions are totally ruled out based on travel times. The computed synthetic acceleration records confirm our hypothesis that the large vertical accelerations probably result from slip after the rupture penetrates the sediments. We have relocated the hypocenter of the Imperial Valley earthquake. The new hypocenter is about 2.5 km closer to the US-Mexico border and 2.0 km shallower than the currently accepted hypocenter. The precise hypocenter and origin time may be refined with the inclusion of more S-wave data. At present, our hypocenter is at 115° 19.80W 32 39.50 N with a depth of 8.0 km and origin time of 23:16:54:40.

An analysis of source parameters for the 1980 Mammoth Lakes mainshock-aftershock sequence has almost been completed. The earthquakes we recorded span 6 orders of magnitude in seismic moment. The main conclusions are; (1) the earthquakes were primarily strike-slip on East-West planes; (2) the stress drops of earthquakes with $M_L \geq 3.0$ generally fall between 20 and 200 bars; (3) a main shock with $M_L \approx 6.3$ had a stress drop of 319 bars and produced peak horizontal accelerations of about 400 cm/sec^2 (instrument clipped at 375 cm/sec^2) at a hypocentral distance of 20 km and 90 cm/sec^2 at a hypocentral distance of 25 km; (4) the most surprising result was that 1×10^{21} dyne-cm is almost constant while the corner frequency for earthquakes with $M_0 > 1 \times 10^{21}$ dyne-cm systematically changes with M_0. The implication is that for the small earthquakes ($M_0 < 1 \times 10^{21}$ dyne-cm) the stress drop depends on the moment whereas for large earthquakes the stress drop is independent of moment.

Reports

Mueller, C., Spudich, P., Cranswick, E., and Archuleta, R., 1981, Preliminary analysis of digital seismograms from the Mammoth Lakes, California, earthquake sequence of May-June, 1980: U.S. Geological Survey Open File Report 81-155.

Cranswick, E., P. Spudich, C. Mueller, and R. Archuleta, 1980, Locations and source parameters of the 1980 Mammoth Lakes earthquake sequence: EOS, v. 61, p. 1040.

National Strong Motion Data Center

9940-02085

Lawrence M. Baker
Branch of Ground Motion and Faulting
U.S. Geological Survey
345 Middlefield Road, MS-77
Menlo Park, California 94025
(415) 323-8111, ext. 2982

Investigations

The National Strong Motion Data Center provides investigators with a convenient, state-of-the-art tool for studies of earthquake sources, wave propagation, ground response, and strong motion. Projects hosted include field investigations of major earthquakes, routine processing for permanent installations, and studies of synthetic earthquakes. Incoming field data is transferred to on-line disk storage from several digital playback units (through parallel and serial interfaces), from in-house digitizers (through cards or IBM-compatible floppy disks), and from outside sources (on 9-track magnetic tape). Using familiar, industry standard Fortran techniques, real and synthetic data are analyzed, printed on terminals and line-printers, or displayed on Tektronix graphics terminals and Versatec or CalComp plotters.

Results

The National Strong Motion Data Center consists of a Digital Equipment Corp. PDP-11/70 minicomputer and associated peripherals running under the vendor supplied real-time operating system, RSX-11M-PLUS. Center personnel are responsible for the maintenance of the system and preparation of applications software for the processing of strong motion records.

1. Hardware: The installation of additional dedicated serial lines from the PDP 11/70 to a terminal room in an adjoining office building has enabled the system to support up to 13 simultaneous users. Four existing editing terminals are being upgraded to perform both editing and graphics functions. An order has been placed for a direct memory access terminal interface, which will be utilized for faster interactive graphics, and will add 16 additional ports in all to the online terminal capacity.

An additional 128K words of core memory has been added, bringing the system total to 384K words (approximately 280K words available for user programs). An order has been placed for a solid state disk drive (a peripheral that appears like a disk to the CPU but responds as fast as core memory) which will be used for holding swapping space and heavily used libraries.

The arrival of two CDC 9766 disk drives has increased online storage capacity by 512M bytes, allowing users to maintain substantial datasets online. Previously, users were forced to wait for access to the RP04 disk pack in order to mount specific datasets.

The two TE16 tape drives (45 IPS, 1600 BPI) will be replaced by two STC 1953 tape drives (125 IPS, 6250 BPI) in the near future, which will help to alleviate both the amount of magnetic tape needed and the time required for disk backup operations.

2. Application software: The following programs were either developed or modified to run on the PDP-11/70:

PAL--Fast PDP-8 cross assembler for GEOS field recorder.
VIEWER--Interactive plotting interface capable of directing graphic output either to any graphics device or to a disk file for later off-line plotting.

Two subroutine packages were purchased: Programs for Digital Signal Processing from IEEE, which includes subroutines for filtering, interpolation, and decimation; and the IMSL Subroutine Library, which includes subroutines for integration, differentiation, and smoothing.

3. System software: The vendor supplied RSX-11M operating system was upgraded in December to RSX-11M-PLUS, which utilizes more features of the PDP-11/70 and added the following capabilities to the system: multiple batch streams for long, CPU-intensive jobs; support for sharing common memory areas among heavily used programs; and resource accounting to acquire resource usage statistics on a per-user basis.

The vendor-supplied networking software (DECNET) arrived and will be used to communicate with a PDP 11/34 running under RSX-11M. The 11/34 is located at Scripps, and will be used to monitor digital data telemetered from Anza in real time. Software is being developed to buffer the real-time data.

The following system software was written or modified:

CSH--Checkpoint space handler to show paging space information and to forcibly deallocate paging space from a disk.
TXTT17--Communications software for interfacing with the adjacent PDP-11/70 UNIX system.
GEOPLT--Comparison software to TXTT17 to allow the transfer of plotting files created under UNIX to be plotted on the CalComp plotter.
Virtual Disk Package--allows a file of any size to be created on a disk, and used as a separate disk.

Teleseismic Determination of Earthquake Source Parameters

9940-03011

John Boatwright
T. C. Hanks
Steve Hartzell
Branch of Ground Motion and Faulting
U.S. Geological Survey
345 Middlefield Road, MS-77
Menlo Park, CA 94025
(415) 323-8111, exts. 2063, 2184, 2133

Investigations:

1. A technique has been developed which combines the information in the long and short period WWSSN records (simultaneous deconvolution), thereby extending the frequency band which may be obtained from WWSSN records to frequencies above 1 Hz.

2. An interactive computer analysis for both time-domain and spectral measurements of body-wave arrivals has been programed along with new inversion techniques which return an extended set of source parameters. The new techniques provide robust estimates of the source geometry from a suite of pulse duration estimates, as well as estimates of the dynamic stress drop, average rupture velocity and the radiated seismic energy. The broad-band SRO recordings of five large events in the foreshock sequence of the 1978 Miyagi-Oki earthquake are being analysed for possible premonitory changes of source parameters.

3. The tradeoff of the corner frequency shift between S and P waves and the attenuation suffered in teleseismic propagation has been analysed in order to determine a range of appropriate source models and allowable attenuation models for the earth.

4. SRO recordings of the body-waves radiated by the 1979 Imperial Valley earthquake are being analysed, in comparison to the strong motion recordings, to provide detailed constraints on the mechanics of faulting.

Results:

1. A minimal distortion filtering algorithm has been determined for the simultaneous deconvolution of the short and long period WWSSN data. The algorithm also matches the relative amplitude and phase delay of the two components over the crossband, making the deconvolutional process substantially more stable than in any previous form.

2. Estimates of dynamic stress release (rather than static stress release), in particular, the dynamic stress drop and the apparent stress, indicate a marked increase in the loading stress leading up to the mainshock. The inversion for rupture areas using both direct and reflected

teleseismic arrivals returns adequate estimates of overall source size for events which have a sufficient range of bodywave takeoff angles. The estimates of radiated energy, which require a suitable description of the attenuation suffered by the body-wave, indicates that for small events (m_b 6.5) recorded teleseimically, the appropriate t*'s are substantially less than those inferred from analyses of long period surface waves.

3. Inversions for shear-wave attenuation obtained from analyses which use identical P and S wave pulse shapes were shown to be in serious error, requiring an important reappraisal of the body wave attenuation models in present observational use.

Reports:

Hanks, T.C., 1981, The corner frequency shift, earthquake source models, and Q: Bull. of the Seis. Soc. of Amer., vol. 71, no. 3.

Choy, G.L. and Boatwright, J., 1981, The rupture characteristics of two deep earthquakes inferred from broad-band SRO data: Bull. of the Seis. Soc. of Amer., vol. 71, no. 3.

Boatwright, J., Choy, G.L., and Cormier, V.F., 1980, The use of short period waveforms to infer earth structure (abs.): EOS, vol. 61, no. 46, p. 1047.

Ground Motion Prediction At Selected Strong Motion Sites

9940-01168

D. M. Boore
Branch of Ground Motion and Faulting
U.S. Geological Survey
345 Middlefield Road, Mail Stop 77
Menlo Park, California 94025
415 323-8111, Ext. 2698

Investigations

Study site amplification effects at stations in the Imperial Valley (with C. S. Mueller).

Results

1. Spectral amplitude ratios show that a local site effect is responsible for the high vertical accelerations recorded at station #6 of the USGS El Centro strong-motion array during the October 15, 1979, Imperial Valley earthquake. Station #6 recorded a peak acceleration greater than 1.7 g, a factor of 2.5 greater than nearby stations. Smoothed spectra from the high amplitude parts of vertical component mainshock seismograms at station #6 show a consistent spectral peak, a factor of three or four times greater than at stations #5 and 7, at 8 Hz. Ratios from coda both before and after the strongest shaking duplicate the spectral peak, implying that the soil column behaved linearly during the strongest shaking. Some spectra indicate that records at station #6 are deficient in frequencies above 10 Hz, perhaps owing to higher attenuation in the wedge between the Imperial and Brawley faults. A similar study of three aftershocks recorded at the same stations confirmed these results. An aftershock recorded by temporary stations HUS, 0.3 km west of station #6, and IVC, 0.4 km southwest of station #7, yielded vertical component spectral ratios with a peak near 12 Hz. The results from HUS and IVC may indicate a lateral thinning of the structure responsible for the amplification at station #6.

Reports

Boore, D. M., and Porcella, R. L., 1980, Peak horizontal ground accelerations from the 1979 Imperial Valley earthquake: comparison with data from previous earthquakes: U.S. Geological Survey Professional Paper on The Imperial Valley Earthquake [in press].

Boore, D. M., and Fletcher, J. B., 1980, A preliminary study of selected aftershocks on the 1979 Imperial Valley earthquake from digital acceleration and velocity recordings: U.S. Geological Survey Professional Paper on The Imperial Valley Earthquake [in press].

Lindh, A. G., and Boore, D. M., 1980, Control of rupture by fault geometry: the 1966 Parkfield, California, earthquake: Bulletin of the Seismological Society of America, v. 71, p. 95-116.

Boore, D. M., and Porcella, R. L., 1980, Peak horizontal ground accelerations from recent earthquakes in western North America: Bulletin of the Seismological Society of America, v. 70, p. 2295-2297.

Daniel, R. G., and Boore, D. M., 1980, Anomalous shear wave travel time delays and surface wave velocities at Yellowstone Caldera, Wyoming: Journal of Geophysical Research [in press].

Dunbar, W. S., Boore, D. M., and Thatcher, W., 1980, Pre-, co- and post-seismic strain changes associated with the 1952 $M_L = 7.2$ Kern County, California, earthquake: Bulletin of the Seismological Society of America, v. 70, p. 1893-1905.

Boore, D. M., Kanamori, H., Harding, S., and Sims, J., 1980, The Montenegro earthquake of April 15, 1979: source orientation and strength: submitted to Physics Earth Planetary Int.

Anicic, D., Berz, G., Boore, D., Bouwkamp, J., Hakenbeck, U., McGuire, R., Sims, J., and Wieczorek, G., 1980, Reconnaissance Report--Montenegro, Yugoslavia, earthquake, April 15, 1979 (R. B. Matthiesen, coordinator, A. Leeds, editor): Earthquake Engineering Research Institute.

Boore, D. M., Harmsen, S. C., and Harding, S. T., 1981, Wave scattering from a step change in surface topography: Bulletin of the Seismological Society of America, v. 71, p. 117-125.

Mueller, C. S., and Boore, D. M., 1981, Site amplification at El Centro strong motion array station #6 (abs.), Earthquake Notes, v. 52, p. 84.

Global Accelerograph Program (GAP)

9940-02689

Roger D. Borcherdt
Branch of Ground Motion and Faulting
U.S. Geological Survey
345 Middlefield Road, MS-77
Menlo Park, CA 94025
(415) 323-8111, Ext. 2755

Investigations:

The Global Accelerograph Program was initiated in FY-80 to accelerate the acquisition of near-source ground motion data via either temporary or permanent arrays in regions around the world with high probability for large earthquakes. An important emphasis of the program is the rapid deployment of instruments and personnel. To date a detailed plan has been completed, reviewed by State Department representatives of the Office of Cooperative Science and Technology Programs, transmitted via U.S. State Department to embassies in 10 countries with suggestions regarding participation of institutions and scientists and engineers.

Results:

During this report period an enthusiastic response to the GAP plan was received from several of the institutions and interest expressed by others. A formal agreement has been drawn up for proposal to the various institutions and submitted by C. Rojahn for OES review. The formal agreement emphasizes 1) rapid deployment of instruments and personnel for acquisition of strong motion data from large aftershocks ($M > 6.5$), 2) exchange of post-earthquake investigation teams, 3) exchange of available strong motion data, and 4) development of additional permanent arrays depending on funding availability.

"Hybrid Ray-Mode Method for Synthetic Seismology"

by

Leopold B. Felsen

POLYTECHNIC INSTITUTE OF NEW YORK
MICROWAVE RESEARCH INSTITUTE

Prepared for

U.S. Geological Survey
Contract No. 14-08-0001-19107

The hybrid ray-mode formulation[1] developed previously for propagation in tropospheric ducts, underwater acoustic ducts,[2] and on concave surfaces has now been generalized and applied successfully to the prediction of a seismic event based on a simple earthquake model. The model consisted of a homogeneous sedimentary surface layer above a semi-infinite homogeneous bedrock, with a line source of SH motion located in the bedrock and the resulting SH motion observed at the earth's surface. Parameters and source functions were chosen so as to conform with previous studies of the same event by Heaton and Helmberger,[3] who used a Cagniard ray analysis, and by Swanger and Boore,[4] who used guided modes. The results are summarized in Fig. 1. An exact reference solution for observation times from 0-48 secs after the first arrival was generated by summing up to 14 Cagniard rays and convolving these with the triangular source function. Our hybrid solution consisted of two Cagniard rays, the first two modes trapped inside the surface layer, and a remainder integral. Since these constituents were evaluated numerically, the hybrid method is likewise exact and was found to agree completely with the Cagniard ray sum. Also shown for comparison is the effect of omitting the remainder. This introduces some distortion near the arrival time of the second ray because the ray series is truncated there. At later times, the influence of the remainder diminishes. Finally, the motion was calculated by including only the two trapped modes. This description is clearly inadequate at early times but predicts the motion well at later times. The small displacement of the two-mode curve from the exact curve at later times is believed to be due to the omission of the continuous mode spectrum, which has not been included. For the indicated positions of source and observer, the continuous spectrum turns out to be non-negligible. A manuscript,[5] wherein these results are derived and discussed in detail, is in preparation.

---

[1] L. B. Felsen, "Hybrid Ray-Mode Fields in Inhomogeneous Waveguides and Ducts," to be published in J. Acoust. Soc. Am.

[2] L. B. Felsen and T. Ishihara, "Hybrid Ray-Mode Formulation of Ducted Propagation," J. Acoust. Soc. Am., March 1979.

[3] T. H. Heaton and D. V. Helmberger, "A Study of the Strong Ground Motion of the Borrego Mountain, California, Earthquake," Bull. Seismol. Soc. Amer. 67 (1977), 315-330.

[4] H. J. Swanger and D. M. Boore, "Simulation of Strong-Motion Displacements Using Surface Wave Modal Superposition," Bull. Seismol. Soc. Amer. 68 (1978), 907-922.

The example demonstrates clearly the advantages of the hybrid approach. By combining rays and modes appropriately, one exploits the ray-like character of the early arrivals and the mode-like character of the late arrivals within a single concise formulation that allows the continuous monitoring from the first arrival to long observation times. The transition from the ray phase to the modal phase is accounted for smoothly and automatically by the hybrid field. Neither the ray formulation alone nor the mode formulation alone possesses these attributes. The hybrid form is evidently much simpler since the ray series, while inherently exact, requires an increasingly large number of contributions as time progresses. Not least of the virtues of the hybrid formulation is the cogent physical insight gained, which should be helpful in identifying features exhibited by actual seismograms or by synthetic seismograms constructed by other (for example, purely numerical) techniques.

Extensions of the hybrid method to other seismic propagation environments are under consideration.

---

[5] A. Kamel and L. B. Felsen, "Hybrid Ray-Mode Analysis of SH Motion in a Two-Layer Earth," in preparation.

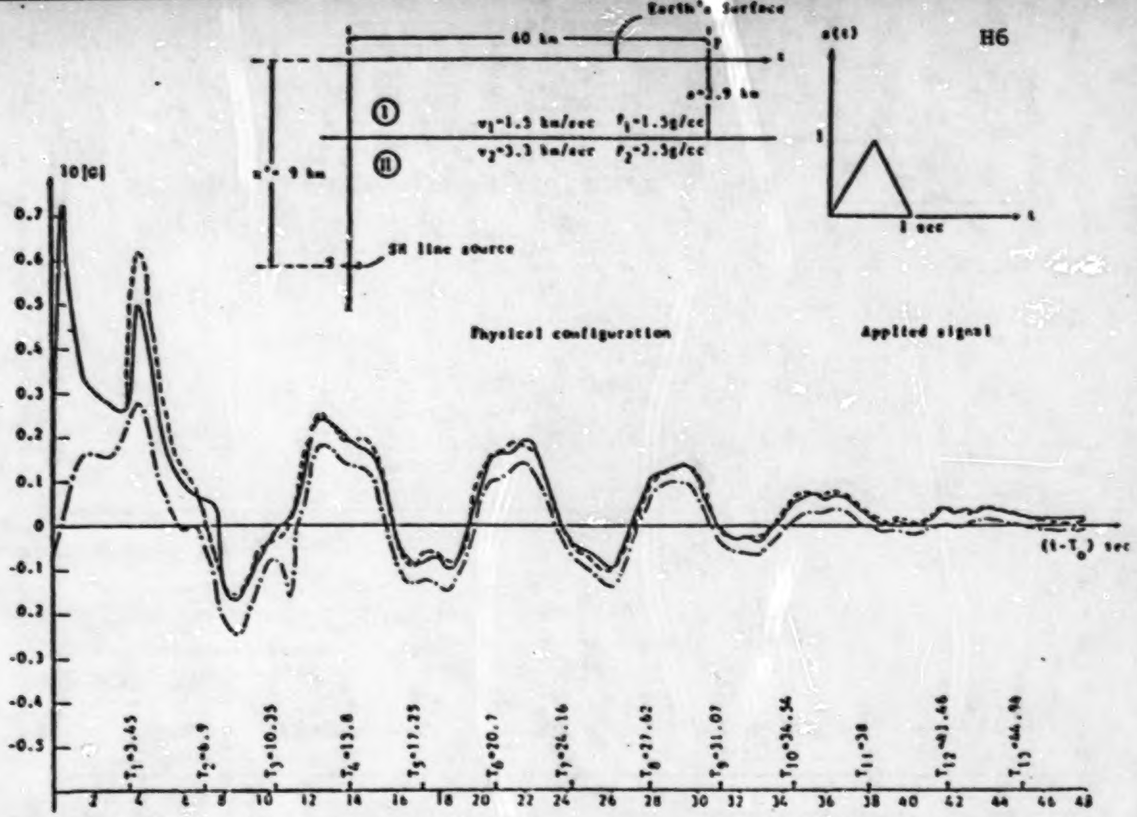

Fig. 1. SH motion G(t) in a two-layer earth model with a homogeneous sedimentary layer of width "a" and a homogeneous bedrock half space. A line source of SH waves, with source function S(t), is located in the bedrock. The parameters employed are shown in the upper portion of the figure. The solid curve represents the exact solution obtained either by summing Cagniard-DeHoop rays or by the hybrid method; both coincide to within the accuracy of the drawing. The ray solution, referred to as the reference solution, has the form:

$$G(t) = \sum_{\ell=0}^{L(t)} \tilde{G}_{\ell}(t)$$

where $\tilde{G}_{\ell}(t) = \tilde{G}^{o}_{\ell}(t) * S(t)$ (* denotes convolution), $\tilde{G}^{o}_{\ell}(t)$ is a Cagniard ray for an impulsive source, and ℓ denotes the number of ray reflections at the bedrock-sediment interface. The number of rays L(t) depends on the observation time, with T_{ℓ} denoting the arrival time of ray $\tilde{G}^{o}_{\ell}$. For a time span of 48 secs from the first arrival at time $T_o = 19.99$ secs, one finds $L_{max} = 13$ (i.e., 14 rays). The hybrid solution includes the first two Cagniard rays $\ell = 0, 1$, two trapped modes $\overline{G}_m(t)$ excited by evanescent tunneling, and a remainder Rem(t)

$$G(t) = \tilde{G}_o(t) + [(1/2)\tilde{G}_1(t) + \overline{G}_1(t) + \overline{G}_2(t) + \mathrm{Rem}(t)]U(t-T_1)$$

where U(t) is the Heaviside unit function. The dashed curve shows the hybrid solution without the remainder Rem(t). The dot-dash curve shows the contribution from the two trapped modes only.

Strong Ground Motion Data Analysis

9940-02676

J. B. Fletcher
A. McGarr
T. C. Hanks
Branch of Ground Motion and Faulting
U.S. Geological Survey
345 Middlefield Road, MS-77
Menlo Park, CA 94025
(415) 323-8111, Exts. 2881, 2708, 2184

Investigations:

1. A general theoretical model has been derived for the acceleration field radiated by an incoherent rupture process, using the results of Madariaga (1977) for the high frequency radiation for crack models of faulting and a simple statistical model. Robust approximations are determined for the relation between the dynamic stress drop and the rms acceleration, averaged over the pulse durations.

2. An analysis of over 300 horizontal components of ground acceleration was undertaken to investigate the character of high-frequency strong ground motion. Included in the analysis are records from the San Fernando earthquake, 8 other moderate-to-large California earthquakes, and seven Oroville aftershocks. This data was analyzed with a particular model in mind that represents ground acceleration as band-limited, white, Gaussian noise within the S-wave arrival window: the band limitation is defined by the spectral corner frequency f_0 and f_{max} the highest frequency passed by the accelerograph or the earth's attenuation operator.

3. Source parameters were determined for ten digitally-recorded earthquakes and 3 others which were recorded by a strong motion accelerograph at Monticello reservoir, S. C.: a site of induced seismicity. These source parameters were then compared to the in-situ stress data of Zoback (1979).

Results:

1. Using a dynamic source model with a component of incoherence, the peak acceleration of a pulse radiated by a single starting or stopping event depends on the dynamic stress drop, the change in rupture velocity and the abruptness of the behavior of the rupture front. By comparing the rms acceleration in the P wave to that in the S waves, the rupture velocity changes associated with the radiation of the acceleration pulses can be estimated directly. Using these results estimates of the dynamic stress drop and the rupture velocity will be determined for a set of small, multiply-recorded earthquakes near the Monticello Dam, South Carolina (Fletcher, 1981).

2. If ground acceleration is modelled as band-limited, white, Gaussian noise, where the high frequency decay of the displacement spectra is ω^{-2}, then the rms acceleration is:

$$a_{rms} = 0.85 \; \frac{(2\pi)^2}{106} \; \frac{\Delta\sigma}{\rho R} \sqrt{\frac{f_{max}}{f_o}}$$

where $\Delta\sigma$ is the earthquake stress drop, ρ is density, R is hypocentral distance. All 16 earthquakes yielded stress of about 100 bars (± a factor of 2) when $\Delta\sigma$ is determined from the a_{rms}. Thus a_{rms} depends solely on the parameter $1/\sqrt{f_o}$.

We can also estimate the peak acceleration a_{max} for a finite duration record given that $\Delta\sigma$ = 100 bars and $1/\sqrt{f_o}$. The relation is:

$$a_{max} = a_{rms} \sqrt{2 \ln \frac{2f_{max}}{f_o}} \quad ,$$

where a_{rms} is defined as above. With less accuracy, this relation fits the peak acceleration set of Hanks and Johnson (1976) as well. At a fixed, close distance, we determine the magnitude dependence of a_{max} to be log a_{max} ~0.3 M for $4 \leq M \leq 6\ 1/2$, which is remarkably close to that recently determined empirically by Joyner et al (1981) for $5 \leq M \leq 7.7$; their coefficient on M being 0.28 ± 0.04. In the model presented here, the magnitude-dependence of peak acceleration is a function of faulting duration alone; larger earthquakes have larger peak accelerations because they last longer not because they are intrinsically more powerful.

3. Locations for the earthquakes recorded by the array of five digital recorders were mostly at the western edge of the reservoir near the site of the first hole in which an in-situ measurement of the stress was made. Depths range from near the surface to about 1.5 km depth. Focal mechanisms for all ten events are thrust, but the strike and dip of the nodul planes varies considerably. Moments calculated for the P and S waves separately for each event agree within 1 standard deviation from 9 out of the 10 events. For the S wave data the moments range from 3.3×10^{17} to 4.7×10^{18} dyne-cm. Stress drops range from .3 to about 4 bars.

The earthquakes for which strong motion accelerograms were obtained are located near the south end of the reservoir within 2 km of the dam. Moments for these events range from 2 to 6×10^{20} dyne-cm. Estimates of stress drop calculated from each component scatter considerably, but suggest that several tens of bars are being released in these larger events.

From the measurements Zoback (1979) made of the principal stresses and pore pressure at Monticello, it appears that several tens of bars of shear stress are available to be released from a depth of 0.2 km down to a 1 km depth. An inconsistency between the mode of faulting predicted by the in-situ measurements (thrust at 0.2 km depth; strike-slip and normal faulting below) and the observed fault plane solutions (all thrust), however, can not be resolved as no directions were determined for the principal stresses. Thus it appear that where only about 1/10 of the available tectonic shear stress is being released by the smaller events, roughly the same amount of shear stress as the tectonic shear stress is being released by the larger events (magnitude from 2.4 to 3). It is interesting to note that after about 3 years of induced seismicity at Monticello, the largest events to occur there are about magnitude 3.0.

Reports:

Fletcher, J. B., R. Zepeda, and D. M. Boore, Digital Seismograms of Aftershock of the Imperial Vally, California Earthquake of October 15, 1979, U.S. Geological Survey Open-File Report 81-655, 1981.

Compilation of Regional Geological and Seismic Site Characteristics

9940-02087

J. F. Gibbs
Branch of Ground Motion and Faulting
U.S. Geological Survey
345 Middlefield Road, M/S 77
Menlo Park, California 94025
(415) 323-8111, Ext. 2910

Investigations

1. Collect seismic velocity data, physical property data, and geologic data in drill holes to develop an improved data base for seismic zonation of the metropolitan Los Angeles Basin.

2. Provide site characteristics (shear and compressional wave velocities, geologic logs, etc.) at locations of important strong motion records.

3. Compare recorded earthquake time histories to measured shear wave velocities to determine site dependent ground motion parameters.

Results

1. Nineteen locations in the Los Angeles area were logged for shear and compressional wave velocities during this report period. This brings the total number of locations to 65 in the Los Angeles area. Physical property data and velocity data together with detailed Quaternary geologic mapping are being used to differentiate geologic units into seismically distinct velocity units.

2. Sixteen of these locations have recorded time histories from the San Fernando earthquake. Together with the shear wave velocity logs, geologic logs and physical property data will provide a comprehensive definition of site properties. From data of this type ground motion prediction equations can be developed. These can be used for predicting the parameters of strong motion in future earthquakes given local magnitude, source distance, and site conditions.

Reports

Fumal, T. E., Gibbs, J. F., and Roth, E. F., 1981, In situ measurements of seismic velocities at 19 locations in the Los Angeles, California, region: U.S. Geological Survey Open-File Report 81-399.

Comparison of Empirical and Theoretical Peak Parameters for Scaling Strong Ground Motion for Distance, Fault Orientation, Magnitude and Crustal Structure

Contract No. 14-08-0001-19131

David M. Hadley
Sierra Geophysics, Inc.
150 N. Santa Anita Ave.
Arcadia, California 91006
(213) 574-7052

Investigations

1. Peak Acceleration Scaling. A hybrid technique using computed transfer functions and empirical source functions has been developed for studying the behavior of peak acceleration vs. distance for the magnitude range M_S = 4.5 to 7.0 for strike-slip faulting.

2. Effective Crustal Attenuation. The observed behavior of M_L and peak acceleration, for the magnitude range of M_L = 4 to 5, provide constraints on the range of acceptable values of Q_β. These constraints have been used to bracket the effective crustal attenuation.

3. Model Studies of M_L. The Wood-Anderson response to the simulated accelerogram from Part 1 have been examined for consistency with Richter's A_o correction for distance.

Results

1. An acceleration time history can be decomposed into a series of operations that transfers energy from each point on the fault to the recording station:

$$ACC(t) = S*R*E*Q$$

Where S is the source time function, R represents rupture over a finite fault, E is the elastic propagation through the earth, Q is the path attenuation, assumed to be linear, and * indicates convolution. If these operators were exactly known, a deterministic approach to predicting strong ground motions would be straightforward. For this study E was computed from a velocity model that incorporates a stiff sedimentary layer over a Southern California crust. A range of realistic rupture velocities have been obtained by other investigators and are incorporated into the simulation. Assumptions of the path averaged attenuation are discussed in Part 2 of this report. Assumptions of S can be avoided by using real sources derived from accelerograms recorded at small epicentral distances (epicentral distance/source depth < 1). Using these operators, accelerograms have been simulated for four magnitudes: 4.5, 5.5, 6.5, 7.0; at eight distances: 5, 10, 15, 20, 30, 50 and 70 km; for five different rupture geometries.

An example of the range of peak acceleration values obtained for the $M_S = 6.5$ simulation is shown in Figure 1. For each magnitude range a simple regression curve was fit to the simulated peak acceleration values. The simulations indicate that peak accelerations tend to saturate with increasing magnitude. The shape of the regression curves for the four magnitudes studied, normalized to 10 km, is shown in Figure 2.

2. Assumptions of the path averaged attenuation, Q_β, can be tested by comparing estimated peak acceleration and M_L to observational data as a function of distance. This provides a check on both the high frequency (5-10 hz) and long period (~1 sec) behavior of the operators $E * Q$ discussed above. Simulations for the case $Q_\beta = \infty$, $M_L \sim 4.5$, resulted in values of peak acceleration that decayed much too slowly with distance and values of M_L that systematically increased with distance. We have found that values of Q_β in the range 200-300 bring the trends of peak acceleration and M_L into agreement with the observations.

3. The parameter Q_β was found to effect the linear trend with distance of the computed value of M_L. However the general shape of the computed M_L curve was not significantly altered. Figure 3 shows the computed values of M_L for both SV and SH, for three source depths and nine distances. The values for each depth and wave type have been normalized by the mean value over the nine distances. The Q_β value used in the simulation was 300 and the fault orientation was vertical strike-slip. These simulated values show a systematic decrease of 0.1 to 0.2 units of M_L at about 20 km. These results suggest that the A_o correction term for M_L is slightly in error for short epicentral distances. These results are being examined for sensitivity to fault orientation.

Reports

Hadley, D.M., D.V. Helmberger and J.A. Orcutt, 1981, Peak Acceleration Scaling Stuides, submitted to Bull. Seism. Soc. Am.

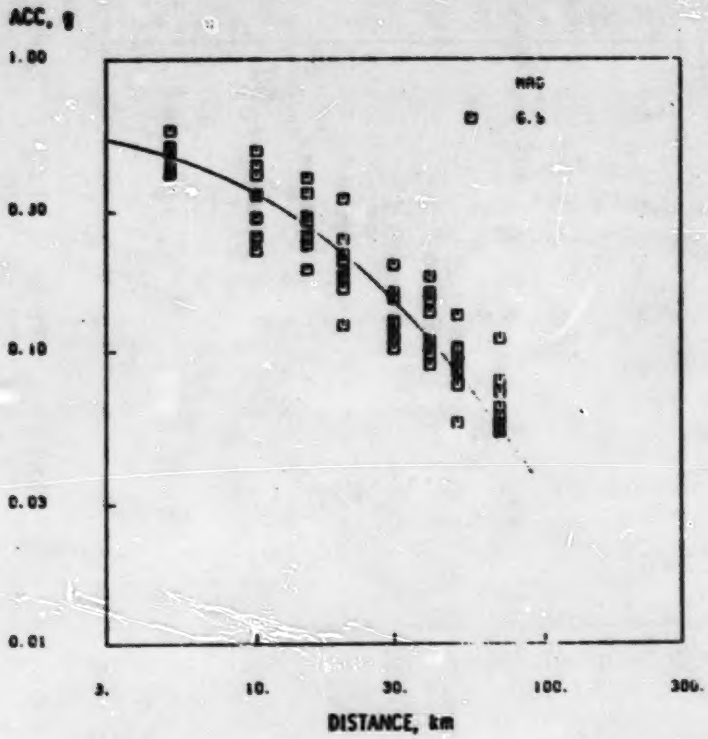

Figure 1. Simulated peak acceleration for the magnitude M = 6.5.

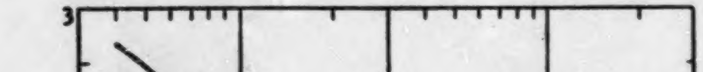

Figure 2. Summary of normalized attenuation curves for simulated peak acceleration.

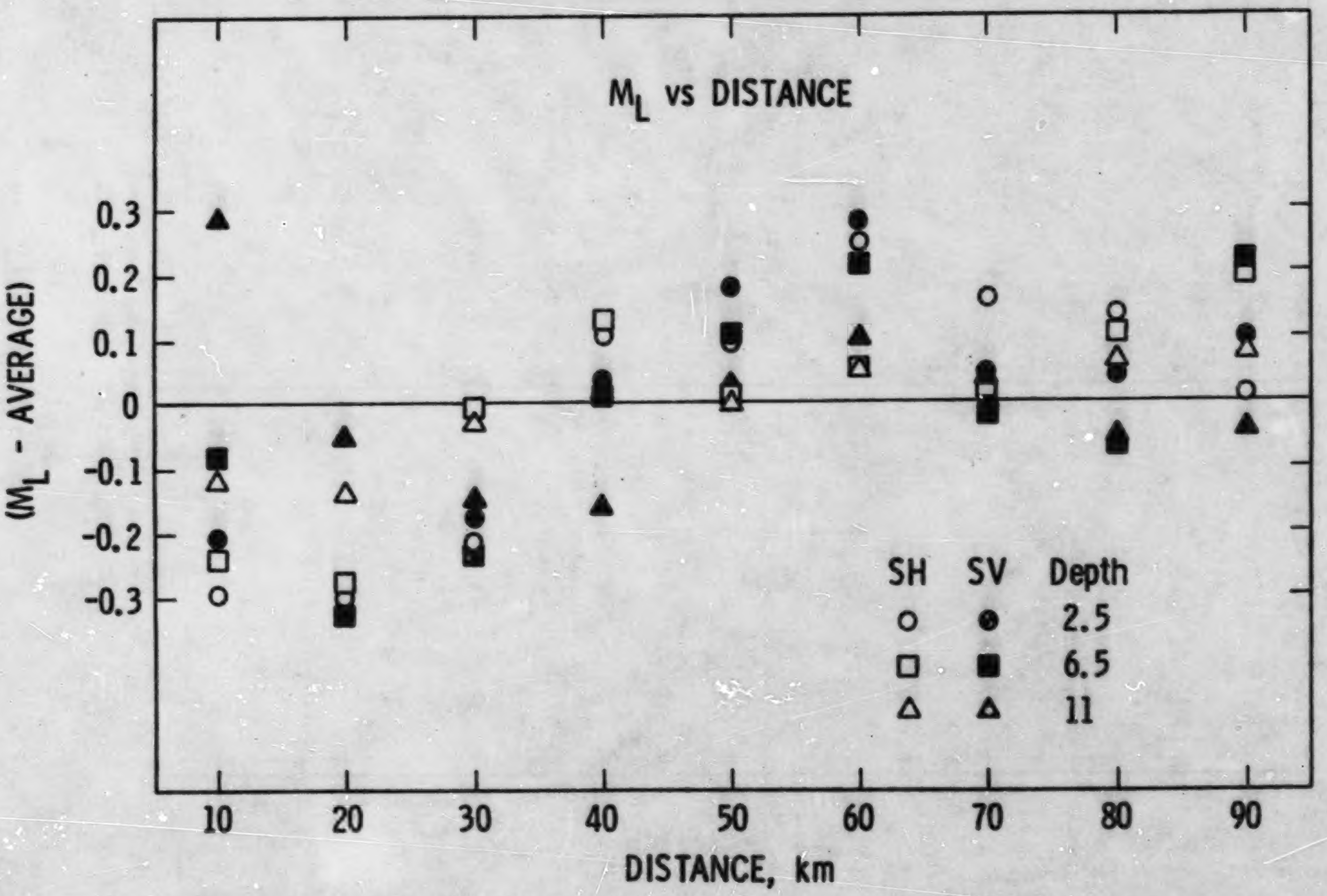

Figure 3. Simulated behavior of M_L for strike-slip faulting for three source depths and nine distances.

STRONG GROUND MOTIONS IN TWO SEISMIC GAPS: SHUMAGIN ISLANDS, ALASKA AND NORTHERN LESSER ANTILLES, CARIBBEAN

Sponsored by USGS Award No. 14-08-0001-19130

Klaus H. Jacob and William R. McCann

Lamont-Doherty Geolgical Observatory of Columbia University
Palisades, New York 10964

The objective of this project is the instrumentation of two major seismic gaps with a sufficient minimum number of seismic strong-motion accelerographs to obtain a good strong-motion coverage from future great earthquakes in these gaps and from any incidental moderate to large earthquakes nearby. To date a total of ten strong motion recording sites are operated by Lamont-Doherty Geological Observatory in the Shumagin Gap region of the eastern Aleutian arc, Alaska; of these, six sites were newly established in 1980. Trigger signals from five remote sites in the Shumagin gap are interfaced with the Shumagin seismic network and centrally recorded at Sand Point for accurate determination of accelerograph trigger times. A magnitude 5.8 earthquake near Nagai Island occurred in late August 1980, only three weeks after installation of the new Shumagin Islands strong motion accelerographs. The central trigger monitor at Sand Point indicated that strong motion instruments at apparently four sites were triggered by this event. Retrieval of the strong motion records from these remote sites will occur during the field season in summer 1981.

A total of 5 strong-motion instruments are presently operated in the Caribbean, none of these are presently interfaced with the L-DGO-operated Caribbean seismic network for transmission of trigger signals. At both strong-motion arrays, in the Aleutians and the Caribbean, preparations are underway to adopt a new system of trigger-moment monitoring by central digital event-recording techniques.

Seismological Field Investigations

9950-01539

C. J. Langer
Branch of Earthquake Tectonics and Risk
U. S. Geological Survey
Denver Federal Center, MS 966
Denver, CO 80225
(303) 234-5091

Investigations

1. Puerto Rico seismicity study--regional investigation of the seismicity on and near the island of Puerto Rico.

2. Argentina aftershock study--regional investigation of the magnitude-7.4 (M_s) earthquake of November 23, 1977.

Results

1. Support of the Puerto Rico Seismic Program (9950-01502) data analysis and interpretation has been assumed by the Seismological Field Investigations Project for FY 81 because of the limited amount of USGS and outside funds necessary to continue the program at its previous level. A considerable amount of work has been accomplished during this fiscal year and was summarized in a presentation by Richard Dart at the 1981 SSA meeting in Berkeley.

2. The magnitude-7.4 (M_s) western Argentina earthquake of November 23, 1977, occurred at the northern end of Sierra Pie de Palo, approximately 70 km northeast of the city of San Juan (see Figure 1). The region surrounding the main shock is one of considerable geomorphic and geologic complexity. Sierra Pie de Palo as well as the neighboring Sierra La Huerta and Sierra Valle Fertil to the east, are composed of Precambrian metamorphic and intrusive rocks. They rise more than 3,000 m above sea level whereas the adjacent valley floors are at an elevation of 500-700 m. These valleys encircle Sierra Pie de Palo and form basins filled with more than 6 km of Recent and Pleistocene sediments. Extending both north and south from Sierra La Huerta and Sierra Valle Fertil are sedimentary rocks of Cenozoic age. These rocks rise to elevations above 3,000 m and form a somewhat continuous north-south mountain system with the Precambrian features.

Across the basin to the west of Sierra Pie de Palo is the city of San Juan and the Paleozoic highlands. Elevations in these highlands exceed 4,000 m in places while the floors of several small alluviated valleys that they enclose are at 500-1,000 m. Faulting is extensive throughout the entire region and has a predominent strike that generally trends north-south. The Precambrian mountains are largely bounded by northerly-striking faults, but some east-west crosscutting faults are also present (see Figure 1).

Analysis of the aftershock data, obtained by the 10-station seismograph network installed around Sierra Pie de Palo, required the development of a regional velocity model and calculation of adequate network station corrections. This, in and of itself, represented a major problem since five seismograph stations (SNO, CHU, MAY, VIC, and CFA) were located on Precambrian rocks, one station (VIL) was on Mesozoic (?) sandstone, and four stations (MOG, SAJ, BRR, and SAM) were on the basinal alluvium (see Figure 1).

With the obvious near-surface velocity variations present in the epicentral region, it was fortunate that the results from a number of refraction profiles were made available by the Argentina Instituto Nacional de Prevencion Sismica. These profiles, 26 in total, were virtually all reversed and gave the sedimentary column and Precambrian velocities. Also, two wells were drilled in the northern part of the study area and their sonic logs agreed with the refraction velocity results obtained in that vicinity. The wells did not bottom in Precambrian and thus they did not add significant new velocity data to this study.

The average sedimentary-column velocities (one-way vertical travel-times) were determined for the center point of each refraction profile and then contoured. They exhibit variations from less than 2.5 km/sec to more than 4 km/sec. When combined with the thickness of the sediments, the contours of the sedimentary travel-times range from 0.0 sec to more than 1.5 sec. Contours of the refraction measurements showed that the velocity at the top of the Precambrain was also variable within the range of 5.30 km/sec to 6.23 km/sec.

A velocity model for the region was developed in two stages from the above results. First, the area was grided at quarter-degree intervals. At each of the resulting 45 grid points, the average sedimentary velocity, sedimentary thickness, and Precambrian velocities were determined by interpolation between the respective contours. Next, averages were obtained for each parameter to produce a generalized velocity model for the study area. This model is:

Velocity (km/sec)	Thickness (km)
2.87	2.41
5.88	7.59

The second stage of the velocity model development was to determine the sedimentary travel-time difference between the above model and the individual stations. For this, the "actual" travel-times were determined from the sedimentary travel-time contour map that was derived from the average velocity contour map and the depth-to-basement contour map. The differences between the "actual" and model travel-times were then considered to be station corrections. Thus, the complete model consists of a generalized velocity model for the region plus station corrections to adjust individual station locations to the velocity model. Unfortunately, there were no reliable crustal velocity data available other than the refraction data. To complete our model, we have assumed the following: 6.2 km/sec from 10 to 32 km, and 7.3 km/sec from 32 to 55 km. A P_n velocity of 8.1 km/sec was assumed for the uppermost part of the mantle. These estimated velocities and depths incorporate the work done by F. Volponi (National University of San Juan, written communication, 1978) who used teleseismic data recorded at seismograph stations near San Juan, Argentina.

The above assumptions state that the Precambrain velocities, calculated from refraction profile data, begin at the depth of 2.41 km and end at a depth of 10.0 km. Given that thickness, the one-way vertical travel-time through the upper two layers of the velocity model is:

$$(2.41\ \text{km}/2.87\ \text{km/sec}) + (7.59\ \text{km}/5.88\ \text{km/sec}) = 0.84\ \text{sec} + 1.29\ \text{sec} = 2.13\ \text{sec}$$

Example station correction calculations follows:

1. Station Correction for MOG (Basin Location)
   From our contour maps, the "actual" sedimentary travel-time at MOG is estimated to be 1.8 sec., the sedimentary thickness is estimated at 6.2 km, and the Precambrian velocity is 6.0 km/sec. Extending to the base of the Precambrian gives the total "actual" travel-time of 2.43 sec. Since the velocity model expects a time of 2.13 sec., a correction of -0.30 sec must be applied to arrival times at MOG.

2. Station Correction for MAY (Mountain Station)
   The station elevation at MAY, which is located on Precambrain rocks in the Sierra La Huerta, is 0.71 km. The estimated Precambrian velocity from our contour map is 6.0 km/sec. Thus, the "actual" travel-time is: 10.71 km/6.0 km/sec = 1.79 sec. Because of the model travel-time is 2.13 sec, a correctin of +0.35 sec is applied to travel-times at MAY.

It turns out that the above velocity model plus station corrections still do not account for all the travel-time complexities of the region. Station delay corrections were also determined in an attempt to "calibrate" the hypocentral location process to the Sierra Pie de Palo region. These corrections were calculated using the following procedure:

1. Select a 20-event subset from the entire sample of aftershocks recorded by the network. These 20 events are all well-recorded and fairly evenly distributed throughout the entire aftershock zone.

2. Locate the selected aftershocks using P-wave arrival times from those stations located on bedrock (VIL, CFA, VIC, MAY, CHU, SNO) and S-wave arrival times recorded by the Wood-Anderson seismographs in San Juan (SAJ).

   Results of this location process demonstrated that significant travel-time residuals (approximately 1/2 to 1 sec) exist at stations located on thick alluvium (MOG, BRR, SAM). An average of those residuals serve as the initial delay corrections.

3. Relocate the 20 selected events using initial delay corrections and the S-wave arrival times at the network stations on bedrock sites. Probe for the P/S velocity ratio that tends to minimize S-wave residuals.

4. Average the residuals at all stations again to arrive at final delay corrections.

5. Relocate all aftershocks using the sum of both the velocity model corrections and the delay corrections. Those sums are:

Station	Total Correction (sec)
BRR	-0.25
CFA	+0.47
CHU	+0.32
MAY	+0.48
MOG	-1.27
SAJ	+0.03
SAM	-0.48
SNO	+0.30
VIC	+0.39
VIL	+0.35

Figure 1 shows the epicenters of 188 aftershocks located to date by an interative version of HYPO71 using the previously described velocity model and travel-time corrections. An average of the root-mean-square (RMS) errors of the travel-time residuals for these locations is 0.11 sec. Averages of the hypocentral standard errors indicate accurracies of about ± 0.39 km in latitude, ± .38 km in longitude, and ± 1.34 km in depth. These events were recorded during a 12-day time period from December 6, 1977 to December 17, 1977. The largest event of the aftershock series ($M_s = 5.9$) occurred on December 6 after all but two of the network stations (SAM and BRR) were installed. The other located aftershocks had duration magnitudes between 4.4 and 2.1.

Most of the aftershocks originated along the eastern half of Sierra Pie de Palo and in the basin to the east and southeast. The epicentral zone roughly defines a north-south rectangular pattern, approximately 100 km long by 40 km wide, with some aftershocks splaying to the east and southeast of Bermejo. Hypocentral depths throughout the zone generally range from about: 2 to 28 km in the northern third, 7 to 35 km in the central section, and 9 to 30 km in the southern part. Eight earthquakes were located at depths of 110 to 120 km, the largest of which is approximately magnitude 3.5. It is not clear what the relationship is, if any, between these deep events and the seismicity associated with the main shock.

The distribution of hypocenters along with the mapped and inferred faults indicate a high degree of geologic and seismotectonic complexity. Composite focal mechanism solutions, as well as focal mechanisms determined from teleseismic data for the main shock and largest aftershocks, suggest that the region is predominately influenced by east-west compressive stresses resulting in both dip-slip and strike-slip motion along several faults within the study area.

Reports

Arabasz, W. J., Richins, W. D., Langer, C. J., 1981, The Pocatello Valley (Idaho-Utah border) earthquake sequence of March-April, 1975: Seismological Society of America Bulletin, v. 71, no. 3, [in press].

Barrows, L., Langer, C. J., 1981, Gravitational potential as a source of earthquake energy: Tectonophysics, v. 75 [in press].

Carver, D., Langer, C. J., Richins, W. D., 1981, Fine details of the aftershock process following the September 30, 1977, Uinta Basin, Utah, earthquake [abs.]: Earthquake Notes, v. 52, no. 1, p. 62.

Dart, R. L., and Tarr, A. C., 1981, Seismicity and regional stress in Puerto Rico [abs.]: Earthquake Notes, v. 52, no. 1, p. 66.

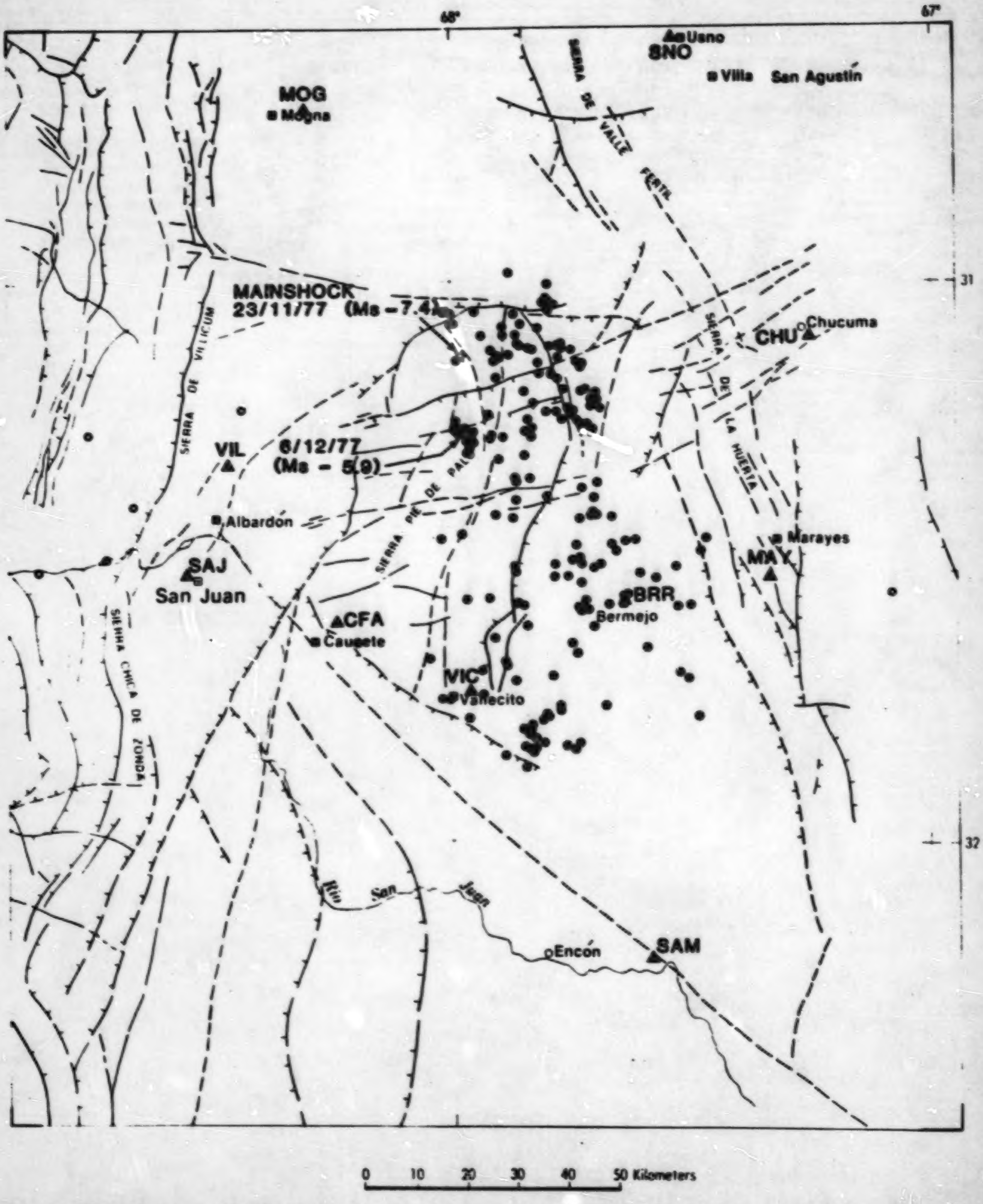
68°
67°
Usno
SNO
Villa San Agustín
MOG
Mogna
SIERRA DE VALLE FERTIL
MAINSHOCK
23/11/77 (Ms - 7.4)
SIERRA DE VILLICUM
CHU
Chucuma
SIERRA DE LA HUERTA
31
VIL
6/12/77
(Ms - 5.9)
SIERRA PIE DE PALO
Albardón
SAJ
San Juan
Marayes
MAY
BRR
Bermejo
CFA
Caucete
SIERRA CHICA DE ZONDA
VIC
Vallecito
32
Rio San Juan
Encón
SAM
0 10 20 30 40 50 Kilometers

Figure 1.--Distribution of aftershocks of the M_S = 7.4 western Argentina earthquake of Nov. 23, 1977. Triangles indicate locations of seismograph network stations, open circles are epicenters of earthquakes deeper than 110 km, and solid dots are aftershock epicenters.

Nonlinear Response of Soft Clay Sediments to High-Strain Earthquake Ground Motions

14-08-0001-19106

Geoffrey R. Martin, Chan-Feng Tsai and Trevor Matuschka
Ertec Western Inc., Long Beach, CA 90807

The objective of this research program is to provide an improved understanding of the nature of earthquake ground motions on soft cohesive soil deposits in the near field of large magnitude earthquakes, where the effects of non-linear response and soil failure can play a significant role.

Investigations

1. A literature review was conducted with effort concentrated on identifying the response of soft cohesive sediments during the 1906 San Francisco earthquake.
2. Appropriate sites were selected in the San Francisco region and the site soil conditions determined. This information was utilized to better understand the observed response of soft cohesive sediments during the 1906 earthquake.
3. Analytical modelling of the response of soft cohesive sediments under strong earthquake shaking was performed in a parametric manner to provide necessary information to better quantify the response of soft cohesive sediments under high-strain earthquake ground motion.
4. Based on the results of the above three investigations guidelines will be developed for the potential effects of the non-linear and yielding response characteristics of soft cohesive soils during strong ground motion.

Results

The extensive literature review revealed that during the 1906 earthquake numerous ground failures of one form or another were reported. Most of the observed soft cohesive sediment failures were found on areas where no structures were nearby. Structures founded on soft cohesive sediments suffered various degrees of structural damage. One possible reason for this difference is the depth of the foundation.

Three different site areas in the San Francisco Bay area were selected to carry out insitu strength measurements and undisturbed sampling. These sites were the Suisun Marsh (northwest of Grizzly Bay), the marsh area at the head of San Pablo Bay between Vallejo and Tubbs Island and at Foster City. At each site a minimum of 2 cone penetrometer records were obtained down to a depth of 100 feet. In addition, undistrubed soil samples were obtained from the Suisun Marsh site.

Using the results from the literature review and the insitu and laboratory testing program, four different idealized soil profiles were used to study the effects of a range of earthquake ground motions on the overall response. At the present time the final stage of the analytical study is underway.

Report

To be completed in June 1981.

Strong-Motion Interpretations for Structural Engineering

9910-02759

R.B. Matthiesen
Branch of Seismic Engineering
U.S. Geological Survey
345 Middlefield Road, MS-78
Menlo Park, CA 94025
(415) 323-8111 x2881

Investigations

1. Evaluate current seismic zone criteria relative to recorded building response and propose criteria for seismic zonation for building design.

2. Develop models to represent the nonlinear structural response and nonlinear soil-structure interaction that is evident in the existing records of building response.

3. Correlate these studies with the on-going efforts in the Structural Engineers Association of California (SEAOC) to upgrade the current building design practice.

Results

1. The current state of seismic design zonation in California has been reviewed relative to a) current design criteria, b) current design practice, c) the acceptable risk implied by such criteria and practice, d) the current state of knowledge regarding the occurrence of strong ground motions, and e) the format in which seismic design zonation might be presented. A draft "commentary" on this material has been prepared and discussed with SEAOC Committees relative to what might be adopted in forthcoming revisions of the SEAOC "Recommended Lateral Force Requirements".

2. Simple models of building frame systems have been studied utilizing limit analysis concepts to develop a "feeling" for the nonlinear range of structural behavior for comparison with recorded response of structures. These studies need to be carried out for more complex framing systems, but some significant implications relative to a parameter proposed for use in structural design are already evident. Currently this parameter is based on judgement as to the response of buildings. These studies indicate that the parameter can be derived analytcally and that there is a significant range of variation in the value of the parameter for one class of building frame system.

3. The SEAOC Seismology Committee has established a schedule for preparing an extensive rewritting of their Recommendations. Through participation as Chair of the Steering Committee, the studies indicated above are being integrated with this overall effort. The outline of the Recommendations

has been revised so that it more nearly conforms to the order in which a designer utilizes the information, and much of the existing material from recent studies of the seismic design process has been assembled into a resource document which the numerous committees involved will work with in preparing revisions to the various sections of the Recommendations.

Data Processing, OES, Golden

9940-02088

Robert B. Park
Branch of Ground Motion and Faulting
U.S. Geological Survey
Mail Stop 978, Box 25046
Denver Federal Center
Denver, Colorado 80225
(303) 234-5070

Investigations

1. The purpose of this project is to provide the day-to-day management and systems maintenance and development for the Golden Data Processing Center. The Center supports Golden based OES investigators with a variety of computer services. The systems include a PDP 11/40, an EAI 680 Analog Computer, Honeywell Level 6 RJE, a RJE, a PDP 11/70, three PDP 11/30s, a PDP 11/23, a VAX-780 and a PDP 11/34. Total memory is 2.4 Mbytes and disk space will be approximately 600 Mbytes. Peripherals include three plotters, seven mag-tape units, an analog tape unit, three line printers, 5 CRT terminals with graphics and a Summugraphic digitizing table. Dial-up is available on all the major systems and hard-wire lines are available for user terminals on the upper floors of the building. Operating systems used are RSX11 (11/40 and 11/23), Unix (11/70 and 11/34), RT11 (11/03) and VMS (VAX).

The three major systems are to be shared by the Branch of Global Seismicity, Branch of Earthquake Tectonics and Risk, and the Branch of Ground Motion and Faulting.

Results

Wave form data was processed (from analog tape, digital cassette tape, and real time phone input) from networks in South Carolina, Nevada, and various U.S. Net stations. The PDP 11/70 has been used primarily for processing global net "day tapes" for ARPA.

The U.S. Net event detection system is being developed on a PDP 11/23 system after preliminary software development on the PDP 11/40. The VAX system is up for time share use. The PDP 11/34 has been accepted and is expected to be on line monitoring the NTS network by October, 1981.

Reports

Rogers, A. M., Covington, P. A., Park, R. B., Borcherdt, R. D., and Perkins, D. M., 1980, Nuclear event time histories and computed site transfer functions for locations in the Los Angeles Region: U.S. Geological Survey Open-File Report.

Earthquake Maps for Developing Areas

San Francisco Bay Area

Contract No. 14-08-0001-19108

Jeanne B. Perkins
Donald A. Olmstead

Association of Bay Area Governments
Hotel Claremont
Berkeley, California 94705
(415) 841-9730

INTRODUCTION

In this project, ABAG extended the computer-based earthquake hazard mapping capability developed in an earlier contract (which focused on the San Mateo County area) to selected areas of significant development pressure. Specific applications for this mapping capability have been extended and refined. The results are being made available in forms useful to a variety of people working for and with local governments in the San Francisco Bay Area.

PROJECT COMPONENTS

1. Selection of a target area.
2. Development of map files.
3. Manipulation of map files.
4. Various applications for these files.
5. Communication of the information.

DISCUSSION OF RESEARCH PROGRESS

1. Target Area Selection

Although many of the basic data map files and hazard map files previously developed were for the entire nine county Bay Area, several were developed only for or only in detail for San Mateo County. The first task in this project was to choose study areas of significant development pressure. The study areas chosen were fifteen 7-1/2 minute quadranges in Petaluma and its vicinity and the ridgelands areas of the East Bay hills.

2. File Development

Three basic data map files have been extended to or refined in those fifteen quadrangles either by digitizing maps or by obtaining existing machine readable data sets. These files include:

- geologic materials
- existing landslides
- digital elevation models

3. File Manipulation

These upgraded basic data map files were used to produce more refined hazard maps for those fifteen quadrangles.

- Information needed to produce more detailed ground shaking intensity files was collected. New maximum ground shaking intensity maps and several risk of ground shaking damage maps were not produced because of the possibility that the shaking attenuation and damage relationships to be used will be modified by mid-1981. Such a change would have made these maps obsolete shortly after they were produced. These maps will be produced in mid-1981.
- The geology, landslide, and topography information, as well as information on vegetation and precipitation, was examined to create a method of extending both the rainfall-induced and earthquake-induced landslide susceptibility mapping beyond San Mateo County. Because of the decrease in the work required on the ground shaking intensity files, much effort was made in perfecting the slope and slope aspect data used in the landslide susceptibility models.

4. Application of Files

These upgraded hazard maps, as well as hazard maps of liquefaction susceptibility, fault surface rupture, and tsunami and dam failure inundation, were used in sample applications:

- as maps for local general plans
- to refine and extend ABAG's ability to develop an automated regional environmental assessment document to serve as a background report for local Environmental Impact Reports (EIRs)

- to compile composite maps of earthquake hazards for the fifteen quadrangles being studied

- to assess the vulnerability of existing and projected land uses and population to damage from a major earthquake.

5. Communication of the Information

Much effort has been made to ensure that this information is effectively communicated and disseminated to a variety of professionals working for and with local governments in the San Francisco Bay Area.

- A series of ten working papers developed previously to document the mapping capabilities was extended to include the documentation of this contract.

- Tools were developed to aid in presentations.

- Talks were given at professional societies.

- Meetings were conducted with local staff.

- Descriptions of ABAG's mapping capabilities were provided to various newsletters and magazines.

- A procedure for producing these products was integrated into ABAG's administrative structure.

- The working papers on ground shaking intensity mapping have been integrated into a draft report for possible publication by USGS.

Classification and Mapping of Quaternary Sedimentary Deposits for Purposes of Seismic Zonation, South Coastal Los Angeles Basin, Orange County, California

14-08-0001-19199

Roger W. Sherburne, Senior Seismologist
David R. Fuller, Geologist
Judy W. Cole, Geologist
Richard B. Greenwood, Geologist
Henry A. Mumm, Senior Program Analyst
Charles R. Real, Seismologist
Gordon W. Chase, Geophysicist

California Division of Mines and Geology
1416 Ninth Street, Room 1341
(916) 445-1923

Objectives of this continuing investigation are to define the spatial distribution and physical characteristics of young near-surface sediments within the study area and to provide an estimation of the probable response of these discriminated sediments to seismic impact. Geologic and seismic data from other investigations have been located and collected for use in this investigation. These collected data have been augmented by refraction seismic surveys, shallow drilling to obtain sediment samples for physical properties analyses and downhole measurement of seismic velocities in these boreholes. An electronic data processing program is being developed which will store, selectively retrieve and graphically display specified geotechnical parameters collected during this investigation.

Traveltime curves and preliminary S-wave velocities from seven downhole SH wave velocity surveys, conducted in February and August 1980, are included in this report. This data, along with geologic interpretation from the second year of study, will result in the production of liquefaction and differential settlement susceptibility maps this contract year. Additionally, map displays of reported intensities of selected historical earthquakes will be prepared and preliminary correlations among geologic and seismic parameters will be undertaken.

Classification and Mapping of Quaternary Sedimentary Deposits for Purposes of Seismic Zonation South Coastal Los Angeles Basin, Orange County, California

14-08-0001-19199

E.C. Sprotte, D.R. Fuller, R.B. Greenwood,
H.A. Mumm, C.R. Real, R.W. Sherburne

California Division of Mines and Geology
1416 Ninth Street, Room 1341
Sacramento, California 95814

Interim Report-Second Year of Investigation

Valid and meaningful estimations of the severity and extent of ground shaking in an area resulting from earthquake energy release, and the secondary effects which may occur as a result of this ground response, must necessarily consider the thickness, configuration and material properties of the unconsolidated near surface sediments. Included in this report are map displays of the historically shallowest ground water occurrences, the distribution and character of discriminated surficial sediments and thicknesses of Holocene and Quaternary age sediments.

The response of near surface sediments to seismically induced shaking is a function of sediment characteristics, materials properties and the velocities of seismic waves through these sediments. Downhole velocity surveys have been conducted in existing boreholes. Additionally, the drilling, logging, sampling for bulk density and the downhole measurement of P- and S-wave traveltimes in a 200 foot hole have provided a means of estimating the clastic properties of the near surface sediments. Because many of the available boreholes in the area of investigation are surrounded by asphalt it was desirable to determine what effect an asphalt layer at the ground surface introduces to the traveltime curve. At the location of the 200 foot hole drilled during this year's effort, it was possible to measure downhole traveltimes from a source generated on soil and from a source generated on asphalt. Comparison and analysis of S-wave traveltimes data from these two sources are presented with the conclusion that when the source is on asphalt, the measured traveltime is less than the measured traveltime on soil at shallow hole depths. Based on this simple test, S-wave traveltime disparity diminishes with increasing depth, and traveltime curves for energy sources on soil and asphalt closely approach each other.

In order to expediently collect and expeditiously analyze the mass of subsurface data accumulated for this investigation an electronic data processing management program has been developed to store, selectively retrieve and graphically display accumulated stratigraphic sample data and geotechnical measurements taken from holes in the ground. The current system can only store point data representing a measured value at some point in space and time. The system does not preclude adding range data. The system consists of two major functions, an edit-audit-update function (input) and a data retrieval function (output). The input function assures that only data that is usable and consistent with user-specified requirements reaches the storage file. The output function provides a variety of services related to obtaining and displaying information from the storage file. The edit-audit-update function is driven by a user-coded input form, while the data retrieval function is driven by a user-coded query. Description of the processing capability of this developed program is contained in the report.

Rupture process and wave propagation effects of the Coyote Lake earthquake and its aftershocks

9940-03010

Paul Spudich
Branch of Ground Motion and Faulting
U.S. Geological Survey
345 Middlefield Road, MS-77
Menlo Park, CA 94025
(415) 323-8111, Ext. 2395

Investigations

1. Computational techniques for combining earthquake source models with general wave propagation methods were investigated for accuracy and efficiency.

2. We studied the feasibility of using collocation methods, which have been developed to solve two-point boundary value problems, to calculate theoretical seismograms in cylindrically symmetric earth models.

3. Comprehensive processing of digital recordings of Coyote Lake earthquake aftershocks was initiated.

4. Digital recordings of events in the 1980 Mammoth Lakes earthquake sequence were processed, located, and analysed.

5. We conducted a numerical study of the effects of the ocean on earthquake-induced seafloor motions.

Results

1. We found that calculation of extended-source seismograms in the frequency domain proved to be computationally simple and economically optimal. This is because at each frequency a surface integral over the fault of a source term and a wave propagation term must be done. At any frequency each term satisfies a smoothness criterion which then can be used to determine the minimum sampling required of each term over the fault in order to calculate the integral accurately.

2. It appears that collocation methods may be used to solve the elastic wave propagation equation $du/dz = Au$, where u is a stress-displacement vector, z is depth, and A is a matrix of coefficients. We have written, in collaboration with Dr. Uri Ascher, a computer program to solve these equations for a cylindrically symmetric earth model in which P and S velocity, density, and attenuation may be smoothly varying functions of depth or have discontinuities. The equation is solved without approximation, yielding complete theoretical seismograms. Both group velocity and phase velocity windowing are permitted.

3. Approximately 6000 digital seismograms from 1500 Mammoth Lakes events were processed. Of these, 150 events were locatable, and their epicenters formed a diffuse pattern not correlated with mapped surface faulting. A cluster of hypocenters defined a vertically dipping plane parallel to the south lip of the Long Valley caldera, and fault plane solutions indicated right-lateral strike slip motion on this plane. The May 27, 1980, 1450 GMT event ($M_L = 6.3$) had a peak horizontal acceleration on our instruments of 0.4 g at a hypocentral range of 16 km.

4. Comparison of theoretical seismograms calculated for the subaerial and submarine environment indicates that earthquake-induced motions of the seafloor are relatively depleted in high frequencies and have larger surface waves with greater durations than earthquakes recorded on land. This may be an important difference for such long-period structures as drilling platforms.

Reports

Spudich, P., 1980, Linear inversion of seismograms to obtain slip functions over a fault plane: EOS, v. 61, p. 1050.

Cranswick, E., Spudich, P., Mueller, C., and Archuleta, R., 1980, Locations and source parameters of the 1980 Mammoth Lakes earthquake sequence: EOS, v. 61, p. 1040.

Spudich, P., and Orcutt, J., 1981, Estimation of earthquake ground motions relevant to the triggering of marine mass movements: Proc. NATO Workshop on Marine Mass Movements, S. Saxov, ed., Plenum, New York.

Spudich, P., Cranswick, E., Fletcher, J., Harp, E., Mueller, C., Navarro, R., Sarmiento, J., Vinton, J., and Warrick, R., 1981, Acquisition of digital seismograms during the Mammoth Lakes earthquake sequence of May-June, 1980: U.S. Geological Survey Open-File Report 81-38.

Mueller, C., Spudich, P., Cranswick, E., and Archuleta, R., 1981, Preliminary analysis of digital seismograms from the Mammoth Lakes, California, earthquake sequence of May-June, 1980: U.S. Geological Survey Open-File Report 81-155.

EARTHQUAKE HAZARD EVALUATION OF THE GREATER HELENA AREA, MONTANA

Contract No. 14-08-0001-19135

Michael C. Stickney
Montana Bureau of Mines and Geology
Montana College of Mineral Science and Technology
Butte, Montana 59701
(406) 496-4332

INVESTIGATIONS

Detailed mapping of Tertiary and Quaternary deposits at a scale of 1:12,000 within the seismically active Helena Valley, site of the state capitol, is intended to provide: 1) a modern data base for identifying and locating all active or potentially active faults and to evaluate their potential for generating damaging earthquakes; 2) knowledge of the distribution and properties of foundation materials where strong ground motion may create a substantial hazard from liquefaction or rapid loss in strength; and 3) a delineation of areas of potential slope instability in the event of a strong local earthquake.

RESULTS

During the second six months of this research project, personnel have completed mapping the unconsolidated deposits within, and surrounding the Helena Valley and the faulting which disrupts these deposits. Low-sun-angle photographs at a scale of 1:12,000 were used as a base for all field mapping. The mapped geology has been transferred to topographic maps with a scale of 1:24,000, and a final version of the Helena Valley geologic map at 1:24,000 scale is 80 percent completed.

The Helena Valley and surrounding foothills are underlain by argillite, quartzite, and calcareous siltstone of the Precambrian Belt Supergroup; fine-grained fluviatile (in part lacustrine?), arkosic silt, gravelly silt, and volcaniclastic sandstone and conglomerate of late Tertiary age; and a thin sequence of pediment gravel; moderately sorted, uncemented alluvial plain deposits of middle Quaternary to Holocene age and minor amounts of thinly-bedded, fine sand and silt deposited in Glacial Lake Great Falls. The Tertiary and Quaternary deposits lie within a fault-bounded structural and topographic basin that first began to take its present form during the middle to late Tertiary and has continued to form through vertical movement and downwarping to the present. The Helena Valley fault zone is a major belt of down-to-the-southwest faults that forms the northeast valley margin. This fault zone splays into two distinct branches to the southeast of Lake Helena and is less than 100 meters wide and very linear northwest of Lake Helena. The Helena Valley fault zone is over 35 kilometers long and is marked by subparallel scarps of middle Quaternary to Holocene(?) age which range in height from less than one meter up to about 10 meters. The Prickly Pear fault zone lies near the southwest margin of the Helena Valley and exhibits down-to-the-northeast displacement.

The Prickly Pear fault zone cuts Quaternary alluvial fan deposits on the northeast flank of the Scratchgravel Hills but lies buried beneath Holocene alluvial plain deposits as far southeast as East Helena. Southeast of East Helena, the Prickly Pear fault zone is composed of early to middle Quaternary scarps several meters to several tens of meters high which bring Tertiary deposits into contact with Paleozoic and Mesozoic rocks or, in some places, cuts only Paleozoic and Mesozoic rocks. Together, the Helena Valley and Prickly Pear fault zones form a northwest trending graben nearly 30 kilometers long by 10 kilometers wide which contains Tertiary and Quaternary deposits nearly 1800 meters thick at its deepest point. Northeast trending fault scarps 0.5 to 1.0 kilometers long with maximum offsets of 0.75 meters at the south end of the Scratchgravel Hills appear to be the youngest faulting in the Valley.

The numerous fault traces mapped along the northeast, southwest, and north-central flanks of the Valley transect middle to late Quaternary pediment and alluvial plain deposits and are viewed as potentially active. No historic movement has been observed on any of these faults, although several occur in areas of present day microearthquake activity. The Quaternary faults mapped as part of this project are associated with major basin boundaries that have existed since at least Miocene(?) time, and as such record continuing and generally consistent movement histories over approximately the last 20 million years.

Earthquake Hazard Maps
# of the Vista and Steamboat
7½-Minute Quadrangles, Nevada

14-08-0001-19116

D. T. Trexler and M. R. Nichol
Nevada Bureau of Mines and Geology
University of Nevada, Reno
Reno, Nevada 89557
(702) 784-6691

Investigations

Development of earthquake hazard maps for the Vista and Steamboat 7½-minute quadrangles is based upon the suspected response of the geologic units to seismic loading and the spatial distribution and recency of movement of faults. The probable response of the geologic units to earthquake-induced stresses is inferred from shear-wave (SH-wave) velocity and bulk density. These parameters, when combined, produce the rigidity product.

Earthquake hazard maps provide information to planners and other public officials about the suspected or probable response of the geologic units to seismic loading. Previous geologic mapping by Trexler and McKinny, 1980 and Trexler and Pease, 1980 provide the base from which the earthquake hazard maps are produced.

Determination of the recency of faulting is an important aspect in the preparation of earthquake hazard maps. By using soil maps prepared by the USDA Soil Conservation Service and applying the technique developed by Trexler and Bell, 1979, faults that are Pleistocene age or younger are divided into categories based on soil development. Faults of Holocene age (<12,000 years B.P.) displace entisol soils which are characterized by a youthful AC profile. Late Pleistocene age faults (approximately 12,000-35,000 years B.P.) displace soils identified as Haplargids and Argixerolls. Faults of Early to mid-Pleistocene age (approximately 100,000 - 1.8 m.y. B.P.) displace Durargid, Paleargid and Durargixeroll soils or equivalents.

Results

A. Vista Quadrangle

Seismic velocity measurements were performed at 24 sites on 10 geologic units. SH-wave velocities range from 594 ft/sec for fluvial-lacustrine deposits to a maximum of 4320 ft/sec for competent unaltered Kate Peak andesite. The low mean SH-wave values of 714 ft/sec for the fluvial-lacustrine deposits was derived from 4 measurements.

Intermediate SH-wave velocities ranging between 912 and 1411 ft/sec were measured in alluvium, Tahoe outwash, and older alluvium. The highest SH-wave velocity of 1741 ft/sec was obtained from the Washington Hill rhyolite.

The geologic unit having the lowest mean rigidity product value (1000) in the Vista quadrangle is the fluvial-lacustrine deposits. The next lowest calculated rigidity product was for mainstream gravels which occupy the channels of the Truckee River and its tributaries. Mean rigidity product values for young alluvium is 1459 and ranges from 1067 to 1632 due to the range in SH-wave velocities. The youngest alluvial fans have mean rigidity product values of 2171. Other geologic units exhibiting intermediate rigidity product values are Tahoe outwash, older alluvium, and older alluvial fan deposits. The rigidity product calculated for the Washington Hill rhyolite was low and the result of slow SH-wave velocities and the low density.

The geologic units within the Vista quadrangle are grouped into six shaking categories based on the suspected seismic response. Geologic units with low rigidity products and saturated within 3 m (10 ft) of the surface have the lowest ranking shaking category (low ranking = most severe shaking). The alluvium and Tahoe outwash are identified as shaking category II when saturation due to groundwater is within 3 m (10 ft) of the surface. When groundwater levels are greater than 3 m (10 ft) the units are classified as shaking category III.

Unconsolidated deposits and sediments of the Truckee formation with rigidity product values in the range of 1800-2700 are included in shaking category III when depth to groundwater is less than 3 m (10 ft) the classification of probable shaking characteristics is elevated to shaking category IV.

Bedrock units consisting of Mesozoic metamorphic rocks and granitic intrusives and Tertiary volcanic rocks comprise shaking category V. Based on the SH-wave velocity measurements, this category should have the least severity of shaking.

Hydrothermally altered Tertiary volcanic rocks are included in shaking category VI. This category of response to earthquake loading will undoubtedly vary over a wide range because variable response in the physical properties of the rocks due to alteration.

Low sun-angle photography interpretation aided in the delineation of subtle fault scarps in the quadrangle. Based on soil development and scarp morphology, none of the faults in the quadrangle are Holocene in age. The northeast trending faults in the east-central portion of the quadrangle are subparallel to the trend of Olinghouse fault located 26 km (16 mi) to the east. There is no evidence of recent movement along these faults in the Vista quadrangle.

B. Steamboat quadrangle

Seismic velocity measurements were performed on 15 sites representing 8 geologic units. The geologic unit with the lowest SH-wave velocity is the fluvial-lacustrine deposits. The mean SH-wave velocity is 555 ft/sec. The lower values are probably due to the presence of peat and intercalated organic matter. Intermediate SH-wave velocities range from 1263 to 1507 ft/sec. Units represented by this range in velocities are mainstream gravels, alluvium, Donner Lake outwash and alluvial fan deposits.

Three seismic velocity measurements were made on Kate Peak andesite, a map unit that represents approximately 75% of the bedrock in the quadrangle. One determination was made on unaltered andesite and resulted in a SH-wave velocity of 4320 ft/sec. Two measurements were made on bleached and altered andesites. SH-wave velocities ranged from 1533 to 2044 ft/sec. The mean SH-wave velocity for the two measurements was 1789 ft/sec or 2.5 times less than unaltered andesite.

Geologic units in the Steamboat quadrangle are grouped into 5 shaking categories based on their calculated rigidity products. Units with low rigidity products, such as, fluvial-lacustrine deposits, eolian sand and hot spring sinter are grouped in category I. This category is suspected to have the most severe shaking from seismic loading as compared to other categories. All other unconsolidated deposits have intermediate rigidity product values ranging from 1800 to 2567. The deposits include alluvium, older alluvial fan deposits and Tertiary sediments. Shaking categories II and III are assigned to these units based upon the depth to groundwater. If saturation of the deposits occurs within 10 m (33 ft) of the surface the shaking characteristics will probably be more severe and the lower shaking category is used. Conversely, if the depth to groundwater is greater than 10 m (33 ft) the higher classification is used.

The remaining geologic units which comprise shaking categories IV and V are bedrock units consisting of intrusive and extrusive igneous rocks and metamorphosed sediments. Fresh unaltered rock comprise category IV and have rigidity products of 3800 or greater. Category V is made up of the Kate Peak and Alta formation rocks which have undergone hydrothermal alteration. A rigidity product of 3600 was calculated for these altered rocks. Due to the range of physical characteristics of these bleached and altered rocks they are assigned to category V, which has a range of potential shaking characteristics.

Faulting in the Steamboat quadrangle can be divided into three categories based on age of last movement. The youngest fault activity is characterized by faults which displace deposits which have soils that are older than 10,000 years and younger than 35,000 years. The next age that can be assigned to fault activity in the quadrangle is that which displaces soil of Sangamon age. These ages are based on correlations between the development of the Cocoon soil which is pre-Tahoe age (pre-80,000 years).

Other faults in the Steamboat quadrangle are pre-Tertiary in age. Based on slope morphology, none of the faults appear to be Pleistocene age or younger. Trenching of youthful appearing scarps indicated that the age of last movement along these faults occurred during mid-Pleistocene time (Trexler and Pease, 1980).

References

Trexler, D.T. and Bell, J.W., 1979. Earthquake hazard maps of Carson City, New Empire and South Lake Tahoe quadrangles. Final report U.S. Geol. Survey grant no. 14-08-0001-G-494.

Trexler, D.T. and McKinny, R.F., 1980. Geologic map, Steamboat quadrangle, Nevada: U.S. Geol. Survey open file rpt.

Trexler, D.T. and Pease, R.C., 1980. Geologic map, Vista quadrangle, Nevada: U.S. Geol. Survey open file rpt.

Development of General Earthquake Observation Systems

9940-03009

John Van Schaack
Branch of Ground Motion and Faulting
U.S. Geological Survey
345 Middlefield Rd., MS 77
Menlo Park, CA 94025
(415) 323-8111, ext. 2584

Investigations

This project will fully develop a dependable, low power, wide dynamic range, portable, digital recording system. The system is software based for easy use in a wide variety of applications. The system will record 6 channels of 16 bit data at a rate of 200 samples per second per channel. The maximum rate will be 1200 samples per second on one channel. The minimum sample rate will be 1200 divided by 4096. Data will be recorded on a cartridge tape recorder. Data capacity is 1.25M 16 bit words, or approximately 17 minutes at the maximum sampling rate.

Results

Testing and modifications of the hardware are almost completed. All parts have been ordered and all the mechanical layout has been designed. Tests have been run of the prototype unit and, after extensive modification, the dynamic range has been increased from 12 bits to between 15 and 16 bits. All the basic software has been completed and modifications are being made to enhance its operation.

Instrument Development and Geotechnical Studies

9940-02089

R. E. Warrick
Branch of Ground Motion and Faulting
U.S. Geological Survey
345 Middlefield Road, MS-77
Menlo Park, CA 94025
(415) 323-8111, Ext. 2757

Investigations

1. The development of techniques for the improvement of field data acquisition specifically in the application of triggered digital recording systems to aftershock studies.

2. Methods for improving the generation, recording and interpretation of stress waves for deep downhole surveys.

Results

1. a. A search for the ideal sensor for use with the new generation of microprocessor controlled recording systems continues. The dynamic range available in the recording systems can be covered by either velocity sensors or accelerometers. The dynamic range provided by the earth, from microearthquakes to near-field moderate to large earthquakes, requires a selection of sensor to match the range of anticipated earth motions.

b. The triggered recording systems (DR-100's) have been made more versatile by the addition of a pre-programmable timing and control system recently developed by Sprengnether. Gene Sembera made the modifications to our systems to incorporate this addition which will allow a choice of recording times and durations and a choice of operating periods for the internal trigger function.

c. Some preliminary field tests of different sensor emplacement methods were made in conjunction with the earthquake simulation experiments being conducted at Camp Parks by SRI International. Preliminary interpretations indicate that acceleration in excess of 1/2 g were recorded near the sources. Analysis of the data is in progress.

d. As a result of recent efforts to rapidly assemble field instrumentation for aftershock studies a vehicle has been assigned to Gene Sembera. Gene has modified the truck to allow the transportation of five recording units and the associated test equipment.

2. a. A winch was assembled to handle the 300 meter logging cable. The initial test by Porcella and Acosta on a 245 meter hole at El Centro suggested some improvements to simplify the process of velocity logging.

b. The Nimbus digital tape system is being tested by Hsi-Ping Liu and Gray Jensen. Initial tests have shown that the system operates as intended. Tests of the transfer process to the 11/70 system are planned.

REALISTIC MODELING OF GROUND AMPLIFICATION EFFECTS

Contract Number USGS 14-08-0001-19761

Hung Leung Wong
Department of Civil Engineering
University of Southen California
Los Angeles, California 90007

Investigation on effects of irregular layers on the amplification of incident waves is underway using two methods: (1) A finite element method with transparent boundaries. (2) A hybrid finite element and boundary integral equation method. The computational procedures developed are applied in three-dimensional problems and they perform best for thin and elongated layers which exist in most important alluvial basins. Derivation of both methods (1) and (2) are based more on physics rather than mathematics and thus are well suited for the wave propagation problems posed.

Method (1) uses the standard finite element modeling technique enhanced by a vanishing boundary to eliminate unwanted wave reflections from the artificial boundaries. The method for transmitting the outgoing waves is based on a straightforward simulation of the wave propagation process which predicts the future boundary value from present and previous values away from the boundary. This simulation is consistent with the wave equation and the Huygen Principle. No differential form of boundary conditions are necessary for the artificial boundary and thus making this formulation different from those introduced previously. The error caused by unwanted reflections from the boundary can be reduced to an arbitrarily small number by using more values from past time steps for the estimation. For each additional time step saved, the accuracy of the calculation will be improved one order of magnitude. Some results were compared to an exact solution and the comparisons were excellent. It has been shown that the size of finite element model can be reduced significantly even for long duration transient wave calculation. This method is presently being applied to realistic geometries.

Method (2) combines the advantages of finite elements for detailed modeling and the advantages of boundary integral equations for wave radiation into the far field. The most difficult obstacle, the numerical evaluation of the stiffness matrix for an embedded layer interface, was reduced to one with a flat boundary with the aid of a finite element extension. The original method, called "substructure deletion", was developed by Dasgupta (1979). Having a flat integration surface for the boundary integral equation, the source and observation points for the Green's function are at the same elevation, making the formulation exceptionally simple numerically. Several refinements have been added to the substructure deletion method to make the integral equation compatible with the finite element formulation, e.g., an average displacement and uniform stress loading is used instead of one that uses nodal forces and displacements. Elevated topographies such as an earth dam and subsurface irregularities are both being studied with this method.

REFERENCES

DASGUPTA, G. (1979). Foundation impedance matrices for embedded structures by substructure deletion, pp 742-745, Proceedings of A.S.C.E. Specialty Conference, Austin, Texas.

REPORTS

WONG, H.L., M. Dravinski, and L.C. Wellford (1981). Response of a dam to plane P, SV, and Rayleigh waves. to be submitted to the International Journal of Earthquake Engineering and Soil Dynamics.

LIAO, Z.P., and H.L. Wong (1981). A method for creating vanishing boundaries for the finite element method, to be submitted to the Bulletin of Seismological Society of America.

Development of a
Liquefaction Susceptibility Map
for Davis County, Utah

Contract No. 14-08-0001-19127

by

Loren R. Anderson[1]

Jeffrey R. Keaton[2]

Introduction

A liquefaction susceptibility map has been compiled for Davis County, Utah. The map was developed from a combination of existing data, available in the files of private and government agencies, and data obtained by drilling test borings in selected areas. Liquefiable deposits, as identified by soil type were found virtually throughout Davis County. To further classify the liquefaction susceptibility of the soil deposits, the results of existing data and a supplementary subsurface investigation were used to compute the critical ground surface acceleration that would be required to induce liquefaction at each soil boring location. Based on these critical accelerations, a liquefaction susceptibility index value was assigned to each boring location and plotted on a map. Boundaries were then drawn on the map delineating various levels of liquefaction susceptibility. Consideration of ground slope allowed further classification regarding probable type of ground failure (Youd and others, 1975).

Methodology

Standard penetration results were obtained from soil boring data. The blow count, N_1, corrected to an overburden pressure of 1 Ton/ft^2, and the relationship proposed by Seed, Mori and Chan (1977) were used to obtain the cyclic stress ratio, $(\tau/\bar{\sigma}_o)$, required to cause liquefaction was then computed from,

$$a_{max} = \left(\frac{\tau_{ave}}{\bar{\sigma}_o}\right)\left(\frac{\bar{\sigma}_o}{\sigma_o}\right)\left(\frac{g}{0.65 r_d}\right)$$

---

[1] Assoc. Prof. Utah State University, Logan, Utah

[2] Senior Engineering Geologist, Dames & Moore Engineers

where,

a_{max} = maximum acceleration at ground surface

$\left(\frac{\tau_{ave}}{\bar{\sigma}_o}\right)$ = cyclic stress ratio required to cause liquefaction (Seed, Mori and Chan, 1977)

$\bar{\sigma}_o$ = total overburden pressure on sand layer under consideration

σ_o = effective overburden pressure on sand layer under consideration

r_d = a stress reduction factor varying from a value of 1.0 at the groundsurface to 0.9 at a depth of 30 ft.

Qualitative descriptions of liquefaction susceptibility were assigned on the basis of exceedance probability for a 100-year return period. A recent probabilistic evaluation representative of Davis County was available (Dames & Moore, 1978). An acceleration of approximately 0.12 g corresponded to a 50 percent exceedance probability and was taken as a 10 percent exceedance probability which corresponded to approximately 0.20 g. "Low" susceptibility was taken as a 5 percent exceedance probability of approximately 0.30 g. Critical accelerations exceeding 0.30 g were considered to have a "very low" liquefaction susceptibility.

The boundaries between the various zones of liquefaction susceptibility were field checked and and compared with topography and geologic conditions.

Results

In assessing the liquefaction susceptibility in Davis County, Utah four maps have been developed: 1) Soil Data and Ground Water Map, 2) Critical Acceleration and Ground Slope Map, 3) Geologic Ground Failure Map and 4) Liquefaction Susceptibility Map. The Liquefaction Susceptibility Map identifies areas of high, moderate, low and very low liquefaction susceptibility, and can be used in conjunction with the soil data and ground slope maps to suggest the most likely type of liquefaction induced ground failure.

Behavior of Weakly Cemented Sands Under Seismic Loading

14-08-0001-18380

G. Wayne Clough
Civil Engineering Department
Stanford University
Stanford, California 94305
(415) 573-9556

Investigations

The project involves laboratory, field and computer studies. Laboratory work is directed at determining the behavior of weakly cemented sands when subjected to static and dynamic loadings and defining the nature of the cementation. Naturally cemented specimens are obtained from two Bay Area sites, while artificially cemented specimens are manufactured to model the observed behavior of the natural soils. Tests are performed in both the dry and saturated conditions. The field studies directed at defining the response of slopes in cemented sands involve an observational program as well as detailed topographic and geologic studies. Historical documents have also been consulted for several sites to determine how they behaved in past seismic events. In order to determine how to properly define the properties of the cemented sands, a variety of in-situ testing methods and sampling techniques were tried at a nearby field site. Finally, computer analyses are being used to study response of cemented soil slopes under gravity and seismic loading. The basic objective of the laboratory, field and computer work is to define how a small degree of cementation can serve to increase the resistance of sands to seismic loading, and how these soils can be properly tested to ascertain their actual strength levels.

Results

The laboratory strength tests show that all the cemented sands tested have a number of common characteristics: (1) Their drained failure envelope is essentially a straight line in compression, exhibiting both a cohesion intercept as well as a friction angle. The friction angle is about the same as would be expected for an uncemented sand; (2) In tension, the failure envelope is curved, with a tensile strength about one-tenth that of the unconfined compression strength; and, (3) In undrained cyclic loading they do not develop pore pressures as rapidly as uncemented sands, but when they fail, it is by a sudden collapse during which the pore pressures accelerate at a high rate. Differences in behavior of the cemented sands are found in failure modes and strength levels, and they are related to the degree and types of cementation. Thin section analyses of the sands show the cementing agents vary with environment and geologic deposition sequence.

The field studies show that in essentially homogeneous cemented sands slope failures are shallow and generally initiate in the upper half of the slope. During earthquake loading spalling type failures are common; these are apparently due to tensile stresses formed as a result of the steep slope inclinations. In some areas deep-seated failures are observed to occur, but here the cemented sands are underlain by clays or shales. The underlying materials form an impervious barrier to downward water flow which ultimately creates high water pressures in the overlying cemented sands, leading to deep slope failures

Field investigation of conventional drilling and sampling techniques show that significant disturbance is likely to occur no matter how carefully the sampling is done. Test data illustrate that regardless of the procedure, the soil is densified and its stress-strain response distorted. Of the in-situ testing techniques, only the pressuremeter was successfully adapted to quantitatively defining cemented sand properties. Special adaptations to a self-boring pressuremeter were required to successfully apply it to cemented sands, but the results clearly indicated that this device could be used to obtain properties representative of the undisturbed cemented sand behavior.

Computer studies of slope response in cemented sands involved limit equilibrium analysis as well as finite element analysis. The former method is useful to evaluate overall stability while the latter one can define local stress conditions as well as stress concentration areas. An extensive suite of finite element analyses have been performed to investigate actual field cases as well as hypothetical problems. Nondimensionalized charts have been developed which allow a user to calculate stress levels in a variety of conditions for static and seismic loading. The results show that during an earthquake, tensile stresses will develop if the cemented soil slope is relatively steep. This finding is consistent with the field observation of tensile spalling failures. The level of tensile and shear stresses is found to be a function primarily of slope inclination, magnitude of the earthquake, and the degree of matching which exists between the natural frequency of the slope and the characteristic frequency of the earthquake. All of these parameters are reflected in the charts published in the project research reports.

Reports

Sitar, N. and Clough, G. W., 1979, Behavior of slopes in weakly cemented soils under seismic loading, Proceedings, 2nd International Conference on Earthquake Engineering, Stanford University, p. 1006-1015.

Clough, G. W., Sitar, N., Bachus, R. C., and Shafii-Rad, N., 1981, Behavior of cemented sands under static loading, to be published in the Jour. Geotech. Engineering Division, ASCE.

Sitar, N., Clough, G. W., and Bachus, R. C., 1980, Behavior of weakly cemented soil slopes under static and seismic loading conditions, The John A. Blume Earthquake Engineering Center Report No. 44, Stanford University, 166 p.

Clough, G. W., 1978, A study of the behavior of cemented soils under seismic loading, A Six Months Progress Report, 31 p.

Clough, G. W., Sitar, N., and Bachus, R. C., 1979, A study of the behavior of cemented soils under seismic loading, A Six Months Progress Report, 35 p.

Clough, G. W. and Shafii-Rad, N., 1980, A study of the behavior of cemented soils under seismic loading, A Six Months Progress Report, 40 p.

Evaluation of Liquefaction Susceptibility in the San Diego, California Urban Area

14-08-0001-19110

Andrew W. Dawson
Maurice S. Power
Woodward-Clyde Consultants
3467 Kurtz Street
San Diego, California 92110
(714) 224-2911

Investigations

The liquefaction susceptibility of deposits in the San Diego urban area is being assessed based on the distribution of geologic materials, the geologic and engineering characteristics of these materials, and the depth to ground water. Geologic maps and cross sections have been prepared showing the ages and mode of deposition of various deposits in the San Diego area. Logs of borings made for numerous projects in the San Diego area have been examined to aid in this mapping. Data from the borings on ground water levels and the engineering characteristics of the deposits, including penetration resistances (blow counts) and grain size and plasticity characteristics, have been compiled and analyzed. Criteria and rating schemes are being utilized to rate the susceptibility to liquefaction of the various deposits.

Results

Geologic maps have been prepared using seventeen City of San Diego base maps at a (reduced) scale of 1 inch to 1800 feet. Thirty-eight cross sections have been prepared to aid in the mapping and to illustrate the vertical extent of the deposits. Emphasis in the mapping has been on Holocene deposits, including hydraulically placed fill, fluvial, deltaic and estuarine deposits, because of the relatively high liquefaction susceptibility of these deposits. Late Pleistocene sediments have also been mapped according to mode of deposition. Early Pleistocene and older formational deposits have been mapped as undifferentiated because of their relatively low susceptibility to liquefaction. Data from approximately 3000 borings have been compiled and analyzed.

Criteria and rating schemes that are based on both geological classifications and engineering data are being utilized to characterize the liquefaction susceptibility of the geologic units and areas. The rating scheme based on geological age and mode of deposition is from the correlations described by Youd and Hoose (1977) and Youd and Perkins (1977). The rating scheme based on engineering data (principally the standard penetration resistance (blow count), and depth to ground water) uses the correlation developed by Seed (1979).

References

Seed, H. B., (1979), Soil liquefaction and cyclic mobility evaluation for level ground during earthquakes: Journal of the Geotechnical Engineering Division, v. 105, no. GT2, February.

Youd, T. L., and Hoose, S. N., (1977), Liquefaction Susceptibility and Geologic Setting: Sixth World Conference on Earthquake Engineering, New Delhi, India.

Youd, T. L., and Perkins, D. M., (1977), Mapping of liquefaction potential using probability concepts: The Use of Probabilities in Earthquake Engineering, ASCE, San Francisco, California, October.

H7

Soil Micromorphology and Faulting

14-08-0001-18320

Lowell A. Douglas

Department of Soils and Crops
Rutgers - The State University
New Brunswick, N. J. 08903
201-932-9800

Investigations

Undisturbed samples were obtained of paleosols and fault breccia associated with an unnamed fault at the Kerns Rock Co. gravel quarry (Figure 1), about 20 km. south of Bakersfield, Calif. Samples were returned to the laboratory for preparation of polished blocks and thin sections.

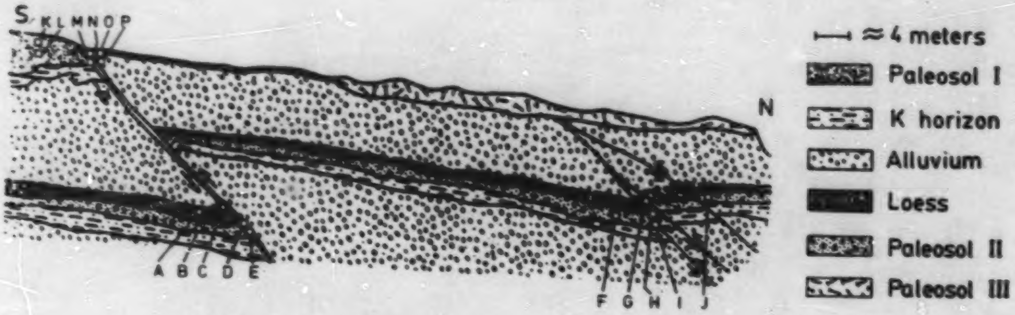

Figure 1. Faults and paleosols in the Kerns Rock Co. quarry, Calif. (Letters indicate sampling locations.)

Results

1. Micromorphometry. After air drying, the samples were vacuum impregnated with a polyester resin that included an ultra-violet fluorescent dye. Pore data were obtained by photographing the polished block under ultra-violet light. The resulting photograph showed pores (light colored) against a black background. Points representing ends of straight sections of soil pores were entered into a computer, from these photographs, using a stylus actuated digitizer. Three-dimensional representations of pore orientations were obtained utilizing a modification of Lafeber's (1965) techniques. Polished serial sections were obtained by photographing a face of a polished block. About 150 μm was removed from the face, using a Lapmaster polishing machine, a second photo taken, and pore data recorded, etc. A computer program based on the concepts of Kalkani and von Frese (1979) was written, which took the pore data from the serial sections and plotted numbers of pores by orientation on a steriographic projection.

Steriographic projections, utilizing equal area nets representing pores of sample B (Paleosol II) and sample D (drag zone of Paleosol II), are shown in Figure 2. The normal soil showed a moderate amount of orientation of soil pores while the drag zone showed a high degree of pore orientation with elongation in the direction of displacement within the drag zone.

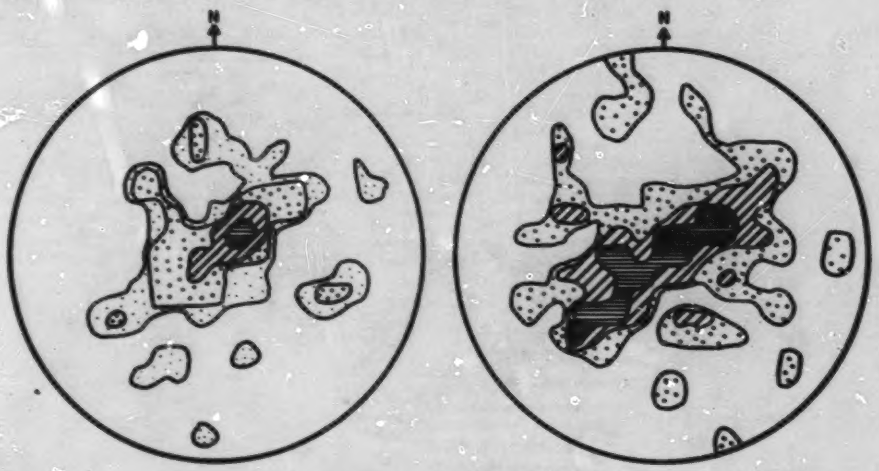

Figure 2. Equal area projections of densities of pores of similar orientation. Paleosol II left (sample B) and drag zone of Paleosol II right (sample D).

2. Micromorphology. Factors that were compared included: the prefaulting soil micromorphology, the effect of the relation of the sampling site to the fault (near, far, drag-zone, etc.) on micromorphology, and postfaulting pedological development.

Soil breccia zones have a unique micromorphometry and micromorphology. These zones are usually apedal, voids are ortho, and void argillans are absent. Assumed orientations are common with principal directions related to the direction of movement of the fault. Postfaulting pedological development may obscure fault induced characteristics. Care must be used when studying potential soil breccias because pedorelicts may be numerous; consequently, large thin sections must be used.

Literature cited:

Kalkani, E. C. and R. R. B. von Frese. 1979. An efficient construction of equal-area fabric diagrams. Computers & Geosciences 5: 301-311.

Lafeber, D. 1965. The graphical representation of planar pore patterns in soils. Australian J. Soil Res. 3: 143-164.

Papers presented:

Sole-Benet, A., L. A. Douglas and D. W. Platt. 1980. Three-dimensional pore distribution in faulted soils. Soil Science Society of America Meetings, Detroit.

Manuscripts prepared:

Douglas, Lowell A., Albert Sole-Benet, Alison J. Low and David W. Platt. Faulting and soil micromorphology. Submitted to: International Working Meeting in Soil Micromorphology, London.

Low, Alison J., Lowell A. Douglas and David W. Platt. Soil pore orientation and faults. To be submitted to: Proceedings of the Soil Science Society of America.

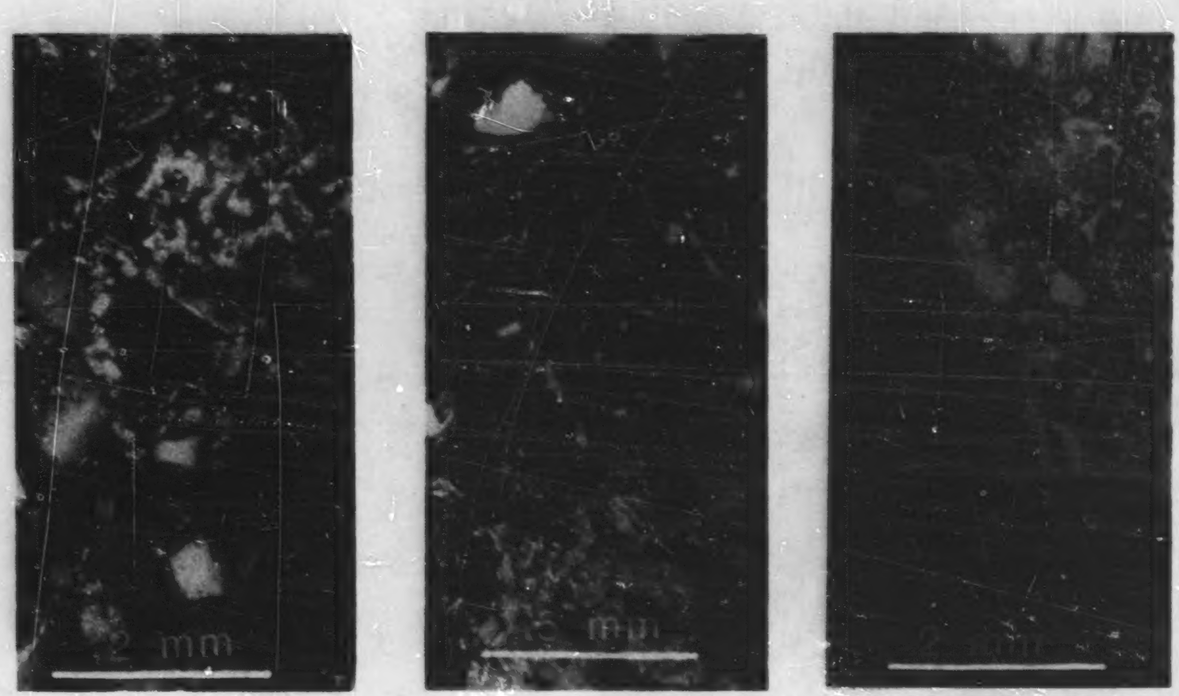

Plate 1. (a) Paleosol II, fabric. (b) Paleosol II, fault zone with recarbonation. (c) Paleosol I, fault zone, assumed orientation with direction of orientation parallel to movement of the fault.

Seismic-Induced Ground Failure

9550-01452

Edwin L. Harp
U.S. Geological Survey MS 98
Branch of Engineering Geology
Menlo Park, CA 94025
(415) 856-7124

Investigations

1. Compiled map at 1:62,500 of landslides resulting from the May 25-27 Mammoth Lakes, California earthquake sequence using conventional and military reconnaissance airphotos.

2. Re-calibrated and tested dynamic piezometers for scaling earthquake-induced pore-pressure records of aftershocks from Mammoth Lakes, California earthquakes. Processed and analyzed pore-pressure records. Compared them with equivalent strong motion records obtained at the same site.

3. Additional cone penetrometer data and samples were collected from Brawley, California from an area which underwent slumping along the New River from the 1979 Imperial Valley earthquake.

Results

1. A map at 1:62,500 scale of landslides from the May 25-27 Mammoth Lakes earthquake sequence depicts the distribution and morphology of individual landslides throughout the area most heavily affected. The mapping has shown that the landslides are concentrated most heavily along the mountain crests with the largest and most dense concentration coming from the Paleozoic metamorphics. However, landslides were also extensive within the Sierra granite with extensive regional joint systems exerting a strong control on landslide distribution within these rocks. Volcanic rocks showed a wide variation in landslide susceptibility. Weakly indurated tuffs shed numerous rock falls and slides; more throughly indurated, blocky tuffs exhibited markedly fewer failures; and massive andesites produced almost no failures.

2. Eight records of pore water pressure during aftershocks from the Mammoth Lakes earthquakes were gathered from piezometers emplaced within lake sediments that sustained liquefaction-induced lateral spread failures during the largest shocks. The eight pore pressure records are accompanied by strong motion records of the same aftershocks at the same site. Analysis is preliminary at this point, but inspection of the records indicates that frequencies of pore pressure fluctuations are similar to frequencies of strong motion for the first few seconds. After this, most of the pore pressure records show a loss of some of the higher frequency components as compared to the strong motion.

3. Additional drilling and cone penetrometer soundings of a large river-bank slump near Brawley, California from the 1979 Imperial Valley earthquake have

Ground Failures Caused by Historic Earthquakes

9550-02161

David K. Keefer
U.S. Geological Survey
Engineering Geology Branch
345 Middlefield Road M/S 98
Menlo Park, California 94025
(415) 856-7115

Investigations

1. Compilation and review of data on ground failures in historic earthquakes has been completed, and a review paper is being prepared.

2. Post-earthquake reconnaissance was conducted in collaboration with Ken Lajoie following the earthquake (M_L = 7.0) in Humboldt County, California, on 8 November 1980.

3. The compiled record of landslides in historic earthquakes was applied to the assessment of earthquake-induced landslide hazards in the Puget Sound region, Washington.

Results

1. Relative abundances of various types of landslides were determined for the 40 earthquakes chosen for complete analysis. Rock falls, soil slides, and rock slides from steep slopes are the most common types of earthquake-induced landslides. Soil slumps, block slides, and lateral spreads are also abundant. Eight other types of landslides, including large rock avalanches and submarine landslides, occur in smaller but still-significant numbers.

2. A bibliography containing citations to original sources of data on ground failures in earthquakes has been prepared for release as an open-file report.

3. The main structural and geologic effects of the 8 November 1980 Humboldt County earthquake were partial collapse of a freeway-overpass bridge, a few failures that occurred when wood-frame houses walked off their foundations, some broken chimneys, some minor landslides, ground cracks in several areas, and soil liquefaction at two sites. No unambiguous evidence of surface rupture along Quaternary faults was observed. The lack of major structural damage, landslides, or liquefaction in this M 7.0 earthquake is probably due to the depth and offshore location of the hypocenter.

4. Data from the 13 April 1949 (M_s = 7.0) and 29 April 1965 (M_s = 6.5) Puget Sound earthquakes were combined with analyses of other historic earthquakes to define geologic environments in the Puget Sound region susceptible to earthquake-induced ground failure. Environments with high susceptibilities include poorly compacted artificial fills; Holocene alluvial, lacustrine and beach sediments; river deltas; and slopes steeper than 35°.

refined our knowledge of the subsurface geotechnical conditions. A third profile across the failure gives greater control on the location of a subsurface sand that underwent liquefaction during the earthquake. The location of this sand with respect to the failure indicates that liquefaction of parts of it during the earthquake was probably the cause of the failure. Analysis of overlying silty clay and artificial fill also shows that failure confined within them would have been unlikely.

Reports

Bennett, M. J., Youd, T. L., Harp, E. L., and Wieczorek, G. F., 1981, Subsurface investigation of liquefaction, Imperial Valley earthquake, California, October 15, 1979, U.S. Geological Survey Open-File report 81-502, 82 p.

Harp, E. L., Bennett, M. J., and Keefer, D. K., 1981, Lateral-spread landslides from the May 25-27, 1980, Mammoth Lakes, California earthquake sequence--a geotechnical investigation, abs., Geological Society of America, Abstracts with Programs: v. 13, no. 2, p. 59.

Harp, E. L., and Keefer, D. K., 1981, Rock falls and rock slides near Mammoth Lakes, California triggered by the May 25-27, 1980 earthquake sequence, abs., Geological Society of America, Abstracts with Programs: v. 13, no. 2, p. 59.

Harp, E. L., 1980, Seismic-induced landslides in Ellingwood, B. R., (ed.), An investigation of the Miyagi-ken-oki, Japan earthquake of June 12, 1978: U.S. Department of Commerece, National Bureau of Standards, NBS Special Publication 592, p. 209-223.

Reports

Harp, E. L., Bennett, M. J., and Keefer, D. K., 1981, Lateral-spread landslides from the May 25-27, 1980, Mammoth Lakes, California earthquake sequence--a geotechnical investigation, [abs.],. Geological Society of America, Abstracts with Programs: v. 13, no. 2, p. 59.

Harp, E. L., and Keefer, D. K., 1981, Rock falls and rock slides near Mammoth Lakes, California triggered by the May 25-27, 1980 earthquake sequence, [abs.], Geological Society of America, Abstracts with Programs: v. 13, no. 2, p. 59.

Keefer, D. K., 1980, Liquefaction and damage to dikes in Ellingwood, B. R., (ed.), An investigation of the Miyagi-ken-oki, Japan, earthquake of June 12, 1978: U. S. Department of Commerce, National Bureau of Standards, NBS Special Publication 592, p. 195-208.

Keefer, D. K., and Tannaci, N. E., Bibliography on landslides, soil liquefaction, and related ground failures in selected historic earthquakes: U.S. Geological Survey Open-File Report 81-572 [Director's Approval].

Lajoie, K., and Keefer, D. K., 1981, Investigations of the 8 November 1980 earthquake in Humboldt County, California: U.S. Geological Survey Open-File Report 81-397, 30 p.

Youd, T. L., and Keefer, D. K., 1981, Earthquake-induced ground failures, in Hays, W. W., and Clarke, P. F., eds., Facing geologic and hydrologic hazards: U.S. Geological Survey Earth Science Special Report 2 in press

H7

Interactions Between Ground Motion and Ground Failure

9550-01628

Raymond C. Wilson
Engineering Geology Branch
U.S. Geological Survey
345 Middlefield Road MS 98
Menlo Park, California 94025
(415) 856-7126

Investigations

1. Developed a normalized "design curve" for displacement of a landslide mass versus the critical acceleration as an approximation of the Newmark seismic slope stability analysis.

2. Analysed the correlation between the displacement of the landslide mass calculated from the Newmark seismic slope stability analysis and the Arias seismic intensity parameter.

Results

1. A major strength of the seismic slope stability analysis developed by N. Newmark is its use of actual instrumental records, rather than an idealized theoretical model, to represent seismic ground motion. A major obstacle to practical application of the Newmark analysis is the lack of strong-motion records outside of a very few, heavily instrumented areas such as Japan and Southern California. For example, some method for preparing "design curves" of seismic slope stability (as expressed by displacement versus critical acceleration of the landslide mass) is necessary for regional mapping of susceptibility to earthquake induced landsliding in areas which are seismically active, but lack an inventory of strong-motion records (Alaska, Hawaii, the Intermountain West, and the Eastern U. S.).

The first step in the development of these "design curves" was to "normalize" the curves of displacement versus critical acceleration previously calculated for a number of existing strong-motion records. That is, to approximate these curves using a simpler relationship based on a few seismic "index" parameters (peak acceleration, duration, etc.). A normalized curve of displacement versus critical acceleration was derived from an analysis of the idealized case of a single, "sawtooth" pulse of acceleration, for which:

$$U = U0\ (1 - a_c/\hat{a})^3\ (1 + \tfrac{1}{2}(\hat{a}/a_c - 1)) \qquad (1)$$

where $\hat{a}$ = peak acceleration of the pulse, a_c = critical acceleration, and $U0$ = a "normalized" displacement. (CGS units for all variables.)
For the case of a single, "sawtooth" pulse,

$$U0 = \tfrac{1}{4}\ \hat{a}\ t_o^2 \qquad (2)$$

where t_0 = the duration of the single pulse (seconds). Most of the curves of displacement versus critical acceleration calculated from actual accelerograms may be closely fit by the curve in equation (1), using the actual value of the peak acceleration and a "normalized displacement", $U0$, "found" by letting $U0$ = the displacement calculated for a critical acceleration such that $a_c/\hat{a} = 0.258$ where $U = U0$ in eq. (1). Since the actual accelerograms are multiple, rather than single, pulse events, the calculation of $U0$ in eq. (2) no longer holds, but rather, $U0$ becomes a somewhat more complex function of the root mean square of the acceleration and the duration of the ground motion. The normalized displacement parameter, $U0$, may in fact be taken as a linear measure of "shaking intensity" (see next section), while eq. (1) represents the non-linear dependence of the Newmark displacement on the ratio of critical acceleration to peak acceleration, $a_c/\hat{a}$. Using only three "index" parameters--a_c, representing the static slope stability, and $\hat{a}$ and $U0$ to represent the intensity and duration, respectively, of the earthquake, the "normalized" relationship defined in equation (1) provides a good approximation to the far more complicated algorithm for calculating displacement from an actual strong-motion record.

2. As a further attempt to develop design curves with which to apply the Newmark seismic slope stability analysis to areas which lack adequate strong-motion records, an investigation was conducted to determine if the displacement calculated from the Newmark analysis correlates with the Arias intensity. Arias intensity is an instrumental measure of seismic shaking intensity derived from a strong-motion record and the relation:

$$I_A = \frac{\pi}{2g}\int_0^{T_o}(a(t)^2\,dt \qquad (3)$$

where: g = acceleration due to gravity, $a(t)$ = acceleration as function of time (from the strong-motion record), and T_0 = duration of the strong motion record. The Arias intensity is usually expressed in MKS units.

The first step in this study was to plot, for a given value of a_c, displacements calculated by the Newmark analysis from several strong-motion records, versus the Arias Intensities calculated for the same records. Statistically significant (98% level) correlations were found between the displacements and Arias Intensity. Further, the slopes of the regression lines of displacement versus Arias Intensity were found to be a reciprocal function of the critical acceleration, so that the entire suite of displacement/intensity curves may be approximated by

$$U = 1.53\ I_A/a_c \qquad (4)$$

where U is in cm., a_c in g's, and I_A in m/sec.

The relationship in eq. (4) suggested a correlation between Arias intensity and the displacement normalization parameter, $U0$, discussed in the previous section. This correlation is also statistically significant (95% level) and may be expressed as

$$U0 = 3.0\ I_A/\hat{a} \qquad (5)$$

where $U0$ is in cm., I_A in m/sec., and $\hat{a}$ in g's.

By combining eq. (5) with eq. (1) from the previous section, the entire curve of displacement versus critical acceleration (U vs a_c), for a given "design" earthquake may be approximated using only the two parameters, peak acceleration and Arias Intensity, from the resulting relationship:

$$U = (3.0\ I_A/\hat{a})(1 - a_c/\hat{a})^3(1 + \tfrac{1}{2}(\hat{a}/a_c - 1)) \qquad (6)$$

Therefore, even in areas where strong-motion records are lacking, the Newmark seismic slope stability analysis may now be applied, if both the expected peak acceleration and the Arias Intensity can be estimated. A number of published design formulas and graphical representations of both parameters as a function of magnitude and distance are already available.

Additional project studies are underway to select the most reliable magnitude/distance curves for peak acceleration and Arias Intensity as well as to attempt a direct correlation between magnitude/distance and displacement/critical-acceleration curves using the existing "library" of strong-motion records. The design curves which result from these studies should allow a greatly expanded application of the Newmark seismic slope stability analysis to practical mitagation measures and hazards mapping in those areas which currently lack an adequate strong-motion data set.

Reports

Youd, T. L., Wilson, R. C., and Schuster, R. L., 1981, Stability of blockage in the North Fork of the Toutle River, in Lipman, P. W., and Mullineaux, D. R., eds., Eruption of Mount St. Helens: U.S. Geological Survey Professional Paper 1250, 18 ms. p. (in press).

Harp, E. L., Wilson, R. C., and Wieczorek, G. F., 1981, Landslides from the February 4, Guatemala earthquake: U.S. Geological Survey Professional Paper 1204-A, 40 p. (in press).

Wieczorek, G. F., Wilson, R. C., and Harp, E. L., Seismic slope stability map of San Mateo County, California: U.S. Geological Survey Miscellaneous Geologic Investigations I-Map, scale 1:62,500 (now being revised after technical review).

Wilson, R. C., and Keefer, D. K., Dynamic analysis of a slope failure from the Coyote Lake, California, earthquake using strong-motion records: Seismological Society of America Bulletin (in technical review).

Experimental Mapping of Liquefaction Potential

9550-01629

T. Leslie Youd
Branch of Engineering Geology
U.S. Geological Survey, MS 98
Menlo Park, CA 94025
(415) 856-7117

Investigations

1. Continued compilation of a liquefaction potential map for San Mateo County, California.

2. Conducted subsurface investigations including cone and standard penetration soundings and sampling with an Osterberg sampler at two sites where liquefaction occurred during the 1979 Imperial Valley, California, earthquake.

3. Began compilation of logs for drill holes and soundings beneath strong motion instrument sites in the Imperial Valley, California.

Results

Subsurface investigations were made to study the geotechnical properties of soils that liquefied and did not liquefy during the October 15, 1979, Imperial Valley, California, earthquake ($M=6.6$). Investigations were made at Heber Dunes County Park 16 km southeast of El Centro and at River Park in the southwest part of Brawley. Highly detailed profiles were constructed from cone penetration and standard penetration results and from examination of disturbed and undisturbed samples. Liquefaction effects including sand boils, ground cracks, and lateral spreading occurred at the Heber Dunes site in a 5-m deep, loose, channel-sand deposit. That deposit lies in an abandoned channel that is part of an ancient delta. One bank of the channel contains a moderately dense overbank deposit; the other bank contains a dense point bar deposit. Other than a few sand boils over a buried pipeline, no surficial liquefaction effects occurred in the denser sand deposits outside the channel. Hundreds of sand boils erupted on the flood plain at River Park. Sand boils originated from both a 3-m deep, loose, sandy-sand layer, and from 6-m deep, medium-dense channel sand deposit. A 1.5-m thick, soft, clay layer is sandwiched between the two layers that liquefied. The behavior of the sands that did and did not liquefy at both sites are in general agreement with behavior predicted by standard engineering analyses.

Reports

Bennett, M.J., Youd, T.L., Harp, E.L., and Wieczorek, G.F., 1981, Subsurface investigations of liquefaction, Imperial Valley Earthquake, California, October 15, 1979: U.S. Geological Survey Open-File Report 81-502, 82p.

Herd, D.G., Youd, T.L., Meyer, H., Arango, J.L., Person, W.J.and Mendoza, C., 1981, The great Tumaco, Colombia earthquake of 12 December 1979: Science, v. 211, p. 441-445.

A Time and Space Dependent Model for Earthquake Occurrences

14-08-0001-19155

Anne Kiremidjian and Thalia Anagnos
Stanford University
Stanford, CA 94305
(415) 497-3664

This research is concerned with modeling the spatial and temporal dependencies that often make a Poisson Process inadequate for describing the seismicity on a fault or in an area. Effort is being made to include certain aspects of the physical mechanism in the model formulation and parameter determination. Examination of the current literature on energy accumulation and release mechanisms for earthquakes, has led to a model description which incorporates the cumulative energy on a fault as a factor in the determination of the time and location of an event. Since uncertainty exists about the true mechanism which underlies earthquake occurrences, a probabilistic description of the mechanism is necessary. Therefore, a Markov Renewal Process has been chosen to model earthquake events. At present, the formulation includes only the temporal dependence, but spatial dependence may be included by dividing a fault into segments and modelling the energy in all of the segments simultaneously.

The Markov Renewal Process was chosen because, unlike the Poisson Process, it incorporates memory in its transition steps. The memory is "one-step". That is, given the past history of level changes and the times of their occurrences on the fault, the next transition depends only on the present energy level. Using the assumption that energy along the fault is accumulated at a constant rate, temporal dependence is introduced into the earthquake histories.

As the process evolves in time, pairs of random variables are produced which describe the level of energy and the times at which transitions occur. A schematic of the process is shown in Figure 1. In order to describe the process the following random variables must be defined:

Y_n = level of energy at the nth transition

T_n = time to the nth transition

$X_n = T_n - T_{n-1}$ = time between nth and $(n-1)^{st}$ transition

τ_m = time to mth energy release, or earthquake

$M_m = Y_n - Y_{n-1}$ = magnitude of mth earthquake

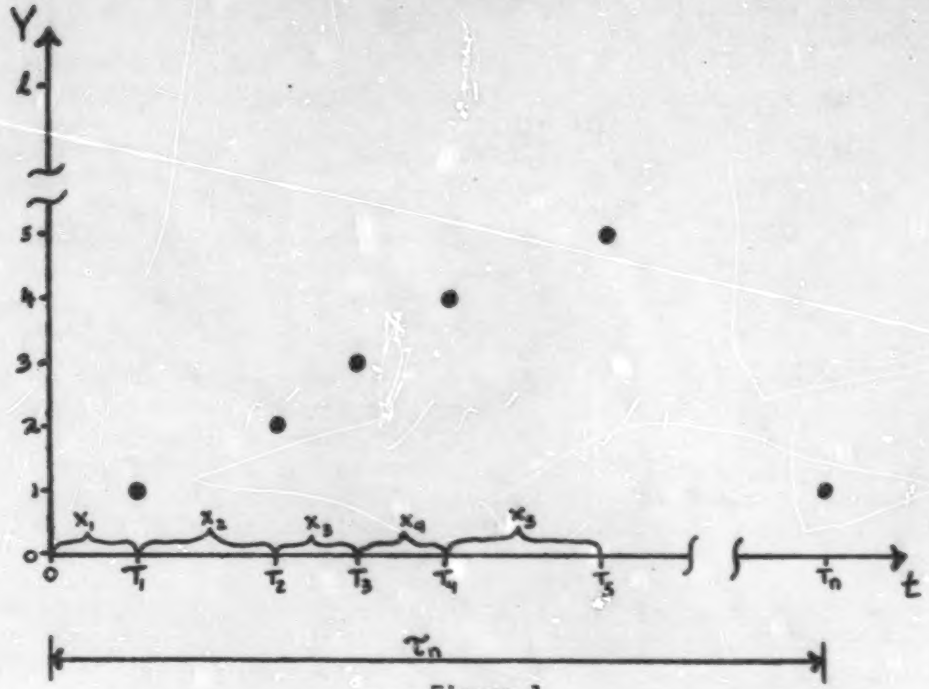

Figure 1

At each transition the pair (Y_n, T_n) are determined. When $Y_n < Y_{n-1}$, the level of energy decreases and an earthquake has occurred. The movement of the process in time is governed by the following equation:

$$P[Y_{n+1} = j, T_{n+1} - T_n \leq x \mid T_n, T_{n-1} \cdots T_0, Y_n, Y_{n-1} \cdots Y_0]$$

$$= P[Y_{n+1} = j, T_{n+1} - T_n \leq x \mid Y_n = i] = p_{ij} F_{ij}(x)$$

where p_{ij} = probability that the next level is j, given the present level is i, and

$F_{ij}(x)$ = probability that the conditional holding time in state i is $\leq x$ given the next jump is to state j

The transition probability, p_{ij}, is used to determine the next energy level, then the time of the next transition is determined through the conditional holding time distribution. Assuming that the fault can only increase energy one level at a time, the matrix of transition probabilities would have zeros above the superdiagonal. If energy release is assumed to be total at the occurrence of an earthquake, many of the transition probabilities below the diagonal will also have zero values.

$$(p_{ij}) = \begin{bmatrix} p_{00} & p_{01} & 0 & 0 & \cdots & 0 \\ p_{10} & p_{11} & p_{12} & 0 & \cdots & 0 \\ p_{20} & p_{21} & p_{22} & p_{23} & \cdots & 0 \\ \cdot & & & & & \\ \cdot & & & & & \\ \cdot & & & & & p_{n-1,n} \\ p_{no} & \cdot & \cdot & \cdot & & p_{nn} \end{bmatrix}$$

At the present time, the transition probabilities are being determined. The distributions on the holding times are determined from intensity functions also known as failure rate distributions. The intensity function, $r(t)$, is defined as the probability of an earthquake occurrence in a finite interval of time, x, given that no earthquake has occurred up to time t. Then, if $G(t)$ is the failure distribution,

$$r(t) = \lim_{x \to o} \frac{G(t+x) - G(t)}{x[1 - G(t)]} .$$

If $r(t)$ is known, then $G(t)$ can be determined from

$$1 - G(t) = \exp [- \int_0^t r(u)du].$$

The work that is now being done concerns specification of parameters for the model and sensitivity analysis. The Weibull and extreme value distribution are both being examined to describe the holding times for large events. The exponential distribution seems appropriate for smaller events. Energy accumulation and release mechanisms are being examined to determine the transition probabilities.

Laboratory and Field Investigations of Fault Gouge

14-08-0001-17677

John M. Logan
Center for Tectonophysics
Texas A&M University
College Station, Texas 77843
(713) 845-3251
30 October 1980

Investigations

The overall objective of this project is to investigate fault mechanics of gouge-host rock systems through controlled laboratory experiments and correlated field studies with the emphasis on understanding the operative physical principles that govern shallow-focus earthquakes. In this report we discuss the results of investigations into two areas: (1) field studies of natural fault zones and (2) laboratory studies of time-dependent friction behavior.

Results

Field studies of natural fault zones. Field studies are still in progress along the Palochic fault zone in Guatemala. A part of the zone which is actively creeping is being studied to characterize the physical properties. Correlation of the field data with the results of current laboratory studies will be used to infer mechanical processes. As the field work is still in progress final results will be delayed until a later time, but presently some tentative observations can be made. The original trace of the fault had one very large and several broad sinusoidal bends to it. As the fault displaced one block overrode the other, forming depositional basins. The rocks in the depositional basins have subsequently been faulted to form slivers which give the fault a braided form. The active displacement zone appears to get progressively narrower as slip progresses. This will produce higher shear strains. This model is similar to that proposed by Crowell for segments of the San Andreas and other faults. It also agrees with observations of experimental studies of simulated fault zones. Further petrofabric studies of samples should provide insights into the operative mechanical processes.

Laboratory studies of time-dependent friction behavior. During the latter part of this contract period we have directed our effort toward developing a physical basis for some of the complex phenomena observed in friction experiments from both our and other laboratories. A model is proposed which follows closely that of Dieterich (1978, 1979) and of Johnson (1980), but which, in addition, is strongly influenced by the earlier works of Rabinowicz (1957) and Kragelskii (1965). The model attempts to provide an explanation for the observed phenomena of (1) the strengthening of frictional surfaces with increasing time of contact (Dieterich, 1978; Teufel and Logan, 1978) and (2) the weakening of intact rocks with increasing time of deformation (Stesky et al., 1974). The model is then compared with the experimental data of this laboratory and other workers. The conclusions of this analysis are:

(1) A necessary but not sufficient condition for the occurrence of stick-slip in a frictional system is that the system must exhibit an inverse dependence of shearing resistance on shear strain rate or shear displacement rate, at the conditions under which it is being deformed.

(2) In order that the system may possess this characteristic, the strain rate sensitivity of the applied stress must be greater for deformation of asperities normal to the surface than for shear, by an amount which exceeds the reciprocal of the exponent in the geometric distribution function describing the variation of asperity heights across the surface.

(3) It might be expected that inverse strain-rate effects are more often associated with polished, than with rough, surfaces.

(4) Condition (2) (above) is most readily met when a positive gradient in the mechanical properties with depth exists, such that, for a given stress, the constitutive relation for creep of adhesive junctions leads to higher strain rates than that for creep of the bulk material, and the two relations are independent of each other.

(5) Inverse strain-rate effects lead to a microstructure that is characterized by discrete zones of relative displacement, and which is therefore highly heterogeneous. Evidence that a shear zone has deformed only by homogeneous flow, precludes the possibility that the zone may have undergone unstable frictional slip, and is therefore diagnostic of stable deformation. Conversely, regions of a fault that have deformed unstably should display heterogeneous deformation features, i.e., discrete slip zones within relatively undeformed material.

Reports

Logan, J. M., N. Higgs, M. Friedman, and H. Gatto-Baver, 1979, Preliminary investigation of core material from U.S.G.S. Dry Valley No. 1 well, San Andreas fault, EOS, 60, 956.

Higgs, N. G., and J. M. Logan, 1979, Effects of temperature on the deformation of experimental quartz-clay shear zones, EOS, 60, 956.

Dengo, C. A., and J. M. Logan, 1979, Correlation of fracture patterns in natural and experimental shear zones, EOS, 60, 955.

Teufel, L. W., 1979, Critical velocity for stick-slip sliding, EOS, 60, 956.

Shimamoto, T., J. Handin, and J. M. Logan, 1980, Specimen-apparatus interaction during stick-slip in a triaxial compression machine: a decoupled two-degree-of-freedom model, Tectonophysics, 67, 175-205.

Teufel, L. W., 1980, Precursive pore pressure changes associated with premonitory slip during stick-slip sliding, Tectonophysics, 69, 189-199.

Seismic Damage Assessment for High-Rise Buildings

14-08-0001-19111

Roger E. Scholl
URS/John A. Blume & Associates, Engineers
130 Jessie Street (at New Montgomery)
San Francisco, California 94105
(415) 397-2525

Investigations

The objectives of this research work are to improve quantitative reliability and refine earthquake damage prediction procedures for high-rise buildings. The research effort consists of three one-year phases made up of five major tasks, as follows:

Task I	Data collection
Task II	Building categorization and calculation of theoretical motion-damage relationships
Task III	Estimation of engineering intensity from seismological intensity data
Task IV	Evaluation of empirical motion-damage relationships
Task V	Correlations between theoretical and empirical motion-damage relationships

Task I was largely completed during the first phase. Work on Task II was initiated during the first phase and is scheduled for completion during the third (current) phase. Task III was completed recently. Initiated during the second phase, Task IV will be completed during the current phase. Task V is to be performed entirely during the third phase and will complete the research.

Results

Task I: In this task, seismic motion-damage data from past earthquakes worldwide were collected for high-rise buildings. For each building, the collected data include a description of the earthquake, the ground motion, local geology, and building characteristics, and the extent of damage. A computerized data base, HIRISE, was created, and the data collected are stored in this data base. The data base allows statistical processing, updating, and accessing the stored information in any sequence; these capabilities enable studies correlating various parameters to be performed easily.

Task II: Categorization of major building systems and description of subsystems under each category has been accomplished; this information was used to structure the data base. There is a current trend in damage prediction technology toward predicting losses to building components such as structural frame, partitions, glass, mechanical components, etc., the losses being calculated in terms of local structure response, floor by floor. Earlier in the project, three buildings damaged by the San Fernando earthquake (the Bank of California, and two Holiday Inn buildings) were analyzed with the intention of relating the calculated responses of these structures to local component damage. However, studies show that the available information does not allow a floor-by-floor assessment of component damage. A discussion of the work performed will be provided in our final report, although it may be considered inappropriate to include the analyses themselves.

Our continuing research into current trends in damage prediction technology has resulted in the development of some new concepts. Currently, experimental data relating local response to component damage are being compiled. These data and the theoretical procedures for utilizing them in damage prediction will be included in the final report.

Task III: The work on this task has been completed. We have acquired and stored on magnetic tape the two horizontal response spectra obtained from each of 520 ground motion records. A computer code was developed to sort these records by magnitude, site geology, site intensity, peak ground acceleration, epicentral distance, and strong motion duration. Another code was developed to compute the mean and mean plus one standard deviation response spectra for any selected group of records. Using the seismological data and the computer codes, we computed mean and mean plus one standard deviation spectra for various Modified Mercalli Intensity (MMI) levels and site geological conditions. These spectra are used to correlate MMI scale with Engineering Intensity Scale (EIS) for various period bands.

Task IV: Various empirically derived motion-damage relationships, or damage matrices, are currently being developed from data base HIRISE. The principal indicators of damage to be calculated are the damage factor (DF), defined as the ratio of dollar damage to replacement value, and the damage ratio (DR), defined as the ratio of the number of buildings damaged to the total number of buildings in a given area. These damage parameters will be correlated with motion identified in terms of EIS level. Finally, these empirical motion-damage relationships will be calculated for various building categories -- including subclasses for various types of structural and nonstructural components -- as the available data permit.

Reports

URS/John A. Blume & Associates, Engineers, *Seismic Damage Assessment for High-Rise Buildings; Semiannual Technical Report: October 1978*, San Francisco, California, 1978.

_______, *Seismic Damage Assessment for High-Rise Buildings: Annual Technical Report, April 1979*, San Francisco, California, 1979.

_______, *Seismic Damage Assessment for High-Rise Buildings; Semiannual Technical Report: October 1979*, San Francisco, California, 1979.

_______, *Seismic Damage Assessment for High-Rise Buildings; Annual Technical Report: August 1980*, San Francisco, California, 1980.

A Stochastic and Bayesian Model for Seismic Hazard Mapping

14-08-0001-17767

Haresh C. Shah
Craig Schoof
Christian P. Mortgat
Martin W. McCann, Jr.
The John A. Blume Earthquake Engineering Center
Dept. of Civil Engineering
Stanford University
Stanford, CA 94305
(415) 497-4150

Two general tasks were investigated under USGS project No. 14-08-0001-17767, titled, "A Stochastic and Bayesian Model for Seismic Hazard Mapping". Task I was to develop a stochastic model for seismic hazard analysis with geophysical input. Task II was to critically investigate the currently used Bayesian models in seismic hazard analysis. This task also developed priors based on theoretical geophysical models and on subjective knowledge of experts.

In Task I, a nonhomogeneous Poisson model was used to model earthquake occurrence. Weibull distribution can be viewed as an extension of the Poisson process for seismic occurrence model. Probabilistic power spectral density of the acceleration for a site was developed by using geophysical model rather than empirical attenuation laws. Finally, time history and response spectra for given sources and site conditions were obtained by using random vibration theories. (Savy et al., 1980).

The second task involved the use of statistical Bayesian theory to complement the available historical and geological data on occurrence and size of past events by means of prior or subjective knowledge about the two variables. Probabilistic seismic hazard estimation based on historical data alone has been subjected to criticism from geologists, engineers and seismologists. Use of Bayes theorem permits the analyst to use information from other sources. In the literature, many researchers have used the term "Bayesian Analyses" rather loosely. Any time some subjective information on source geometry, upper cutoff magnitude, attenuation or recurrence has been used in a quantitative sense, people have labelled the method as Bayesian. One should be careful in calling such procedures as Bayesian. Only when one uses the Bayes theorem in the context of equation 1 can one label the procedure as that of Bayes.

$$P'' = NLP' \qquad \text{Eq. 1}$$

where

P" is the posterior probability distribution on the variable of interest

L is the data based likelihood function about the variable of interest

P' is the apriori or subjective information about the variable

N is the normalizing constant

In the work performed under the subject project, Bayes theorem was used for complementing occurrence of events and magnitude (or size) of events. Other information on source geometry, attenuation, uncertainties on source and site parameters was complemented by quantifying subjective information but not in the context of Bayes theorem.

A questionnaire was developed to obtain subjective information on the following parameters;

1. Source zone configuration
2. Maximum earthquakes
3. Earthquake occurrences
4. Attenuation

A total of 23 questions were developed. Six experts who are familiar with the San Francisco Bay Area seismicity were questioned. An average time of about two hours was taken by each expert to answer fully the 23 questions covering the four areas mentioned above. Using the above subjective information and the available data, a detailed sensitivity analysis for probabilistic seismic hazard estimation for a site within the Bay Area was carried out. Based on the experience gained in obtaining subjective information and using such information in Bayesian and non-Bayesian context for seismic hazard analysis, the following points can be made:

- Development of a questionnaire to extract subjective information from experts should be made with extreme caution and with minimum of ambiguity in individual questions as well as in consistency between questions.

- When subjective information is obtained, its weight (or level of confidence) with respect to historical data should be carefully evaluated. This particular aspect is important and should be further investigated. As an example, how does one weigh the 100 yr. occurrence data for a given source with the subjective information on creep rate of the fault or the geologic evidence on fault displacement?

- When an expert assigns a probability distribution or confidence on a given variable (say the size of the maximum event) he may not realize that a weight is automatically given to the quality of his information vis-a-vis the available historical evidence.

- Many experts find it difficult to assign probability distributions on variables about which they are interviewed. This makes it difficult for using Bayes formulation in a consistent manner.

- An expert, while answering various questions does not realize that he may be giving inconsistent answers to two related questions.

- When many experts are interviewed to get their subjective input, it is almost impossible to weigh respouse of one expert with that of the other or with the data base information. In such cases, it is best to obtain results by combining the prior of each individual with the likelihood function separately. The posterior obtained in this manner from all the experts can then be compared.

- It is difficult to separate systematic errors from random errors in the experts response. However techniques are available to minimize this problem.

- Use of the Bayes' theorem forces the analyst in getting additional information and in systematizing his analysis procedures.

- Information gathered in this manner facilitates the evaluation of sensitivity in seismic hazard estimation.

- Consistency check between data, geologic evidence and opinion of various experts is possible.

- From a practical and pragmatic point of view, using this approach makes the evaluation of seismic hazard a lot more acceptable to engineers and earth scientists. It gives a perception (to the user of results) that all the available information was utilized in arriving at the hazard estimate.

Finally, McCann (1981) used the Bayesian method to incorporate geophysical model for seismic hazard analysis. The root mean square acceleration parameter was used to update the data base information with the information from geophysical model. The result of the model is a probabilistic power spectral density function at a site due to an event of a given size.

References

1. Savy, J.B., Shah, H.C. and Boore, D., 1980, Non-Stationary Risk Model with Geophysical Input, Journal of Structures Division, Proceedings of the American Society of Civil Engineers, Vol. 106, No. ST1. Pages 145-163.

2. McCann, M.W., Jr., 1981, A Bayesian Geophysical Model for Seismic Hazard, Technical Report No. 47. The John A. Blume Earthquake Engineering Center, Dept. of Civil Engineering, Stanford University, Stanford, CA

On-Line Seismic Processing

9970-02940

Rex Allen
Branch of Network Operations
U.S. Geological Survey
345 Middlefield Road - MS-77
Menlo Park, California 94025
(415) 323-8111, ex. 2240

Investigations

The investigations for this period have centered on improvements of the Real-Time Picker (RTP) both in hardware and software to obtain greater versatility and reliability. The picker program has been improved, and is still being upgraded to obtain more accurate magnitude estimates. The supervisor-associator program has undergone several improvements and has recently been modified to allow it to run in read-only memory (ROM) in a standard microcomputer configuration. This will make the system cheaper, simpler, and much more reliable.

We are nearing completion of the 120-station installation for the University of Washington, and are preparing to start work on a system for the Hawaii Volcano Observatory.

Results

The Real Time Picker (RTP) is now in operation with a full complement of 32 processors, each monitoring 8 seismic lines, for a total of 256 seismic stations. This includes all of the California Network west of the Great Valley from Parkfield to the Oregon border plus a selection of stations from other nets in the Sierra and southern California. Comparison of results from the RTP with Calnet handpicks indicates that the RTP picks are superior in sensitivity and timing accuracy. This conclusion is based on a comparison of rms residuals from the two systems and also on a pick-by-pick comparison of identical phase lists.

RTP phase card output is routed to a PDP11/70 computer for immediate location and also to an 8-track magnetic tape as a backup device. RTP results are being routinely used in Calnet processing under procedures developed by Jerry Eaton which allow evaluation of results and a gradual increase of reliance on the RTP as it proves itself and we learn to make proper use of it.

Seismic Source Mechanism Studies in the Anza-Coyote Canyon Seismic Gap

14-08-0001-18397

Jonathan Berger and James N. Brune

Institute of Geophysics & Planetary Physics
Scripps Institution of Oceanography
University of California, San Diego
La Jolla, CA 92093
(714) 452-2889

Seismic Studies

While awaiting the deployment of our telemetered array, we have been operating digital event recorders in the Anza area for extended periods of time. We operated an array of seven instruments for a period of about three weeks after the February 25, 1980 earthquake ($M=5.5$). We also have been operating an array of four digital event recorders for the last few months. We are able to make some preliminary comparisons between these data and data recorded earlier, in 1977 and 1978. Spectra and corrected ground motion for three typical aftershocks of the February 25, 1980 earthquake show very simple pulses, quite similar to what is theoretically expected for a simple dislocation, indicating that as expected the Anza area is an ideal site to study the mechanism of earthquakes because of its structural homogeneity, high Q, and shallow events.

One of the main objects of the research is to understand the nature of the high frequency energy in local earthquakes, since this is important in understanding strong motion for larger earthquakes. In particular, we would like to understand the high frequency spectral fall-off and coherency. To give a preliminary idea of the nature of the data which will become available, we have studied in more detail the spectra of some of the larger events we have recorded so far on digital seismographs in the Anza Area. In order to see if the high frequency energy in the spectra is signal or noise, we have filtered the time series through band-pass Parzen filters (Figure 1). The original seismograms are shown at the top of each figure, and the filtered traces below. As can be seen, the filtered seismograms clearly show the P-waves and the S-waves. This illustrates the necessity of the high sample rate we have specified in the telemetered array if we are to be confident of recording the higher frequency energy radiated by earthquakes at Anza. This high frequency energy will hopefully tell us about the details of the slip process during faulting, e.g., the roughness of the fault plan and the complexity of the faulting.

Instrumentation

The first year of this project was devoted to instrument design and prototype construction and testing. Our decision to utilize high sample rate digital telemetry and return all the data in real time back to our La Jolla labs resulted in the initiation of a new generation of seismic equipment. We have been working with Dr. W. E. Farrell, of Systems, Science and Software in La Jolla, and Dr. Paul Passmore, of Refraction Technology in Dallas, in the design and construction of this equipment. A one-station prototype has been constructed and tested and orders for the complete equipment for 10 stations will be placed as soon as we have our VHF telemetry frequency assignments (about March 1981). Station locations have been chosen and remotely recording seismic stations operated at most sites. Deployment of the telemetered array will begin in the spring with full operation planned by summer.

The design of the ANZA seismic array allows for up to 16 three component remote digital stations, each channel (seismic component) being sampled 250 times per second and digitized with a 16 bit A/D. In order to transmit the data from the seismic stations (spread over the Anza area) to a central recording site in La Jolla, a relay station is necessary due to the local topography. Fortunately, a nearby peak on Santa Rosa Mountain (Toro Peak) has a clear line of sight to the Anza area, Piñon Flat Observatory, and down to San Diego. The plan, then, is to transmit the seismic data *via* VHF radio link to Toro Peak, multiplex the data, and relay it to IGPP *via* Mt. Soledad at La Jolla over a microwave link. The overall scheme is illustrated in Figure 2.

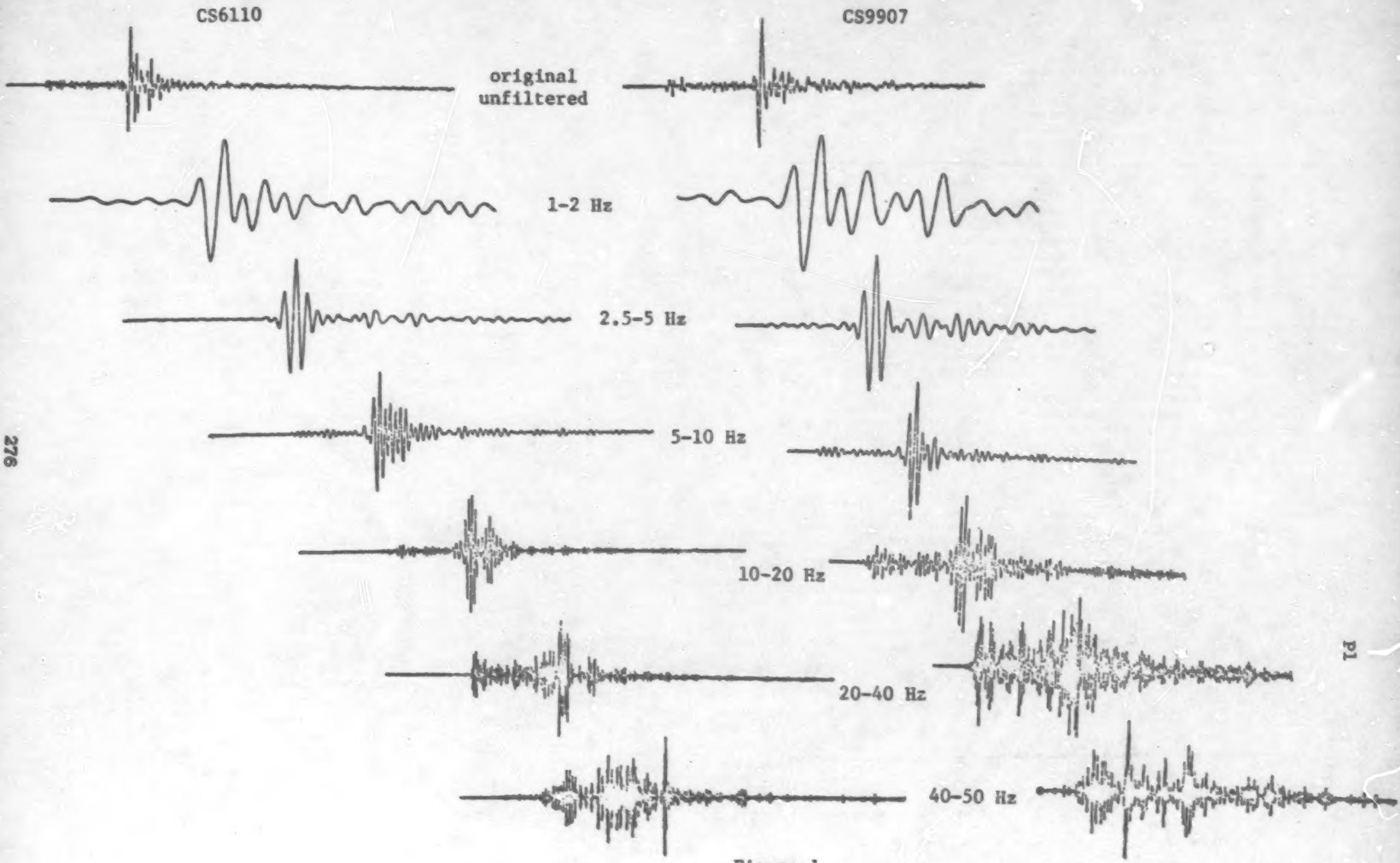
CS6110
CS9907
original unfiltered
1-2 Hz
2.5-5 Hz
5-10 Hz
10-20 Hz
20-40 Hz
40-50 Hz

Figure 1.

P1

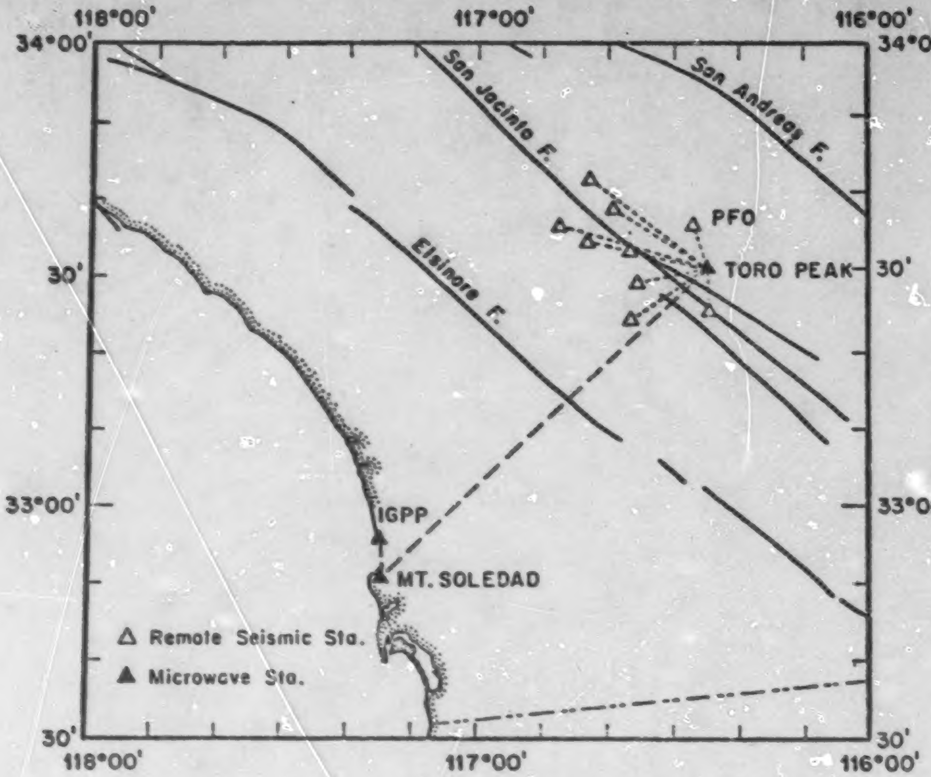
118°00'
117°00'
116°00'
34°00'
30'
33°00'
San Jacinto F.
San Andreas F.
Elsinore F.
PFO
TORO PEAK
IGPP
MT. SOLEDAD
△ Remote Seismic Sta.
▲ Microwave Sta.

ANZA DIGITAL SEISMIC DATA LINK

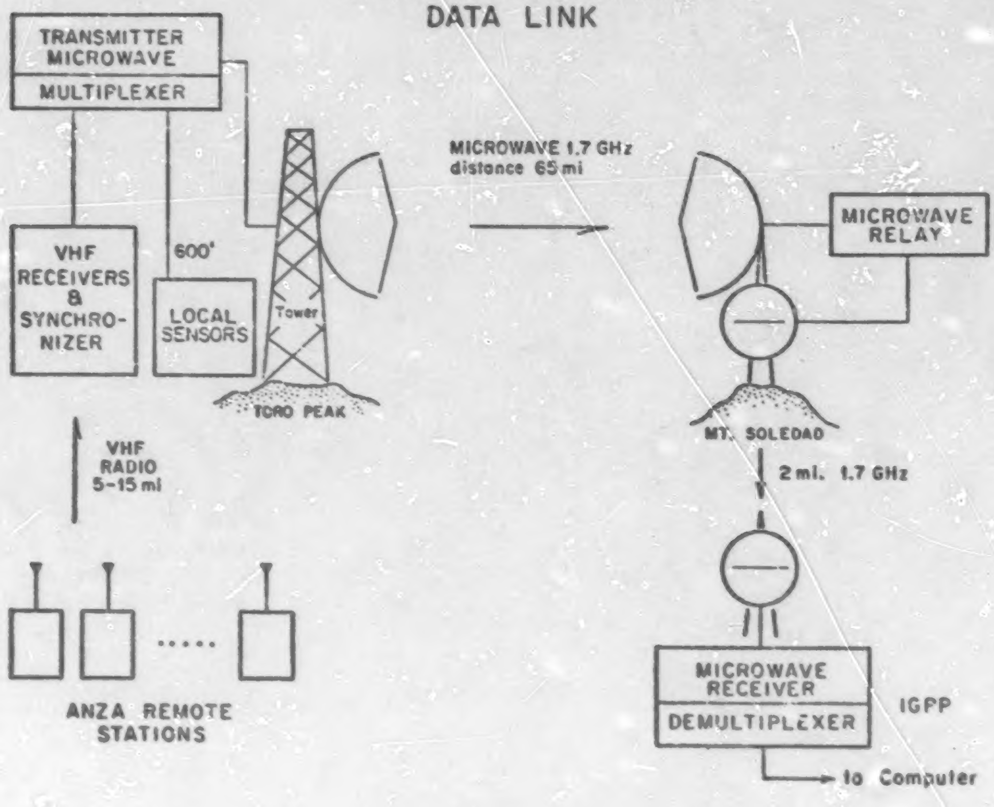
TRANSMITTER MICROWAVE
MULTIPLEXER
VHF RECEIVERS & SYNCHRONIZER
600'
LOCAL SENSORS
Tower
TORO PEAK
VHF RADIO 5-15 mi
ANZA REMOTE STATIONS
MICROWAVE 1.7 GHz distance 65 mi
MICROWAVE RELAY
MT. SOLEDAD
2 mi. 1.7 GHz
MICROWAVE RECEIVER
DEMULTIPLEXER
IGPP
to Computer

Very Long Period Seismic Studies in the U.S.S.R.

14-08-0001-18328

Jonathan Berger and Freeman Gilbert

Institute of Geophysics & Planetary Physics
Scripps Institution of Oceanography
University of California, San Diego
La Jolla, CA 92093
(714) 452-2889

Under the US/USSR "Agreement on Cooperation in the Field of Environmental Protection," we have operated two very long period seismic stations which we installed in the USSR. The data from the IDA array are being used in studies of variations in the long period spectral content of local earthquakes, possibly premonitory to large events; temporal changes in tidal admittances associated with changes in local elastic properties; and properties of tsunamigenic earthquakes.

The operation of the station in Yuzhno-Sakalinsk has been unproductive and that equipment has been returned to us by the Soviets (March 1981). When the opportunity to install a station in the People's Republic of China at Kunming was presented to us, USGS gave us permission to use travel funds, originally designated for the now closed station in USSR, to defray costs to travel to China to install this new station. This station went into operation October, 1980.

Political conditions in 1980 seemed to keep us from travelling to the station at Garm; however, we recently received almost a year's worth of data, sent by Dr. Nersesov while visiting in the United States. Dr. Nersesov told us that the data logger from Garm is being sent to us for repair. After receiving the data logger and repairing it, it is our intent to travel to Garm to re-calibrate the equipment and set up the recorder for our new 10 second format.

Crustal Deformation Observatory
Part D - Data Logging Facilities

14-08-0001-18365

Jonathan Berger, Principal Investigator
Frank Wyatt, Associate Investigator
Institute of Geophysics & Planetary Physics
University of California, San Diego
La Jolla, CA 92093
(714) 452-2019

In the past year considerable progress has been made at Piñon Flat Observatory (PFO) in providing facilities and field assistance for independent investigators. This effort was undertaken as part of the multi-institutional Crustal Deformation Observatory (CDO) project. The overall aim of the program is to evaluate existing and proposed instrumentation for measuring long period (days to years) ground deformation in an area of active tectonic deformation. Based on historical observations and current seismic studies the adjacent San Jacinto fault zone is a prime candidate for a moderate ($\sim M_L$ 6) in the near future. The experiment is being conducted by operating an array of differing instruments at PFO, each of which should record consistent tectonic signals. The various techniques will be evaluated by attempting to understand and reduce sources of noise in the instrumentation and instrument/earth interface.

Improvements in the CDO facility include:

1. Extensive electrical and signal wiring has been installed at the site (in excess of 10 km of cabling) interconnecting the new vaults and enclosures with the recording facility.

2. Design and construction of standardized signal amplifiers (drivers) and filters (receivers) have reduced the problems normally associated with reliably transmitting low level analog signals over moderate distances.

3. A digital cassette data logger has been fabricated and installed, capable of recording up to 30 channels of information with 12-bit resolution.

4. Programs have been written to decode (unpack) the digital cassettes and to correct timing errors in the data series. A standard "station tape" format has been adopted for distribution of the data to all the investigators.

5. Multiplexed visual recorders have been fabricated to continuously monitor the status of the various instruments.

6. A resident care-taker has assisted in the construction, operation, and recording of the new instrumentation.

Much of our effort at PFO has involved attempting to assist independent investigators in their difficult assignments of establishing an experiment at a remote field site. We intend to continue this operational support in the coming year. We hope this will encourage additional investigators to participate in the CDO program. Table 1 lists the current cooperative studies at PFO.

Table 1.

Cooperative Studies Activities
Piñon Flat Observatory Janaury, 1981

Investigator	Institution	Activities
D. Jackson	University of California, Los Angeles	Management, monument testing
A. Sylvester	University of California, Santa Barbara	Precision geodesy, monument testing
G. Cabaniss	Air Force Geophysics Laboratory	Borehole tiltmeter
F. Wyatt J. Berger	University of California, San Diego	Field support, data collection long baseline strainmeters, long baseline tiltmeter, laser optical anchors, shallow borehole tiltmeters, environmental monitoring
R. Bilham	Columbia University	Long baseline tiltmeter
G. King	Cambridge University	Long baseline tiltmeter
B. Clark	Leighton & Associates	Stressmeters
L. Slater	C.I.R.E.S.	Two-fluid tiltmeter, monument testing
S. Sacks	Carnegie Institute	Borehole strainmeters
R. Allenby	NASA	ARIES - TLRS
L. Hothem	NGS	Satellite positioning

Crustal Deformation Measurements near Yakataga, Gulf of Alaska and the Shumagin Islands, Alaska Peninsula

14-08-0001-19745

Roger Bilham and John Beavan
Lamont-Doherty Geological Observatory of Columbia University
Palisades, New York 10964

Investigations

1. Seven 17 m-long carbon-fiber strainmeters were installed in shallow surface sites near the coast of the Gulf of Alaska within the Yakataga seismic gap. All the instruments are located above the forecast rupture zone. Hourly-mean strain data are telemetered via the Landsat 3 satellite for analysis in N.Y. The least-count resolution is approximately 10^{-9} strain.
2. The Yakataga coastline was found to be unsuitable for the continuous operation of existing tide gauges. We have investigated alternative methods for monitoring mean sea-level to provide a measure of vertical crustal deformation in the region.
3. We have investigated a vibratory method for driving steel rods into sand-and-gravel to provide stable vertical-control marks for use in the Yakataga region.

Results

1. Transmissions have been received from six of the strainmeters since November 1980. One transmitter and two strainmeters had early malfunctions and a third strainmeter ceased operation in January 1981. Three strainmeters continue to transmit data of good quality.

   The load tide signal has a maximum peak amplitude of 4×10^{-7} strain. Superimposed on the tidal signal are strain rates that vary from 10^{-8}/day lasting for as long as 30 days and strain rates of 5×10^{-7} day lasting less than 5 days. The higher strain rates are probably associated with temperature, rainfall and ground expansion during freezing processes. Our ability to distinguish tectonic signals amid these large atmospherically-induced strains depends on the magnitude and spatial geometry of likely precursory strainfields. Since storm conditions are essentially synchronous across the Yakataga coastline we cannot use temporal coherence alone to search for possible tectonic signals within the strain time series. In order that we may detect unambiguously a strain precursor, the magnitude of the precusory tectonic strain rate must either exceed the maximum observed strain-noise rate (e.g. 10^{-6}/day) or we must be able to distinguish the precursory strain signal from the noise by virtue of its spatial geometry. The nature of a short-term strain precursor to a magnitude 8.1-8.3 earthquake cannot be surmised from historical data since no continuous strain data from within the epicentral region of an event of this magnitude have been reported. Moreover, the spatial form of strainfields generated by fast-moving storms are likely to be difficult to predict. Because of the large size of strain precursors that have been reported for twenty out of forty documented precursory strain events (Bilham, 1981), we remain optimistic about our detection capability.

2. A newly designed sea-level instrument is to be installed in Alaskan seismic gaps in 1981 to monitor crustal movements associated with future seismicity. The device consists of two ceramic pressure gauges; one to monitor barometric variations and the other installed in shallow water on the coast to measure sea-level variations. The instruments have a resolution of approximately 1 mm over a range of more than 10 m. Sea-level, barometric pressure and sea water temperatures will be averaged for 12 minutes, stored for up to three hours and telemetered via the GOES satellite. In each region we will install two permanent gauges and one portable gauge. The portable gauge will be operated for variable lengths of time in order to establish several vertical-control points within and near each seismic gap. These control points will be reoccupied yearly.

The sea level monitors are unusual in that the sensor may be operated above or below sea-level. A flexible tube connects the sensor to deep water, and a six-conductor cable connects the sensor to an electronics package on land. For winter operation in the Gulf of Alaska the sensor must be installed below the lowest low-water mark in order to prevent freezing. The permanent gauges will thus be installed below the lowest low-tide level during the summer months, which is approximately 1 m lower than the low tides in the winter. The portable gauges will be operated above the high-water tide level, or in the intertidal zone, to simplify site preparation.

In both configurations the sensor must be bolted to a datum that is vertically stable. The entry point of the flexible-tube does not affect the stability of the measurement unless a density contrast exists between the sea-water inside and outside the tube. In the portable gauges the temperature of the flexible tube where it emerges above sea-level must be known to within 2°C for errors to be less than 1 mm. The tube will be buried beneath beach sand to provide thermal stability. The sensors will be bolted to bedrock where possible and to a steel-rod driven to refusal where rock is not present.

Three of the new sea-level monitors will be operated in the Shumagin Islands seismic gap and three in the Yakataga seismic gap during the summer 1981 field season. The three Shumagin Islands instruments will occupy sites that were initially occupied by stilling-well gauges in 1977.

3. The difficulty of transporting drilling or excavating machinery to the Yakataga region has led to our developing a vibratory pile driver weighing less than 100 lbs. The device is bolted to the end of a 1 1/2" diameter pipe and driven by a 4 HP gasoline engine at a frequency that sets the system in resonance. The pipe sinks rapidly into sand and gravel. Additional pipe sections are added until further sinking ceases.

Reports

Bilham, R., and Beavan, J., 1980, Strain measurements in the Yakataga seismic gap, EOS, Trans. Am. Geophys. Un., vol. 61, p. 1030.

Bilham, R., 1981, Delays in the onset times of near-surface strain and tilt precursors to earthquakes, Earthquake Prediction - An International Review, Maurice Ewing Series, vol. 4, edited by D. W. Simpson and P. G. Richards, AGU, Washington, D.C.

Fault Slip Measurements

9960-02943

R.O. Burford and P.W. Harsh
Branch of Tectonophysics
U.S. Geological Survey
345 Middlefield Road, M/S-77
Menlo Park, California 94025
(415) 323-8111, Ext. 2574

Investigations

The surface tectonic effects of the M = 7.3 Algerian earthquake that struck near El Asnam on October 10, 1980 were studied in the field during November 5-15. Repeat surveys of several alinement arrays along the San Andreas fault near Parkfield in Cholame Valley were conducted during December, 1980. Analysis of data on the distribution, duration, and amplitude of afterslip along the Imperial fault following the October 1979 Imperial Valley earthquake was undertaken.

Results

1. The October 10, 1980 El Asnam earthquake was caused by slip on a reverse or thrust fault that generally emerged along a 32-km-long surface break as a low-angle thrust. The center of the area of surface effects was about 36° 13'N, 1° 33'E. The main surface rupture strikes about N 42° E and dips between 8° and 25° to the northwest at sites where direct measurements were possible. However, dips as high as 60° were estimated or measured at a few sites, and those values are more consistent with the 55° to 60° dip reported by S.T. Harding for the main-shock fault-plane solution. In this respect as well as in regard to other general characteristics, the faulting associated with the El Asnam earthquake was similar to that of the February 9, 1971 San Fernando earthquake. The maximum vertical component of surface displacement across the main fault was 2.6 m, and thus a maximum dip slip of more than 5 m would be represented for an assumed dip of 30° (3.4-m dip slip assuming 50° dip).

   A zone of shallow normal faulting developed roughly parallel to the central and northeast sections of the main thrust break within 1 to 2 km to the northwest into the hanging-wall block. Scarps along these normal faults above the shallow part of the thrust were often more conspicuous, if not larger, than the scarps along the trace of the main fault. A complex zone of predominantly normal faulting, mixed in several places with landslide effects, occurred in an arcuate pattern within the hanging-wall block about 6 to 7 km northwest of the main thrust break. The arcuate fracture pattern nearly duplicates the fracture pattern mapped by Jean-Pierre Rothe during a field investigation of the magnitude 6.7 1954 Algerian earthquake. Similarities of the fault plane solutions for the 1954 and 1980 mainshocks derived by S.T. Harding and A.F. Espinosa plus the regeneration of the arcuate pattern of normal fault breaks indicate that the 1980 earthquake sequence can be considered a repeat of the 1954 sequence, even though there was no evidence for surface breakage along the trace of the thrust reported from the 1954 investigation.

2. The distribution of slip rates through December 1980 along the San Andreas fault from Slack Canyon, 25 km northwest of Parkfield, to Palo Prieto Pass, 12 km southeast of Cholame, shows an inflection point within the Middle Mountain section at a point about 8 km northwest of Parkfield. This point of increased slope in the trend of average creep-rate decline from northwest to southeast is associated with a slight bend in the main fault trace (concave to southwest).

3. Monitoring of slip activity along the Imperial fault during a 2.5-month period following the Imperial Valley earthquake of 15 October 1979 determined initial afterslip rates of up to 20 mm/day which decayed to 1 mm/day by early January, 1980 at the end of the period of monitoring, producing up to 0.18 m of additional slip across the surface break.

Reports

Burford, R.O., Harsh, P.W., and Espinosa, A.F., 1981, 7.3 quake in Algeria reviewed, Geotimes, 26, 18-20

Harsh, P.W., 1981, Distribution of afterslip along the Imperial fault, *in* The Imperial Valley Earthquake of 15 October 1979, R.V. Sharp, ed., U.S. Geol. Surv. Prof. Paper, in preparation.

Evans, K.F., Burford, R.O., and King, G.C.P., 1981, Propagating episodic creep and the aseismic slip behavior of the Calaveras fault north of Hollister, California, Jour. Geophys. Res., v.86 (in press)

Burford, R.O., Nason, R.D., and Harsh, P.W., 1981, Results of fault-creep studies in central California, U.S. Geol. Surv. Earthquake Info. Bull., v.13 (in press)

Remote Monitoring of Source Parameters for Seismic Precursors

9920-02383

George L. Choy

Branch of Global Seismology
U.S. Geological Survey
Denver Federal Center, MS 967
Denver, CO 80225
(303) 234-4041

Investigations

The digitally recording instruments of the GDSN comprise a global array that provides a broad-band teleseismic data base that has not yet been utilized in source studies. We sought to design and implement techniques to use information in the frequency band from several Hz to tens of seconds to extract source parameters and to describe the rupture process of earthquakes. We then sought to extend these methods to monitor the changes in source parameters before large earthquakes.

Results

1. A program has been developed that reconstructs broad-band records of ground displacement and velocity by the simultaneous deconvolution of the long- and short-period vertical channels of the GDSN instruments. We demonstrated that information in this intermediate frequency band is suitable for studies of frequency dependent attenuation and permits quantifying directivity effects associated with seismic sources.

2. We have developed a method of synthesizing seismograms that combines the full wave theory with a realistic rupture model to describe propagation and source effects. Using this program we succeeded in determining the complete rupture history of two deep earthquakes, including constraints on the dynamic and static stress drops, the rupture velocity and the rupture complexity.

3. We are examining the rupture characteristics of a suite of 4 large (m_b>5.5) earthquakes that encircled and preceded over a period of 2 years the eventual rupture zone of the Miyagi-Oki earthquake of June 12, 1978. The dynamic stress drops of these earthquakes rose 1.5 times above background just before the mainshock. This rise was not mirrored in the apparent stress drop. Other preliminary indications are that rupture duration, complexity and the direction of rupture propagation also changed systematically with time.

Reports

Choy, G. L., and Boatwright, J., 1981, The rupture characteristics of two deep earthquakes inferred from broad-band GDSN data: Seismological Society of America Bulletin, v. 71, p. 691-711.

Harvey, D., and Choy, G. L., 1981, Broad-band deconvolution of GDSN data, submitted to Geophysical Journal of Research of the Astronomical Society.

Central California Network Processing

9930-01160

Rob Cockerham
Branch of Seismology
U.S. Geological Survey
345 Middlefield Road, MS 77
Menlo Park, California 94025
(415) 323-8111, ext. 2963

Investigations

Signals from 300 stations of the multipurpose Central California Seismic Network are telemetered continuously to the central laboratory facility in Menlo Park where they are recorded, reduced, and analyzed to determine the origin times, magnitudes, and hypocenters of the earthquakes that occur in or near the network. Data on these events are presented in the form of lists, computer tape and mass data files, maps, and cross sections to summarize the seismic history of the region and to provide the basic data for further research in seismicity, earthquake hazards, and earthquake mechanics and prediction. A magnetic tape library of "dubbed" unprocessed records of the network for significant local earthquakes and teleseism is prepared to facilitate further detailed studies of crust and upper mantle structure and physical properties, and of the mechanics of earthquake sources.

Results

1. Summary catalogs of earthquakes located by the network from 1969 through September 1977 have been published. Preliminary results for late 1977 through June 1980 are accessible in various forms, and work on completing and publishing the summary catalogs for these years has high priority. Results for July through December 1980 have been finalized.

2. Routine analysis of the network data has been transferred from the MULTICS system to the PDP 11/70 computer under the UNIX system. Processing procedures have been revised to include the merging of P-phase data provided by the real-time picker system developed by Rex Allen and Jim Ellis. The addition of these data has substantially decreased the amount of time required to process earthquake to catalog quality.

3. Implimentation of routine processing of $M \geq 2.5$ earthquakes on the ECLIPSE computer system is continuing. These data contain P and S (when S is timeable) arrival times and the maximum amplitude and associated period record from the horizontal components. Since ECLIPSE processing produces digitized seismograms, these records are archived onto magnetic tape.

4. The Mammouth Lakes, California, region was shaken by three strong earthquakes on May 25-27, 1980--a M 6.0 shock at 1633 GMT, a M 6.3 shock at 1945 GMT on May 25, and a M 6.0 shock at 1451 GMT on May 27. They were preceded and followed by hundreds of smaller quakes _ M 3. Within the first 48 hours, teams from the U.S. Geological Survey, University of Nevada, Reno (UNR), California Institute of Technology, and California Division of Mines and Geology installed over 20 portable seismographs in the Mammoth Lakes-Long Valley region. Preliminary analysis of data from these instruments and UNR permanent stations reveals the following pattern: the three large shocks and most of the accompanying seismicity are confined to a NSW-trended band that is located along the mapped trace of the Laurel-Convict fault, which is within the Sierra Nevada, 5 km west of the edge of Long Valley. A patch of seismicity (including a M 5.2 event) was located east of this zone, on the trace of the Hilton Creek fault, near the point where ground breakage was observed. Most of the aftershocks appear to be shallow, at at depth less than 10 km. The western seismicity band cannot be placed on the subsurface projection of the Hilton Creek fault because the fault is believed to be an eastward-dipping normal fault. Most of the fault-plane solutions derived for the aftershocks indicate strike-slip movement, with a NNE plane corresponding to left-lateral motion. The seismicity pattern is surprising, as the Laurel-Convict fault has not been known to be active in Quaternary time. The Hilton Creek fault is known to be recently active, but it does not presently appear to be the causative fault for the Mammoth earthquakes.

Analysis of these data as well as monitoring of this area has been restricted to ≥ M 3 earthquakes and has been completed to May 1981.

5. To study the aftershocks of the November 8, 1980, Eureka earthquake, the seismic network of the U.S. Geological Survey in central California was augumented at its north end between Eureka and Crescent City by 8 portable three-component stations. Although the aftershocks were offshore outside of the network, abundant S-wave data from the portable stations permitted reliable epicenter determinations for nearly 250 aftershocks of ≥ M 2 from November 10 through December 3. The epicenters define a 120-km-long linear zone that extends northeastward from a point near the Mendocino fault about 100 km west of Cape Mendocino to a point about 25 km northwest of Trinidad Head. The N 53° E trend of the aftershock zone agrees with one of the nodal planes (left-lateral strike slip) for the main shock determined from stations in northern California and Oregon.

Reports

Marks, S. M. and Lester, F. W., 1980, Catalog of earthquakes along the San Andreas fault system in central California, January-March 1977: U.S. Geological Survey Open-File Report 80-1233, 47 p.

Marks, S. M. and Lester, F. W., 1980, Catalog of earthquakes along the San Andreas fault system in central California, April-June 1977: U.S. Geological Survey Open-File Report 80-1264, 43 p.

Murphy, J. M. and Lester, F. W., 1981, Preliminary catalog of earthquakes in central California for March 1979: U.S. Geological Survey Open-File Report 81-520.

Riley, L. M. and Lester, F. W., 1981, Preliminary catalog of earthquakes in central California for April 1979: U.S. Geological Survey Open-File Report 81-519.

Cockerham, R. S., Ryall, A. S., and Corbett, E. J., 1980, The Mammouth, California, earthquakes of 1980, (abs.): EOS, American Geophysical Union Transaction, v. 61, no. 46, p. 1041.

Eaton, J. P., 1981, Distribution of aftershocks of the November 8, 1980, Eureka earthquake (abs.): Earthquake Notes, v. 52, no. 1, pp. 44-45.

Teleseismic Search for Earthquake Precursors

9920-02142

J. W. Dewey
Branch of Global Seismology
U. S. Geological Survey
Denver Federal Center, MS 967
Denver, Colorado 80225

(303) 234-4041

Investigations

C. Mendoza and J. W. Dewey have continued study of seismicity associated with the Colombian earthquake of December 12, 1979 ($M_S \cong 8$) by relocating pre-1964 earthquakes from the epicentral region.

Results

As noted in our previous semi-annual report, the immediate hypocentral region of the 1979 main shock was quiescent for $m_b \geq 4.8$ during the last fifteen years preceding the main shock, but had been a zone of intense aftershock activity following the great earthquake of January 19, 1958. Kanamori and McNally (1980, EOS, 61, p. 1044) have suggested that the hypocentral region of the 1979 earthquake corresponds to an asperity or barrier in the thrust fault zone. This asperity is thought to have blocked the 1958 earthquake rupture from propagating further to the north, and the subsequent failure of the asperity in 1979 is thought to have caused the 1979 shock. We relocated the 1958 aftershocks together with the 1979 main shock, using joint hypocenter determination, and find that the 1979 and 1958 epicenters together define a seismic cluster with dimensions of about 20 kilometers. Assuming that the cluster of 1958 and 1979 shocks is a map of the asperity, we estimate the dimensions of the asperity to be 20 km or less. The lack of significant prior seismicity in the region of the inferred asperity in the 15 years leading up to the earthquake of December 12, 1979, and the scarcity of 1979 aftershocks in the region of the inferred asperity, suggest that the asperity was a rather simple region with high resistance to fault slippage, rather than a heterogeneous region consisting of many fault patches with widely varying resistances to slippage.

Reports

Mendoza, C. and Dewey, J. W., 1981, Prior seismicity and aftershocks of the December 12, 1979 Colombian earthquake (abs), Earthquake Notes, v. 51 no.1, p. 68.

Seismic Studies for Fault Mechanics

9930-02103

W. L. Ellsworth, P. A. Reasenberg, S. M. Marks and B. L. Moths
Branch of Seismology
U.S. Geological Survey
345 Middlefield Road, MS 77
Menlo Park, California 94025
(415) 323-8111, ext. 2778

Investigations

The analysis of seismicity in central and southern California has been the principal subject of investigation during this period. A preliminary investigation into the possibility of determining the state of stress from focal mechanism data has also been conducted.

Results

1. The hypothesis that plate margin seismicity follows a cyclic pattern that is controlled by great earthquakes, as advanced by the work of Fedotov and Mogi, appears to be compatible with the known history of earthquakes in California. Results that we have reported earlier for northern and central California support a three stage model of seismicity: quiescence following a great earthquake, renewed activitity of moderate-sized events during the latter half of the time period between great earthquakes, and finally the next great earthquake. The historic record in southern California, although not as complete or extensive as that for the north, tentatively supports the identification of the same stages of seismicity. Our reanalysis of historical reports during the period from 1857 to 1920 has failed to uncover any events as large as M 6 in the southern California region at latitudes parallel to the 1857 surface rupture, and indicates that magnitude values of several previously reported M 6 are overestimated. The pattern that emerges is one of relative quiescence at the M 6 level throughout the breadth of the San Andreas system in the region that is parallel to the 1857 earthquake until about 1920. Since that time there have been at least seven M 6 events. Seismicity in southernmost California, parallel to the segment of the San Andreas fault that has not ruptured in a large earthquake in historic time, has been at a high level since at least the 1890's, when the reliable record begins.

2. Microearthquakes from along the San Andreas fault near San Juan Bautista, at the southern terminus of faulting in the 1906 earthquake, has been reanalyzed to determine the spatial and temporal relationship of these events to the transition zone between the locked and creeping segment of the fault. Relocated hypocenters reveal that shallow seismicity terminates abruptly some 10 km northwest of San Juan Bautista, at Pajaro Gap. Unusually deep activity (10 to 15 km) begins north of this point and dies out altogether some 20 km to the north. Seismic

activity along the Sargent fault, located a few km to the east of the San Andreas fault follows precisely the same spatial pattern. Temporal variations in the rate of seismicity indicate that this region has been unusually active since mid-1979. The increase in activity apparently began with an intense swarm of activity that occurred on the San Andreas fault four days before the M_L 5.8 Coyote Lake earthquake that ruptured the Calaveras fault immediately to the east of the region.

3. Hypocenters and fault plane solutions for 311 aftershocks of the 1979 Coyote Lake earthquake on the Calaveras fault near Gilroy, California, were examined in detail. A model for hypocenter relocation was developed from inversion of aftershock P-wave and calibration shot data. The relocated hypocenters of the main shock and aftershocks reveal two distinct zones of seismicity between 36° 55' and 37° 10' north latitude. A 5° bend and complication in the surface faulting at 37° demarcates the tranisition between these two faulting regimes. South of 37°, the aftershock hypocenters describe a narrow, vertical planar zone between 2 and 5 km depth that parallels the surface trace of the fault. The seismicity north of 37° reveals a more complicated spatial pattern that is concentrated between 4 and 8 km depth. The hypocenter of the mainshock is located in this zone. The structure can be generally described by a plane dipping 80° to the northeast, parallel to the surface expression of the fault zone. The existence of a set of subparallel quasiplanar imbricate-slip surfaces within this zone is suggested by the seismicity. The complexity of faulting structure in this zone coincides with a zone of en echelon step faulting seen on the surface between 37° and 37° 05'. Fault plane solutions are consistent with the hypothesis that two distinct faulting regimes were active during the aftershock period.

4. Completion of earthquake catalogs for 1977 continues at a good rate of progress. Open-file reports for the first half of the year are complete, and the second half of the year should be finished during the current fiscal year.

5. An exact, linear relationship between the shear stress acting on a fault and the slip direction on that fault has been used to develop a linear inversion method that produces an estimate of the stress field from an ensemble of focal mechanism data. As presently formulated, the method determines the orientation and relative magnitudes of the principal stress components that produce the best match to slip vector data for a suite of events. Results from data collected at Rangely, Colorado and at several locations in Utah and Nevada are encouraging.

Reports

Ellsworth, W. L., Lindh, A. G., Prescott, W. H., and Herd, D. G., 1981, The 1906 San Francisco earthquake and the seismic cycle: Maurice Ewing Symposium, 3rd, Mohonk Lake, New Platz, 1980, Earthquake Prediction Proceedings, ed. by Simpson, D. W., and Richards, P. G.: American Geophysical Union, Washington, D. C., 30 p., (in press).

Marks, S. M., and Lester, F. W., 1980, Catalog of earthquakes along the San Andreas fault system in central California, January-March 1977: U.S. Geological Survey Open-File Report 80-1233, 47 p.

Marks, S. M., and Lester, F. W., 1980, Catalog of earthquakes along the San Andreas fault system in central California, April-June 1977: U.S. Geological Survey Open-File Report 80-1264, 43 p.

Ellsworth, W. L., and Xu Zhong-huai, 1980, Determination of the stress tensor from focal mechanism data (abs.): EOS, American Geophysical Union Transactions, v. 61, p. 1117.

Herd, D. G., Ellsworth, W. L., Lindh, A. G., Prescott, W. H., and Shedlock, K. M., 1981, The next large San Francisco Bay area earthquake (abs.): Earthquake Notes, v. 52, p. 4-5.

Moths, B. L., and Ellsworth, W. L., 1980, The California earthquake of 1857 and the seismic cycle (abs.): EOS, American Geophysical Union Transactions, v. 61, p. 1030.

Olson, J. A., Lindh, A. G., and Ellsworth, W. L., 1980, Seismicity and crustal structure of the Santa Cruz Mountains, California (abs.): EOS, American Geophysical Union Transactions, v. 61, p. 1042.

Olson, J. A., Lindh, A. G., and Ellsworth, W. L., 1981, Microseismicity on the San Andreas fault near the 1906 epicenter (abs.): Earthquake Notes, v. 52, p. 12.

Precursory Strain/Seismic Anomaly Studies on a Strike-Slip Fault System

9930-02393

E. T. Endo
Branch of Seismology
U.S. Geological Survey
Geophysics Program AK-50
University of Washington
Seattle, Washington 98195
(206) 543-9024

Investigations

1. Deformation: No field work undertaken during the last six months. Level lines EDM arrays and crack stations to be remeasured during summer of 1981.

2. Seismic: On the more than 500 large magnitude Kaoiki and south flank Kilauea earthquakes initially selected for a focal mechanism study, approximately 80 percent produced solutions. Problem events were earthquakes with focal depths less than 5 km. In addition to crustal earthquakes, upper mantle earthquakes were included in the study. The direct ray paths for most stations helped to confirm station polarities for the Kaoiki and south flank Kilauea mechanism study. The 1959-1979 Kaoiki focal mechanism study was expanded to include large magnitude earthquakes from 1979-1981.

Miscellaneous software tools to present results of the study are being developed on both the University of Washington CDC and DEC 11/70 computer systems.

Results

1. Deformation: None for deformation studies since no new measurements were completed during the past year.

2. Seismic: Preliminary results of the Kaoiki focal mechanism study indicate two dominant mechanism types. The most common type of solution is nearly pure strike-slip. When the trend of the Kaoiki is used in selecting a preferred nodal plane, right-lateral strike-slip faulting appears to be taking place on the pre-existing Kaoiki structure. This type of faulting is consistent with the ground deformation mapped during 1979. A second less common type of faulting is low-angle normal faulting to the southeast (again using the trend of the Kaoiki structure in selecting a preferred nodal plane). Horizontal first-motion data appears to support slip to the southeast. The largest magnitude ($M_L = 4.1$) Kaoiki earthquake during the first five months of 1981 has the second type of focal mechanism solution. At this point in the analysis of the Kaoiki earthquakes, there is not sufficient evidence to indicate that a change in focal mechanism parameters may be used as a prediction tool.

Reports

Crosson, R. S., and Endo, E. T., Focal mechanisms of earthquakes related to the November 29, 1975 Kalapana, Hawaii earthquake: The effect of structure models: Seismological Society of America Bulletin (in press).

Garm Source Mechanism Studies

9930-02100

F. G. Fischer
Branch of Seismology
U.S. Geological Survey
345 Middlefield Road - MS-77
Menlo Park, California 94025
(415) 323-8111, ex. 2321

Investigations

U.S. participation in this joint US-USSR project resumed in February with travel to the Garm, USSR study area. During this visit needs of the 1981 network rebuilding program were noted. Develocorder records of relatively deep earthquakes were collected for refinement of the velocity model published in 1980. A survey was also made of the possibly unique earthquake prediction methods currently in use by the Soviets.

Results

Solar electric panels and regulated DC-DC converters were delivered to Garm to eliminate all primary batteries from the seismic network.

Data on seventeen earthquakes with depths ranging from 12 to 24 km were returned to Menlo Park for inclusion in an inversion program to refine the Garm seismic velocity model.

Several tools under active study by the Soviets for earthquake prediction are P-wave velocity anomalies, effective stress variations infered from S-wave to P-wave amplitude ratios, and increases in the low frequency (LF) radio background noise. A narrowband LF radio receiver is now monitoring 62 KHz in Menlo Park, California in an effort to duplicate a Soviet study. Based on the Russian study, we expect a 25 dB increase in noise level two minutes prior to any magnitude 6 earthquake within 500 km.

There were no reports for this period.

Central California Network Operations

9970-01891

Wes Hall
Branch of Network Operations
U.S. Geological Survey
345 Middlefield Road - MS-77
Menlo Park, California 94025
(415) 323-8111, ex. 2509

Investigations

Maintenance and recording of 403 seismometer, 34 tiltmeter, 16 magnetometer, 8 strainmeter, 33 creepmeter, and 14 radio receiver sites located in northern and central California and in Oregon. This is a total of 447 data gathering field sites and the area covered is approximately 101,000 square miles.

Making preparations for new California Network telemetry terminal installation at Pasadena.

Results

1. The Stanwick Corporation under contract 14-08-0001-1945 is responsible for the maintenance of seismic, tiltmeter, magnetometer, creepmeter, and strainmeter field sites; inside maintenance of low frequency digital equipment; installation of new seismic stations, and final testing of J402 VCO/AMPS.

2. The Stanwick team consisting of ten members has far exceeded maintenance goals set by the reference contract (95% operational). Maintenance delays greater than 48 hours were attributable to weather, transporation, or access problems.

3. New seismic stations, installation of:
   1 single component stations in Bear Valley area.
   1 multi-component station in Calaveras area.
   7 single component stations in Lassen/Shasta area.
   5 single component stations in Melones/Merced area.

4. Assumed COR responsibility of Northern California, Southern California, Southern Nevada Stanwick contract.

Central American Historical Earthquakes

9930-01163

David Harlow
Branch of Seismology
U.S. Geological Survey
345 Middlefield Road, MS-77
Menlo Park, California 94025
(415) 323-8111, ext. 2570

Investigations

A list of major historical earthquakes in Central America since 1540 has been compiled. A historian was contracted to search the Archivo General de Indias in Seville, Spain for detailed descriptions of damage caused by these earthquakes. We have received his report and are beginning to translate a large number of original accounts. The goal of this work is to locate and estimate the magnitude of historical earthquakes in Central America so that recurrance intervals can be accurately determined. These results will be used to evaluate the potential for the occurrence of large earthquakes within several "seismic gaps" that have been identified along the seismically active Pacific Coast of Central America.

Results

Preliminary results indicate that intensity contours can be constructed from existing archival information for large earthquakes in Central America. The intensity contours can then be used to estimate magnitude. Detailed descriptions of the extent of damage were found in petitions to the King of Spain for tax relief for those communities that suffered damage. Death records were also somewhat useful, but more often reflected the occurrence of epidemics following a disastrous earthquake. One result is that a large destructive earthquake occurred in 1816 on the Polochic fault in west-central Guatemala. The Polochic is a left-lateral strike-slip fault that forms part of the plate boundary between the North American and Caribbean plates. Although this fault is young and microearthquakes have been recorded along it, no large historic earthquakes on the Polochic had previously been reported in the literature.

Report Received

Fieldman, L. H., 1981, Master list of historic (pre-1840) earthquakes and volcanic eruptions in Central America with a list of Legajos checked at the Archivo General de Indias.

DEEPWELL MONITORING OF STRAIN-SENSITIVE PARAMETERS OVER THE SOUTHERN CALIFORNIA UPLIFT

14-08-0001-18383

Thomas L. Henyey
Ta-liang Teng
Douglas E. Hammond
Charles G. Sammis
University of Southern California
Department of Geological Sciences
Los Angeles, California 90007

SUMMARY

Over the past few years, we have reclaimed a set of abandoned wildcat oil wells in the western Mojave Block in which to monitor groundwater variations. The wells are located in a variety of geologic terrane and range in depth from 500' to 5500'; they were selected from a much larger well population after extensive investigations and work-over operations by commercial rigs.

We have developed a set of water level, turbidity and temperature sensors for use in these wells. Development has emphasized

1) deployment in deep as opposed to shallow wells;
2) compatibility with multiple sensors down-hole;
3) long term down-hole service;
4) high resolution and low drift.

Figures 1 to 3 are representative data sets from our network. We have not observed any activity which might be characterized as "unusual" or related to seismic activity. A small (M = 2.5) earthquake occurred near the Del Sur and Fairmont wells on Day 357 of 1980. However, no pre- or coseismic signals were seen in the Fairmont data (figure 1); the Del Sur recorder was "down" during this time.

Figure 1 shows daily averages of water level in the Fairmont well together with barometric pressure from nearby Fox Airport. The lines on either side of the water level curve represent the 4-sigma band, due, almost exclusively, to the diurnal and semi-diurnal variation. The correlation with barometric pressure is high, with virtually no secular or short term change in water level seen once the pressure induced level changes are accounted for. Note that the barometric efficiency factor is on the order of 0.5 for periods on the order of one - two weeks. We plan to monitor this factor with time, and as a function of excitation frequency inasmuch as it reflects bulk aquifer properties.

Figure 2 shows similar barometric pressure and daily-averaged water level for the Del Sur well. The barometric efficiency is somewhat higher for this aquifer. Also shown is the daily-averaged turbidity; the decreasing trend during the first 30 days indicates a decrease in turbidity. This is probably the result of settling of particulate matter in the water column after emplacement of the sensors on day 312. Particles are probably sediment fines, rust, etc. which adhere to the casing and are loosened by the cables and water turbulence.

Finally, figure 3 is representative of the thermistor data. Data from the two thermistors are plotted on two ordinate scales for the post-insertion equilibration period. The apparent variability seen in the lower two curves represents the least count resolution of the datalogger and as such is not real. Thus resolution of these units is ∿ ± 0.015°C. Resolution is determined by the desired range, which in this case is ∿ 25°C. For stable holes we plan to reduce the range to ∿ 2°C, thereby gaining a resolution $\underset{\sim}{\sim}$ ± 0.001°C.

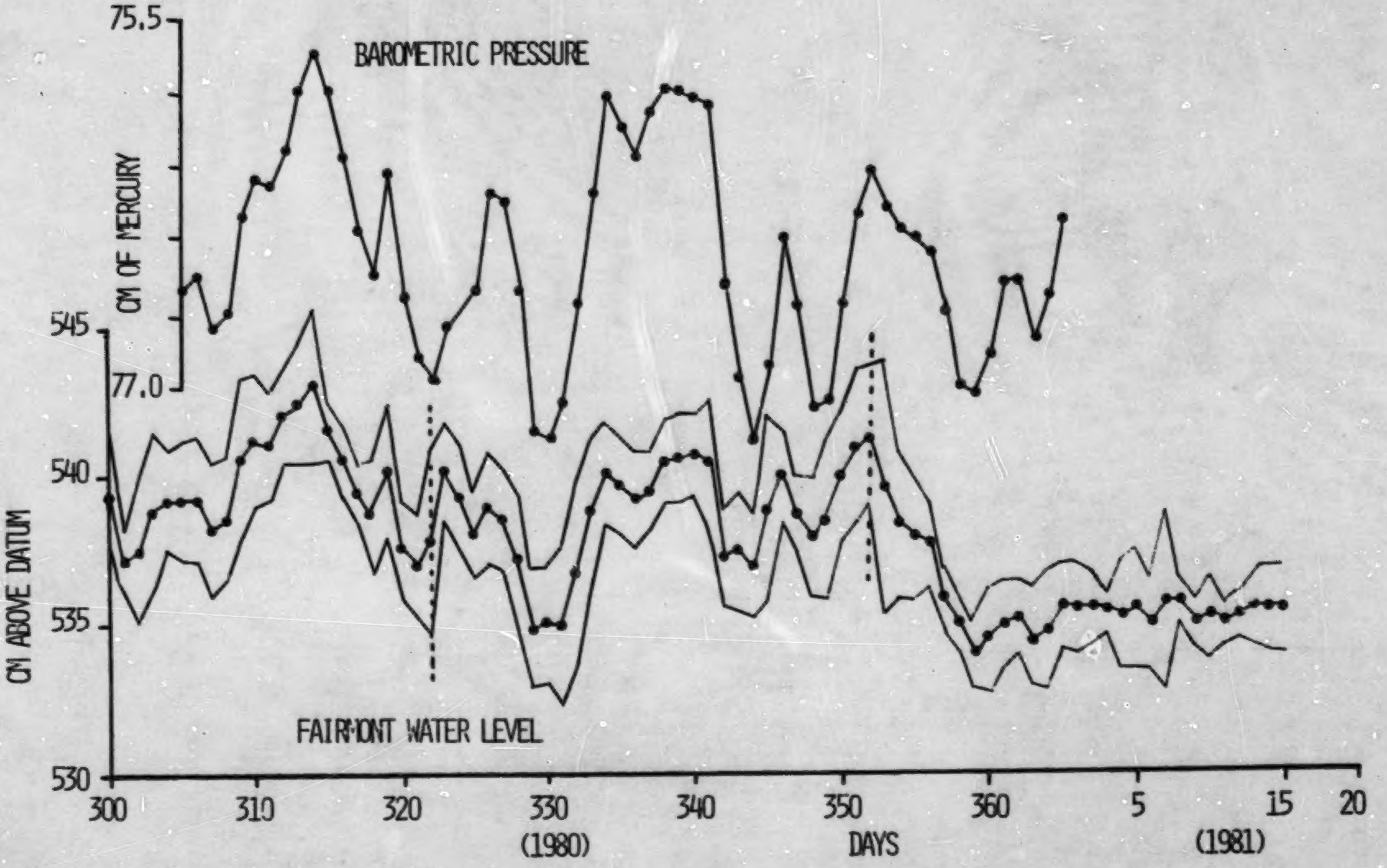
75.5
BAROMETRIC PRESSURE
CM OF MERCURY
77.0
545
540
535
530
CM ABOVE DATUM
FAIRMONT WATER LEVEL
300
310
320
330
340
350
360
5
15
20
(1980)
DAYS
(1981)

FIGURE 1

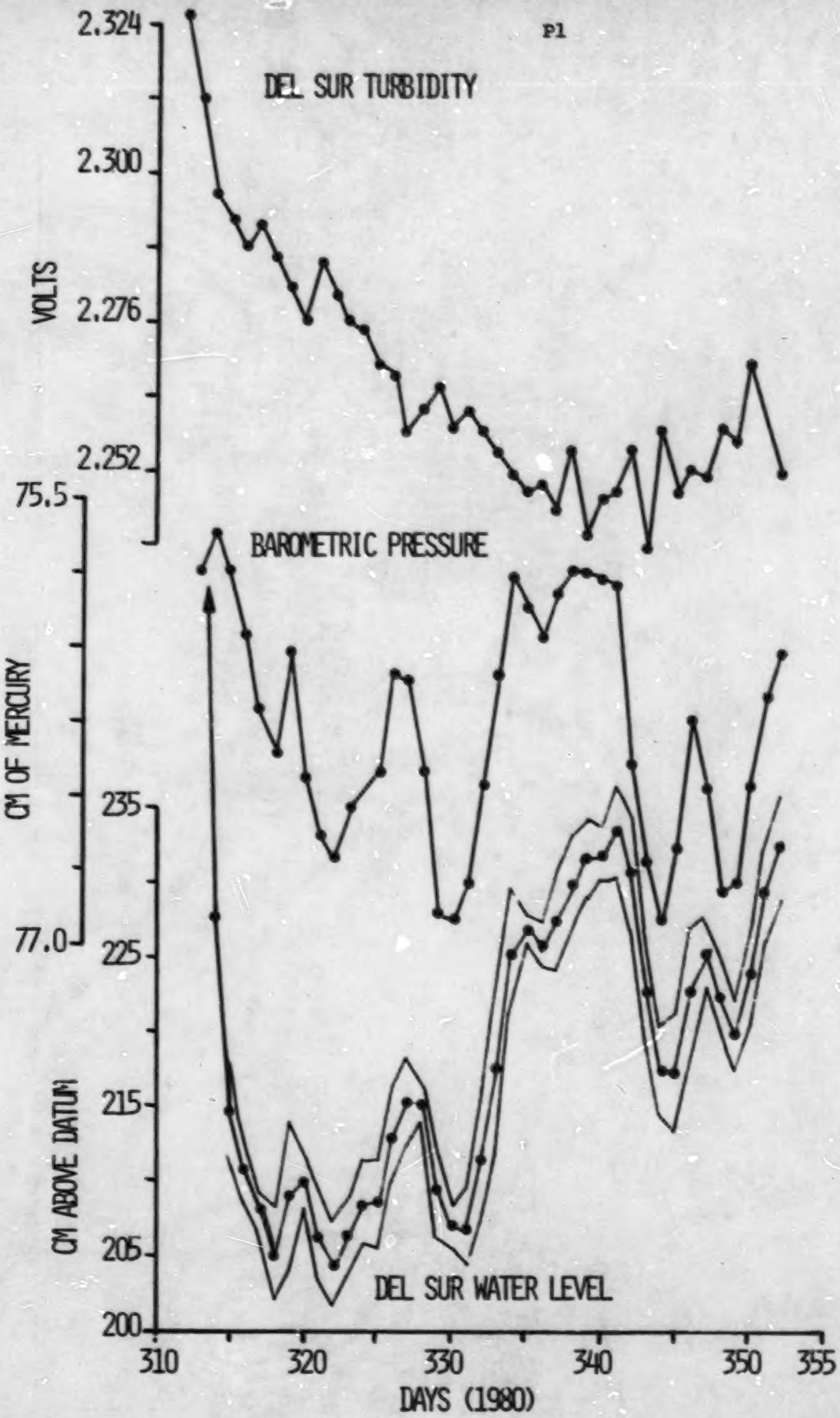
P1
DEL SUR TURBIDITY
VOLTS
2.324
2.300
2.276
2.252
75.5
BAROMETRIC PRESSURE
CM OF MERCURY
77.0
235
225
215
205
200
CM ABOVE DATUM
DEL SUR WATER LEVEL
310
320
330
340
350
355
DAYS (1980)

FIGURE 2

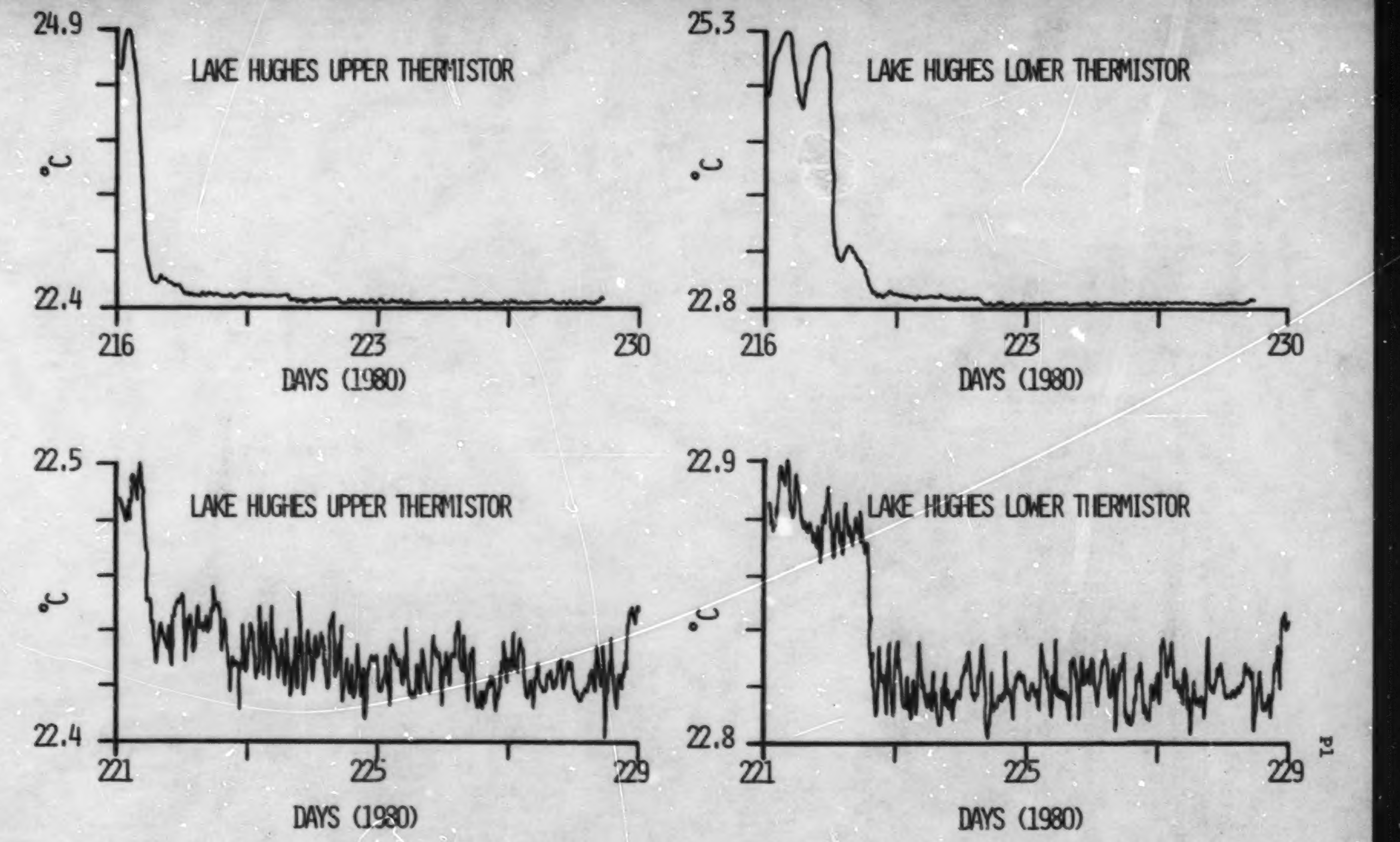
24.9
LAKE HUGHES UPPER THERMISTOR
°C
22.4
216
223
230
DAYS (1980)
25.3
LAKE HUGHES LOWER THERMISTOR
°C
22.8
216
223
230
DAYS (1980)
22.5
LAKE HUGHES UPPER THERMISTOR
°C
22.4
221
225
229
DAYS (1980)
22.9
LAKE HUGHES LOWER THERMISTOR
°C
22.8
221
225
229
DAYS (1980)

P1

FIGURE 3

Tilt Measurements in the New Hebrides Island Arc: Search for Aseismic Deformation Related to Earthquake Generation in a Major Zone of Lithosphere Subduction

14-08-0001-18350

Report prepared by B.L. Isacks, Principle Investigator,
R. Cardwell, J.-M. Marthelot, and M. Bevis
Department of Geological Sciences
Cornell University
Ithaca, New York 14853
(607) 256-2307

Investigation and Results

During the period covered by this report, no earthquake with magnitude greater than 5.4 occurred inside the network. Outside of the network at a distance of 280 km from the nearest seismograph station there was a sequence of large events which occurred in the southern New Hebrides arc in October 1980. The sequence included earthquakes with magnitudes (Ms) equal to 6.7, 6.7, 7.2, and 6.5 which occurred in a period of 1.5 days. Numerous aftershocks, including events which appear from the PDE listing to be located in the oceanic plate, occurred throughout the six month period. The PDE bulletin did not list any precursory seismic activity in the immediate vicinity of the sequence. The last shocks located in the area occurred in July 1980, 7 days after the major Santa Cruz earthquake (Ms = 7.9). They had magnitudes (Ms) of 5.8 and 5.3 and had the same epicenter as the first shock in the October 1980 sequence. Fifteen days before the beginning of this sequence a swarm of earthquakes occurred in the back-arc region between Erromango and Tanna islands at a distance of 300 km to the north of the sequence. Although this swarm occurred inside the southern network, it was not recorded by the southern network because the batteries were exhausted and the political situation in the southern New Hebrides Islands prevented their replacement at that time. Thus, only the largest events in the swarm, also listed by the PDE bulletin, were located by the northern New Hebrides network. An earthquake with magnitude Ms = 5.9 occurred 50 km to the north of the network in December 1980. This event will be analyzed in more detail when the preliminary locations for the month are completed by ORSTOM.

The space-time analysis of the events located by the PDE bulletins in the New Hebrides arc has continued to be updated. No precursory anomaly was recognizable in the rate of occurrence of earthquakes in the epicentral region of the October 1980 sequence in the southern New Hebrides. This sequence occurred in a segment of the arc which has been quite active for the past 20 years in comparison with an adjacent segment which exhibits a long-term quiescence. A manuscript describing the results of the space-time study will shortly be submitted for publication.

The local seismograph and tiltmeter networks continued to work well although they did suffer some downtime. Political unrest associated with the independence of the New Hebrides Islands (now called the Republic of

Vanuatu) during July 1980 made inter-island travel almost impossible during the months from July through October. Therefore, some stations that had been scheduled for periodic maintenance during this time could not be reached and their batteries went dead. Political unrest was also responsible for the station at Tanna being removed and the equipment still has not been recovered. The major relay station for the telemetry network on Mt. Bernier was hit by lightning at the end of December, and all of the equipment there was damaged. The network was down for approximately 2 weeks until spares could be installed. Lightning protection equipment was installed on Mt. Bernier and will be installed for the whole network this summer. Finally, a cyclone hit the central portion of the island arc on February 12, 1981 and damaged several of our VHF antennas causing another week of downtime. In spite of these difficulties the network is presently running well (except for the southern sub-network) now that the political trouble has been settled and all repairs have been completed.

A local magnitude scale has been developed for the New Hebrides based on the total duration of the seismic signal and the distance of the earthquake. The magnitudes are being used in a study of the variation of b-values for specific regions along the arc.

The microprocessor-based trigger and delay hardware for the network was installed in late October, 1980. The ROM based program for the system was written at that time but testing and debugging is not yet finished. A microprocessor-controlled digitizing table was also installed to improve the speed and accuracy of picking phase arrival times from the seismograms of the network.

The long baseline, liquid-level tiltmeter was serviced in late October and included replacing the fractured Lexan end caps with stronger, better designed plexiglass end caps, and general maintenance. The stalactite growth on the water-sensing probe tip mentioned in earlier reports still seems to be a problem. The instruments ran until late December when the water-sensing electronics were damaged by lightning. Lightning protection circuitry has been designed and will be installed this summer.

Another leveling was performed at the Devils Point and Ratard benchmark arrays, bringing the total number of surveys to 15 and 14, respectively. Both new levelings indicate that the arrays have not diverged from the tilt trends established over the last five years. Bevis and Isacks (1981) have summarized the leveling observations obtained through 1980 and their paper is in press.

Reports

Isacks, B.L., R. Cardwell, J.-L. Chatelain, M. Barazangi, J.-M. Marthelot, D. Chinn, and R. Louat, 1981, Seismicity and tectonics of the central New Hebrides island arc, in *Earthquake Prediction*, D. Simpson and P. Richards, eds., A.G.U. Ewing Series 3, (in press).

Coudert, E., B.L. Isacks, M. Barazangi, R. Louat, R. Cardwell, A. Chen, J. Dubois, G. Latham, and B. Pontoise, 1981, Spatial distribution and mechanisms of earthquakes in the southern New Hebrides arc from a temporary land and ocean bottom seismic network and from worldwide observations, *J. Geophys. Res.*, in press.

Bevis, M., and B.L. Isacks, 1981, Leveling arrays as multicomponent tiltmeters: Slow deformation in the New Hebrides island arc, *J. Geophys. Res.*, in press.

Southern California Repeat Gravity Studies

9730-01034

Robert C. Jachens
U.S. Geological Survey
345 Middlefield Road
Menlo Park, CA 94025
(415) 323-8111, ext. 2168

Investigations

Parts of the southern California high-precision gravity network, established during the fall of 1976, were remeasured during November 1980, and February 1981. These surveys constituted the sixth and seventh partial reoccupations during the past four years. As in previous surveys, during the November survey 12 stations of the secondary reference station network scattered over an area of 45,000 km^2 were remeasured. The rest of the November survey and the February survey were conducted in the vicinity of Lucerne Valley and Homestead Valley.

Results

1. Results from the last two surveys indicate that the temporal gravity anomaly that developed in the vicinity of Lucerne Valley and Homestead Valley between the fall of 1976 and May 1980, reversed sign sometime between May 1980 and November 1980. In this area, gravity had been decreasing systematically since the initial survey in 1976 and reached its lowest value (-60 μGal with respect to assumed invariance at Riverside) at Homestead Valley in May 1980. Gravity at other stations in the area decreased by about 20-40 μGal during the same period. Between May and November 1980, gravity at stations throughout the area increased by 20-30 μGal, typically recovering in 6 months 30-60% of the change that had accumulated during the previous 3.5 years.

   The cause of the temporal gravity anomaly is not known but it does not appear to be related to changes in the distribution of groundwater. The gravity stations are situated on crystalline bedrock outcrops and water level records from adjacent alluvial filled valleys indicate that the elevation of the water table has changed less than 70 cm during the observation period. Water table elevation changes of this magnitude should cause gravity changes of only a few μGals.

2. Oscillatory short term gravity changes (with respect to assumed invariance at Riverside) at a station near Lebec, California correlate strongly with elevation changes determined by level surveys between Glendale and Lebec. Level surveys conducted during January-April 1978, March-April 1979, and May-June 1980 show that the relative elevation at Lebec first decreased by approximately 6 cm, then increased by approximately 12 cm. Corresponding gravity changes were +11 μGal and -18 μGal with computed standard errors of 6-7 μGal. Considering the uncertainties associated with the

gravity measurements, the relationship between gravity change and elevation change for the event appears to be the Bouguer relationship of -2 μGal/cm. Based on the gravity measurements, the 1979-1980 changes occurred between December 1979 and May 1980. Both the magnitude and timing of the gravity changes have been confirmed by independent determinations of the relative gravity between San Fernando and Lebec (J. Evernden, written communication 1981).

Instrument Development and Quality Control

9970-01726

E. Gray Jensen
Branch of Network Operations
U.S. Geological Survey
345 Middlefield Road - MS-77
Menlo Park, California 94025
(415) 323-8111, ex. 2050

Investigations

This project supports other projects in the Office of Earthquake Studies by designing and developing new instrumentation and by evaluating and improving existing equipment. During this period the development of the GEOS microprocessor event recorder became a separately funded project (9940-03009). Some personnel from this project were assigned to the GEOS project as well to project 9930-02392 during this time.

Results

A playback system to allow digitizing of 1" Calnet tapes was installed at Caltech. This system includes a Bell & Howell tape transport, discriminators, a patch panel, a strip chart recorder and a computer interface to a PDP 11/34. Sixty-four Calnet stations have been connected to a PDP 11/34 at the Menlo Park playback center. Seismic events are currently being digitized on these stations and the number of stations will soom be expanded. A combined tape ID/hex footage counter for playback recorders has been built and more are under construction. A tick-mark generator which allows 5-day tape recordings to be played-back and displayed on a smoke drum recorder has been implemented. Some maintenance of playback center and computer systems has been provided by this project.

Research and development has been done on radio receivers to study the relationship of background radio noise and seismic events. This group has provided maintenance support for the Seismic Cassette Recorder (SCR) system during several field programs and in the office. Development of a radio-controlled trigger for the SCR system is nearing completion and radios and parts for implementation are being acquired. A new cassette playback deck which automatically corrects tape speed errors has also been developed and installed on the system. Personnel from this project aided in the construction and testing of a 256 channel real-time microprocessor seismic analyzer system for this office and another 128 channel system for the University of Washington.

Alignment and repair of 140 radio transmitters and receivers was completed as well as calibration of approximately 100 seismometers. One hundred fifty seismic VCO/preamp field units have been constructed and deployed as replacements or in new stations. Construction of 200 discriminators has been completed and 120 of them are tuned, calibrated and ready for installation.

Southern California Cooperative Seismic Network

9930-01174

Carl Johnson
Branch of Seismology
U.S. Geological Survey
Seismological Laboratory 252-21
Pasadena, California 91125
(213) 356-6947

Investigations

1. Routine processing using stations of the southern California cooperative seismic network were continued for the period October 1980 through March 1981. Routine processing includes timing of phases using the interactive CEDAR analysis system, event location, preliminary and final catalog production. During the first quarter of FY81, event analysis was conducted using an interactive system running under the UNIX operating system on a PDP 11/70. No earthquakes larger than $M_L = 5.0$ were recorded during the reporting period. For a detailed discussion of the results of this investigation refer to C. R. Allen, southern California seismic arrays, 14-08-0001-16719.

2. A study of the 1971 San Fernando earthquake has been completed in which we have modeled strong motions, teleseismic body waves, and static offset data. A complex three-dimensional finite-fault model was constructed to explain these data. The goal is to discover models of faulting time history which are compatible with as many different types of data as possible.

3. We are proceeding with the development of a southern California earthquake prediction data base. Geophysical data (e.g., seismicity, strain, tilts, radon, water levels) are collected from a variety of researchers in southern California. These data are cataloged and included in a computer data base. Plots of these data are made on a common time scale and copies are made available to other workers.

4. We are continuing operation of a system for the timely recognition of anomalous activity of southern California water wells. Yearly requests are mailed to private and municipal water companies requesting that anomalous activity be immediately reported to our staff. These data are logged and, if necessary, further investigation is conducted.

5. We are conducting a study of the influence of solid earth tides on earthquake occurrence. Earthquakes whose source mechanisms are well-studied are collected from the geophysical literature. Tidal shear stresses which are sympathetic to failure, are calculated for these earthquakes to discover whether a relationship exists between earth tides and earthquake occurrence.

Results

1. We have found evidence that the 1971 San Fernando earthquake may have been a double event on two separate, subparallel thrust faults. A model was developed in which the first event occurs at depth on the Sierra Madre fault zone. The second event initiates about 4 s later on the San Fernando fault zone. Rupture occurs between depths of 16 km and 3 km on the Sierra Madre fault zone and between a depth of 8 km and the earth's surface on the San Fernando fault zone. The moments of the first and second events are 0.7×10^{26} dyne-cm and 1.0×10^{26} dyne-cm, respectively.

2. The development of automated network event detection and analysis has continued with the implementation of the second generation online detection system running on a PDP 11/34 minicomputer. This system extends the first generation system presently in use at Menlo Park, the University of Washington, St. Louis, CIRES, Lamont, and the University of Utah. New capabilities include the augmentation of channel capacity to 256 signals, a more flexible tape format, and a more adequate user interface. Changes in the event detection logic has nearly doubled the number of events recorded over the original system based on the same network configuration. This system has been in full operation since January 1, 1981.

3. The CUSP (Caltech-USGS Seismic Processing) system has been implemented on a PDP 11/70 minicomputer under the RSX-11M operating system with all source code written in FORTRAN. This approach provided a substantial improvement in throughput, analysis features, system integrity, and simplicity of overall design as compared to the UNIX-based, "C"-coded system developed during FY80 under this project and presently in routine use at Menlo Park, the University of Washington, and St. Louis. The approach represents the first in the current series that fully integrates processing from digital records through catalog production and digital archiving. Running in southern California, the CUSP system, with a 5-person staff, provides a production rate of 80-120 events per day, substantially exceeding the background seismicity of roughly 35 detections per day. This system is now fully operational and will be integrated into routine processing at Caltech during the second half of FY81.

Publications

Moslem, K., Amini, A., Anderson, J. G., and Heaton, T. H., 1981, Mammoth Lakes aftershock accelerograms recorded on a temporary array (abs.): Earthquake Notes, v. 52, no. 1, p. 21.

Hutton, L. K., and Johnson, C. E., 1981, Summary of seismicity in southern California region, 1978 through 1981 (abs.): Earthquake Notes, v. 52, no. 1, p. 63.

Corbett, E. J., and Johnson, C. E., 1981, Evidence for mid-crustal horizontal shearing in the Western Transverse Ranges, California (abs.): EOS, American Geophysical Union Transactions, v. 61, no. 46, p. 1042.

Corbett, E. J., and Johnson, C. E., 198 , The Santa Barbara, California, earthquake of August 13, 1978: Seismological Society of America Bulletin (in press).

P1

Seismicity Studies for Earthquake Prediction in Southern California Using a Mobile Seismographic Array

14-08-0001-19266

Hiroo Kanamori
Karen C. McNally
Seismological Laboratory
California Institute of Technology
Pasadena, California 91125
(213) 356-6919

Eight Caltech seismograph trailers are being used to monitor spatial-temporal variation in locations and mechanisms of small earthquakes in southern California, especially near the Palmdale area, where anomalous changes in strain rate and seismicity were observed recently. The records obtained by this field survey together with those obtained from permanent stations are being analyzed in an attempt to understand physical processes leading to an earthquake. Long-term seismicity patterns (since 1932) in southern California, and detection capability of the permanent array, form the basis for selecting special study areas using the mobile array.

Large quarry blasts in southern California are being monitored with a precision of up to 10 msec to detect any temporal changes in P velocity in the crust.

Earthquake Mechanisms and Patterns in Seismic Activity Concurrent with the Short-Term Strain Changes in Palmdale, Cal

To better understand the relationship between seismicity and temporal changes in crustal deformation of the big bend region of the San Andreas, we examined the patterns in seismicity since the initiation of the Juniper Hills swarm (November 1976, McNally *et al.*, 1978) and determined focal mechanisms of the larger events ($M_L \geq 2.0$) in this area and compared these to horizontal strain measured by Savage *et al.*, (1981) on the U.S.G.S. Palmdale trilateration network. Increased microearthquake activity along the big bend of the San Andreas fault, which began with the Juniper Hills swarm, abruptly decreased to the NW and SE of the Juniper Hills area around the beginning of 1979. This change in activity occurred around the time of rapid dilatation reported by Savage *et al.*, (1981) and MacDoran and the ARIES team (personal communication). In November 1980, activity along the entire big bend region of the San Andreas began to increase. Results of the focal mechanism study suggest a relationship between the type of fault mechanism and temporal changes in surface strains observed at Palmdale, California. During periods of relative North-South compression, the stress field may be more favorable to thrust-type mechanisms on East-West striking planes (#9, 11, 20) and during periods of relative extension, the stress field may be more favorable to strike-slip type mechanisms (#14, 15, & 21) (Figure 1).

Investigations of Seismic Quiescence and Microearthquakes Along the Southern San Andreas Fault: Coachella Valley, California

A 100 km section of the southern San Andreas fault between the Salton Sea and Desert Hot Springs was the focus of an intensive microearthquake field survey, using a mobile array of eight seismographic trailers, between February and August 1979. This southernmost portion of the San Andreas has not undergone any significant rupture in historic time as documented by instrumental recordings and historic accounts. This area has not experienced a major break for the past 230 years (K. Sieh, personal communication) and has the potential to be the site of a large earthquake.

Activity along the San Andreas fault through the Coachella Valley is very low compared to other regions for which microearthquake activity levels are known. Of particular interest is the fact that even with mobile seismographic trailer stations augmenting the permanent network coverage, we do not see activity clearly associated with the San Andreas. Earthquake activity in the Coachella Valley exhibits very marked patterns of occurrence. Events tend to be aligned along east-west trending features to the San Andreas; and earthquakes commonly occur in "clusters" of closely related events which occur as very local features along the east-west lineations. Twelve days following the Imperial Valley earthquake of 15 October 1979 (the most recent large event near the Coachella Valley) a cluster of 85 events was observed as part of an investigation of "sympathetic slip" noted by geologists. We conclude that although this activity occurred just after the Mexicali event, it does not appear to represent a change from normal seismic activity.

In contrast to the big bend region of the San Andreas fault near Palmdale, microearthquake activity in the Coachella Valley does not appear to be exhibiting changes in either the rate of activity or the nature of the clustered activity in response to recent changes in the patterns of regional strain. Without the microearthquake data of this work, we would not have been able to document this "non-response" since supplemental coverage by the temporary array was necessary in order to make true comparisons between the earthquake data sets.

Rates of seismic activity ($M_L \geq 3.0$) in the Coachella Valley since 1932 have fluctuated from 0.8 to 10.0 events per year. A decrease in the rate of seismic activity was observed prior to the large events in 1940 (Imperial Valley) and 1968 (Borrego Mountain). In contrast, for the Desert Hot Springs event in 1948, which occurred on the northern edge of the Coachella Valley, no change in the rate of activity was observed prior to the mainshock. Between 1970 and 1980, the seismicity of the study area ($M_L \geq 3$) appears to be fairly constant.

Large, Late Aftershocks Following $M_L \geq 6.0$ Events In Southern California, and Implications for Expectd Future Activity.

We have evaluated the time, space and magnitude relationships of the mainshock-aftershock sequences for twelve earthquakes of $M_L \geq 6.0$ which have occurred in southern California since 1932, in order to identify and characterize the occurrence of large, late events in the aftershock activity. Our results indicate that such aftershocks have occurred in 64 percent, or 7 out of 11 sequences, since 1932 and prior to 15 October 1979. The magnitudes of these late occurring shocks appear to be $M_L \geq 5.0$; they are observed to occur 37.4 ± 26.6 months after the mainshock and to be located 36.4 ± 15.9 km distant. From this work it appears that the occurrence of large, late aftershocks is significant in southern California. Future shocks of this type can be identified as particularly likely in those local areas which have previously exhibited such patterns, e.g., the Imperial Valley, the southern San Jacinto fault and northern Baja, California. For this reason, three areas in southern California merit special consideration at this time with regard to expected aftershocks. These include the aftershock regions of the 15 October 1979 ($M_L = 6.6$) earthquake, the Mammoth Lakes earthquake aftershock area (25 May 1980, $M_L = 6.5$), the region of the 9 June 1980 ($M_L = 6.1$) earthquake in northern Baja along the Cerro Prieto fault. In this light, further study of the rupture patterns of these events should be undertaken in a specific effort to ascertain the failure mechanism, approximate size and location of the expected aftershocks. In particular, features of "complex rupture", inferred fault asperities, and large, late aftershocks should be compared with complexities in the mapped surface geology and general aftershock distributions.

Sauber, J., McNally, K. C., Pechmann, J., H. Kanamori, 1981, Earthquake mechanisms and patterns in seismic activity concurrent with the short-term strain changes in Palmdale, California, Geophy. Res. Letters, to be submitted.

Leitner, B., McNally, K., and H. Kanamori, 1979, Investigations of seismic quiescence and microearthquakes along the southern San Andreas fault; Coachella Valley, California. Bull. Seism. Soc. Am., to be submitted.

Leitner, B. J., McNally, K. C., Richter, C. F., and H. Kanamori, 1981, Large late aftershocks following M_L 6.0 events in southern California, and implications for expected future activity, Bull. Seismol. Soc. Am., to be submitted.

Corbett, E. J., and McNally, K. C., 1980, Seismicity of the Borrego Mountain region 1960-1968: Earthquake Notes, Seismological Society of America, 50, 883.

Leitner, B. J., Humphreys, E., McNally, K. C., and Kanamori, H., 1979, Investigations of seismic quiescence and microearthquakes along the southern San Andreas fault; Coachella Valley, California: EOS Trans, AGU, 60, 883.

McNally, K. C., H. Kanamori, J. C. Pechmann and G. Fuis (1978) Earthquake swarm along the San Andreas fault near Palmdale, southern California, 1976 to 1977, Science, v. 201 p. 814-817.

McNally, K. C., Richter, C. F., Leitner, B. J., and Kanamori, H., 1980, Aftershock sequences and minor seismicity in southern California and Mexico: Relationship to the Mexicali earthquake ($M_L = 6.6$, $M_s = 6.8$) of 15 October 1979: Earthquake Notes, Seismological Society of America, 50, 52.

Sauber, J., Pechmann, J., Bryan, C., McNally, K. C., and H. Kanamori, 1980, Earthquake Mechanisms and patterns in seismic activity concurrent with the short-term strain changes in Palmdale, California: EOS Trans., AGU, 61, 1053.

Savage, J. C., W. H. Prescott, M. Lisowski, N. E. King (1981) Strain accumulation in southern California, 1973-1980, Science, v. 211 p. 56-58.

Wallace, R. E., McNally, K. C., and J. F. Davis, 1981, Problems of earthquake prediction terminology and communication: Earthquake Notes, Seismological Socieity of America, 51, in press.

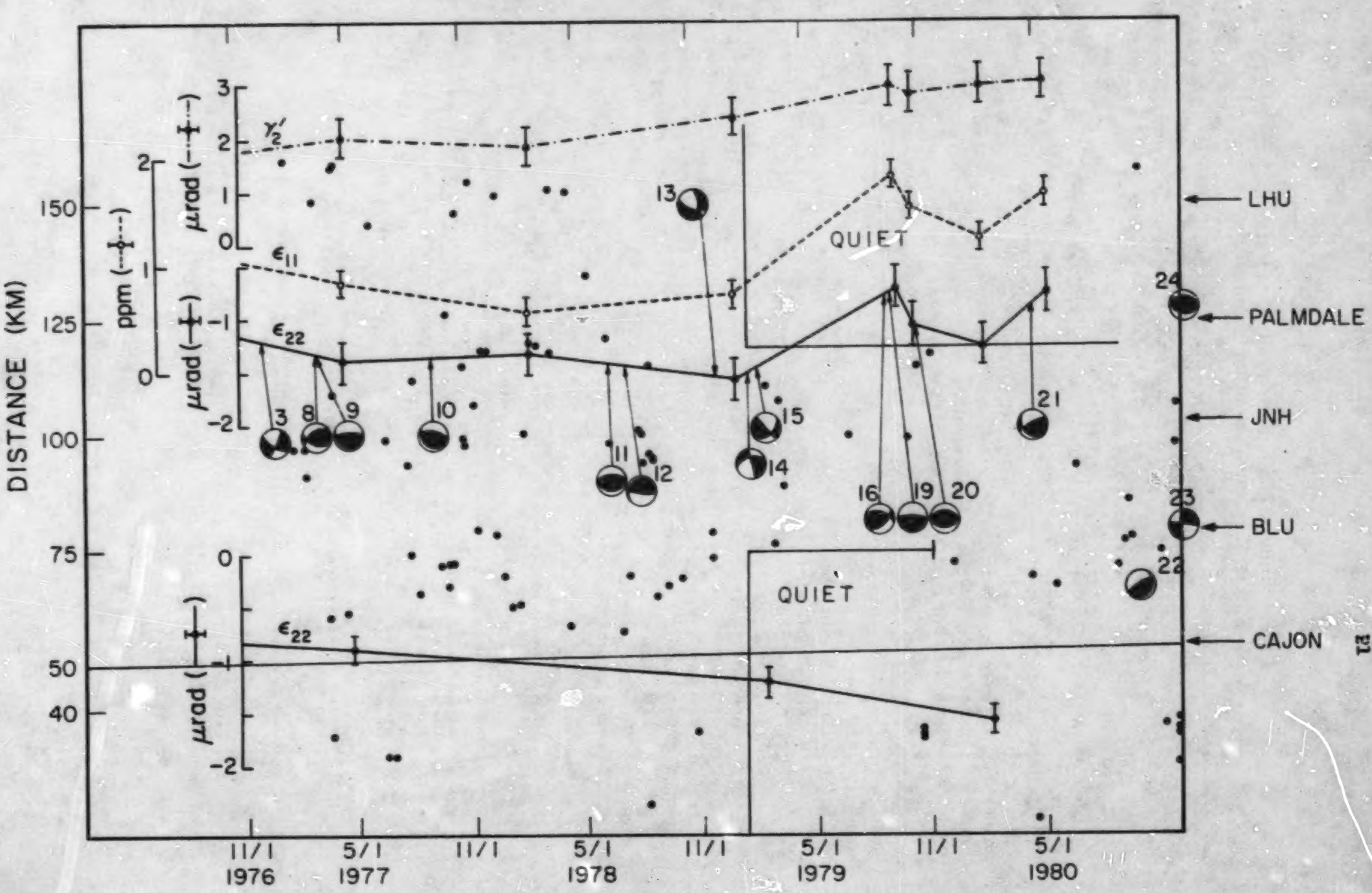
DISTANCE (KM)
150
125
100
75
50
40
ppm (- - -)
μrad (—)
μrad (-·-·-)
μrad ( )
3
2
1
0
-1
-2
γ'₂
ε₁₁
ε₂₂
ε₂₂
QUIET
QUIET
3
8
9
10
11
12
13
14
15
16
19
20
21
22
23
24
LHU
PALMDALE
JNH
BLU
CAJON
11/1
1976
5/1
1977
11/1
5/1
1978
11/1
5/1
1979
11/1
5/1
1980

FIGURE 1

A Field Study of Earthquake Prediction Methods in the Central Aleutian Islands

14-08-0001-19272

C. Kisslinger
S. Billington

Cooperative Institute for Research in Environmental Sciences
Box 449
University of Colorado
Boulder, CO 80309
(303) 492-8028

Network Operation and Data Analysis.

The efforts made during 1979 and 1980 to harden the field installation against adverse weather in the Adak region are proving effective. A wind storm typical of those that had caused serious damage to the network in the past happened in December, 1980, with no effects noted. Two out of the 32 components monitored are out of service and will remain so until the stations can be reached by helicopter. The analogue magnetic tape recording system is working well.

Routine analysis of Adak network data was shifted to the use of digital data for all events since January 1, 1981. A number of problems have been made the full realization of this change difficult, but most of the routine work is being done from digital seismograms. Digitizing of the analogue tapes from the network is now routine on the PDP 11/34 and the tapes can be recycled to Adak in a timely way. The success of this approach depends critically on the reliability of the triggering algorithm which picks the events to be stored.

Program PING, developed at the University of Washington, has been modified to meet the needs of this project and is now used routinely for reading the seismograms. A useful change made was the addition of filtering to take out the severe wind noise which is often present in the data.

Investigations and Results.

Earthquake locations are complete for 1980 and a substantial part of the first few months of 1981. Monthly seismicity maps and graphs of cumulative numbers of earthquakes vs. time are routinely plotted as a means of displaying and monitoring space-time patterns of seismicity.

The cooperative study with the University of Texas, Galveston, based on simultaneous observations with their OBS and our island-based stations, is nearly completed. The principal conclusions are:

1) Events located between a line about 100 km north of the trench axis and the volcanic islands are detected well by the island stations. Events southward from the trench axis are not recorded reliably by the island stations. These conclusions are based on a comparison of detections by the island and OBS stations.

2) Generally, the epicenters of events within the range of reliable detection by the island stations, calculated from island observations alone, are not far (about 3 km on average) from the locations based on the combined data set. However, the depths based on island data alone, especially for events deeper than 70 km, differ substantially from those based on the combined data set.

3) The flat-layer velocity model that has been used to locate Adak zone events seems to be satisfactory and no modifications have been required by the combined data.

The work still to be done is the completion of focal mechanism studies and cooperation with outside investigators using ray tracing techniques to test for mislocations and to explain the failure to detect on the islands the events seaward of the trench.

Computational procedures for calculating focal mechanisms from body-wave amplitude data are developed. These codes have been tested of several sets of real and synthetic data. Listings of the programs (Fortran for the Unix operating system on the PDP 11/70) are available on request.

Another case of re-orientation of the focal mechanism of small earthquakes before a larger one has been found. The earthquake, July 15, 1980, occurred very near to an event of February 22, 1976 that was throughly studied as part of this project. The earlier event not only showed a precursory change in focal mechanism orientation, but also was preceded by seismicity changes (3 1/2 months of quiescence followed by a burst of foreshocks). No patterns were seen in the seismicity before the more recent earthquake. The focal mechanism change showed up primarily as a change in the ratio $(SV/P)_z$ at one station.

Reports.

Bowman, R., and C. Kisslinger (1981). Changes in focal mechanism of small earthquakes before an m_b 4.6 earthquake in the central Aleutian seismic zone (abstract), **Earthquake Notes, 52, 69.**

Chen, A. T., C. Frohlich, G. V. Latham, R. K. Cardwell, and S. Billington (1980). Is there seismic activity within the accretionary prism? (abstract), **EOS, 61,** 1044-1045.

Billington, S., E. R. Engdahl, and S. Price (1981). Changes in the seismicity and focal mechanism of small earthquakes prior to an M_S 6.7 earthquake in the central Aleutian island arc, in press, Ewing Series Vol. 4: **Earthquake Prediction.**

Microearthquake Data Analysis

9930-01173

W. H. K. Lee
Branch of Seismology
U.S. Geological Survey
345 Middlefield Road - MS-77
Menlo Park, California 94025
(415) 323-8111, ext. 2630

Investigations

1. The primary focus of this project is the development of state-of-the-art computation methods for analysis of data from microearthquake networks.

2. The principal effort during the past six months has been devoted to
(a) proof-reading the book "Principles and Applications of Microearthquake Networks" by Lee and Stewart, and preparing a Glossary, an Author Index, and a Subject Index for it, and
(b) preparing two invited talks for the Workshop on Computational Seismology.

Results

The following two talks were delivered at the Workshop on Computational Seismology, Salishan Lodge, Gleneden Beach, Oregon on March 23, 1981:

1. Lee, W. H. K., Some seismological applications of ray-tracing and optimization, and

2. Luk, F., and Lee, W. H. K., A shooting method for seismic ray-tracing.

Seismic Data Library of WWSSN Seismograms

9930-01501

W. H. K. Lee
Branch of Seismology
U.S. Geological Survey
345 Middlefield Road - MS-77
Menlo Park, California 94025
(415) 323-8111, ext. 2630

This is a nonresearch project, and its main objective is to keep the WWSSN seismograms up to date and properly filed. Everything is now up to date.

Worldwide Earthquake Research Database

9930-02104

W. H. K. Lee
Branch of Seismology
U.S. Geological Survey
345 Middlefield Road - MS-77
Menlo Park, California 94025
(415) 323-8111, ext. 2630

Investigations

The main goal of this project is to provide up-to-date information which will facilitate research on earthquakes. Two major topics now under investigation are:

1. Establishment of a seismogram library of significant earthquakes, especially those before 1963.

2. Organization and maintenance of a bibliographic data base and retrieval system on current earthquake literature.

Results

Seismogram library: Under contract from this project, the National Geophysical and Solar-Terrestrial Data Center, NOAA, has been filming historical seismograms from key U.S. stations.

Bibliographic database and retrieval system: The Current Earthquake Literature (CEL) database has been maintained and kept up to date. Quarterly indexes are being distributed on schedule, but the Annual Index for 1980 has been delayed due to a printing backlog.

Reports

Hayashida, B. S., Kauffmann, M. L., and Lee, W. H. K., Index to current earthquake literature (quarterly issues).

A Study of Earthquake Prediction and the Tectonics of the Northeastern Caribbean: A Continuing Experiment in Two Major Seismic Gaps

14-08-0001-16748

W. R. McCann, A. L. Kafka, and L. R. Sykes
Lamont-Doherty Geological Observatory of Columbia University
Palisades, New York 10964

Investigations

During the period November 1977 through October 1980 Lamont-Doherty Geological Observatory continued to operate a network of 17 seismograph stations in the northeastern Caribbean. Throughout this period several significant improvements to the detection and recording equipment were implemented. In March 1979 a digital recording system with an event-trigger was installed at the central recording site on St. Thomas, and this system has operated without failure since then.

Several changes in the configuration of the network occurred during the three year period covered by this report. At present 6 of the 17 stations are 3 component short period sites. One station (SJV - St. John, Virgin Islands) has an experimental response which is proportional to displacement and which enhances the long periods and attenuates the higher frequencies. Station VST (St. Thomas, Virgin Islands) has 3 components with a broad band response in addition to 3 components with short period response.

Results

The focal mechanisms of four earthquakes which occurred in the northeastern Caribbean have been determined. These results, combined with other focal mechanism results from the literature and the seismicity recorded by the network indicate that a wide variety of seismotectonic deformation is presently occurring in the northeastern Caribbean.

Focal mechanisms in the southern portion of the Lesser Antilles are consistent with a simple model of the North American plate subducting beneath the Caribbean plate. As the northern end of the Lesser Antilles arc is approached, however, several deviations from a simple subduction model are observed. These deviations, as well as the regional seismicity and other geological and geophysical observations, can at least partly be explained by a new model of the recent tectonic framework of the northeastern Caribbean. This model postulates that the normal subduction processes in this region were recently perturbed by the subduction of a bathymetric feature (the Barracuda ridge).

The microearthquakes along the northeastern margin of the Caribbean plate are not evenly distributed along the main seismic zone. Most shocks of magnitude 3 or greater are confined to limited portions of the inner wall of the Puerto Rico trench north of the Virgin Islands. Another zone of relatively high seismic activity is further down-island in the vicinity of the northern Leser Antilles. These two segments of the seismic zones are portions of the plate boudary which are presently interacting with ridges on the downgoing seafloor. There appears to be a dichotomy in the mode of seismic energy release between the up-island and down-island clusters of seismicity. Whereas, the down-island cluster is characterized by main shock - aftershock sequences, the up-island cluster is characterized by swarms.

The digital seismograms collected by the network are being used to study the source parameters of earthquakes in the area and the attenuation of seismic radiation. By combining stress drop results with hypocentral locations of swarm events we have obtained a detailed picture of the spatial variability of stress drop on a scale of hundreds of meters. The results of this study show that static stress drops of the swarm events (all of which occurred within 1 km of each other) increased systematically with their seismic moments and varied by an order of magnitude (from 0.2 to 2 bars).

The spectral fall-off of earthquakes in the region were used to estimate seismic attenuation. We obtained a Q for P-waves of 390 ± 30 and a Q for S-waves of 670 ± 70. These values of Q are valid over the frequency range of 10 to 30 hertz. It is notable taht, for these frequencies, Q_s exceeds Q_p. This observaton implies that the attenuation mechanism at these high frequencies differs from the mechanism at longer periods where $Q_p < Q_s$.

Geodetic Strain Monitoring

9960-02156

Arthur McGarr
Branch of Tectonophysics
U.S. Geological Survey
345 Middlefield Road, M/S 77
Menlo Park, California 94025
(415) 323-8111, Ext. 2708

Investigations

1. A portable two color laser geodimeter (Terrameter) was ordered in 1978 for the purpose of high resolution trilateration surveys in selected areas of the San Andreas fault system.
2. A cooperative program is underway with Dr. Larry Slater of the University of Colorado, CIRES, to observe crustal deformation near Pearblossom, California which is within the region of the "Palmdale Bulge".
3. Recent observations indicate that there are substantial changes in the state of stress in a short distance between two large provinces where the state of stress shows no horizontal variation. We have solved some of the theoretical aspects of this problem.

Results

1. The terrameter, ordered in 1978, was put through a third series of acceptance tests in December, 1980 and January, 1981; the other two tests have been described in the two previous reports. The results of the January test indicate that the terrameter was not stable over a 20 hour interval to the specified one part in ten million in observed distance. A similar result occurred in the test in July 1980. The terrameter has been sent back to the factory where factory personnel have found a series of problems resulting from interference of its microwave oscilators.
2. On the basis of failure of the terrameter during acceptance test performed in July, 1980, and the need to closely monitor the strain in the region of the Palmdale Bulge, we cooperated with Dr. Larry Slater and moved the University of Colorado's two color geodimeter from Hollister, California, to Pearblossom, California. Since October, 1980, we have constructed an observatory to house the instrument and we have initiated a program to make frequent measurements of distances to 13 benchmarks that are distributed radially from the observatory. Currently, line length measurements are taken about twice a week on most of the baselines. Portable retro reflectors are used as targets on all the baselines with the exception of two baselines which have permanent reflectors since the benchmarks have difficult access. The baselines range from 3.2 km to 8.1 km in length and 8 of the baselines cross the trace of the San Andreas fault.

As of the end of March, 1981, the pattern of strain inferred from our measurements indicates that it is fairly uniform over the region. In detail, the build-up of right lateral shear strain is not quite at the level of 2 standard errors of significance; the rate is 0.08 ± 0.05 μstr/year with no significant short period departures from this trend. The components of strain orthagonal to the local strike of the San Andreas and the dilatation show a six month trend of contraction with 2 significant episodes of accelerated contraction. So far, the long term dilatation is -1.36 ± 0.09 μstr/year and the contraction normal to the fault is 0.95 ± 0.07 μstr/year. These rates were primarily governed by two periods of contraction; during the month of December the area was compressed by an amount of 0.55 ± 0.07 μstr and the normal component of strain contracted by 0.48 ± 0.05 μstr. During the month of March, a similar episode of shortening occurred. Areal compression was 0.82 ± 0.07 μstr and the normal component of strain contracted by 0.33 ± 0.05 μstr. Clearly, the second episode differs from the first episode since a significant amount, 0.49 ± 0.05 μstr of contraction occurred in a direction parallel to the strike of the fault, where as the value of this strain component, which is inferred from the data taken in December, is not significant at a level of 0.1 μ strain.

We expect to continue to closely monitor the strain changes near Pearblossom and compare our measurements to other crustal deformation data taken nearby including the Sachs-Evertson volumetric strainmeters and geodetic measurements taken in the Palmdale network.

3. The transition in stress state between adjacent domains is mediated by a stress field within a zone between the provinces that can be determined by solving the equations of force equilibrium and stress compatability. These solutions indicate that the states of stress in adjacent domains are coupled; a change in the stress field of one province is generally accompanied by changes in the other domain as well as in the intermediate transition zone. For example, the alignment of the horizontal principal stresses of one domain parallel and perpendicular to the boundary implies the same directions for these stresses in the adjoining province. Most importantly, the solutions provide a clear indication that the change in the state of stress from one province to another is caused by a shear stress acting on the base of the elastic layer of the transition zone in a direction normal to the trend of the boundary. The magnitude of this basal shear stress is proportional to the change in horizontal stress multiplied by the ratio of the thickness to the width of the transition zone. The coincidence of many transition zones with boundaries between provinces defined by heat flow or topography suggests convincingly that the basal shear stresses are the result of subjacent mass transport in the direction of increasing horizontal stress. For instance, the horizontal flow of subjacent material from a region of high to low heat flow gives rise to a basal shear stress, which, in turn, causes the horizontal stress in the region of low heat flow to be larger than in the high heat-flow province. In general, this analysis provides a quantitative relationship between changes in the stress field measured in the upper portion of the crust and shear stresses acting on the base of the elastic layer. Such basal stresses are perhaps the most plausible cause of crustal deviatoric stresses that increase linearly with depth, in accord with the observations.

Reports

Langbein, J., M. Linker, L. Slater, and A. McGarr, 1981, Strain accumulation near Palmdale, California, measurement with a two color laser geodimeter; preliminary results: Terra Cognita, No. 1, p. 30, 1981. Presented at the Congress of European Union of Geosciences.

Slater, L. E., A. McGarr, J. O. Langbein, and M. F. Linker, 1981, Initial MWDM measurements on the Palmdale uplift: EOS, vol. 62, no. 17, p. 393. Presented at spring AGU meeting.

Crustal Strain

9960-01187

W. H. Prescott, J. C. Savage, and M. Lisowski
Branch of Tectonophysics
U.S. Geological Survey
345 Middlefield Road, M/S 77
Menlo Park, California 94025
(415) 323-8111, Ext. 2701

Investigations

Analysis of deformation in tectonically active areas of the Western United States was the principal subject of investigation.

Results

1. At the northern end of the creeping section of the San Andreas fault, near San Juan Bautista, California, north-south contraction is taking place at a rate of 0.37 ± 0.03 μstrain/a. This deformation, observed between 1973 and 1981, appears to be occurring at a uniform rate with no significant time variations. Displacement across the northern end of the net (near Corralitos, California) is about 6 mm/a. Since the network covers primarily the western side of the fault this result is consistent with a slip rate of 12 mm/a at depth near the San Andreas fault.

2. A new technique for extracting crustal deformation information from geodetic observations was developed. This technique allows a more satisfactory treatment of the rotation part of the deformation field. The amount or rate of relative motion observed is very sensitive to the treatment of rotation. The new technique, an 'outer coordinate' solution, finds the rotation of the network that minimizes the components of displacement normal to the fault. Since motion along a strike slip fault is generally expected to be parallel to the fault, the displacements obtained with the outer coordinate solution are more reasonable than those obtained with other techniques.

3. Periodic measurements of fault-crossing networks with a side length of 1 to 3 km are being made to monitor deformation across fault zones in California. The distance measurements, made with a Hewlett-Packard 3800 or 3808 electronic distance meter, have a maximum standard deviation of 5 mm. Deformation meaured within networks that span the San Juan Bautista-Cholame segment of the San Andreas fault in central California yields slip rates similar to those meaured across a 100-300 m wide zone by repeated alinement array surveys. Fault slip rates increase from near 0 to 32 mm/yr between San Juan Bautista and Bitterwater Valley in steplike

increments. From Bitterwater to Slack Canyon slip rates vary between 26 and 32 mm/yr. Slip rates decrease southwestward of Slack Canyon to 3 mm/yr at Cholame. In contrast, Geodolite measurements of deformation across a 20-km-wide zone are consistent from San Juan Bautista to Slack Canyon and imply a 32 ± 2 mm/yr slip rate. Deformation across the Calaveras fault accounts for the difference between Geodolite and near-fault slip rates between San Juan Bautista and Bear Valley, although the zone of deformation is wider than 2.5 km just south of Hollister. At Bear Vallley, measurements of a short-range network crossing the Paicines fault imply a slip rate of 10 ± 3 mm/yr during the period 1976 to 1979. From Slack Canyon to Cholame, Geolodite measurements show a constant decrease in the rate of shallow slip.

4. A 15-station geodetic control network extending 10 km north and 40 km south of the Motagua fault in Guatemala was reobserved 2 years after the February 4, 1976 $M_S = 7.5$ earthquake. The initial first-order triangulation was observed in two parts: the Guatemala-Honduras border arc completed in 1935 and the Motagua Valley arc completed in 1953. Both angles and distances were observed in the 1978 resurvey. The angle changes between the combined 1935-53 survey and the 1978 resurvey were used to calculate earthquake-related fault slip on two dislocation models of the rupture surface. Dislocation modeling of the geodetic data indicate left-lateral slip of 0.8 ± 0.1 m near the surface, increasing to 2.1 ± 0.5 m in the intermediate 5 to 15 km section. The model was consistent with the 0.9-1.1 m of accumulated slip and afterslip observed near the network by Bucknam *et al*. (1978) and with the 2 meter of slip derived by Kanamori and Stewart (1978) from a long period seismic surface wave estimate of the seismic moment.

5. Plate motion below the seismogenic layer along the San Andreas fault system in California is generally assumed to occur by aseismic slip along a deeper extension of the fault. It is also possible that below the seismogenic layer, deformation is distributed laterally over a zone. Several observed features of the San Andreas fault in California have implications about the mode of accommodation of relative motion along the plate boundary beneath the seismogenic zone: the shallow depth of all earthquakes in California, the depth of which coseismic slip occurred during the 1906 San Francisco earthquake, the broad zone of strain accumulation, the broad heat flow anomaly, and the existence of widely separated parallel faults. The observations strongly imply that below the seismogenic zone, relative motion is distributed over a zone and occurs by inelastic flow rather than by aseismic slip on discrete fault planes. The existence of multiple faults further suggests that tractions at the base of the brittle layer are significant over time periods of years to hundreds of years.

Reports

Prescott, W. H., and Nur, A., 1981, The accommodation of relative motion at depth on the San Andreas fault system in California: Journal of Geophysical Research, v. 86, no. B2, p. 999-1004.

Prescott, W. H., and Lisowski, M., 1980, Vertical deformation at Middleton Island, Alaska: Bulletin of the Seismological Society of America, v. 70, no. 5, pp. 1887-1892.

Savage, J. C., Lisowski, M., Prescott, W. H. and Sanford, A. R., 1980, Geodetic measurement of horizontal crustal deformation across the Rio Grande rift near Socorro, New Mexico, Journal of Geophysical Research, v. 85, n. B12, pp. 7215-7220.

Prescott, W. H., 1980, The accommodation of relative motion along the San Andreas fault system in California, Ph.D. thesis, Stanford University, 195 pp.

Prescott, W. H., Lisowski, M., and Savage, J. C., 1980, Geodetic measurement of crustal deformation on the San Andreas, Hayward and Calaveras faults near San Francisco, EOS, Trans Am Geophys Union, v. 61, no. 46., p. 1126.

Savage, J. C., Prescott, W. H., Lisowski, M. and King, N., 1980, Strain accumulation in Southern California, EOS, Trans Am Geophys Union, 61, (46), 1127.

King, N. E., Savage, J. C., Lisowski, M., and Prescott, W. H., 1980, Geodolite measurements near the epicenter of the 1978 Bishop earthquake and the 1980 Mammoth Lake earthquakes in Owens Valley, California, EOS, Trans Am Geophys Union 61 (46), 1127.

King, N. E., Savage, J. C., Lisowski, M., and Prescott, W. H., 1981, Preseismic and coseismic deformation associated with the Coyote Lake, California, earthquake, Journal of Geophysical Research, v. 86, no. B2, p. 892-898.

Savage, J. C., Lisowski, M., and Prescott, W. H., 1981, Strain accumulation across the Denali fault in the Delta River Canyon, Alaska, Journal of Geophysical Research, v. 86, no. B2, p. 1005-1014.

Savage, J. C., Lisowski, M., Prescott, W. H., and King, N. E., Strain accumulation near the epicenters of the 1978 Bishop and 1980 Mammoth Lakes, California, earthquakes, Bulletin of the Seismological Society of America, v. 71, no. 2, pp. 465-476, 1981.

Lisowski, M. and J.C. Savage, 1980, Horizontal strains in the Shumagin Islands and Cape Yakataga, Alaska, Seismic gaps, EOS, Trans. Am. Geophys. Un., 61, no. 46, p. 1110.

Savage, J.C., W.H. Prescott, M. Lisowski, and N.E. King; 1981. Strain on the San Andreas fault near Palmdale, California: Rapid, aseismic change, Science 211, 56-58.

Comparative Study of Continental Convergence Zones: The Himalaya, The Apennines and the Appalachians

14-08-0001-19123

Leonardo Seeber
Lamont-Doherty Geological Observatory of Columbia University
Palisades, New York 10964
(914) 359-2900

Investigations

Earthquake data, from a local network, from teleseismic stations and from historic reports, are used to infer the active structures and their significance for seismic hazard. This study has been extended to other continental convergence zones, both active and fossil, with the scope of comparing the fundamental features of this kind of plate boundary.

Results

Earthquake data as well as surface data on morphology and structure along the Himalaya indicate a remarkably homogeneous pattern of faulting which traces a small circle along the central portion of the Himalayan arc. We have developed a detailed model where the great Himalayan earthquakes rupture a shallow-dipping detachment below a wide sedimentary wedge, the most forward expression of the convergence zone. Intermediate-magnitude earthquakes, instead, are concentrated on a narrow thrust belt which separates the sedimentary wedge from the thicker and more rigid backward portion of the overriding plate (Seeber et al., 1981).

According to these and other constraints, convergence along the Himalaya can be modeled by a single tectonic phase in which cratonic India subducts a thick and wide wedge of sediments formerly along its very old passive margin. The intensity data for the great Himalayan earthquakes suggest a space-time distribution consistent with the gap concept. Accordingly, we have drawn tentative conclusions about the distribution of future great earthquakes (Figure 1; Seeber and Armbruster, 1981).

The structural elements associated with plate convergence in the Himalayan are remarkably similar to the elements in other convergence zones, for example in the fossil convergence zone along Eastern North America and in the active oceanic convergence zone in Alaska (Figure 5) and the arc continent collision zone in Italy and New Guinea. We have recently applied to the Appalachians some of the concepts developed for the Himalaya, and have proposed that tectonic activity in the southeastern U.S., including the 1886 Charleston earthquake, is associated with a backward slip on the Appalachian detachment (Figure 2) (Seeber and Armbruster, 1981).

The continental arc collision now active in New Guinea, at the northeastern margin of the Indo-Australian plate (Hamilton, 1980), may resemble closely the early (Subathu, Upper Eocene) collisional stage at the northern margin of greater India (Klootwijk, 1979). Nevertheless, the present Himalayan structure is still remarkably similar to the structure in New Guinea where incipient MBT- and MCT-like faults can be recognized (Seeber and Gornitz, in preparation). The similarity between the early collisional structure in New Guinea, and the more mature continent collision structure in the Himalaya support the concept of a steady state tectonic regime where the major features evolve simultaneously rather then in a succession of different tectonic phases (e.g. LeFort, 1975).

The Italian arc is probably the site of an arc-continent collision (Giese and Ruetter, 1978). A rapidly subsiding foredeep extends continuously along the arc and marks the limit of the fold and thrust belt toward the Adriatic foreland. Some of the historic earthquakes in Italy are associated with very large mezoseismal areas, for example, the 1857, 1456 and 1703 earthquakes in south-central Italy (Figure 4). Reliable modern hypocenters in this area of Italy are all shallow and these historic events are probably associated with very large shallow ruptures. In analogy with the Himalayan convergence structure (Figure 4), we hypothesize an active detachment below the thrust and fold belt of the Italian arc (the Apennines), which can generate great earthquakes.

Reports

Armbruster, J.G., L. Seeber, R. Quittmeyer, and A. Farah, Seismic network data from Quetta, Pakistan, Rec. Geol. Surv. Pakistan, 49, 1-5, 1979.

Gornitz, V., and L. Seeber, Morphotectonic analysis of the Hazara arc region of the Himalayas, N. Pakistan-N.W. India, Tectonophysics, in press, 1980.

Seeber, L., J.G. Armbruster, The 1886 Charleston, South Carolina earthquake and the Appalachian detachment, submitted to J. Geophys. Res., 1980.

Seeber, L., J.G. Armbruster, and R.C. Quittmeyer, Seismicity and continental subejction in the Himalayan arc, Interunion Commission on Geodynamics Working Group 6 Volume, 1981.

Seeber, L., and J.G. Armbruster, Continental subduction and great earthquakes of the Himalayan arc, Maurice Ewing Series, Earthquake Prediction, 4, Amer. Geophys. Union, Washington, D.C., 1981.

Seeber, L., R. Quittmeyer, and J. Armbruster, Seismotectonics of Pakistan: A review of results from network data and implications for the Central Himalaya, Structural Geology of the Himalaya, P.S. Saklani (editor), Univ. of Delhi, 1979.

Seeber, L., J. Armbruster, and S. Farhatulla, Seismic activity at the Tarbela dam site and surrounding region, in Proceedings of the International Committee on Geodynamics, Group 6, R.A.K. Tahirkheli, M.Q. Jan, and M. Majid (editors), University of Peshawar, Peshawar, 1980.

References

Baratta, M., I Terremoti d'Italia, second print (1979), 1981.

Cook, F.A., D.S. Albaugh, L.D. Brown, S. Kaufman, J.E. Oliver, and R.D. Hatcher, Thin-skinned tectonics in the crystalline southern Appalachians; COCORP seismic-reflection profiling of the Blue Ridge and Piedmont, Geology, 7, 563-567, 1979.

Hamilton, W., Tectonics of the Indonesian region, U.S. Geol. Surv. Professional Paper 1078, 1979.

Klootwijk, C.T., A summary of paleomagnetic data from extra-peninsular Indo-Pakistan and south-central Asia: Implications for collision tectonics, in Structural Geology of the Himalaya, P.S. Saklani (editor), New Delhi, 1979.

LeFort, P., Himalayas: The collided range. Present knowledge of the continental arc, Amer. J. Sci., 275A, 1-44, 1975.

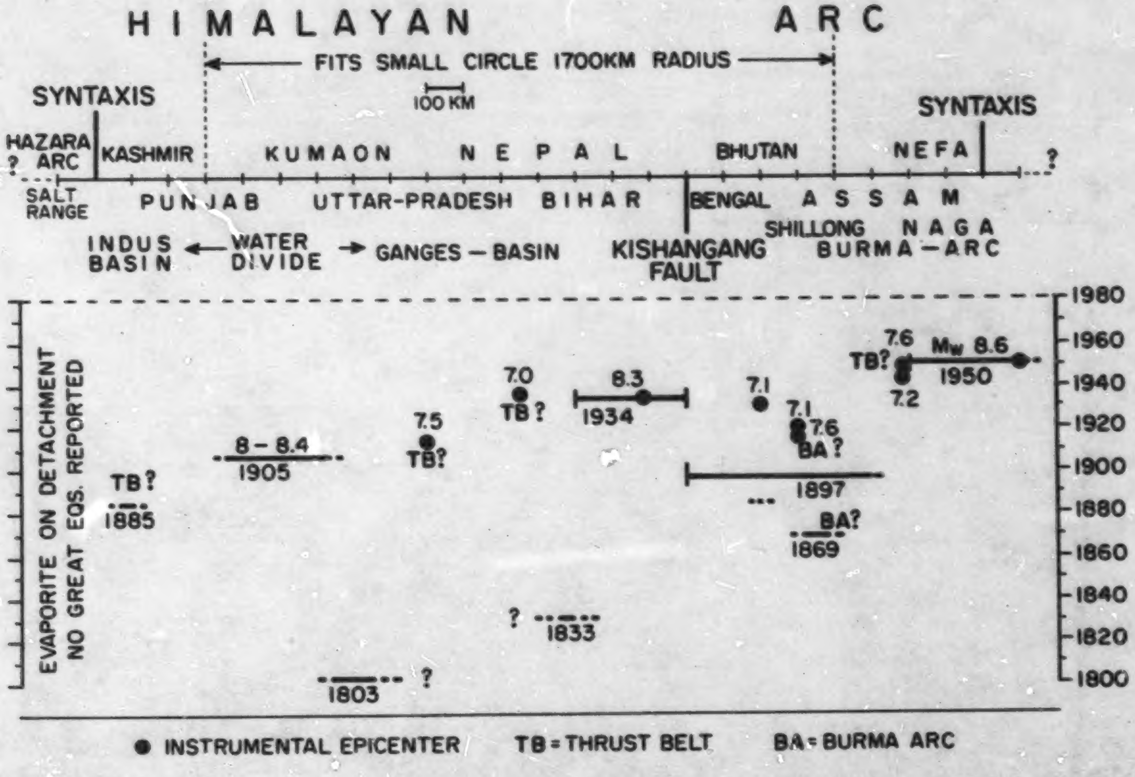

Figure 1. Space-time diagram of detachment ruptures along the Himalayan arc after 1800. The data are very scanty for the period before 1897 and may be incomplete. The most likely gaps unruptured since 1800 are in Kashmir and in Uttar Pradesh, between the 1833 and 1803 ruptures. The gap between the 1897 and 1950 ruptures was probably filled by the 1943 and 1947 earthquakes. If the 1833 and 1803 ruptures abut, the entire Himalayan detachment, excluding Hazara and Kashmir where aseismic slip may play an important role, has probably ruptured since 1800. (From Seeber and Armbruster, 1981).

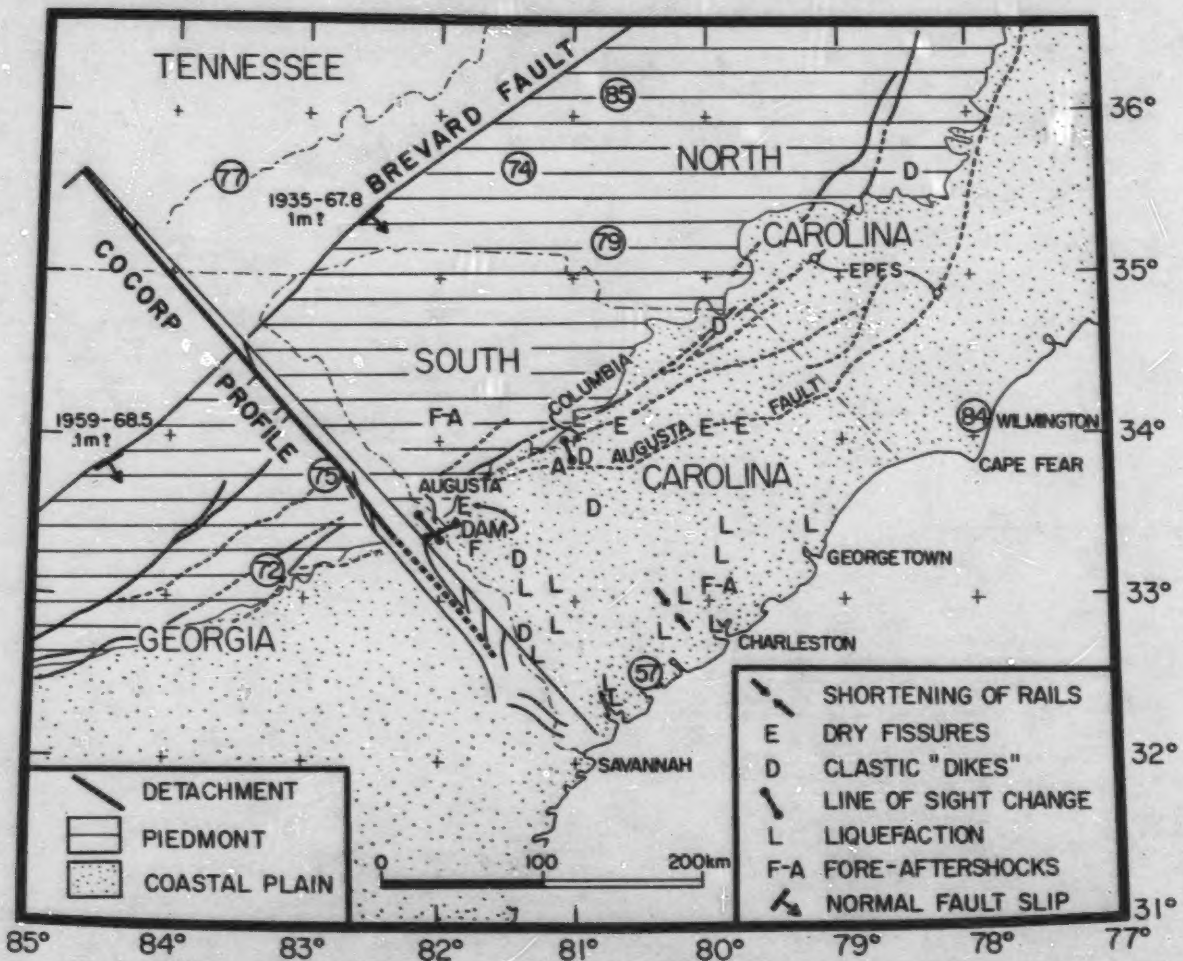
TENNESSEE
BREVARD FAULT
85
74
77
79
NORTH
CAROLINA
1935-67.8
1m?
COCORP
PROFILE
SOUTH
CAROLINA
1959-68.5
.1m?
F-A
COLUMBIA
AUGUSTA FAULT
EPES
84
WILMINGTON
CAPE FEAR
AUGUSTA
DAM
75
72
GEORGIA
GEORGETOWN
CHARLESTON
57
SAVANNAH
DETACHMENT
PIEDMONT
COASTAL PLAIN
0
100
200km
SHORTENING OF RAILS
E DRY FISSURES
D CLASTIC "DIKES"
LINE OF SIGHT CHANGE
L LIQUEFACTION
F-A FORE-AFTERSHOCKS
NORMAL FAULT SLIP
36°
35°
34°
33°
32°
31°
85°
84°
83°
82°
81°
80°
79°
78°
77°

Figure 2. Particular effects of the 1886 earthquake (changes in line-of-slight not to scale). Liquefaction and dry fissuring as well as foreshocks and aftershocks are not limited to the Charleston-Summerville area. Prehistoric clastic dikes, are found along the belt of 1886 dry dissuring and beyond. Earthquakes before 1886 (56) (Mercalli intensity ≥ are shown by circles numbered by the last two digits of the year. There is a suggestion of a doughnut pattern around the meizoseismal area forming in the 14 years before 1886. The normal fault displacements along the Brevard are modelled from releveling data (Citron and Brown, 1979). The COCORP profile (no vertical exaggeration) is from Cook et al. (1979).

P1

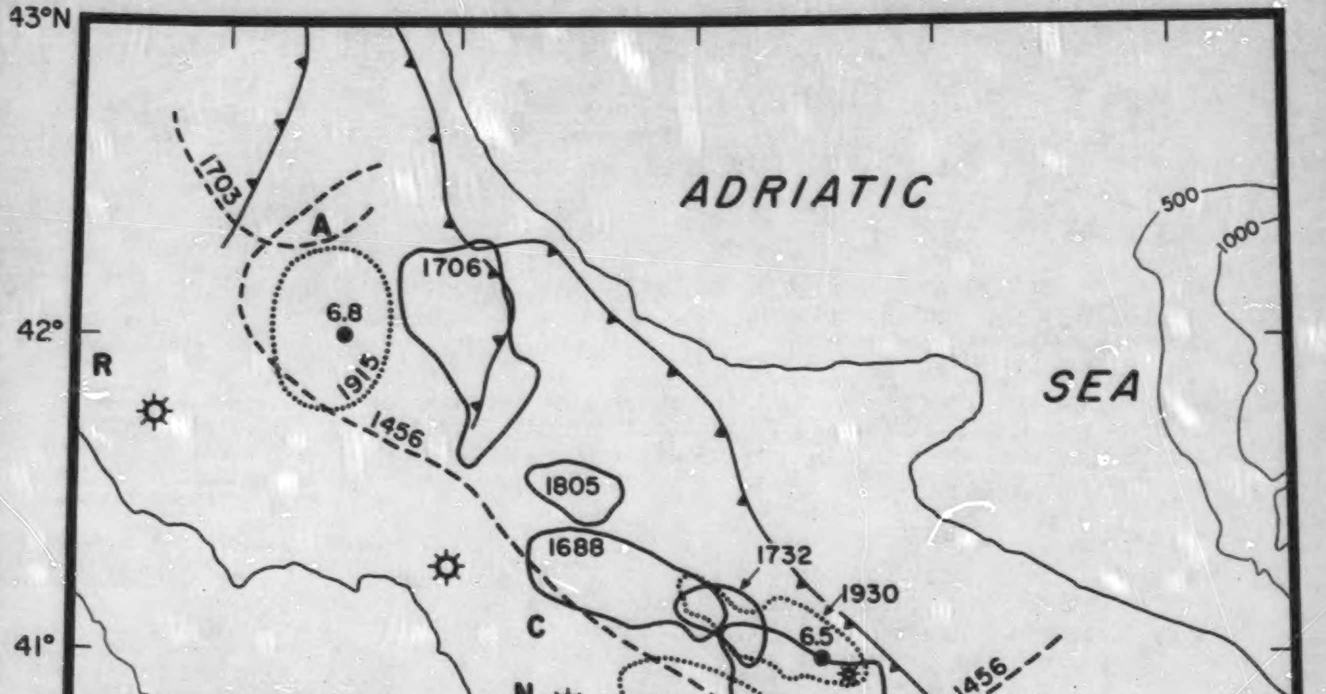
43°N
42°
41°
40°
39°
13°
14°
15°
16°
17°E
ADRIATIC
SEA
TIRRENIAN
SEA
IONIAN
SEA
1703
A
1706
6.8
1915
R
1456
1805
1688
1732
1930
6.5
C
N
1980
6.8
P
1694
1857
500
1000
1000
1000
0
50
100 KM
BORDER THRUST:
ALLOCHTHONOUS APENNINES
OVER FOREDEEP
QUATERNARY VOLCANOES
1000 DEPTH CONTOURS, METERS
MEIZOSEISMAL AREAS OF
LARGE EARTHQUAKES
POSSIBLE GREAT
DETACHMENT EQS
INTERMEDIATE MAGNITUDE EQS
BEFORE 1900
INTERMEDIATE MAGNITUDE EQS
AFTER 1900

Figure 3. Large earthquakes in south-central Italy in the second part of the second milleninium. This sample should include most of the crustal earthquakes with magnitude $M \geq 6.5$. In the 1456 earthquakes villages that suffered total destruction are scattered over a zone approximately 300 km long. (Data is from Baratta, 1901). A - Aquila, R - Rome, C - Caserta, N - Napoli, P - Potenza.

Minicomputer Systems Development

9970-02118

Peter R. Stevenson
Branch of Network Operations
U.S. Geological Survey
345 Middlefield Road - MS-77
Menlo Park, California 94025
(415) 323-8111, ex. 2572

Investigations

The major goal of this project is to assist the Office of Earthquake Studies in efficiently processing data by means of minicomputer hardware/software.

A minicomputer-based seismic data processing system has been developed to process local earthquakeks from the USGS central California network's analog tape recording system. The goal of the system is to provide preliminary hypocenters and associated waveform data on a routine basis.

The system is designed to process events involving hundreds of seismic stations. To accomplish this, it creates a dubbed analog library tape from five 14-track, online analog tapes. Information is recorded on those tapes in Frequency Division Multiplexing format (FDM) which allows up to 112 stations per tape.

The data flow within the system is controlled by an operator who, with the help of computer-updated files, invokes the appropriate processor as the events pass through the system. The current processing status of all events is accounted for from the time of the request until the event has been either copied onto a digital archive tape or processing has been discontinued.

The events are detected initially either by manually scanning microfilm or by an independent online earthquake detection system which produces request cards for the first stage of the system. The processing consists of reading the request cards, creating the dub library tape, selecting the analog channels to be processed, digitizing and displaying those channels, interactively picking first arrivals and other seismic parameters, locating the hypocenters, and creating a digital archive tape.

Results

Processing continues to be done by various groups and individuals. The biggest users at this time are CALNET digitizing (McHugh), Oregon Network Processing (Rite), and SPRINT file generation (Pelton/Bakun). The focus of the CALNET digitizing has been changed. Only events of magnitude 2.5 or greater are digitized. In addition, all multicomponent stations of those events are digitized. Also, amplitudes are being measured in addition to the standard phase-picking.

Software development and maintenance continued at a modest level during the report period.

An extensive revision involved the replacement of EVCON12, EVDIG12, and DMUX2 with NPCON, NPDIG, and DMUX3. The main purpoe of this change is to allow the processing of events which have dubs from Network tapes D and E. Because of memory limitations, it was necessary to redesign the data structure, hence the necessity for rewriting the demultiplex routine. Another feature of NPCON is its ability to run unattended, being driven by a file of event ID's.

A new program (WSPRINT) was developed to write small ASCII files containing phase, station, and waveform data. These files, called SPRINT files contain pieces of the trace data extracted from the CALNET binary (-.TR) files. One use of the SPRINT files is to write them to a TAR tape, so that they can be utilized on the UNIX system, and hence on Bill Bakun's Tekronix 4051 smart terminal.

Another use is as input to a Spectral analysis program SPEKTRA which has been developed on the Eclipse.

Reports

Stevenson, P. R., 1981, Programs WSPRING and VIEW, a method for creating small ASCII waveform files on the Eclipse minicomputer: U.S. Geological Survey Open-File Report (in review).

Stevenson, P. R., 1981, Programs SPEKTRA and RPLOT, How to display seismic amplitude spectra and spectral ratios on the Eclipse: U.S. Geological Survey Open-File Report (in review).

McHugh, C., 1981, Earthquake processing on the Eclipse, a beginners manual: U.S. Geological Survey Open-File Report (in preparation).

Crustal Inhomogeneity in Seismically Active Areas

9930-02231

S. W. Stewart
Branch of Seismology
U.S. Geological Survey
345 Middlefield Road, MS-77
Menlo Park, California 94025
(415) 323-8111, x2525

Investigations

1. Development of an online, realtime earthquake waveform data acquisition system for the Central California Microearthquake Network has taken a new direction. The PDP 11/34 computer, and the recently delivered Tustin high-speed digitizing system, will continue to serve as the hardware components of the system. The software, however, will take full advantage of Carl Johnson's very extensive and successful development at Caltech, for the Southern California Seismic Network. This development follows directly from the strategy to acquire and distribute similar computer systems to certain universities and laboratories engaged in seismic network data acquisition and analysis, as envisioned and carried out by Pete Ward.

2. Final details of preparing the book, "Principles and Applications of Microearthquake Networks", by W. H. K. Lee and S. W. Stewart are continuing.

Results

1. In late November, 1980, Alex Bittenbinder of the University of Washington, and Carl Johnson from the U.S. Geological Survey Pasadena office, gave us a copy of an early version of their online earthquake detection and data acquisition system. We brought this up on our PDP 11/34 without any programming changes at all (Hurray for real compatibility!). Presently we are monitoring 61 seismic stations from the Parkfield region of the seismic network. Detected events are written out to magnetic tapes. There have, of course, been some hardware maintenance problems, and a software problem was corrected. This is just a preliminary system, whose operation is intended to get us conversant with all aspects of this mode of data acquisition. The detection algorithm works very well. The number of nonearthquake events detected and written out to magnetic tape is low enough to be tolerable, although exact numbers are not yet available.

Off-line, interactive processing of the data tapes is being done by Bob Dollar on the UNIX 11/70 system, using software developed by Steve Malone and associates at the University of Washington. Al Lindh is watching over the results of this processing.

2. The book, by Willie Lee and me, will be published as Supplement No. 2 to the Advances in Geophysics series. During this report period we have completed extensive revisions to the text, and have started to correct the page proofs.

Reports

None.

Crustal Deformation Observatory, Part B: Precision Geodesy

14-08-0001-18366

Arthur G. Sylvester
Department of Geological Sciences and
Marine Science Institute
University of California
Santa Barbara, California 93106
(805) 961-3156

Investigations

An L-shaped leveling array, 1168 m long, was established at Pinon Flat Geophysical Observatory to provide a means of geodetically monitoring tilt. The array is comprised of 31 permanent, steel rod benchmarks. Two 6-point dry tilt arrays were also established. The arrays were surveyed in October 1979, January, July and August 1980.

Results

Elevation changes as great as 2 mm for single benchmarks and for the line as a whole characterize the data for FY 1979-80. We have not observed these kinds of changes in any one of a number of lines established elsewhere in southern California since 1969. Thus we interpret the Pinon Flat data as due to benchmark instability, and also because the tilts that may otherwise be inferred from the data do not coincide with other kinds of strain data collected by other investigators at Pinon Flat.

Geodetic Modeling and Monitoring

9960-01488

Wayne Thatcher
Branch of Tectonophysics
U.S. Geological Survey
345 Middlefield Road, M/S 77
Menlo Park, California 94025
(415) 323-8111, Ext. 2120

Investigations

Analysis and interpretation of repeated geodetic survey measurements relevant to earthquake-related deformation processes operative at or near major plate boundaries. Principal recent activities have been:

1. Analysis and interpretation of co- and post-seismic deformation measurements relevant to the 1979 M_L 5.2 Homestead Valley, California earthquake sequence.

2. Modeling of effects due to asthenospheric readjustment following the great 1964 Alaska earthquake.

Results

1. An unusually dense network of coordinated precise geodetic measurements, including leveling, triangulation, trilateration, and gravity, were undertaken prior to and following the M_L 5.2 Homestead Valley, California earthquake sequence of 15 March 1979. The observations are modeled as dislocations in an elastic half-space; they provide evidence for time-dependent rupture with no more than one quarter of the total moment released seismically. During the first 1 1/2 years following a 3-hr, 4-shock sequence (M_L 4.5-5.2), the initial 5 x 6 km^2 (depth x length) slip surface yielded bilaterally along strike to 5 x 30 km^2, accompanied by the propagation of aftershocks. The seismic slip averaged 60 cm in the initial 5 x 6 km^2 region, with less than 2 cm of additional post-seismic slip. Rupture barriers at the ends of the seismic patch did not slip appreciably at any time and remained continuously aseismic. The geodetic observations suggest that ductile or viscous behavior in the upper lithosphere can be triggered by rather small earthquakes. (R. Stein and M. Lisowski).

2. The expected surface deformation effects due to asthenospheric flow following the great 1964 Alaska earthquake have been computed. The coseismic dislocation model of Hastie and Savage (1970) has been used to determine the faulting parameters in the lithosphere, and the computational schemes developed by Rundle (1978, 1981) were employed to determine the resulting time-dependent surface movements. It appears that the high tilt rates on Middleton Island observed by Prescott and Lisowski (1980) can be explained by this mechanism, although a rather short

relaxation times for the asthenospheric readjustment is required. The 5 microradian/yr down to the NW tilts during 1974-79 can only be matched in magnitude if the relaxation time τ is about 3 years or less ($\tau = 2\eta/\mu$, where η = asthenospheric viscosity, μ = average shear modulus of lithosphere and upper asthenosphere). This compares with values of 20 to 60 years determined from postseismic observations from Japan (Thatcher and Rundle, 1979; Thatcher et al, 1980). In principle, data from points further landward could test the plausibility of such a short asthenospheric relaxation time. However, scarcity of data, unmodeled complexities in the coseismic faulting, probable landward thickening of the elastic lithosphere, and complicating effects due to postearthquake buried slip (Brown et al, 1977) all conspire to frustrate the formulation of any stronger tests of the relaxation model (W. Thatcher and J. B. Rundle).

Reports

Dunbar, W. S., D. M. Boore, and W. Thatcher, 1980, Pre-, co-, and post-seismic strain changes associated with the 1952 M-7.2 Kern County, California, earthquake, Bull. Seismol. Soc. Amer., 80, 1893-1905.

Lisowski, M.,, and W. Thatcher, 1980, Geodetic determination of horizontal deformation associated with the Guatemala earthquake of February 4, 1976, Bull. Seismol. Soc. Amer., 71, in press.

Rundle, J. B., and W. Thatcher, 1980, Speculations on the nature of the southern California uplift, Bull. Seismol. Soc. Amer., 70, 1869-1886.

Stein, R. S., 1981, Discrimination of tectonic displacement from slope-dependent errors in geodetic leveling from southern California, Proceedings, Fourth Maurice Ewing Symposium on Earthquake Prediction, in press.

Stein, R. S. and W. Thatcher, 1981, Seismic and aseismic deformation associated with the 1952 Kern County, California, earthquake, and relationship to the Quaternary history of the White Wolf fault, J. Geophys. Res., 86, in press.

Thatcher, W., 1981, Crustal deformation studies and earthquake prediction research, Proceedings, Fourth Maurice Ewing Symposium on Earthquake Prediction, in press.

Thatcher, W., and T. Matsuda, 1981, Quaternary and modern crustal movements in the Tokai district, central Honshu, Japan, J. Geophys. Res., 86, in press.

Thatcher, W., T. Matsuda, T. Kato, and J. B. Rundle, 1980, Lithospheric loading by the 1896 Riku-u earthquake, northern Japan: Implications for plate flexure and asthenospheric rheology, J. Geophys. Res., 85, 6429-6435.

Seismicity and Earthquake Prediction Studies in Turkey

14-08-0001-19772

M. Nafi Toksöz
Department of Earth and Planetary Sciences
Massachusetts Institute of Technology
Cambridge, Massachusetts 02139
(617/253-6382)

Investigation

The program on seismicity and earthquake prediction studies in Turkey involves data acquisition analysis and related studies for the assessment of seismic hazards and for long range prediction of earthquakes along the North Anatolian fault zone. The North Anatolian fault zone is a major right-handed, strike-slip fault geologically very similar to the San Andreas.

Results

In this study we report on the earthquake migrations and time-dependent viscoelastic relaxation after strike-slip earthquakes. There has been a westward migration of large earthquakes along the North Anatolian fault zone after the 1939 earthquake. There is some evidence of an eastward migration as well.

The migration may be due to time-dependent viscoelastic stress "diffusion". This question was investigated theoretically using three-dimensional finite element models. The effects of lateral heterogeneities, finite fault and non-uniform fault slip are included. Models of a great earthquake and a medium size earthquake are constructed using a set of possible viscosity structures (Fig. 1). Deformation change after an earthquake is found to be sensitive to the viscosity structure located beneath the fault zone (see Fig. 2). The presence of low viscosity beneath the fault concentrates the horizontal displacement near the fault zone and completely changes the character of vertical deformation. Thus leveling, in addition to horizontal geodetic measurements after a strike-slip event, is important in determining the viscosity structure near fault zones. The shear stress in front of the fault tip increases significantly within several decades after the event for models with a shallow low viscosity zone beneath the fault. This accelerated stress accumulation is consistent with the observed phenomenon of earthquake migration along the North Anatolian fault zone.

Publications

Toksöz, M.N., A.F. Shakal and A.J. Michael, Space-time migration of earthquakes along the North Anatolian fault zone and seismic gaps, PAGEOPH, 117, 1258-1270, 1979.

Yang, M., and M.N. Toksöz, Time-dependent deformation and stress relaxation after strike-slip earthquakes, J. Geophys. Res., in press, 1981.

P1

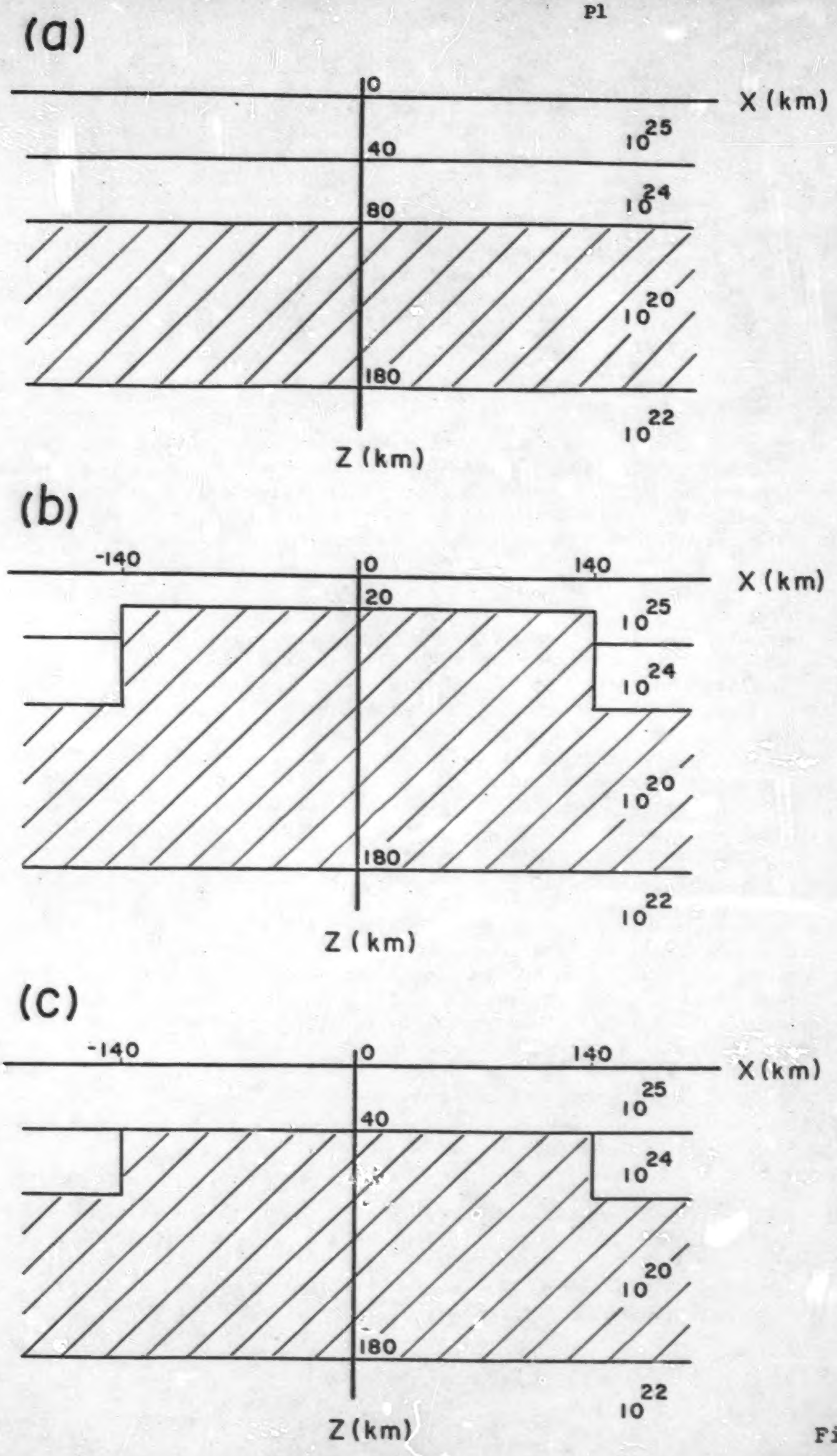
(a)
0
X (km)
10^{25}
40
10^{24}
80
10^{20}
180
10^{22}
Z (km)
(b)
-140
0
140
X (km)
20
10^{25}
10^{24}
10^{20}
180
10^{22}
Z (km)
(c)
-140
0
140
X (km)
10^{25}
40
10^{24}
10^{20}
180
10^{22}
Z (km)

Fig. 1

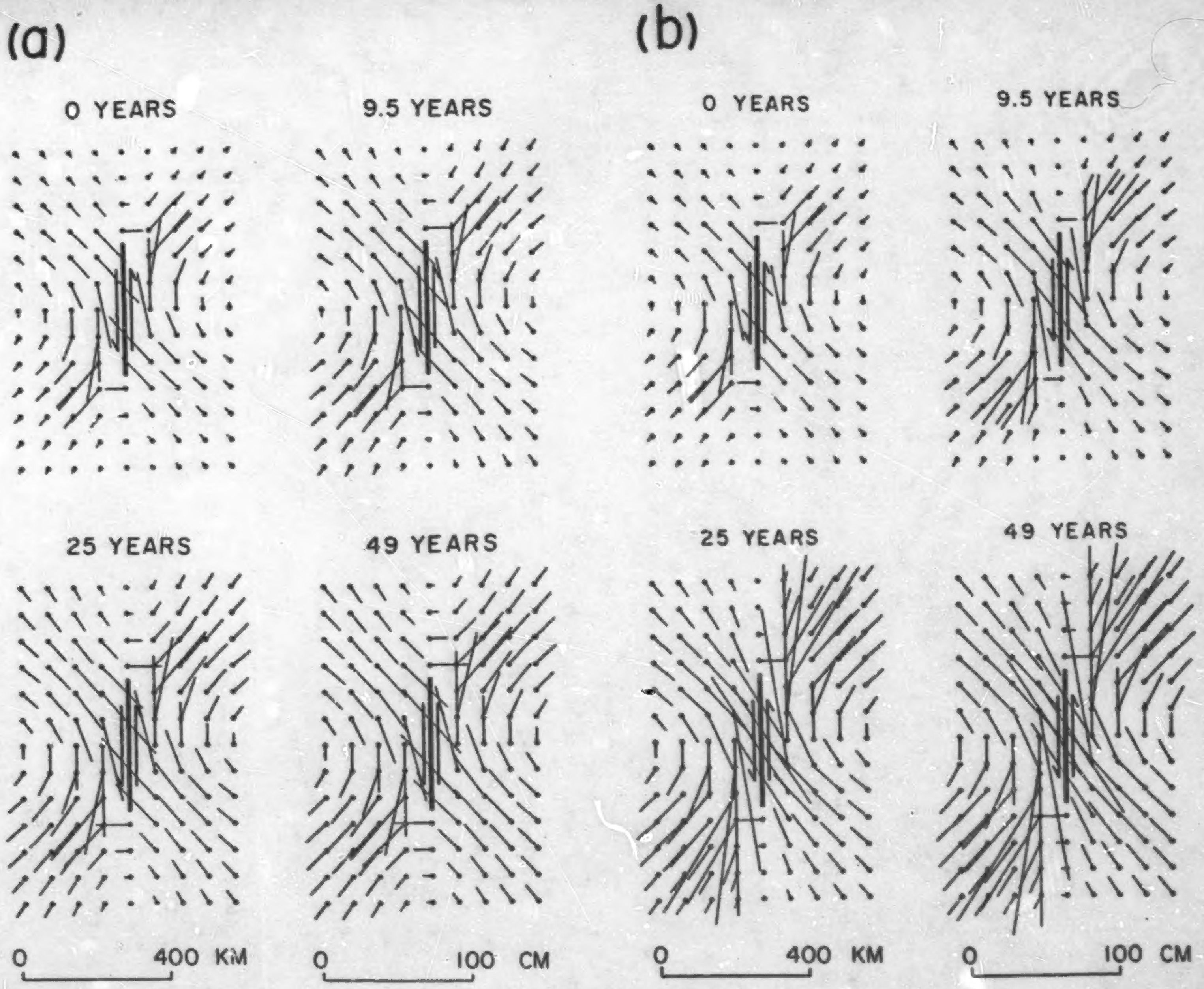
(a)
(b)
0 YEARS
9.5 YEARS
0 YEARS
9.5 YEARS
25 YEARS
49 YEARS
25 YEARS
49 YEARS
0 400 KM
0 100 CM
0 400 KM
0 100 CM

Fig. 2

Field Experiment Operations

9970-01170

John Van Schaack
Branch of Network Operations
U.S. Geological Survey
345 Middlefield Road - MS-77
Menlo Park, California 94025
(415) 323-8111, ext. 2584

Investigations

This project performs a broad range of management, maintenance, field operation, and record-keeping tasks in support of seismology and tectonophysics networks and field experiments. Seismic field systems that it maintains in a state of readings and deploys and operates in the field (in cooperation with user projects) include:

a. 5-day recorder portable seismic systems
b. Smoked paper-recorder portable seismic systems
c. Seismic refraction trucks
d. "Cassette" seismic refraction trucks
e. Portable digital event recorders

This project is responsible for obtaining the required permits from private landowners and public agencies for installation and operation of network sensors and for the conduct of a variety of field experiments including seismic refraction profiling, aftershock recording, teleseism P-delay studies, volcano monitoring, etc.

This project also has the responsiblity for managing all radio telemetry frequency authorizations for the Office of Earthquake Studies and its contractors.

Results

Network augmentation. Installation of about 40 stations in southern California is almost complete. This augmentation is the completion of the work started in 1980; delays have been due to phone line installation problems.

Seismic refraction. Profiles were shot, using the seismic cassette recorders, from Benicia to Mt. Hamilton to Salinas, California. Shots were also recorded near Palmdale, California.

Portable networks. Eleven 5-day recorders have been deployed for 3 months around San Luis Obispo, California. Five units were previously deployed near Parkfield, California. Eight 5-day recorders and 6 digital-event recorders were deployed in extreme northern California immediately after the Eureka, Calif. earthquake of November 10, 1980.

Tiltmeters. Modifications have been made to approximately half of the operating tiltmeter systems to improve the stability of the electronics. Stability has been improved 5 to 10 times on some systems. All systems show some improvement.

Data Processing Center Operations

9970-01499

John Van Schaack
Branch of Network Operations
U.S. Geological Survey
345 Middlefield Road - MS-77
Menlo Park, California 94025
(415) 323-8111, ex. 2584

Investigations

This project has general housekeeping, maintenance and management authority over the Earthquake Prediction Data Processing Center. Its specific responsibilities include

1. day-to-day operation and performance quality assurance of 5 network tape recorders,

2. day-to-day management, operation, maintenance, and performance quality assurance of 2 analog tape playback stations,

3. day-to-day management, operation, maintenance and performance quality assurance of the USGS telemetered seismic network event library tape-dubbing facility (for California, Alaska, Hawaii, Oregon, and Yellowstone National Park), and

4. projection of usage of critical supplies, replacement parts, etc., maintenance of accurate inventories of supplies and parts on hand, and reordering of these items on a schedule that insures uninterrupted operation of the Data Processing Center.

Results

Procedures and staff for fulfilling its assigned responsibilities have been developed, and the Data Processing Center is operating smoothly and serving a large variety of scientific user projects.

Adequate and Timely Data Processing

9930-02392

Peter Ward and Jim Herriot
Seismology Branch
U.S. Geological Survey
345 Middlefield Road - MS-77
Menlo Park, California 94025
(415) 323-8111, ext. 2838

Investigations

1. Operate PDP 11/70 for use by prediction branches.
2. Develop modular hypocenter program for locating earthquakes.
3. Develop general-purpose plotting programs for display of geophysical data.
4. Develop interactive language and database.
5. Improve general distribution of the UNIX Timesharing Operating System.

Results

1. The 11/70 has serviced an average of 15 people continuously all day and is providing more than $500K worth of computing time per year measured in Multics dollars.

2. A modular version of HYPO71 and HYPO79 has been developed in conjunction with Willie Lee and has been tested. Documention of HYPO81 is being written and an open-file report should be issued by fall 1981.

3. Geoplot has been extended to include output on the Printronix matrix printer and Calcomp plotter. An overlayed version including 20 map transformations is nearly complete.

4. Geolab and geobase are being merged into one well-integrated process.

5. Numerous improvements and extensions to UNIX have been developed or integrated from work done at U.C. Berkeley and a common distribution is planned by mid-1981 not only among USGS-supported sites but the general UNIX users community. Substantial improvements have been made to the manuals.

Cooperative Earthquake Prediction Research with Institute of Geophysics,State Seismological Bureau, People's Republic of China

14-08-0001-19141

Francis T. Wu
Professor of Geophysics
State University of New York
Binghamton, New York 13901

Ta-liang Teng
Professor of Geophysics
University of Southern California
Los Anageles, Ca 90007

Investigations

1. Studies on precursors of large Chinese earthquakes.
2. Earthquake prediction studies in Beijing-Tienjin-Tangshan area.

Results

1. Preliminary studies of some of the precursors of the 1976 Tangshan earthquake show that significant precursors in shortline geodetic levelling across faults to a distance of 200 km from the causative fault (figure 1) as well as in waterwell level (figure 2), electrical resistivity, etc can be seen. Such data, if processed in time to remove disturbances generated by changes in ambient conditions and displayed in suitable synoptic fashion, should be useful for mid-term to short term predictions.

2. Testing of data-transmission and receiving equipment in progress in the vicinity of Beijing-Tienjin-Tangshan. Seismic network expansion plan has been made.

Reports

Wu, F. T., and Dayu Han, Shortline deformation data before and after the Tangshan earthquake of July 29, 1976, submitted to JGR, March, 1981.

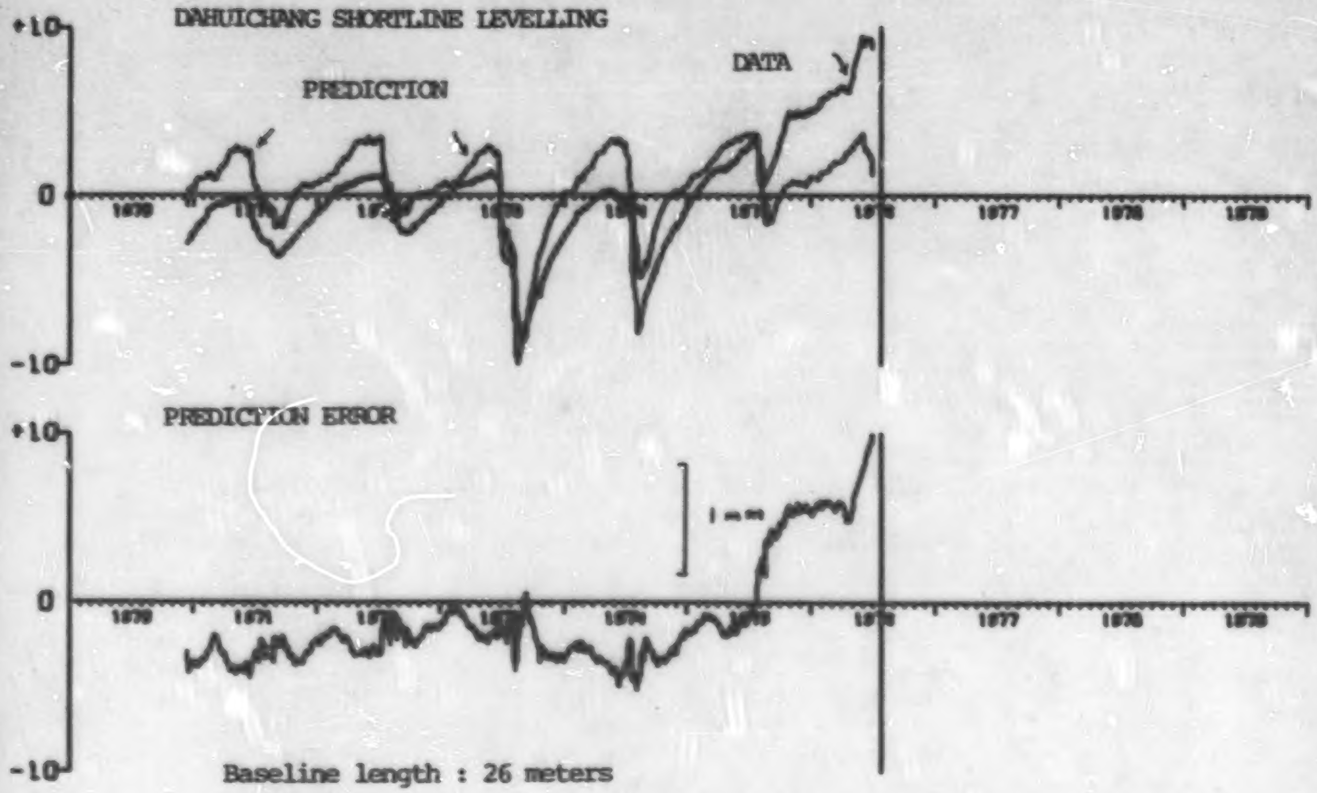

Figure 1. Shortline levelling across the Babaoshan fault west of Beijing(180 km to the west of the Tangshan epicenter). The raw data show clear effects of yearly rainfall and temperature variations. Using Wiener predictive filtering techniques, we have removed the effects and the "prediction errors" indicate the strain changes across the fault before and after the earthquake. The vertical line marks the time of the Tangshan mainshock. The "anomaly" disappeared gradually after the event.

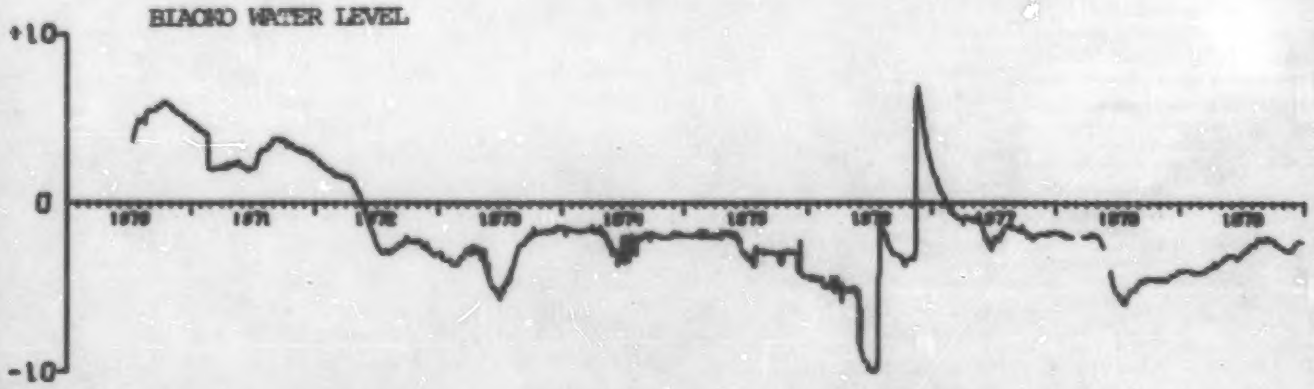

Figure 2. Biaoko waterwell (100 km southwest of Tangshan) before and after the Tangshan (July 27, 1976) and the Ninghe (November 15, 1976). The Ninhe event is closer to the station than the Tangshan event.

Precursory Seismicity Patterns

14-08-0001-18366

Max Wyss
CIRES and Dept. of Geological Sciences
University of Colorado, Boulder, CO 80309
(303) 492-8020

Investigations

The detection and quantitative definition of seismicity quiescence was the purpose of this project. The main data base was the teleseismic catalogue of world activity compiled by NOAA. In some studies this data set was supplemented by local catalogue data. To our disappointment we discovered that the NOAA file does not improve with time in resolution since 1963. Instead there are marked decreases in reporting of smaller events in 1968 and 1974. Nevertheless we were able to show that significant and unique episodes of quiescence existed before some earthquakes, while no such episodes were detectable before other main shocks using this data set.

Results

Consistency of Teleseismic Reporting Since 1963. Changes in the rate of occurrence of smaller events have been recognized in the rupture zones of upcoming large earthquakes in several post–earthquake and one pre–earthquake study. A data set in which a constant portion of the events in any magnitude band are consistently reported through time is crucial for the recognition of seismicity rate changes which are real (related to some process change in the earth). Such a data set is termed a homogeneous data set.

The consistency of reporting of earthquakes in the NOAA Hypocenter Data File (HDF) since 1963 is evaluated by examining the cumulative number of events reported as a function of time for the entire world in eight magnitude bands. It is assumed that the rate of occurrence of events in the entire world is roughly constant on the time scale examined here because of the large size of the world–wide earthquake production system.

The rate of reporting of events with magnitudes above $m_b = 4.5$ has been constant or increasing since 1963. Significant decreases in the number of events reported per month in the magnitude bands below $m_b = 4.5$ occurred during 1968 and 1976. These decreases are interpreted as indications of decreases in detection capability because they occur at times of constant rates of reporting of larger events, and because similar decreases have been described in the teleseismic data reported by the International Seismological Center.

During 1968 the detection decreased in the United States, Central and South America and portions of the South Pacific. This decrease is probably due to the closure of the VELA arrays, BMO, TFO, CPO, UBO, and WMO. During 1976 the detection decreased in most of the seismically active regions of the western hemisphere, as well as in the region between Kamchatka and Guam. The cause of this detection decrease is unclear.

These detection decreases seriously affect the amount of homogeneous background period available for the study of teleseismic seismicity rate changes. If events below the minimum magnitude of homogeneity are eliminated from the teleseismic data sets, the resulting small numbers of events render many regions unsuitable for study. Many authors have reported seismicity rate decreases as possible precursors to great earthquakes. Few of these studies have considered detection decreases as possible explanations for the results. This analysis indicates that such considerations can not be avoided in studies of teleseismic data.

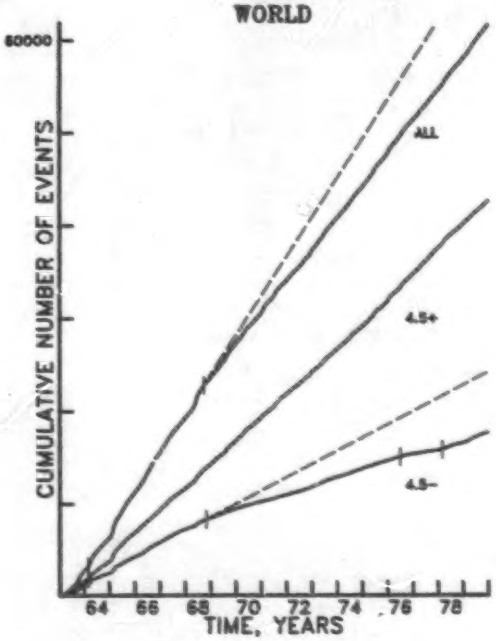

Figure 1: Cumulative number of events reported in the NOAA HDF for three magnitude bands. Changes recognized at the 99% confidence level are marked by vertical bars. ALL events are all events with m_b's assigned. Note the decrease in this set during 1968, the dashed line shows the curve expected on the basis of the 1964 to 1968 rate. Because the entire world is considered, this decrease must be due to changes in detection and reporting. Events with $m_b \geq 4.5$ show a constant rate of listing since 1963. This is interpreted as an indication of constant occurrence, detection and reporting rates for these relatively large events. the curve for ALL events.

Precursory Seismicity Patterns: Stalking the Mature Seismic Gap. Mature seismic gaps are defined here as gaps in which a possible precursor to a future event has been identified. The seismic potential of these seismic gaps is enhanced relative to immature seismic gaps. The seismic gap hypothesis by itself provides an excellent means of narrowing spatial limits along plate boundaries within which the great earthquakes of the next several decades are expected. To narrow the temporal limits on these forecast events, identified gaps must be monitored for signs of maturity. Decreased seismicity rates (number of events reported/unit time) have been reported before over fifty large earthquakes. Seismicity rates measured teleseismically are tested as a possible indicator of maturity by examining data from the NOAA HDF in the regions of eleven recent large events. These events were chosen as test cases because they occurred in previously recognized seismic gaps.

Many previous seismicity studies lack quantitative evaluation of patterns or changes of patterns which are proposed as precursors. This makes many of the results unconvincing. In this work seismicity data is quantified by studying seismicity rates, the number of events per month. Changes in rates are evaluated using the normal deviate (z) test for a difference between two means. Several techniques for appling this test to seismicity data are proposed. These techniques offer various approaches to quantitatively defining seismicity rate changes and evaluating their temporal and spatial uniqueness.

Two of the eleven events examined (Sitka, 1972 and St. Elias,1979) occurred in regions for which the teleseismic seismicity was too sparse to allow study of seismicity rates. Rates preceding two events in the Hokkaido corner, the South Kuriles 1969 and Nemuro–oki 1973 earthquakes, could not be evaluated because of the complex seismicity of the region. Of the remaining seven events, the Tokachi–oki 1968, Colima 1973, and the Oaxaca 1978 earthquakes were preceded by temporally and spatially unique seismic quiescence. The Kamchatka 1971 event was preceded by a precursory cluster of events. The Lima 1974 and Solomon Islands 1978 events were preceded by clusters which may reflect similar phenomena but neither case was as clear as the Kamchatka 1971 case. Only the Guerrero 1979 event was not preceded by a recognizable seismicity anomaly.

The multiple asperity model for earthquake precursors predicts that two types of precursors will be observed in upcoming rupture zones. High–stress precursors (dilatancy related velocity anomalies and increased seismicity) occur in locked portions of the upcoming rupture (asperities). Seismic quiescence occurs in regions of the rupture zone which experience precursory displacement and decreased stresses. The ratio between locked and unlocked areas of the future rupture (Rl) may be important in determining what type of seismicity precursors will occur. Possible differences in Rl for different ruptures offers a speculative explanation for the occurrence of different types of precursory anomalies.

Seismic Hazard in the Hellenic Island Arc. The seismicity of the Hellenic arc was studied as a function of space and time by two methods. First data on large and great historic earthquakes were reinterpreted with the purpose of identifying seismic gaps along this plate boundary. We found that the 8 great and 3 large earthquakes which occurred along the Hellenic arc between 1805 and 1926 can be interpreted as shallow sources along the plate boundary. Based on macroseismic data we propose approximate locations and size of these earthquakes. Individual rupture lengths of the largest events were approximately 100 to 150 km. It appears that the entire Hellenic plate boundary can be considered to be a seismic gap of class 1,2, and 3 depending on the segment. Second a systematic analysis of the shallow seismicity (< 100 km) showed that the rate decreased by about 80% in the western third and portions of the eastern third of the arc. These anomalies started in 1962 and 1966 respectively, they lasted to the present, and they can be interpreted as earthquake precursors. Combining the seismic gap and the seismicity rate data we suggest that ruptures of about 120 ± 40 km lengths ($M = 7\ 3/4 \pm 1/2$) may be expected to occur along the Hellenic plate boundary near 22.5 to 23.5° E and 26.5 to 27.5° E between now (1980) and 1990. Along the other segments of the Hellenic arc we were not able to define seismicity anomalies. Nevertheless, based on estimates of the stored strain derived from the approximate slip-rate one may conclude that large earthquakes may be expected there also. At the present stage of rudimentary understanding of earthquake preparatory processes, predictions like the above may be changed or rendered obsolete by new discoveries which may show that assumptions or hypotheses used may not be valid.

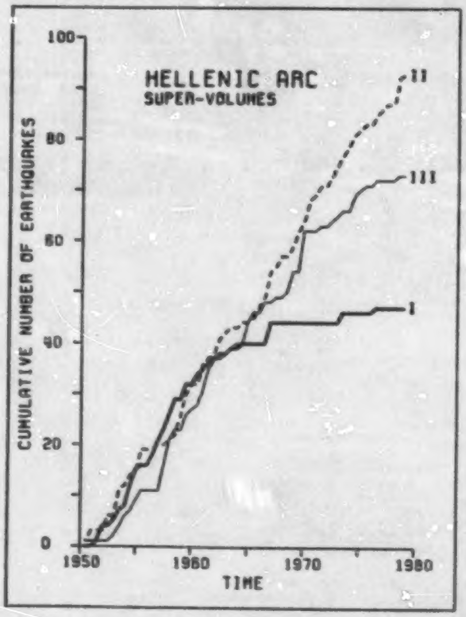

Figure 2: Seismic quiescence in the western third of the Hellenic island arc (curve I) existed since about 1962 and contrasts sparply with the seismicity rate in the central (curve II) and eastern (curve III) segments.

Articles Prepared

The following articles were produced with support of this contract:

1. Seismic quiescence in the Western Hellenic arc suggests large earthquakes are in preparation, *Nature*, 289, 785-787, 1981.
2. Earthquake hazard in the Hellenic arc, Ewing Symposium on Earthquake Prediction, Proceedings, May, 1981.
3. Precursory seismicity patterns: Stalking the mature seismic gap, Ewing Symposium on Earthquake Prediction, Proceedings, May, 1981.

Parkfield Prediction Experiment

9930-02098

Allan Lindh, John Estrem, Jean Olsen,
Bob Dollar, Tricia Mutch, Sandi Ball
Branch of Seismology
U.S. Geological Survey
345 Middlefield Road - MS-77
Menlo Park, California 94025
(415) 323-8111, ext. 2042

Investigations

Seismic data are being analyzed in conjunction with geodetic observation to develop the ability to predict the next magnitude 5.5 Parkfield earthquake. Our immediate goal is to use this information to build a strong working hypothesis against which slip and stress distribution along this segment of the San Andreas can be predicted and measured.

Results

We have maintained an up to date record of all Parkfield earthquakes. Seismicity patterns continue to support our geological and geophysical models of the Parkfield region, that the 1966 Parkfield earthquake ($M \sim 5.5$) was controlled by two physical discontinuities along the fault: a slight ($\sim 5°$) bend in the fault plane to the north of Parkfield (point of initiation) and a 1-km offset in the fault plane to the south (point of termination).

Attempts are being made to automate the earthquake selection and location process by sending the telemetered seismic signals directly into a computer for analysis.

2. An extensive medium-range geodetic network ($\sim$ 300 sq km) has been installed across the San Andreas fault in the Parkfield region. Being the transition zone between the "freely" creeping section of the fault to the north and the stuck portion to the south, we expect to see a definite pattern of slip distribution and consequently strain accumulation.

3. We have been experimenting with a new compact, easily transportable laser distance meter (Hewlett-Packard 3850A) for making regular trilateration surveys with relatively high precision and simplicity. This would allow greater possibility for repeating surveys, as well as reduce the time interval for seeing any real sip ('strain') at depth along the fault.

3. We plan to eventually connect the laser distance meter to a small field computer. This would allow possibly hundreds of length measurements to be taken per minute, potentially increasing the precision further.

4. The several kms of level lines installed last summer are being remeasured. This data in conjunction with lateral slip data should present a fairly complete 3 dimensional strain accumulation pattern.

Reports

Lindh, A., Motooka, C., Ball, S., and Dollar, B., 1980, Current seismicity of the central California coastal region from Point Muchon to Point Piedras Blancas: A preliminary report: U.S. Geological Survey Open-File Report 80-44, 25 p.

Red River Fault Study, Yunnan Province, China

Contract No. 14-08-0001-19271

Clarence R. Allen, Alan R. Gillespie, and Kerry E. Sieh
Division of Geological and Planetary Sciences
California Institute of Technology, Pasadena 91125
(213-356-6904)

Investigations

This study is being carried out under the Protocol between the State Seismological Bureau of the People's Republic of China and the National Science Foundation and the U. S. Geological Survey of USA for scientific and technical cooperation in earthquake studies. The principal Chinese investigators include Zhang Buchun of the State Seismological Bureau and Han Yuan and Zhu Chengnan of the Bureau of Seismology of Yunnan Province.

Results

The principal investigators spent six weeks in China, from 10 February to 23 March 1981, pursuing field work along the Red River fault zone together with Chinese colleagues. In January 1981, five Chinese geologists, including three who subsequently joined us in Yunnan, spent one month in a counterpart visit to the United States, and this contract also supported part of their expenses here.

Our field work in China was concentrated along the principal linear segment of the Red River fault from about 50 kilometers north of the Viet Nam border north to Xiaguan, although limited reconnaissance was also carried out along branches of the fault system north to the Jinsha (Yangtze) River. We stayed for varying periods in county hostelries and rural commune headquarters in Jianshui, Honghe, Yuanjiang, Mosha, Gasha, Xiaguan, Lijiang, and Chuxiong.

The puzzling aspect of the Red River fault that had led to our original research proposal was the fact that, although it is one of the most spectacular regional faults of China as viewed on satellite images, no large historic earthquakes are known from the principal segment of the fault (south of Midu). Thus, our objective was to determine its degree of activity and seismic hazard, if any. There had also been considerable debate concerning strike-slip vs. vertical displacements. As a result of the joint study, we all now agree that there is abundant evidence of Neogene and probably Quaternary horizontal displacements, and many of us argue that this movement has continued well into Holocene time as well. It also turned out that the fault which is so obvious on satellite images (bounding the Ailaoshan metamorphic block) is not the prinicipal active fault in many areas; another previously unmapped parallel fault lies within the Neogene basin which borders the Ailaoshan on the northeast.

Exposures are surprisingly good, and this plus the availability of excellent aerial photographs and topographic maps permitted accurate delineation of the fault traces. There are numerous localities of impressive fault gouge and horizontal slickensides, and everywhere that we saw major branches of the fault, they were near-vertical. Drainages have been consistently right-laterally offset about 5 km subsequent to the time of the most recent river incision -- presumably in late Neogene or early Quaternary time -- although the 5-km offset is in some places distributed between 2 branches of the fault. Numerous abandoned channels can be neatly fitted to their former headwaters. The smallest offsets are on the order of several meters, which some of us feel must represent late Holocene displacement. Shutter ridges and scarps are abundant, although there is a marked absence of closed depressions. Our tentative feeling is that the Red River fault has a significantly lesser degree of activity than that of the San Andreas, although direct comparisons are difficult because of climatic differences, as well as the fact that major incision and erosion have characterized the late Quaternary history of the Red River. We found no evidence pertaining to the total displacement on the fault, nor were we really looking for such, inasmuch as we concentrated our attention on young deposits rather than on the older rocks.

North of Midu and Xiaguan, the Red River faults splits into a number of branches of more northerly trend and predominantly normal displacement. Some of the resulting scarps are truly spectacular, such as the 2000-meter-high mountain front just north of Xiaguan itself. Alluvial gravels and fan surfaces are clearly broken in some places. Prominent glacial moraines of at least two stages on the slopes of the 5600-meter peak near Lijiang may be faulted. Field studies of active normal faults in this region appear very promising indeed.

A joint manuscript of our field studies of the Red River fault is in preparation.

Earthquake and Seismicity Research Using SCARLET and CEDAR

Contract No. 14-08-0001-19270

Clarence R. Allen
Donald V. Helmberger
Hiroo Kanamori
Karen C. McNally

Seismological Laboratory, 252-21
California Institute of Technology
Pasadena, California 91125

Investigations

Research performed under this contract to date has included three major areas of investigation:

1. A comparative study of waveform, frequency content, and first motion for preshocks and aftershocks of the October 15, 1979 M_L 6.6 Imperial Valley earthquake.

2. Analysis of aftershocks of the August 13, 1978 M_L 5.1 Santa Barbara earthquake.

3. Determination of P_n velocity as a function of azimuth in the central Transverse Ranges and in the eastern Mojave Desert.

Results

1. Preliminary results of our Imperial Valley work suggest that waveforms of small earthquakes may be a more sensitive indicator of stress conditions within the crust than spectra or first motion data. We examined seismograms of eight preshocks and five aftershocks (M_L 2.0-2.8) from a 4 1/2 by 1 1/2 km area near the epicenter of the mainshock. These events cover the time period Aug., 1977 to May, 1980. The study area was chosen to include the only three events to occur within 15 km of the impending mainshock epicenter during the 3 1/2 months of relative quiescence which preceded the mainshock (Johnson and Hutton, 1979). The preshocks exhibit remarkable similarity in waveform, whereas the aftershocks show much more variability from event to event. This observation is illustrated in Fig. 1, which shows at three different stations the maximum correlation between the seismogram of an event and that of the previous event, plotted as a function of time. Although the clear change at the time of the mainshock is encouraging, the physical interpretation of these results and their significance for earthquake prediction depend on the longer-term behavior of the function plotted in the figure. Frequency content of P, pP (sP?), S, and the entire record was studied for the same data set using bandpass filtering techniques. No systematic temporal changes in frequency content were

found. P-wave first motions were not sufficient to constrain the focal mechanisms, but remained constant with time throughout the preshock-mainshock-aftershock sequence.

2. A study of the 1978 M_L 5.1 Santa Barbara earthquake and its aftershocks has revealed important details about the rupture process. During the first 20 minutes after the mainshock, all of the aftershocks were located in a cluster 7 km WNW of the mainshock epicenter. During the next 24 hours the aftershock zone grew to 11 km in the WNW direction and 4 km in the N-S direction. Eventually the zone extended to 12 by 6 km. This temporal-spatial development may indicate that the initial rupture propagated 7 km unilaterally to the WNW and that the initial rupture plane was considerably smaller than the eventual aftershock zone. Theoretical stress drops for this smaller area may be hundreds of bars, and the theoretical displacements would be about 1 m. In cross-section, the aftershock hypocenters outline a nearly horizontal plane (dipping 15° or less) at 13 km depth. Focal mechanisms for the mainshock and 46 aftershocks indicate compression in a generally N-S direction. The preferred fault plane for the mainshock strikes N 80° W and dips 26° NNE, indicating north-over-south thrusting with a component of left-lateral movement. For most of the aftershocks, the north-dipping nodal plane dips 25° or more which is significantly steeper than the plane delineated by the hypocenters themselves. Hence, the aftershocks and the initial mainshock rupture might represent movement on a complex series of imbricate thrust faults that flatten northward into a nearly horizontal plane of primary slip.

3. Strong azimuthal variation of P_n velocity in the central Transverse Ranges can be explained by a combination of moho dip (2° to N 40° W) and a three to four percent anisotropy of subcrustal material, with the fast axis oriented N 50° W. The isotropic velocity of P_n is 7.8 km/sec. In contrast, a higher (8.1 km/sec) P_n velocity is found in the Mojave block, with no indication of anisotropy. These observations are consistent with a subcrustal model of the Pacific-North America plate boundary where ductile flow is characterized by simple shear in a vertical plane with strike parallel to the direction of relative plate motion.

Reports

Pechmann, J. C., J. B. Minster and H. Kanamori, Search for Seismological Precursors to the 1979 Imperial Valley Earthquake, EOS 61, 1053 (abstract).

Corbett, E. J., and C. E. Johnson, Evidence for Mid-Crustal Horizontal Shearing in the Western Transverse Ranges, California, EOS 61, 1042 (abstract).

Vetter, U. and J. B. Minster. P_n Velocity Anisotropy in Southern California, EOS 61, 1025 (abstract).

Vetter, U., and J. B. Minster. P_n Velocity Anisotropy in Southern California. Submitted to Bull. Seism. Soc. Am.

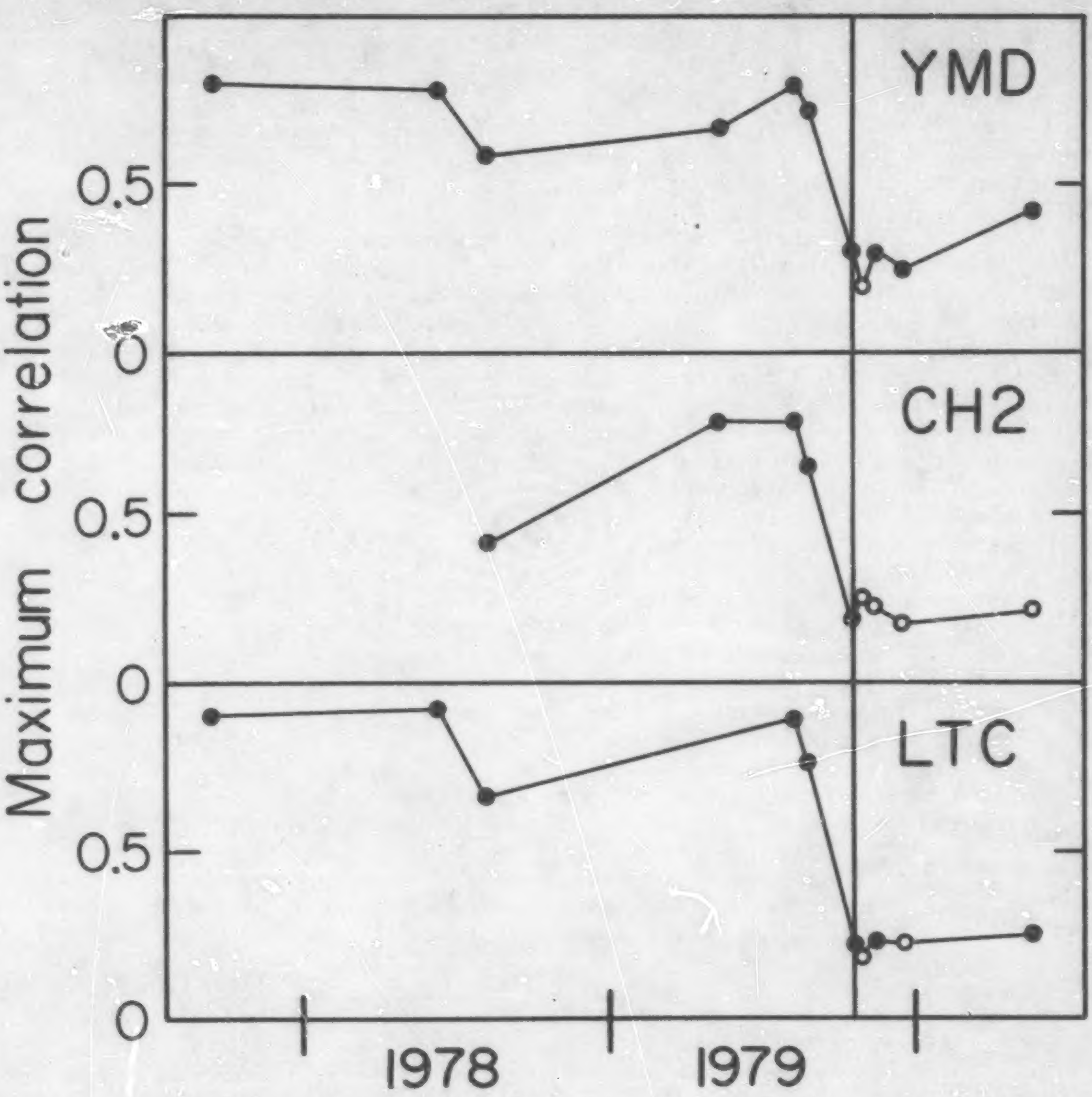

Fig. 1. Maximum correlation between the seismogram of an event and that of the previous $M_L \geq 2.0$ event in a small (4 1/2 by 1 1/2 km) source area near the epicenter of the 1979 Imperial Valley earthquake. The vertical bar marks the time of the mainshock. Approximate station distances and azimuths are: YMD, 68 km, 95°; CH2, 76 km, 355°; LTC, 99 km, 11°. Solid circles are correlation coefficients corresponding to time lags where the phases are properly aligned. Open circles correspond to lags where the phases are not properly aligned, and hence represent upper limits to the maximum correlation in the sense that these numbers would decrease if the range of allowable lags (± 7.5 sec) was decreased. Thirty seconds of record was used in the cross-correlation calculations. The instrument response was deconvolved in the passband 1-16 Hz. before performing this analysis.

P2

REAL TIME MONITORING OF RADON AS AN EARTHQUAKE PRECURSOR IN ICELAND

Contract #14-08-0001-17726

W.S. Broecker, J.G. Goddard and Egill Hauksson

Lamont-Doherty Geological Observatory
Palisades, New York 10964

We report radon data collected during 1980 from geothermal wells in Iceland. Discrete radon samples are being collected weekly from nine stations in the Southern Iceland Seismic Zone (SISZ) and two stations in the Northern Iceland-Tjornes Fracture Zone (TFZ) to determine the potential for earthquake prediction. We also monitor volume ratio of gas to water, wellhead temperature and chloride content of the water to enable us to constrain the possible mechanism involved in radon anomalies.

We report a possible strain event in April that caused both changes in radon emission and a small earthquake swarm. An eruption at Hekla in August was not preceded by any distinctive radon anomalies. Swarm activity occurring close to Selfoss and Oxnalaekur appeared to be associated with possible low amplitude (<30%) precursory radon anomalies in April and October.

We present the first data from our ALOKA-continuous radon meter at Fludir. The data show no anomalies and no earthquakes have been reported.

Chloride and radon data from Bakki and Dalvik indicate that an inverse correlation exists between them at longer periods. Therefore, we feel that in the case of a large earthquake the chloride data could tell us something about the mechanism of radon anomalies.

During 1980 three major eruptions and two subsurface migration events occurred at Krafla, north Iceland. All of these events were followed by an increase in radon emission except for the event in July when no data were collected.

INVESTIGATION OF RADON ON HELIUM AS POSSIBLE FLUID-PHASE PRECURSORS TO EARTHQUAKES

14-08-0001-19227

Y. Chung, H. Craig, J. E. Lupton
S. Damasceno and R. Poreda

Scripps Institution of Oceanography
University of California, San Diego
La Jolla, California

(714) 452-3260

This report includes new data on radon and helium in thermal wells and springs along our Southern California network, for the period October, 1980, to March, 1981. Other dissolved gases (N_2, Ar, CH_4) data have not been completely updated. Graphs of data measured from currently active sites since 1975 are included as appendices.

Two sites, Arrowhead Hot Springs and Hot Mineral Well, were of special interest during 1979 and 1980. Arrowhead Hot Springs showed a large increase in radon and helium (plus all other gases) in early 1979, prior to the Big Bear earthquakes (M=4.8). The observed increases represent an increase in the "deep" component of gases in a two-component mixture with atmospheric gases dissolving into the exposed hot-spring surface water. The radon and helium levels at Arrowhead have returned to normal baseline levels since early 1980, a year after the initial anomalies were observed.

We observed two "valleys" in conductivity in early 1978 and early 1980 at Arrowhead, but these valleys were not correlated with radon or any other dissolved gases. Chloride measurements were made recently at Arrowhead in order to check the conductivity data. It is found that chloride mimics conductivity very closely, showing identical valleys. Conductivity is linearly correlated with chloride with a slope of 16.7 μmho/ppm and an intercept of 266 μmho at zero chloride. It seems that these valleys might have been caused by dilution of rain waters from rainy seasons which appeared to be heavier than normal during 1978 and 1980.

At the south end of the San Andreas, in the Salton Sea geothermal area, Hot Mineral Well and Bashford's Baths Well, two 60°C hot wells in continual use, both showed 37% increases in radon concentration relative to previous baselines, beginning in February, 1980. These increases were not accompanied by any increases of helium, nitrogen or argon. At Hot Mineral Well both radon and helium showed a significant drop in March: radon seems to indicate a return to normal baseline; helium reaches its minimum. At Bashford's Bath Well, a "valley" of radon in September, 1980 was also observed in helium.

Frink Springs has undergone a steady increase in helium concentration since 1975, approximately 5% per year over a six-year period. This 30% increase in helium is not matched by increases in radon, nitrogen, or argon. Nor has there been any change in the He^3/He^4 isotopic ratio during this time. A significant component of mantle helium appears to be present, since the He^3/He^4 ratio is twice the atmospheric ratio.

We have finalized the stable isotopes (D/H, O^{18}/O^{16}), radium-226 and lead-210 data which are included in this report. [illegible] paper discussing the spatial variations of radium, radon and their activity ratio, has been completed and accepted for publication in the Geophysical Research Letters.

Joint work with the Peking SSB is continuing. Two Chinese scientists visited our laboratory for one month during December and January to study laboratory and field collection techniques. A program for a very extensive study of crustal fluids throughout China is being developed as a joint long-term study involving helium, radon, other gases, stable isotopes, and chemistry, in a variety of tectonic regimes where significant earthquake hazards are present.

P2

Continuous Gravity Measurements in the Region of the Palmdale Uplift

14-08-0001-18353

John M. Goodkind
Department of Physics
University of California, San Diego
La Jolla, California 92093
(714) 452-3666

Investigations

In late 1978 a superconducting gravimeter was installed near Lytle Creek, California (34.23°N, 117.48°W). The site is located near the intersection of the San Andreas and San Jacinto faults, about 50 Km southeast of Palmdale. Operation was ended and the instrument removed September 1980. All of the useable gravity record has been analyzed.

Results

The analysis of the data included subtraction of the theoretical tide, compensation for gravity changes caused by variations in the local barometric pressure, and digital low pass filtering. The result is the upper curve of Figure 1. Segments of data which were severely disturbed by rainfall induced tilting of the pier have been deleted.

Although this tilting resulted in large apparent gravity changes during rainy periods, the true gravity change between any two points in time could be determined by readjusting the tilt to the local vertical at those two times. The effect of slowly varying tilt is also removed in this manner. The instrument at Lytle Creek was releveled at intervals and the lower curve of Figure 1 (displaced for clarity) is a linear interpolation of the data between those times when the tilt was readjusted. Since the tilt as a function of time between these points is unknown, all of the meaningful information about slow variations of gravity at Lytle Creek is contained in the interpolated curve. The curve shows a 124 μgal decrease in gravity over the 647 days of operation. The decrease is monotonic, but the slope is larger at the center of the record than at the ends. A local earthquake of magnitude 4.1 occurred in October 1979 during the period of largest slope.

Since this information is obtained from a single instrument, we do not have independent proof that the change of gravity was real. However, we have operated seven of these instruments in the field, and during the past 9 months we have been making extensive tests with simultaneous operation of instruments in the laboratory. None of the instruments at any other location has revealed a steady decrease in gravity such as this. No instrumental mechanism that we have examined could lead to drift such as shown in Figure 1.

Local gravity surveys by Fett and Jachens in this area during the same time period do not reveal a change of gravity at Lytle Creek with respect to other stations in the San Gabriel Mountains or within 2° East-West and 1° North-South of Lytle Creek. However, measurements over a greater distance by Whitcomb, et al claim to show a gravity decrease of about 50 μgal of Lytle Creek with respect to Goldstone. All of this data would be consistent if it resulted from a regional phenomenon greater than 300 Km in extent. Other measurements of surface strain, by space techniques as well as by surface geodimeters, and of radon in well water also provide evidence of regional phenomena during 1979, but there is no model at present to relate these various observations.

With all information presently available to us we are unable to attribute our results to anything other than a true variation in gravity. Thus, pending further results at other locations and additional results from laboratory tests, we conclude that during the period of our observations there occurred a large regional variation in gravity.

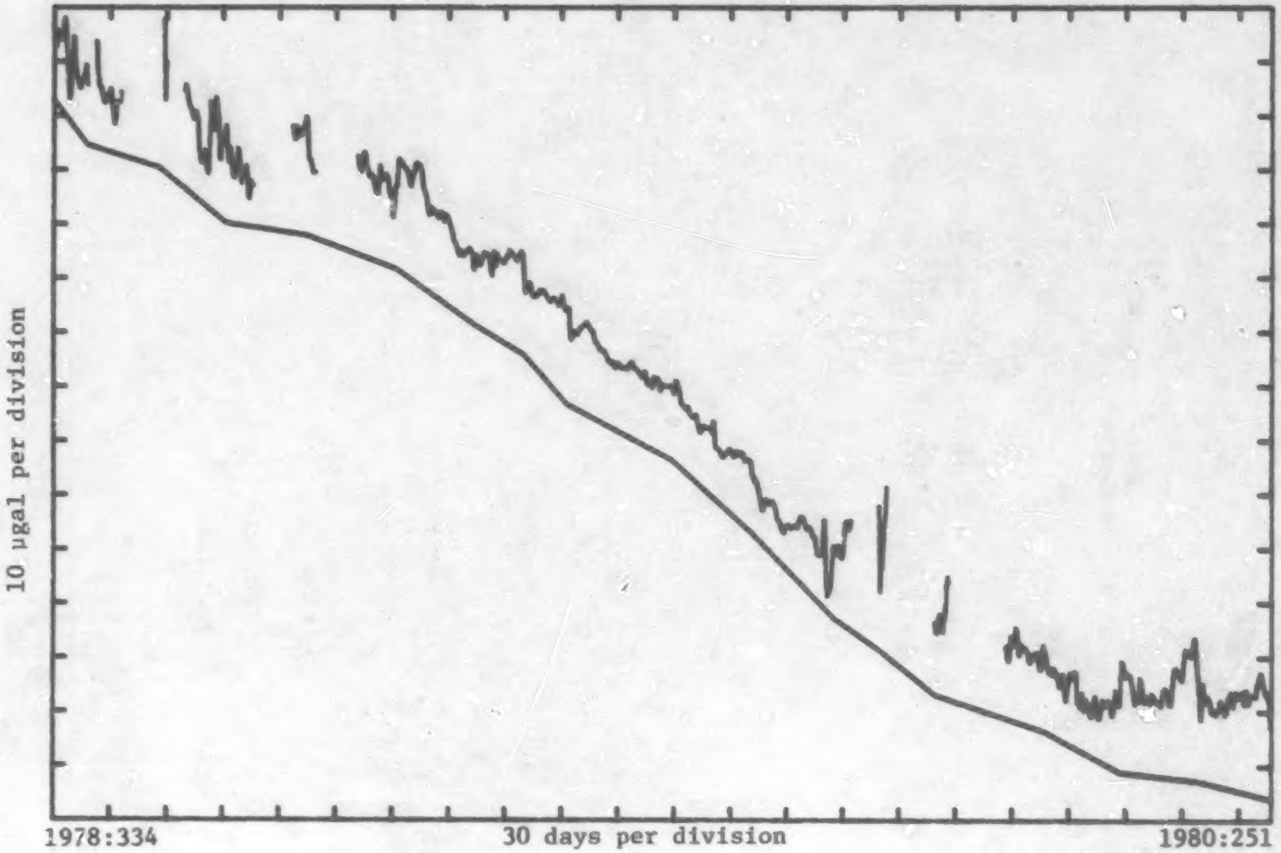

Figure 1. Gravity residual at Lytle Creek.

Support of the Southern California
Geophysical Data and Analysis Center

14-08-0001-19267

David G. Harkrider
Seismological Laboratory, 252-21
California Institute of Technology
Pasadena, California 91125
(213)356-6910

This report covers the six-month period from October 1, 1981 to March 31, 1981.

Goals

1. To support the data collection and processing activities of the CEDAR (Caltech Earthquake Detection And Recording) system and CROSS (Caltech Remote Observatory Support System).

Results

1. CEDAR

CEDAR operations was originally developed and supported by this contract and its predecessors (contracts # 14-08-0001-16629,17642, 18330), and is now an element of the joint USGS-Caltech SCARLET system (Southern California Array for Research on Local Earthquakes and Teleseisms). As such its product is a component of the results produced by the contract "Southern California Seismic Arrays", contract # 14-08-0001-19268. The result of this effort is the recording and processing of earthquake data effecting a digitized data base of seismic events stored on "Archive" 800 BPI magnetic tapes.

2. CROSS

This contract supplies continuing operational support for CROSS developed under the predecessor contracts (given above). During this reporting period nine data logging (TIM) units have been on site. They are as follows:

SITE LOCATION	TYPE of MEASUREMENTS	PRINCIPAL INVESTIGATOR
Anza	water well	Lamar/Merifield
Caltech campus	tilt	T. Ahrens
Hollister	tellurics	T.A. Madden
Kresge Lab.	tilt,gravimeter	Test site
Lake Hughes	tilt	L. Teng, T. Ahrens
Palmdale	tellurics	T.A. Madden
Palmdale	water well,baro. pressure	Lamar/Merifield
Riverside	Radon	L. Teng
Valyermo	water well	Lamar/Merifield

Note: Some sites listed in previous reports have been removed from service by the P.I.'s for operational reasons.

The data at these Southern California sites is collected once a day via the telephone telemetry polling procedure and is being accumulated as a data base on the Caltech Seismo. Lab. PRIME computing system. The data is available externally via a modem port on the computer system but the current method of data delivery for non-Caltech investigators is by use of magnetic tape.

Low Frequency Data Network

9960-01189

J. Herriot, S. Silverman, J. York
Tectonophysics Branch
U.S. Geological Survey
Menlo Park, California 94025
415/323-8111, Ext. 2932

Investigations

1. Continued collection, analysis, and interpretation of tilt, strain, magnetic, telluric, and other data within the San Andreas fault system and other areas for the purpose of understanding and anticipating crustal deformation and failure.

2. Development and enhancement of innovative computer controlled monitoring and telemetry systems.

3. Further development of interactive research tools.

Results

1. Data from low frequency instruments in both southern and central California have been collected and archived using the Low Frequency Data System. In the last six months six million measurements from 230 channels have been received and subsequently transmitted on the OES 11/70 UNIX computer.

2. The data from the Network have been made available to investigators in real time. Data only minutes old can be plotted. Events such as creep events can be monitored while they are still in progress.

3. The working prediction group of the Branch has made extensive use of the timely plots which are produced routinely by the System.

4. A new algorithm for removing non-geophysical signals from the data has been developed. Data can be "cleaned" removing telemetry noise and offsets due to field adjustments quickly and efficiently on the 11/70. Preliminary results indicate approximately 98 percent effectiveness.

5. Historical data is being processed using this new algorithm in order to produce near-error-free daily records of each of the tilt and strain instruments for the past several years.

6. Historical data which was stored heretofore in the USGS Multics computer have been transfered to UNIX special purpose data bases. More than 100 megabytes have been moved.

7. In order to accomodate the large data volume on the smaller 11/70 machine a new algorithm was developed for compressing data files into one third the space. This makes possible the storage of the entire historical data set in the limited disk space. Files can be quickly decompressed ("thawed") to their normal state and are bit-for-bit identical to the original file before compression.

8. Graphics have been improved on the 11/03 Data System such that routine plotting of instrumental data can be done with a minimum of human interventation. A plotting sequence can be initiated to make hundreds of plots in one command.

Reports

Cutler, V., Silverman, S., Johnston, M.J.S., and Herriot, J. 1980. Real-time Crustal Monitoring - the On-lin acquisition, Display, and Testing of Low-Frequency Geophysical Measurements along the San Andreas Fault, Earthquake Note, 52, 16- .

Tilt, Strain, and Magnetic Measurements

9960-02114

M. Johnston, R. Mueller and V. Keller
Tectonophysics Branch
U.S. Geological Survey
Menlo Park, California 94025
(415) 323-8111, Ext. 2132

Investigations

This project concerns continuous monitoring of various types of crustal deformation parameters throughout the San Andreas fault system. Sample rates with digital telemetry are typically 6 per hour. Data are immediately available in an interactive minicomputer for testing, plotting and checking. Precursor algorithms can be routinely run on the data but await demonstration of reliable relationships between earthquakes and the various parameters. The goal is to understand the mechanics of earthquakes by analyzing tilt strain and magnetic field variations which occur as a result of fault activity and by comparing the variations with expectations from the various fault models.

Results

1) Three volume strainmeters have each been installed at a depth of 600 feet in granite basement rock in southern California. The instruments are at distances of 3, 16 and 30 km along a line perpendicular to the San Andreas fault near Pearblossom. These instruments can resolve strains of less than 10^{-10}. Solid earth tides are presently the most dominant short period signal in the record. Drift rates due to cement curing are presently less than 10^{-8}/day.

2) The crustal tilt rate obtained by linear regression on differential lake level measurements in San Andreas lake near San Francisco from 1978 to 1981 is $0.7 \pm 0.4 \mu$ rad/a down to the north.

3) Simultaneous measurements of geodetic and magnetic arrays installed across active segments of the Red River fault system in Yunnan, China, have been reduced. Following a M4.8 on November 20, 1980, the nets were remeasured. No change is expected, however, since the hypocentral distance is about 30 km from the nets.

4) A prototype deep-hole differential strain meter has been operating beside the PD2S strainmeter for three months. The instruments produce similar records of the solid earth tide and presently show the same strain rate. The strain rate for the new instrument has shown an expotential decrease to the present rate of 3×10^{-8}/day.

5) The electronics for two deep hole tiltmeters has been tested also for 3 months. No changes greater than the equivalent of 6×10^{-9} rad have occurred.

6) An analysis of differential proton magnetometer data indicated a standard deviation that varies with site separation of

$$\sigma = a L + b$$

where $a = 0.097 \pm 0.02$, $b = 0.003 \pm 0.001$ and L is the site separation kilometers. At separations of a few meters in seismically and culturally quiet sites, the precision approaches the theoretical instrument limitation of 0.1 nT at a 0.25 nT sensitivity and 0.05 nT at a 0.12 nT sensitivity.

7) Effects of uniform and non-uniform secular variation due to internal currents in the core have been identified and removed from the magnetic field records. External currents in the magnetosphere and ionosphere induce changes in the difference fields due to contrasting inpedances at different magnetometer sites. These changes have been removed using methods of multichannel predictive filtering. The remaining fluctuations of up to several nT are attributed to crustal magnetization changes. Evidence that they are stress related includes the precursive variations prior to the Busch fault (1974) earthquake and the 1979 Coyote earthquake.

Reports

Cutler, R., Silverman, S., Johnston, M. J. S., and Herriot, J., 1981. Real-time Crustal Monitoring--the On-line acquisition Display and Testing of Low-Frequency Geophysical Measurements along the San Andreas Fault, Earthquake Note, 52, 16- .

Dvorak, J., Okamura, A. and Johnston, M. J. S., 1981, Tiltmeter measurements on Mt. St. Helens, U.S. Geological Survey Prof. Paper, in press.

Cutler, R. and Johnston, M. J. S., 1981, An Interrogatable Data Collection Node (D.C.N.): A Microprocessor Based System for Collection and Transmission of Law=Sample Rate Geophysical Data, U.S. Geological Survey Open File Report 81- .

Davis, P. M., Johnston, M. J. S., and Mueller, R. J., 1980, Localized magnetic field variations in central and southern California, Trans. Am. Geophys, Un., 61, 1118, 1980.

Dvorak, J., Johnston, M. J. S., and Okamura, A., 1980, Tilemeter measurements on Mt. St. Helens, Trans. Am. Geophys. Un., 61, 1134, 1980.

Johnston, M. J. S., Mueller, R. J., and Dvorak, J., 1980, Volcano magnetic observations during eruptions of Mt. St. Helens May-August 1980, Trans. Am. Geophys. Un., 61, 1134, 1980.

Johnston, M. J. S., Mueller, R. J., and Keller, V. C., 1981, Preseismic and and coseismic magnetic field measurements near the Coyote Lake Earthquake of August 6, 1979, J. Geophys, Res., 86, 921-926.

Mueller, R. J., Johnston, M. J. S., and Keller V., 1981, U.S. Geological Survey magnetometer network and measurement techniques in western U.S.A., U.S. Geological Survey Open File Report No. 81.

Silverman, S. and Johnston, M. J. S., 1980, Have large scale magnetic changes of crustal origin occurred within the San Andreas fault system, 1974-1980, Trans. Am. Geophys., Un., 61, 1118, 1980.

Johnston, M. J. S., Mueller, R. J., and Dvorak, J., 1981, Volcanomagnetic Observations During Eruptions of Mt. St. Helens, May-August 1980. U.S. Geological Survey Prof. Paper (in press).

Fault-Zone Water and Gas Monitoring

9960-01485

Chi-Yu King
Branch of Tectonophysics
U.S. Geological Survey
345 Middlefield Road, M/S 77
Menlo Park, California 94025
(415) 323-8111, Ext. 2706

Investigations

1. Radon in soil gas. Radon content of subsurface soil gas was continuously monitored by the Track Etch method in capped shallow holes at about 80 sites along several active faults between Santa Rosa and Cholame in central California, and at 35 sites in southern California (in cooperation with UCSD and UCSB). Radon has also been monitored since June 1980 at 44 new sites in Livermore and Parkfield areas with thermoluminescent dosimeters in cooperation with Westinghouse Research and Development Center.

2. Radon in groundwater. Radon content of groundwater was continuously monitored at an artesian well in San Juan Bautista, California (in cooperation with University of Tokyo). Radon was also monitored in four other wells by the Track Etch method.

3. Water level. Water level was continuously recorded at eight wells in central California.

4. Water quality. Temperature, salinity, conductivity, and pH were periodically measured at eight wells and two springs in central California.

5. Water samples were collected from the above-mentioned wells and springs for chemical and isotopic analyses by two USGS groups (I. Barnes and J. R. O'Neil).

6. Soil-gas samples were periodically collected near nine radon-monitoring sites for helium measurement by G. M. Reimer of USGS in Denver, Colorado.

7. Mercury in soil gas. Mercury content of soil gas was monitored at nine radon-monitoring sites in the San Francisco Bay area (in cooperation with Arizona State University).

Results

1. Soil-gas radon anomalies. Increased radon emanation was recorded at many stations (using both Track Etch detectors and thermoluminescent dosimeters) before most earthquakes of magnitude >4.0 that occurred during the past one-year interval between San Juan Bautista and the San Francisco Bay area.

2. Anomalous chemical changes at the Chabot well in Oakland. Preliminary results of chemical analysis of water samples taken from the Chabot well, where water level showed anomalous changes in August 1980 before a magnitude 3.9 earthquake (see the previous report), indicate that the water chemistry underwent significant changes also.

Reports

King, C.-Y., Evans, W. C., Presser, T., and Husk, R. H., 1980, Anomalous groundwater changes before a magnitude 4.8 earthquake (abs.), EOS (Trans. Am. Geophys. Union) v. 61, p. 1034.

O'Neil, J. R. and King, C.-Y., 1980, Deuterium anomalies in groundwater as precursors to seismic acitivty in California (abs.), EOS (Trans. Am. Geophys. Union), v. 61, p. 1033.

King, C.-Y. and Wakita, H., 1981, Anomalous radon changes in an artesian well and possible relation to earthquakes (abs.), Earthquake Notes, v. 52, No. 1, p. 71.

King, C.-Y., 1981, A special collection of reports on earthquake prediction: Hydrologic and geochemical studies, Geophys. Res. Lett., v. 8, No. 5, in press.

King, C.-Y., Evans, W. C., Presser, T., and Husk, R. H., 1981, Anomalous chemical changes in well waters and possible relation to earthquakes, Geophys. Res. Lett., v. 8, No. 5, in press.

O'Neil, J. R. and King, C.-Y., 1981, Variations in stable-isotope ratios of groundwater in seismically active regions in California, Geophys. Res. Lett., v. 8, No. 5, in press.

Water-Level Monitoring Along San Andreas and San Jacinto Faults Southern California, During First Half of Fiscal Year 1981

14-08-0001-18358

D. L. Lamar and P. M. Merifield
Lamar-Merifield, Geologists
1318 Second Street, Suite 27
Santa Monica, California 90401
(213) 395-4528

Investigations

Currently, over thirty wells are being monitored along the San Andreas fault between Palmdale and Valyermo and along the San Jacinto fault zone between San Jacinto Valley and Ocotillo Wells. Ten wells are monitored continuously with Stevens Type F recorders; an additional three recorders have been modified to operate on the Caltech Remote Observatory Support System (CROSS). The remaining wells are probed weekly, or in some cases semi-weekly or daily, by volunteers. Weekly water-level data are displayed on computer-generated hydrographs for each well. Rainfall and earthquakes are plotted on the graphs for direct comparison with water levels. The hydrographs are updated and reviewed weekly. Weekly hydrographs are also prepared from recorder charts on two wells maintained by W. R. Moyle, Jr., of the U.S. Geological Survey, Water Resources Division Office, Laguna Niguel, California.

Geochemical parameters, including radon utilizing the track-etch technique, temperature, salinity and conductivity, are being measured in ten selected wells at the time the water level charts are changed. Six additional wells are being prepared for CROSS or satellite platforms. These telemetry units enable receipt of the data in near real time.

Results

A M3.6 event occurred 30 August 1980 in the Anza area. The epicenter was 3.5 km (2.2 mi) west of well 7S/3E-23B1. The long-term hydrograph for this well is shown in Figure 1 and the continuous record from CROSS is shown in Figure 2. It is this well that showed the unusual water-level fluctuations prior to the Imperial Valley earthquake of 15 October 1979 (Lamar and Merifield, 1980). The water level was rising during the spring and summer of 1980, evidently in delayed response to earlier rains. Superimposed on the general rise are unusual fluctuations, the most prominent of which is the rise and fall of about one foot (30 cm) between 2 August and 23 August. Barometric pressure made no significant contribution to this fluctuation, because it varied less than 0.2 inches of mercury during this period. To our knowledge, there are no wells in the vicinity that are pumped for other than single-family domestic purposes; however, the possibility that the short-term declines were caused by pumping wells unknown to us cannot be ruled out. Some rain fell in the area near the end of July, but this well had not shown a short-term response to individual rains in the past. Therefore, a causal relationship between the M3.6 earthquake and the anomalous water-level fluctuations in the preceding weeks remains a possibility. Several other earthquakes between M3.0-4.0 occurred in late 1980 and early 1981. These events were farther from the wells, viz., over 13 km (8 mi). No unusual water-level fluctuations were associated with these events.

Anomalous high-frequency water-level fluctuations were recorded by the Steven's device on well 11S/6E-1C1 between 22 July and 21 August 1980 (Merifield and Lamar, 1981). The origin of the fluctuations remains unexplained; however, the record is similar to one from a well in which gases were observed bubbling up the well (Chi-Yu King, personal communication, 1980). No seismic activity, during or after, can be correlated with this record.

Long-term water-level changes in eight wells in the Palmdale-Valyermo area appeared anomalous during 1979 and 1980 because they were not clearly related to a seasonal cycle (Merifield and Lamar, 1981). With the longer records now available, these changes can be explained reasonably well by a combination of rainfall patterns and local hydrogeologic conditions, in particular the effect of three years of above average precipitation following a long drought. If the water-level changes were related to the change in strain pattern in 1979 (Savage et al, 1981), water levels should have returned to normal in 1980. In general, however, the water wells have maintained higher levels from early 1979 through the spring of 1981.

References

Lamar, D. L. and P. M. Merifield, 1980, Water-level monitoring along San Andreas and San Jacinto faults, southern California, during fiscal year 1979, Summaries of technical reports, volume IX, Open-file report 80-6, p. 361-364.

Merifield, P. M. and D. L. Lamar, 1981, Water-level monitoring along San Andreas and San Jacinto faults, southern California, during second half of fiscal year 1980, Summaries of technical reports, volume XI, Open-file report 81-167, p. 365-368.

Savage, J. C., W. H. Prescott, M. Lisowski and N. E. King, 1981, Strain on the San Andreas fault near Palmdale, California: rapid, aseismic change, Science, volume 211, p. 56-58.

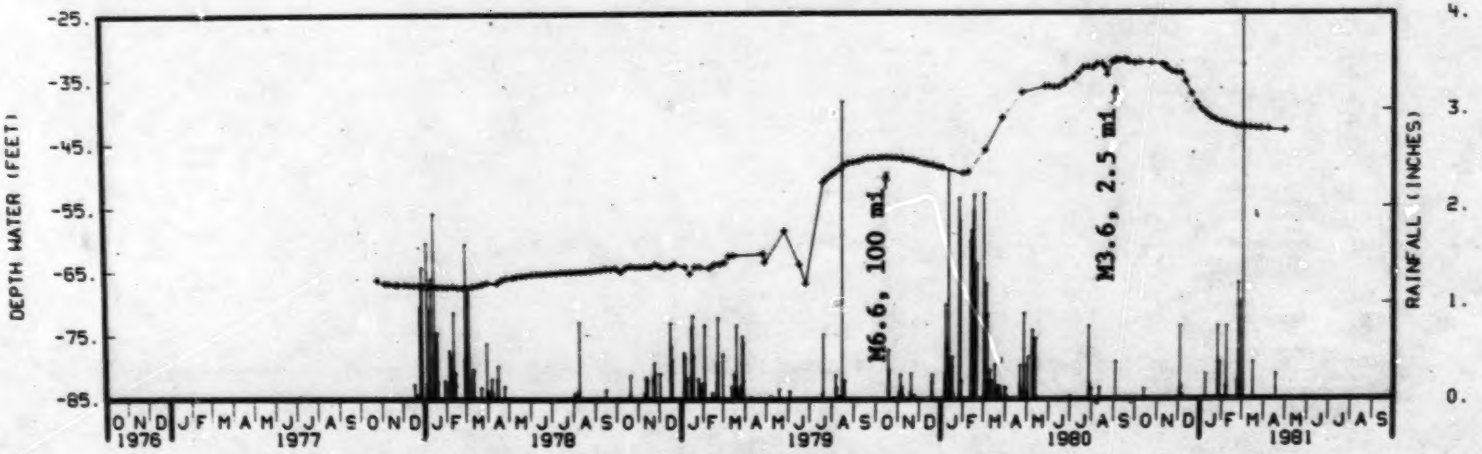

Fig. 1 - Weekly observations of water level (+) and rainfall (.) in well number 07S/03E-23B01 during 1976-1981, Anza area.

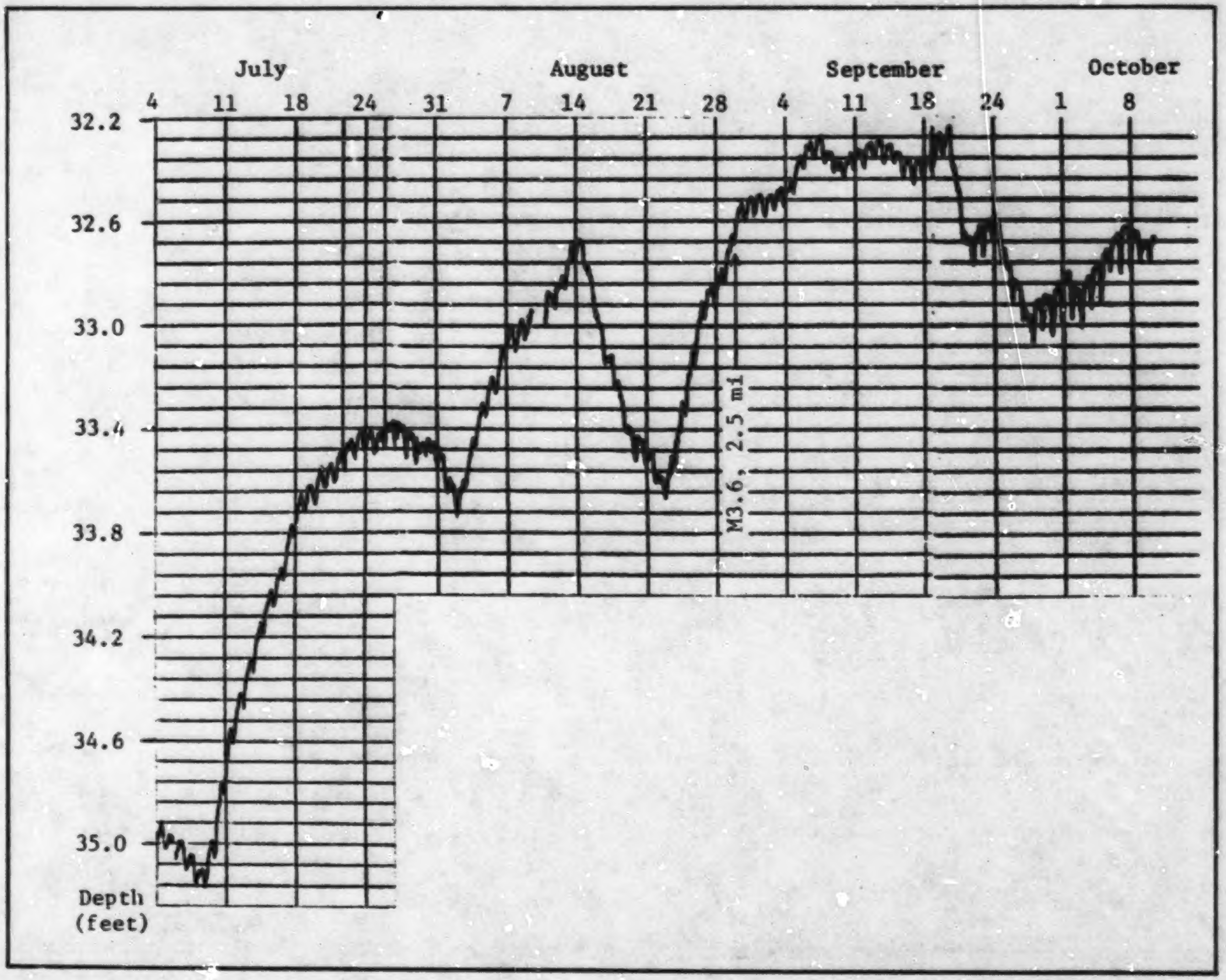

Fig. 2 - Continuous hydrograph of well number 07S/03E-23B1 recorded by CROSS, July to October 1980.

P2

UNIVERSITY OF CALIFORNIA, LOS ANGELES

BERKELEY • DAVIS • IRVINE • LOS ANGELES • RIVERSIDE • SAN DIEGO • SAN FRANCISCO SANTA BARBARA • SANTA CRUZ

Institute of Geophysics and Planetary Physics
Los Angeles, California 90024

Contract #14-08-0001-17686 MOD 3

Can Animals Predict Earthquakes?
A Search for Correlations Between Changes in the Activity Patterns of Captive Fossorial Rodents and Subsequent Seismic Events

Robert G. Lindberg, Principal Investigator
Durward D. Skiles, Co-Principal Investigator*
Page Hayden, Research Associate

This project is an experimental investigation of the possibility that certain animals may behave in unusual ways immediately prior to nearby earthquakes. Specific objectives of the study are:

1. to establish animal monitoring facilities within seismically active regions;
2. to continuously monitor (a) the daily and long term activity of small rodents under controlled conditions of light and temperature and (b) the daily and seasonal activity of small rodents in artificial burrow systems buried in the ground and exposed to the natural environment;
3. to determine whether any correlations exist between changes or anomalies in the activity of these animals and subsequent seismic events;
4. to record baseline patterns of animal activity in the absence of seismic events: and to determine whether correlations exist between changes or anamalies in the activity patterns and changes in non-earthquake related environmental parameters such as temperature, rainfall, humidity, insolation, barometric pressure, and atmospheric electrostatic fields.

Towards these ends, we are continuously monitoring the activity of a small number of individuals of a few species of captive burrowing rodents. At a facility located on the Big Morongo Wildlife Reserve in San Bernardino County, California, we have the capability of monitoring 20 animals housed individually in running wheel cages in an indoor, temperature controlled room, and 11 animals housed individually in fabricated burrow systems located out of doors. We also have installed a second burrow system facility in Stone Canyon, San Benito County, California. The latter facility has the capability of monitoring 10 rodents.

---

*Address: Seismographic Station, University of California, Berkeley CA 94720.

The burrow systems located out of doors at Morongo Valley were seriously damaged by the winter rains of 1979-80. These have been repaired and reinstalled. No seismic activity was reported in the vicinity of the Morongo Valley site during the reporting period.

The animal monitoring facilities at both sites now are providing continuous and reliable animal activity data. Minor seismicity occurred in the vicinity of Stone Canyon but it is clear that a casual examination of the data collected during the reporting period provides no clear evidence for the hypothesis that impending earthquakes precipitate events of unusual animal behavior. No conclusion whatsoever can be drawn regarding large and moderate earthquakes since none has occurred near either monitoring facility.

Air-gun Seismic Velocity and Attenuation Measurements in the San Andreas Fault Zone

9960-02413

Hsi-Ping Liu
Branch of Tectonophysics
U.S. Geological Survey
345 Middlefield Road, M/S 77
Menlo Park, California 94025
(415) 323-8111, Ext. 2731

Investigations

1. Effect of tidal stress on seismic wave velocity and amplitude in fractured granite rocks adjacent to the San Andreas fault zone near Hollister, California.

2. Laboratory measurement of rock internal friction. For a detailed discussion of the results of this investigation, refer to Rocks under Geothermal Conditions, 9960-01490.

3. Numerical evaluation of Hilbert transform by the Fast Fourier Transform technique and its applicability to fault creep problems.

Results

1. Analysis of the air-gun seismic data collected in fractured granite rocks adjacent to the San Andreas fault zone near Hollister, California reveals that: (i) The single shot accuracy and repeatability of travel time over a distance of 600 m is ±0.1 ms ($\Delta t/t = \pm 0.02\%$) for the first higher frequency arrival after the onset of body waves; (ii) A systematic error exists in the Sprengnether recorder when its internal clock is synchronized (reset) by an external reference clock. Specifically, the external reference clock resets only the counter which puts time marks on the seismic record. It, however, does not reset the sample and start convert counter. Because two recorders with independent clock drift rates were reset by a third reference clock in our experiment (Liu 1981), this systematic error in clock resetting represents a systematic error in travel time of ±1.66 ms. The clock resetting error was not mentioned either in the specifications or in the manual of the Sprengnether recorder. We are asking the Sprengnether Instrument, Inc., to modify a circuit board which would allow resetting of the sample and start convert counter by an external reference clock. The effect of tidal stress on seismic wave velocity and amplitude experiment will be repeated after correction of this seismic recording instrument problem.

2. The diesel engine-air compressor unit which supplies the compressed air for air-gun field operation has been automated and modified to start with an air-motor starter. The present modification enables field operation of the air-gun equipment over an extended period without the intensive care of an operator.

3. The Hilbert transform appears frequently in geophysics, e.g., connection between seismic wave phase velocity dispersion and amplitude attenuation, construction of synthetic seismograms, phase response and amplitude response of seismic recording systems, and quasi-static slip problems on a two-dimensional fault. Three Fast Fourier transform numerical methods computing the Hilbert transform integral have been evaluated for their accuracy by numerical examples. All three methods have the common feature that the property that Hilbert transform is a convolution is employed. The first method uses the result that the Fourier transform of $1/\pi x$ is $-i\,\mathrm{sgn}(\omega)$. The second method is based on a discrete Hilbert transform introduced by Saito. The third method, introduced by us, uses linear interpolation to transform the Hilbert trnsform integral into a discrete convolution. The last method is shown by numerical examples from fault dislocation models to be more accurate than the other two methods when the Hilbert transform integral has high frequency components.

Reference cited

Liu, H. -P., 1981, Air-gun seismic velocity and attenuation measurements in the San Andreas fault zone, in Summaries of Technical Reports, Vol. XI, U.S.G.S. open-file report 81-167, 406-407.

Report

Liu, H. -P., and D. D. Kosloff, 1981, Numerical evaluation of Hilbert transform by the fast Fourier transform (FET) techniques, Geophys. J. R. astr. Soc., in press.

Department of Earth and Planetary Sciences
Massachusetts Institute of Technology
Cambridge, Massachusetts 02139

High Sensitivity Monitoring of Resistivity and Self-Potential Variations in the Palmdale and Hollister Areas for Earthquake Prediction Studies

Contract No. 14-08-0001-19249

Principal Investigators: Theodore R. Madden and M. Nafi Toksoz

New electrodes have been installed on both the Palmdale and Hollister arrays. These electrodes are again AgCL:KCL electrodes but incorporating a larger fluid reservoir and a more reliable air seal.

New data and changes in the analysis have modified the picture concerning long period trends of resistivity noted in our last semi-annual report. The data is shown in Figure 2. At Hollister, we still see what are probably significant differences between the dipoles emanating from Paicines (B and F) and the rest of the array. The drift determinations shown in parentheses were made omitting two segments in late 1980 that were not remote referenced with respect to Palmdale. At Palmdale we have had greater noise problems, and are now less sure of our original result that no drifts were occurring. We are counting on the new electrodes to reduce this noise.

Figure 3 shows the first month of self potentials on the Hollister array after installation of the new electrodes, but without 60 cycle decoupling. Some settling in drifts may still be occurring but never the less the electrode behavior seems superior to what we have seen in the past and we are hopeful of maintaining a self potential sensitivity of 0.1 -0.2 mv/km for the array.

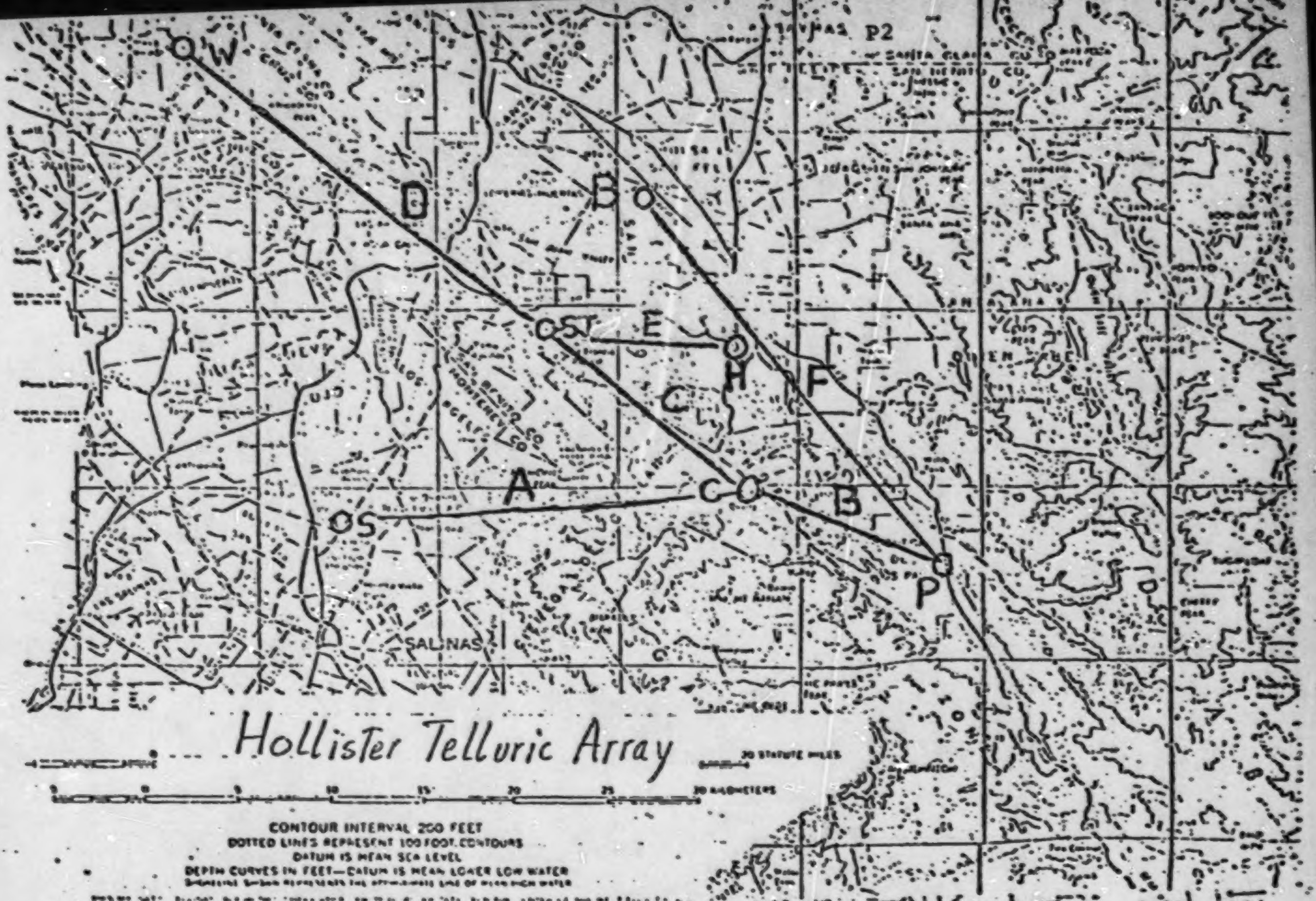
W
D
B
CST
E
H
F
C
A
OS
C
B
P
SALINAS
P2
20 STATUTE MILES
30 KILOMETERS
CONTOUR INTERVAL 200 FEET
DOTTED LINES REPRESENT 100 FOOT CONTOURS
DATUM IS MEAN SEA LEVEL
DEPTH CURVES IN FEET—DATUM IS MEAN LOWER LOW WATER

Hollister Telluric Array

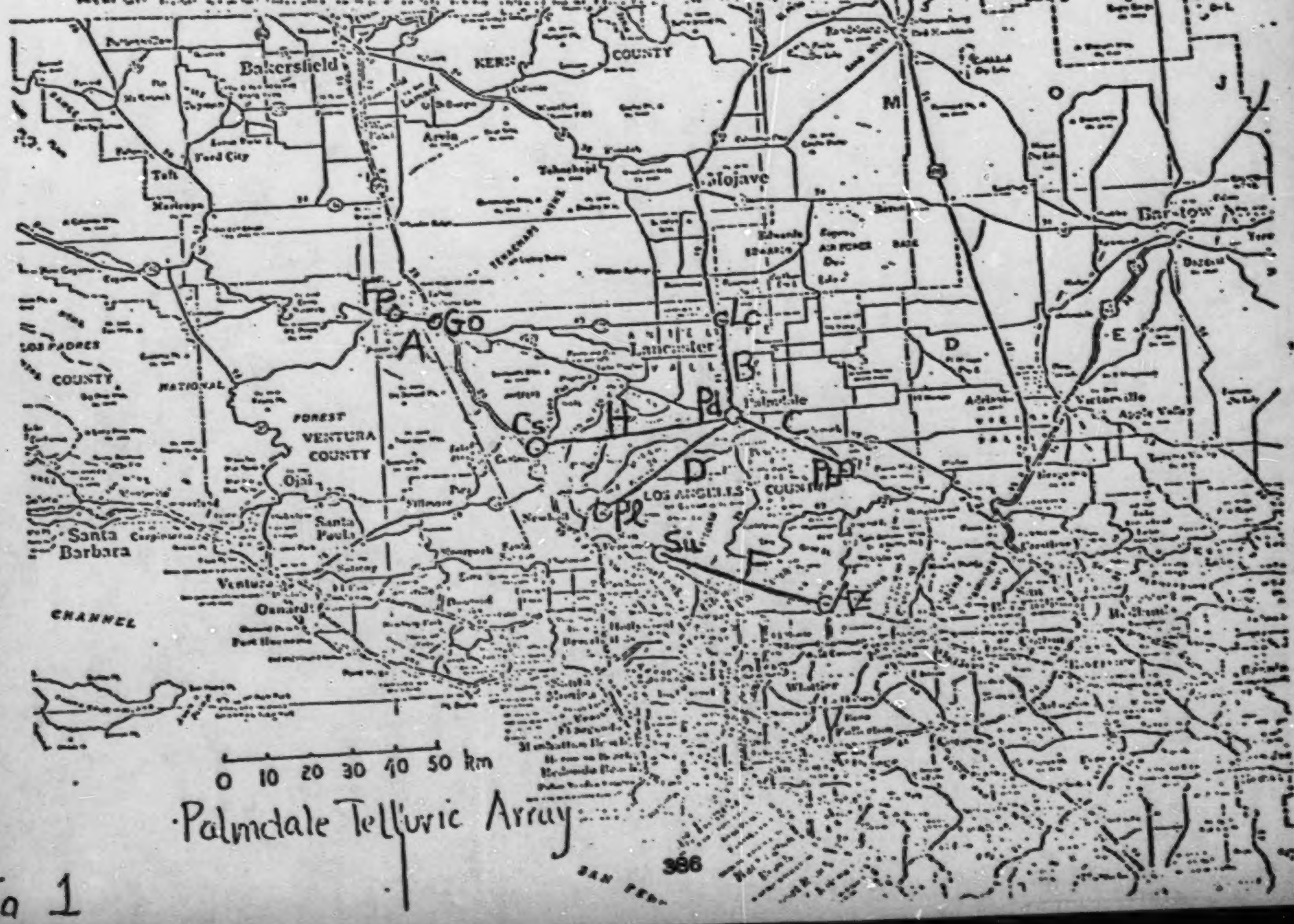
Bakersfield
KERN COUNTY
Taft
Tehachapi
Mojave
Barstow
M
O
J
Lancaster
Palmdale
Victorville
Apple Valley
FPo
Go
A
Lc
B
Pa
H
Cs
C
D
Pb
E
CPl
Su
F
Az
LOS PADRES NATIONAL FOREST
VENTURA COUNTY
LOS ANGELES COUNTY
Ojai
Santa Paula
Santa Barbara
Ventura
Oxnard
CHANNEL
0 10 20 30 40 50 km

Palmdale Telluric Array

ig 1

P2

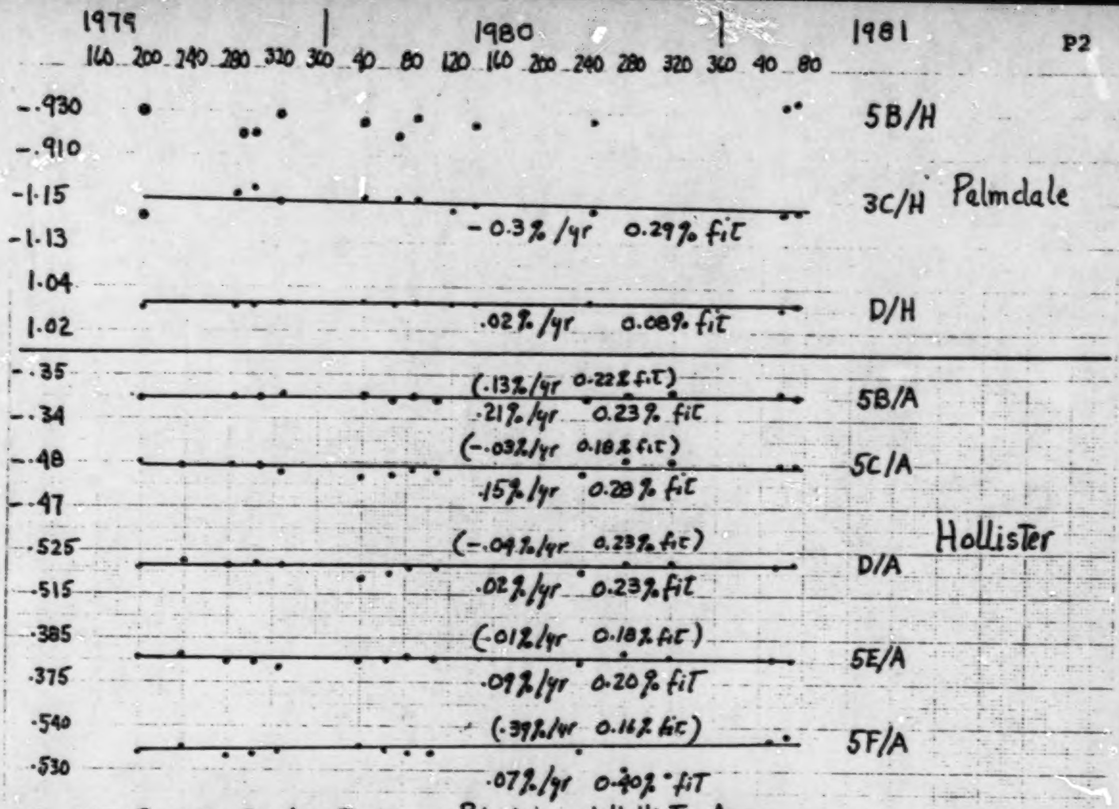

Fig 2 Resistivity Variations on Palmdale and Hollister Arrays
Undamped Inversions of 1-2 week segment averages

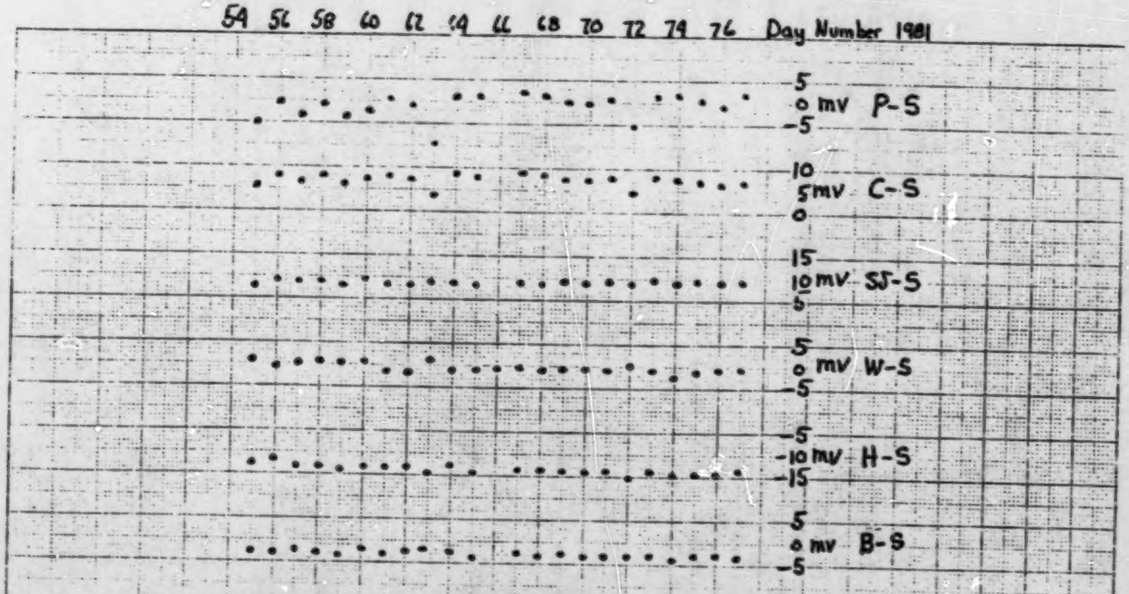

Self Potential Variations Hollister Array

Fig 3

A SEARCH FOR PRECURSORY SEISMIC VELOCITY ANOMALIES NEAR PALMDALE, CALIFORNIA OVER FIXED BASELINES

#14-08-0001-19262

Peter E. Malin
Peter C. Leary
Thomas L. Henyey
University of Southern California
Department of Geological Sciences
Los Angeles, California 90007

SUMMARY

Our project consists of monitoring the travel times of several seismic phases along and across the San Andreas fault near Palmdale, California. The seismic source is a 1000 cu. in. airgun mounted in Bouquet Reservoir (see Figure 1). Signals are received on deep borehole geophones and transmitted by phone line to the experiment controlling computer at the Reservoir. Travel time measurements to three receiver sites established several years ago have been successfully repeated. A new receiver site, 52 km from the source and 0.9 km deep, has been instrumented and an initial timing point for at least two phases has been taken.

The source-receiver lines that had been measured earlier are shown as solid lines in Figure 1. The propagation paths of various phases over them has been discussed by Malin et al. (1980). The direct P and S waves that are being monitored penetrate between 1.5 and 2.5 km into the crust, while a third phase may represent a reflection from as deep as 10 km. As indicated in Table 1 below, in the past 28 months, the first arrival time to the Del Sur site has not changed within the experimental error of .1%. While still under scrutiny, the times of other phases to this and the remaining sites also have not varied. Travel times to the Anaverde and Chief Paduke sites, indicated as dashed lines, were measured in the spring of 1981, but have not been reoccupied. Our present data suggests that no premonitory velocity changes are occurring in the upper 10 km of crust along the San Andreas near Palmdale.

The region covered by our measurements was significantly increased when we demonstrated that timing measurements could be made to the 52 km distant Crystalaire borehole (XTLR in Figure 2). Substantial effort was put in accessing and instrumenting this site. In addition to the first arrival, at least one secondary phase was observed. Both phases were timed to a precision of several milliseconds.

TABLE 1.

Date	Travel Time of First Arrival (ms) at Del Sur
November, 1978	3,414. ± 4
April, 1979	3,410. ± 5
December, 1979	3,406. ± 4
May, 1980	3,410. ± 4
March, 1981	3,411. ± 3

References

Malin, P. E., M. H. Gillespie, P. C. Leary, and T. L. Henyey, 1980, Refraction Profiles Using Borehole Determined Ray Parameters Parallel and Transverse to the San Andreas fault, EOS, Vol. 61, p. 1025.

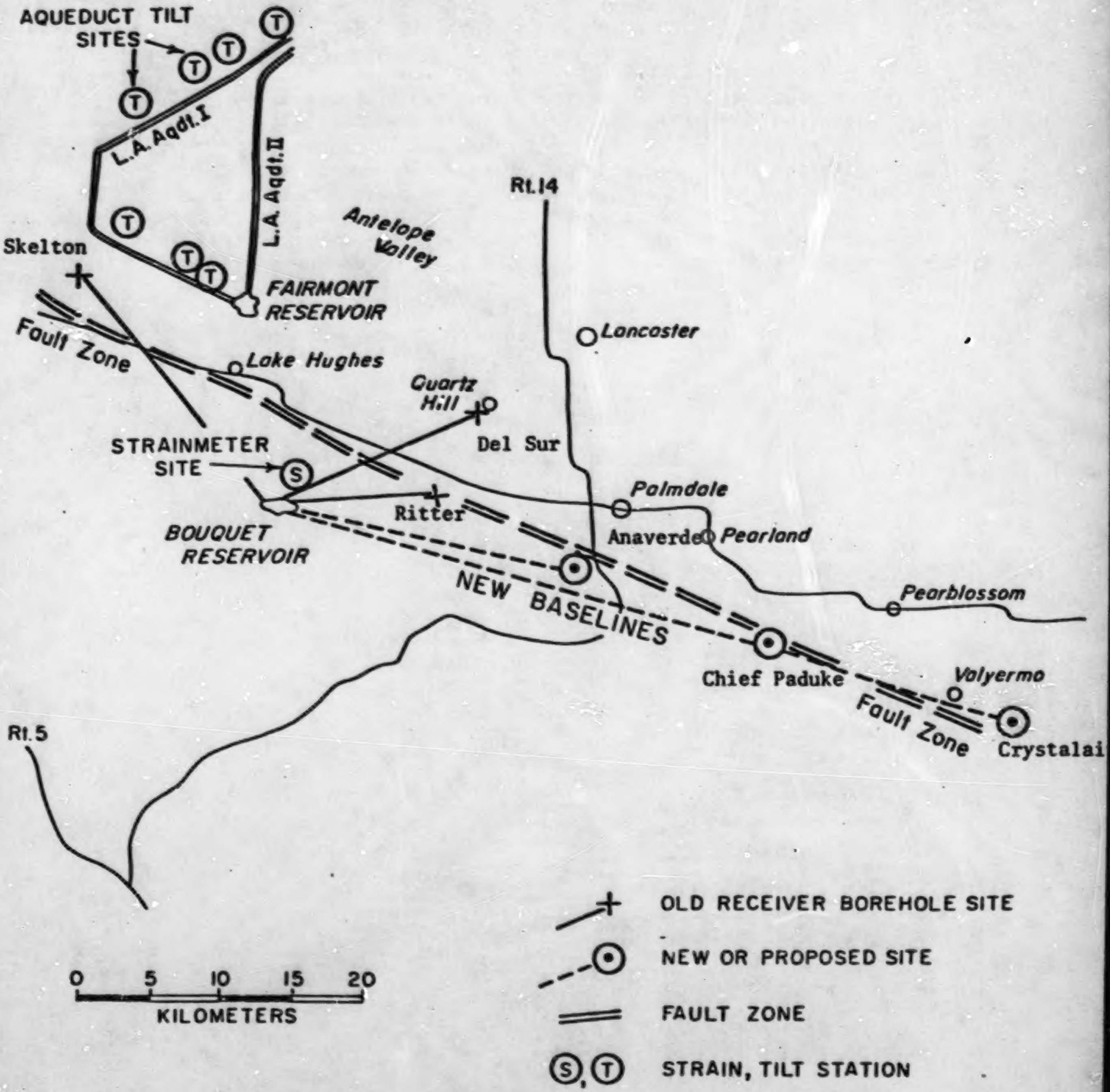
AQUEDUCT TILT SITES
L.A. Aqdt. I
L.A. Aqdt. II
Antelope Valley
Rt. 14
Skelton
FAIRMONT RESERVOIR
Fault Zone
Lancaster
Lake Hughes
Quartz Hill
Del Sur
STRAINMETER SITE
Palmdale
Ritter
BOUQUET RESERVOIR
Anaverde
Pearland
NEW BASELINES
Pearblossom
Chief Paduke
Valyermo
Fault Zone
Crystalai
Rt. 5
0
5
10
15
20
KILOMETERS
OLD RECEIVER BOREHOLE SITE
NEW OR PROPOSED SITE
FAULT ZONE
STRAIN, TILT STATION

Figure 1. Location map of borehole sites with respect to Bouquet Reservoir.

FIGURE 2

52 Km. BASELINE, .05% PRECISION TRAVEL MEASUREMENT ALONG THE SAN ANDREAS FAULT

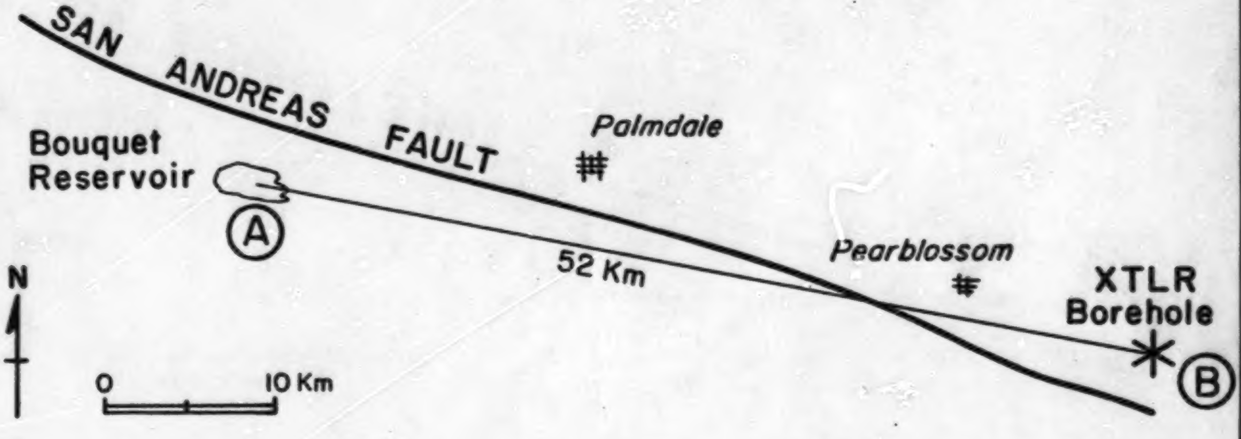
SAN ANDREAS FAULT
Bouquet Reservoir
Palmdale
Ⓐ
52 Km
Pearblossom
XTLR Borehole
Ⓑ
N
0
10 Km

Ⓐ

AIRGUN SOURCE SIGNAL AT BOUQUET RESERVOIR $\Delta \sim 0.3$ Km

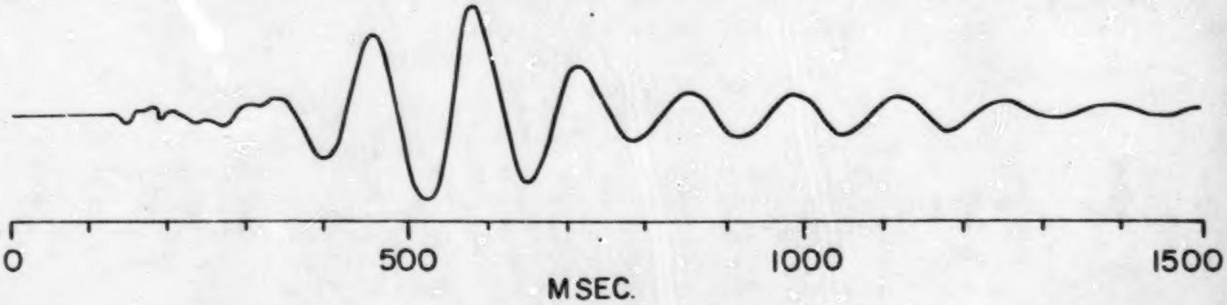

Ⓑ

STACK OF 64 SIGNALS IN 1Km DEEP XTLR BOREHOLE

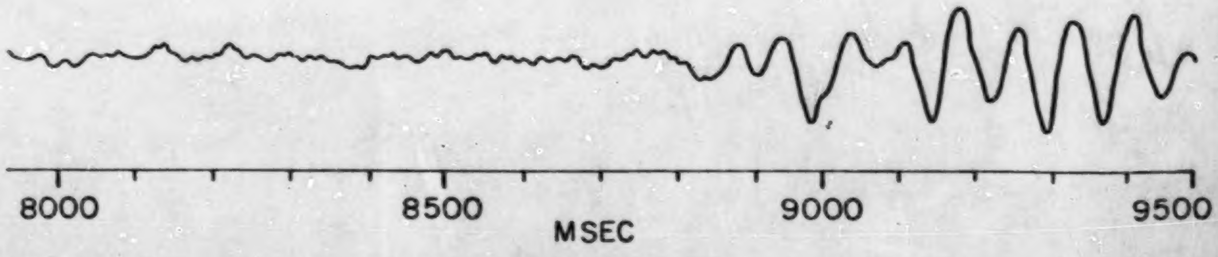

Fault Zone Tectonics

9960-01188

Gerald M. Mavko
Branch of Tectonophysics
U.S. Geological Survey
345 Middlefield Road, M/S 77
Menlo Park, California 94025
(415) 323-8111, Ext. 2756

Investigations

1. Maintained and upgraded creepmeter array in California.
2. Updated archived creep data on PDP 11/70 computer and improved software for data reduction and plotting
3. Searched for distinctive fault creep prior to earthquakes.

Results

1. Telemetry was added to creepmeter CRR1 near Parkfield, California. Six new sites on the Calaveras and Hayward faults were identified for creepmeter installations during the next year. This is part of increased attention given to instrumenting the faults of the San Francisco East Bay region. Currently 39 extension creepmeters operate; 25 of the 39 have on-site strip chart recorders; and 19 of the 25 are telemetered to Menlo Park.
2. Fault creep data from all 39 USGS creepmeter sites on the San Andreas, Hayward, and Calaveras faults have been updated (through January, 1981) and stored in digital form (1 sample/day). Software was written for filtering telemetered data and plotting it superimposed on the longterm archived data. A report of all data from recently operating U.S.G.S. creepmeters was completed up to the review stage.
3. Some of the most striking anomalies of the creep data that have been noted during this period include the following deviations from the apparent long term creep date:

   a. A decrease in rate at XSJ2 (San Andreas fault near San Juan Bautista) from 9 mm/yr to 3.5 mm/yr beginning in early 1976 and continuing to the present.

   b. A gradual increase in rate at HWR1 (Hayward fault, City of Hayward) from 4 mm/yr to 6 mm/yr beginning in 1976.

c. A significant decrease in rate at CRR1 (San Andreas fault near Parkfield) from 10 mm/yr to nearly 0 mm/yr since 1977. This is the first lag of its kind at CRR1, which has kept at a remarkably steady rate since 1969. The lag was interrupted by a large creep event in March, 1981, but the creep is still significantly behind the long term trend.

Reports

Schulz, S., and Mavko, G., 1980, Long term trends in fault creep rate determined from the USGS network, EOS Transactions American Geophysical Union, 61, 1126.

Study of the Foreshock-Mainshock-Aftershock Sequence of the 1978 Oaxaca Earthquake

14-08-0001-18371

Karen C. McNally
Hiroo Kanamori
Seismological Laboratory
California Institute of Technology
Pasadena, California 91125
(213) 356-6919

The recent Oaxaca, Mexico earthquake 1978 November 29 ($M_W = 7.6$, $M_s = 7.8$, seismic moment, $M_o = 3.2 \times 10^{27}$ dyne-cm), is of special interest because of its location within a pre-determined seismic gap. The event excited long-period (100-200 sec) multiple Rayleigh and Love waves which were well-recorded by the WWSSN. These data along with P-wave first-motion data and P waveforms were used to constrain the source mechanism. The results indicate an oblique thrust mechanism consistent with subduction of the Cocos plate to the northeast beneath Mexico (dip = 14^o, strike = N 90^oW, rake = $+54^o$); hence this event is indeed of the type anticipated by Ohtake et al. (1977). A local network of stations, installed in a joint University of Mexico-California Institute of Technology program, began operation 20 days prior to the mainshock [Gonzalez (1979), McNally et al. (1980) and Ponce et al. (1980)]. Forty-three foreshocks of magnitude $M \geq 2.8$ were recorded by the network in a period of 20 days prior to the mainshock. These events show an interesting spacial and temporal pattern, which culminates in the last 1.8 days of the sequence with an apparent migration of activity towards the epicenter of the impending earthquake. This pattern can be interpreted as a buildup of stress or migration of stress towards a fault zone asperity. With supplemental stations, the network continued operation until 12 December 1978 [Singh et al. (1980)], and provided good hypocentral control for the more than 169 aftershocks of magnitude $M \geq 2.8$. The area of the aftershock zone determined from these events is 5525 km^2 (85 km by 65 km). In spite of its large size, P-waves for the Oaxaca event indicate an extremely simple source, at the period range of the WWSSN long-period seismographs. This simplicity suggests that the P-waves were generated by a limited portion of the rupture surface, perhaps by the breaking of a fault zone asperity. This result may be further supported by the discrepancy between the large surface wave moment compared with that determined from body waves. Such simplicity also appears to be the case for the 1965 and 1968 Mexican earthquakes on the adjacent eastern and western ends of the Oaxaca aftershock zone, respectively (Chael et al. 1980). This type of body wave simplicity for a large subduction zone earthquake is an important characteristic of the mode of strain release along some subducting plate boundaries. (Stewart et al. (1980).

The seismic activity and patterns of large earthquake occurrence have been investigated for the region of the Oaxaca, Mexico earthquake

(29 November 1978), and adjoining areas for the period 1964 to 1973. The JHD method was employed to relocate the hypocenters show reduced scatter with greater concentration along the coast of Mexico near the Middle America trench. We have also found that the standard single event locations cause aftershock areas to be enlarged by about 30%. Large earthquakes which occured in Oaxaca in 1965 and 1968 have been relocated by about 40km at S15°W and 50 km at S50°W respectively, to the original epicentral determinations. These improved locations allow better definition of seismic gaps and slip calculations. It appears that two sections of the fault in Oaxaca may remain unbroken by the recent earthquakes in 1965, 1968 and 1978. Furthermore, the seismic slip in these events is less than half that calculated for each of the major sequences in Oaxaca at the turn of the century in 1899/1903 and again in 1928/1931. The relocations also indicate that faulting in this area is bilateral as opposed to updip unilateral propagation typical of subduction zones elsewhere (Tajima and McNally, 1980).

The largest shallow earthquakes ($M_s \geq 7.0$ which have occurred along the Middle American trench since the installation of the WWSSN network are the 1965, 1968, and 1978 Oaxaca events, the 1970 and 1973 events and the 1979 Petalan event. All have been studied to identify similarities and differences that may lead to a better understanding of fracture and subduction processes with relationship to precursory seismicity patterns. The events have seismic moments ranging from 1.0×10^{27} dyne-cm for the 1968 event to 3.2×10^{27} dyne-cm for the 1978 Oaxaca event. All events are of predominantly thrust type, consistent with subduction of the Cocos plate to the northeast. Body waves of the 1965, 1968, 1978 and 1979 events along the trench indicate rather simple faulting processes. These events all had focal depths of 15 to 20 km and stress drops on the order of 10 bars. The 1970 and 1973 events, the eastern- and westernmost, respectively, of the events studied here, show greater complexity in their body waves, perhaps representing a transition to regions of more complicated tectonics (Chael et al. 1981).

The earthquakes in 1965, 1973, 1978 and 1979 were preceded by relative seismic quiesence of ≥ 24 months, in contrast with those in 1968 and 1970. Short term "foreshock type" activity occurred 28 days and 73 days before the 1970 and 1979 events, respectively. The rates of background activity are about double in the regions with no prior seismic quiescence; this correspondence suggests the possibility of predicting the type of precursory pattern for different regions. Seismic quiescence has prevailed for more than three years near Acapulco, Mexico (McNally, 1980).

Revised estimates of seismic slip rates along the Middle America Trench are lower on the average than plate convergence rates, but match them locally (e.g., Oaxaca). Along the Cocos-North American plate boundary this can be explained by nonuniformities in slip at points of aseismic ridge or fracture zone subduction. For at least 81 years (and possibly several hundred years) no major ($M_s \geq 7.5$) shallow earthquake is known to have occurred near the Orozco Fracture Zone and Tehuantepec

Ridge areas. Compared with the average recurrence period for large earthquakes (33 ± 8 y. since 1898 and 35 ± 24 y. between 1542 and 1979), this suggests that either a large ($M \geq 8.4$) event may be anticipated at such locations, or that these are points of aseismic subduction. At least three large coastal terraces are found onshore from the Orozco Fracture zone; these terraces may point to uplift of tectonic origin at this location. The large discrepancy between plate convergence and seismic slip rates along the Cocos-Caribbean plate boundary is more likely due to decoupling and downbending of the subducted plate.

The statistical evidence available is consistent with a possible forthcoming episode of more intense seismicity, characterized by larger events. On the basis of our analyses, three areas stand out as being sufficiently anomalous to deserve special attention: 1) Colima/ Jalisco (~104-105°W) 2) Oaxaca NW (~97.2-97.7°W), 3) Guatemala coast (~90-92°W). In these three cases, at least 48, 52 and 53 years, respectively, have elapsed since the last significant earthquakes. Recent activity has been low in Colima/ Jalisco, Oaxaca, and Acapulco. Based on a series of comparisons with carefully delineated aftershock zones, we conclude that the zone of anomalous seismic activity can be identified by a systematic, automated analysis of the worldwide earthquake catalog ($m_b \geq 4$) (McNally and Minster, 1980).

At roughly 18.5°N, 104.5°W, the trend of the Rivera fracture zone intersects the Middle American trench. This fracture zone represents the boundary between the Rivera plate, subducting under North America at about 2.1 cm/yr, and the Cocos plate, subducting under North America at about 5.4 cm/yr. A segment of the East Pacific Rise intersects the Rivera Fracture Zone from the south at 18°N, 106°W, so that the western branch of the fracture zone represents the boundary between the Pacific and Rivera plates. Seismicity near the western branch of the Rivera fracture zone follows the trend of the fracture zone, but along the eastern branch approaching the coast of Mexico it is more diffuse. Earthquakes near the eastern Rivera facture zone were jointly relocated in an attempt to clarify the location of the plate boundary as determined by the seismicity. The great earthquake of 1932 in Jalisco, Mexico, is the largest historic event of that area. The seismic moment of the main shock on June 3, M_s=8.2, is 1.5×10^{28} dyne-cm. A more accurate epicenter for the 1932 event was found in order to locate the Jalisco earthquake on either the Rivera plate or the Cocos plate. Since the subduction rates of these plates are different, the results of the location of the 1932 event is crucial for estimating the repeat time and current seismic potential for an earthquake of this size in the Jalisco area. We conclude that this earthquake was north of the extension of the rivera Fracture Zone and was probably caused by subduction of the Rivera plate under North America. Hence, the repeat of a 1932 type event may not be likely in the immediate future. (Eissler and McNally, 1980).

References

Chael, E., Stewart, G. and K.C. McNally, 1981, Recent large earthquakes along the Middle American trench, J. Geophys. Res., to be submitted.

Chael, E.P., Stewart, G.S., Singh, S.K., and McNally, K.C., 1980, Recent large earthquakes along the Middle America trench and their implications for the subduction process: EOS Trans., AGU, 61, 297. Del Castillo, Alonso, 1980, Le estadistica de Poisson y el Modelo de dona en la actividad sismica anterior al terremoto de Oaxaca (M_s=7.8) de Noviembre 29 de 1978, U.N.A.M, Tesis, (in Spanish).

Drowley, D., McNally, K. C. and Gonzales, L., 1979, a dipping gradient layer velocity model for southern Mexico: Geofisica Internacional, v.17,2, p. 109-126.

Drowley, D., McNally, K.C. and Vazques, E., 1979, A dipping gradient layer velocity model for southern Mexico: Earthquake Notes, Seismological society of America, 49, 64.

Eissler, H.K., and K.C. McNally, 1980, Seismicity of the Rivera Fracture Zone, and the great Jalisco earthquake of 1932, Proceedings of Simposium Los Riesgos Sismicos y los Asentamientos Humanos (Mexico, Centroamerica y el Caribe), SAHOP, in press.

Gonzalez, J. 1979, Some characteristics of the foreshocks (M 4.0) to the Oaxaca earthquake (M_s=7.8) of the 29 November 1978, professional Thesis, UNAM (in Spanish).

McNally, K.C., 1980, Non-uniform seismic slip rates along the Middle American Trench...(earthquake prediction research and human settlements in Mexico and Central America): Simposium: "Los Riesgos Seismicos y los Asentamientos Humanos," (Mexico, Centroamerica y el Caribe), in press.

McNally, K.C., 1980, Plate subduction and prediction of earthquakes along the middle America trench, Third Maurice Ewing Symposium, New York.

McNally, K.C., 1981, Plate subduction and prediction of earthquakes along the Middle America trench, Maurice Ewing Series 3, Earthquake Prediction, A.G.U., in preparation.

McNally, K.C., 1980, The status of earthquake hazard reduction: Proceedings of the Mexico-California symposium of "Human Settlements in the San Andreas fault Zone", State of California and Baja, California; Sacramento, California, p. 240-251.

McNally, K.C., Alt, J., Helmberger, D.V., Lomnitz, C., and Sieh, K., 1980, New observations of coastal uplift patterns near the Middle America trench, Mexico, Science, to be submitted.

McNally, K.C., Chael, E., and Ponce, L., 1979, The Oaxaca, Mexico, earthquake (M_s=7.8) of 29 November 1978: New "pre-failure" observations: EOS Trans. AGU, 60, 322.

McNally, K.C. and Hearn, T., 1980, A "master catalog" of large shallow earthquakes along the Middle America trench (1898-1979): Bull. Seism. Soc. Am., in preparation.

McNally, K.C., and Minster, J.B., 1980, Non-uniform seismic slip rates along the Middle America trench, J. Geophys. Res., in press.

McNally, K.C., and Minster, J.B., 1979, Non-uniform seismic slip rates along the Middle America Trench: EOS Trans. AGU, 60, 884. Ponce, L., McNally, K.C., Gonzalez, J., del Castillo, A., and Chael, E., 1979, The Oaxaca, Mexico earthquake of 29 November 1979: Foreshock activity: Earthquake notes, Seismological Society of America, 49, 48.

Ponce, L., McNally, K.C., Sumin de Portilla, V., Gonzalez, J., del Castillo, A., Gonzalez, L., Chael, E. and French, M., 1979, report on spatio-temporal pattern of preceding seismic activity and mainshock relocation, Geofisica Internacional, v. 17,2, p.109-126.

Singh, S.K., Haskov, J., McNally, K., Ponce, L.; Hearn, T., and Vassiliou, M., 1979, The Oaxaca, Mexico, earthquake of 29 November 1978: A preliminary report on aftershocks: Earthquake Notes, Seismological Society of America, 49, 48.

Singh, S.K., Haskov, J., McNally, K.C., Ponce, L., Hearn, T., and Vassiliou, M., 1980, The Oaxaca, Mexico, earthquake of 29 November 1978: A preliminary report on aftershocks: Science, v. 2007, p 1211-1213.

Stewart, G.S., Chael, E.C., and McNally, K.C., 1980, the 29 November 1978 Oaxaca earthquake: A large simple event: J. Geophys. Res., in press.

Sumin de Portilla, V., Ponce, L., Kochneva, N.T., Igem, A.M., Rodriguez-Lopez, S. and McNally, K.C., 1979, Geomorphostructural analysis of Oaxaca, Mexico, and its relation to seismicity: Earthquake Notes, Seismological Society of America, 49, 45.

Tajima, F., Kikuchi, M., and K.C. McNally, 1980, Seismic rupture pattern in Oaxaca, Mexico (Part II): EOS Trans., AGU, 62, in press.

Tajima, F., and McNally, K.C., 1980, Seismic rupture patterns in Oaxaca, Mexico: EOS Trans., AGU, 61, 288.

P2

Experimental Tilt and Strain Instrumentation

9960-01801

C.E. Mortensen
Branch of Tectonophysics
U.S. Geological Survey
345 Middlefield Road, M/S-77
Menlo Park, California 94025
(415) 323-8111, Ext. 2583

Investigations

1. Project investigators continued to operate and monitor tiltmeter and strainmeter arrays in central and southern California, totaling 56 sites, and a tiltmeter array in Alaska consisting of three doubly instrumented sites. The purpose of these networks is to provide a continuous monitor of crustal deformation near active faults in order to contribute to a thorough understanding of fault mechanics. Observed signals in the records are checked against meterological and other data to assure validity, are compared with other records to determine coherence and possible correlation with seimicity, and are tested against various fault models to estimate source parameters.

2. A cluster of five shallow borehole tiltmeters is operated at Gold Hill, near Parkfield, California, to determine the coherence of detectable tilt changes among closely spaced instruments in shallow boreholes over periods that might be of interest in earthquake prediction. This experiment should provide an estimate of the lowest possible noise level of tilt measurements made in shallow boreholes with short base length instruments.

3. A system that monitors a difference in water level is operated continuously at San Andreas Lake near Belmont, California. The system uses sensitive pressure transducers to monitor the "tilt" of the lake, and provides a continuous measurement with excellent long-term stability.

4. Twenty-one tiltmeter sites have been retrofitted with electronics circuits that have been modified and tuned to reduce thermal response and drift, and to improve linearity.

5. Prototype long-baseline tiltmeters are operated at two sites in central California. These instruments use a tubular column to extend the baselength of borehole tiltmeters to approximately 60 m. Damping and thermal tests are being conducted on these instruments.

6. A deep borehole differential strainmeter has been designed and a prototype constructed in conjuction with Malcolm Johnston's Tilt, Strain and Magnetic Measurements project. Stability testing is being conducted at the San Francisco Presido Vault.

7. Two shallow borehole tiltmeters were installed at the Geysers geothermal field in conjuction with Dave Oppenheimer's geothermal project. The purpose of these instruments was to monitor possible episodic subsidence within the field. A paucity of potentially good sites for shallow borehole instrumentation in the area lead to siting the instruments in a location with poor drainage, which resulted in flooding during winter rains. Repair of the instruments is underway and the plan is to resite the instruments in available adits.

8. Three volumetric strainmeters were installed in the Mojavi Desert, in the general region of Palmdale, California, in conjunction with Malcolm Johnston's project and the Carnegie Institute. Assistance was provided in emplacing the instruments and establishing telemetry links. It is expected that maintenance of the instruments and assistance in evaluating the data will continue to be provided by this project.

Results

1. The instrument near Anza, California, has consistently produced some of the lowest noise level records among similar shallow-borehole tiltmeters throughout central and southern California. In January 1978 a sequence of distinctive tilt signals, with wave-like character, not apparently related to rainfall or instrumental causes, appeared in the record and persisted for approximately ten days. After some loss of data, the signals reappeared intermittently in August 1978 increasing in frequency and amplitude, culminating in two swarms of tilt events in February and March 1979. Subsequently these signals gradually became smaller and less frequent, with only minor intermittent events occurring as late as July 1979. The record since that time shows only one small event in February 1981, which occurred during a period of heavy rainfall. The tilt events in 1978 and early 1979 are similar in waveform, amplitude and timescale to signals observed at tiltmeters in central California at the times of nearby recorded surface creep events. A continuously recording water well gage on the opposite side of the fault and 3 km east of the Hamilton School tiltmeter shows no clear aperiodic, event-like behavior. Thus, if the tilt signals were caused by creep events, these events had to be confined to a section of the fault northwest of the monitored water well. Visual inspection of the fault trace near Hamilton School shows no evidence of recent surface creep; however, soil condition in the area would likely obscure small offsets. There is no apparent correlation of the tilt events with local seismicity.

   Modeling of several typical tilt events, using dislocation models in an elastic solid to simulate propagating creep sources, indicates that slip zones may have nucleated close to the Hamilton School instrument and propagated away from it. The creep events may have had amplitudes on the order of 3 cm, depending on slip zone geometries and other parameters.

2. An experiment involving a cluster of five closely spaced instruments, together with the results of several different tests of linearity, calibration and thermal response, provides some conclusions regarding the stability and noise level of tilt measurements made in shallow boreholes with short baselength tiltmeters.

   a) Tilt changes with periods greater than diurnal tend to be incoherent between shallow-borehole, short-baseline tiltmeters spaced as closely as 5 m. The ultimate noise-level for such installations appears to be on the order of 1/2 μradian per week, notwithstanding the amount of care exercised in installing and tuning the instrument.

   b) The dominant source of thermal noise in the tiltmeter data from shallow boreholes is thermoelastic response coupled through topography or minor asymmetries in the ground immediately surrounding the instrument. The thermal response of the tiltmeter electronics circuit, when operating properly, cannot account for the major thermal features in the tiltmeter data.

   c) Modification and careful tuning of the tiltmeter electronics circuits to minimize thermal response provides some improvement in data quality, particularly at sites where circuits have not previously been tuned. However, the general character of the long-term tilt data does not appear to be significantly effected. This conclusion is supported by the cluster experiment and by preliminary results from the retrofitting of existing tiltmeter sites with the modified electronics packages.

3. Preliminary tests of a prototype diffential strainmeter conducted in the San Francisco Presido vault indicate sensitivity and stability comparable to horizontal invar-wire strainmeters operating in the vault environment.

Reports

Myren, G.D., Mortensen, C.E., Murray, T.L., and Iwatsubo, E.Y., 1980, Tiltmeter observations at Cape Yakataga, Alaska, preceding the Saint Elias Earthquake, M=7.7, of February 28, 1979: Bull. Seismol. Soc. America, v.70, n.5, p.1661-1665.

Mortensen, C.E., and Iwatsubo, E.Y., 1980, Short-term tilt anomalies preceding local earthquakes near San Jose, California: Bull. Seismol. Soc. America, v.70, n.6, p.2221-2228.

Dvorak, J., Okamura, A., Mortensen, C., and Johnston, M., 1981, Summary of electronic tilt studies-Mount St. Helens, 1980: U.S. Geological Survey Professional Paper (in press).

Mortensen, C.E., and Myren, G.D., 1981, Short-term tilt events near Anza, California (abs.) Earthquake Notes, SSA, v.52, no.1, p.24.

Stable Isotope Analyses

9740-00383

J. R. O'Neil
Branch of Isotope Geology (MS 18)
U.S. Geological Survey
345 Middlefield Road
Menlo Park, CA 94025
(415) 323-8111, ext. 2598

Investigations

1. Analyses of D and ^{18}O are made of ground waters collected bimonthly at several sites along active fault systems in California with the aim of tracing changes in local hydrological regimes that precede or accompany earthquakes.

2. In a search for geochemical precursor phenomena, soil gases at several sites along the San Andreas fault are being analyzed for amount and isotopic compositions of CO_2 and H_2.

3. The isotopic compositions and water contents of fault gouge are being analyzed with the aim of learning the physical chemical conditions of formation and the porosity of such material.

Results

1. Encouraging isotopic results were observed for waters from three sites near San Juan Bautista: Mission Farm Campground, St. Francis Retreat, and Cienaga Winery. The importance of these measurements lies in the fact that during the last two years the seismicity in the area changed significantly. There were no earthquakes of magnitude $\geq$4.0 from the beginning of the study until March, 1980 when a sequence of earthquakes occurred. As a consequence, these analyses provide an excellent background of data for observing variations in the isotopic compositions of ground waters and testing the relations to seismic activity. The data for the 18-month period emcompassing these earthquakes are shown in Figure 1 for the site at Mission Farm Campground. There was a clear-cut lowering of both the $\delta^{18}O$ and δD values of the water about one month prior to the largest and closest event (magnitude 4.8). Inasmuch as both isotopic ratios changed in the same direction, another ground water must have entered the system, possibly by the (temporary?) creation of a connection between two aquifers. That such a process occurred is well substantiated by the dramatic concurrent changes in the chemistry of the fluids (King, pers. comm.). The case for the connection between the seismicity and the changes in chemical and isotopic compositions of this water is strengthened by the fact that after the changes occurred, δD values increased steadily while the $\delta^{18}O$ values remained constant, as in the previous Oroville Dam study. The differences observed in the isotopic signature of the water are shown more clearly on a

plot of δD versus $\delta^{18}O$ (Fig. 2). The dramatic changes occurred at about the same time as the magnitude 4.0 earthquake, 25 km. away, of 3-6-81 and about one month prior to the larger (m=4.8) and closer (6 km.) earthquake of 4-13-81. After almost a year the $\delta^{18}O$ values have not recovered but the δD value dropped significantly about two weeks prior to the events on 6-18-80 and the closely spaced events on 1-17-81 and 1-27-81. The hydrological regime at this site is undoubtedly delicate but the deuterium anomalies observed there so far look promising for earthquake prediction.

2. There are very large variations in the concentration of CO_2 in soil gases from the three sites (above) near San Juan Bautista. The variations are generally correlated from site to site, but no relation to local seismic activity is evident. ^{13}C and ^{18}O contents of this gas vary by over 5 permil but, again, without obvious relation to seismic activity. Unlike observations made along the Yamaski fault in Japan, no H_2 has been detected in the soil gas at sites along the San Andreas fault near San Juan Bautista.

3. Determinations have been made of the D and ^{18}O contents of San Andreas fault gouge collected by Mark Zoback. Water, separated by vacuum distillation, varies from 9.0 to 25.1 weight percent of the samples and is clearly of local groundwater origin. $\delta^{18}O$ and δD values of the water range from -5.0 to +2.6 and -50 to -21 respectively, and correlate well with depth (to 1305 feet). $\delta^{18}O$ and δD values of the gouge (primarily clay minerals) vary from 16.9 to 14.9 and -73 to -64 respectively. There is a good balance between the ^{18}O lost by the rock and gained by the water, implying that the water/rock ratio in the gouge has been low throughout the formation history of the clays. The deuterium data is in agreement with this conclusion. Thus the fault gouge is not being flushed through with fresh supplies of water from above. This is in keeping the geophysical data that indicate that the gouge is quite impermeable. With additional measurements on mineral separates, it may be possible to estimate formation temperatures of the clays.

Reports

O'Neil, J. R., and Hanks, T. C., (1980), Geochemical evidence for water-rock interaction along the San Andreas fault in central California, Jour. of Geophys. Res., v. 85, p. 6286-6297.

O'Neil, J. R., and King, C.-Y., (1980) Deuterium anomalies in groundwater as precursors to seismic activity in California, EOS, vol. 61, p. 1033.

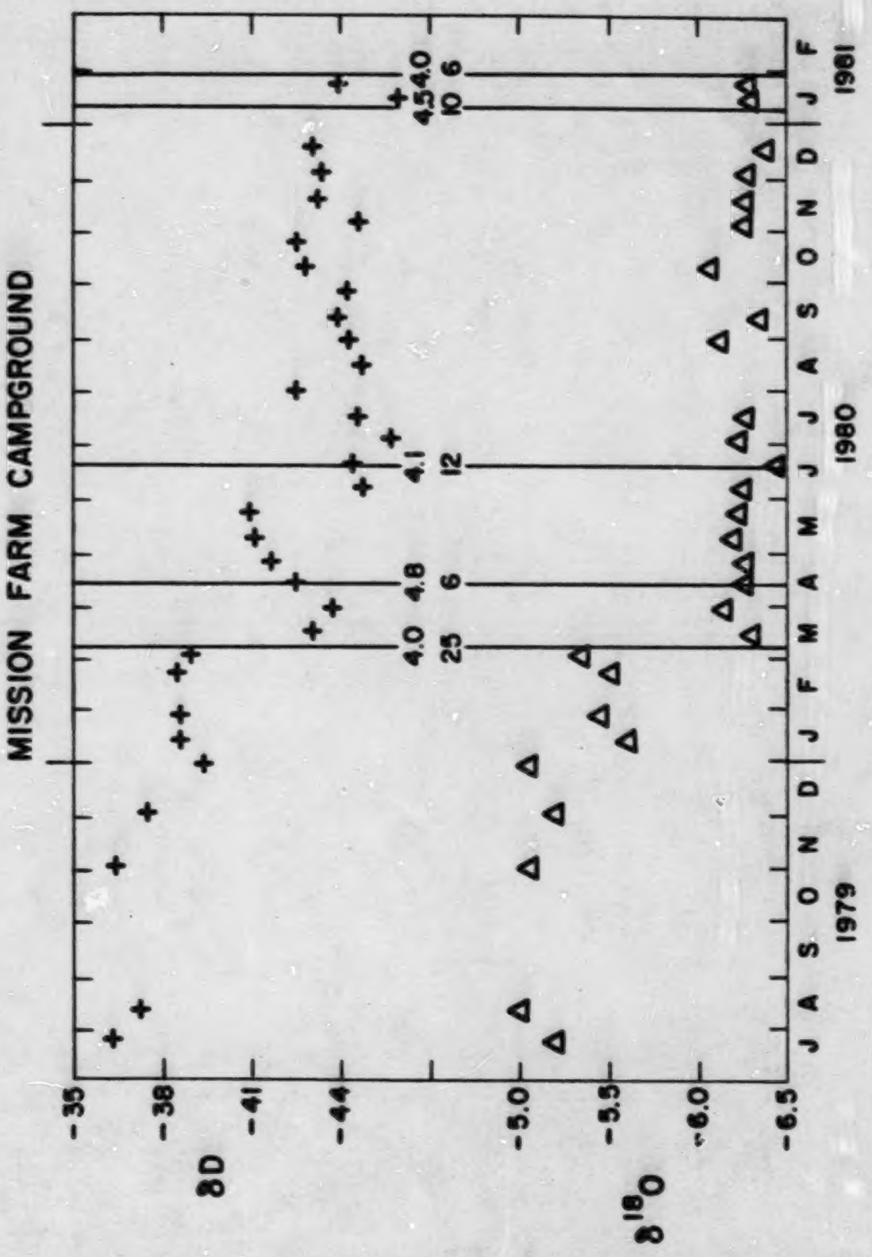

Fig. 1. Time series of δD and $\delta^{18}O$ of water at Mission Farm Campground. Vertical lines indicate occurrence of earthquakes of magnitude ≥4.0; labeled are magnitude and epicentral distances in km.

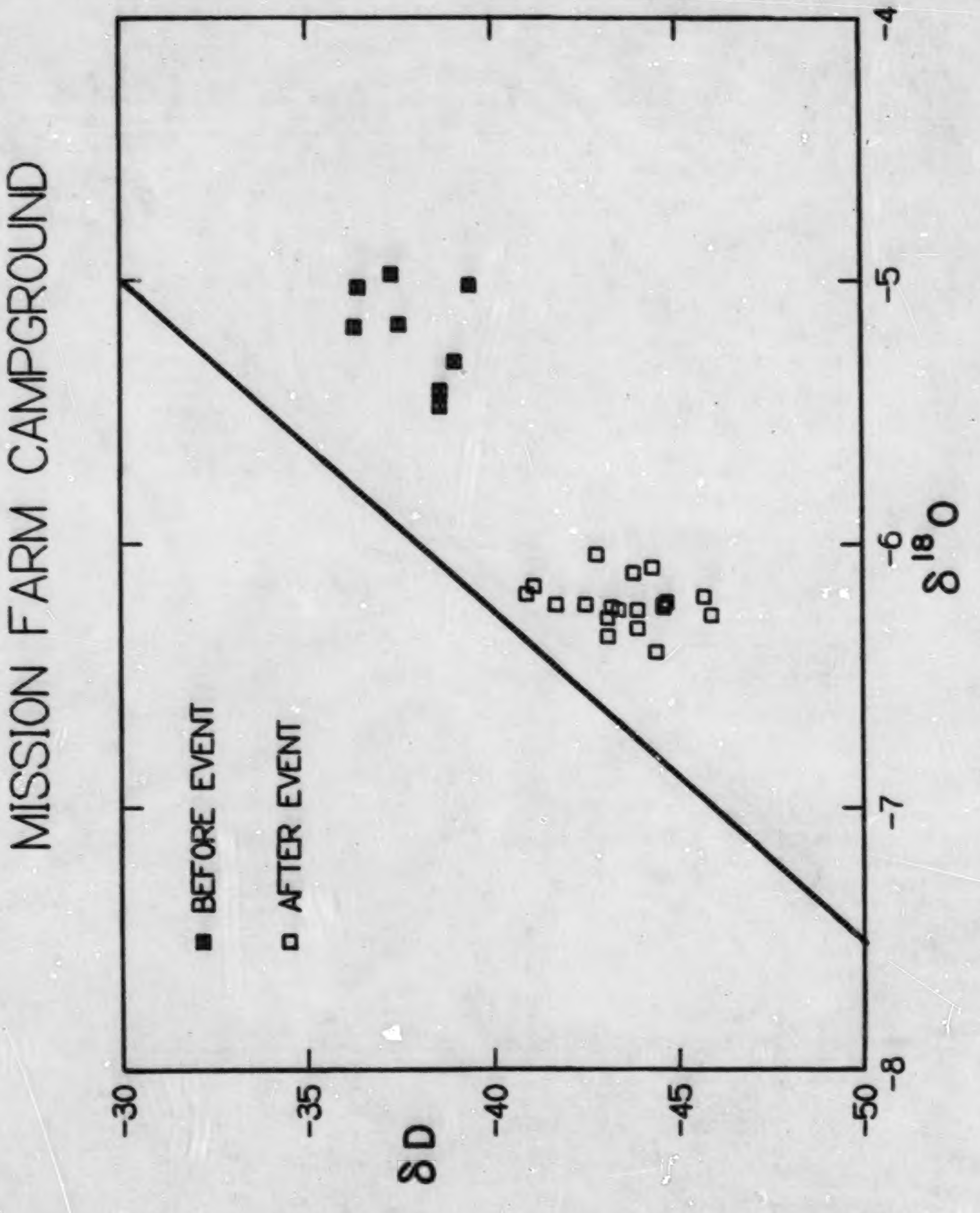

Fig. 2. δD vs. δ^{18}O for the water samples collected before and after the isotopic anomaly related to the largest and closest earthquake at Mission Farm Campground. The straight line shown is the "meteoric water line".

Biological Premonitors of Earthquakes:
A Validation Study

14-08-0001-19112

Leon S. Otis
William H. Kautz
SRI International
333 Ravenswood Avenue
Menlo Park, California 94025
(415) 326-6200

Popular reports of anomalous animal behavior before earthquakes are common and extend through most of recorded human history up to the present. Birds, household pets, fish, and farm animals are cited most frequently, with occasional mention of dozens of other animals with which man has contact.

Unfortunately, these reports are of little scientific value because they are anecdotal and subject to the inaccuracies of observation, recall, and assessment of significance that usually accompany laymen's reports of disasters. Moreover, the reports provide scanty data, and the credentials of the observer are rarely provided.

Efforts are currently in progress in the United States to gather animal behavior data before and after earthquakes. The recent successful short-term predictions of earthquakes in the People's Republic of China have impressed U.S. seismologists, and a principal element of the Chinese program is reports of unusual behavior of animals by volunteer observers.

The purpose of this research is to determine whether unusual animal behavior may serve as a biological premonitor of earthquakes. Our approach was designed to test this hypothesis and incorporates some features of the Chinese program. Specifically, a network of qualified volunteer observers has been established along seismically active areas of California. These volunteers are collecting daily observational data on the behavior of animals with which they are in daily contact through their employment or hobbies.

A toll-free (WATS) hot line at SRI operates for 24 hours a day, 7 days a week. Each call is automatically recorded on tape; an independent circuit also records the date and time the call is received. Volunteer observers are instructed to call the hot line on a designated day once weekly to check in, and to use it any time they observe an instance of unusual animal behavior. Only hot line reports received prior to earthquakes are treated as valid information for purposes of data analysis.

Observers are given 30-day log sheets on which they rate the behavior of their animals daily on a scale of 0 to 4. Zero denotes typical behavior, 1 slightly atypical behavior, 2 clearly atypical behavior, 3 very atypical behavior, and 4 behavior never previously observed. Log sheets are mailed to SRI when completed. The reliability of observer reporting is assessed, in part, by comparing log sheet entries with transcripts of hot line calls; observers are instructed to report on the hot line all behaviors that are rated 2 or more on the log sheets.

Observers are categorized as 1, 2, 3, or 4 on the basis of their performance in checking-in weekly on the hot line, and returning the monthly log sheets to SRI. Category 1 observers are the most reliable, categories 2 and 3 are progressively less so, and category 4 observers have discontinued voluntarily or have been dropped because of unacceptable performance.

Since January 1978, we have recruited approximately 1600 volunteer observers in selected seismically active areas of California, principally in Humboldt County, the San Francisco Bay area (extending south to Hollister and Santa Cruz, and north to Santa Rosa), Los Angeles and Ventura Counties, and San Diego County. About 400 observers were recruited during 1980. The attrition rate was approximately 24%; most of these were individuals who received all of the materials but never started. During all or part of 1980, 1197 volunteer observers were active.

Approximately 250 species of house pets and other domestic and wild animals are being observed, including arthropods, fish, reptiles, amphibians, birds, and mammals. Reports of unusual behavior typically refer to unexplained or prolonged vocalization; restlessness; a change in regularly occurring habits; pacing, running, or attempts to escape from enclosures; immobility, refusal to enter normal housing; hiding; and unexplained absence from a usual locale.

Eight hundred and thirty of the 1197 active observers reported one or more instances ($\bar{X} = 2.4$) of unusual animal behavior during 1980. A total of 2026 calls were received. The mean and standard deviation of the baseline rate of reporting was approximately 5.56 ± 0.84 per day for all of California and ranged from zero to 3.7 per day for different map sections* in the reporting network. Our working assumption is that the frequency of reports will increase significantly above the baseline level just before a major earthquake. Other possible causes will be excluded before such an increase in reporting behavior is considered relevant to the animal hypothesis.

Past reports of anomalous animal behavior before earthquakes do not indicate clearly the distance from the epicenter, the pre-earthquake time period or the minimum magnitude range over which the phenomenon may be occurring. Consequently, a nonparametric statistical method has been devised for determining whether an increase in the frequency of hot-line reports received just before an earthquake from the vicinity of the epicenter is sufficiently higher than the background level of reporting to constitute evidence in support of the animal-behavior hypothesis. The background level is established from a control group of reports from the same region that are not associated with the earthquake in question or any other. All reports occurring within an assumed distance and time period after earthquakes are disregarded. This analysis is based on an evolving predictive model in which the sizes of the pre- and post-earthquake vicinities (in both time and space), as well as the minimum earthquake magnitude and minimum observer report rating to be included, are treated as unknown parameters of the hypothesis. That is, they initially are assigned various values, and those that lead to the strongest results are retained for testing against future data.

---

*For purposes of data analysis the state is divided into 60 map sections; each is bounded by 1° latitude and 1° longitude.

A total of 350 earthquakes (excluding aftershocks) of magnitude ≥ 3.0 occurred in California during 1980. None of those of magnitude ≥ 4.0 occurred within the observer network. Nevertheless, 14 were selected for analysis because they either occurred on the fringes of the network or were of large magnitude ($M \geq 5.0$).

For certain provisional values of the parameters of our model the number of reports preceding 4 of these events (the earthquakes near Livermore on 24 and 26 January, near Prunedale on 12 April, and off the coast of Trinidad in Humboldt County on 8 November) differed significantly from chance ($p \leq 0.05$). For other values, however, the results were not statistically significant. Because the earthquakes that were the most appropriate for evaluation occurred on the fringes of the observer network, the data were too sparce to make a meaningful determination as to which set of parametric values are the most appropriate. This can only be determined when one or more earthquakes of a reasonable magnitude ($M \geq 5.0$) occur well within the network. Nevertheless, we now have a set of values that have resulted in significant findings and whose appropriateness can be tested against future earthquakes.

A survey questionnaire mailed to 260 observers residing within approximately 165 km (100 miles) of the epicenter of the 24 January earthquake near Livermore revealed that 95% of the 195 (75%) observers who responded were around their animals during the two-week priod preceding this earthquake, and that 56 (29%) observed unusual animal behavior. Only 32, however, reported such behavior on the hot line before the quake; the remaining 24 reported it after the earthquake so that their data could not be used in the analysis. Three others in the network also made post-earthquake reports. These data indicate that laxity in observer reporting of unusual behavior as soon as it is observed may contribute to our failure to find significant results in some cases. We are continuing our efforts to improve observer reporting practices.

Most routine network operations are automated, including maintenace of records of the performance of each observer, the mailing of additional logs, praise and delinquency notices, and the preparation of weekly and monthly management and statistical reports. A cadre of non-observer volunteers in the Menlo Park area handle other non-automatable functions.

Our experience to date indicates that members of the community may participate constructively in data collection for certain kinds of earthquake research, suggesting that this potential resource may be useful for other geophysics research programs.

Analysis and Evauation of Strinmeter and Tiltmeter Data

9960-02942

J. H. Pfluke
Branch of Tectonophysics
U.S. Geological Survey
345 Middlefield Road, M/S 77
Menlo Park, California 94025
(415) 323-8111, Ext. 2041

Investigations

1. Data from several taut wire strainmeters have been collected in Central California over the past 6 years. Analysis of the data is encumbered by frequent data loss and several instrumental defects. The instrument output, once cleaned of equipment effects, must be examined for meteorological and geologic-site effects. If identified such effects must be extracted as well as possible in order to observe the residual tectonic effect on the datum trace. The resulting residual trace is interpacted with the goal of recognizing patterns that are precursors to earthquakes and interpreting such patterns via physical models.

2. Surface tiltmeter data are being collected under external research contract with St. Larris University at or near sites where the USGS is collecting data from dilatometers installed at depth. These data are analyzed, much along the lines described above, in the attempt to integrate the tiltmeter data into a coherent picture of the local tectonics.

Results

1. Plans are completed for the installation of four of the SLU tiltmeters at two sites in Southern California. The installations should be completed by mid-summer.

2. Strainmeter records from the two installations at San Juan Bautista have been studied in detail. While most of the fluctuations can be attributed to rainfall there are exeptions. Occasional sharp change in trend of the strain traces take place with no apparent correlation to meteorology. These are being investigated for possible correlation with other geophysical phenomena, principally with perterbations in the seismicity along nearby faults.

Electrical Conductivity Sounding Experiments on the San Andreas Fault

14-08-0001-17763

Wayne J. Phillips
A. F. Kuckes
School of Applied and Engineering Physics
Cornell University, Ithaca, NY 14853

The electrical conductivity structure of the San Andreas Fault in Central California has been studied by means of an electromagnetic induction experiment. The source utilized was the University of California, Berkeley grounded electric dipole located on the Law Ranch near the town of Paicines (1). Horizontal and vertical magnetic fields and horizontal electric fields were measured at a series of sites running roughly perpendicular to the strike of the fault. The transmitter is oriented nearly parallel to the strike of the fault. The location of the transmitter and receiver sites are shown in Fig. 1.

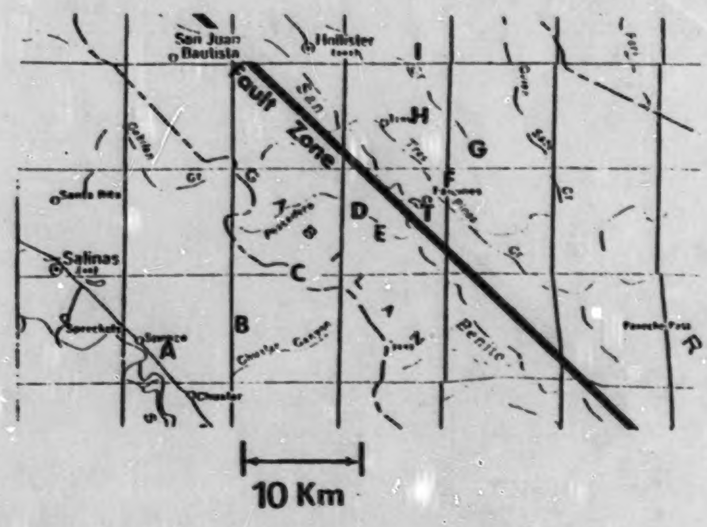

Figure 1.
Map showing the location of the transmitter and measurement sites.

The transmitter was operated in a square wave mode with periods of 1 and 10 seconds. For each of these two periods, Fourier analysis of the magnetic and electric fields at the receiver sites yielded data at the odd harmonics up to the 9th harmonic.

The electrical conductivity structure is derived from the observed fields by calculating apparent resistivities ($\rho_a = \frac{1}{\mu_0\omega} |E|^2/|H|^2$) at each site and fitting these to two-layer magnetotelluric sounding curves. The resulting two-layer models are placed side-by-side to construct a two-dimensional map of the conductivity structure. This is shown in Fig. 2.

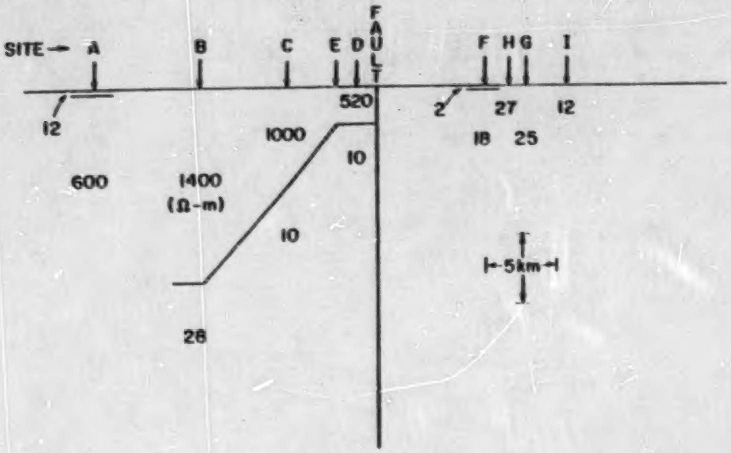

Figure 2.
Conductivity structure obtained by placing two-layer models side-by-side.

At the surface the region is characterized by a large contrast in conductivity across the fault. Conductivities on the West side being about 50 times larger than those on the East side. The results also indicate the presence of highly conducting materials beneath the Gabilan range on the West side while the conductivity on the East side is nearly independent of depth at least in the upper 8 Km or so.

The results agree with the geology of the area. In central California the San Andreas fault marks the eastern edge of the Salinian block, a terrain of granitic and metamorphic basement rocks encompassing most of coastal California between San Francisco and Los Angeles. The high resistivities observed on the West side of the fault are associated with the granites of the Gabilan range, one of the major granitic plutons of the Salinian block. The granitic plutons of the Salinian block range in age from ≈ 80-100 m.y. which places them at the end of the Mesozoic era (2). Granites of this era have resistivities which are typically 500-2000 Ω-m (3) which compares favorably with the observed values of 520-1400 Ω-m.

On the East side of the fault lie Franciscan rocks and younger sediments. The Franciscan complex is primarily a collection of marine sediments with some mafic and ultra mafic plutonic and volcanic rocks which account for about 10% of the total. Resistivities of Mesozoic marine sediments are typically 5-20 Ω-m and those volcanic rocks of the same age are 20-500 Ω-m (3). Resistivities on the East side of the fault average ≈ 20 Ω-m.

As on the West side, resistivities observed on the East side of the fault compare well with values one would expect based on the kinds of rocks seen at the surface.

The presence of highly conducting material beneath the Gabilan range correlates well with results of seismic and gravity surveys in this area. On the basis of gravity measurements, Pavoni (4) concludes that there exists a wedge of low density rocks beneath the eastern rim of the Gabilans. The position of these rocks correlate well with the high conductivities seen at depth at sites D and E (see Figs. 2 and 3). Pavoni interprets these rocks as a continuation of the Franciscan rocks and other sediments that lie to the East of the fault. The conductivity data is certainly compatible with this hypothesis. Alternatively, it is possible that this wedge of low density, highly conducting rocks is fault gouge. The fact that gouge is a very porous aggregate of small grains of rock could account for both the low density and high conductivity. It is worthwhile to note here that the epicenters of earthquakes in this vicinity are systematically displaced a few kilometers to the West of the surface trace of the fault (5). Pavoni (4) suggested that the hypocenters may actually be within the low density zone. Interpretation of these rocks as fault gouge is certainly consistent with this possibility. It has been pointed out, however, that the displacement of epicenters may be artifact of the complex velocity structure of the fault zone and attempts to take into account the influence of the velocity structure in locating epicenters have been successful in relocating them onto the surface trace of the fault (5,6).

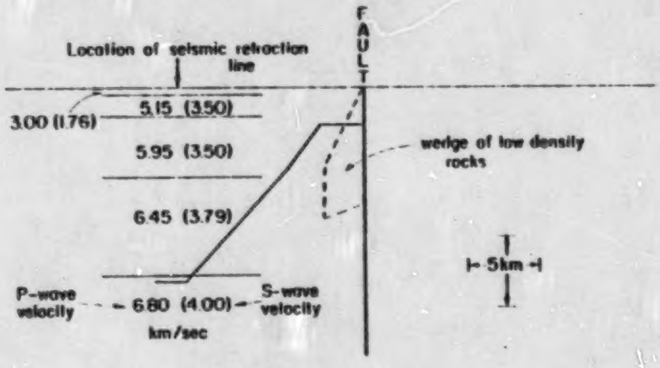

Figure 3.
Seismic, gravity and conductivity structures superimposed.

Seismic velocities in the Gabilan range have been determined by a seismic refraction survey (7) and by analysis of arrival times of seismic waves generated by earthquakes in the vicinity (8). The location of the refraction survey and the velocity structure are shown in Fig. 3. The increase in seismic velocity to 6.8 Km/sec, a feature observed on both the East and West sides of the fault, seems to correlate with the increase in conductivity at 13 Km at site B. Stewart and Peselnick (9) suggest oceanic crust is responsible for the jump in seismic velocities. The high conductivities observed beneath the Gabilans can be attributed to the presence of oceanic crust if the rocks have been subjected to some degree of serpentinization. Serpentinization is a hydrothermal alteration of some of the minerals commonly found in oceanic crust (particularly pyroxene and olivine) to yield serpentinite which is a porous, highly conducting mineral. As a result, serpentinization can dramatically increase the conductivity of ocean rocks (10).

References

1. Morrison, H.F., Corwin, R.F., and Chang, M., High Accuracy Determination of Temporal Variations of Crustal Resistivity, in The Earth's Crust, A.G.U. Monograph 20, Heacock, J.G., ed., 593-614 (1977).
2. Howell, D.G. and Vedder, J.G., Late Cataceous Paleography of the Salinian Block, California, in Mesozoic Paleography of the Western U.S., Soc. Econ. Paleontologists and Minearologists, Pacific Sec., Pacific Coast Paleography Symposium 2, Howell, D.G. and McDogall, K.A., eds., 523-534 (1978).
3. Clark, S.P., Jr., Handbook of Physical Constants, The Geological Socity of America Inc., 562 (1966).
4. Pavoni, N.A., A Structural Model for the San Andreas Fault Zone Along the Northeast Side of the Gabilan Range in Proc. of Conf. on Tectonic Problems of the San Andreas Fault System, Stanford University series in Geological Sciences, 13, Kovach, R.L. and Nur, A., eds. 259-267 (1973).
5. Boore, D.M. and Hill, D.P., Wave Propagation Characteristics in the Vicinity of the San Andreas Fault, in Proc. of Conf. on Tectonic Problems of the San Andreas Fault System, Stanford University series in Geological Sciences, 13, Kovach, R.L. and Nur, A., eds., 215-223 (1973).
6. Engdahl, E.R. and Lee, W.H.K., Relocation of Earthquakes by Seismic Ray Tracing, J. Geophys. Res. 81, 4400-4406 (1976).
7. Stewart, S.W., Preliminary comparison of seismic travel times and inferred crustal structure adjacent to the San Andreas Fault in the Diablo and Gabilan Ranges of Central California, in Proc. of Conf. on the Geologic Problems of the San Andreas Fault System., Stanford University series in Geological Sciences 11, Dickinson, W.R. and Grantz, A., eds., 218-230 (1968).
8. Healy, J.H. and Peake, L.G., Seismic Velocity Structure along a section of the San Andreas Fault near Bear Valley, California, Bulletin of the Seismological Society of America, 65, 1177-1197 (1975).
9. Stewart, R. and Peselnick, L., Velocity of Compressional Waves in Dry Franciscan Rocks to 8 kbar and 300°C. J. Geophys. Res. 82, 2027-2039 (1977).
10. Stesky, R.M. and Brace, W.F., Electrical Conductivity of Serpentinized Rocks to 6 Kb., J. Geophys. Res. 78, 7614-7621 (1973).

Earthquake Hazard and Prediction in NW Mexico and California/Mexico Border

14-08-0001-19163

Michael Reichle and James N. Brune
Institute of Geophysics and Planetary Physics
Scripps Institution of Oceanography
University of California, San Diego
La Jolla, California 92093

Recent seismicity in the Imperial and Mexicali Valleys has somewhat changed the direction our research has taken during the first 6 months of the current contract. Our primary interest has been installation of the Northern Baja California telemetering array. Our efforts during the six months have been principally concentrated in these areas: maintenance of temporary stations in Northern Baja California and analysis of that data; completion of the study of the Oaxaca and Petatlan mainshocks, cataloguing and analysis of digital data collected following the 15 October 1979 Mexicali and the 9 June 1980 Victoria earthquakes.

The most interesting new data come from aftershocks of the 9 June 1980 M_L = 6.2 earthquake located 11 km southeast of the town of Guadalupe Victoria. A portable array of up to 7 analog and 12 digital recorders operated in the aftershock zone from 4 hours to one month after the main event. Over 50 smoked paper records and 60 digital cassettes were obtained. The data is being analyzed with that obtained following the Mexicali earthquake. The two earthquakes have interesting similarities and differences which might be clarified by analysis of the digital data. Victoria aftershocks are clustered aboug 15 km northwest of the instrumental epicenter, with few events in the epicentral region. A number of events are also found scattered throughout the area between the southern end of the Imperial fault and the northern end of the Cerro Prieto fault. Similar phenomena characterized aftershocks of the Mexicali earthquake. The primary differences between the two events are in surface characteristics. The 1979 Mexicali earthquake has surface displacements of up to 80 cm (including the first 10 days of afterslip) displacement along 30 km of the Imperial fault. The Victoria earthquake, on the other hand, had very little direct superficial faulting. A maximum of about .5 cm of right-lateral displacement was located along one segment of the Cerro Prieto fault, but this could not be followed through adjacent fields. At several sites, small left-lateral motion along conjugate faults was found, but those could not be followed for any distance either. Even after several months, the displacement had not creeped to the surface. Hopefully, a careful analysis of local and teleseismic data will clarify these basic differences in faulting characteristics.

Helium Monitoring for Earthquake Prediction

9440-01376E

G. M. Reimer
Mail Stop 916
U.S. Geological Center
Denver Federal Center
Denver, Colorado 80225
(303) 234-5146

Investigations

Four additional soil-gas monitoring stations have been established at locations extending from Daly City to Menlo Park. Each new station consists of two probes and will provide an opportunity to evaluate sample collecting variability as well as influence of seasonal factors. The new locations are approximately 120 km northwest of the previously established stations near Hollister.

Results

1. Nearly two year's worth of data has been collected for soil-gas stations near Hollister. A seasonal pattern is apparent for the two years and will be used to establish a baseline reference from which future helium analyses will be compared.

2. Soil moisture may play a lesser role in the seasonal pattern than previously thought. While the influence of moisture is substantial on a short-term basis, as previously documented, the yearly cycle of helium soil gas concentration is maintained even during periods of abnormal precipitation.

3. A helium decrease and increase cycle of several months duration was observed to correspond with the recent cluster of earthquake activity near San Juan Bautista. It appears that some fine structure is present in the actual measurements and may hint at resolution of the specific seismic events. However, the uncertainties in linking helium decreases to specific events are large considering the samples are collected only about once each week.

Reports

Reimer, G. M., 1981, Helium soil-gas variations associated with recent central California earthquakes: Precursor or coincidence?: Geophysical Research Letters (in press).

Graph showing a 3-point moving average of the helium concentration of soil gas from stations around Hollister, California for the period May 1979 to April 1981. Also plotted are earthquakes of magnitude 4 or greater that occurred within a 160 km radius of the sample stations. The data extending above the earthquake bars are for convenience to locate the intersection with the helium plot.

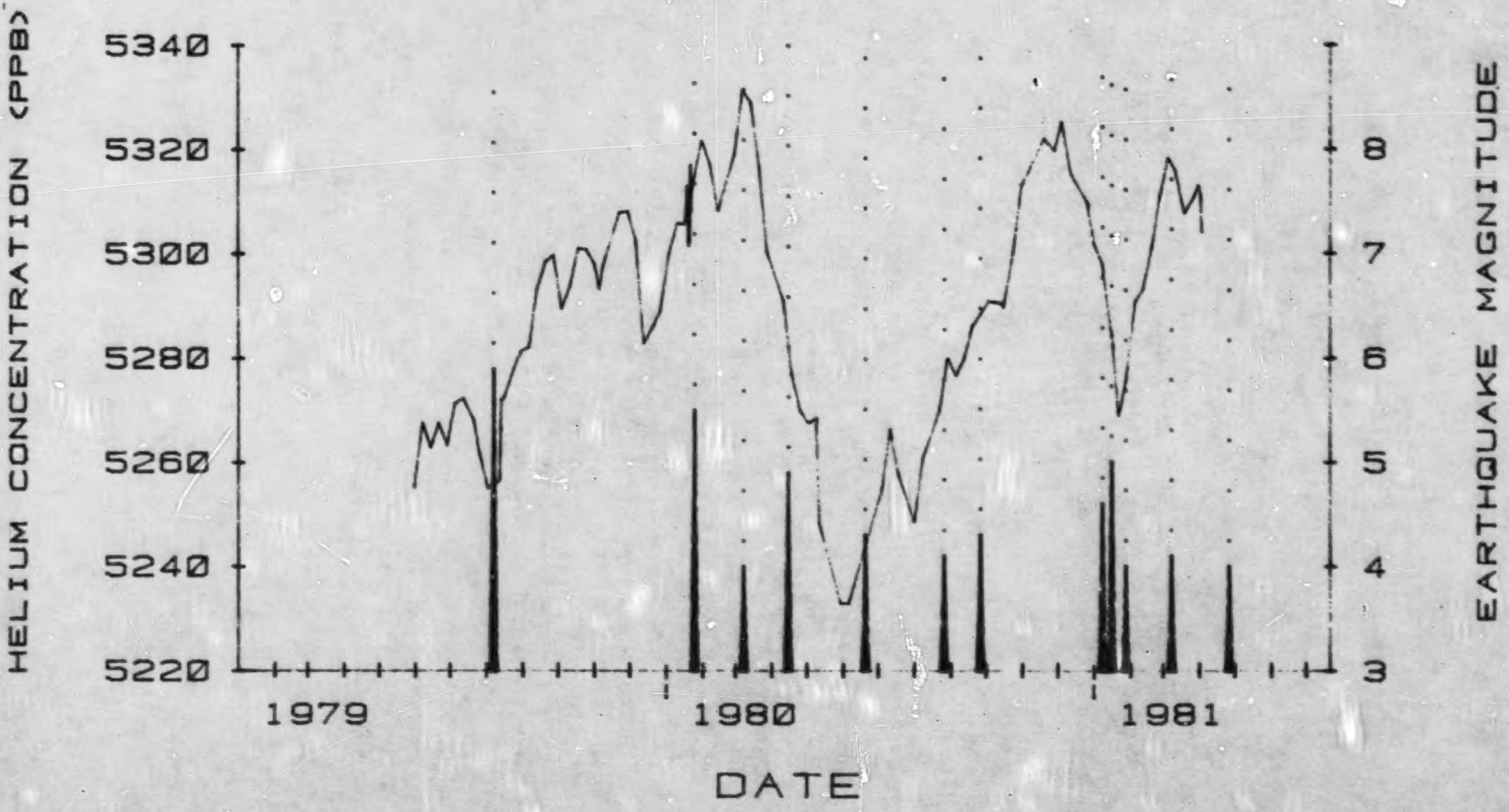

Hydrogen Monitoring

9710-02773

Motoaki Sato and K. A. McGee
Branch of Experimental Geochemistry and Mineralogy
U. S. Geological Survey
M/S 959, National Center, Reston VA 22092
(703)860-6600

Investigations

Hydrogen gas can be generated by the reaction of rock-forming minerals with ground water when frictional stress causes local heating. Hydrogen is extremely mobile and non-cumulating, and thus may prove to be one of the best chemical indicators of the highly stressed state of the crust. We explore techniques for reliable and economical monitoring of hydrogen emission along active seismic faults and implement the field testing and data collection.

Results

Our effort so far has been concentrated on (1) reconnaissance survey of H_2 emission on San Andreas and Caraveras faults between Hollister and Cholame; (2) experimental continuous H_2 monitoring at Melendy Ranch; and (3) development of H_2 sensors suitable for monitoring on seismic faults.

(1) Our surveys at 9 locations show that H_2 emission occurs, but at a very slow rate, and at very low concentration levels (at most 50 ppm by volume). We did not encounter such high levels of H_2 as those reported by Wakita et al. (1980) along Yamasaki fault in central Japan.

On December 17, 1980, guided by S. Schultz (OES), Sato and McGee visited Shore Road (SHR1), Wright Road (WRT1), Mission Vineyard Road (XSJ2), Hollister Hills (XHR1), and Melendy Ranch (XMR1). On each site, the trio dug a hole 4 to 5 feet deep and buried the sensor probe of a newly acquired H_2 detector (International Sensor Technology solid-electrolyte H_2 sensor, 100 ppm full scale sensitivity). Except at Melendy Ranch, no H_2 was detected in 15 minutes after the burial of the sensor. At Melendy Ranch, a slight movement of the meter needle was detected. We left a membrane-type sensor (developed by Sato at USGS) in a 5-foot plastic pipe buried in the ground and covered the top with a plastic sheet.

On December 18 the trio visited Jack Ranch (XGH1), Work Ranch (WKR1), Slack Canyon (SXC1), and again Melendy Ranch. At Jack Ranch, we failed to detect any H_2 in 15 minutes. At Work Ranch, we noticed a slight movement of the meter needle on the IST detector in 15 minutes, and decided to wait for a longer period. Within 45 minutes after burial, the H_2 concentration on the IST sensor registered 13 ppm. The USGS sensor (which we buried also at this site) showed 20 ppm.

At Slack Canyon, 15 ppm H_2 was registered by the IST sensor and 13 ppm by the USGS sensor in 40 minutes. At Melendy Ranch, the USGS sensor left for 24 hours in a plastic pipe registered about 50 ppm.

Apparently H_2 escapes from the soil rapidly when a hole is dug, and accumulates slowly in the soil after the burial of the sensor. The fact that we did not wait for more than 15 minutes in locations where H_2 was not detected may have caused the negative results. On the other hand, serpentine fragments were recognized at Work Ranch and Slack Canyon, and Melendy Ranch is not far from an exposed serpentine mass, suggesting a possible connection between serpentine and H_2 degassing.

(2) Sato and McGee established a continuous H_2 monitoring station based on the USGS sensor at Melendy Ranch on December 21, 1980. A solar panel and lead storage battery supply the power for the pump which sends air into the sensor as a reference gas. The sensor output stabilized by Dec. 23, and started showing diurnal variations similar to those observed on radon by Chi-yi King (pers. commun.). Selected examples of the recorded data collected at Menlo Park and plotted from the computer memory by S. Schultz are shown in Figure 1.

The sensor went dead on Feb. 18, 1981. McGee visited the ranch on March 6, and repaired the open sensor wire connection. Apparently the soil column filling the pipe settled down because of rain and pulled a wire solder connection apart. In future, the sensor will be set at the bottom of a hole and a slack will be left in the cable. Lighter filling material such as plastic bubbles may also be tried.

The cause for the diurnal variations is probably the orographic winds (vertical air currents which occur daily around a mountainous terrain). Similar diurnal changes have been observed at Mount St. Helens during summer months (Sato and McGee, 1981). The diurnal changes observed at Melendy Ranch diminish on rainy days supporting the above hypothesis.

(3) The results obtained to date of the experiment at Melendy Ranch suggest that the USGS membrane-type electrochemical sensor has enough sensitivity, and that the use of more complicated detectors such as the IST solid-electrolyte sensor, the Magna ion-pump sensor, an automated gas chromatograph, and a compact mass spectrometer, are not required at this stage of investigation. Rather, the direction to go is to simplify the presently used system, such as eliminating the air pump and solar panel. Development of a sensor which does not require any electrical power or uses only extremely low power (10 mA at most) so that it can be operated on small primary batteries seems to be highly desirable.

Future Plans

Our effort in the next 6 months wll be devoted to the following goals.

(1) Developiong a membrane-type sensor system which uses no, or very little, electrical power.

(2) Instrumenting several sites from Hollister to Chalome, along San Andreas and Caraveras faults. This will probably be done during the summer.

(3) Developing the capability to extract the data stored in the Menlo Park computer memory directly in Reston through the Multics system. This would facilitate the processing of the data such as obtaining the daily average H_2 concentration to eliminate the diurnal effect.

(4) Testing and experimenting with other sensors as back-up units in case higher sensitivities are required under certain conditions.

(5) Theoretical studies on the possible role of serpentinization of ophiolitic peridotites in generating hydrogen along active faults, eventually leading to the design of laboratory experiments on the determination of hydrogen fugacity during serpentinization.

References

Sato, M. and McGee, K.A. (1981) Continuous hydrogen monitoring on the south flanck of Mount St. Helens: USGS Prof. Paper, The 1980 Eruption of Mount St. Helens.

Wakita, H., Nakamura, Y., Kita, I., Fujii, N., and Notsu, K. (1980) Hydrogen degassing: a new appraoch to fault movement: Science, v. , p. .

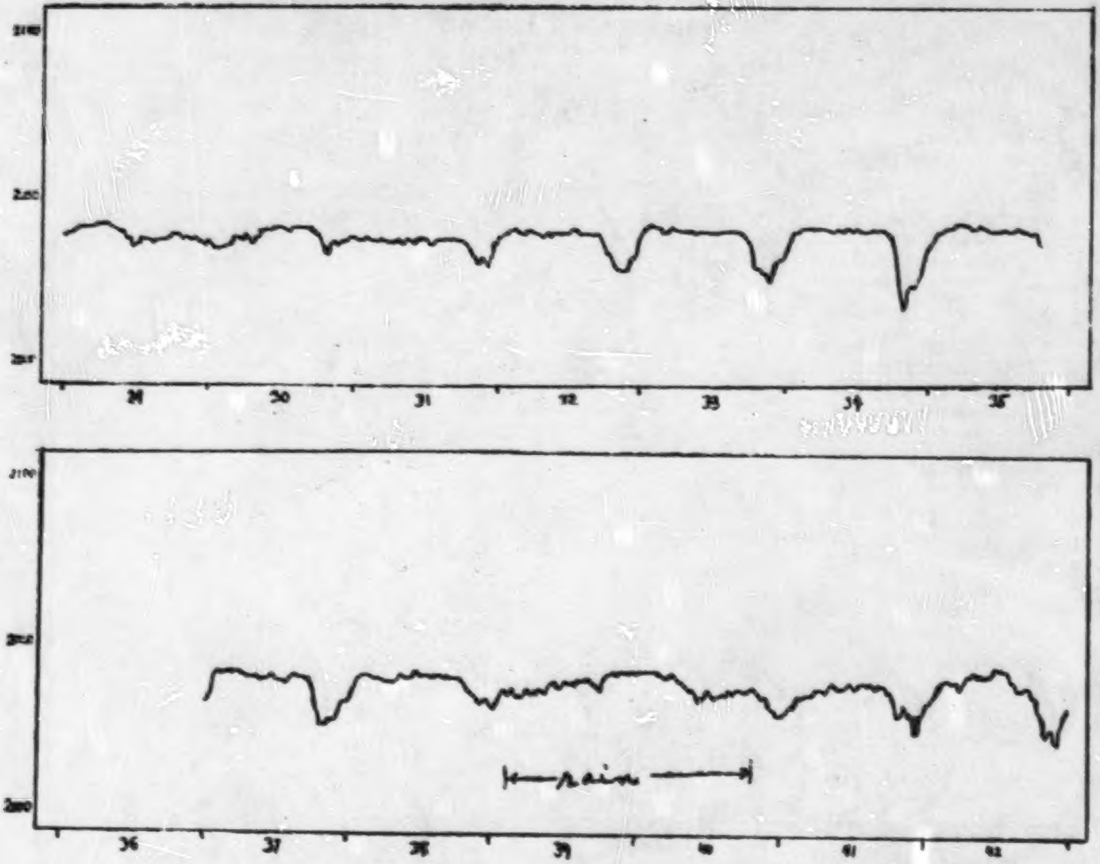

Fig. 1. Selected H_2 gas data monitored at Melendy Ranch along the San Andreas fault. The numbers on the horizontal axis indicate the julian days and those on the vertical axis the number of counts registered on the telemetry system. The data show diurnal changes in H_2 emission, the magnitude of which diminish on rainly days. The concersion of the telemetry counts to H_2 concentration has not been completed.

COMPARISON OF RADON MONITORING TECHNIQUES, THE EFFECTS OF THERMOELASTIC STRAINS ON SUBSURFACE RADON, AND THE DEVELOPMENT OF A COMPUTER OPERATED RADON MONITORING NETWORK FOR EARTHQUAKE PREDICTION

14-08-0001-17734

M.H. Shapiro, J.D. Melvin, and T.A. Tombrello
W.K. Kellogg Radiation Laboratory-Caltech
Pasadena, California 91125
(213) 356-4277

INVESTIGATIONS

During FY80 the Caltech automated radon-thoron monitoring network was expanded to include new sites at Pacoima Dam, Lake Hughes Forestry Station, Sky Forest Ranger Station, and Ft. Tejon State Historical Park. Among the technical improvements to the system during this period have been the incorporation of bi-directional telephone communication with the new monitors, improved capability for the control and monitoring of external instrumentation, and the installation of water level monitoring equipment at new sites. At the Pacoima site, in collaboration with Gulf Research, we have installed an automated gas chromatograph for the measurement of hydrogen and helium from the borehole.

Improvements also have been made in the software for routine data analysis which permit the more rapid dissemination of radon data updates to other investigators. In addition to the conventional time series presentation of the data, we now carry out spectral analysis of radon and other data on a regular basis in an attempt to better define anomalous patterns.

In collaboration with visiting scientists from the China, an expanded program of hydrogeological field work and geochemical analysis has been undertaken with the aim of determining hydrological and geochemical profiles of existing and future monitoring sites.

RESULTS

The large radon anomalies that were observed at the Kresge and Dalton Canyon sites during the second half of FY79 subsided during the early part of FY80 then reappeared in early summer and have continued to the present. In addition, there has been a substantial change in the level and character of data from the Stone Canyon Reservoir site during much of FY80. Data from the other sites appear to be following normal seasonal trends. (See Fig. 1) The 1979 radon anomalies coincided with several other anomalous geochemical, geophysical, and geodetic data, and it now appears likely that these phenomena were caused by a regional strain event to which the 6.6 M Imperial Valley earthquake may have been related.

The reappearance of the substantial radon anomaly coincides with a return to tensional strain across the San Andreas as determined by laser geodimeter and VLBI techniques. This, together with continued high levels of seismicity throughout California, would suggest that the strain event which began in 1979 is continuing. Examination of historical seismicity data suggests that such events occur sporadically, typically are of about two years duration, and are accompanied by relatively high levels of seismicity.

Several intense rainstorms occurred in southern California during the first half of FY80. Although difficult operating conditions were encountered during the winter, the automated radon-thoron network collected data with very few interruptions. As a result, the response of several sites in the system to major changes in hydrology has been determined reasonably well. The 1980-81 winter has been very dry to date. This has allowed us to continue site development and to collect data without weather related problems.Publications and Talks

REPORTS

M.H. Shapiro, J.D. Melvin, N.A. Copping, T.A Tombrello, and J.H. Whitcomb, Automated radon-thoron monitoring for earthquake prediction research, in Natural Radiation Environment III--DOE Conf-780422 (Vol. 1) 1980 p. 137.

M.H. Shapiro, J.D. Melvin, T.A. Tombrello, and J.H. Whitcomb, Automated radon monitoring at a hard-rock site in the southern California Transverse Ranges, J. Geophys. Res., 85, 3058, 1980.

M.H. Shapiro, J.D. Melvin, T.A. Tombrello, M.H. Mendenhall, P.B. Larson, and J.H. Whitcomb, Relationship of the 1979 southern California radon anomaly to a possible regional strain event, J. Geophys. Res., in press. (W.K. Kellogg Radiation Lab. preprint LiAP-36, 1980).

Jiang Fong-liang and Li Gui-ru, The application of geochemical methods in earthquake prediction in China, W.K. Kellogg Radiation Lab. preprint LiAP-37, 1980.

Jiang Fong-liang and Li Gui-ru, Experimental studies of the mechanisms of seismo-geochemical precursors, W.K. Kellogg Radiation Lab. preprint LiAP-39, 1980.

M.H. Shapiro, Comparison of radon monitoring techniques, the effects of thermoelastic strains on subsurface radon, and the development of a computer operated radon monitoring network for earthquake prediction, U.S.G.S. Open file report 80-896, 1980.

P2

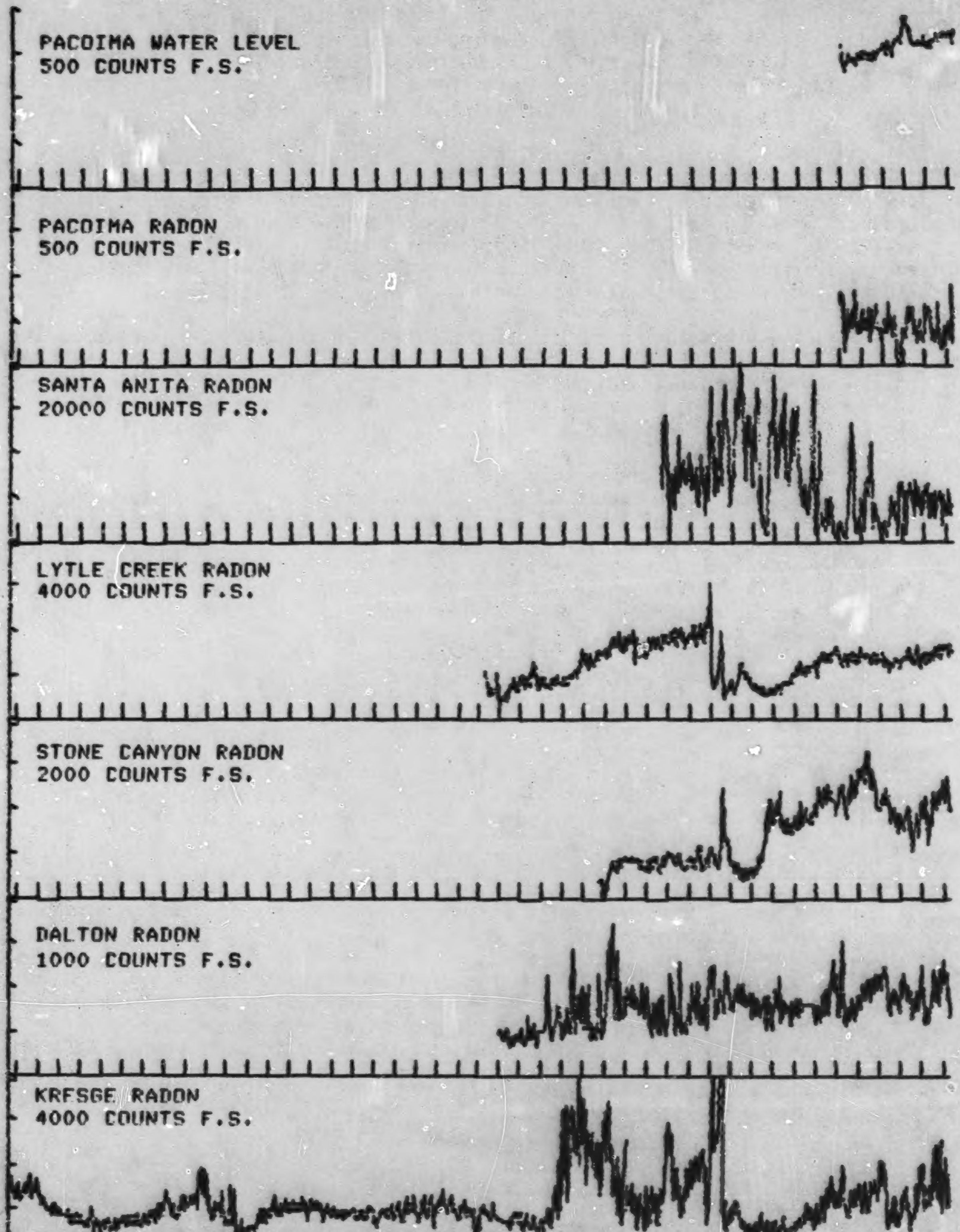
PACOIMA WATER LEVEL
500 COUNTS F.S.
PACOIMA RADON
500 COUNTS F.S.
SANTA ANITA RADON
20000 COUNTS F.S.
LYTLE CREEK RADON
4000 COUNTS F.S.
STONE CANYON RADON
2000 COUNTS F.S.
DALTON RADON
1000 COUNTS F.S.
KRESGE RADON
4000 COUNTS F.S.
1-JAN-78
1-JUL-78
1-JAN-79
1-JUL-79
1-JAN-80
1-JUL-80

GROUNDWATER RADON AND CHEMISTRY STUDIES FOR EARTHQUAKE PRECURSORS

#14-08-0001-19264

Ta-liang Teng and Douglas E. Hammond
Department of Geological Sciences
University of Southern California
Los Angeles, California 90007
(213) 743-6124

There have been no anomalies at 12 of our 13 monitoring sites during the period from October 1, 1980 to March 31, 1981. The only interesting data and possible anomaly comes from the Big Pines site at Wrightwood. This 30 meter well is in the San Andreas Fault Zone; one million liters of water are pumped each week from the well. There has been no change in the well water level (10 m) since we began sampling the well in 1976.

Figure 1 shows the radon data at Big Pines for the period between 2/10/81 and 3/17/81. A U.S.C. designed continuous radon monitoring device was installed at the site in January, 1981. The system is activated when the pump is turned on. The system counts radon for four minutes each hour during the sampling periods. The counting technique should be viewed as a relative measurement of radon content.

During the first four pumping periods shown in the figure (2/10, 2/11, 2/12, 2/14 - 2/16), the radon counts averaged 11,500 after the 2-3 hour start-up period for the instrument. This was the average mean since system start-up in January. The radon count dropped off during the sampling on 2/21, 2/23 and 2/28 and averaged 7,500 counts. During the 3/9 to 3/11 sampling period, counts rose to 9,500. During the 3/16 - 3/17 sampling counts rose to 13,500. On March 17 at 10.07 pm PST, an M=4.2 earthquake occurred at Mill Creek Canyon (34°6'N, 117°0'W). This earthquake is near the epicenter of the June 28, 1979 Big Bear earthquake (M=4.8). While we do not understand the dropoff in counts during the 2/21 to 3/10 period, a similar phenomenon was observed at our SHS site during the period of the January 1, 1979 Malibu event. After the earthquake, the radon count returned to the 9,500 level.

Before the Big Bear event, radon anomalies were observed at the Big Pines, Arrowhead Springs, and Mormon Springs sites. However, there were no similar anomalies at Arrowhead or Mormon before the Mill Creek Canyon event.

PUBLICATIONS

Teng, T. L., L. F. Sun, and J. K. McRaney (in press), Correlation of Recent Groundwater Radon Levels with Earthquakes in the Greater Palmdale Bulge Area, Geophysical Research Letters.

Hammond, D. E., T. L. Teng, L. G. Miller, and G. Haraguchi (in press), A Search for Co-variance between Groundwater Radon, Groundwater Chemistry and Seismicity in Southern California, Geophysical Research Letters.

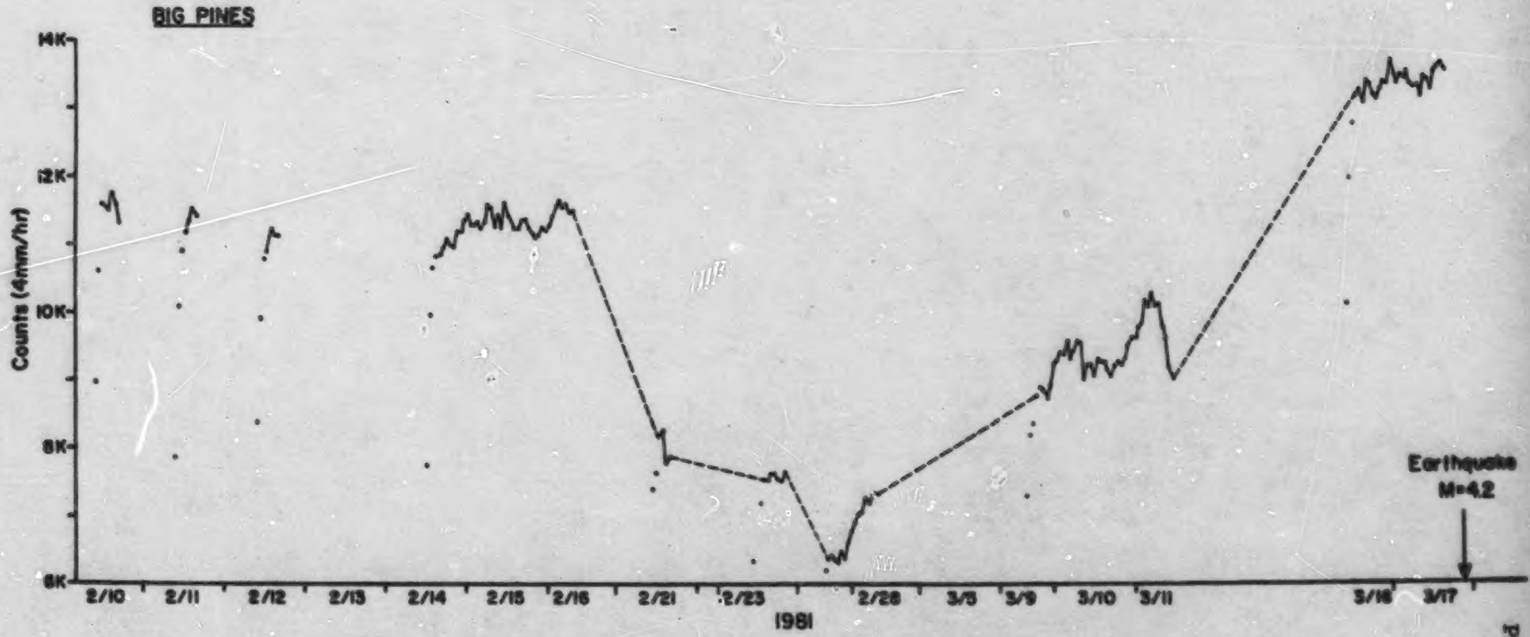

Figure 1. Data from a continuous radon meter at the Big Pines site, Wrightwood, California.

A STUDY OF TECTONOMAGNETIC METHODS AND INSTRUMENTS

14-08-0001-19140

R.H. Ware
CIRES
University of Colorado
Boulder, CO 80309
303 492-8028

Emphasis was placed on a direct field comparison of self-calibrating rubidium magnetometers (SCRs), and proton magnetometers (PMs) used by the USGS for tectonomagnetic studies. The SCRs are accurate to 0.01 nT and the PMs to 0.25 nT. Three PMs were operated at the SCR sites in Colorado. We found that the noise levels for the SCR differences were 40 db below those for the PMs, as seen in Figure 1. It is evident that the local noise levels in Colorado are considerably below the 0.25 nT PM instrument noise level. If local noise levels are comparable in California, the use of high accuracy magnetometers may increase our ability to resolve coseismic magnetic events by 40 db.

In order to explore this possibility, two SCR sites were set up in California, near San Juan Batista (SJ) and the Harris Ranch (HA). Initial results indicate that local noise levels at periods from several seconds to one hour are similar in Colorado and California. However, we have identified an additional component in the California noise spectrum at longer periods which we attribute to ocean tides. Figure 2 shows the frequency spectrum of the difference HA-QS from central California, measured by USGS PMs. The site HA is 30 km from the coast and QS is 20 km further inland. We attribute the M2 component, with a period of 1/2 lunar day, to ocean tides.

For periods greater than 1 hour, the high accuracy SCR data from SJ-HA is dominated by atmospheric and tidal noise. We intend to remove the atmospheric noise using vector data from the NASA fluxgates at HA in conjunction with a transfer function (Ware, 1979) or Weiner filter (Davis, 1980). Recent calculations show that the tidal noise correlates with the gravitational potential, and we intend to remove it using a transfer function or a filter.

Davis, P.M., D.D. Jackson, C.A. Searls, and R.L. McPherron, Detection of Tectonomagnetic events using multi-channel predictive filtering, submitted to JGR, 1981.

Ware, R.H., Precise magnetic gradiometer measurements and improved noise reduction techniques in a non-seismic zone, JGR, 84, 6291, 1979.

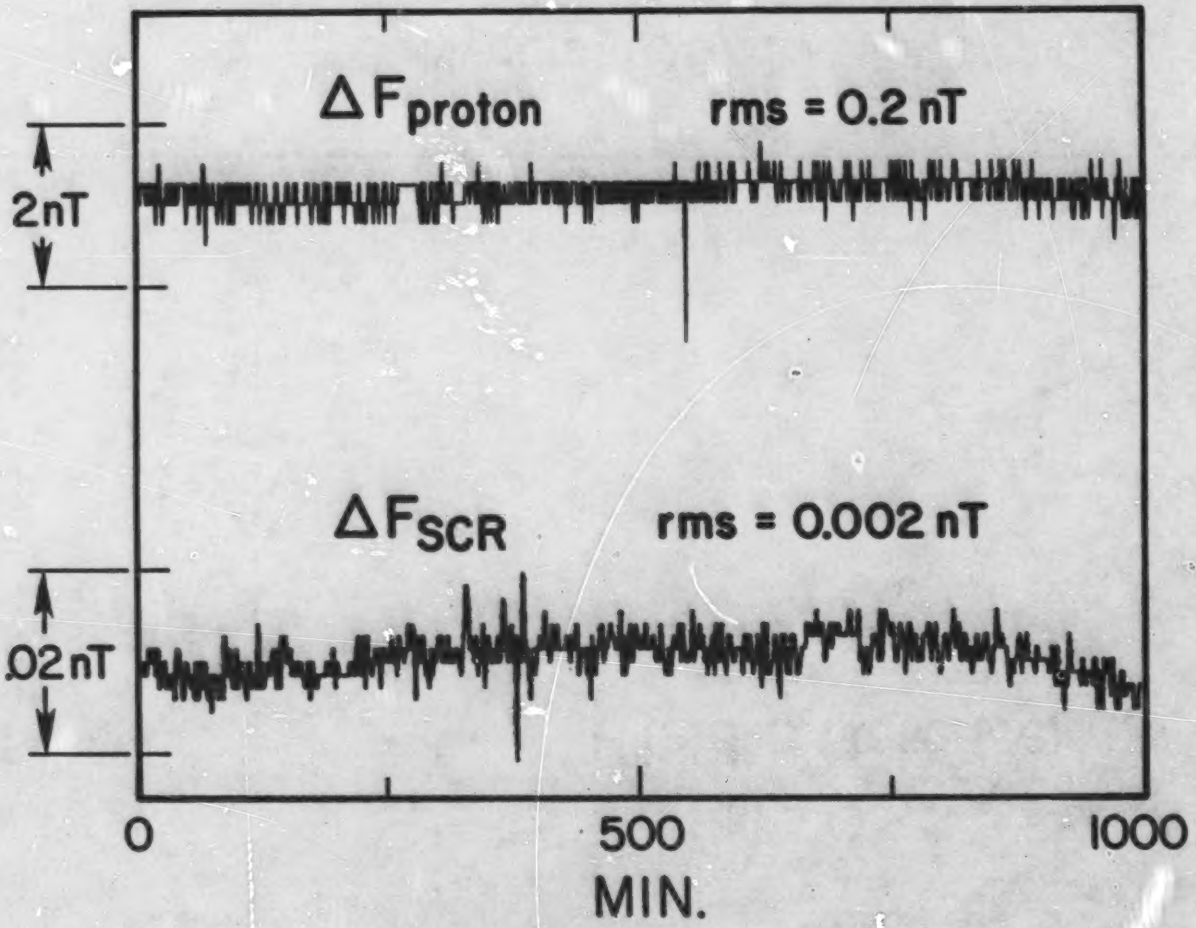

Figure 1. Total field differences observed by proton and SCR magnetometers at the same site. Baselines were 50m (PM) and 80m (SCR). The two differences were not observed simultaneously.

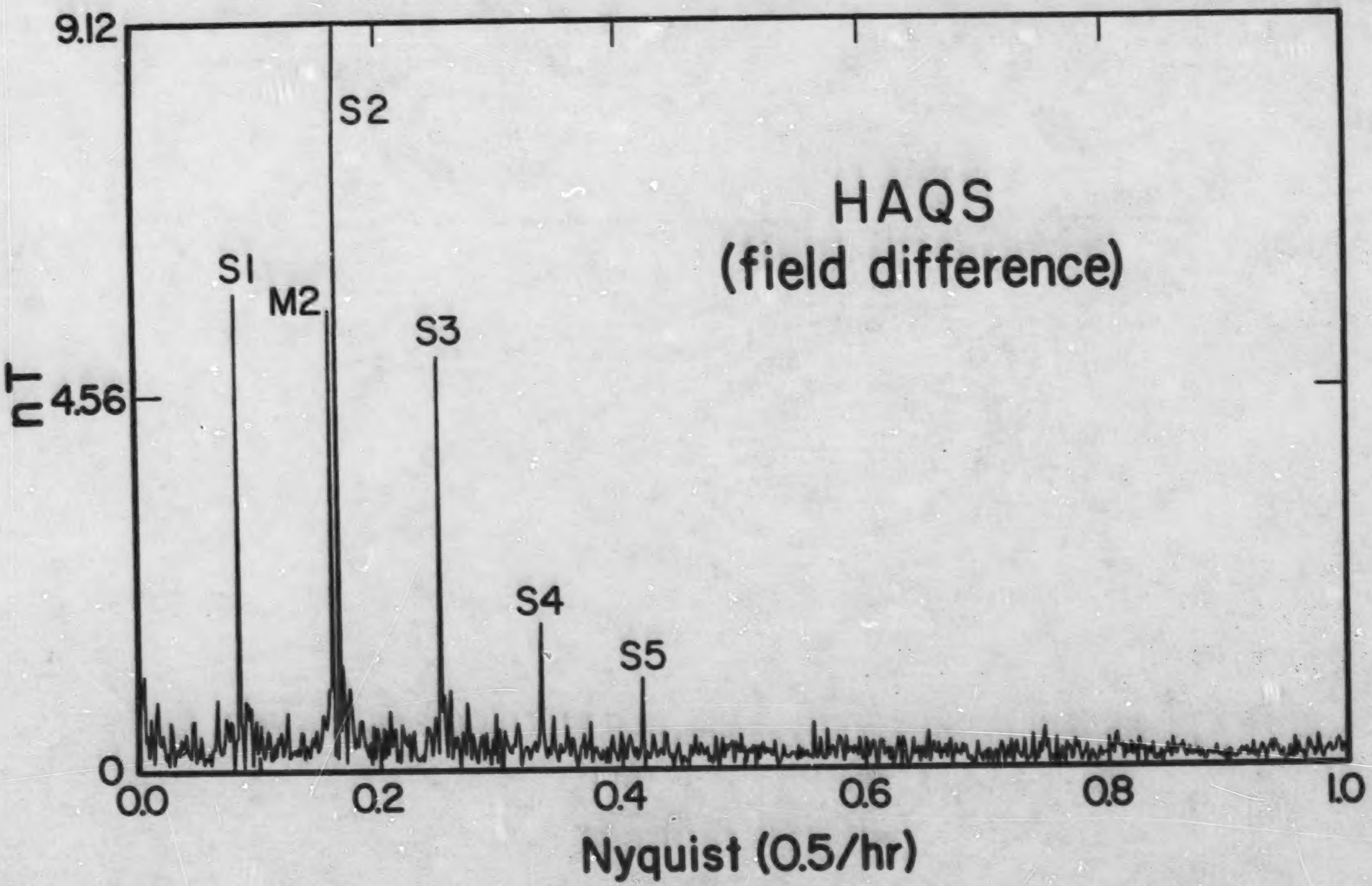

Figure 2. The amplitude spectrum for HA-QS. Two months of hourly averages, starting on 1 May 1977, were transformed. The labels on the peaks refer to lunar and solar harmonics.

F2

STOCHASTIC SIGNAL PROCESSING OF WATER LEVEL DATA

14-08-0001-18379

P. R. Westlake and J. A. Dracup
Environmental Dynamics, Inc.
1024 Pico Blvd., #101
Santa Monica, CA 90405
(213) 399-9135, -36

INVESTIGATIONS

This Semi-Annual Technical Report describes the status of the U.S.G.S. Contract #14-08-0001-18379 with Environmental Dynamics, Inc. It has been shown that precursory groundwater anomalies frequently occur prior to major earthquakes. This contract was entered into with the intention of demonstrating that contemporary stochastic processing techniques can enhance the usefulness of ground water level data by isolating any such earthquake precursors that might occur against a background of other influences which might otherwise mask the precursors.

EDI receives records from twelve wells in Southern California in which the water levels are continuously recorded. An additional 40 wells are sampled for water level on the average of once a week.

We take as input:

1) Water level
2) Barometric pressure
3) Three component tides (calculated from a NOAA Fortran program which calculates the tidal attraction).

The water level and barometric pressure records are digitized prior to processing. Details of the various procedures involved in this digitizing and the difficulties encountered are covered in this Semi-Annual Report.

BACKGROUND

Originally a considerable quantity of water level data was processed by multiple regression techniques based on an autoregressive-moving average (ARMA) process. While this ARMA model accounted for the data to within 98-99% of the fluctuation variance, it presented some difficulties. The chief difficulty was that the autoregressive terms (i.e., the water level lags) did not permit the separation of the water level precursors from the background noise level. We determined this fact by adding in various artificial precursors and examining the residuals.

RESULTS - NEW METHODOLOGY

Because of these difficulties we were forced to go to a new approach. Extensive modifications to the software were required in order to make provision for this new methodology which also permits the routine inclusion of three different types of precursors along with whatever combination of differencing, lags and trends which are appropriate. The new software to accomplish this is given in the report.

Knowing that all the regression terms had a daily deterministic component, the 34th differences were taken of all terms in a new model (34 X 42 minutes = 1 day, where 42 minutes is the sample period) prior to processing the regressions. The lags that were included in the model were based on cross-correlation calculations, and other considerations. This new model accounts for better than 90-95% of fluctuation variance. The total variation that has been accounted for is actually better than this value of R^2 (the multiple correlation coefficient) by the amount by which the 34th differencing procedure has reduced the total fluctuation variance.

This model was tested against three different kinds of artificial precursors of varying complexity and arbitrary time constants. In each case, detection of the artificial precursors in the presence of other influences was easily done.

Figure 1 shows such a combined plot of water level, water level with added artificial precursor #1 (the simplest of the artificial precursors), and artificial precursor #1. Figure 2 shows a combined plot of the residuals without this artificial precursor, residuals with this artificial precursor and the differenced artificial precursor for comparison. Figure 2 shows how readily the artificial precursor stands out in the residual time series. It is expected that anomalies will show up even more clearly as the methodology is more finely tuned.

This method, which includes the capability of generating and processing artificial precursors, allows each well to be suitably calibrated as to its sensitivity in picking up potential precursors.

This report describes the programs and procedures that are routinely used in calibrating the well sensitivity and the options that are available for the normal examination of data for the true water level anomalies. Procedures that are used for selecting the appropriate lagged variables for the regression are also enumerated.

After many problems with both the software and hardware, EDI is now progressing swiftly on the data. New software that has recently been installed at UCLA includes a new APL implementation (i.e., VSAPL) which permits much larger workspaces.

As an example of the extent to which our processing methods have been automated, when the edited files of the data are lined up in order, and have been suitably preprocessed, and we are familiar with the well characteristics, it takes only 8-12 commands at a terminal keyboard to obtain a weeks or months dataset, the regression, its statistics and any or all of 6-9 relevant plots with hardcopy on a Tektronix 4015 terminal. Software which permits all of these plots to be produced with a single command is also listed in this report.

Our methods are shown to be effective in capturing any significant water level anomalies that might occur in the presence of masking influences.

1 PLS [illegible] (Command which produces plot.)

Figure 1.

PLOT NO. 1---WATER LEVEL, WATER LEVEL WITH ART PRE. AND PRE for well #5N-12W-4H1 for the week of 1-8 May 1977
(No. 1 Precursor added in for comparison)

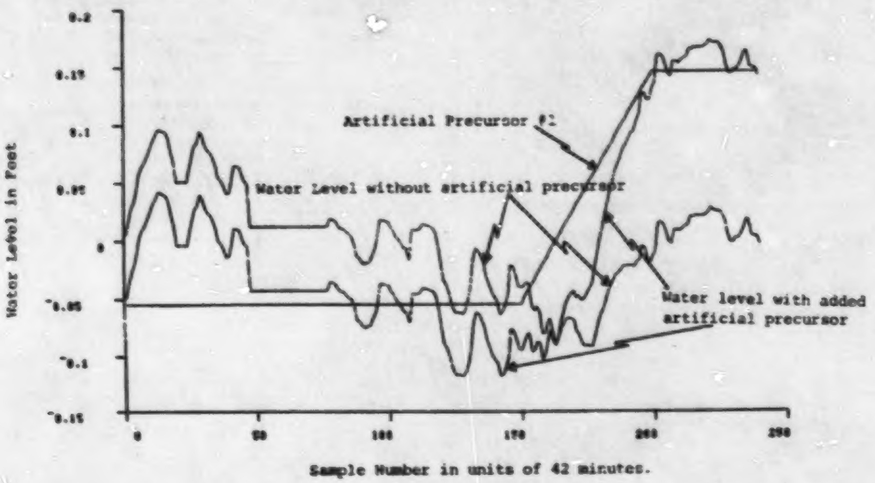

* PRE is the abbreviation for artificial precursor.

1 PLS [illegible] (command which produces plot)

Figure 2. Results of Regression for Well 5N-12W-4H1 for the Week of 3-10 May 1977.

PLOT NO.3---RES* WITH ART PRE.** RES NO PRE. PRE (WITH TREND)

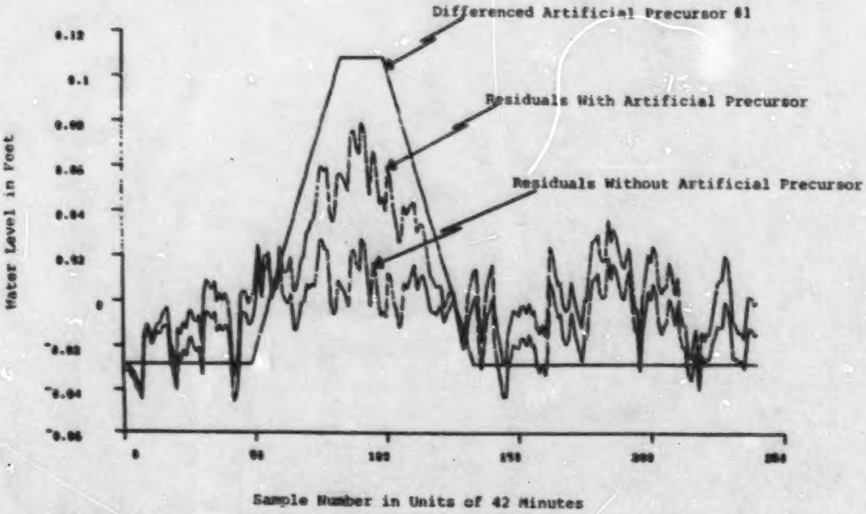

*RES is the abbreviation for RESiduals
** ART PRE is the abbreviation for ARTificial PREcursor

Digital Signal Processing of Seismic Data

9930-02101

W. H. Bakun
Branch of Seismology
U.S. Geological Survey
345 Middlefield Road, M/S 77
Menlo Park, CA 94025
(415) 323-8111, ext. 2777

Investigations

Seismograms from main shocks of earthquake sequences in 1922, 1934, and 1966 on the San Andreas fault near Parkfield, Calif. are compared to deduce differences in source characteristics, in particular differences in the velocity of rupture propagation.

Results

The epicenter of the mainshock of the 1922 Parkfield sequence lies within 7 km northwest of the common epicenter of the mainshocks of the 1934 and 1966 Parkfield sequences. The similarity in reported surface breaks extending southeast along the trace of the San Andreas fault from the common epicenter in 1922, 1934, and 1966 suggest that southeast unilateral rupture was a source characteristic common to all three shocks. Comparisons of the Love wave spectra recorded at Berkeley imply that the velocity of rupture was greater in 1922 and in 1934 than in 1966. The greater velocity of rupture in 1934 explains the greater azimuthal disparity of M_L for 1934 (M_L 6.0 for CIT vs. M_L 5.2 for BRK) than for 1966 (M_L 5.8 for CIT vs. M_L 5.5 for BRK).

Reports

Bakun, W. H., and McEvilly, T. V., 1981, Source directivity for main shocks near Parkfield, California (abs.): Earthquake Notes, v. 52, no. 1, p. 82.

Determination of Average Stress Levels on Faults in Southern California by Finite-Element Modeling

14-08-0001-19142

Peter Bird
Department of Earth and Space Sciences
University of California
Los Angeles, CA 90024
(213) 825-1126

Investigations

1. Compilation from the geologic and geophysical literatures of limits on rates of slip of southern California faults in Pliocene-Recent time.

2. Field reconnaissance of a lineament in the Little San Bernadino Mts., California.

3. Assembly of a block-model approximation of Recent southern California tectonics.

4. Testing of isoparametric- and fault-element additions to the plane-stress, nonlinear-rheology finite-element code that will be used in further modeling.

Results

1. A search was made for separations of distinctive rocks of Late Miocene to Recent age. Historic offsets determined geodetically were not included because they do not average enough earthquakes. Offsets of older rocks were not included because rates proabaly changed at the beginning of the Pliocene. Separation was assumed equal to slip on strike-slip faults, and equal to the vertical component of slip on dip-slip faults. Within these limits, some 63 references to upper, lower, or paired limits on fault slip rate were found; these are shown in Figure 1. After discounting inconsistent or redundant information, some 30 useful values remain.

2. A prominent valley lineament from Yucca Valley to Durmid, California which was suspected of being an active but unmapped fault was investigated. Four days of field work revealed that the lineation is due to preCambrian(?) bedding surviving through Mesozoic intrusive events. Uncut Pleistocene(?) gravel terraces prove that there is no Recent slip on this feature.

3. In order to provide boundary velocity conditions for the upcoming finite element models, the block model of Fig. 2 was compiled as an approximation of Recent tectonics. The RM2 Pacific/No.American pole of Minster and Jordan (1978) was used as a constraint. Interesting features include the rapid Transverse Ranges thrusting and lack of rotation except in the Mojave.

4. Isoparametric elements with curved sides proved error-free in uniform strain tests. Fault elements with nonlinear resistance are being programmed.

Report: Bird, Peter (1980) EOS Trans. AGU, 61, #46, p. 1125-6 (abstract).

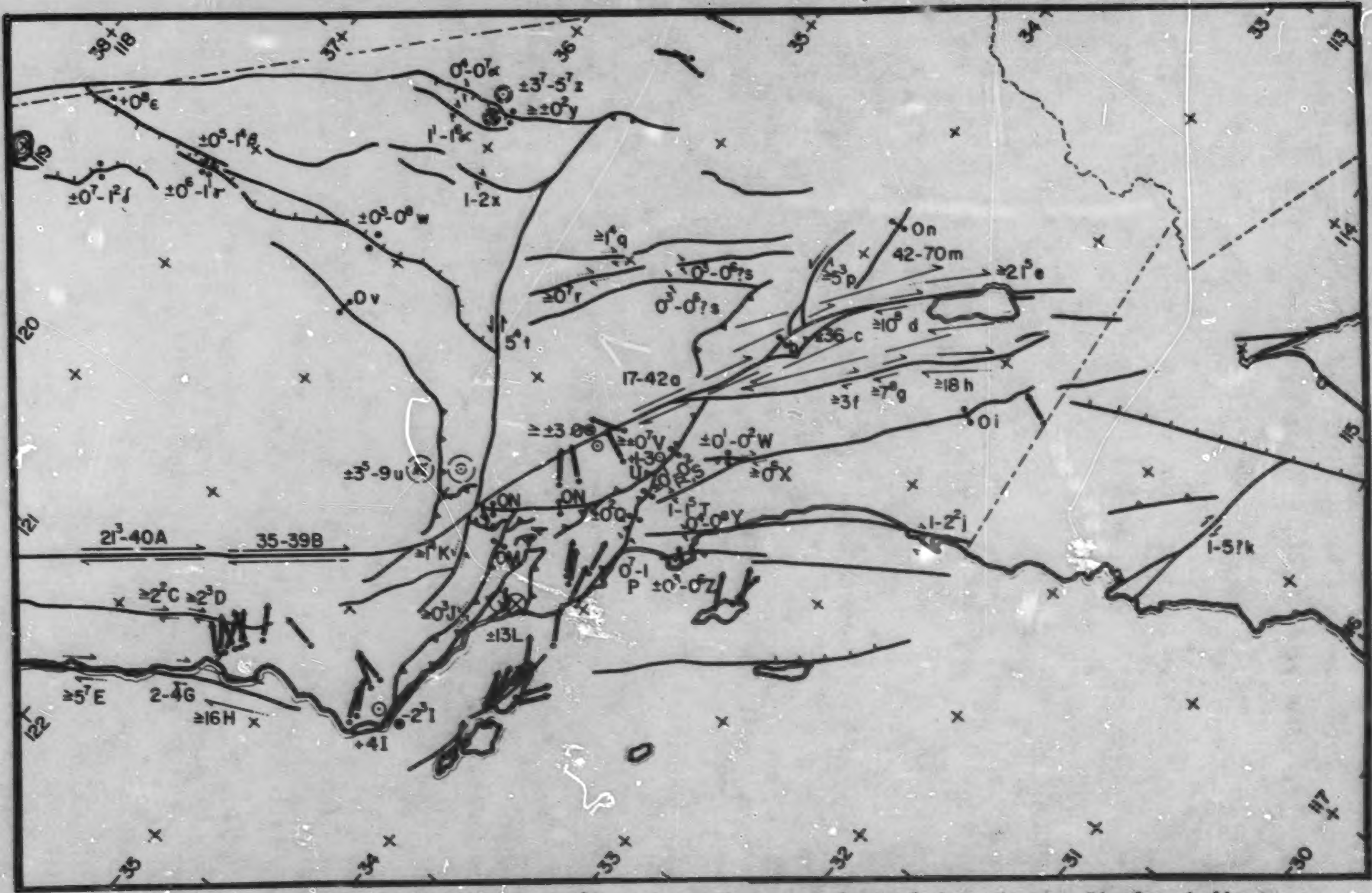
38 118
37
36
35
34
33
113
119
120
121
122
114
115
117
$0^6-0^7\kappa$
$\pm3^7-5^7z$
$\geq\pm0^2y$
$1^1-1^6\kappa$
1-2x
$+0^8\epsilon$
$\pm0^5-1^4\beta$
$\pm0^7-1^2\delta$
$\pm0^6-1^1\gamma$
$\pm0^3-0^8w$
0v
5^4t
$\geq1^4q$
$\geq0^7r$
$0^3-0^6?s$
0n
42-70m
$\geq5^3p$
$\geq21^5e$
$\geq36c$
$\geq10^8d$
17-42a
$\geq3f$
$\geq7^6g$
$\geq18h$
0i
$\geq\pm3.0a$
$\geq\pm0^7V$
$\pm0^1-0^2W$
$\geq0^6X$
$\pm3^5-9u$
0N
$1-1^5T$
0^4-0^9Y
$1-2^2j$
$1-5?k$
21^3-40A
35-39B
$\geq1^6K$
0W
0^7-1
P
$\pm0^5-0^8Z$
$\geq2^2C$
$\geq2^3D$
$\pm0^3J$
$\pm13L$
$\geq5^7E$
2-4G
$\geq16H$
+4I
-2^3I
35
34
33
32
31
30

Figure 1. Compiled rates of fault slip in mm/a. Superscripts are decimal fractions. Circles indicate vertical components and arrows indicate strike-slip components proportional to their size. A sign indicates absolute vertical motion and ± indicates relative motion. Heavy arrows are paleomagnetic declinations from the literature. Letters are keys to references in the full version of this report.

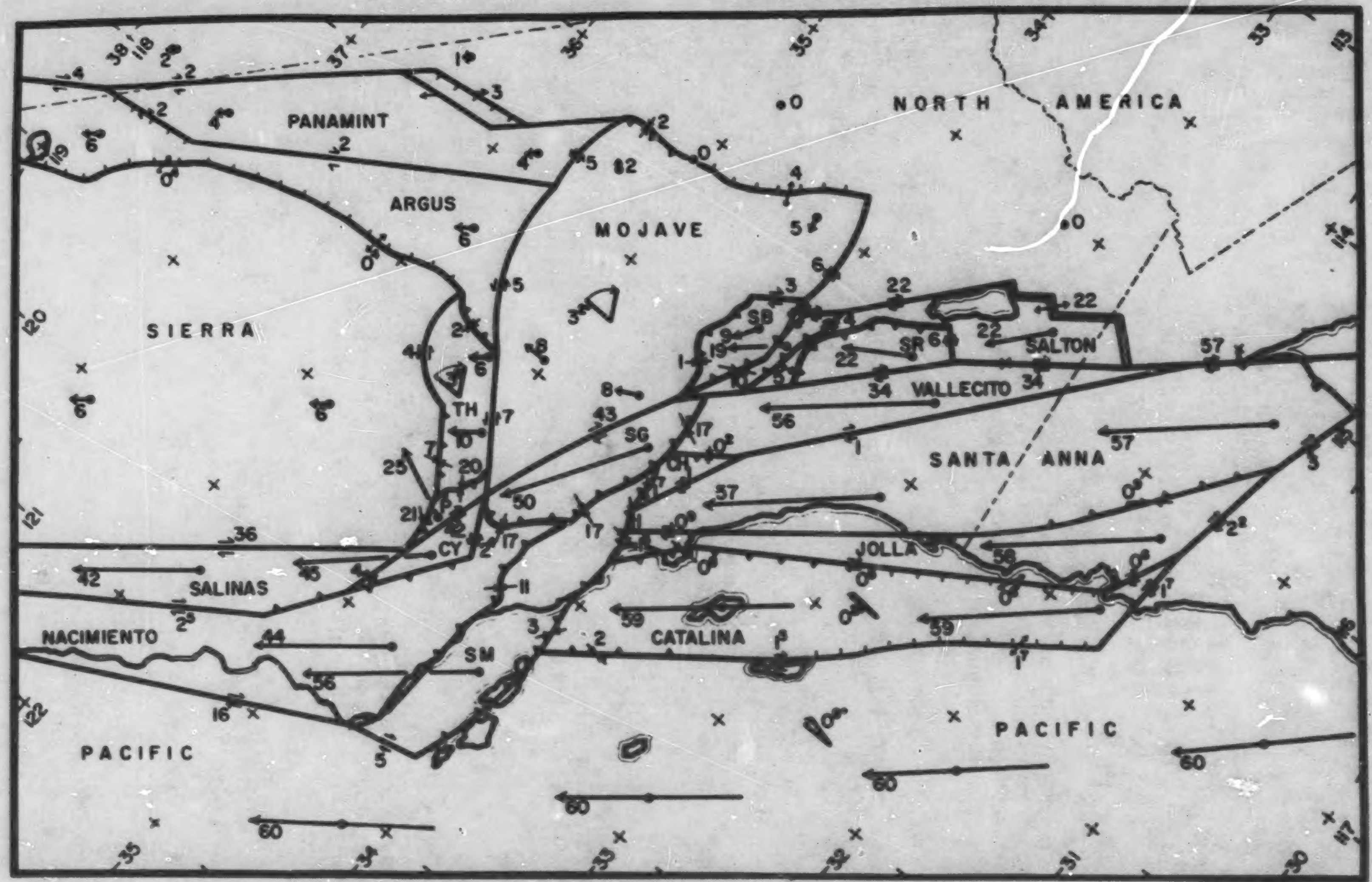

NORTH AMERICA
PANAMINT
ARGUS
MOJAVE
SIERRA
TH
SB
SR
SALTON
VALLECITO
SG
CH
SANTA ANNA
CY
JOLLA
SALINAS
NACIMIENTO
SM
CATALINA
PACIFIC
PACIFIC

Figure 2. A block model approximation of Recent southern California tectonics. All rates in mm/a, with decimal fractions as superscripts. Internal vectors are motion with respect to North America at the point indicated. They have length proportional to magnitude; relative motion vectors do not. Rotation rates for the Mojave, Tehachipi, and Catalina blocks in degrees/10^6 years; others do not rotate.

ROCK MECHANICS

9960-01179

James D. Byerlee
Branch of Tectonophysics
U.S. Geological Survey
345 Middlefield Road, M/S 77
Menlo Park, California 94025
(415) 323-8111, Ext. 2453

Investigations

Laboratory experiments are being carried out to study the physical properties of rocks at elevated confining pressure, pore pressure, and temperature. The goal is to obtain data that will help us to determine what causes earthquakes and can we predict or control them.

Results

Changes in permeability of granite were measured as water flowed through samples in a temperature gradient. Temperature was maintained between 200 and 300°C, in a borehole of a cylindrical sample. Confining pressures of 30 and 60 MPa, with corresponding pore pressures of 10 and 20 MPa, simulated depths of burial of 1.2 and 2.5 km, respectively, A small pore pressure gradient enabled distilled water to flow from the borehole (high temperature) to the outside of the sample (low temperature). Tests were run for intact samples with initial permeabilities of several hundred nanodarcies, and for samples containing through-going fractures, with initial permeabilities of a millidarcy. In all cases, permeability decreased between one and two orders of magnitude at a rate that increased with higher temperatures. At 200°C, permeability dropped by an order of magnitude over a one month period, whereas at 310°C, permeability dropped sharply within a few days to 5% of the initial value. The dissolution of quartz and feldspar and redeposition of these minerals within cracks at lower temperature was found to be the major cause of reduction of permeability.

Chemical analyses were made of the aqueous fluids flowed through samples of Barre Granite and Westerly Granite held in a temperature gradient. Deionized and redistilled water was used in all experiemtns. The pH of the recovered solutions at room temperature ranged between 6.7 and 7.8. To date, analyses have been conducted for the cations Na^+, K^+, Ca^{2+}using atomic absorption techniques, and for the anions Cl^- and HCO_3 using an ion chromatograph and carbon analyzer, respectively. For nearly all fluid samples collected from Barre Granite, $Na \geq Ca >> K >> Mg$, and $Cl > NCO_3$. For fluid samples from Westerly Granite, $Ca > Na > K > Mg$, and $HCO_3 > Cl$. High initial concentrations was as much as 750 ppm (for Cl from Barre Granite in a T gradient of 250-80°C) of each dissolved species were found in all experiments, followed by rapid decreases for as much as 6 days. Thereafter, the rate of decrease slowed considerbly, and final concentrations were stabilized at 5-20 percent of the initial values. These changes in ionic concentrations are directly correlated with the measured permeability decreases for the experiments. For the same granite type, the final permeabilities and ionic concentrations are slightly higher for higher T experiments. For the same conditions of T and confining and pore pressure, higher total ionic concentrations but lower permeabilities were obtained with Barre than with Westerly Granite. The marked decrease of dissolved materials in the fluids with decreasing permeability may be due to the correspondingly greater amount of time for chemical reaction at low temperatures in the samples. The final concentrations may represent "equilibrium" solubilities at the low-temperature, outlet sides of the samples, these solubilities increasing with increasing outlet temperature.

The permeabilities of 4 clay-rich San Andreas fault gouges (taken from surface and borehole depths to 408 m), a serpentinite fault gouge from San Francisco, and 2 pure clays were measured at confining pressures from 5 to 200 MPa and during shearing with shear displacement up to 9 mm at 200 MPa confining pressure. Samples consisted of 1 mm thick gouge layers placed between 30° sawcut surfaces of sandstone cylinders 25.4 mm in diameter and 63.5 mm in length. Permeability was strongly dependent on grain size distribution. Homogeneous, fine-grain San Andreas gouge (98.6% grain diameters < 0.075 mm) taken from borehole depth of 408 m, had a permeability < 1.0 nD at 200 MPa confining pressure, whereas the serpentinite gouge with mixed grain sizes (grain diameters ranged from 0.09 mm to 1 mm) was 2 orders of magnitude more premeable. Permeabilities for San Andreas gouges ranged from 2.1 to 22 nD at 50 MPa confining pressure and from 0..3 to 2.3 nD at 200 MPa. Only a fraction of the permeability (typically 50%) was recoverable, upon unloading confining pressure. In addition, samples were deformed in steps and at each step permeability was measured in 2 ways: at constant differential stress and after unloading differential stress. The permeabilities obtained by these two methods were in close agreement with each other. In all cases, application of differential stress reduced premeability (23 to 87%). This reduction in permeability was primarily due to increased normal stress and was nearly independent of the amount of shearing. That is, most of the decrease in permeability occurred when differential stress was first applied and normal stress was increasing rapidly.

We have studies the shear deformation of thick layers of granular silicate aggregates at high confining pressure. Increased strain rates resulted in increased frictional strength for confining pressures greater than 100 MPa. This result is consistent with a physical model of macroscopic shear being produced by time dependent cracking causing dilatancy and rearrangement of gouge grains. At very low normal stresses other workers have found the opposite effect, that is, increased strain rates resulted in decreased frictional stress. In an attempt to reconcile these seemingly contradictory results we have conducted a series of deformation experiments on granular silicate aggregates at low confining pressure. Specimens consisted of cylindrical samples, 63.5 mm long and 25.4 mm diameter, of 20-30 mesh quartz sand. Time dependent compaction at confining pressures to 400 MPa was studiedunder constant pore water pressure of 2 MPa. Pore pressure, monitored with a servo-controlled pressure generator, decreased with increased confining pressure in all cases. The loss of pore volume, however, was greatest at low pressure (from 2 cm^3 at 20 MPa confining pressure to 0.1 cm^3 at 380 MPa confining pressure from an initial pore volume of 10 cm^3. Time dependent shortening of cylindrical specimens of granular quartz was studies at 30 MPa confining pressure and under both dry conditions, and at constant pore water pressures of 2 MPa. At low differential stress creep resulted in little or no grain cracking and pore volume decreases. Large amounts of grain cracking and pore volume increases occurred at elevated differential stresses. These results suggest that the dominant process controlling the shearing of granular silicate aggregates at low confining pressures and differential stresses may be time dependent compaction and grain rearrangement.

Reports

Morrow, C., Lockner, D., Byerlee, J. D., 1980, Fluid flow through granite in a temperature gradient: I. Permeability (abs.): EOS, American Geophysical Union Transactions, v. 61, no. 46, p. 1112.

Moore, D., Morrow, C., Byerlee, J. D., 1980, Fluid flow through granite in a temperature gradient: II. Fluid chemistry (abs.): EOS, American Geophysical Union Transactions, v. 61, no. 46, p. 1112.

Solberg, P., Byerlee, J. D., 1980, Deformation of granular silica aggregates, (abs.): EOS, American Geophysical Union Transactions, v. 61, no. 46, p. 1116.

Shi, L. Q., Morrow, C., Moore, D., Byerlee, J. D., 1980, Permeability of fault gouges under confining pressure and shear stress (abs.): EOS, American Geophysical Union Transactions, v. 61, no. 46, p. 1120.

Baker, P., Kastner, M., Byerlee, J. D., Lockner, D., 1980, Pressure solution and hydrothermal recrystallization of carbonate sediments--an experimental study, Marine Geology, v. 38, pp. 185-203.

Earthquakes and the Statistics of Crustal Heterogeniety

9930-03008

B. R. Julian
Branch of Seismology
U.S. Geological Survey
345 Middlefield Road - MS-77
Menlo Park, California 94025
(415) 323-8111, ex. 2931

Investigations

Most efforts have been directed toward obtaining information on spatial coherence of seismic waves, from which information about crustal heterogeneity can be inferred.

1) Toward the end of the period, I have participated in a branch-wide effort to quantify various aspects of earthquake magnitudes, with the aim of understanding the physical wave-scattering process responsible for coda waves.

2) In addition, methods for inferring earthquake focal mechanisms and in-situ stress orientation from seismic data have been improved.

Results

1) An elaborate computer system for organizing, analyzing and displaying digital seismic data has been obtained from M.I.T.'s Lincoln Laboratory and brought into operation on the UNIX computer system in Menlo Park. This system has been modified in several ways to handle USGS seismic data, take adavantage of high-speed graphics hardware, measure spectral levels interactively, etc.

2) Linear programming methods for inferring earthquake focal mechanisms have been extended to use seismic wave amplitude data (either signed or absolute) as well as first motions.

3) The problem of inferring in-situ stress orientation from seismic-wave first motions has been formulated as a quadratic programming problem.

Project Title: Stress Analysis of Deeply Eroded Analogs of the San Andreas Fault (A Renewal)

Contract Number: 14-08-0001-19119

Principal Investigators: David L. Kohlstedt (607-256-7144)
John M. Bird (607-256-6437)

Institution: Cornell University
Ithaca, New York 14853

We have been studying deformation-induced microstructures in quartzo-feldspathic rocks from the Nordre Stromfjord shear zone in western Greenland. The shear zone extends for 150 km, from the west coast of Greenland towards the ice cap. The width of the shear zone decreases from $\sim$15 km at the coast to $\sim$6 km at the ice cap. Rocks from the western half of the shear zone are metamorphosed to granulite facies; rocks from the eastern half of the shear zone are metamorphosed to amphibolite facies. We are studying microstructures in samples from three measured collections across the shear zone, one section made in granulite facies rocks, one section in amphibolite facies rocks, and one section near the transition from granulite to amphibolite facies. The rocks in this shear zone are primarily biotite gneisses composed of plagioclase (An_{25-40}), quartz, alkali feldspar, biotite, and, in the granulite facies rocks, orthopyroxene. We have been studying the microstructures in quartz, plagioclase, and hornblende grains from our three measured collections.

Rocks from the western part of the shear zone (granulite facies) are strongly deformed. Quartz grains are elongated and show undulatory extinction, deformation bands, and extensive subgrain development. Feldspar grains are somewhat elongated and show development of deformation twins and subgrains. Both the quartz and feldspars are commonly recrystallized along grain boundaries; as much as 30% of many samples are recrystallized. Samples from the eastern part of the shear zone (amphibolite facies) appear to be less deformed. Quartz and feldspar grains are more equant and are not recrystallized. We suggest that the rocks from the eastern part of the shear zone may have undergone more extensive post-deformational annealing than rocks from the western part of the shear zone, possibly because of the higher water content in the amphibolite facies rocks.

We have made a detailed transmission electron microscopy study of defects in plagioclases in order to evaluate the possibility of using microstructural data from the plagioclases as a paleopiezometer. Many quartzo-feldspathic rocks can be viewed as being built up of a stress-supporting framework of feldspars with quartz (and other minerals) situated in interstices in the framework. It is, therefore, probably more appropriate to use the microstructural data from feldspars rather than from quartz in order to apply paleopiezometers to quartzo-feldspathic rocks. For quartz the free dislocation density usually varies by a factor of two among grains in any sample. However, for plagioclase the free dislocation density may vary by factors of up to fifteen among grains in any sample. We have, therefore, decided that it is not possible to use dislocation densities from the plagioclases to evaluate stress levels along the shear zone. We have measured dislocation densities in quartz grains in samples from the three measured sections across the shear zone. In quartz grains from the granulite facies rocks the free dislocation density varies from 5 to $10x10^8 cm^{-2}$, corresponding to a differential stress of 1.5 to 2.0 kbar. The free dislocation density in quartz grains from amphibolite facies rocks varies from 3.5 to $8x10^8 cm^{-2}$, corresponding to a stress of 1.2 to 1.9 kbar. At the transition between the two facies the free dislocation density in quartz grains varies from 1 to $5x10^8 cm^{-2}$, corresponding to a stress of 0.7 to 1.5 kbar. We have found no difference in dislocation density between samples from within the shear zone and samples in the regions outside the shear zone.

These results suggest that there is no stress concentration in the shear zone and that there is a stress minimum at the transition from amphibolite to granulite facies rocks within the shear zone. It is known that the dislocation density is easily altered by post-deformational annealing or by a late, high-stress pulse, so that stress levels obtained from measuring free dislocation densities may not reflect the stress level of the main deformation event along the shear zone. In order to check this possibility we have begun measuring subgrain sizes in quartz grains from the same samples in which we measured free dislocation densities. In quartz from granulite facies rocks the average subgrain size is 4 microns, corresponding to a differential stress of 0.5 kbar. In quartz grains from the transition zone (from amphibolite to granulite facies) the average subgrain size is 5 microns, corresponding to a stress of 0.4 kbar. Subgrain sizes in samples collected outside the shear zone, but in the same region as the transition zone, average 10 microns, corresponding to a stress of 0.2 kbar.

We are continuing this study of subgrain sizes in quartz and will measure subgrain sizes in the amphibolite facies samples. We believe that the subgrain sizes more accurately reflect the differential stress during the major deformation event along the shear zone. The results of the subgrain study suggest that there might have been a stress gradient going from amphibolite facies to granulite facies deformation. By completing this detailed study of subgrain sizes we should be able to determine the paleostress distribution across and along the shear zone during the main deformation event.

Publications

Kohlstedt, D.L., and Weathers, M.S., 1980, Deformation-induced microstructures, paleopiezometers, and differential stresses in deeply eroded fault zones: Jour. Geophys. Res., v. 85, p. 6269-6285.

Olsen, T.S., and Kohlstedt, D.L., 1981, Dislocations in some naturally deformed plagioclase feldspars: Trans. Amer. Geophys. U., v. 62, p. 395.

Large Scale Laboratory Contained Fracture Experiment

9960-02941

David A. Lockner
Branch of Tectonophysics
U.S. Geological Survey
345 Middlefield Road,, M/S 77
Menlo Park, California 94025
(415) 323-8111, Ext. 2479

Investigations

1. Determination of source parameters during unstable sliding on a fault. Producing contained fracture events by altering the stress field along the fault.

2. Measuring heat generated during unstable sliding on a fault and relating this to the total energy released during sliding.

Results

1. Water injection system which will be used to alter the local stress field on the fault is in final stages of construction. The sample is currently instrumented and awaiting installation of the pore pressure system.

2. Temperature transients accompanying unstable sliding have been measured at distances from 0.3 to 1.1 cm from the fault. Heat generated was proportional to total energy release over the entire range of experiments (up to 6.5 mcal/cm^2; and normal stress up to 4.4 Mpa). Comparison to temperature data to results of a 1-dimensional numerical heat flow model indicates that heat generated is 85 to 95 percent of the total work done. This suggest that seismic efficiency is 5 to 15 percent.

   Analysis of the numerical model also indicated that the temperature rise on the fault is sensitive to the precise sliding history, but that to a first approximation, it is 0.1°C per mcal/cm^2 total energy release.

Reports

Lockner, D. A. and Okubo, P., 1981, Laboratory measurements of heat generated during unstable sliding in granite, (abs.) EOS: (Trans. of the Amer. Geophys. Journal), v. 62, no. 17, p. 400.

Theoretical Mechanics of Earthquake Precursors

9960-02115

Gerald M. Mavko
Branch of Tectonophysics
U.S. Geological Survey
345 Middlefield Road, M/S 77
Menlo Park, California 94025
(415) 323-8111, Ext. 2756

Investigations

1. Constructed and performed parametric studies on two-dimensional models of faults in the Hollister, California, area. The models simulate the elastic (and geometric) interaction of faults and predict, in particular, the effects of localized earthquake slip on nearby creep and geodetic measurements.

2. Studied theoretical models of one-dimensional and two-dimensional faults, incorporating fault zone constitutive laws inferred from laboratory measurements of frictional sliding.

Results

1. Model simulations were made to help clarify the relations among seismicity, fault creep, and fault trace geometry. In the model, fault strength obeys a pressure dependent law, which is assumed to have the form of a constant coefficient of friction. A steady slip rate model was found that predicts the spatial variation of slip rate in the region of interaction of the Calaveras, Paicenes, and San Andreas faults, in close agreement with geodetically determined slip rates. The distribution of fault stress and the orientations of maximum shear stress predicted by the model will be used to interpret observed seismicity and earthquake focal mechanisms.

2. These model simulations were made to explore the effect of laboratory-inferred friction laws on the sliding behavior of in situ-scale faults. The fault zone "frictional" strength is characterized by two competing effects: an instantaneous dependence of fault strength on velocity (strength increases with velocity); and also an inverse dependence of strength on velocity that takes full effect only after a finite amount of slip has occurred. 2-D simulations in a plate predict recurring rapid

strike-slip events, similar in size to the 1906 San Francisco earthquake, separated by periods of strain accumulation. The modeled slip rate and frictional dissipation rate in the rupture zone fall off as 1/(time) during the year or so after each event similar to the observed frequency of aftershocks. The predicted slip rate in the rupture zone then drops to an order of magnitude or more below the long term average slip rate, giving the appearance of a locked fault. Finally, the model predicts accelerated slip from the surface down to seismic depths during the year preceding the next earthquake.

Reports

Mavko, G., 1980, Simulation of creep events on a spatially variable model, EOS, Transactions American Geophysical Union, 61, 1120.

Bounds on Lower Crustal Rheology

9960-02414

Marcia McNutt
Branch of Tectonophysics
U.S. Geological Survey
345 Middlefield Road, M/S 77
Menlo Park, California 94025
(415) 323-8111, Ext. 2479

Investigations

Topography on the earth's surface represents a departure from hydrostatic equilibrium which must be supported by stress differences within the earth. Gravity anomalies correlated with topography provide clues as to the magnitude and distribution of deviatoric stress and thus place lower bounds on the strength of crustal and upper mantle materials. The purpose of this investigation was to develop simple means of parameterizing observations to compare with theoretical predictions from proposed rheological models. Topography and gravity data from oceanic regions were selected for the initial study because the simple geologic and thermal history of the ocean basins increases the signal-to-noise ratio in the data.

Results

Wherever the oceanic lithosphere is sharply bent, such as at convergence zones and under the weight of islands and seamounts, the surrounding region is deformed into obvious deeps and arches which show up distinctly in the topography and in the gravity data. The deformation pattern is commonly interpreted in terms of elastic-plate flexure, which nevertheless is an unsatisfactory model from the standpoint that it assumes unbounded strength and predicts deviatoric stresses exceeding 10 kbars in the oceanic lithosphere. Attempts to model the deformation with more realistic brittle/elastic/ductile rheologies are time consuming and to some extent inconclusive in that enough new, free parameters are introduced to ensure consistency with the data.

In this study we parameterized the flexure data in terms of the moment and curvature at the first zero crossing of the gravity or bathymetry profile seaward of the subduction zone or seamount load. The observed moment consists of the integral of the gravity anomaly weighted by the distance from the zero crossing, and it can be directly compared to theoretical moments from rheological models describing strength as a function of depth within the lithosphere. The advantage of this technique is that it places tighter constraints on parameters in the rheological models because moment/curvature observations from many regions must be simultaneously satisfied.

The principal conclusion from this study is that the oceanic lithosphere is just a little bit weaker than extrapolation of laboratory experiments would lead us to believe. The activation energy for ductile flow, Q, measures how hard it is to deform earth materials. The commonly quoted value for a dry olivine rheology is Q = 125 kcal/mole. We find that the ratio Q/RT, where R is the gas constant and T is temperature in °K, is of the order of 60 (dimensionless units). Taking into account published geotherms for the oceanic lithosphere based on heat flow, geothermometry, and thermal plate models, we conclude that Q for the oceanic lithosphere is no more than 100 kcal/mole. This low value for the activation energy implies that either trace amounts of water must be present in the upper mantle to significantly weaken the rocks, or additional dislocation mechanisms not observed at laboratory strain rates must contribute to deformation at low temperatures over geologic time scales.

Reports

McNutt, M. K. and H. W. Menard, Improving estimates of the temperature at the base of the elastic lithosphere from flexure studies, EOS, Trans. Amer. Geophys. Union, 61, 1123, 1980.
(manuscript to be submitted to Geophys. J. Roy astr. Soc by 7/1/81.)

Rocks under Geothermal Conditions

9960-01490

L. Peselnick and H.-P. Liu
Branch of Tectonophysics
U.S. Geological Survey
345 Middlefield Road, M/S 77
Menlo Park, California 94025
(415) 323-8111, Ext. 2393

Investigations

1. Development of direct stress-strain apparatus for determination of internal friction of rocks at seismic frequencies (0.01 to 1 Hz) and at seismic strain amplitudes (0.01 to 1.0 microcm/cm).

2. Construction of linear compressibility apparatus for determination of elastic anisotropy of rocks resulting from cracks.

Results

1. The frequency range of internal friction (1/Q) measurements was extended by a factor of 10. The range is now 0.01 Hz to 1.0 Hz. This was accomplished by maintaining constant temperature in the apparatus to within 0.001 degrees C.

2. At present there is no standard material for Q's in the range of 10 to 200 for purposes of calibration. The Q of a sample of lucite was obtained for the frequency range of 0.01 to 2.0 Hz. The frequency dependence of Q for the lucite was observed to have a single maximum at about 0.4 Hz. The results do not agree with measurements by Spencer (1981). The discrepencies could be a result of differences in annealing, sample size and geometry, if the dominant mechanism is theromoelastic loss.

3. A minicomputer was acquired for automatic processing of the internal friction data. This permits rapid reduction of the data.

4. An apparatus has been completed to determine linear compressibility as a function of direction in rocks for strains less than 1 microcm/cm. Testing of the apparatus is underway.

Reports

Spencer, J. W., Stress relaxations at law frequencies in fluid-saturated rocks: attenuation and modulus dispersion, J. Geophys. Res. 86, 1803-1812, 1981.

Mechanics of Geologic Structures Associated with Faulting

9960-02112

David D. Pollard, Paul Segall and Atilla Aydin
Branch of Tectonophysics
U.S. Geological Survey
345 Middlefield Raod, M/S-77
Menlo Park, California 94025
(415) 323-8111, Ext. 2932

Investigations

1. Field mapping and thin section investigation of strike-slip faults and related structures in granitic rocks.

2. Field and theoretical investigation of the process of fracture and jointing in granitic rocks.

3. Investigation of the geometry of strike-slip and normal faults, and the nature of geometric discontinuities along fault zones.

4. Investigation of source mechanisms for volcanic tremor.

Results

1. Several excellent exposures of fractures in granite have been mapped in detail, within the Mt. Abbot quadrangle (central Sierra Nevada). Fractures within a given area typically form a parallel, northeast trending set, with separations between fractures small compared to average fracture lengths. Individual fractures display left-lateral strike-slip offsets of 0-2 meters. It has been possible to demonstrate that the fractures initially formed as extensional cracks. Subsequent to this, the region was subjected to shear, and the resulting deformation concentrated on the pre-existing fractures. The shearing induced large inelastic deformation, both within the fracture-filling minerals and the host granodiorite. This process eventually led to the formation of narrow mylonite zones. Secondary fracturing also acted to link individual shear cracks together, forming fault zones of ~1 meter in width with offesets of ~10 meters. In addition, the left-lateral shear was accompained by buckling of the granite into kink structures. The kinks are defined by the buckling of the fault surfaces, and may represent complementary right lateral strains of ~40%. Analysis of field data is continuing. A manuscript detailing the formation of strike-slip fault zones and related structures is in preparation.

2. Detailed fracture mapping in the Sierra Nevada batholith reveals the following about joints in crystalline terrains: (1) joint sets are composed of many subparallel cracks; (2) observed crack lengths vary from less than .01 meters to nearly 100 meters; (3) crack surface displacements, observed both at outcrop and thin-section scales, reflect extension, not shear; (4) crack terminations show no dynamic propagation effects, such as bifurcation; (5) spacing between joints is variable, not periodic, and; (6) crack density correlates inversely with average crack length. Observed joint dilations indicate an extensional strain due to jointing of approximately .01 percent. The wide range of observed crack lengths is interpreted to reflect the growth of macroscopic joints from smaller cracks. The nature of the joint terminations, together with the absence of dynamic features, strongly suggest a quasi-static mode of joint growth.

   Quasi-static growth of distributed cracks in an elastic medium subjected to remote strain is investigated to ascertain; why cracks stop once propagation initiates, what parameters influence final crack geometry, and what rates of crack propagation are expected. The driving force for crack growth is found to depend on four independent parameters: (1) the instantaneous crack lengths; (2) the total applied strain; (3) local elastic interaction with neighboring cracks, and; (4) stress relaxation due to crack growth. The first two effects increase the driving force, the latter two tend to decrease the driving force. Crack propagation ceases due to the combined effects of stress relaxation and crack interaction. The final (observed) crack geometry is a predictable consequence of the initial conditions, applied strains, and material behavior. For identical material properties and applied strains the final crack lengths are predicted to correlate inversely with the number of cracks per unit outcrop area, as observed in the Sierra Nevada. Crack propagation rates start from rest, increase rapidly, pass through a maximum, and finally decrease to zero. For reasonable choices of initial and boundary conditions, crack propagation rates are quasi-static at all times during joint formation.

3. Rhomb grabens and horsts along major strike-slip fault systems in the world are generally associated with the horizontal slip across the faults. Simple models suggest that the width of the rhombs is controlled by some initial geometry whereas the length increases with increasing fault displacement. We have tested this model by analyzing the shapes of about 40 well defined rhomb like pull apart basins, ranging from tens of meters to tens of kilometers in length, associated with several major strike-slip faults in the western U.S., Israel, Turkey, and New Zealand. In clear conflict with the model we find that the length to width ratio of these basins, is roughly constant, with a value of approximately 3. Consequently, these basins become wider as they grow longer with increasing fault offset.

Two possible mechanisms responsible for the increase in width are suggested: 1. Coalescence of neighboring rhomb grabens as each graben increases its length. An elongated basin from Northwest of Corona through the Elsinore Lake to southeast of Temecula along the Elsinore fault in southern California is a good example of coalesced rhomb grabens. 2. New faults form parallel to the existing ones when large displacement needs to be accommodated. This promotes interaction among the new faults and between the new and preexisting faults on a larger scale. Increasing displacement, consequently, increasing width of the faulted zone will result in wider pull-apart basins. Salton Sea-Imperial Valley depression appears to be an example of this type.

4. An emprirical correlation between volcanic tremor and igneous intrusion or eruption has encouraged the use of tremor in forecasting volcanic activity, yet the origin of this seismic signal remains obscure. The discovery of tremor at Mount St. Helens that is similar to tremor at Kilauea casts doubt upon the general applicability of source mechanisms which rely on magma flow in cracks because viscosities of dacitic and basaltic magmas differ by many orders of magnitude. However, water is common to both volcanoes. We suggest that periodic opening and closing of a vertical crack tip containing water vapor could produce tremor. Slowly moving magma wedges open the crack tip, providing a low-pressure sink for water lodged in the surrounding rock (or perhaps a vapor exsolved from the magma). The magma supplies heat that raises vapor pressure and drives the opening phase; pressure drops as vapor expands into the dilating crack tip and heat is transferred to the crack walls. A theoretical analysis of a crack subject to linear gradients in driving pressure has identified an instability in the rate of crack dilation with change in vapor pressure that could excite vibration of the magma reservoir. Escape of steam from ground cracks preceding fissure eruptions in Kilauea and the steam eruptions and fumarolic activity at Mount St. Helens support this mechanism. Further evidence comes from the presence of hydrothermally altered rock in cracks above basaltic dikes.

Reports

Pollard, D.D., and P. Segall, 1980, Observations of joints in granite, (abstract), Trans Am Geophys Union, v. 61, p. 1111.

Segall, P. and D.D. Pollard, 1980, Development of joint sets, (abstract), Trans Am Geophys Union, v.61, p.1111.

Pollard, D.D., and K. Aki, 1981, A new source mechanism for volcanic tremor, (abstract) Trans Am Geophys Union, v.62, p.400.

Aydin, A., and A. Nur, 1981, Evolution of pull-apart basins, (abstract) Trans Am Geophys Union, v.62, p.393.

Segall, P., Formation and growth of extensional fracture sets in massive crystalline rock, (abstract) Fourth Int. Conf. on Basement Tectonics 1981, in press.

Aydin, A., and P. D. Pollard, Origins of zig-zag patterns of normal faults in rift valleys, (abstract) Fourth Int. Conf. on Basement Tectonics, 1981 in press.

P3

FUNDAMENTALS OF DEFORMATION AND RUPTURE PROCESSES IN POROUS GEOLOGICAL MATERIALS

Contract 14-08-0001-17664

Professor James R. Rice, Principal Investigator
Division of Engineering
Brown University
Providence, RI 02912
(401) 863-2868

Investigations

Studies carried out under this project have dealt with the mechanics of pre-instability deformations and slip motions in earthquake fault zones on different scales and are grouped accordingly into:

1. Tectonic scale stressing and rupture propagation at plate boundaries.

2. Fault instability in relation to constitutive descriptions for inelastic rock deformation and frictional slip.

Results

1.1 An analysis has been completed of the role played by viscoelastic lithosphere/asthenosphere coupling in the time-dependent redistribution of stress along plate boundaries or other seismic lineaments following great earthquakes [Lehner, Li and Rice, 1980.] The study is based on a generalization by Rice of Elsasser's model of stress diffusion [Rice, 1980] in which general elastic plane stress deformations are allowed in lithospheric plates which are coupled in an elementary way to a (Maxwellian) viscoelastic asthenosphere. Solutions are developed which describe the large-scale quasistatic distribution of thickness-averaged stresses in the lithosphere at or near stationary or travelling rupture zones, modelled here by either crack-like zones of fixed stress drop or dislocation-type slip zones. Sudden ruptures shed load onto the asthenosphere which is gradually transferred back to the lithosphere by a slow relaxation process. The spatial and temporal characteristics of the predicted stress alterations suggest a significant role of lithosphere/asthenosphere coupling effects in triggering interactions of great earthquakes, patterns of prolonged aftershock activity, and the breaking of barriers or gaps by time-dependent stressing.

1.2 The generalized Elsasser model has also been used to study the large-scale response of the lithosphere to periodic slip at a transform or subduction-type plate boundary, as described by an appropriate limit cycle solution [Lehner and Li, 1980.] The periodic behavior of displacements and stress, their decay away from the plate boundary, and a resolution into co-seismic and post-seismic stress alterations are obtained and their dependence on plate velocity, recurrence time, and a characteristic relaxation time investigated. Post-seismic stress alterations of equal sign as co-seismic stress jumps appear gradually at distances beyond one lithosphere thickness and become progressively more important than the latter. They are followed by a much slower post-seismic stress recovery, extending typically over 80% of the cycle length. These results also suggest a new interpretation of post-seismic strain rate data to be taken along a survey line perpendicular to a transform fault, which would provide independent estimates of lithosphere and asthenosphere parameters.

1.3 A tectonic scale great earthquake model has been developed for a long segment of a strike slip fault on which a crack-like zone of slippage grows vertically upwards from the base of the lithosphere [Li and Rice, 1980.] It is found that the shear fracture energy variation with depth determines when the overall stress (τ) versus slip (Δu) relation for the faulted plate boundary reaches the slip softening regime, so that the boundary is amenable to catastrophic unloading, an earthquake analog. The model also predicts that slippage at depth is terminated while the upward tip of the slip zone continues to move until instability occurs; this locking mechanism may in part explain the apparent shallow depth of earthquake foci. Exactly when instability is reached depends both on the constitutive behavior of the plate boundary, embodied in the τ versus Δu relation as computed from crack growth considerations, as well as the unloading stiffness of the adjoining lithospheric plates. A time-dependent stiffness is formulated based on the generalized Elsasser model. It is thus found that seismic failure does not occur immediately when the slope of the slip softening curve for the plate boundary equals the (viscously relaxed) unloading stiffness of the surroundings. Instead, the coupling to viscous asthenosphere response leads to an accelerated creep which terminates in an instability when the slope reaches the unrelaxed unloading stiffness of the surroundings. The model describes time-dependent processes leading to large scale rupture and the associated fault slip.

2.1 A study into elastic-brittle behavior of compressed rock has been completed [Doctoral Thesis by Kachanov, 1980.] It examines the hypothesis that frictional sliding on microcracks, accompanied by the growth of secondary (tensile) cracks, is the dominant mode of inelasticity. The constructed model of rock inelasticity--based on a random field of branching frictional sliding cracks--is tested from the point of view of its ability to explain the basic features of macroscopic behavior. Chapter I surveys the results of microscopic observations and identifies the range of stresses (up to several kbars) which is considered and is usually known as brittle-elastic range. Macroscopic behavior of rocks in this interval of pressures is briefly reviewed. Basic assumptions of the model are introduced. The first stage of inelasticity, when the driving force $\tau-\mu\sigma$ acting on cracks (τ,σ = shear and normal tractions; μ = friction coefficient) is positive, but not high enough to initiate local tensile crack propagation, is considered in Chapter II. Macroscopic stress-inelastic strain relations, obtained by summation of individual slidings, are analyzed. The basic features of these relations include: stress-induced anisotropy, existence of a wide cone of path independence, increase of the apparent value of Poisson's ratio in triaxial compression. The stress interval, corresponding to the first stage of inelasticity, can be of considerable length. The second stage of inelasticity--propagation of secondary (dilatant) microcracks--is considered in Chapter III. A three-dimensional crack configuration is treated as a set of two-dimensional cross-sections. Based on analysis of results for a kinked crack, modified with account of pressure normal to the kink, simple expressions for the microstrains associated with a propagation of a branched crack are derived. The macroscopic stress-strain relations obtained by averaging over the crack orientations provide a description of many inelastic effects. However, dilatancy, predicted by the model, is much lower than the experimentally observed values. A modified version of the model, incorporating uplifting at asperities as an additional mechanism of dilatancy, is introduced. It provides a generally satisfactory description of experimental data. Time-dependent micro-crack growth (stress corrosion cracking) is also considered in the framework of the model (Chapter IV).

2.2 An investigation into friction laws and fault instability forms the subject of a Doctoral Dissertation of A. Ruina [1980]. Motivated by failures of traditional friction laws, this study proposes an internal variable representation for a memory dependent friction law. Conditions are stated for the validity of a description with one internal variable and found to be approximated by, but technically in disagreement with experimental results which require two internal variables for accurate description. The internal variable friction laws predict the following results: Stability of massless elastic systems in contact with a boundary governed by a memory dependent law depends largely on $v(d\mu^*(v)/dv)/d_c$ where v is slip velocity, $\mu^*(v)$ is the steady state dependence of coefficient of friction μ on v and d_c is a characteristic displacement of the memory. Stability also depends on the ratio of elastic compliance to normal stress. At neutral stability a spring and massless block system may oscillate steadily. A simple one dimensional fault allows propagating creep waves. A limited class of internal variable friction laws yield a scaling rule that predicts, for example, that in some experiments 'time dependence' of static friction must be scaled by previous and successive slip velocity. An extension of a one internal variable friction law to continuous deformation predicts localization of deformation before any elastic unloading instabilities.

References

Kachanov, M.L., 1980, "Microcrack model for rock inelasticity," Ph.D. Thesis and Report No. 20 under NSF Grant EAR78-1294801 and U.S.G.S. Contract 14-08-0001-17664, Division of Engineering, Brown University.

Lehner, F.K., V.C. Li and J.R. Rice, 1980, "Stress diffusion along rupturing plate boundaries," Report No. 19 under NSF Grant EAR78-1294801 and U.S.G.S. Contract 14-08-0001-17664, Division of Engineering, Brown University (to appear in J. Geophys. Res.)

Lehner, F.K. and V.C. Li, 1980, "On the stressing of the lithosphere in an earthquake cycle," EOS, Vol. 61, No. 46, p. 1051

Li, V.C. and J.R. Rice, 1980, "Time-dependent tectonic scale earthquake instability model for a strike-slip boundary," EOS, Vol. 61, No. 46, p. 1050.

Rice, J.R., 1980, "The mechanics of earthquake rupture," in Physics of the Earth's Interior, A.M. Dziewonski and E. Boschi (eds.), Italian Physical Society, North Holland Publ. Co., pp. 557-649.

Ruina, A.L., 1980, "Friction laws and instabilities: a quasistatic analysis of some dry frictional behavior," Ph.D. Thesis and Report No. 21 under NSF Grant EAR78-1294801 and U.S.G.S. Contract 14-08-0001-17664, Division of Engineering, Brown University.

FUNDAMENTAL STUDIES ON FAULT MECHANICS AND EARTHQUAKE PRECURSORY PROCESSES

Contract 14-08-0001- 19793

James R. Rice
Division of Engineering
Brown University
Providence, RI 02912
(401) 863-2868

Investigations

Studies carried out under this project have dealt with the mechanics of pre-instability deformations and slip motions in earthquake fault zones on different scales and are grouped accordingly into:

1. Fault instability in relation to constitutive descriptions for frictional slip.
2. Tectonic scale stressing and rupture at plate boundaries, asthenospheric coupling, and relation to seismicity patterns.
3. Electrical effects preceding rupture, including resistivity changes before mine rockbursts and electrokinetic phenomena.

Results

1.1 We have considered the class of slip rate ($\dot{\delta}$) and surface state dependent frictional constitutive relations suggested in work of Dietrich (1978,79,80) and Ruina (1980), and evaluated the manner in which these predict instabilities of steady slip (Rice, 1981; Ruina and Rice, 1981). This is done both for the instability of a steadily translating spring-block arrangement, and for the emergence of growing creep waves at the interface of elastic bodies in sliding contact. The results extend earlier stability analyses by Ruina (1980). Assuming that state can be characterized adequately by a finite set of variables $\underline{\phi}$ (Ruina, 1980) the shear stress τ for sliding at constant normal stress σ has the form $\tau = f(\dot{\delta},\underline{\phi})$. State is assumed to evolve according to $\dot{\underline{\phi}} = \underline{g}(\dot{\delta},\underline{\phi})$. The Dieterich-Ruina experiments suggest that (i) $\partial f(\dot{\delta},\underline{\phi})/\partial\dot{\delta} > 0$ (ii) for fixed $\dot{\delta}$, $\underline{\phi}$ evolves stably towards a unique associated steady state $\underline{\phi}_{ss}(\dot{\delta})$; and (iii) $df[\dot{\delta},\underline{\phi}_{ss}(\dot{\delta})]/d\dot{\delta} < 0$, at least for the range of response leading to possible instabilities. Results show that according to linearized stability analysis, carried out for the above class of constitutive models, the spring-block arrangement goes unstable by a flutter mode (growing oscillations of $\dot{\delta}$ about the steady slip value) when the spring spring constant k is less than a critical value k_{cr}; k_{cr} depends on details of the constitutive functions and may, in general, depend on σ and the steady slip speed. Further, the instability is in the form of a Hopf bifurcation (e.g., Howard, 1979), such that a solution with finite amplitude periodic oscillations of $\dot{\delta}$, containing contributions from higher harmonics, exists for values of k in a one-sided neighborhood of k_{cr}. These periodic oscillations are either stable or unstable, according to whether the neighborhood of their occurence in $k<k_{cr}$ or $k>k_{cr}$. Conditions for existence of propagating, small-amplitude creep waves have also been established for *elastic* bodies in sliding contact. In the case of elastic half spaces in contact, the conditions are met by considering wavelengths λ of a velocity perturbation such that (shear modulus)/ λ has a value proportional to k_{cr} of the spring-block analysis. Waves grow in amplitude as they propagate for longer λ , decay for shorter. In the case of a particular 2-state-variable constitutive model, which Ruina (1980) found to fit his experiments on quartzite, the speed of creep wave propagation at critical conditions is found to be $\approx 100(G/\sigma)\dot{\delta}$. For reasons related to the fact that finite amplitude periodic oscillatory solutions are exhibited by the spring-block arrangement for k in a neighborhood of k_{cr}, it appears also that elastic half-spaces allow finite amplitude *spatially* periodic propagating velocity distributions for wavelengths λ in some one-sided neighborhood of λ_{cr}. Explicit solutions of this type have not yet been determined.

2.1 A tectonic scale model of great earthquakes has been developed for a long segment of a strike slip plate boundary on which a crack-like slip zone grows vertically upwards from some depth of the lithosphere (Li and Rice, 1980). Constitutive behavior of the plate boundary, describing the relation of overall lithosphere thickness average stress to overall slip, is obtained by crack growth considerations and an assumption of a fracture energy that varies with depth. Instability occurs when the effective unloading stiffness of the adjoining lithospheric plate falls below that of the faulted boundary. However, due to viscoelastic coupling to the asthenosphere (Rice, 1980; Lehner et al., 1980), the time dependent stiffness of the plate stabilizes the boundary for a precursory period, during which the fault is self-driven and anomalously high fault creep (and perhaps associated secondary effects) may be observed before dynamic failure. An estimate of the rate of upward progression of the slip zone, based on a fracture energy of depthwise Gaussian distribution which was adapted from Stuart (1979), shows that no appreciable acceleration occurs during the precursor period. However, fault slip rate, which is more amenable to observation, accelerates during the precursor period and becomes unbounded at failure. Slip histories have been computed based on various assumed values of tectonic loading rate, fracture energy, lithospheric thickness, brittle zone size, rupture length and relaxation time of the asthenosphere. These parameters are not very well constrained, especially the fracture-related ones, but with the range of values assumed it is found that the precursor period ranges from several days to about a year. It is also found that with other parameters equal, a longer percursor period is associated with a longer rupture, which appears to be consistent with observations.

2.2 Features of seismicity patterns, including quiescence periods, observed before some large earthquakes have been modeled by inhomogeneities on the fault plane (Li and Dmowska, 1981). The patterns have been interpreted in the context of the upward progression of a zone of slip, towards the earth's surface, from some depth of the lithosphere at a plate boundary. The slip zone may be blocked by local strength asperities which may be of higher inherent strength, or which are currently stronger due to a local slowdown of a basically rate-dependent frictional response. For any segment (between two asperities) that is relatively shorter than adjacent ones, a higher stiffness would result in diminishing of slippage in the blocked region, producing a spatial contrast of reduced seismicity. Quiescence over space and time would be maintained until stress concentration forces slip through one of the asperities, initiating a rupture from one end of the gap zone. This model, supported by seismicity evidence such as doughnut-shaped patterns of seismicity (Mogi, 1969), precursory clustering of seismic activity at the two ends of a gap zone, and propagation of rupture into the quiet region (Kelleher and Savino, 1975), suggests lower b-values and different waveforms and frequency content of seismic events that cluster around the future hypocenter, in comparison with the same characteristics of background seismic activity. For earthquake prediction purposes, the model emphasizes both the spatial and temporal considerations of seismicity changes preceding the main event.

3.1 Electric effects accompanying deformation and rupture processes have been studied. In particular, the work on rock resistivity changes related to strain changes and occurrence of rockbursts in a mine has been completed (Dmowska and Stopinski, 1980). The work has been conducted in cooperation with the Institute of Geophysics, Polish Academy of Sciences, Warsaw, and concerned rock resistivity changes occurring in a copper mine in Lubin, Poland. The work was aimed towards continuous monitoring of electrical resistivity changes of a rock mass caused by mine works (approaching exploitation front, mine blasts, etc.) and/or rockbursts occurring in the region of the mine, with the future possibility of prediction of rockbursts. A new recording instrument has been developed and used, allowing precise measurements of apparent rock resistivity at up to 20 measuring sites per mine section ($\sim 3 \times 400$ m^2), with the use of graphite electrodes providing very high electrode-rock contact and electrochemical stability. The changes of strain of the rock mass caused by mine works and/or approaching rockbursts were traced, in the best cases up to a distance of 400 m. Changing pattern of rock resistivity has been separated into short (1 hour to half-day), middle (half-day up to a few days), and long type changes. The measurements show that characteristic patterns of resistivity change accompany approaching rockbursts, as well as follow rock blasts and roof detachments. Resistivity is found to increase over a period of a few days before a nearby rockburst; sometimes a peak occurs shortly before the failure. Resistivity generally decreases with occurrence of the rockburst, and also after blasts at times of enhanced resistivity.

References

Dieterich, J.H., 1978, "Time-dependent friction and the mechanics of stick slip," PAGEOPH. 116, pp. 790-806.

Dieterich, J.H., 1979, "Modelling of rock friction," J. Geophys. Res. 84 (B5), pp. 2161-2175

Dieterich, J.H., 1980, "Constitutive properties of faults with simulated gouge," in Solid Earth Geophysics and Geotechnology, ed. S. Nemat-Nasser, ASME-AMD Vol. 42, pp. 21-29.

Dmowska, R. and Stopkinski, W. 1981, "Rock resistivity in the Lubin (Poland) copper mine and its relation to variations of strain field and occurrence of rock bursts," abstract for AGU Spring Meeting (Baltimore, May 1981), EOS, Vol. 62, No. 17, p. 323. [Also, manuscript by Stopinski and Dmowska, in preparation for PAGEOPH.]

Howard, L.N., 1979, "Nonlinear oscillations," in Lectures in Applied Mathematics, Vol. 17, ed. F.C. Hoppensteadt, Amer. Math. Soc., Providence.

Kelleher, J. and J. Savino, 1975, "Distribution of seismicity before large strike slip and thrust-type earthquake," JGR, Vol. 80, No. 2, p. 260-271.

Lehner, F.K. and V.C. Li, 1980, "On the stressing of the lithosphere in an earthquake cycle," EOS, Vol. 61, No. 46, p. 1051.

Lehner, F.K., V.C. Li and J.R. Rice, 1980, "Stress diffusion along rupturing plate boundaries," J. Geophys. Res., in press.

Li, V.C. and J.R. Rice, 1980, "Time-dependent tectonic scale earthquake instability model for a strike-slip boundary," EOS, Vol. 61, No. 46, p. 1050.

Li, V.C. and Dmowska, R., 1981, "Aperity model for precursory seismicity patterns for some large earthquakes," abstract for AGU Spring Meeting (Baltimore, May 1981), EOS, Vol. 62, No. 17, p. 329.

Mogi, K., 1969, "Some features of recent seismic activity in and near Japan: Activity before and after great earthquakes," Bull. Earthq. Res. Inst., Vol. 47, p. 395-417.

Rice, J.R., 1980, "The mechanics of earthquake rupture," in Physics of the Earth's Interior, A.M. Dziewonski and E. Boschi (eds.), Italian Physical Society, North Holland Publ. Co., pp. 557-649.

Rice, J.R., 1981, "Studies on the stability of frictional slip," abstracts for AGU Spring Meeting (Baltimore, May 1981), EOS, Vol. 62, No. 17, p. 328, and for Soc. Engr. Sci. Annual Meeting (Providence, Sept. 1981).

Ruina, A.L., 1980, "Friction laws and instabilities: a quasistatic analysis of some dry frictional behavior," Ph.D. Thesis, Brown University.

Ruina, A.L. and Rice, J.R., 1981, "Sliding instabilities due to slip-rate and surface-state dependent friction laws," abstract for IASPEI Gen. Assembly (London, Canada, July 1981).

Stuart, W.D. and G.M. Mavko, 1979, "Earthquake instability on a strike-slip fault," JGR, Vol. 84, p. 2153-2160.

THEORETICAL STUDIES OF RUPTURE PROCESSES IN GEOLOGICAL MATERIALS

14-08-0001-19146

J. W. Rudnicki
Department of Theoretical and
Applied Mechanics
University of Illinois
Urbana, IL 61801

During the first six months of the contract we have accomplished some work in each of the three areas proposed for study: (i) interaction of slipping zones on faults; (ii) inception of shear rupture; and (iii) effects of coupling between deformation and pore fluid diffusion on rupture.

Interaction of Slipping Zones

Rudnicki and Kanamori (1981) have used existing quasi-static solutions for collinear shear cracks to examine quantitatively the effects of fault slip zone interaction on determinations of moment stress drop, and static strain energy release. In addition, these calculations provide specific numerical examples of the general relations between moment and stress drop derived by Madariaga (JGR, 84, 2243-2250, 1979) and illustrate the extent to which small strong asperities or barriers can control the pattern of stress release.

The strain energy change due to introducing collinear slip zones or to breaking the asperities between them is shown to be given by the usual formula for an isolated slip zone with the stress drop replaced by the effective stress. Significant interaction between slip zones occurs only if the length of the separating ligament is less than half the length of the adjacent slip zones. For the case of two collinear slip zones, fracture of the asperity between them produces a relatively large moment because of the additional displacement induced on the adjacent slip zones. For example, if the length of the ligament between two adjacent slip zones of length ℓ is 0.05ℓ, then fracture of the ligament causes a moment almost 1.8 times the moment due to introducing an isolated slip zone of length ℓ. For two collinear slip zones, the local stress drop due to fracture of the separating asperity is shown to become unbounded as the asperity length goes to zero, but in the same limit the stress drop averaged over the entire fault length is approximately equal to the apparent stress drop inferred for an isolated fault of the same moment and total length. The apparent stress drop is approximately equal (within a factor of 2 or 3) to the effective stress and hence can be used in the usual formula to give a good estimate of the strain energy change. For two collinear slip zones of length ℓ separated by a ligament of length 0.2ℓ, the ratio of apparent stress drop (calculated on the assumption of an isolated slip zone) to true stress drop is 0.5 whereas for a ligament length equal to slip zone length this ratio is 0.24.

As a preliminary to an examination of the dynamic effects of slip zone interaction, Rudnicki and Freund (1980) have reexamined the relationships among various expressions for the energy radiated by elastodynamic seismic sources. Both farfield representations and Kostrov's (Izv. Earth Physics, 1, 23-40, 1974) representation of radiated energy in terms of fault surface traction and particle velocity are examined. In particular, Kostrov's representation is arranged in various forms to reveal the source of radiated energy as the deviations of the fault surface tractions and particle velocities from the values that would occur during quasistatic fault motion between the same end states. Moreover, the excess of the static strain energy change over the work done by the fault surface tractions, called W_o by Kanamori (JGR, 82, 2981-2987, 1977), is shown to be a good approximation to the radiated energy when fault propagation speed is near the Rayleigh wave velocity and the time rate of change of fault surface tractions is small. Because Kanamori has shown that for large earthquakes W_o is approximately equal to the Gutenberg-Richter energy, one possible inference is that the conditions for which W_o is approximately equal to the radiated energy are satisfied for large earthquakes.

Inception of Shear Rupture

Our work in this area has concentrated on an extension of Rice's (JGR, 80, 1531-1536, 1975) analysis of the stability of dilatant hardening for a layer subjected to simple shear. In particular, we are examining the response in the case of a finite-size nonuniformity in the form of a sublayer already weakened, perhaps by past faulting. An analysis that linearizes the response of the weakened layer and that of the surrounding material about undrained (no change in fluid mass content) homogeneous deformation demonstrates the competing effects of increasing tectonic stress and pore fluid diffusion in aggravating and mitigating, respectively, the tendency for the deformation to concentrate in the weakened layer. A second approximate analysis, which simplifies the diffusion aspects of the analysis but retains the full nonlinear material behavior, leads to a set of coupled nonlinear ordinary differential equations for the ensuing response. Rudnicki is investigating the numerical solution of these equations while a graduate student G. L. Bowers has been formulating a direct numerical solution of the problem.

Coupled-Deformation Diffusion Effects

In addition to the above-mentioned work on dilatant hardening, which also involves coupled deformation diffusion effects, we have accomplished some additional work in this area.

Rudnicki (1980) has reviewed predictions for processes preparatory to earthquakes based on an inclusion model of earth faulting (Rudnicki, JGR, 82, 844-854, 1977; Rice and Rudnicki, JGR, 84, 2177-2193, 1979) for both dry and fluid-saturated rock masses. This review includes an interpretation of recent experimental results by Martin (GRL, 7, 404-406, 1980) on the stabilization by dilatant hardening of failure in Westerly granite.

Rudnicki (1981) has also obtained a useful rearrangement of Cleary's (Int. J. Solids Struc., 13, 785-808, 1977) solution for the sudden application of a point force at the origin in a linear fluid-infiltrated porous elastic solid. In particular, the stress and displacement fields are demonstrated to comprise a time independent portion, the classical elastic solution based on the undrained (short-time) moduli, and a time dependent portion, the solution for a continuous fluid mass dipole. A corollary of this result is that the time dependent functions entering the point force solution can be obtained from a single function entering the displacement solution for a fluid mass source. Rudnicki has used singular solutions constructed from the point force solution to reconstruct, by placing appropriate point singularities at the origin, the solution of Rice, Rudnicki, and Simons (Int. J. Solids Struc., 14, 289-303, 1978) for the response of a fluid-infiltrated porous elastic solid containing a spherical cavity or inclusion. It is hoped that this technique may be used to obtain solutions for more complex geometries.

Publications

Rudnicki, J. W. and H. Kanamori, Effects of fault interaction on moment, stress drop, and strain energy release, J. Geophy. Res., 86 in press, 1981.

Rudnicki, J. W. and L. B. Freund, On energy radiation from seismic sources, submitted to BSSA, 1980.

Rudnicki, J. W., An inclusion model for processes preparatory to earthquake faulting. In Solid Earth Geophysics and Geotechnology, edited by S. Nemat-Nasser, Applied Mechanics Division Vol. 42, Am. Soc. Mech. Eugn., New York, pp. 39-52, 1980.

Rudnicki, J. W., On "Fundamental solutions for a fluid-saturated porous solid" by M. P. Cleary, Int. J. Solids Struc., to appear, 1981.

A Time-Dependent, Finite Element Model of Southern California Strain Fields

14-08-0001-18368

Albert T. Smith
Earth Sciences Board
University of California
Santa Cruz, CA. 95064
(408) 429-2504
(415) 422-9739

INVESTIGATIONS

Integrating the geodetic data for Southern California requires development of a numerical model. Our approach uses the finite element method for a linear viscoelastic continuum and non-linear properties along the faults. The mesh configuration is based on the existing horizontal and vertical geodetic network in Southern California.

RESULTS

An effective, out-of-core solution method has been developed for both three-dimensional problems and plates. Infinite elements at the boundaries have helped to compress the problem size; however, an alternate computer system was needed for large three-dimensional solutions. A Cray-1 computer at Lawrence Livermore National Laboratory is overcoming the problems of computer storage and CPU time. The finite element programs have been optimized for vector operations and the architecture of this machine. In addition, a version will be operating on a Prime 750 with virtual memory.

A relatively simple plate model of Southern California has been developed to test the feasibility of the procedures. The model contains approximately 500 two-dimensional elements with a configuration corresponding to the principal elements of the Southern California geodetic network. A viscoelastic foundation approximates the asthenosphere, and non-linear behavior is allowed along the fault zones. The relative plate motion is incorporated through the boundary conditions on the model.

Large Scale Rock Fracture Experiment

14-08-0001-19166

Carl H. Sondergeld
Hartmut A. Spetzler
Cooperative Institute for Research in Environmental Sciences
University of Colorado
Boulder, Colorado 80309

Investigations

Through the cooperative US-USSR exchange program, we were able to carry out a large scale uniaxial compression test on a granite using the 445 MN loading frame in Moscow. During the test acoustic velocities, emission, strain, resistivity, electrical potential, and stress were monitored. The sample was loaded to failure.

Results

Failure of the rock specimen was not catastrophic. A single macrocrack was created as the load suddenly dropped. The crack was contained within the 70 cm cubic sample. Failure stress was estimated to be 140 MPa which was in excess of the strength obtained on smaller samples. This may be an artifact of the sample geometry. Approximately 530 acoustic emission (AE) events were captured and stored in digital form on floppy disks. This data is just beginning to be analyzed. Among the findings to date are: (1) an optimum sample size exists for detailed AE studies which is much smaller than the 0.7 m cube used in this test; (2) severe attenuation of high frequencies limits the usefulness of the recorded data; and (3) simple envelope detection scheme could be used to crudely locate the regions of incipient failure.

Report

Sondergeld, C. H., Desirable sample dimensions for detailed acoustic emission studies, Geophys. Res. Lett., paper #140508, 1981.

A Study of the Role of Fault Gouge in the Mechanisms of Faulting

14-08-0001-18213

Francis T. Wu
Department of Geological Sciences
State University of New York
Binghamton, New York 13901
(607) 798-2512

Investigations

As clays have been found to be a significant component of fault gouge in fault zones, it is important to understand the properties of clays under triaxial conditions. In this work, five different types of clays have been tested. These are Ca-montmorillonite, Na-montmorillonite, well-crystalline and poorly-crystalline kaolinites and a high temperature smectite, hectorite. Tests are performed at Dr. Randy Martin's laboratory at Pennsylvania State University under confining pressures of 2 to 4 kilobars and undrained conditions. The samples were precompressed under confining pressures identical to that for the triaxial tests. All experiments were performed under a nearly constant strain rate of 3×10^{-4}.

Results

Sample results for different clays under a confining pressure of 3 kilobars are shown in figure 1. The maximum shear strengths of the clays range from about 200 bars for Ca-montmorillonite under 2 kilobars to about 1.5 kilobars for kaolinite under 4 kilobars. The hectorite samples have strength up to about 2 kilobars under 4 kilobars confining pressure; the difference here is probably due to the difference in crystal structures — hectorite is a trioctahedral clay while the others are dioctahedral clays. In general, the strength of the clays with similar structures seems to depend on the cation exchange capacity: the more prone a clay is to cation exchange the weaker it is (figure 2).

Reports

Wang, C. Y.., N. H. Mao, and F. T. Wu, 1980, Mechanical Properties of clays at high pressure, Jour. of Geophys. Res., v. 85, pp 1462-1468.

Wu, F. T., H. Roberson, C. Y. Wang and N. H. Mao, Fault zones, Gouge and mechanical properties of clays under high pressure, Proc. Conf. VIII, Analysis of Actual Fault Zones in Bedrock, NEHRP, USGS, 1979.

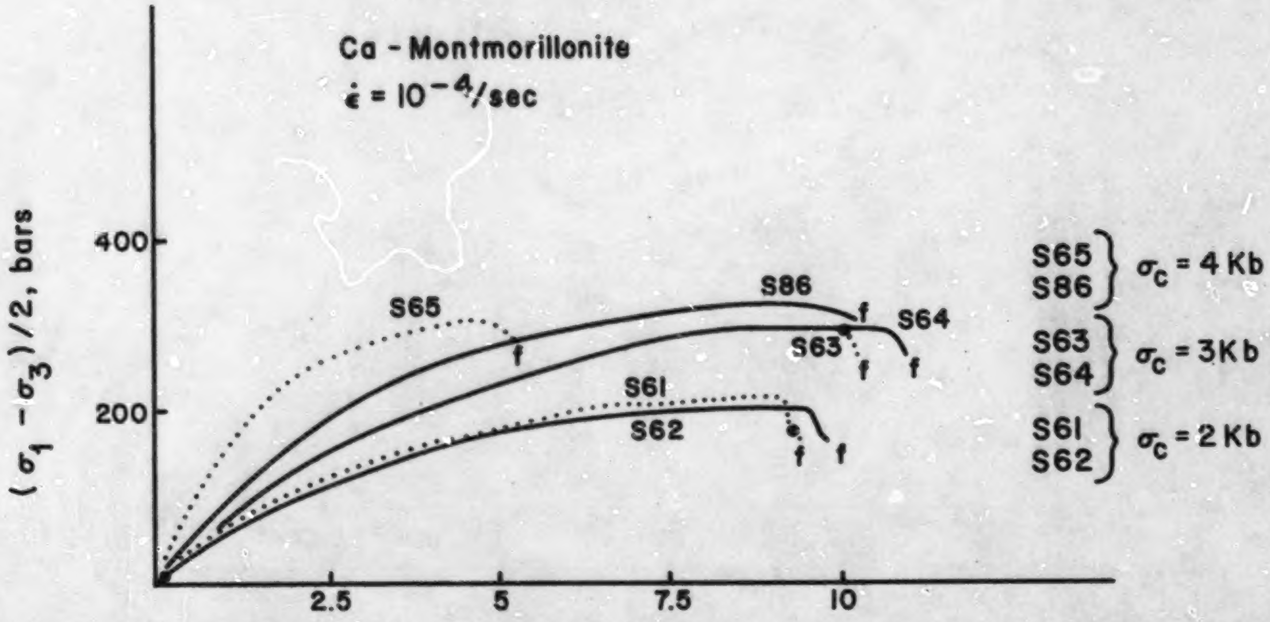

Figure 1. Stress-strain relations for Ca-Montmorillonite under various confining pressures. The samples failed at the end of the experiment.

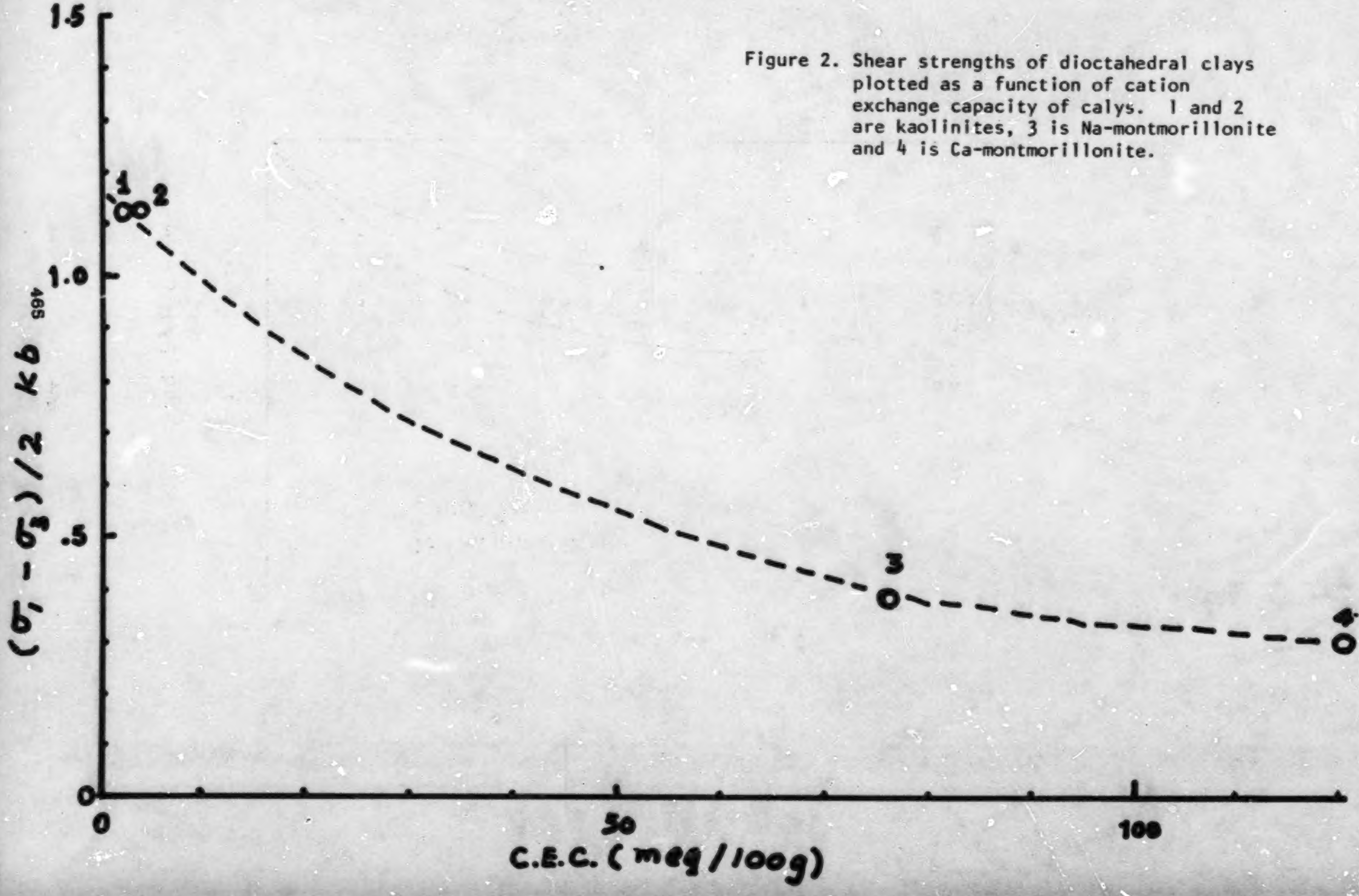

Figure 2. Shear strengths of dioctahedral clays plotted as a function of cation exchange capacity of calys. 1 and 2 are kaolinites, 3 is Na-montmorillonite and 4 is Ca-montmorillonite.

A STUDY OF MYLONITIC ROCKS FROM MAJOR FAULT ZONES

14-08-001-17757
James R. Anderson
Department of Geological Sciences
SUNY-Binghamton
Binghamton, New York 13901
(607)798-2736

Investigations

1. Further field sampling accomplished in June by the Principal Investigator was primarily centered in the northeastern San Gabriel Mountains in southern California. A number of excellent exposures of the Punchbowl fault zone in Prairie Fork were extensively sampled. The nearby Vincent thrust zone was also sampled.

   Mary Davis, a graduate student working on the project, conducted field work during July and August along the Carthage-Colton mylonite zone, also known as the Highland-Lowland Boundary fault, in the northwest Adirondacks of New York. Mylonitic rocks of a variety of types and equivalent rocks were sampled.

2. Prepared thin sections of samples were petrographically examined to determine minerals present, what reactions have occurred, and whether the reactions may have accompanied shearing. A suite of samples from the eastern Peninsular Ranges mylonite zone have been analyzed for whole-rock chemistry using rapid silicate analysis methods. Samples from other studied zones were analyzed as well. Also, selected samples were analyzed with the electron microprobe.

Results

1. Samples examined since the last Technical Report are consistent with previously studied samples in that retrograde metamorphism is observed to have accompanied shearing in the sampled fault zones. No evidence of prograde dehydration or decarbonation reactions has been found. The extent of retrogradation is variable from zone to zone, reflecting differences in depths of exposure and perhaps in other factors. The least hydration of the studied zones is found in the eastern Peninsular Ranges zone, although a small degree of retrogradation is persistently present and appears to have accompanied mylonitization.

2. Whole-rock chemical analysis of a suite of mylonitized rocks of eastern Peninsular Ranges zone indicate that the rocks have been chemically changed during mylonitization. Many of the mylonites of the zone were originally granites, granodiorites, and tonalites of the Peninsular Ranges batholith. The mylonites have been compared to unmylonitized rocks of the batholith that were analyzed by Larsen (1948) in his classic study.

In general, the mylonitized granitic rocks have been depleted in Na_2O and enriched in K_2O relative to the suite of Larsen (1948). There may also have been some depletion in CaO in the mylonites. The initial results do not indicate any relative change in the other major components. Total alkali ($Na_2O + K_2O$) is not significantly different in the mylonites when compared to the unmylonitized suite. Similar behavior for K_2O and Na_2O have been found by Muller (1980, Ph.D. thesis, SUNY-Binghamton) in mylonitized Agua Fria granodiorite from his study area in Guatemala.

The behavior of the alkalis in mylonites of these zones seems to indicate the former presence of an intergranular fluid phase (and an interconnected pore space) which could provide the required diffusion medium. Since the effects are apparently uniform in sense (depletion or enrichment) for each element, the process cannot be a strictly locallized one. Further study is needed on this problem, including the collection of a suite of unmylonitized batholith rocks from areas near the eastern Peninsular Ranges zone.

Crustal Deformation Observatory, Part F

14-08-0001-19742

Roger Bilham and John Beavan
Lamont-Doherty Geological Observatory of Columbia University
Palisades, New York 10964

Activities

A 510 m long half-filled, water-tube tiltmeter has been constructed at Pinion Flats Observatory. The ends of the tiltmeter are referenced to subsurface points 30 m deep via invar rod extensometers installed within cased-boreholes. The water surface in the half-filled tube tiltmeter is continuous from one end to the other. Equalization of air pressure above the water surface is assisted by a second 82 mm diameter tube interconnected with the lower half-filled tube at 20 m intervals. Water-height at each end is monitored by an equal-arm Michelson interferometer using a He/Ne laser and monitored by fringe-counting electronics. The water height resolution is 0.95 μm corresponding to 1.86 x 10^{-9} radians tilt resolution. A water-wave initiated at one end of the tiltmeter takes 15 minutes to travel the length of the tiltmeter. This imposes a high-frequency limit to the data acquired by the tiltmeter.

Two improvements are planned before the instrument is fully commissioned. The East-end transducer is significantly more sensitive to thermal variations than is the West-end transducer. The source of this sensitivity appears to be fluid-tube misalignment near the East end transducer which we intend to correct in June. An improved water-height measurement system has been built and tested. it uses a microprocessor-controlled fringe-counting system to monitor water-height and to automatically compensate for degradation of the optical conditions within the interferometer. The least digital count is equivalent to 1.86 x 10^{-9} radians, but the introduction of artificial dither in the new system makes it possible to monitor tilt signals smaller than 10^{-10} radians. The new transducers will be installed in June.

It appears probable that three parallel 510 m long tiltmeters will be operating simultaneously from June 1981 onward. The two other tiltmeters have been constructed by groups from IGPP and Cambridge, U.K. using somewhat different design concepts. It is planned to search the data for mutual coherence.

Reports

Beavan, J., and Bilham, R., 1977, Thermally induced errors in fluid tube tiltmeters, J. Geophys. Res., vol. 82, p. 5699-6704.

Bilham, R., Plumb, R., and Beavan, J., 1979, Design considerations in an ultrastable long baseline tiltmeter - results from a laser tiltmeter, Proc. Conf. Terr. Space Techniques Earthquake Pred., Strasbourg, Sept. 1978, Vieweg Verlag Wiesbaden/FRG, p. 235-254.

Plumb, R., Bilham, R., and Beavan, J., 1978, A stable long baseline fluid tiltmeter for tectonic studies, USGS Conf. Measurement of Ground Strain Phenomena Related to Earthquake Pred., Carmel. Sept., Open File Report 79-370, p. 47-83.

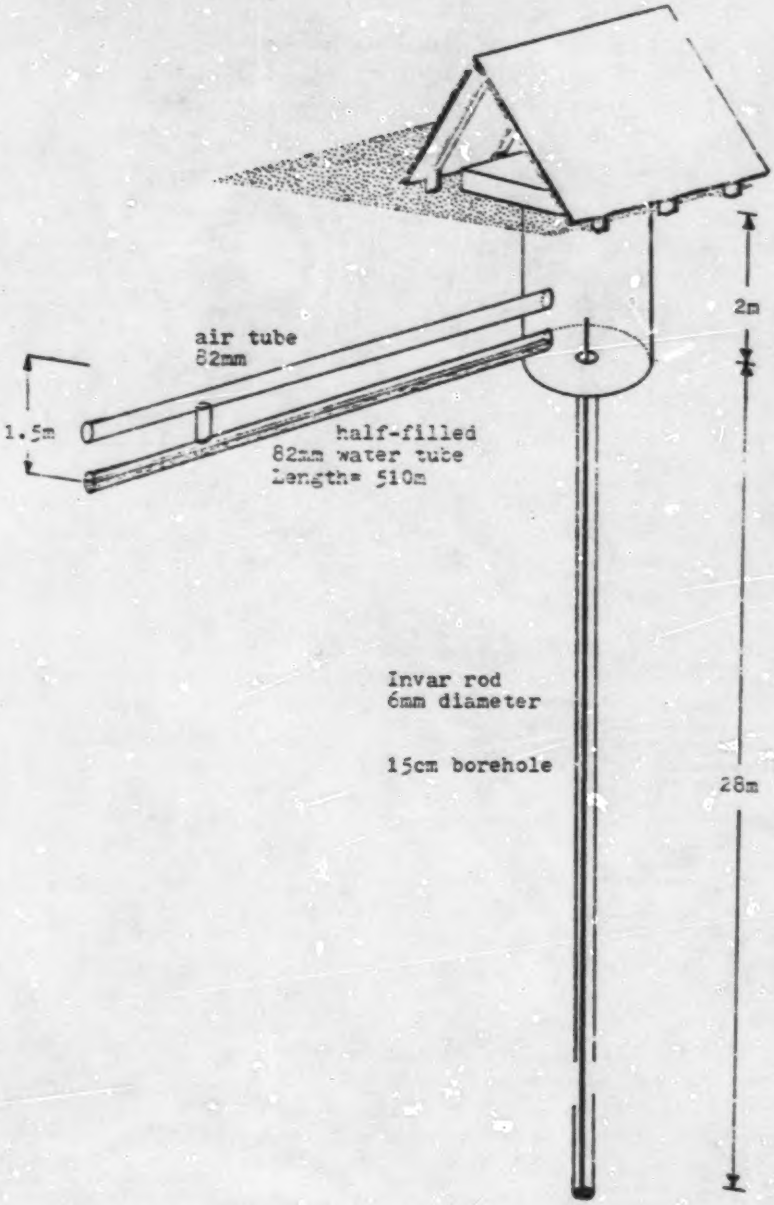
air tube
82mm
1.5m
half-filled
82mm water tube
Length= 510m
2m
Invar rod
6mm diameter
15cm borehole
28m

Figure 1: One end of the 510 m Lamont-Doherty tiltmeter at Pinion Flats Observatory. The borehole extends to twice the depth shown. A similar underground chamber without a borehole exists at the center of the tiltmeter to house the Cambridge differential pressure transducer.

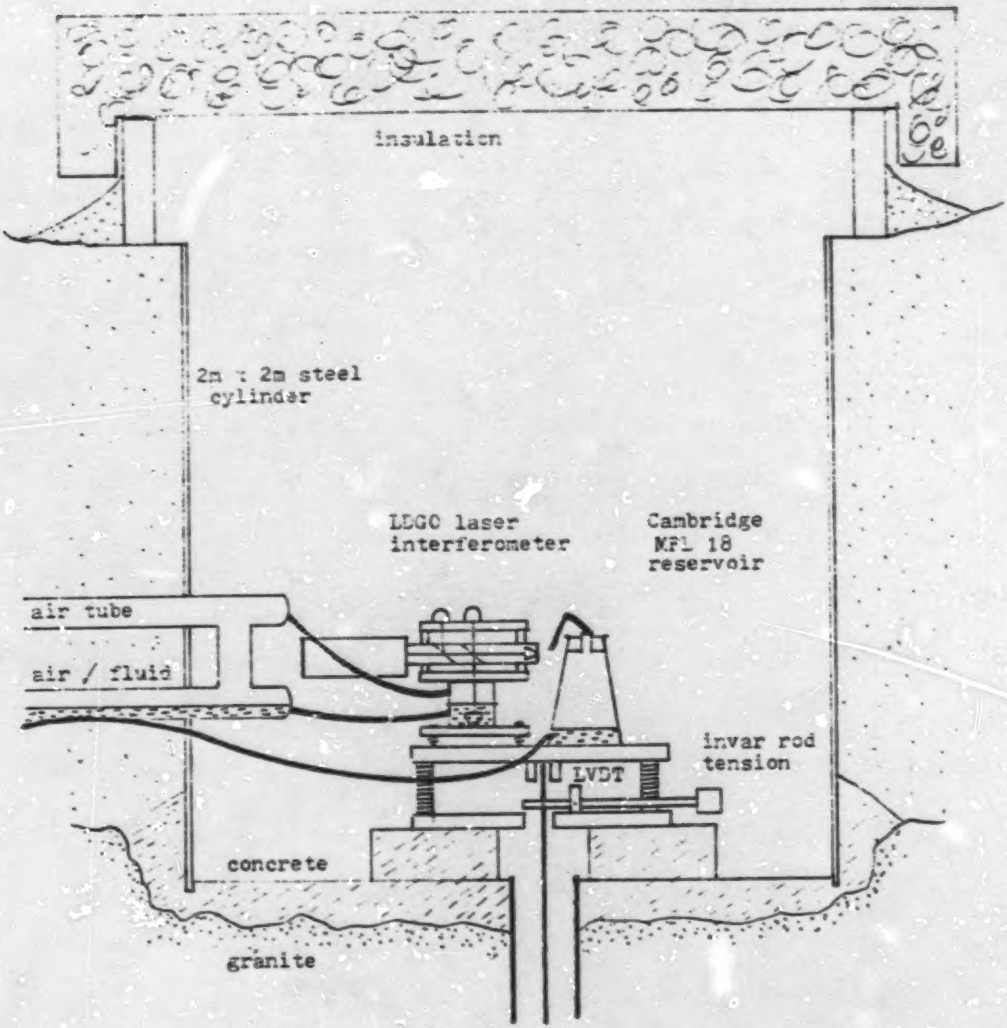
insulation
2m x 2m steel cylinder
LDGO laser interferometer
Cambridge MFL 18 reservoir
air tube
air / fluid
invar rod tension
LVDT
concrete
granite

Figure 2: Arrangement of tiltmeter end units relative to the invar reference rod. An LVDT monitors vertical displacements of the end units relative to a point 30 m below ground level.

Use of a Transportable VLBI Electronics System to Monitor the Rotation of the Earth and Transcontinental and Intercontinental Strain Accumulation

14-08-001-18388

Professor Charles C. Counselman III
Professor Irwin I. Shapiro
Massachusetts Institute of Technology
Cambridge, MA 02139
(617)253-7902

During September and October, 1980, the transportable VLBI terminal was used in a series of multi-station experiments involving a total of 11 days of observation and participation by a total of three American and four European stations. In these experiments the transportable terminal was placed successively at Effelsberg, Germany; at Werthoven, Germany; and at Chilbolton, England. In November, the terminal was sent to Goddard Space Flight Center for upgrading, and then to the Jet Propulsion Laboratory for use in southern California.

Preliminary examination of the data from these experiments showed that interference fringes were obtained on all baselines. Continuing analyses of data from experiments in November 1979 and July 1980 have yielded, respectively, determinations of geodetic coordinates, and the discovery of and a probable correction for a systematic error in the phase calibration of our VLBI receiver affecting the observations at the centimeter level.

MEASUREMENT AND ANALYSIS OF THE NEAR SURFACE STRESS FIELD IN THE VICINITY OF ACTIVE FAULTS IN SOUTHERN CALIFORNIA

14-08-0001-17703

Terry Engelder
Lamont-Doherty Geological Observatory
of Columbia University
Palisades, New York 10964
(914) 359-2900

The objective of this research project is to successfully measure the regional stress field in a tectonically active area using the near-surface strain relief method, an in-situ technique originally developed by the U. S. Bureau of Mines.

During the summer of 1980, about fifty strain relief measurements were made at two sites near Palmdale, California, one 2 km SW of the San Andreas fault (site L) and the other 20 km to the NE (site I). Previous near-surface data indicated that measurements made within 6 m of the surface might be unreliable for predicting tectonic stress in this region, perhaps due to thermal stresses in the upper few meters associated with large seasonal temperature variations. In an effort to address this question. measurements were made successively to depths of 29 m at both sites.

Results of successful measurements are attached. Both the orientation and magnitude inferred for the maximum horizontal compressive stress (P) are plotted vs. depth (up is also North), and shown for reference are the respective lithostats, or estimates of the vertical stress, at each site. For measurements made below 6 m, a very consistent NNW orientation for P was obtained. The rose diagrams also shown reflect the averages and standard deviations obtained at sites I and L. A N23°W orientation for P is in excellent agreement with tectonic stress orientations inferred by Zoback et al. (1980) from deep hydrofracture measurements to depths of 800 m at sites within 2 km of our site L. It is also in agreement with orientations inferred from strain accumulation on the Palmdale and Pearblossom trilateration nets (Lisowski and Savage, 1979).

"Recrystallized Grainsize in Ductile Fault (Mylonite) Zones as an Indicator of Palaeostress Magnitudes During Faulting"

Contract No. 14-08-001-19179

M. A. Etheridge
B. E. Hobbs
G. H. Edward
Department of Earth Sciences,
Monash University,
Clayton, Victoria, 3168,
Australia.

Investigations

(i) To develop a model for dynamic recovery and recrystallization which yields a stress/strain size relationship suitable for use as a palaeostress indicator.

(ii) To test and calibrate the stress/grain size relationship by experimentally deforming minerals (principally quartz) under a range of controlled conditions.

Results

Examination of quartzite mylonites and experimentally deformed pyroxenes by optical and transmission electron microscopy has shown that both minerals have a subgrain structure, particularly in the regions of more intense recrystallization. The subgrain structure ranges from strongly developed walls with closely spaced dislocation to short, incomplete sections of wall with widely spaced dislocations and low misorientation angles.

The observations suggest that recrystallization is occurring by a 'subgrain rotation' mechanism, and so a model for subgrain formation is being developed, as subgrain formation is a precursor to rotation recrystallization. The model can explain the material dependence of the subgrain-size/stress relationship that is seen in the published data for metals, and has the potential to explain environmental effects in tectonic recrystallization

Fault Zone Structures

9930-01725

John H. Healy/Walter D. Mooney
Branch of Seismology
U.S. Geological Survey
345 Middlefield Road, MS 77
Menlo Park, CA 94025
(415) 323-8111, Ext. 2535/2476

Investigations

1. Study of P-wave velocity structure of the Edwards Air Force Base region, Mojave Desert, California, using time-term analysis.
2. Development of techniques and computer software for displaying and analyzing seismic amplitudes.
3. Development of procedures and techniques to improve preliminary data processing to the point of producing seismic record sections.
4. Analysis of seismic refraction data from the Mississippi embayment (with R. M. Hamilton).

Results

1. In June 1980 a temporary array of portable seismographs was deployed in a cross-shaped pattern in the Mojave Desert and shots were fired at the ends and center of this cross. P-wave first arrivals were picked using an interactive computer picking program and time terms were computed for each plot and recorder site. Time term values varied from about 0.0 s to 0.3 s and seem to be strongly correlated with site geology; i.e., large time terms were observed over sedimentary basins and small time terms on hard rock sites. The inferred sedimentary basin depth is about 0.25 to 0.50 km. The computed refractor velocity is 5.5 km/s which agrees with well logs and other refraction work done in this area.

   In an attempt to determine if anisotropy is present in upper crustal rocks, plots were made of apparent refractor velocity versus azimuth for each shot-recorder combination. Variations in velocity were observed, but it seems that the variations may be explained equally well by structure as by anisotropy.

2. Techniques have been developed for plotting true amplitude record sections with an apparent accuracy control of about 25-50%. These record sections have proved valuable in analyzing data from the Mojave Desert and elsewhere, since existing raytrace and synthetic seismogram programs can be used to predict amplitudes for theoretical models. Amplitude control has also been improved by the design and installation of new calibrators in the portable seismic records.

3. Many minor changes have been made to the programs and procedures for preliminary data processing. These include:

a) Construction of an improved cassette playback system with automatic gain control and tape speed control.
b) Simplification of data entry procedures which allows greater speed and improved error checking.
c) Hardware modification of pen plotter controller to increase plotting speed.
d) Development of high speed disk access software.
e) Installation of a new and faster FORTRAN compiler.
f) Development of software to plot at hgih speed on a Tektonix 4014 terminal. This allows one to preview data before plotting on a pen plotter.
g) Digital filtering techniques have been improved.

4. Aeromagnetic and seismic reflection data suggest that the main structural feature of the New Madrid seismic zone underlying the northern Mississippi embayment is a northeast-striking rift about 200 km long and 80 km wide. The pattern of recent seismicity defines a linear trend about 100 km long which coincides wth the rift axis. Previous refraction data along the northwest margin of the embayment, together with regional gravity data, indicate that the embayment is underlain by mafic material. In September 1980 we began a seismic refaction study designed to test this model using 100 portable seismographs and multiple shotpoints. Thirty-four shots were recorded by these instruments which were deployed parallel and perpendicular to the axis of the rift zone. Profiles along the axis indicate a four-layer crustal structure with velocities of 1.9, 5.9-6.1, 6.6, and 7.1 km/s overlying a mantle with a velocity of 8.0 km/s. Extremely high apparent velocities (6.4-7.5 km/s) are observed from shallow layers in some regions. We believe these are indicative of mafic intrusions (laccoliths) at 3-5 km depth. True amplitude record sections show a low amplitude zone ranging from 10 to 70 km from the shotpoints. We believe that the amplitude decrease is indicative of a pronounced upper-crustal low velocity zone. The 7.1 km/s arrivals are generally much stronger that both the 6.6 and 8.0 km/s arrivals, indicating that the discontinuity to 7.1 km/s is the most persuasive. Analysis is proceeding using two-dimensional raytracing of arrival times for reflected and refracted phases and synthetic seismogram modeling of true amplitude record sections.

Reports

Fuis, G. S., Mooney, W. D., Kohler, W. M., and Moos, D., 1981, A seismic-refraction survey in the western Mojave Desert, California, Earthquake Notes, v. 52, no. 1, p. 50.

Fuis, G. A., Mooney, W. D., Healy, J. H., Lutter, W. J., and McMechan, G. A., 1980, Seismic-refraction results in the Imperial Valley region, California, and implications for plate tectonics, EOS, (American Geophysical Union Transactions), v. 61, no. 46, p. 1025.

Healy, J. H. and Kohler, W. H., 1980, Anisotropy of upper curstal rocks, EOS, (American Geophysical Union Transactions), v. 61, no. 46, p. 1025.

Wegener, S. S., Hamilton, R. M., and Healy, J. H., 1980, Seismic refraction study in the New Madrid, Missouri, seismic zone, EOS, (American Geophysical Union Transactions), v. 61, no. 46, p. 1026.

NEW MADRID SEISMIC STUDY, 1980

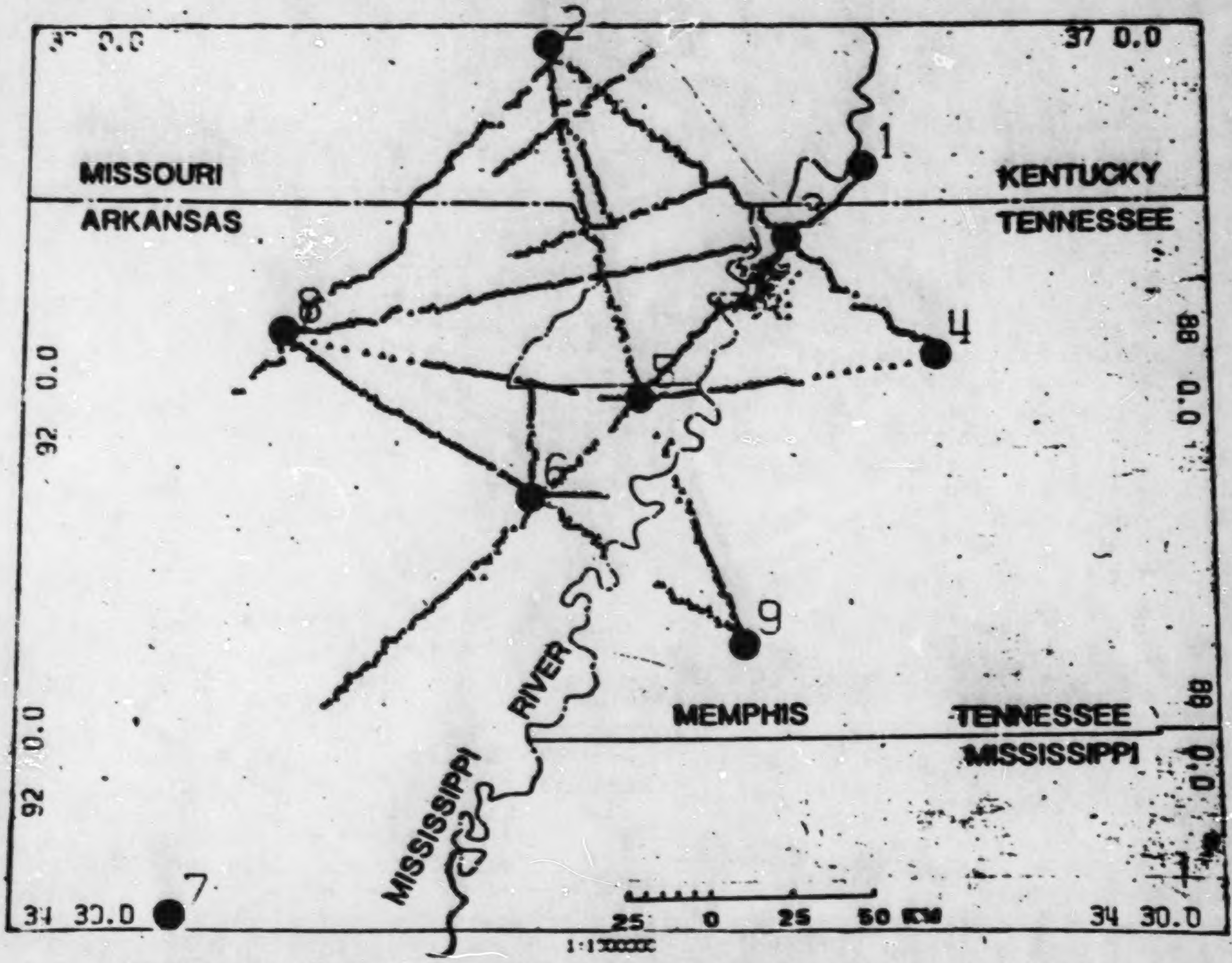
37 0.0
37 0.0
MISSOURI
ARKANSAS
KENTUCKY
TENNESSEE
1
2
3
4
5
6
7
8
9
92 0.0
92 0.0
88 0.0
88 0.0
MEMPHIS
TENNESSEE
MISSISSIPPI
MISSISSIPPI RIVER
34 30.0
34 30.0
25 0 25 50 KM

Location map of shot and instrument sites occupied by the October 1980 U.S. Geological Survey Missouri seismic refraction study. The 9 shot points are represented by black dots. Triangles indicate the location of the 1100 instrument sites.

In-Situ Stress Measurements

9960-01184

John H. Healy
Branch of Tectonophysics
U.S. Geological Survey
345 Middlefield Road, MS 77
Menlo Park, CA 94025
(415) 323-8111, Ext. 2535

Investigations

During the first half of this year, work has been concentrated in the Mojave Desert in the area south of Edwards Air Force Base and north of the San Andreas fault. Five holes were drilled for the installation of the Sacks volumetric strainmeter, and a deep hole, greater than 2000 feet, was drilled for in-situ stress measurements.

Seismic velocity, televiewer, and caliper logs were taken in these holes whenever possible and these data combined with data taken earlier provide a basis for an aerial picture of the physical properties of these granitic rocks.

In addition, in-situ stress measurements were made in a 2,000 foot deep hole 13 miles east of the Wasatch fault near Spanish Fork, Utah.

Results

1. More than 12 holes have been drilled in this region of the Mojave Desert where our study is currently concentrated. These holes have been drilled as seismic shot holes, as holes for instrument emplacement, or deeper holes for in-situ stress measurements. There is great variation in the drilling characteristics of the rock and the quality of results obtained in each of the holes. It now appears that the rocks above 300 feet are much more friable than the rocks encountered at greater depth. There are individual fracture zones which account for the tendency of the holes to collapse at shallow depth, but closer inspection shows the rocks have weakened through their whole mass. This surficial zone might be called a weathered zone, but at this time we have no independent evidence that suggests penetration of weathering to depths of more than 200 feet. Below this depth, the rock is harder and has a seismic velocity between 5.7 and 6.1 km/s; it is broken occasionally by fracture zones indicated by extremely friable material that ranges in thickness from 1 to 10 feet. Some of these fracture zones produce a considerable amount of water during the drilling operation. During drilling the rock appears to be dry except for the water introduced through these larger fracture zones.

2. An examination of stress measurements in the hole drilled last year at Crystallaire, near the San Andreas fault, suggests that there is a correlation between the magnitude of the observed stress and the square

of the seismic velocity. If this correlation is supported by future measurements it would imply that a constant strain imposed on the system is producing a variable stress that reflects the elastic properties of the rocks in different sections of the hole. A careful analysis of this phenomenon is needed to correctly estimate the stress at greater depth from measurements in relatively shallow holes. Thus we are concentrating on measurements to define the elastic properies of the rocks on a regional basis and to correlate these elastic properties with stress measurement wherever possible. It appears from the examination of rock cuttings that there is no significant change in rock type throughout this region. The rock is composed of quartz, orthoclase, and plagioclase feldspar, with some blocky biotite masses. Other minerals are present in very small quantities, less than 1%. Any changes in physical properties based on composition, therefore, would be related to the relative abundance of potassium, calcium, and sodium feldspar minerals, and we estimate that these changes in composition should not change the elastic properties by more than a few percent.

3. We believe that physical properites are dominated by the distribution of fractures, both macrofractures and microfractures, which affect the rock on a scale of individual grains. Current effort is directed toward a detailed study of these fracture patterns on a regional basis in the hopes that the spatial distribution of the fracture patterns may provide a clue to their origin and physical significance.

4. The stress measurements made at 1,090 to 2,000 foot depths in the hole near the Wasatch fault indicate the direction of maximum horizontal compression to be approximately N17°W (±15°), sub-parallel to Quaternary normal faulting in the region. A large difference was observed between the two horizontal principal stresses, with the maximum horizontal principal stress being approximately equal to the vertical principal stress computed using sample densities. The difference between the vertical principal stress and the minimum horizontal principal stress is approximately that required for frictional sliding on optimally-oriented fault planes wth a coefficient of friction of 0.8.

Discussion

One might take the view that random fractures in the near surface granitic rocks are not important. They could, afterall, have resulted from some process in the distant geologic past that bears no relationship to modern tectonics. We suspect, but cannot yet prove, that the open fractures are the result of recent or current tectonic activity, and that they may play a critical role in the shaping of many earthquake precursors by acting in some way as a strain amplifier to generate water level, radon, and apparently random local stress anomalies. In any case, we have to learn enough about these fractures to determine the reliablity of our measurements and decide on the depths required for the installation of instruments and the reliable measurement of in-situ stress.

Reports

Hickman, S. and Zoback, M. D., 1980, Bulk permeability measurements in fractured crystalline rock, Eos, (American Geophysical Union Transactions), v. 61, no. 46, p. 1032.

Zoback, M. D., Hickman, S., and Moos D., 1980, In-situ measurements in a ∿ 1 km deep well near the San Andreas fault in the western Mojave Desert, Eos, (American Geophysical Union Transactions), v. 61, no. 46, p. 1032.

Anderson, R. N. and Zoback, M. D., 1981, Permeability, underpressure, and covection in layer 2A near the Costa Rica rift, EOS, (American Geophysical Union Transactions), v. 62, no. 17, p. 308.

Anderson, R. N. and Zoback, M. D., 1981, The implications of fracture distribution and reflectivity from borehole televiewer imagery for the structure and stratigraphy of the oceanic crust on the Costa Rica rift, eastern equatorial Pacific, EOS, (American Geophysical Union Transactions), v. 62, no. 17, p. 308.

Fuis, G. S., Mooney, W. D., Kohler, W. M., and Moos, D., 1981, A seismic-refraction survey in the western Mojave Desert, California, Earthquake Notes, v. 52, no. 1, p. 50.

Moos, D., Kovach, R., and Nur, A., 1981, Measurements of seismic velocity and attenuation at the East Mesa KGRA, Imperial Valley, California, EOS, (American Geophysical Union Transactions), v. 62, no. 17, p. 334.

Seeburger, D. A. and Zoback, M. D., The distribution of natural fractures and joints at depth in crystalline rocks, submitted to JGR.

Zoback M. D. and Zoback, M. L., 1981, State of stress and intraplate earthquakes in central and eastern United States, Science, in press.

Zoback M. D., Zoback, M. L., Svitek, J., and Liechti, R., 1981, Hydraulic fracturing stress measurements near the Wasatch fault, central Utah, EOS, (American Geophysical Union Transactions), v. 62, no. 17, p. 394.

A MULTI-PURPOSE CRUSTAL STRAIN OBSERVATORY, DALTON TUNNEL COMPLEX SAN GABRIEL MOUNTAINS

Contract No. 14-08-0001-19263

Thomas L. Henyey, Ta-liang Teng, Peter C. Leary
(213) 743-6123

EARTH AND SPACE SCIENCES INSTITUTE
UNIVERSITY OF SOUTHERN CALIFORNIA
LOS ANGELES, CALIFORNIA 90007

Two Bilham-King carbon fiber strainmeters are operating at Dalton. An orthogonal pair of strainmeters, recording since July, 1980 appear to respond to a seasonal thermal cycle to the exclusion of other sources. The east-west (SDE) instrument (Figure 1) is more exposed to surface heating and has a greater temperature response compared with the north-south instrument (SDN, Figure 2). The thermal effect is probably borne by the rock since tunnel air temperatures appear stable to ± .01 degrees centigrade. An exception to the air temperature stability can be seen in Figure 3, where a sample of the daily strain and temperature record is shown. Entry into the tunnel induces a pronounced temperature and strain excursion. Also shown in Figure 3 is the daily temperature record at one foot depth in the rock face of the canyon wall. The seasonal excursion is 4 to 5 times the daily variation and penetrates far more effectively into the rock mass. Aside from occasional events associated with seismic energy, we have not seen signals that can be related to tectonic activity.

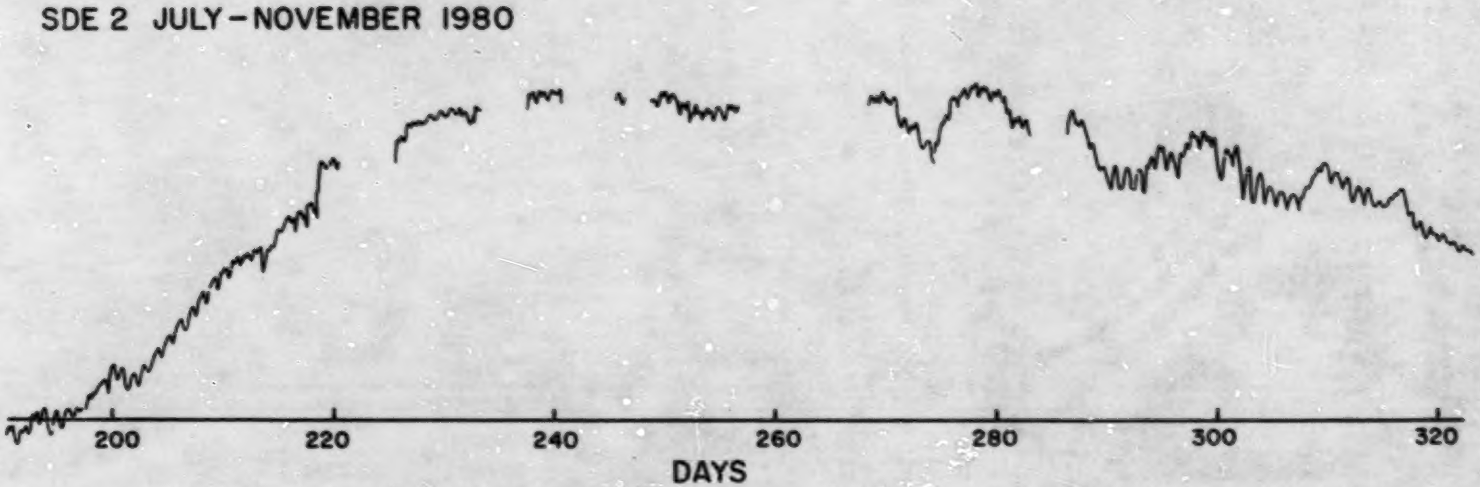

Figure 1. Dalton Tunnel carbon fiber strainmeter record, July-November, 1980; S30E orientation; parallel to canyon face; 200' long.

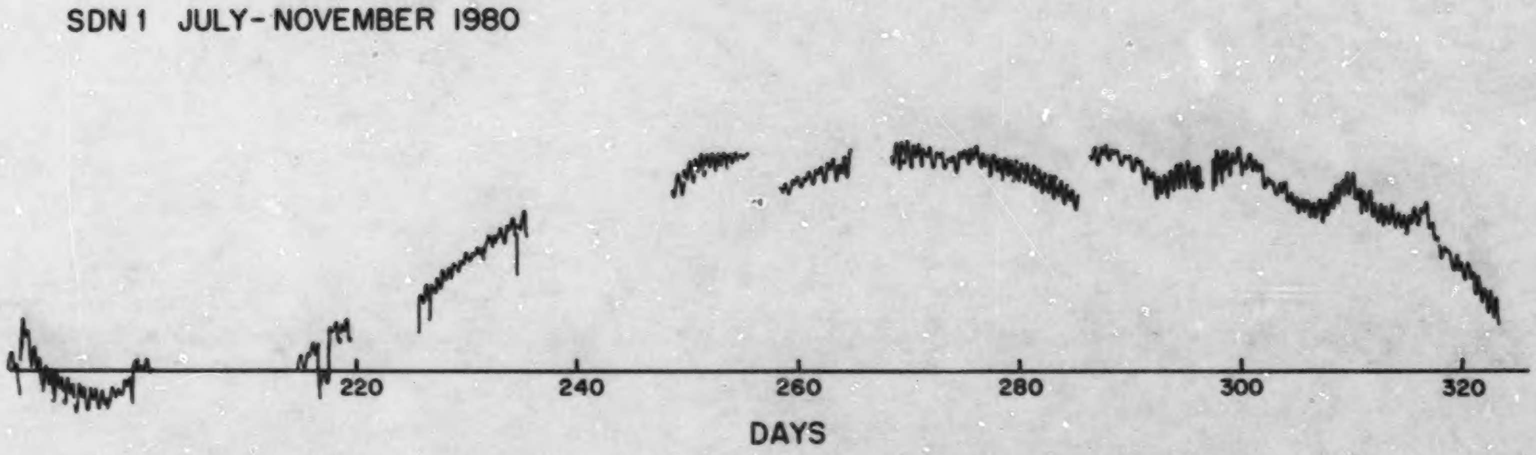

Figure 2. Dalton Tunnel carbon fiber strainmeter record, July-November, 1980; N30W orientation, perpendicular to canyon face; 100' long.

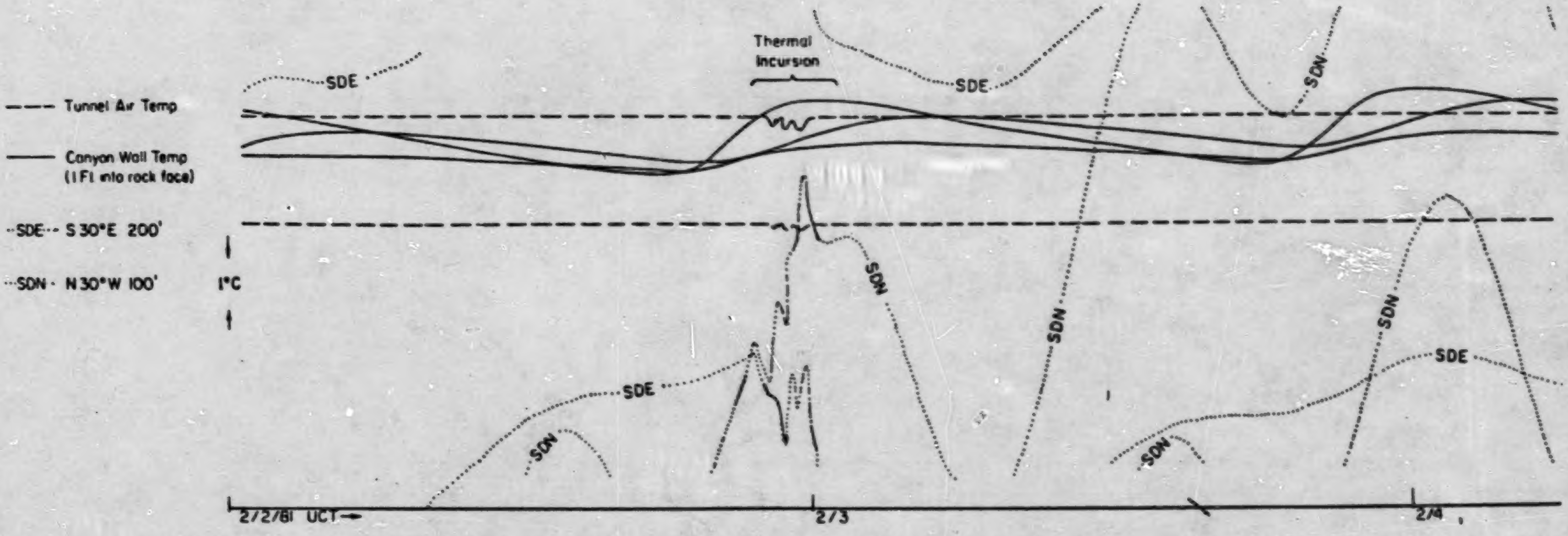

Figure 3. Daily strain and temperature records for Dalton Tunnel. Dashed lines indicate tunnel air temperature, including a period of work in which access door was left open. Solid lines indicate rock face temperature measured at a depth of 1 foot; the temperature variation maximun occurs at 1600 hours local time. The dotted lines show the strain for the two carbon fiber strainmeters, SDN and SDE.

Project Title: Stress Analysis of a Deeply Eroded Analog of the San Andreas Fault

Contract Number: 14-08-0001-17772

Principal Investigators: David L. Kohlstedt (607) 256-7144
John M. Bird (607) 256-6437

Institution: Cornell University
Ithaca, New York 14853

We have been studying deformation-induced microstructures in quartz-bearing rocks from shear zones which might be deeply-eroded analogs of the San Andreas fault. Studies of deformation-induced microstructures in single crystals and in polycrystalline materials indicate that the grain size, sub-grain size, and free dislocation density are, to a good approximation, dependent primarily on differential stress, and are related to temperature and strain rate only as the stress, temperature, and strain rate are coupled through a flow law. We suggest that analyses of deformation-induced microstructures might allow us to place major constraints on the range of stress levels that exist during large-scale geologic deformation phenomena. We have chosen four faults for this study of deeply eroded shear zones: the Ikertôq and Nordre Strømfjord shear zones in Greenland, the Idaho Springs - Ralston shear zone in Colorado, and the Mullen Creek - Nash Fork shear zone in Wyoming. We have made collections across three of these shear zones; we will collect samples from the Nordre Strømfjord shear zone during the summer of 1980.

The Ikertôq shear zone trends ENE for over 150 km from Holsteinsborg on the west coast of Greenland to Søndre Strømfjord. The shear zone is ∿40 km wide and cross-cuts Precambrian granodioritic to quartz dioritic gneisses which have been metamorphosed to granulite facies. The gneisses are cross-cut by two sets of basic dikes which are progressively deformed going into the shear zone. Quartz grains within the gneisses are deformed, showing undulatory extinction and recrystallization along sub-grain boundaries. Measurements of free dislocation densities, sub-grain sizes and recrystallized grain sizes in quartz grains in the gneisses have yielded differential stresses of 50-110 MPa, 20-40 MPa, and 20-40 MPa, respectively. We have interpreted the microstructure of the gneiss as indicating that a significant amount of post-deformational recovery has occurred and that the stresses indicated by the sub-grain size and recrystallized grain size reflect recovery following deformation. The dislocation density might reflect a late, short-term, high stress pulse. We do not think that any of the differential stress measurements reflect the stress level during the major episode of deformation along the shear zone. The textures of the dikes within the shear zone also indicate that a significant amount of post-deformational recovery has occurred. The dikes show extensive development of boudinage. However, petrographically, the dikes show no effect of the deformation. In contrast to quartz grains from the gneiss, quartz grains in the dikes show very little undulatory extinction and no recrystallization. Amphibole grains commonly form 120° triple junctions. Such textures are common in rocks that have undergone significant recovery.

We have also been studying the difference in style of deformation in quartzite samples from two shear zones in the western U.S. Quartzites from the Idaho Springs - Ralston shear zone in Colorado show microstructures typical of those developed in quartz mylonites from regions such as the Moine thrust. Within the quartzite unit, we have observed several completely recrystallized bands which are a few meters in width and are spaced a few meters to a few tens of meters apart. Midway between two completely recrystallized zones, relict quartz grains have aspect ratios of up to 10:1; samples are ∿25 to 35% recrystallized to 15-micron grains. Samples taken closer to the recrystallized bands show more extensive elongation of relict quartz grains, with aspect ratios of greater than 100:1 and a greater percentage of recrystallized grains. The variation in aspect ratios of relict quartz grains, approaching the recrystallized bands, suggests a variation in strain. However, the differential stress during deformation appears to have been constant across the shear zone. The recrystallized grain size is ∿15 microns. The sub-grain size varies from 0.5 to 4.0 μm, and averages about 2 microns. The dislocation density ranges from 3.5 to $6.0 \times 10^8 \text{cm}^{-2}$. Because the recrystallized grain size, sub-grain size, and dislocation density all indicate a stress of about a kilobar, we suggest that along this shear zone, there was a long-term deformation event at a differential stress of ∿1 kbar during which time the observed microstructure was generated.

The quartzite from the Mullen Creek - Nash Fork shear zone shows a very different style of deformation from that exhibited by the quartzite from the Idaho Springs - Ralston shear zone. Relict quartz grains are angular, with aspect ratios of not greater than ∿7:1. The quartz shows extensive polygonization and sub-grain development, but very little recrystallization. Sub-grain size in quartz grains from across the shear zone are generally constant, averaging ∿1.7 microns. The free dislocation density, measured in quartz grains, shows a definite trend to lower values near the center of the shear zone and much higher values near its margins. The dislocation density decreases from $13 \times 10^8 \text{cm}^{-2}$ at the western margin of the shear zone to $\sim 4 \times 10^8 \text{cm}^{-2}$ near its center, and increases again to $\sim 11 \times 10^8 \text{cm}^{-2}$ at the eastern margin. These dislocation densities correspond to a stress of more than 2 kbar at the margins of the shear zone, and less than 1 kbar at the center. The sub-grain size suggests a constant stress of about 1 kbar. It is possible that the sub-grain size represents the stress during the main episode of deformation along the shear zone and the trend in dislocation density reflects a later, high-stress pulse, with the dislocations becoming progressively annealed from the center of the shear zone. We have done preliminary IR spectroscopy on samples from both shear zones to determine if water-content could have affected the styles of deformation. Thus far our results have been inconclusive. However, we are continuing to investigate possible reasons for the difference in style of deformation between the two shear zones.

Publications:

Kohlstedt, D.L., Cooper, R.F., Weathers, M.S., and Bird, J.M., 1979, Paleostress analysis of deformation-induced microstructures: Moine thrust fault and Ikertoq shear zone: in Proceedings of Conference VIII, Analysis of Actual Fault Zones in Bedrock, U.S.G.S. Open-File Report 79-1239, p. 394-425.

Weathers, M.S., Bird, J.M., Cooper, R.F., and Kohlstedt, D.L., 1979, Microstructure and stress analysis of the Mullen Creek - Nash Fork shear zone, Wyoming: in Proceedings of Conference VIII, Analysis of Actual Fault Zones in Bedrock, U.S.G.S. Open-File Report 79-1239, p. 426-447.

Cooper, R.F., and Kohlstedt, D.L., 1979, Dislocation recovery in naturally deformed quartz: Trans. Amer. Geophys. U., v. 60, p. 370.

Weathers, M.S., Cooper, R.F., Pierson, D.D., Bird, J.M., and Kohlstedt, D.L., 1979, Microstructural deformation and stress analysis of a Precambrian shear zone: Trans. Amer. Geophys. U., v. 60, p. 384.

Weathers, M.S., Cooper, R.F., Bird, J.M., and Kohlstedt, D.L., 1979, Deformation-induced microstructures in the Ralston Buttes - Idaho Springs shear zone: Trans. Amer. Geophys. U., v. 60, p. 948.

Project Title: Stress Analysis of Deeply Eroded Analogs of the San Andreas Fault (A Renewal)

Contract Number: 14-08-0001-19119

Principal Investigators: David L. Kohlstedt (607) 256-7144
John M. Bird (607) 256-6437

Institution: Cornell University
Ithaca, New York 14853

We are continuing our study of petrofabrics and microstructures of deformed rocks from several major shear zones which are considered to be deeply-eroded analogs of the San Andreas fault system. The faults included in this study are the Ikertoq and Nordre Strømfjørd shear zones in western Greenland, the Idaho Springs - Ralston shear zone in Colorado, and the Mullen Creek - Nash Fork shear zone in Wyoming. During the summer of 1980, I. van der Molen and T.S. Olsen made collections across the Nordre Strømfjord shear zone. The rocks from this shear zone are metamorphosed to amphibolite facies. We are comparing microstructures in these samples with granulite facies gneisses collected from the Ikertoq shear zone. Van der Molen also mapped several dikes in the Ikertoq shear zone at Søndre Strømfjord. During the same period of time, M.S. Weathers made several additional collections across the Idaho Springs - Ralston shear zone in the quartzite unit. Our preliminary study of the quartzite from this shear zone had shown the presence of several narrow (1-2 m), completely recrystallized zones within the quartzite. We are studying the microstructures of these collections to better characterize the occurrence of, and mechanisms of formation of these recrystallized zones.

Van der Molen mapped several boudinaged dikes within the shear zone at Søndre Strømfjord to try to determine the deformation history of the dikes and the magnitude of the strain within the shear zone subsequent to intrusion of the dikes. The regional structure immediately after intrusion of the dikes would have to be known to determine the magnitude of later strain and to evaluate the type of deformation causing it. Escher et al. (1975) calculated a shear strain of $\gamma = 6$ associated with post-intrusive thrusting for a part of the southern margin of the Ikertoq shear zone between Søndre Strømfjord and Holsteinsborg, where there is evidence that dikes now within the shear zone had originally the same orientation as those in the Archean to the south. The same can not be assumed for the dikes at Søndre Strømfjord. Where pre-emplacement or syn-emplacement deformation can be demonstrated, intrusion may have occurred preferentially along existing planes of weakness, different in orientation from the attitudes attained in undeformed Archean (e.g. Watterson, 1974). The observed parallelism of dikes is not indicative of high strains; it may be an original feature.

The horizontal component of layer-parallel extension reflected in the separation of boudins varies widely from one dike to the next. For some dikes it is only ∿10%. Other dikes, with the same strike and in the same exposure, show boudin separations adding up to 50%. If dike parallelism is considered to be original, it might be concluded that the E-W horizontal strain component varies widely from one dike to the next. More likely, however, similar large horizontal extensions were imposed on all dikes. In some, this has been achieved by early boudinage followed by separation of boudins; in others plastic deformation continued for a longer period of time prior to separation of the dike into boudins. The structural evidence does not require a two-stage deformation history for the Ikertoq shear zone gneisses at Søndre Strømfjord.

We have continued our study of deformation-induced microstructures in quartzite from the Idaho Springs - Ralston shear zone. The sheared quartzite shows periodic development of recrystallized zones, 1-2 m wide and spaced several meters to several tens of meters apart, in the region around Coal Creek. The quartzite exhibits a progressive development of microstructure, approaching the recrystallized zones which is similar to that observed in quartzites from along the Moine thrust (Christie, 1963). Aspect ratios of relict quartz grains increase to >100:1, approaching the recrystallized zones. The increasing aspect ratios indicate an increase in strain and suggest that the recrystallized bands represent regions of maximum strain within the shear zone. The differential stress during deformation was apparently constant across the shear zone. The average recrystallized grain size is ∿15 microns and the average sub-grain size is ∿2 microns. The dislocation density varies from ∿3.6 to 6.0 x $10^8 cm^{-2}$. All three microstructural parameters indicate a differential stress of ∿1 kbar.

Several aspects of our project are still in the preliminary stages of investigation. Specifically, we are trying to evaluate the role of water during the deformation processes along several faults. We are presently comparing the microstructures in a collection of amphibolite facies rocks collected across the Nordre Strømfjord shear zone with the microstructures observed in the granulite facies rocks collected across the Ikertoq shear zone. Etheridge and Wilkie (1979) have suggested that there may be a correlation between recrystallized grain size and water-content of the rocks. Such a relationship would affect the paleostress scales used to estimate differential stress during deformation. We are also using IR spectroscopy to determine the water content in quartzite samples from two shear zones showing very different styles of deformation. The Mullen Creek - Nash Fork shear zone in Wyoming is part of the same belt of shear zones as is the Idaho Springs - Ralston shear zone. However, sheared quartzites from this fault zone show very little elongation of relict grains and almost no recrystallization. It has been suggested that a lower water content in this quartzite may have resulted in a style of deformation different from that exhibited by the quartzite from the Idaho Springs - Ralston shear zone.

References:

Christie, J.M., 1963, The Moine Thrust zone in the Assynt region, northwest Scotland: Univ. Calif. Publ. Geol. Sci., v. 40, p. 345-439.

Escher, A., Escher, J.C., and Watterson, J., 1975, The reorientation of the Kangamiut dike swarm, West Greenland: Can. J. Earth Sci., v. 12, p. 158-175.

Etheridge, M.A., and Wilkie, J.C., 1979, The geometry and microstructure of a range of QP-mylonite zones--A field test of the recrystallized grain size paleopiezometer: U.S.G.S. Open-File Report 79-1239, p. 448-504.

Watterson, J., 1974, Investigations on the Nagssugtoqidian boundary in the Holsteinsborg district, central West Greenland: Rapp. Gron. geol. Unders., v. 65, p. 33-36.

Publications:

Kohlstedt, D.L., 1980, Paleostress levels in deeply eroded fault zones based on analyses of deformation-induced microstructures: U.S.G.S. Open-File Report 80-625, p. 648-664.

Kohlstedt, D.L., and Weathers, M.S., 1980, Deformation-induced microstructures, paleopiezometers, and differential stresses in deeply eroded fault zones: Jour. Geophys. Res., v. 85, p. 6269-6285.

P4

Heat Flow and Tectonic Studies
9960-01176

Arthur H. Lachenbruch
Branch of Tectonophysics
U.S. Geological Survey
345 Middlefield Road
Menlo Park, California 94025
(415) 323-8111, ext. 2272

Investigations:

Twenty holes were drilled in the Salton Trough - southern San Andreas fault - southern California Batholith region. Fifteen of the holes were drilled in unconsolidated sediments as part of a site-specific study of the Glamis and East Brawley Known Geothermal Resources Areas. The remainder were drilled in crystalline rocks to fill in gaps in the regional coverage of southern California. A continuous temperature-monitoring system with sensitivity better than .001°C was designed and built in our laboratory and has been installed in the hole at Stone Canyon. Others currently are being readied for installation in the Mojave region in conjunction with John Bredehoeft's satellite-monitoring system. The remainder of field activities were focussed on obtaining near-equilibrium temperature data in southern California and Arizona, on temperature logging at NTS and Utah in support of studies of sites proposed for Nuclear Waste Isolation, and on the initiation of a cooperative study with WRD of the heat flow and hydrology of the region surrounding the San Francisco Peaks. Laboratory and office facilities have been engaged primarily in supporting this field activity and ongoing interpretive studies of the Sonoran-Mojave region, Alaska, the Northern Great Basin, the Sierra - Basin and Range transition and the California Cascades.

Results:

1. Southernmost San Andreas fault (see also Salton Trough). The thermal regime of the part of the San Andreas fault south of San Bernardino is markedly different from that to the north and west. This region of the San Andreas and associated faults is characterized by more abundant thermal springs and more variable, generally higher heat flow attributable at least in part to the segment of spreading center presumed to exist beneath the Salton Trough. From preliminary data, the heat-flow pattern appears complicated as a result of a combination of tectonic energy sources and hydrothermal sources and sinks.

2. Salton Trough. A broad heat-flow anomaly with maximum of about 300 mWm^{-2} (~7 HFU) is centered between Glamis and East Brawley and is superimposed on a regional heat flow high in excess of 100 mWm^{-2} (>2.5 HFU). From preliminary data, heat flow in the crystalline rocks surrounding the Salton Trough appears high and variable, with much of the variability attributable to hydrothermal convection. The deltaic sedimentary material comprising the upper ~100 m of the Salton Trough generally is poorly sorted and high in quartz resulting in quite high thermal conductivities (averaging 2.0 Wm^{-1} K^{-1} as opposed to 1.2 to 1.7 for typical "alluvium").

3. Temperature monitoring near the San Andreas fault. Earliest results from the Stone Canyon well show a background temperature variation of a few hundredths of a °C, with as yet no clearly definable thermal "events". At some levels in the Menlo Park hole (MP-1), background is much quieter (~1 millidegree C) and a number of thermal events with amplitude ~.01°C have been detected; one of them coincident with an earthquake in the East Bay.

4. Great Central Valley of California. Temperature profiles from about 70 wells (mostly shallower than 200 meters) in the Sacramento and San Joaquin Valleys have provided data pertinent to the heat flow and hydrology of the region. Very few of the wells are suitable for heat-flow determinations. An attempt to contour near-surface temperature confirms a steep lateral thermal gradient on the west side of the valley, as suggested by widely scattered heat-flow measurements.

5. Mono Craters - Bodie Area. Detailed heat-flow measurements indicate the expected transition from low-normal values (~1 HFU) in the Sierra Nevada to high values (~2 to 2.5 HFU) characteristic of the Basin and Range modified extensively by a number of fault-controlled hydrothermal systems. East of the Mono Craters, an extensive zone of hydrologic recharge for both the Mono and Long Valley systems is indicated. A significant positive anomaly with a maximum greater than 10 HFU coincides with warm spring activity and travertine deposits to the east of Mono Lake.

6. Sonoran Desert. The portion of the Basin and Range Province to the west of the Colorado Plateau (the Great Basin) has high and variable heat flow (~2.1 HFU ± 40%) and there is a very rapid transition to low heat flow (about 1 HFU) at its western boundary with the Sierra Nevada. Preliminary analysis of recent data in the part of the Basin and Range Province to the south of the Colorado Plateau (the Sonoran Desert) shows that it has similarly high and variable heat flow which undergoes a rapid transition to moderate heat flow (about 1.6 HFU) at its western boundary with the Mojave block, MB. This boundary, which coincides with the projection of the Death Valley fault zone and with the eastern limit of active seismicity probably separates a region of San Andreas-type strike-slip tectonics to the west from the region of Basin-and-Range type extensional tectonics to the east. At the eastern boundary of the Great Basin and the northern boundary of the Sonoran Desert, the high heat flow undergoes a gradual transition (modified to some extent by lateral and vertical regional water flow) to moderate heat flow in the relatively stable interior of the Colorado Plateau. Hence in this part of the continent, the region of high and variable heat flow is coextensive with a region of late Cenozoic tectonic extension, as such deformation is characteristic of the Basin and Range Province.

High and variable heat flow is an expectable consequence of prolonged tectonic extension (horizontal dilatation) provided that (as in the Basin and Range Province) such extension does not result in rapid subsidence and massive sedimentation. To maintain isostatic balance and conserve mass, it is necessary that warmer material move upward from depth to replace material that moves laterally in the extending lithosphere. Heat carried convectively by this upward motion could account for the elevated regional heat flow observed. The associated elevated thermal gradients and relatively open fractures in an extending brittle layer could facilitate hydrothermal convection which probably accounts for much of the local variability of heat flow in the Basin and Range Province.

7. Uranium test wells in Arizona. Five deep test wells drilled by the Department of Energy's National Uranium Resource Evaluation (NURE) program in the sedimentary basins of central-western Arizona yielded high quality heat-flow determinations with values ranging from 1.6 to 2.2 HFU. This range of heat flow is in good agreement with values determined in granitic rocks to much shallower depths (~150 meters). Agreement of heat flow at depths up to 1.7 km in sediments with those obtained from the shallow holes in granites greatly increases our confidence in the shallow measurements.

8. San Francisco Peaks, Arizona. Fragmentary thermal results from hydrologic observation wells in the area surrounding San Francisco Peaks have indicated a strong lateral water movement with a significant downward component. Heat-flow estimates indicate a conductive flux on the order of a few tenths of a heat-flow unit, much lower than one would expect in this tectonic environment.

9. Nevada Test Site. Recent heat-flow determinations in and near the Nevada Test Site have confirmed the general shape and extent of the "Eureka Low" as depicted in recent heat-flow maps published by the project. Detailed thermal measurements in the vicinity of Yucca Mountain suggest the potential for both vertical and lateral water movement within the proposed repository. We have not, however, accumulated sufficient data to estimate velocities of the possible flows.

Reports:

Lachenbruch, A. H., 1980, Frictional heating, fluid pressure, and the resistance to fault motion: Journal of Geophysical Research, v. 85, p. 6097-6112.

Lachenbruch, A. H., 1980, Discussion of "A reinterpretation of the linear heat flow and heat production relationship for the exponential model of the heat production in the crust," by R. N. Singh and J. G. Negi: Geophysical Journal of the Royal Astronomical Society, v. 63, p. 791-795.

Lachenbruch, A. H., 1980, Regional thermal structure in the Western U.S. (abstract): EOS, v. 61, p. 1144.

Lachenbruch, A. H., and Sass, J. H., 1980, Heat flow and energetics of the San Andreas fault zone: Journal of Geophysical Research, v. 85, p. 6185-6223.

Mase, C. W., and Sass, J. H., 1980, Heat flow from the western arm of the Black Rock Desert, Nevada: U.S. Geological Survey Open-File Report 80-1238, 38 p.

Mase, C. W., Sass, J. H., and Lachenbruch, A. H., 1980, Preliminary heat-flow investigation of the California Cascades (abstract): EOS, v. 61, p. 1150.

Sass, J. H., and others, 1981, Heat flow from the crust of the U.S., in Physical Properties of Rocks and Minerals, edited by Y. S. Touloukian, W. R. Judd, and R. F. Roy: McGraw-Hill Book Company, p. 503-548.

Sass, J. H., Kennelly, J. P., Jr., Wendt, W. E., Moses, T. H., Jr., and Ziagos, J. P., 1981, In situ determination of heat flow in unconsolidated sediments: Geophysics, v. 46, p. 76-83.

Lachenbruch, A. H., and Sass, J. H., Corrections to 'Heat Flow and Energetics of the San Andreas Fault Zone' and some additional comments on the relation between fault friction and observed heat flow: Journal of Geophysical Research, in press, 1981.

Lachenbruch, A. H., and Sass, J. H., 1981, Heat flow and its implications for tectonics and volcanism in the Basin and Range province, in Tectonic framework of the Mojave and Sonoran Deserts, California and Arizona, edited by K. A. Howard, M. D. Carr, and D. M. Miller: U.S. Geological Survey Open-File Report 81-503, p. 56-58.

Vertical Displacement Measurements in Central California With a Long-Baseline Two-Fluid Tiltmeter

14-08-0001-18224

Howard C. Merchant
Department of Mechanical Engineering
University of Washington, FU-10
Seattle, Washington 98195
(206) 543-5628

A two-fluid multiple leg tiltmeter has been assembled and installed at a test sight near San Juan Bautista, California. The system consists of two legs at 75° with lengths of 243 meters and 193 meters. Each leg has two-fluid lines which are both exposed to the same temperature environment, one containing methyl ethyl ketone and one containing N-butyl alcohol. The fluid and tubing sizes were selected using a number of criteria including accuracy for thermal compensation, dynamic response characteristics, safety, and cost. The reservoirs are supported on thermally compensated piers embedded approximately 4 meters.

The dynamic responses of the system measured in the field compare well with theory. The measurement of tilt at the test site for times of geophysical interests will be carried out in a follow-on program.

Active Seismology in Fault Zones

9930-02102

Walter D. Mooney
Branch of Seismology
U.S. Geological Survey
345 Middlefield Road - MS-77
Menlo Park, California 94025
(415) 323-8111, ext. 2476

Investigations

1. Collection and analysis of seismic refraction data from the greater Bay area: Livermore Valley, Great Valley, Diablo Range, Santa Clara Valley, Gabilan Range.

2. Collection and analysis of seismic refraction data from the Mojave Desert, southern California (with G. S. Fuis).

3. Analysis of existing refraction data from the Diablo and Gabilan Ranges, supplemented by new earthquake record sections of CALNET data (with A. Walter).

4. Analysis of seismic refraction data using slant stacking and downward continuation (with G. McMechan and R. Clayton).

5. Analysis of refraction data from the Mississippi embayment (with W. Kohler, A. Walter, and W. Lutter).

Results

1. The San Andreas fault system in central California lies within the Coast Ranges. Major geologic elements of the Coast Ranges include: 1) the Great Valley sequence, (2) the Franciscan assemblage, (3) granite of the Gabilan Range, and (4) Tertiary marine sedimentary rocks. The velocity structure of these elements is required to locate accurately and model earthquakes within the fault system.

Two-dimensional ray-tracing and synthetic seismograms applied to detailed data collected during the past year indicate strong crustal heterogeneity within the Coast Ranges. For the uppermost part of the crust (0-4 km), typical velocity observations are: (1) Vp=3.8 km/s for Great Valley rocks, (2) Vp=4.8-5.2 km/s for Franciscan metasedimentary rocks, (3) Vp=5.3-5.6 km/s for granitic rocks, and (4) Vp=6.0-6.1 km/s for mafic volcanic rocks associated with the Franciscan assemblage. In addition, we have found new evidence for low velocities (Vp=2.7 km/s) within the Calaveras fault zone.

Variations in velocity in the middle and lower parts of the crust are less marked but still significant and amount to $\sim$0.4 km/s. Average crustal thickness is 27 km, with an apparent northward thinning in the eastern Coast Ranges.

2. In June 1980, the USGS recorded a reversed seismic refraction profile between Rogers Dry Lake in the western Mojave Desert, Calif., and the San Andreas fault zone to the south. This profile was 38 km long and had a station spacing of 0.5 km.

We modeled this profile using a two-dimensional ray-tracing program to match first-arrival traveltimes. Three units are recognized: (1) a unit of low velocity (1.6-1.8 km/s), 0 to 0.4 km thick, corresponding to sedimentary deposits, (2) a unit 0.5 to 2.0 km thick in which velocity increases relatively rapidly from 4.7 to 5.4-5.7 km/s, corresponding to the upper part of the granitic basement, and (3) a unit in which velocity increases relatively slowly from 5.7 to about 6.2 km/s at 10 km depth, the bottom of the model. The thickness of sedimentary basins determined from refraction agrees within 0.1-0.2 km with that determined from wells. The relatively high velocity gradient in the upper part of the granitic basement reflects primarily the rapid closing of cracks with depth. This unit thickens southward toward the San Andreas fault and is thickest beneath the deepest sedimentary basin on this profile.

Preliminary results from preparing a true-amplitude record section indicate that beyond the crossover to the 5.7 km/s branch (at about 10 km), amplitudes decrease with distance (r) as r^{-2}. At closer ranges, amplitudes decrease more slowly with distance. Synthetic seismograms generated for the model show good agreement with the data. Velocity-depth functions determined from sonic logs in three wells along or near the profile agree with our model velocity-depth functions.

3. The compressional-wave velocity structure of the crust of the Coast Ranges of central California has been modeled using seismic refraction data previously reported by Stewart (1968). Heterogeneous velocity structures for both the Diablo Range (east of the San Andreas fault) and Gabilan Range (west of the fault) were derived by iterative two-dimensional ray-trading.

The results indicate that there is a resolvable difference in the crustal velocity structure on either side of the San Andreas fault. Below the sediments and weathered zone, the upper crust (3-8 km) of the Diablo Range has an average velocity of 5.5 km/s while in the Gabilan Range the average velocity is 6.1 km/s. In the middle crust (8-17 km) the Diablo Range has an average velocity of 6.1 km/s) while it is 6.3 km/s in the Gabilan Range. In the lower crust (17-29 km) the average velocity in the Diablo Range is 6.9 km/s while it is 6.5 km/s in the Gabilan Range. These contrasts in velocity with depth are indicative of compositional differences between the two ranges. We conclude that the Diablo Range most likely consists of metagraywacke to a depth of 17 km, and of gabboic material below this depth. The Gabilan Range consists of granitic material to a depth of 17 km and of metagranite (gneiss) in the lower crust, but it is possible that some gabbroic rocks are also present.

A Fortran program was developed to plot earthquake record sections of data digitized from the central California network. The utility of this program was tested by selecting reversing events of magnitude greater than three that were recorded along lines of stations in the Diablo and Gabilan Ranges of the Coast Ranges. Preliminary analysis of the plotted profiles shows clear Pg, Pn, and PmP arrivals. Because clear Pn arrivals are not seen on most explosion profiles previously recorded through this region, the earthquake record sections are an important supplement to the explosion data and provide additional constraints on the velocity structure of the Diablo and Gabilan ranges.

4. Recently, a downward continuation method was presented for the inversion of densely recorded refraction data (Clayton and McMechan, 1981 a,b). This technique transforms the entire recorded data wavefield from the time-distance (t-x) domain into the slowness-depth (p-z) domain. The resulting velocity-depth locus is a focused image in the p-z domain, and the uncertainty in the solution is indicated by the width and coherence of this image. There are two basic assumptions: (1) lateral homogeneity of the velocity structure, and (2) that the data are sufficiently well sampled in the spatial dimension that they can be treated as a wavefield.

We have applied this technique to USGS data from the Mojave Desert. These results have then been compared with those obtained by two-dimensional ray-traing (see item 2). We conclude that a reasonable, average velocity-depth curve can be stably estimated, but the finer details of the curve may be related to lateral rather than vertical velocity variations. These effects are not confined to wavefield analysis, but the wavefield approach has the advantage of being relatively unbiased as the significance of any region of coherent energy in the data is not established until convergence is obtained. Wavefield transformation is seen to be robust, unbiased, and particularly suited to processing large volumes of data. Further development of the method is warranted.

Reports

Mooney, W. D., and Walter, A. W., 1981, Seismic refraction studies in the Coast Ranges, central California: EOS, American Geophysical Journal Transactions, v. 62, no. 17, p. 328.

Fuis, G. S., Mooney, W. D., Kohler, W. M., and Moos, Dan, 1981, A seismic-refraction survey in the western Mojave Desert, California, (abs.), Earthquake Notes, v. 52, no. 1, p. 50.

Walter, A., and Mooney, W. D., 1981, Reinterpreting seismic refraction data from central California: Earthquake Notes, v. 52, no. 1, p. 51.

Mooney, W. D., 1981, IASPEI workshop: Seismic modeling of laterally varying structures: EOS, American Geophysical Union Transactions, v. 61, no. 2, p. 19.

Mooney, W. D., and Luetgart, J. H., (in press), A seismic refraction study of the Santa Clara Valley and southern Santa Cruz Mountains, central California (submitted to Seismological Society of America Bulletin).

McMechan, G. A., Clayton, R. W., and Mooney, W. D., (in press), Application of wavefield continuation to the inversion of refraction data (submitted to Journal of Geophysical Research).

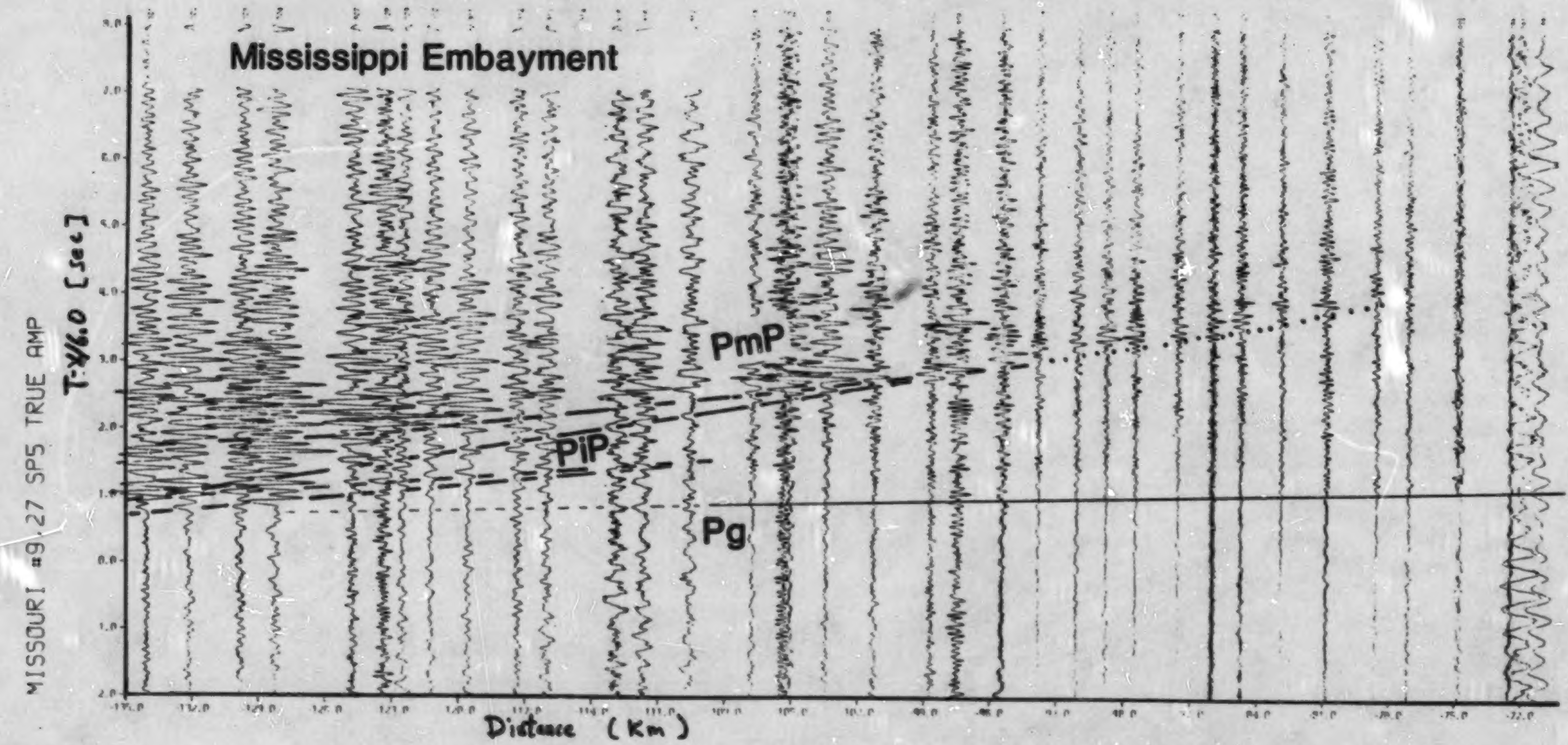

Figure 1. A portion of a true amplitude record section from the 1980 Mississippi Embayment investigation. The profile shows clear reflected arrivals from a deep-crustal and the crust-mantle boundary (PiP and PmP, respectively). The phase Pg is the basement arrival. This section is typical of the data analyzed in this project.

Tiltmeter and Earthquake Prediction Research in S. California and at Adak, Alaska

14-08-0001-19273

Sean-Thomas Morrissey
Department of Earth & Atmospheric Sciences
Saint Louis University
St. Louis, MO 63156
(314) 658-3129

Goals

The overall objective of the program is to detect precursors to larger earthquakes with the data from tiltmeters. The prime area of interest is Southern California, but a joint effort with CIRES includes a tiltmeter array at Adak, Alaska, where instruments have operated since 1976, and 8 are presently installed. The several tasks to achieve this goal are (1) to continue to improve the instrumentation itself (a well-modified TM-1 borehole system) and to seek alternate instruments; (2) to improve the installation method such that data from small arrays is coherent; (3) to monitor the environment of each site to delineate sources of noise in the data; (4) to deploy and operate a digital data acquisition system; (5) to process and interpret the data so as to remove known noise sources, then seek correlation and coherence between the tiltmeters themselves and any tectonic activity.

Accomplishments

Task 1: A new power converter/voltage regulator system was designed for the meteorology sub-system to replace a previous unit that used mercury cells as a reference. These were installed at Adak in January; the unit is stable from +100 to -40°C. A new electronics module is being evaluated for replacing the TM-1 electronics; it costs only $220.00/pair, operates from +12 V at 4 ma, and is designed for very stable transducers.

Task 2: The eight tiltmeters at Adak continue to operate satisfactorily. The noisy units are at sites that would be expected to be noisy. Two units are operating at the CCMO test site near St. Louis. The installation of units in the Palmdale area is delayed because we have determined that, in light of the results of the stress overcoring experiments, the units should be installed 10 meters deep. A cost estimate to prepare two dual unit sites with suitable manholes, etc., considerably exceeded the budget allowance.

Task 3: The environmental monitoring has shown obvious noise in the data from rainfall and temperature, and possibly also barometric pressure contamination. Because of manpower restraints, no serious effort has been made to sort it out. The micro-barometer has been a major power consumer in the system, so we have found a solid-state absolute pressure gauge that is both inexpensive and low power.

Task 4: Data acquisition: Most of the problems with the digital data system have been solved. A nagging habit of the acquisition microcomputer to crash about once a day was finally traced to an apparent error in the DFM software supplied with the system. The clock rates in the remote micro-computers drift excessibly, (a few minutes a year) so an adjustment will have to be provided. A priority control circuit was developed to provide "first come, first served" switching of the incoming digital data to the acquisition microcomputer, thus preventing a later transmission from a remote unit from destroying a transmission already being logged.

Task 5: In order to provide an immediate look at the raw incoming data discs, a series of command scripts to automatically process the data was developed on the 11/70 computer. These scripts call the appropriate programs and pass along the pertinent variables. Some programs are original Fortran creations, but most of the work is heavily dependent on the IGPP time series programs and the LEROY package from CIRES. A mother script was written to call the command scripts, so a disk of 10 days of 56 channels of raw data can be processed into plots with less than 15 minutes of active effort; about 350 commands are called by the script. A sample of the last 3 months of raw data from Adak is in Figure 1.

An event of note occurred at Adak on 21 November 1980, in which an apparent co-seismic tilt was recorded identically on all 8 tiltmeters. The general sense of the event was that the island tilted down to the NW about 3 μ-radians and returned over a 30 minute period. Figure 2 shows some of the data. It is not a transient of the instrument system; the time constant of the tiltmeter bubble is one second, and of the electronics, 20 seconds. We have had many earthquakes of considerably greater intensity at the instrument sites, and have not seen such an event. It is too large to be directly associated with the $\simeq m_b$ 5.0 earthquake 100 km away, so we speculate that it is a pulse from something like a "slow quake" in the subduction zone. Suggestions are welcome.

Reports

Morrissey, Sean-Thomas, (1981). The Adak Winter Field Trip, January 19-24, 1981: A Special Technical Report, Open File, 30 pp.

Morrissey, Sean-Thomas, (1981). A Progress Report: The New Madrid Seismic Telemetry Network, 38 pp.

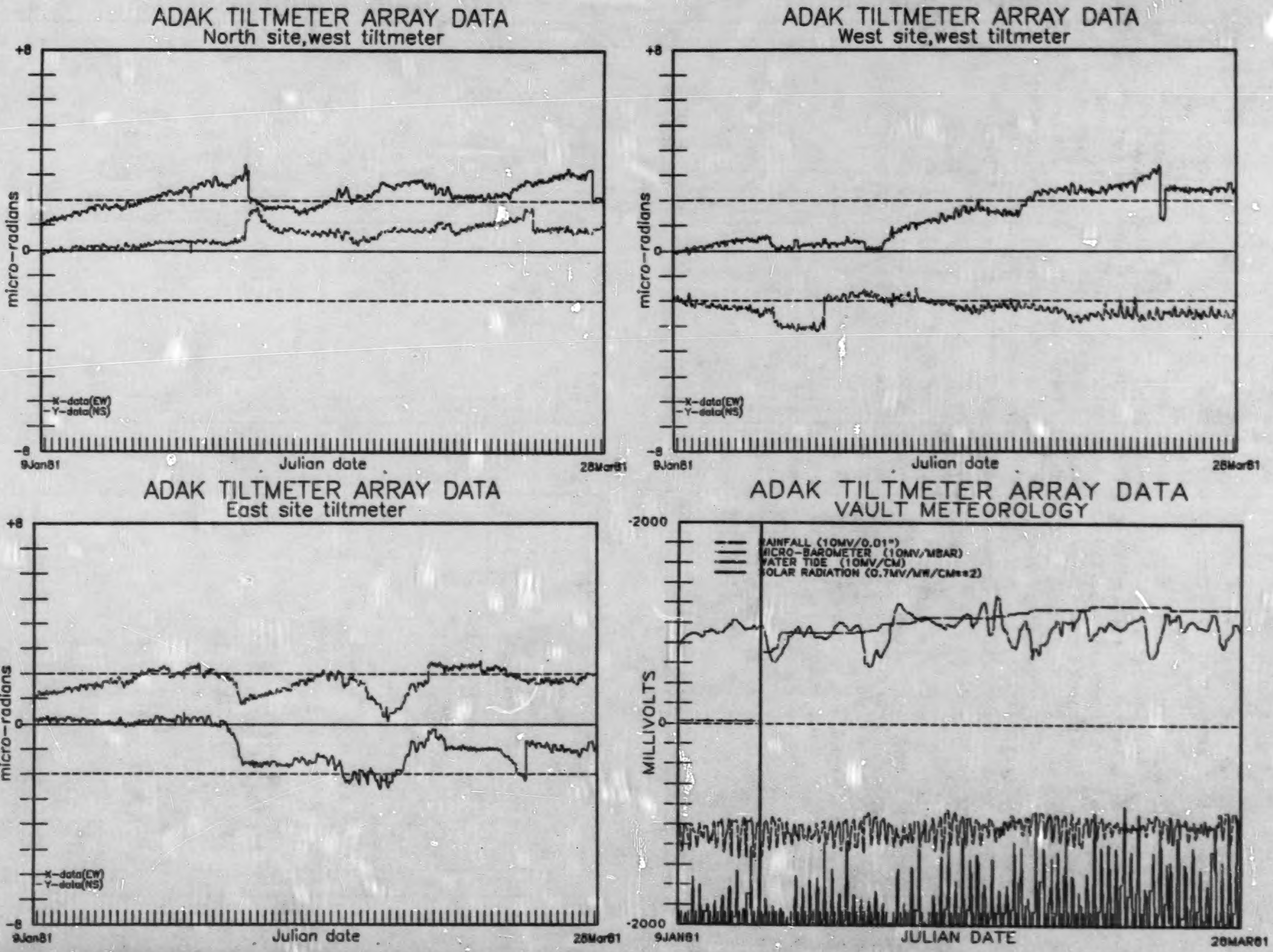

Figure 1: Sample of raw Adak data for 9 January to 28 March 1981.

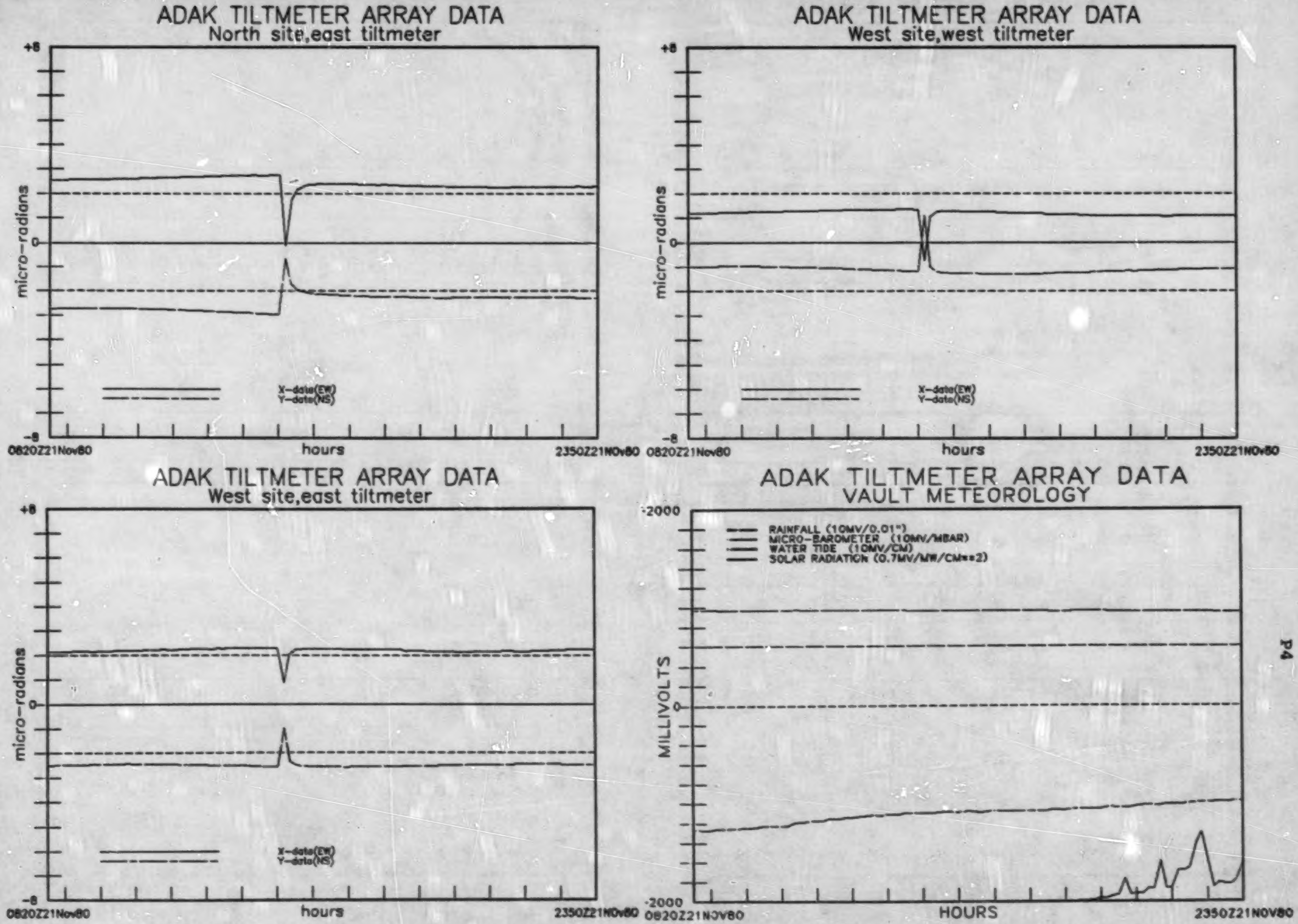

Figure 2: Sample of data for the tilt event of 21 November 1980.

MEASUREMENT AND ANALYSIS OF THE NEAR SURFACE STRESS FIELD IN THE VICINITY OF ACTIVE FAULTS IN SOUTHERN CALIFORNIA

14-08-0001-17705

Marc L. Sbar (602)626-4849
Randall M. Richardson (602)626-4950
University of Arizona
Tucson, Arizona 85721

The objective of this research project is to successfully measure the regional stress field in a tectonically active area using the near-surface strain relief method, an in-situ technique originally developed by the U.S. Bureau of Mines.

During the summer of 1980, about fifty strain relief measurements were made at two sites near Palmdale CA, one 2 km SW of the San Andreas fault (site L) and the other 20 km to the NE (site I). Previous near-surface data indicated that measurements made within 6 m of the surface might be unreliable for predicting tectonic stress in this region, perhaps due to thermal stresses in the upper few meters associated with large seasonal temperature variations. In an effort to address this question, measurements were made successively to depths of 29 m at both sites.

Results of successful measurements are attached. Both the orientation and magnitude inferred for the maximum horizontal compressive stress (P) are plotted vs. depth (up is also North), and shown for reference are the respective lithostats, or estimates of the vertical stress, at each site. For measurements made below 6 m, a very consistent NNW orientation for P was obtained. The rose diagrams also shown reflect the averages and standard deviations obtained at sites I and L. A N 23°W orientation for P is in excellent agreement with tectonic stress orientations inferred by Zoback et al., (1980) from deep hydrofracture measurements to depths of 800 m at sites within 2 km of our site L. It is also in agreement with orientations inferred from strain accumulation on the Palmdale and Pearblossom trilateration nets (Lisowski and Savage, 1979).

The excellent agreement between our near-surface results and the results of others, particularly those sensing to much greater depths, leads us to conclude that we are indeed measuring tectonic stress with this relatively inexpensive technique provided measurements are made below 6 m. The scatter observed in the orientation of P above 6 m is suggestive of a thermally induced stress acting along existing rock fractures or anisotropy. One of the goals of future work will be to more thoroughly understand the effect of this thermal stress. During January 1981, we will redrill one outcrop and compare summer and winter data.

References:

Zoback, M.D., H. Tsukahara, S. Hickman, Stress Measurements in the vicinity of the San Andreas Fault: Implications for the Magnitude of Shear Stress at Depth, submitted to: Journal of Geophysical Research Special Issue on Stress. Manuscript SIS 5352, 1980.

Lisowski, M., J.C. Savage, Strain Accumulation from 1964 to 1977 Near the Epicentral Zone of the 1976-1977 Earthquake Swarm Southeast of Palmdale, California, Bull Seism Soc. Amer, 69, pp 751-756 June 1979.

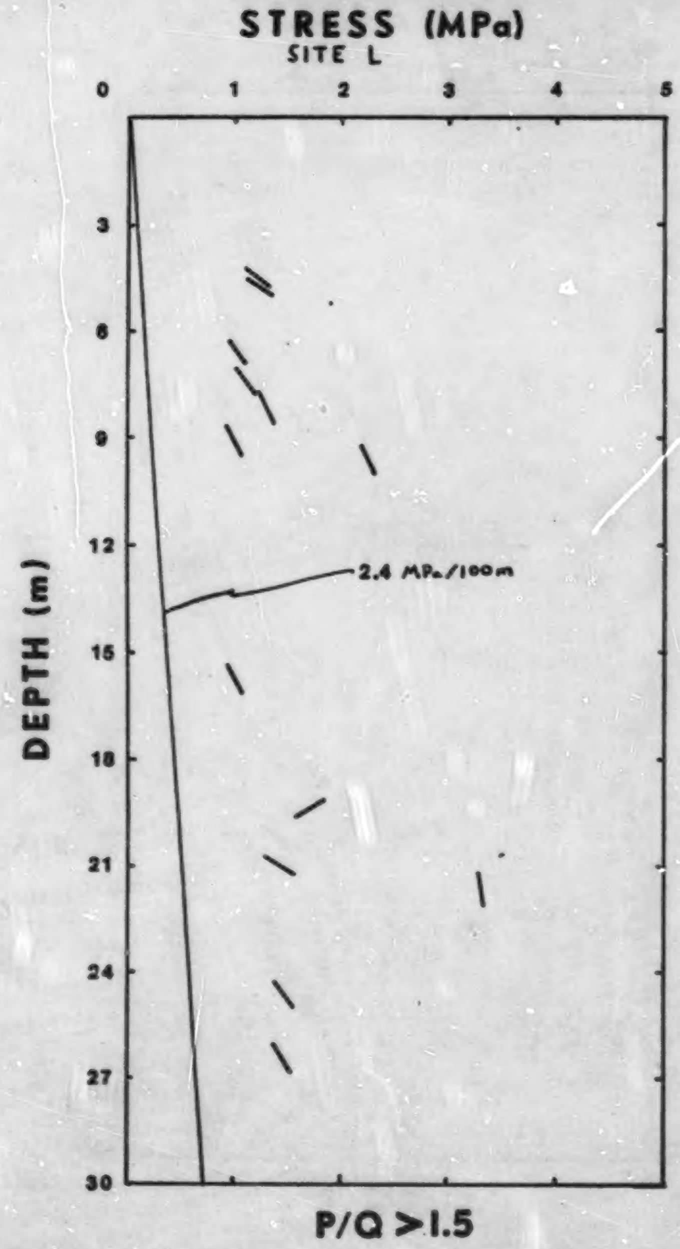
STRESS (MPa)
SITE L
0
1
2
3
4
5
DEPTH (m)
3
6
9
12
15
18
21
24
27
30
2.4 MPa/100m
P/Q >1.5

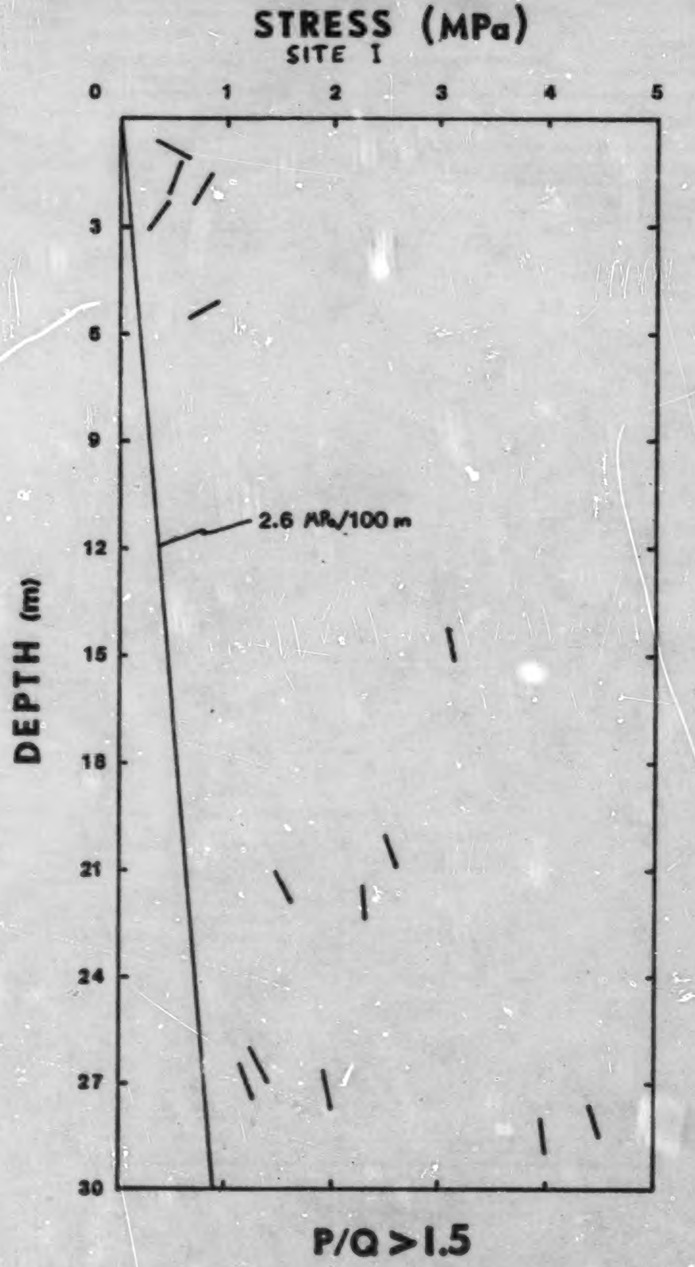
STRESS (MPa)
SITE I
0
1
2
3
4
5
DEPTH (m)
3
6
9
12
15
18
21
24
27
30
2.6 MPa/100 m
P/Q >1.5

P4

ORIENTATION OF P AXIS

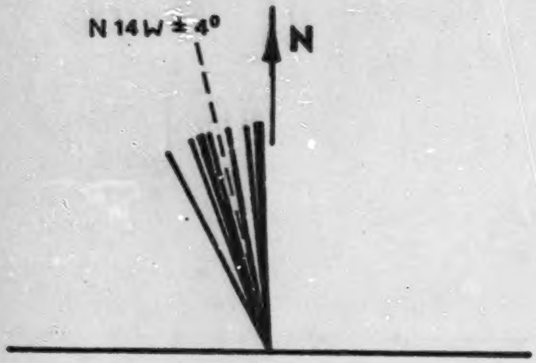

SITE I

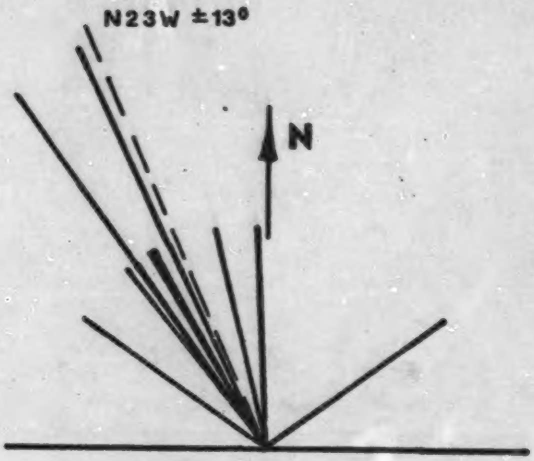

SITE L

Title: Detailed analysis of deformation associated with the Melones fault: A deeply-eroded former plate boundary, western Sierra Nevada, California

Contract Number: USGS 14-08-0001-18376

Principal Investigators: Dr. Richard A. Schweickert
Dr. Terry Engelder

Institution Name and Address: Lamont-Doherty Geological Observatory
of Columbia University
Palisades, New York 10964

Telephone Number of Principal Investigators: 914-359-2900

Field studies along the Melones fault zone in five detailed traverses and five reconnaissance traverses indicate that the fault has had three distinct periods of activity, each characterized by a distinct style of deformation and displacement.

Late Jurassic faulting is typically characterized by very narrow zones (10-20m) of ductile deformation and transposition of hangingwall and footwall rocks. However, where the hangingwall is granodiorite, the zone of ductile deformation is over 1 km wide.

Early Cretaceous faulting, which often does not coincide with Jurassic faulting, is characterized by brittle, gouge-filled shear zones, associated with quartz veins. Sense of displacement is high-angle reverse. Usually the brittle shearing occurs over a wide zone.

Cenozoic faulting, as shown by studies of Woodward-Clyde Consultants, is characterized by narrow gouge or clay-filled seams and brittle shears that slice through or are adjacent to broader zones of fault gouge.

Thus, these results indicate that important Cenozoic reactivation occurs primarily (exclusively?) along the Cretaceous high-angle reverse faults.

In addition, major strike-slip displacements on the Melones fault zone can be ruled out because: 1) the zone of Jurassic ductile deformation is exceedingly narrow, and fault fabrics exactly parallel regional slaty cleavages in footwall rocks, suggesting that the Jurassic fault experienced thrust displacements; 2) Knopf (1929) showed that Cretaceous displacements were typically only on the order of 100 m.

Finally, the character of deformation along the Jurassic fault seems to be strongly dependent upon the nature of lithologies in the hangingwall and footwall.

A Crustal Deformation Observatory Near the San Andreas Fault in Central California

14-08-0001-18370

Larry E. Slater
Cooperative Institute for Research
in Environmental Sciences
University of Colorado
Boulder, CO 80309
(303) 492-8028

Investigations

1. The geodetic array near Hollister, California has been measured almost daily for the last five years using a multiwavelength distance measuring (MWDM) instrument. The array consisted of nine primary lines and several secondary lines covering approximately 100 km^2. The lines were 3 to 9 km in length and radiated from the MWDM instrument site. The Calaveras fault bisected the MWDM array. The operation of the MWDM instrument at the Hollister site was concluded during October 1980.

2. A site near San Juan Bautista has been selected for the Crustal Deformation Observatory. The observatory will utilize both the MWDM instrument and the new 2-fluid tiltmeter. We will be able to collect both horizontal and vertical deformation data simultaneously to high precision.

3. An interim measurement program was begun near Palmdale in Southern California during October 1980 and is continuing at the present time. Rapid changes in strain had been monitored by Savage et. al. (1981) in the region and one of the goals of the MWDM interim effort was to provide a more detailed picture of this deformation. We also wished to establish a high precision geodetic data base as early as possible with the expectation that other MWDM instruments would be available in the near future to continue this effort when the University of Colorado MWDM instrument is moved to San Juan Bautista. This interim work is a cooperative effort between the University of Colorado and the U.S. Geological Survey.

4. The University of Colorado's MWDM instrument was extensively modified during this reporting period. The entire computing and electronic portions of the MWDM instrument have been redesigned and modernized.

Results

1. The Hollister MWDM array was deactivated during this reporting

period after completing over 5 years of high precision measurements in a region spanning the Calaveras fault in central California. The data collected during the 1847 days of the experiment are listed on computer file at the U.S. Geological Survey facility in Menlo Park, California. The long-term changes in line lengths within the Hollister array generally occur in fairly well defined episodes that have been ascribed to slip at depth on the nearby faults. These episodes typically last for several weeks and are intersperced with periods of relative quiescence. An anomalous change in length was observed on several of the lines in the Hollister array that may be associated with the propagation of a creep wave across the array (Slater, 1980). If this interpretation is correct the creep wave propagation velocity was approximately 40 km/a. The analysis and interpretation of the Hollister MWDM array data is ongoing.

2. The construction of the MWDM building will begin soon near San Juan Bautista, California. Completion of the structure is expected within 2 months. Radiating from this site will be approximately 10 lines, each 2 to 8 km in length. Within this MWDM array is the site of the 2-fluid tiltmeter. The installation of the tiltmeter is complete at this time and measurements will begin as soon as instrument evaluation is complete. The tiltmeter is composed of 2 legs joined in the shape of an 'L', one leg is 243 meters in length the other 193 meters in length. The fluid height sensor units are situated on thermally stable benchmarks.

3. During the first 6 months of the interim measurement program we have collected over 600 high precision length measurements from the MWDM site on Holcomb ridge near Palmdale, California. Strain calculations using the recent MWDM data show significant changes in the strain field, particularly in the component that is normal to the San Andreas fault. Changes as large as a micro strain appear over time periods as short as a few months. These changes may be associated with variation in the level of stress across the fault such as those suggested by Slater (1981) within the Hollister MWDM array.

4. Modifications to the MWDM instrument consisted of a complete redesign of the analog servo and all associated control electronics, replacement of the Varian 620/100L computer and various input-output peripherals. A Hewlett-Packard 9815 calculator was interfaced to the instrument and now programs the pulse generators for system timing, reads the frequency counters, and performs the distance calculations. The effect of these modifications has been to produce an instrument requiring much less power, an instrument considerably smaller and lighter than the original, an instrument of high reliability.

References (PI references are listed in Reports section)

Savage, J.C., W.H. Prescott, M. Lisowski, and N.E. King, Strain on the San Andreas fault near Palmdale, California: Rapid, aseismic change, Science, 211, 56-58, 2 Jan 1981.

Reports

Slater, L.E., Multiwavelength EDM measurements near Hollister, California: 1975 - 1980, Transactions American Geophysical Union, 61, no. 46, 1126, 1980.

Slater, L.E., Episodic block motion and convergence along the Calaveras fault in central California, Tectonophysics, 71, 87-94, 1981.

Slater, L.E., A. McGarr, J.O. Langbein, and M.F. Linker, Initial MWDM measurements on the Palmdale uplift, Transactions American Geophysical Union, 62, no. 17, 393, 1981.

AN EXPERIMENTAL STUDY OF THE RHEOLOGY OF CRUSTAL ROCKS

Contract 14-08-0001-15247

J. Tullis and R.A. Yund

Department of Geological Sciences
Brown University, Providence, RI 02912
401-863-2240

The purpose of this study is to gain a more fundamental understanding of the deformation of crustal rocks by determining the grain-scale deformation mechanisms operative at different pressures, temperatures, strain rates, differential stresses, and water contents; to determine both the macroscopic and the microscipic brittle-ductile transitions for these rocks as a function of these variables; and to develop an understanding of the rheology of polyphase aggregates in terms of the flow properties of their principal constituents which will allow extrapolation to natural conditions. Our approach involves detailed petrographic and transmission electron microscope (TEM) analysis of the deformed samples.

During the past year we have submitted two manuscripts which are currently in press, one dealing with the effect of high dislocation density on oxygen diffusion in feldspar, and another dealing with faults produced experimentally at high temperatures and pressures. Another major manuscript on flow laws for granitic and gabbroic rocks and their constituents, including the effect of water, is currently in preparation and should be submitted within a month or two. In addition we have made major advances in sample assembly design. Our results are summarized below.

Experimental High Temperature and Pressure Faults

Recent results from our laboratory (Shelton et al., 1980, in press) show that faulting is not necessarily precluded by high pressure and temperature, and that the presence or absence of trace amounts of water is of major importance. Experiments were done on a fine-grained, polycrystalline albite rock, and two degrees of sample wetness were tested: (1) air drying at 160°C for 12 hours, which leaves about 0.1 weight% water in the samples, and (2) vacuum drying at 800°C for 24 hours, which is believed to leave only about 0.01 weight% water in the sample.

At 15 kb confining pressure, air-dried samples exhibited a transition from cataclastic flow at lower temperatures ($\sim 500^{\circ}C$) to steady state dislocation creep at higher temperatures ($\geq 900^{\circ}C$), as expected. However, vacuum dried samples were tested at temperatures of 900°C to 1125°C; they were much stronger than equivalent air-dried samples, and all failed by the unexpected mechanism of faulting. At 5 kb confining pressure, vacuum-dried samples have not been tested; air-dried samples show expected behavior at lower temperatures, but at 600° to 900°C they show sharp faults (Tullis and Yund, 1977; Tullis et al., 1979) identical in appearance and behavior to those observed in vacuum dried samples deformed at high temperature and pressure.

The high temperature faults at both 5 and 15 kb pressure differ in several important ways from faults produced in the wetter, air-dried material tested at lower temperatures (25° to 500°C) and pressures (5 to 7.5 kb). First, they are oriented at about 45° to σ_1 instead of 30°. Second, the faults are extremely sharp; very little gouge is produced. Third, the failure on these faults is less sudden.

TEM observations show that for the vacuum-dried samples, the temperature of the transition from dominantly microcracking to dominantly dislocation glide and climb is increased by about 500°C compared to that for air-dried samples. This increase brought about by removing approximately 0.1 weight % water can be compared with a decrease of only about 200°C brought about by adding that same amount of water instead (Tullis and Yund, in press).

It is believed that the high temperature and pressure faults may develop as cracks propagating in an orientation of high resolved shear stress. High confining pressure should favor the propagation of shear cracks, because they involve no volume increase. High temperature may also favor shear cracks, as limited dislocation motion may blunt crack tips and thus reduce tensile stress concentrations.

The occurrence of sharp faults at 15 kb also means that the frictional strength of the hypothesized growing shear crack must be lower than that predicted by Byerlee's law. Decreasing frictional strength with increasing temperature has also been found by other workers. None of our high temperature and pressure faults reached steady state sliding, but they do show a lower value of friction than low temperature faults. This temperature dependence suggests that thermally activated processes such as dislocation motion are important. Our proposed model for the high temperature and pressure faults is that initial flaws such as grain boundaries and cleavage planes, which are oriented at high resolved shear stress, are able to slide even at high pressure if the temperature is high enough to reduce friction. Possibly the high temperature permits dislocations to glide through asperities. The sliding concentrates shear stress at the flaw tips and propagates the fracture in a shear mode. Thus the temperature dependence of sliding could impose a temperature dependence on the fracture strength.

Water appears to be very important in the formation of the high temperature and pressure faults through its effect on dislocation glide and climb. At 15 kb pressure, the trace amount of water in the air-dried samples allows them to undergo homogeneous crystal plastic flow at a stress lower than that for faulting, whereas the vacuum dried samples faulted. There is little or no hydrolytic weakening in air-dried samples deformed at 5 kb pressure, presumably because little water dissolves in the crystal at these conditions. Thus these samples also develop high temperature faults.

There are many geologic situations where faulting apparently occurs at pressures which would require extremely high shear stresses according to models of temperature-independent friction or fracture. For example, thrust faults occur at depths of 50 km in down-going oceanic slabs, and would require ~35 kb differential stress by the Coulomb criterion. The recent COCRP seismic profile across the Wind Riber Thrust also shows evidence of the fault at depths of 24 and possibly 36 km. The temperature in both cases is probably 400° to $600^{\circ}C$, and temperature dependent friction with consequent high temperature (dry) faulting may be the most reasonable explanation of these features.

Improvements in Sample Assembly

We have done some further finite element modelling of the sample assembly for the Griggs-type solid confining media deformation apparatus. In addition we have experimented with end pistons having thermal conductivities much lower than the carbide or alumina generally used. Both zirconia and hard-fired pyrophyllite have conductivities almost an order of magnitude lower than that of alumina; use of these pistons reduces the longitudinal temperature gradient in the samples to a few percent. We are currently experimenting with an internal force gage, and the initial results are encouraging.

Flow Laws for Crustal Rocks

Most of the crust consists of polyphase rocks such as 'granites' and 'gabbros', consisting of at least two phases of quite different rheology. Flow laws for such aggregates cannot be measured in the laboratory and reliably extrapolated to natural conditions. Our goal is to express the flow law for polyphase aggregates in terms of the flow properties of its constitutent phases and their volume proportions and geometrical arrangement.

We have determined flow laws for Enfield aplite and for its constituents quartzite and a pure albite aggregate; we have also determined flow laws for Maryland diabase and for its constituents anorthosite and clinopyroxenite. Most of the flow laws were determined for hot-plate dried samples; removal of about 0.1 weight % water by vacuum drying prior to deformation raised the activation energy substantially but did not greatly affect the stress exponent. Addition of water lowers the activation energy; the Adirondack anorthosite contains somewhat more water than the Bushveld anorthosite. Most of the creep tests were done at differential stresses of 1.0 to 6 kb; for all the materials tested there appears to be an increase in the stress exponent with increasing differential stress, and the value of the exponent listed below is for a range of 1-3 kb.

The flow laws for the seven materials we have tested are listed below; a major manuscript discussing these results in detail is currently in preparation.

aplite: $\dot{\epsilon} = 0.5\,\sigma^{3.1}\,e^{-39/RT}$

quartzite: $\dot{\epsilon} = 11.4\,\sigma^{2.0}\,e^{-40/RT}$

albite rock: $\dot{\epsilon} = 5.2\ \sigma^{2.7}\ e^{-55/RT}$

diabase: $\dot{\epsilon} = 1.4\ \sigma^{3.4}\ e^{-62/RT}$

Bushveld anorthosite: $\dot{\epsilon} = 1.2\ \sigma^{2.6}\ e^{-57/RT}$

Adirondacks anorthosite: $\dot{\epsilon} = 3.0\ \sigma^{5.3}\ e^{-48/RT}$ (n at 7kb)

clinopyroxenite: $\dot{\epsilon} = 2.5\ \sigma^{2.6}\ e^{-83/RT}$

Reports

Kronenberg, A.K., and Shelton, G.L., in press, Deformation microstructures in experimentally deformed Maryland diabase: Jour. Struc. Geol.

Shelton, G.L., Tullis, J., and Tullis, T.E., 1980, Faulting at high temperature and pressure: Trans. Amer. Geophys. Union, v. 61, p. 376.

Shelton, G.L., Tullis, J., and Tullis, T.E., in press, Experimental high temperature and high pressure faults: Geophys. Res. Let.

Tullis, J., and Yund, R.A., in press, Hydrolytic weakening of experimentally deformed Westerly granite and Hale albite rock: Jour. Struc. Geol.

Yund, R.A., and Tullis, J., 1980, The effect of water, pressure, and strain on Al/Si order-disorder kinetics in feldspar: Contrib. Mineral. Petrol., v. 72, p. 297-302.

Yund, R.A., Smith, B., and Tullis, J., 1980, Dislocation-assisted diffusion of oxygen in albite: Geol. Soc. Amer. Abstracts with Programs, v. 12, p. 553.

Yund, R.A., Smith, B., and Tullis, J., Dislocation-assisted diffusion of oxygen in albite: submitted to Phys. Chem. Minerals.

Seismicity and Structure of the San Pablo Bay-Suisin Bay Seismic Gap from Calnet and Explosion Data

9930-02938
D. H. Warren
Branch of Seismology
U.S. Geological Survey
345 Middlefield Road, MS/77
Menlo Park, California 94025
(415) 323-8111, ext. 2531

Investigations

1. An overall plot of earthquake epicenters was made of the investigation area, broadened to include the region northwest and southeast of the San Pablo and Suisin Bays, using all events in the Calnet catalogs from 1969 through 1980. A smaller area was defined extending about 60 km northwest and about 40 km southeast of these bays, and six cross sections were plotted, usually along active or dormant faulting, to obtain a fairly complete display of depth distribution.

2. A few stereoplots have been made to study the geometry of active portions of the faults. The presentations are still in the experimental stage.

3. Previous preliminary study of the focal mechanisms of larger earthquakes of magnitude 2.4 and above was made in the immediate vicinity of these bays.

Results

1. Most earthquakes occur in concentrated globular clusters on or near known NNW-SSE-trending faults and many earthquakes occur at widely varying densities along and near faulting elsewhere. The southern boundary of the seismic gap is well defined to be just south of the bay, but the northern boundary is irregular. It extends about 20 km northwest of San Pablo Bay.

2. The stereoplots emphasize the nonuniform nature of the earthquake distributions. They show the prominence of clusters, some dense, some with not many events. Earthquakes near faulting occur in a ragged fashion in a zone on the order of 2-5 km from the fault. Location inaccuracy may contribute to the scatter. Just east of Suisin Bay, earthquakes extend right across the eastern projection of the gap in a nearly north-south zone. The majority of the earthquakes in this zone are deeper than 15 km. Most of the deeper earthquakes are in a 19± km deep cluster just east of the center of Grizzly Island on the northeast side of Suisin Bay. This location may be on the north boundary of the eastern projection of the gap. Some earthquakes occur to the south of the cluster and extend as deep as 25 km.

3. In the immediate vicinity of the San Pablo Bay and Suisin Bay earthquakes of magnitude 2.4 and above from 1969 to 1978 were located mostly along the Hayward and Concord faults south of these bays and in a more diffuse zone extending mostly north of the Sacramento River just east of Suisin Bay. Most focal mechanisms shown NNW-trending, right-lateral, strike-slip motion.

Reports

None.

Studies of the Seismic and Crustal Deformation Patterns of an Active Fault: Piñon Flat Observatory

14-08-0001-18398

Frank Wyatt

Jonathan Berger & James N. Brune, Principal Investigators
University of California, San Diego - La Jolla, California 92093

A collection of nearly twenty instruments is being operated at Piñon Flat Observatory (PFO) in an effort to monitor the ambient strain, tilt, and gravity near an active fault zone. Secondary to this function, the goal of the research program at PFO is to determine the factors limiting the accuracy of observatory-based geophysical instrumentation. Because the signals of interest occur at such low frequencies (e.g., one cycle per year) the process of identifying these factors is not a simple one. Subsequent to performing an experiment, it is often necessary to collect many months of data in order to quantify the results. The array of instruments at PFO provides a data base that is used to accelerate the process.

A comparison of the recent records from the short fluid tiltmeter (50 m) and the Northwest-Southeast strainmeter (731 m) at PFO illustrates the value of simultaneous measurements. Figure 1 presents the tiltmeter observations for the period 1979.64 to 1981.04. Also shown are the instrument fluid temperature, which is in equilibrium with the ground temperature at a depth of .5 m, and the daily precipitation. A feature of this record that stands out is the symmetric cusp in the tilt around the time of a local (M_L 5.3) earthquake. The observed tilt offset at the time of the event, .112 μ radians, is in excellent agreement with the value determined by a simple calculation for the deformation related to the faulting (.106 μ radians). However, the factors responsible for the cusp are not as clear. We believe that both the upward and downward changes in trend were caused by displacements in the materials under the instrument in response to the rainfall that occurred in the preceding weeks.

The evidence for this conclusion is provided by examining Figure 2. This figure displays the uncorrected strain observations and the data corrected for monument displacement at the North-West end (only). These are presented on a time and magnitude scale equal to that of Figure 1. The size of the tidal signals (indicated by the width of the traces) suggests that the vertical scales are different. However, a tiltmeter responds both to accelerations and deformation, which results in the tidal signals being roughly three times greater than the purely deformational signals recorded by a strainmeter. There is no indication of unusual deformation associated with the local earthquake (1980.1 to 1980.2) in the strain records. Indeed, we have evidence that the conspicuous changes in the other portions of the strain record are due to displacements of the South-East reference monument. In particular, the change which occurred near the start of 1980 was due to recementing the South-East monument.

Based on these observations, it is clear that additional instrument improvement is possible. The tiltmeter baselength has recently been extended to 535 m, with vertical strainmeters at each end to monitor the undesirable motions of the near surface monuments. Similarly the strainmeter is to be improved by installing a second "optical anchor" at the southeast end of the instrument. We anticipate that these changes will result in reducing the variance of the low frequency observations significantly.

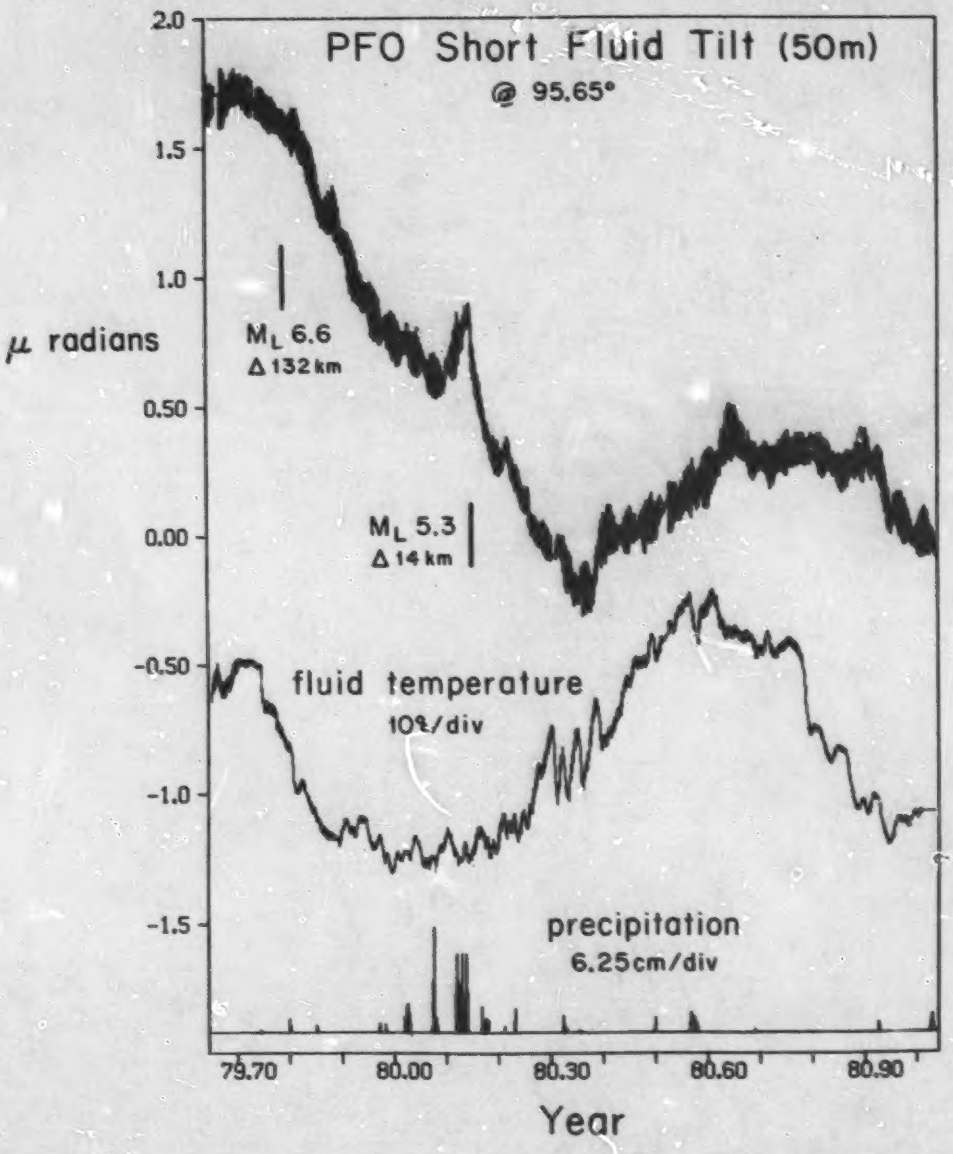
PFO Short Fluid Tilt (50m)
@ 95.65°
2.0
1.5
1.0
0.50
0.00
-0.50
-1.0
-1.5
μ radians
M_L 6.6
Δ 132 km
M_L 5.3
Δ 14 km
fluid temperature
10°/div
precipitation
6.25cm/div
79.70
80.00
80.30
80.60
80.90
Year

Figure 1.

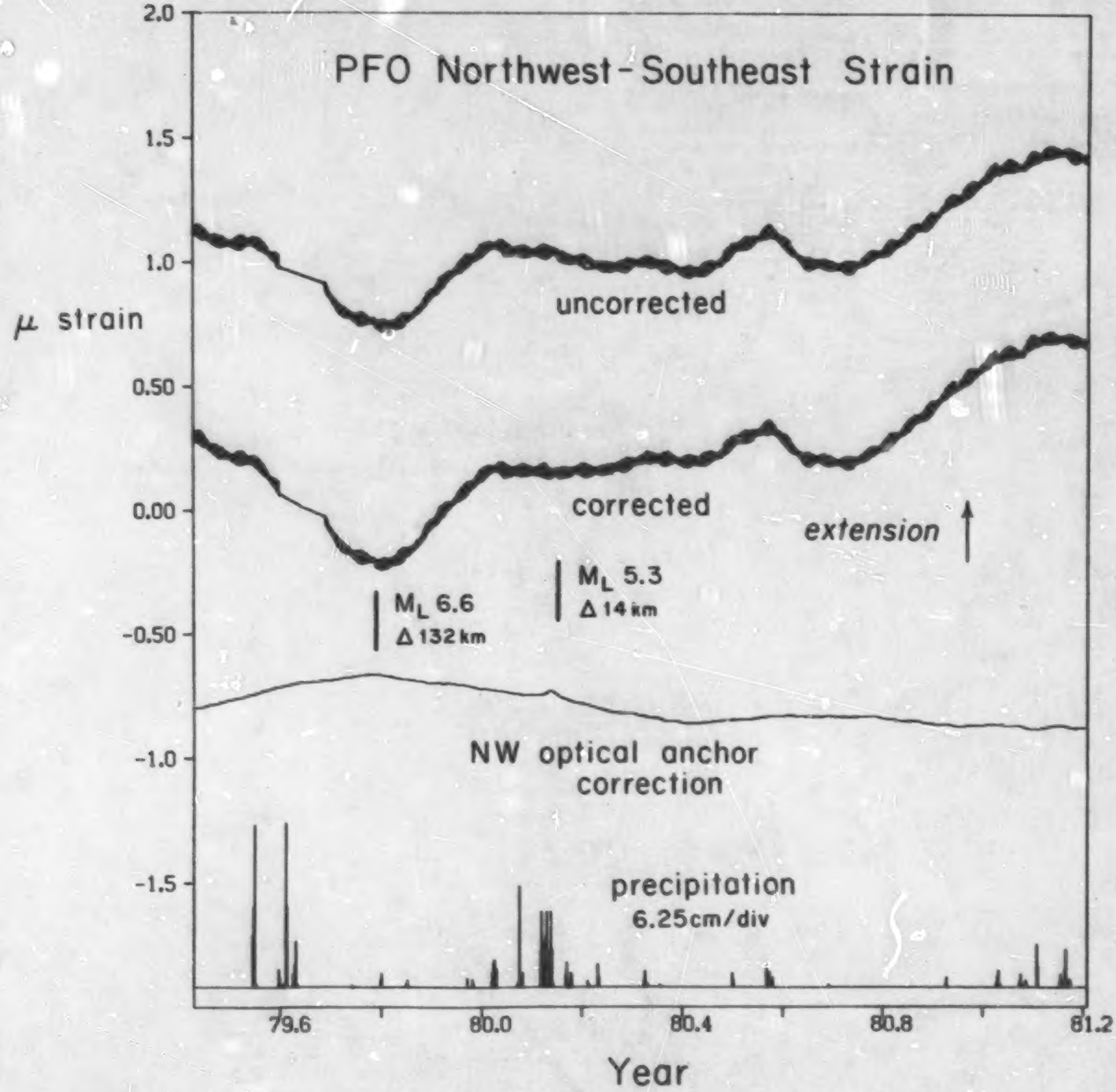
PFO Northwest-Southeast Strain
2.0
1.5
1.0
0.50
0.00
-0.50
-1.0
-1.5
μ strain
uncorrected
corrected
extension ↑
M_L 6.6
Δ 132 km
M_L 5.3
Δ 14 km
NW optical anchor correction
precipitation
6.25cm/div
79.6
80.0
80.4
80.8
81.2
Year

Figure 2.

U.S. Seismic Network

9920-01899

Marvin A. Carlson
Branch of Global Seismology
U.S. Geological Survey
National Earthquake Information Service, Stop 967
Box 25046, Denver Federal Center
Denver, Colorado 80225
(303) 234-3994

Investigations

U.S. Seismicity:
Continuously monitor U.S. Seismicity using data recorded by the U.S. Seismic Network.

Worldwide Seismicity:
Data from the U.S. Seismic Network are used to obtain a preliminary location of significant earthquakes worldwide.

Results

As an operational program, the U.S. Seismic Network operated normally throughout the report period. Data were recorded continuously in real time at the NEIS main office in Golden, Colorado. At the present time, 78 channels of SPZ data are being recorded at Golden on Develocorder film. This includes 9 channels of Alaskan data telemetered to Golden via satellite from the Alaska Tsunami Warning Center, Palmer, Alaska. A representative number of SPZ channels are also recorded on Helicorders to give NEIS real time monitoring capability of the more active seismic areas of the U.S. In addition, 11 channels of LPZ data are recorded in real time on multiple pen Helicorders.

Data from the U.S. Seismic Network are interpreted by record analysts and the seismic readings are entered into the NEIS data base. The data are also used by NEIS standby personnel to monitor seismic activity in the U.S. and worldwide on a real time basis. The data are also used to support the Alaska Tsunami Warning System and the Pacific Tsunami Warning System. At the present time, all earthquakes large enough to be recorded on several stations are worked up using the "Quick Quake" program to obtain a provisional solution as rapidly as possible. Finally, the data are used in such NEIS publications as the "Preliminary Determination of Epicenters" and the "Earthquake Data Report."

Development work is continuing on an event detector to monitor the U.S. Seismic Network in real time. Current plans are to use several PDP 11/03 microcomputers to monitor the data and pass events on to a PDP 11/23 for further processing.

The goals of the U.S. Seismic Network are to upgrade the quantity and quality of the data received to make possible more rapid and accurate location of U.S. earthquakes and significant earthquakes worldwide.

DIGITAL NETWORK-DATA PROCESSING

9920-02217

John P. Hoffman
Branch of Global Seismology
U.S. Geological Survey
Albuquerque Seismological Laboratory
Building 10002, Kirtland AFB-East
Albuquerque, New Mexico 87115
(505) 844-4637

Investigations

1. Data Processing for the Global Digital Seismograph Network. All of the digital data received from the global network is reviewed and checked for quality.

2. Network-Day Tape Program. All the digital data received at the ASL is assembled into network-day tapes which are archived and distributed.

3. International Data Collection Experiment. From October 1-15, 1980, all of the digital and analog data from the Global Digital Seismograph Network was assembled and forwarded to Sweden for special analysis.

4. New Event Detection Software Program for Short-Period Digital Data. Developed a software program to pick onsets of seismic events and measure parameters of the events.

Results

1. Data Processing for the Global Digital Seismograph Network. During the past 6 months, 358 digital tapes from the global network were edited, checked for quality, corrected when feasible, copied and archived in the Albuquerque Seismological Laboratory. Sixty-seven of these tapes were from the digitally recording WWSSN systems installed during the past year. Copies of their station tapes are regularly supplied to six of these stations for their own research programs.

2. Network-Day Tape Program. The network-day tape project is a continuing program which assembles the data from the entire digital network for a specific calendar day on to one magnetic tape. This tape includes all the necessary station parameters, calibration data, and time correction information for each station in the network. The production of these day tapes is normally about 60 days behind the actual recorded date to allow for delays in shipping the data to Albuquerque. As of April 1, 1981, the network day tapes were completed for February 2, 1981. Five copies of the network day tapes are forwarded to various research centers in this country. Individual distribution is handled by the Environmental Data and Information Service in Boulder, Colorado.

3. International Data Collection Experiment. The ad hoc Group of Scientific Experts of the UN Committee on Disarmament initiated a seismic data collection program for the time frame of October 1-15, 1980. All stations in the Global Digital Seismograph Network recorded both short-period and long-period data

on a continuous basis. Ninety-three digital tapes were produced and copies were forwarded to Washington and ultimately to Sweden for final analysis.

All of these tapes were event detected, using a program developed at the ASL, in order that the event data might be included on the network day tapes. A listing of these events was provided to the Group of Scientific Experts for assistance in analyzing the digital data. In addition, 40 additional digital tapes from other U.S. stations containing continuous short-period data were event detected for this program.

4. Event Detection Software Program for Short-Period Digital Data. An event detection program has been developed and tested that measures parameters of short-period seismic signals. These parameters include: (1) the on-set time, (2) the signal-to-noise ratio of the first break expressed as a function of the standard deviation of the background noise, (3) polarity of the first break, and (4) period and amplitude of the signal. Self-evaluating features are employed. Tests demonstrate that the algorithm can be implemented with integer arithmetic. Although the algorithm appears to function better with recursive filters, it functions moderately well (80-90% of clear on-sets picked correctly) without them. We are now testing the possibility of implementing this algorithm on SRO field systems.

Reports

Murdock, J. M., and Jaksha, L. H., 1980, Time-term solutions and corresponding data for the crustal structure of north-central New Mexico, USGS Open-File Report 80-2014.

Murdock, J. M., and Jaksha, L. H., 1980, the P-wave velocity of the uppermost mantle of the Rio Grande rift region of north-central New Mexico, accepted by JGR subject to editorial revisions.

ALBUQUERQUE OBSERVATORY

9920-01260

Lawrence H. Jaksha
Branch of Global Seismology
U. S. Geological Survey
Albuquerque Seismological Laboratory
Building 10006, Kirtland AFB-East
Albuquerque, New Mexico 87115
(505) 844-4637

Investigations and Results:

Sixteen sites along the DICE THROW seismic-refraction line were re-occupied with ASL-2 tape recorders during the fall of 1980. Explosions originating at Morenci, Arizona, Miami, Arizona and Tyrone, New Mexico, were recorded. The Morenci data were digitized and compiled into a record section. A preliminary interpretation of the record section suggests the presence of reflectors in the upper crust beneath the western end of the line. The Conrad Discontinuity beneath the study area is defined by both reflected and refracted phases. The Pn velocity estimated from Morenci is 8.08 km/s. This value, taken in conjunction with that obtained from the 1976 DICE THROW shot (8.06 km/s) suggest that there is no dip along the base of the crust beneath the line.

Nine months of seismicity data from the San Juan basin have been compiled for an informal presentation at the Rocky Mountain section, AAPG meeting. A preliminary interpretation of our refraction studies in the basin will be presented as well.

Work conducted on the seismic networks included installing solar panels at Cedar Rock, Los Pinos, Chaco Canyon and Manzano Tower. An evaluation of a USGS radio-link between the San Juan basin and ASL is being done.

Reports:

Sanford, A. R., Olsen, K. H., and Jaksha, L. H., 1981, Earthquakes in New Mexico, 1849-1977, N.M. Bureau of Mines & Mineral Resources, Circular 171.

GLOBAL DIGITAL NETWORK OPERATIONS

9920-02398

Nicholas A. Orsini
Branch of Global Seismology
U.S. Geological Survey
Albuquerque Seismological Laboratory
Building 10002, Kirtland AFB-East
Albuquerque, New Mexico 87115
(505) 844-4637

Investigations

The Global Network Operations continued to provide technical and operational support to the SRO/ASRO/HGLP observatories, which includes operating supplies, replacement parts, repair service, redesign of equipment, training and on-site maintenance, recalibration and installation. Maintenance is performed at locations as required but also each station is scheduled a visit by a technician every few months for preventative maintenance and training purposes.

Early in this period, the Raytheon O&M contract attained the full compliment of technicians requested; i.e., one team leader and six digital technicians.

There were 18 SRO, 3 ASRO, 2 WWSSN, and 2 DWWSSN station visits made during this period.

The following station maintenance activity was accomplished:

ANMO - Albuquerque - SRO
Station set up for 3 S.P. Channel recording for October data collection experiment.

ANTO - Ankara, Turkey - SRO
Two (2) maintenance visits. One of these included setting up station for October data collection experiment.

BCAO - Banqui, Central African Republic - SRO
One maintenance visit to set station up for October data collection experiment.

BOCO - Bogota, Columbia - SRO
Two (2) maintenance visits. One of these included setting up station for October data collection experiment.

CHTO - Chiang Mai, Thailand - SRO
Six (6) maintenance visits.

CTAO - Charters Towers, Australia - ASRO
One maintenance visit.

GRFO - Grafenberg, West Germany - SRO
Two (2) maintenance visits.

GUMO - Guam - SRO
No visits

KONO - Kongsberg, Norway - ASRO
Two (2) maintenance visits.

MAJO - Matsushiro, Japan - ASRO
No visits.

KAAO - Kabul, Afghanistan - ASRO
No visits.

MAIO - Mashhad, Iran - SRO
No visits.

NWAO - Mundaring (Narrogin), Australia - SRO
One maintenance visit.

SHIO - Shillong, India - SRO
Two (2) maintenance visits.

TATO - Taipei, Taiwan - SRO
No visits.

SNZO - Wellington (South Karori), New Zealand - SRO
One maintenance visit.

WWSSN

SPA - Special project was accomplished November 80 thru February 81 to calibrate, change seismometers, and repair the WWSSN station at South Pole.
BOG - Long standing problem at Bogota, Columbia repaired in conjunction with SRO maintenance visit.

DWWSSN

ALQ - Albuquerque. Two DWWSSN stations installed during this period.
SCP - State College, PA

ASL Repair Facility

Assembly, testing, and shipping of five DWWSSN systems was accomplished.

Results

ASL participation in the ARPA/Swedish special experiment during October was successful. Plan basically called for continuous SP - three component digital data recording for period 1-15 October 1980.

Generally, the network provides improved geographical coverage with highly sensitive short-and long-period seismic sensors with analog and digital magnetic tape recordings.

USGS AND COOPERATIVE OBSERVATORIES

9902-01261

Nicholas A. Orsini
Branch of Global Seismology
U.S. Geological Survey
Albuquerque Seismological Laboratory
Building 10010, Kirtland AFB-East
Albuquerque, New Mexico 87115
(505) 844-4637

Investigations

Field activities consist of occasional visits to the seismic stations for the purpose of maintenance, calibration, or installation of new instrumentation. Stations are provided with advice on operation, maintenance, and calibration. Also all stations are provided with spare parts, operational supplies and replacement modules.

Results

These observatories contribute essential data to the NEIS, both routinely and on a rapid basis when required. The locations were selected to fill gaps in station locations and to provide better coverage for local events. All data are available for other seismologists when required.

WORLD-WIDE STANDARDIZED SEISMOGRAPH NETWORK (WWSSN)

9920-01201

Nicholas A. Orsini
Branch of Global Seismology
U.S. Geological Survey
Albuquerque Seismological Laboratory
Building 10010, Kirtland AFB-East
Albuquerque, New Mexico 87115
(505) 844-4637

Investigations

1. The Global Network Operations continued to provide technical and operational support to the WWSSN observatories as funding and staffing permitted.

2. During this period, 228 WWSSN modules were repaired and 344 separate items were shipped to support the network. Thirty-seven stations were supplied with annual shipments of photographic supplies and emergency shipments were made to five stations.

3. During the period October 6 through October 27, 1980, the usual annual training for the team (Ken Murphy and Allen Tinkham), planning to winter over at the SPA (South Pole) station, was provided. Training was also provided for a Raytheon contract technician during October 20 through November 24, for special modifications to be made to the SPA station. Training of two Raytheon contract technicians was provided during December 15 through December 19, on the WWSSN system. These men will comprise the first team in the DWWSSN upgrade program. An alternate (Ann Rognlie) was trained during January 7 through January 15, 1981, for possible replacement at SPA.

Results

A continual flow of high quality seismic data from the network of 115 observatories for use by the seismological community.

GLOBAL SEISMOGRAPH NETWORK EVALUATION AND DEVELOPMENT

9920-02384

Jon Peterson
Branch of Global Seismology
U.S. Geological Survey
Building 10002, Kirtland AFB-East
Albuquerque, New Mexico 87115

Investigations

1. Work continued on a system design study for a National Digital Seismograph Network, which was initiated under a different project last fiscal year.

2. Work continued on the test and evaluation of the digital WWSSN.

Results

1. Noise tests were completed on two types of accelerometers to determine their suitability for use in the NDSN system. Tests were also completed on one type of broad band seismograph that could be used in the system. A report on the design study has been drafted.

2. Tests on the DWWSSN system have been completed except for the linearity tests. A system has been installed at Albuquerque to provide data for evaluation of calibration stability and other parameters that require analysis of longer-term effects.

Seismic Observatories

9920-01193

Harry Whitcomb
Branch of Global Seismology
U.S. Geological Survey
Box 25046, MS 967
Denver Federal Center
(303) 234-5083

Investigations

Recorded and provisionally interpreted seismological and geomagnetic data at observatories operated at Newport, Washington; Cayey, Puerto Rico; Adak, Alaska; and Guam. At Newport, Washington, and Guam, 24-hour standby duty was maintained to provide input to the Tsunami Warning Service operated at Honolulu Observatory by NOAA. Also, Newport Observatory served as a part of the National Earthquake Information Service's, Early Earthquake Reporting Service during off duty hours by reporting information on felt and damaging earthquakes in the United States and on worldwide events of magnitude 6.5 or greater to government agencies, the news media, and the public.

Results

Continued to provide data on an immediate basis to the National Earthquake Information Service and the Tsunami Warning Service. Supported the Puerto Rico Project of the Branch of Earthquake Tectonics and Risk. Provided geomagnetic data to the Branch of Electromagnetism and Geomagnetism. Responded to requests from the public, interested scientists, state and federal agencies regarding geophysical data and pheonomena.

During early 1981, the Early Earthquake Reporting and the Tsunami Warning functions were moved from the observatory at Newport, Washington, to the NEIS in Golden, Colorado. This resulted in Newport Observatory being removed from 24-hour standby duty and the personnel complement was reduced by one employee.

National Earthquake Information Service

9920-01194

E. P. Arnold
Branch of Global Seismology
U.S. Geological Survey
Denver Federal Center, MS 967
Denver, Colorado 80225
(303) 234-3994

Investigations and Results

The weekly publication, Preliminary Determination of Epicenters (PDE), continues to be published on a weekly basis, averaging about 50 earthquakes. The PDE was taken from the Energy Enterprises DEC-20 computer and placed on our 11/70 at the beginning of March 1981. We have been able to publish a couple of PDEs using the system but are continuing to debug the program. Within a few weeks we should be running smoothly. The monthly summaries and Earthquake Data Reports (EDRs) are being done on the Energy Enterprises DEC-20 computer. We continue to publish all earthquakes which have data available within 30 days of the earthquake. We have had a few improvements on rapid data flow from our foreign contributors, but in order to reach our goal of a 10-day PDE, we will need much faster reporting of seismic data from our contributors, both foreign and domestic.

Those problems are still being worked on and slow but steady improvement is taking place. We continue to receive telegraphic data from the USSR on magnitude 6.5 or greater earthquakes; the latest was the 6.7 Italian earthquake of November 23, 1980. Data from the PR China via the American Embassy in Beijing is still being received including two additional stations for a total of four. One is from southern China.

The Monthly Listings of Earthquakes and Earthquake Data Reports (EDRs) are up to date. To date, the Monthly Listings and EDRs have been completed through November 1980 and are being printed and mailed.

The programs for entering seismic data on the BGS 11/70 computer are completed and operational. Programs for producing the NEIS publications on the 11/70 and ultimately the Golden VAX are well on their way and are operational on the 11/70 for the PDE beginning the first part of March, 1981. All the NEIS programs are being transferred to the VAX and hopefully will be operational by mid-May.

We continue to provide services on recent earthquakes in response to the increasing demands from scientists and the general public.

Reports

Preliminary Determination of Epicenters (24 weekly publications--October 1980 to March 31, 1981--Numbers 37-80 through 08-81). Compilers: W. Leroy Irby, Reino Kangas, John Minsch, Waverly Person, Bruce Presgrave.

Monthly Listings of Earthquakes and Earthquake Data Reports (EDR) (7 publications--May 1980 through November 1980). Compilers: W. Leroy Irby, Reino Kangas, John Minsch, Russell Needham, Waverly Person, Bruce Presgrave, William Schmieder.

Goals

Provide more rapid and comprehensive hypocenter locations to the government and the scientific community using our in-house computers.

Provide more rapid notification of significant or damaging earthquakes to relief agencies, the press, the scientific community, and the general public.

Keep the Monthly Listings and Earthquake Data Reports up to date.

Seismic Review and Data Services

9920-01204

R. P. McCarthy
Branch of Global Seismology
U.S. Geological Survey
Denver Federal Center, MS 969
Denver, Colorado 80225
(303) 234-5080

Investigations and Results

The quality control and technical review were carried out on 121,000 seismograms (660 station-months) generated by the World-Wide Standardized Seismograph Network (WWSSN).

Station performance reports were sent to 50 Station Directors. These reports cover instrumental and station operations which include calibration accuracies, damping, timing precision, noise patterns and intensities, record quality, seismogram backlog, label data, and any unusual problems. Operational standards remained at high levels throughout the system. Over 75 percent of the stations showed timing errors averaging less than 50 milliseconds daily. Polarity problems at Bulawayo (BUL) and Stuttgart (STU) have been corrected.

Kabul (KBL) continues to send its WWSSN and ASRO records. Backlog seismograms from Sanae (SNA) for 1973 through 1979 have been received. Sombrero (SOM) has also sent backlogs for 1974 and 1975. The situation with the Iranian stations remained the same.

The quality of the WWSSN, SRO, and ASRO microfiche film duplicates received from the NOAA microfilming service for the library have improved considerably. Replacement fiche duplicates for the "bad" copies are being sent out by NOAA. The initial shipment to our branch film library has not been received as of this report date.

United States Earthquakes

9920-01222

Carl W. Stover
Branch of Global Seismology
U.S. Geological Survey
Denver Federal Center, MS 967
Denver, Colorado 80225
(303) 234-3994

Investigations

1. Seventy-three earthquakes in 15 states were canvassed by a mail questionnaire for felt and damage data. Forty-three of these occurred in California. The most significant earthquake for this period was in northern California on November 8, 1980, at 41.16N, 124.31W, depth 14 km, magnitude 7.4 MS, 6.2 mb.

2. The United States earthquakes for the period October 1, 1980, to March 31, 1981, have been located and the hypocenters, magnitudes, and maximum intensities have been published in the Preliminary Determination of Epicenters.

3. The seismicity maps for Maine, New York, Pennsylvania, Maryland, and Delaware have been completed and are being printed at a scale of 1:1,000,000. The data for Minnesota, Iowa, North Dakota, Texas, Oklahoma, and Kansas have been compiled.

Results

The maximum Modified Mercalli intensity of VII was assigned to the Fields Landing, California, area for the November 8, 1980, earthquake. The most significant damage was the failure of the southbound lane of Tompkins Hill overpass on Highway 101. Other effects were of a few houses being moved off their pier and post type foundation and reports of people unable to walk across the room because of the shaking.

United States earthquake data for January-June 1980 have been compiled for publication in quarterly circulars.

Reports

Stover, C. W., Minsch, J. H., Reagor, G. B., and Smith, P. K., 1980, Earthquakes in the United States, January-March 1979: U.S. Geological Survey Circular 836-A, 42 p.

Stover, C. W., Hubiak, P., Minsch, J. H., and Person, W. J., 1980, Earthquakes in the United States, April-June 1979: U.S. Geological Survey Circular 836-B, 34 p.

Minsch, J. H., Stover, C. W., Person, W. J., and Smith, P. K., 1980, Earthquakes in the United States, July-September 1979: U.S. Geological Survey Circular 836-C, 39 p.

Stover, C. W., Reagor, B. G. and Wetmiller, R. J., 1980, Intensities and isoseismal map for the St. Elias earthquake of February 28, 1979: Seismological Society of America Bulletin, v. 70, no. 5, p. 1635-1649.

Stover, C. W., Barnhard, L. M., Reagor, B. G., and Algermissen, S. T., 1980, Seismicity map of the state of New Hampshire: U.S. Geological Survey Miscellaneous Field Studies Map MF-1261.

Stover, C. W., Barnhard, L. M., Reagor, B. G., and Algermissen, S. T., 1980, Seismicity map of the state of New Jersey: U.S. Geological Survey Miscellaneous Field Studies Map MF-1260.

Reagor, B. G., Stover, C. W., and Algermissen, S. T., 1980, Seismicity map of the state of North Carolina: U.S. Geological Survey Miscellaneous Field Studies Map MF-1224.

Reagor, B. G., Stover, C. W., and Algermissen, S. T., 1980, Seismicity map of the state of South Carolina: U.S. Geological Survey Miscellaneous Field Studies Map MF-1225.

Stover, C. W., Barnhard, L. M., Reagor, B. G., and Algermissen, S. T., 1980, Seismicity map of the state of Vermont: U.S. Geological Survey Miscellaneous Field Studies Map MF-1262.

Reagor, B. G., Stover, C. W., and Algermissen, S. T., 1980, Seismicity map of the state of Virginia: U.S. Geological Survey Miscellaneous Field Studies Map MF-1257.

Stover, C. W., Barnhard, L. M., Reagor, B. G., and Algermissen, S. T., 1980, Seismicity map of the state of Massachusetts: U.S. Geological Survey Miscellaneous Field Studies Map MF-856.

Reagor, B. G., Stover, C. W., Algermissen, S. T., Steinbrugge, K. V., Hubiak, P., Hopper, M. G., and Barnhard, L. M., 1980, Preliminary evaluation of the distribution of intensity, in Selected papers on the Imperial Valley, California, earthquake of October 15, 1979: U.S. Geological Survey Open-File Report 80-1094.

Reagor, B. G., Stover, C. W., and Hopper, M. G., 1981, Preliminary report of the distribution of intensities for the Kentucky earthquake of July 27, 1980: U.S. Geological Survey Open-File Report 81-198.

Stover, C. W., and von Hake, C. A., 1980, United States Earthquakes, 1978: U.S. Department of Interior, Geological Survey and U.S. Department of Commerce, National Oceanic and Atmospheric Administration, 112 p.

Stover, C. W., Barnhard, L. M., Reagor, B. G., and Algermissen, S. T., 1981, Seismicity map of the state of Connecticut and Rhode Island: U.S. Geological Survey Miscellaneous Field Studies Map MF-1283.

Digital Data Analysis

9920-01788

Ray Buland
Branch of Global Seismology
U.S. Geological Survey
Denver Federal Center, MS 967
Denver, Colorado 80225
(303) 234-4041

Investigations

1. Mantle Wave Magnitude. Develop methods for routine estimation of moment magnitude M_w from long period surface (mantle) waves.

2. Moment Tensor Inversion. Develop methods for inverting body phase wave forms for the best point source description.

3. Computation of Free Oscillations. Develop practical methods for computing free oscillations of the Earth and combining them to construct synthetic seismograms.

4. Computation of Travel Times. Develop practical methods for computing body phase travel times directly from arbitrary, realistic Earth models.

5. Swedish Experiment. Analyze both analog and digital data acquired during the DARPA "Swedish experiment" for the U.S. Delegation to the U.N. Committee on Disarmament.

6. Network Day Tape. Develop portable software for retrieving data from the Global Digital Seismograph "Network Day Tapes".

Results

1. Mantle Wave Magnitude. A method has been developed and tested extensively on synthetic data. It has been applied to one large, well studied event with good results. It is now being re-developed for more routine operation.

2. Moment Tensor Inversion. Two different methods have been developed, both of which work well on complex synthetic events. Initial experiments on real data look promising, but require a) developing error analysis machinery and b) further experiments with real data.

3. Computation of Free Oscillations. Programs have been converted to a local computer and modified to handle transverse isotrophy and physical dispersion as required by the new reference Earth Model.

4. Computation of Travel Times. Two different methods have now been implemented for a spherically symmetric Earth model, one superior in flexibility, one in speed. A little more testing is required before beginning work on an earthquake location scheme based on these methods.

5. Swedish Experiment. All analog and short period digital data have been analyzed. Analysis of the long period digital data should be complete within a few weeks. Note that this work constitutes nearly all of the U.S. Delegation report listed below.

6. Network Day Tape. Portable software is complete and fully documented. A users manual is complete and in technical review.

Reports

U.S. Delegation, 1981, U.S. Contributions to the data collection experiment, report to the U.N. Committee on Disarmament.

Madeleine Zirbes and Ray Buland, 1981, Network day tape software users guide, U.S.G.S. Open File Report, in press.

Earth Structure and its Effects upon Seismic Wave Propagation

9920-01736

George L. Choy
Branch of Global Seismology
U. S. Geological Survey
Denver Federal Center, MS 967
Denver, Colorado 80225

(303) 234-4041

Investigations

1. Use of short-period waveforms to infer Earth structure. Develop a method of generating synthetic seismograms that incorporates the frequency dependent effects that arise from propagation of body waves through the Earth and from source directivity, because at high frequencies, some common assumptions (viz., the description of the source as a point and the frequency independence of attenuation) are incorrect.

2. Source parameters from GDSN data. Extract source parameters from the digitally recorded data of the GDSN by developing techniques of processing digital data to exploit information over a broad band of frequencies and by determining corrections to waveforms in order to distinguish body wave interactions with Earth structure from source directivity.

3. Normal mode interactions with Earth structure. Develop theory and implement computer programs that compute normal modes of Earth models and to construct synthetic seismograms from them.

Results

1. Use of short-period waveforms to infer Earth structure. We have developed a method of synthesizing seismograms that combines the full wave theory with a realistic rupture model to describe propagation and source effects. Synthetic seismograms of body waves that interact strongly with the core structure of the Earth have been generated and compared with a suite of eight PKP body waves generated by one deep earthquake and digitally recorded by the Global Digital Seismograph Network. Strong constraints on the velocity and attenuation structure for the base of the outer core and for the inner core have been obtained.

2. Source parameters from GDSN data. A program that reconstructs high quality broad-band (several Hz to tens of seconds) records of ground velocity by the simultaneous

deconvolution of long- and short-period vertical channels of the GDSN instruments has been converted to a local computer. Frequency dependent attenuation operators derived from a full wave theory have been cataloged for some specific velocity and attenuation models of the Earth. We are examining the rupture characteristics of a suite of 4 large earthquakes (m_b>5.5) that encircled and preceded over a period of two years the eventual rupture zone of the Miyagi-Oki earthquake of 12 June 1978 in the context of a realistic rupture model.

3. Normal mode interactions with Earth structure. Programs have been developed to compute free oscillations of the Earth and to combine them to form synthetic seismograms. Splitting of spectral peaks can be related to lateral heterogeneity. The effects of transverse anisotropy and physical dispersion can be handled.

Reports

Choy, G. L. and J. Boatwright (1981). The rupture characteristics of two deep earthquakes inferred from broadband GDSN data, Bull. Seism. Soc. Am., 71, 691-711.

Boatwright, J., G. L. Choy, V. F. Cormier (1980). The use of short-period waveforms to infer Earth structure, EOS, Trans. A.G.U., 61, 1047.

Harvey, D. and G. L. Choy (1981), Broad-band deconvolution of GDSN data, submitted to Geophy. J. R. Astr. Soc.

TSUNAMI NETWORK SUPPORT

9920-01263

Harold E. Clark, Jr.
Branch of Global Seismology
U.S. Geological Survey
Albuquerque Seismological Laboratory
Building 1002, Kirtland AFB-East
Albuquerque, New Mexico 87115
(505) 844-4637

Investigations

1. Design, develop, and test microprocessor based TSUNAMI related seismic and tide systems.

2. Design, develop, and test GOES satellite related TSUNAMI data transmission techniques and instrumentation.

3. Design, develop, and test microprocessor/computer software programs for TSUNAMI instrumentation and TSUNAMI data retrieval systems.

Results

1. A standard short period TS-4 Seismic System was modified for an audio alarm and was installed at the NASA facility in Chile. This system will operate as a stand-alone unit without a GOES radio set for satellite communication. In the event of selected seismic events, the NASA personnel will start monitoring the NOAA/NWS Tsunami Warning channel 111 from the GOES satellite for the Tsunami tide system data.

2. Five TT-4 Tsunami Tide Systems were designed and assembled at the Albuquerque Seismological Laboratory. Four of these systems were installed by NOAA personnel along the western South American coast. The four installation sites are: Easter Island; Galapagos Islands (Baltra Island); La Punta, Peru; and Antofagasta, Chile. These TT-4 systems will operate with the older float and pulley-type tide meters (Bristol) or new pressure-type sensors. The fifth system is operating at Albuquerque with constant pressure readings. This system will record 20 minutes of tide data with a tide word being recorded every 30 seconds. This time rate, as well as the total storage capacity, is software programmed. The present 40 tide-word capacity can be expanded to 250, if required. These TT-4 systems will respond to interrogation requests from the GOES Satellite system. Data from these TT-4 systems transmit through the GOES Satellite Network channel 111.

SYSTEMS ENGINEERING

9920-01262

Harold E. Clark, Jr.
Branch of Global Seismology
U. S. Geological Survey
Albuquerque Seismological Laboratory
Building 10003, Kirtland AFB-East
Albuquerque, New Mexico 87115
(505) 844-4637

Investigations:

1. Design, develop, and test microprocessor based seismic instrumentation.

2. Design, develop, procure, and test special electronic systems required by seismic facilities.

3. Design, develop, and test microprocessor/computer software programs for seismic instrumentation and seismic data recording systems.

Results:

1. The checkout and field testing of the portable DRS Verify-Playback System has been completed and the system meets all performance specifications. These systems will allow the installing and maintenance teams of the DWWSSN program to completely checkout the quality of recorded DWWSSN Upgrade DRS systems in the field by plotting all recorded channels and by record to record time check programs. In the past these teams had to make a test tape which was sent to the Albuquerque Seismological Laboratory for verification and the results given to the team. This process took many days to complete and the teams had to wait for the results to determine if further maintenance was required or the system was working properly. Now a simple, few-minute test will give these teams the playback and verification of the system. Plans are for more of these DRS Verify-Playback Systems to be built in the next few months.

2. A telemetered version of the DWWSSN Upgrade DRS System is being designed and built for the Jamestown-Berkeley installation. This telemetered DRS System will allow the DWWSSN seismometers with the associated analog to digital conversion unit to be remotely connected to the central recording system by a hardwire circuit. The data rate of this link is 2400 baud and will operate over voice grade telephone lines. In addition, a remote calibrator unit is being designed to allow the central facility to activate 29 different calibration sequences. These 29 calibration sequences will allow SP, IP, LP, and LP-Photo calibration functions of daily step cals, daily sinewave cals, and full frequency response calibrations. It is also possible to get different current levels for each of the function type calibrations. This calibrator unit will be located at the remote site but will be controlled by the central facility operator. A special digital to analog MUX system is being designed and built which will allow all of the received seismic channels to be available in an analog form for helicorder recording or further analog telemetry transmission. This will provide three LP channels, three IP channels, and one to three SP channels of realtime analog seismic data.

3. An earlier analog/digital test unit for the DWWSSN Upgrade DRS is being considered as a test item for each of the DWWSSN maintenance teams. This unit was initially designed for the Upgrade DRS four years ago and is used by the Albuquerque Seismological Laboratory for initial test and system check-out. It has been extremely helpful in checking the ADC unit and will aid the teams in the field during their installation and maintenance visits.

Seismicity and Tectonics

9920-01206

William Spence
Branch of Global Seismology
U.S. Geological Survey
Denver Federal Center, MS 967
Denver, Colorado 80225

(303) 234-4041

Investigations

1. Peru Seismicity and Tectonics. Determine the space-time patterns of aftershocks of the October 3, 1974 Peru earthquake.

2. Mantle Structure Beneath the Rio Grande Rift. Use a 3-D, seismic ray tracing algorithm to invert a set of teleseismic P-wave delay data, with the objective of determining the maximum depth and degree of velocity anomaly in the upper mantle beneath the Rio Grande Rift.

Results

1. Peru Seismicity and Tectonics. The aftershocks of the October 3, 1974 Peru earthquake occurred in two distinct spatial segments. Segment A extends for about 230 km parallel to the coast of Central Peru and is midway between the coast and the axis of the Peru-Chile trench. Segment B is perpendicular to A at its mid-zone and extends about 140 km downdip to beneath the coastal town of Chilca. These aftershocks occur in five main groups with segments A and B. being alternatingly active, to the general exclusion of events in the other zone. When segment A is active, there is a strong tendency for activity to oscillate over mean jump lengths of 80-140 km. Most aftershocks have magnitudes in the mid-4 range and thus these mean jump lengths greatly exceed the rupture length of individual aftershocks. The last main phase appears to have ended with the three events on 9 Nov., 1974 (M_S=7.1), 14 Nov. 1974 (m_b=5.4), and 18 Nov. 1974 (m_b=3.8). The first two of these are the largest aftershocks of the entire series and it is hypothesized that the alternation of zonal activity and the oscillation of aftershocks in segment A reflects a near-critical stress condition that was relieved by the occurrence of these two shocks. Activity following this period is largely confined to the northwest area of segment A and exterior to the entire zone of the two active segments.

2. Mantle Structure Beneath the Rio Grande Rift. The upper mantle beneath the Rio Grande rift, and perhaps eastward as far as the Front Range, has a P-wave velocity that is 4 - 6%

lower than that of the adjoining High Plains Province, down to a depth of 200 km ± 15 km. At a depth interval of 90-130 km beneath a 150 km length of the NE-trending Jemez shear zone (which includes the Jemez volcanic field), there is a layer of concentrated low velocity material. We are now attempting to develop a tractable resolution matrix such that the overall reliability of these apparent results can be quantitatively evaluated.

Report

(p) Langer, C. J. and Spence, W., 1981, Deformation of the Nazca plate related to the gap-filling Peru earthquake series of October-November, 1974: Bull. Seism. Soc. Am. (in press).

Permeability of Fault Zones

9960-90079

J. Byerlee
Branch of Tectonophysics
U.S. Geological Survey
345 Middlefield Road
Menlo Park, CA 94025
(415) 323-8111 x2453

Investigations

Laboratory studies of the permeability of fault gouge were carried out to provide information that will assist us in evaluating whether, in a given region, fluids can migrate to a sufficient depth during the lifetime of a reservoir to trigger a large destructive earthquake.

Results

The permeability and strength of San Andreas fault gouge from the Cienega Valley was measured for confining pressures up to 2 kb. The gouge was almost entirely composed of clay minerals, predominantly monmorillonite and mixed layer clays. Permeability was found to be in the nanodarcy range for both hydrostatic and drained conditions. Permeability did not depend on accumulated strain or creep, but was sensitive to differential stress. The presence of water in the clay lowered the strength, even in the absence of excess pressures.

Reports

(A) Shi, L. Q., Morrow, C., Moore, D., Byerlee, J. D., 1980, Permeability of fault gouges under confining pressure and shear stress (abs.): EOS, American Geophysical Union Transactions, v. 61, no. 46, p. 1120.

Induced Seismic Cogdell Canyon Reef Oil Field

9950-02412

S. T. Harding
U.S. Geological Survey
Denver Federal Center, MS 966
Denver, CO 80225
(303) 234-5087

Investigations

1. Following the m_b-4.7 earthquake of June 19, 1978, close to Snyder, Texas, an eight-station microearthquake network was installed. The subsequent earthquakes fall in or near the Cogdell Canyon Reef oil field. This project has been to determine, if possible, the relationship of the water flooding and earthquake occurrence.

Results

1. Since the network was installed in February 1979, there have been 20 earthquakes with coda length magnitudes, .3 to 3.5, and depth ranging from .95 km to 6.48 km. There has been no additional measurable seismic activity from the oil field in the past 6 months. The network of eight stations has been operating since October 1980 with only 1 or 2 hours of down time. It is planned to remove this network in July and move it to McCook, Nebraska where it is thought that water flooding is inducing earthquakes in a similar manner.

Induced Seismicity and Earthquake Prediction Studies at the Koyna Reservoir, India

9930-02501

H. M. Iyer
Seismology Branch
U.S. Geological Survey
345 Middlefield Road - MS-77
Menlo Park, California 94025
(415) 323-8111, ext. 2685

This project, aimed at setting up 13 portable seismic stations in the Koyna Dam region of Maharashtra State, India, is still awaiting approval of the Government of India. When the required permission is forthcoming, work on installation of the network and data analysis will be started in collaboration with the National Geophysical Research Institute, Hyderabad, India.

Seismological Field Investigations

9950-01539

C. J. Langer
Branch of Earthquake Tectonics and Risk
U.S. Geological Survey
Denver Federal Center, MS 966
Denver, CO 80225
(303) 234-5091

Investigations

Provide technical support to the Induced Seismicity Program for the operation, maintenance, recording, playback, and digitizing of seismic data obtained from a 10-station seismograph network installed around the Monticello, South Carolina reservoir. Purpose of investigation is to study reservoir-induced earthquakes that result from water loading and unloading following reservoir impoundment. Pradeep Talwani, University of South Carolina, Department of Geology, is principal investigator (USGS Contract No. 14-08-0001-19252).

Results

A 20-channel develocorder, complete with galvanometers, date time group assembly, and time fiducial, has been refurbished and delivered to Golden, Colorado. The unit is scheduled for installation at the University of South Carolina sometime in late May or early June. This will provide additional data recording capability for the Induced Seismicity Program in South Carolina which is currently limited to 13 channels plus time on an analog magnetic tape recorder.

According to Bob Park, Golden computer center, approximately 900 Monticello events have been digitized at 130 sps (13 channels). These earthquakes occurred in the time period between October 1979 and December 1980. The computer center is currently working on the 1981 data and should be up-to-date by mid-June. In addition to the digitizing, the University of South Carolina has been provided with about 150 analog and 250 digital plots of the seismic data. The digital plotting had to be curtailed because of excessive use of the DEC-1170 (approximately 75 hours of CPU time). Over 200 hours of CPU time on the DEC-1140 have been used thus far in the analog-to-digital processing.

Routine operation and maintenance of the Monticello network has continued throughout the report period.

COLLECTION OF DATA FOR DATA BANK ON RESERVOIR INDUCED SEISMICITY

Contract No. 14-08-0001-19132

by
Roseanne C. Perman, Kevin J. Coppersmith,
Duane R. Packer, and Lloyd S. Cluff

Woodward-Clyde Consultants
Three Embarcadero Center, Suite 700
San Francisco, CA 94111
(415) 956-7070

Introduction

Research was conducted on reservoir induced seismicity (RIS) to augment the data base developed by Woodward-Clyde Consultants during a 1978-1979 study for the U.S. Geological Survey entitled "Research on Reservoir Induced Seismicity". A major objective of both studies has been to establish a consistent data base for a probabilistic analysis of the interrelationships between certain geologic, hydrologic, and seismologic parameters and the occurrence of reservoir induced seismicity. An ultimate objective is to develop a more reliable method for evaluating the potential for RIS at existing and proposed reservoir locations throughout the world.

Investigations

- Cases of RIS reported in the literature from the end of 1978 through the beginning of 1981 were identified. Data on reservoir size, water impoundment and fluctuation history, regional and local geology, faulting, local stress regime, and seismicity were collected for each case.

- Systematic criteria were used to evaluate each reported case of RIS for placement in one of three categories: 1) accepted cases of reservoir induced seismicity; 2) questionable cases of reservoir induced seismicity; and 3) cases of seismic activity near reservoirs that were not reservoir induced. Where post-impoundment seismicity had a demonstrable spatial and/or temporal relationship to the reservoir, the case for reservoir induced seismicity was classified as accepted. If it was clearly established as being unrelated to the reservoir, the case was classified as not reservoir induced seismicity. If the relationship was unclear because of insufficient data, the case was classified as questionable reservoir induced seismicity. Macroseismicity was considered independently from microseismicity.

- Reservoirs completed between 1976 and 1979 that are deep (minimum water depth of 92 m) and/or very large (minimum water volume of 10^{10} m^3) have been identified. These classes of reservoirs were selected as a base for the study because a relatively higher percentage of these reservoirs exhibit induced seismicity than do smaller or shallower reservoirs. Data on reservoir characteristics, and geologic, hydrologic and seismologic characteristics of the reservoir areas were also collected.

Results

- Approximately 52 new deep and/or very large reservoirs have been identified. There were 234 cases described in the previous study; a population of 286 reservoirs is thus available as a basis for probabilistic analysis of reservoir characteristics and the occurrence of induced seismicity associated with deep and/or very large reservoirs.
- Forty (40) new reported cases of RIS were identified. Of these cases, 25 were assessed to be accepted cases of RIS; 8 cases were recognized as RIS at both macro and microseismicity levels, 10 were recognized at microseismicity levels only, and 7 were recognized at macroseismicity levels only. Of the reported cases, 15 cases were assessed as questionable. In the 1978-1979 study, 45 accepted cases of RIS were identified; the combined total number of accepted cases is therefore 71. The accepted cases of RIS identified in this and the previous study are listed in Table 1.
- Fourteen (14) of the 25 accepted cases of RIS are deep and/or very large reservoirs; 27 were identified in the previous study. Therefore, the total number of deep and/or very large reservoirs with accepted RIS is 41.

TABLE 1
ACCEPTED CASES OF RESERVOIR INDUCED SEISMICITY

No.	Dam Name, Reservoir Name	Country	Classification of RIS	Magnitude Largest RIS Event
1.	Akosombo Main, Lake Volta	Ghana	Accepted, macro	Intensity V
2.	Almendra, Tormes Reservoir	Spain	Accepted, micro	less than 2
3.	Bajina Basta	Yugoslavia	Accepted, micro	less than 3
4.	Benmore	New Zealand	Accepted, macro & micro	5 (?)
5.	Blowering	Australia	Accepted, macro & micro	3.5
6.	Cajaru	Brazil	Accepted, macro & micro	4.6
7.	Camarillas	Spain	Accepted, macro	4.1
8.	Campotosto	Italy	Accepted, macro	5.6
9.	Capivara	Brazil	Accepted, macro	4.4 (?)
10.	Capivari-Cachoeira	Brazil	Accepted, micro	less than 3
11.	Cenajo	Spain	Accepted, macro	4.2
12.	Charvak	USSR	Accepted, macro	3.9
13.	Chicoasen	Mexico	Accepted, micro	3.0
14.	Canelles	Spain	Accepted, macro	4.7
15.	Clark Hill	USA	Accepted, micro (macro?)	4.3 (?)
16.	Contra, Lake Vogorno	Switzerland	Accepted, micro	less than 3
17.	Coyote Valley, Lake Mendocino	USA	Accepted, macro	5.2
18.	Danjiangkou	China	Accepted, macro & micro	4.7
19.	Emosson	Switzerland	Accepted, micro	less than 3
20.	Eucumbene	Australia	Accepted, macro	5 (?)
21.	Fairfield, Lake Monticello	USA	Accepted, micro	2.8
22.	Furnas	Brazil	Accepted, macro	Intensity V
23.	Gordon	Australia	Accepted, micro	2.2
24.	Grancarevc	Yugoslavia	Accepted, micro	less than 3
25.	Grandval	France	Accepted, macro & micro	Intensity V
26.	Hendrik Verwoerd	South Africa	Accepted, micro	less than 2
27.	Hoover, Lake Mead	USA	Accepted, macro & micro	5.0
28.	Huangshi	China	Accepted, micro	2.3
29.	Inguri	USSR	Accepted, micro	less than 3
30.	Itezhitezni	Zambia	Accepted, macro	4 or less (?)
31.	Izvorul Muntelui	Romania	Accepted, micro	less than 3
32.	Jocassee	USA	Accepted, macro & micro	3.2
33.	Kamafusa	Japan	Accepted, micro	less than 3
34.	Kariba	Zambia/Rhodesia	Accepted, macro & micro	6.25
35.	Kastraki	Greece	Accepted, macro	4.6
36.	Keban	Turkey	Accepted, micro	less than 3
37.	Kerr, Flathead Lake	USA	Accepted, macro	4.9
38.	Koyna, Shivaji Sagar Lake	India	Accepted, macro & micro	6.3
39.	Kremasta	Greece	Accepted, macro & micro	6.3
40.	Kurobe	Japan	Accepted, macro & micro	4.9
41.	Long Valley, Lake Crowley	USA	Accepted, macro	6.0
42.	Manicouagan 3	Canada	Accepted, macro & micro	4.1
43.	Marathon	Greece	Accepted, macro	5.75
44.	Miena, Great Lake	Australia	Accepted, macro & micro	3.9
45.	Monteynard	France	Accepted, macro	Intensity VII
46.	Mula	India	Accepted, micro	less than 1
47.	Nanchong	China	Accepted, micro	2.8
48.	Nurek	USSR	Accepted, macro & micro	4.5
49.	Oroville	USA	Accepted, macro	5.7
50.	Oued Fodda	Algeria	Accepted, micro	less than 3
51.	Palisades	USA	Accepted, micro	3.7 (?)
52.	Paraibuna	Brazil	Accepted, macro & micro	3.2
53.	Paraitinga	Brazil	Accepted, macro & micro	3.2
54.	Piastra	Italy	Accepted, macro & micro	4.4
55.	Pieve di Cadore	Italy	Accepted, macro & micro	Intensity V
56.	Porto Colombia	Brazil	Accepted, macro	—
57.	Pukaki High, Lake Pukaki	New Zealand	Accepted, macro & micro	4.6
58.	Santa Ana	Spain	Accepted, macro	4.7
59.	Schlegeis	Australia	Accepted, micro	less than 2
60.	Serpentine, Lake Pedder	Australia	Accepted, micro	2.2
61.	Shenwo	China	Accepted, macro & micro	4.8
62.	Shasta	USA	Accepted, micro	less than 3
63.	Talbingo	Australia	Accepted, macro & micro	3.5
64.	Toktogul	USSR	Accepted, micro	2.5
65.	Vajont	Italy	Accepted, micro	less than 3
66.	Vidra-Lotru	Romania	Accepted, micro	less than 3
67.	Vidraru	Romania	Accepted, micro	less than 3
68.	Volta Grande	Brazil	Accepted, macro	less than 4
69.	Vouglans	France	Accepted, macro	4.4
70.	Xinfengjiang	China	Accepted, macro & micro	6
71.	Zhelin	China	Accepted, macro & micro	3.2

Brittle Tectonics and Reservoir-Induced Seismicity

9510-02389

David C. Prowell
Branch of Eastern Environmental Geology
U.S. Geological Survey
6481 Peachtree Industrial Blvd.
Doraville, GA 30360
(404) 221-4858

Investigations

1. Rock fracture fabrics and geometry of the Wateree Creek fault near Monticello, South Carolina, were studied and compared with those found in USGS borehole #2 at the Monticello Reservoir and in cores from the Cenozoic Belair fault zone in Augusta, Georgia.

2. The distribution of Triassic and younger rocks in the vicinity of the Wateree Creek fault was studied to properly evaluate the movement history along the surface trace of the structure in the Carolina Slate belt.

3. The area around the new R. B. Russell Reservoir (under construction) is being mapped in the hopes of locating and studying evidence of late faulting prior to empoundment of water.

Results

1. The Wateree Creek fault is a northerly-trending fault that dips steeply to the east, making it a near-vertical reverse fault. Several episodes of fracturing are recorded in the fault fabric taken from cored holes along its trace. Generally, the fractured slate has been compacted and recemented by calcite to the point that the rock has internal integrity. Later faulting, however, has fractured the rock and has resulted in a non-cemented breccia and gouge. The nature of the fracturing and accessory mineralization is very similar to that recognized along the Cenozoic Belair fault zone but the evidence of Cenozoic displacement is lacking in the Wateree Creek area. Although the fracturing is somewhat similar to that in Monticello borehole #2, the Monticello fractures show evidence of extensive zeolite invasion and hydrothermal alteration. The relationship of these fracture systems is still under evaluation.

2. An early Mesozoic(?) mafic dike that trends into the Wateree Creek fault was trenched for evidence of late Mesozoic and younger fault displacements but the observations were inconclusive. The data collected do suggest that late Mesozoic movements along the fault would be small and that most of the vertical offset recorded in the Paleozoic slates was probably pre-Mesozoic.

3. Plio-Pleistocene (?) colluvial deposits that cover the trace of the Wateree Creek fault near Chapin, South Carolina, are apparently not affected by any movements along the fault at that locality. The courses of nearby streams do, however, appear to be controlled by the position of the fault but we are uncertain whether this is due to rock type or structural control.

4. The regional delineation of post-metamorphic brittle faults at the R. B. Russell Reservoir and the Monticello Reservoir has been very limited due to the metamorphic conditions and polydeformed nature of the rocks in the two areas. Similarly, efforts to trace the Wateree Creek fault from the Slate belt at Columbia, South Carolina, through the high grade terrane of the Monticello area have been impeded by the same geologic conditions.

Geological Studies in an Area of Induced Seismicity at Monticello Reservoir, South Carolina

14-08-0001-19124

Donald T. Secor, Jr.
Department of Geology
University of South Carolina
Columbia, South Carolina 29208
(803) 777-3120

Project Description

Lake Monticello is a hydroelectric pump storage reservoir, built in conjunction with the V. C. Summer nuclear station in Fairfield County, South Carolina. Lake Monticello is one of the most thoroughly documented cases of induced seismic activity in the United States, and it is the focus of a research effort to understand the seismic activity, to develop a capability for predicting the time of occurrence of induced earthquakes, and hopefully to extrapolate the results to better understand the natural earthquakes that occur in the South Carolina seismic zone (see also project description by P. Talwani, this volume). The goal of the project described here is to determine the geological boundary conditions responsible for the induced seismic activity through a program of geological mapping and geophysical studies in the vicinity of Lake Monticello.

Results

The area under investigation lies partly in the Charlotte belt (amphibolite facies) and partly in the Carolina slate belt (greenschist facies). The stratigraphic sequence is a thick (~10 km) section of metasedimentary and metavolcanic rocks that was deposited in a late Precambrian and Cambrian volcanic arc. This sequence has been affected by at least two major episodes of deformation (D_1, D_2). D_1 was an early to middle Paleozoic episode of regional metamorphism and passive folding resulting in the formation of a major F_1 synclinorium (the Chapin synclinorium) which plunges gently to the northeast through the Carolina slate belt portion of the study area. D_2 was a mid to late Paleozoic episode of flexural folding. L_{0x1}, F_1, and F_2 are northeast trending and approximately coaxial. S_0 and S_1 surfaces have been extensively reoriented by F_2 folding. In the mid to late Paleozoic the Charlotte belt portion of the study area was intruded by several irregular stocks of biotite adamellite and biotite-hornblende adamellite. The latest Paleozoic and Mesozoic history of the study area is characterized by brittle faulting and by the emplacement of a series of northwest trending Jurassic(?) diabase dikes.

Two distinct sets of steeply dipping to vertical faults formed in the study area in latest Paleozoic and Mesozoic time. The oldest set (Set I) is oriented approximately east-west, and the fault zones are characterized by silicification and by irregular extensional gash veins partly infilled with quartz. The character of the displacement along Set I faults is unknown but is generally too small to produce measurable offsets of major stratigraphic units at the 1:24,000 scale. The youngest set of faults (Set II) is oriented approximately north-south and is characterized by intense calcite veining and by dip-slip displacements of approximately 1700 meters. During Jurassic(?) time a series of northwest trending diabase dikes, up to 10 meters in thickness, were emplaced in the study area. Detailed geological studies have been made in the south-central part of the Chapin quadrangle in the region of intersection of a major Jurassic(?) diabase dike and a large Set II fault (the Wateree Creek fault). The diabase dike contains a dextral en echelon offset in the region near the Wateree Creek fault zone, but detailed magnetometer traverses and backhoe trenching indicate that the dike locally penetrates across the fault zone without apparent offset. These results suggest that most and perhaps all of the displacement of the Wateree Creek fault zone occurred prior to the intrusion of the Jurassic(?) diabase dike.

Future Research Plans

During the coming year (3/1/81-2/28/82) detailed geological maps of the Jenkinsville and Pomaria quadrangles will be prepared, and fracture patterns and the pattern of diabase dike emplacement around Monticello reservoir will be studied in order to better understand the geological controls of the induced seismic activity. During the period 3/1/82-2/28/83 geological studies will be undertaken along the northern and southern extensions of the Wateree Creek fault zone and a detailed 1:12,000 scale geologic map will be made of the fault zone in order to further document its geological history.

Induced Seismicity at Toktogul Reservoir and Seismotectonics of the Talas-Fergana Fault

14-08-0001-16844

D. W. Simpson
Lamont-Doherty Geological Observatory of Columbia University
Palisades, New York 10964

Investigations

1. Data from an 8 station telemetered network installed in 1978 have been used to monitor changes in seismicity related to filling of the 215 m deep Toktogul Reservoir.
2. Techniques have been developed to improve depth resolution and determination of velocity structure using data from dense local networks.
3. Geological studies have begun of the reservoir area and the Talas-Fergana fault.
4. In conjunction with the study of induced seismicity at Nurek Reservoir (USGS-14-08-0001-17707), reviews of Soviet geological literature and earthquake catalogs are being used to study the Nurek and Toktogul sites within a framework of the broader tectonic setting of Soviet Central Asia.

Results

1. Induced seismicity is occurring in a narrow zone, 10 km long and 3 km wide oriented along the canyon of the Naryn River, directly beneath Toktogul Dam. The largest earthquake to date near the dam has been magnitude 2.6. The telemetered network was installed in October 1978 when the water level at the dam was 125 m. The most intense activity since installation of the network was in July 1979 when the most rapid increase in water level, from 130 to 155 m, occurred. Although the induced seismicity is concentrated above depths of 7 km, natural seismicity within 50 km of the reservoir extends to depths of 30 km. Most of the deeper activity is concentrated in a narrow zone along the Talas-Fergana fault and in two transverse features extending 10 to 15 km southwest of the fault. No obvious increase in seismicity related to filling of the reservoir has been observed along the Talas-Fergana.
2. In computer processing of large volumes of earthquake data from regional or local networks, gross errors in hypocentral locations, caused by reading errors or inappropriate convergence and model parameters, can often go undetected. We find that simple graphical presentations of arrival time data can be used to detect these errors, provide independent estimates of hypocenter parameters, and obtain additional information on average velocity variation with depth. Wadati diagrams (t_p vs. t_{s-p}) can be used to estimate the origin time and velocity ratio (V_p/V_s). The hyperbolic relationship between travel time (t) and epicentral distance (x) (in the form x^2 vs t^2) provides estimates of focal depth and average velocity. Although the techniques assume

a half-space velocity model, data from earthquakes at various depths can be used to generate a first approximation to a vertical velocity distribution. In applying these techniques to the data from the Toktogul network, we find a significant decrease in V_p/V_s (1.9-1.7) with depth in the upper 20 km. By specifying independent P and S velocity models, rather than the standard assumption of constant V_p/V_s, we find improved stability in hypocentral determination and increased resolution of shallow seismicity patterns.

3. Geological studies of the Toktogul Reservoir area began in 1979 with the visit of three American geologists to the area. Work has since concentrated in the Naryn canyon area near the dam, and adjoining segments of the Talas-Fergana fault. Preliminary reconnaisence of the reservoir basin lakebed deposits (Quaternary) showed that these are gently but strikingly folded -- an immediate substantiation of the existence of recent deformation in the region. Some 400 km^2 have been reconnaisence mapped to an accuracy of 1:100,000. The mapping has shown the dam and lower reservoir to be located in a folded and faulted continental marginal sedimentary sequence of late-Paleozoic age. The youngest of the major deposits in this area is a Permian conglomerate. Consequently, although it is easy to prove the existence of post-Permian faulting, it will be necessary to search for Quaternary and Recent deposits to prove recent surface fault breakage in this area. For the moment, we note that there are many possibly active faults in the area exhibiting maximum induced seismic activity, surrounding and upstream of the dam. A fault-displacement study of the Talas-Fergana near the Naryn canyon mouth has been initiated, with the ultimate goal of determining the historic character of fault displacement along this fault section. Recent alluvial gravels are regularly deposited across the fault by several mountain streams which flow out of the ranges to the south. These are accompanied by numerous landslides and debris flows. Both alluvial and colluvial deposits are distrubed along the fault trace. In such deposits 3 km southeast of the Naryn canyon it is possible to demonstrate right-lateral offsets of several meters. Gravel beds adjacent to the fault trace have been gently warped. Uplift along the north side of the fault (from 1 to 10 m) is pronounced in the alluvial gravels of this area. Some 3 km further southeast along the fault, stream channels have been offset in right lateral sense by up to 10 m.

4. In addition to local seismicity and geology studies at Nurek and Toktogul, we are using seismicity catalogs for Central Asia, published works on Central Asian geology, LANDSAT images, and special studies of recent large earthquakes to investigate the regional setting of Nurek and Toktogul. Soviet catalogs of Central Asian earthquakes, both strong earthquakes (800 events, 250 B.C.-1974 A.D.) and weak earthquakes (over 12,000 crustal earthquakes, 1974-1977) provide considerably more detail than is available from international catalogs. Although the Gissar-Kokshal-Vakhsh fault zone (near Nurek) and the Talas-Fergana fault (near Toktogul) stand out as the major features of crustal seismicity, numerous blocks within the mosaic

of Central Asian geology can be identified by lineations in seismicity. The relationship of this seismicity to the crustal deformation resulting from the India-Eurasia collision and the current intermediate depth activity in the Pamir and Hindu Kush is being investigated.

Reports

Bilham, R., and Simpson, D. W., 1981, Indo-Asian convergence and the 1913 survey line connecting the Indian and Russian triangulation surveys, Royal Geographical Society International Karakorum Project 1980, in press.

Kristy, M., and Simpson, D.W., 1980, Seismicity changes prior to two Central Asian earthquakes, J. Geophys. Res.,vol. 85, p. 4829-4837.

Kristy, M., Burdick, L., and Simpson, D. W., 1980, Focal mechanisms of the Gazli earthquakes, Bull. Seismol. Soc. Am., vol. 70, p. 1737-1750.

Nicholson, C., and Simpson, D. W., 1981, Routine processing of shallow earthquake locations and velocity models, EOS, Trans. Am. Geophys. Un., vol. 62, p. 336.

Simpson, D. W., and Kristy, M. J., 1980, Seismicity changes preceeding Central Asian earthquakes, EOS, Trans. Am. Geophys. Un., vol. 61, p. 293.

Simpson, D. W., and Leith, W. S., 1980, Seismicity, tectonics and topography of the Hindu-Kush, Pamirs, Karakorum and Tadjik Depression, EOS, Trans. Am. Geophys. Un., vol. 61, p. 1031.

Simpson, D. W., Hamburger, M. W., Pavlov, V. D., and Nersesov, I. L., 1981, Tectonics and seismicity of the Toktogul Reservoir region, Kirgizia, USSR, J. Geophys. Res., vol. 86, p. 345-358.

Geological and Geophysical Studies of Induced Seismicity at Nurek Reservoir

14-08-0001-17707

D. W. Simpson, C. M. Keith, and W. Alvarez
Lamont-Doherty Geological Observatory of Columbia University
Palisades, New York 10964

Investigations

1. The catalog of earthquakes from a network of Soviet stations operating near Nurek Reservoir since 1955 has been studied to evaluate changes in seismicity caused by filling of the reservoir and to investigate the correlation between changes in water level and seismicity.
2. Data from an 8 station telemetered network around Nurek Reservoir have been analyzed to determine the location of induced seismicity, especially during a swarm of activity related to the raising of the water level from 120 to 205 m in late 1976.
3. The geological structure and stratigraphy of the immediate reservoir area have been mapped and compared with the induced seismicity.

Results

1. The filling of the 300 m deep Nurek Reservoir has caused a significant increase in the level of seismicity near the reservoir. From the first major stage of filling in 1972 to the end of 1980, the rate of seismicity has averaged more than 4 times the pre-impounding level of activity. During intense bursts of seismicity related to rapid increases in water level in 1972 and 1976, the level of seismicity rose to as high as 15 times the pre-impounding level. Changes in seismicity are closely related to changes in the rate of filling of the reservoir, with increased seismicity following rapid decreases in the rate of filling. Once the water level is more than 10 m above the previous maximum, the potential for increased seismicity is high. Extremely small changes in filling rate can then trigger the onset of activity. For example, the largest earthquakes all followed decreases in filling rate of approximately 0.5 m/day^2. The response in seismicity to decreases in the filling rate is rapid. Increased activity follows abrupt decreases in filling rate with delays as short as 1 to 4 days.
2. Using data from a telemetered network installed in 1975, earthquakes which occurred during a burst in seismicity during the second stage of filling, August-December 1976, can be located with a precision an order of magnitude better than that possible with the Soviet network. Seismicity defines a series of narrow, offset fault zones, with the highest level of seismicity concentrated near the central basin of the reservoir. Composite fault plane solutions show distinct segments with thrust, strike-slip

and normal mechanisms. There is excellent agreement between the strike and dip of the focal planes determined from the fault plane solutions and the lineations visible in the seismicity data. The increased seismicity began directly beneath the reservoir and gradually migrated 10 km southward, extending 8 km beyond the southernmost edge of the reservoir.

3. One of the most important results from the detailed seismicity study is that the active zones seen in the seismicity do not correspond to fault structures observed at the surface. Although at least three active faults have been mapped near the reservoir, none of them shows increased seismicity during the 1976 swarm. There is no surface expression of the four most active segments seen in the seismicity patterns. The location of the induced seismicity during the 1976 swarm appears to be controlled by small scale (order of kilometers) variations in permeability and structure in the immediate reservoir area. The earthquakes occur within a steeply plunging anticline, the core of which outcrops beneath the reservoir. Alternating layers of permeable and impermeable strata allow water to flow to depth along the bedding direction, within the permeable layers, down the plung of the anticline. No seismicity occurs beneath the deepest part of the reservoir, near the dam, where a near-horizontal syncline cups the base of the reservoir and the impermeable layers prevent water from penetrating to depth.

Reports

Keith, C., Simpson, D. W., and Soboleva, O. V, 1981, Induced seismicity and deformation style at Nurek Reservoir, Tadjik SSR, to be submitted to J. Geophys. Res.

Leith, W., Simpson, D. W., and Alvarez, W., 1981, Structure and permeability: Geologic controls on induced seismicity at Nurek Reservoir, Tadjikistan, USSR, EOS, Am. Geophys. Un., vol. 62, p. 329 (also submitted to Geology).

Simpson, D. W., and Negmatullaev, S. Kh., 1981, Induced seismicity at Nurek Reservoir, submitted to Bull. Seismol. Soc. Am.

Reservoir Induced Seismicity

9540-02199

D. E. Stuart-Alexander
Branch of Western Environmental Geology
U.S. Geological Survey
345 Middlefield Road, MS 75
Menlo Park, CA 94025
(415) 323-8111, ext. 2353

Investigations

We continued to update the computer data base of large dams and reservoirs which was created to permit a statistical study of reservoir-induced seismicity world wide. However, no additional data reduction was undertaken during the first half of FY 81. The remaining work and final report writing will be done in the last half of FY 81.

Induced Seismicity and Earthquake Prediction Studies in South Carolina

Contract No. 14-08-0001-17670

Pradeep Talwani
Geology Department
University of South Carolina
Columbia, S.C. 29208
(803) 777-6449

1. Induced Seismicity At Monticello Reservoir, South Carolina.

We have continued to monitor seismicity in the vicinity of the 40 m deep Monitcello Reservoir. The seismicity has been monitored before, during and after its impoundment in December, 1977. In addition to the study of various seismological parameters (hypocentral locations, temporal and spatial variation of seismicity, composite fault plane solutions, source studies, etc.) subsurface data were obtained from two deep boreholes ($\sim$ 1 km) drilled in the hypocentral regions by the USGS. These borehole data include in situ stress, permeability, fracture density and orientation measurements. Additional surface data were obtained from detailed geologic, hydrologic and potential field studies. These efforts have been combined to understand the nature of the observed reservoir induced seismicity (RIS). The results of these efforts include the following:

1. Induced seismicity is limited in both space and time to superficial zones beneath and in the immediate vicinity of the reservoir.

2. Accurate hypocenter depths determined from the 10-station network (magnetic tape data) are all shallow (< 3 km) and the largest magnitude observed is $M_L = 2.8$.

3. There is no evidence of any through-going faults nor any tendency for the induced activity to coalesce along large (reservoir-sized) planes of potential failure.

4. Focal mechanisms for induced earthquakes indicate in situ stress conditions favoring thrust-type faulting.

5. In situ stress measurements in the 2 deep boreholes indicate variable stress levels both vertically and laterally; absolute stress differenes (maximum-minimum) reported by Zoback range from a few bars to approximately 100 bars.

6. The distribution of fracture density and fracture orientations observed in the 2 boreholes is non-uniform and is characterized by local concentrations of fractures in limited depth intervals with different dominant orientations in each; focal mechanisms of nearby induced earthquakes show nodal planes generally corresponding to these orientations.

7. Geological maps, surface magnetic and aeromagnetic anomaly maps, gravity anomaly maps, and radio-metric maps all indicate significant lateral variations in rock properties beneath the site. These variations are associated with plutons that have been intruded into the older metamorphic rocks of the Piedmont Province and that are now near the surface in this area.

8. The close spatial association of the clusters of well-located induced seismic events with boundaries of plutonic bodies as indicated by correlative geological geophysical data (item 7 above) and the association of specific focal mechanisms with different orientations of fractures observed in the 2 boreholes (item 6 above) makes a strong case that the effect of the reservoir impoundment has been to relieve local remanent stresses around the plutons that have, over geologic time, been brought near the surface in this area (i.e., into a stress environment different from that in which the plutons were intitially emplaced). These stresses are highly variable from one point to the other over the area.

9. The lateral and vertical heterogeneity in: rock properties, stress levels and orientations, permeability, and induced seismic activity, coupled with the limited spatial extent laterally and with depth of the induced activity all point to the conclusion that the effects of reservoir impoundment are surficial (top 2-3 km) and reflect minor local adjustments where the effective stress had changed as the pore pressure from reservoir loading has changed.

10. Limited data on the distribution of permeability indicates that there are significant lateral and vertical variations, with higher permeabilities associated with zones of higher fracture density in the boreholes. There is a general decrease of permeability with depth towards the bottom of deep borehole No. 2, the only one with complete data set available.

11. The initial spectral analysis of several of the induced earthquakes indicates average stress drops of a few bars; the maximum reported value is 300 bars, although r.m.s. acceleration values are all less than 30 bars.

12. Frequency-of-occurence vs. magnitude plots for induced activity at Monticello (and elsewhere) are highly atypical compared to the natural tectonic behavior in the region (and elsewhere). The transient nature of the induced activity (non-steady-state) in both time and space is associated with high "b" values.

13. RIS was initiated following the impoundment of the reservoir by a process of pore pressure diffusion. The average hydraulic diffusivity is $\sim 10^4 \mathrm{cm}^2/\mathrm{sec}$.

14. Subsequent seismicity appears to be related to sudden decreases in the reservoir level.

2. Induced Seismicity at Lake Jocassee, South Carolina.

Seismicity at Lake Jocasse has been monitored since October 1975, using portable seismographs and recently three permanent stations. One of these stations, SMT was connected to the state seismograph network in February 25, 1980. In the reporting period there were 9 events with magnitude> 2.0 (8 in 1980, one thru 4/81). Of these, one sequence was associated with geochemical anomalies, described below.

3. Earthquake Prediction Studies at Lake Jocassee.

Together with induced seismicity at Lake Jocassee, radon concentration of spring water, and other geochemical parameters have been measured. Two larger events with M$\sim$2.0 on April 30, 1980 and one on May 4, 1980 occurred at a distance of about 2 km from an observation spring. There was an anomalous increase in both the seismicity and in the radon concentration of water in this spring. No precursory change was observed in the conductivity or cholorinity of this spring water. However, one day after the April 30 earthquakes there was a further 20% increase in Rn, and a day after the May 4 event, there was a large (70%) increase in the cholorinity. No corresponding change was observed in the conductivity. These data suggest that the post-earthquake changes may be associated with a pressure front emanating from the hypocenter and passing through the spring a day later.

4. Earthquake Prediction Studies at Monticello Reservoir.

Here we have begun to monitor water level in the deep USGS wells, and geochemical parameters at four sites. The data are stable, although no spectacular anomaly has been encountered.

Reports

P. Talwani and D. Stevenson, Lake Jocassee Earthquake of August 25, 1979, 51st Annual meeting of Eastern Section, Seismological Society of America, Oct. 1979, (Abstract), Earthquake Notes, 50, no. 3, p. 40.

W. R. Logan, D. C. Amick and P. Talwani, Seismic refraction survey in Bowman area, South Carolina, 51st Annual meeting of Eastern Section, Seismological Society of America, Oct. 1979, (abstract), Earthquake Notes, 50, no. 3, p. 30.

K. B. Taylor and P. Talwani, An isoseismal study of the August 25, 1979 Lake Jocassee earthquake, Oconee County, South Carolina, 51st Annual meeting of Eastern Section, Seismological Society of America, Oct. 1979, (abstract), Earthquake Notes, 50, no. 3, p. 41-42.

Pradeep Talwani, Precursory seismicity, seismicity gaps and Earthquake Predicition studies at Lake Jocassee and Monticello Reservoir, South Carolina, Fall meeting of American Geophysical Union, (abstract), EOS, Transactions, American Geophysical Union, 60, 46, 881, 1979.

P. Talwani, Intraplate seismicity in South Carolina - possible explanations. (Presented at) Penrose Conference on Tectonics and Geophysics of the Applichians, Georgia, April-May 1980.

P. Talwani, Earthquake Prediction studies at Lake Jocassee, South Carolina, (abstract) (presented at) Third Maurice Ewing Symposium on Earthquake Prediction, New York, May 1980.

P. Talwani, The August 25, 1979 Lake Jocassee earthquake and its implications on reservoir induced earthquake, (abstract), EOS, Transactions, American Geophysical Union, 61, 17, 1980.

K. D. Hutchenson and P. Talwani, Source properties of Earthquakes near Monitcello Rservoir, Programs and Abstracts of the Seismological Society of America, Eastern Section 52nd Meeting, October 1980, (abstract), Earthquake Notes, 51, no. 3, p. 23.

A. Robinson and P. Talwani, Ground failure damage and "made ground", Charleston, 1886, Programs and Abstracts of the Seismological Society of America, Eastern Section 52nd Meeting, October 1980, (abstract), Earthquake Notes, 51, no. 3, p. 23.

Pradeep Talwani and R. E. Van Nieuwenhuise, Water Level and Geochemical Anomalies at Lake Jocassee, S. C. (abstract), EOS, Transactions, American Geophysical Union, 61, p. 1035, 1980.

Pradeep Talwani, Association of induced seismicity with Preexisting fracture at Monticello Reservoir, South Carolina, 76th Meeting, Seismological Society of America, April, 1981, (abstract), Earthquake Notes, 52, no. 1, p. 28-29.

Papers

Sauber, Jeanne and Talwani, P., Applications of Keilis-Borok and McNally prediction algorithms to earthakes in the Lake Jocassee area, South Carolina, Physics of the Earth and Planetary Interiors, Vol. 21, p. 267-281, 1980.

Talwani, P., Moore, W. S., and Chiang, Jin, Radon anomalies and microearthquakes at Lake Jocassee, South Carolina, Journal of Geophysical Research, Vol. 85, #B6, p. 3079-3088, 1980.

Rastogi, B. K. and Talwani, Pradeep, Spatial and temporal variations in t_s/t_p at Monticello reservoir, South Carolina, Geophysical Research Letters, Vol. 7, pp. 781-784, 1980.

Talwani, Pradeep, Earthquake prediction studies in South Carolina, to appear in Ewing Series IV, American Geophysical Union on Earthquake Prediction, expected in May 1981.

Tarr, A., Pradeep Talwani, S. Rhea, D. Carver and D. Amick, Results of Recent South Carolina seismological studies, submitted to the Bulletin of the Seismological Society of America, March 1981.

INDEX 1

INDEX ALPHABETIZED BY PRINCIPAL INVESTIGATOR

		Page
Ager, T. A.	U.S. Geological Survey	114
Aggarwal, Y. P.	Lamont-Doherty Geological Observatory	78
Algermissen, S. T.	U.S. Geological Survey	1
Algermissen, S. T.	U.S. Geological Survey	12
Allen, C. R.	California Institute of Technology	26
Allen, C. R.	California Institute of Technology	116
Allen, C. R.	California Institute of Technology	357
Allen, C. R.	California Institute of Technology	359
Allen, R.	U.S. Geological Survey	273
Anderson, J. R.	New York, State University of, Binghamton	466
Anderson, L. R.	Utah State University	242
Anderson, R. E.	U.S. Geological Survey	119
Andrews, D. J.	U.S. Geological Survey	192
Archuleta, R. J.	U.S. Geological Survey	193
Arnold, E. P.	U.S. Geological Survey	532
Baker, L. M.	U.S. Geological Survey	194
Bakun, W. H.	U.S. Geological Survey	431
Barrows, A. G.	California Division of Mines and Geology	123
Behrendt, J. C.	U.S. Geological Survey	80
Bell, J. W.	Nevada Bureau of Mines and Geology	124
Berger, J.	California, University of, San Diego	274
Berger, J.	California, University of, San Diego	278
Berger, J.	California, University of, San Diego	279
Bilham, R.	Lamont-Doherty Geological Observatory	281
Bilham, R.	Lamont-Doherty Geological Observatory	468
Bird, P.	California, University of, Los Angeles	432
Boatwright, J.	U.S. Geological Survey	196
Bonilla, M. G.	U.S. Geological Survey	126
Boore, D. M.	U.S. Geological Survey	198
Borcherdt, R. D.	U.S. Geological Survey	200
Brabb, E. E.	U.S. Geological Survey	30
Broecker, W. S.	Lamont-Doherty Geological Observatory	362
Buchanan-Banks, J. M.	U.S. Geological Survey	34
Bucknam, R. C.	U.S. Geological Survey	35
Buland, R.	U.S. Geological Survey	537
Burford, R. O.	U.S. Geological Survey	284
Burke, D. B.	U.S. Geological Survey	128
Byerlce, J. D.	U.S. Geological Survey	435
Byerlee, J. D.	U.S. Geological Survey	546
Carlson, M. A.	U.S. Geological Survey	522
Castle, R. O.	U.S. Geological Survey	37
Choy, G. L.	U.S. Geological Survey	286
Choy, G. L.	U.S. Geological Survey	539

Chung, Y.	California, University of, San Diego	363
Clark, H. E., Jr.	U.S. Geological Survey	541
Clark, H. E., Jr.	U.S. Geological Survey	542
Clough, G. W.	Stanford University	244
Cockerham, R.	U.S. Geological Survey	287
Counselman, C. C.	Massachusetts Institute of Technology	471
Dawson, A. W.	Woodward-Clyde Consultants	247
Dewey, J. W.	U.S. Geological Survey	3
Dewey, J. W.	U.S. Geological Survey	290
Diment, W. H.	U.S. Geological Survey	81
Douglas, L. A.	Rutgers University	249
Ellsworth, W. L.	U.S. Geological Survey	291
Endo, E. T.	U.S. Geological Survey	294
Engelder, T.	Lamont-Doherty Geological Observatory	472
Espinosa, A. F.	U.S. Geological Survey	13
Etheridge, M. A.	Monash University	473
Felsen, L. B.	Polytechnic Institute of New York	201
Ferrians, O. J., Jr.	U.S. Geological Survey	38
Fischer, F. G.	U.S. Geological Survey	296
Fletcher, J. B.	U.S. Geological Survey	205
Gibbs, J. F.	U.S. Geological Survey	208
Goodkind, J. M.	California, University of, San Diego	365
Hadley, D. M.	Sierra Geophysics, Inc.	209
Hall, N. T.	Foothill-De Anza Community College	129
Hall, W.	U.S. Geological Survey	297
Hamilton, R. M.	U.S. Geological Survey	83
Harding, S. T.	U.S. Geological Survey	16
Harding, S. T.	U.S. Geological Survey	547
Harkrider, D. G.	California Institute of Technology	368
Harlow, D.	U.S. Geological Survey	298
Harp, E. L.	U.S. Geological Survey	252
Hays, W. W.	U.S. Geological Survey	20
Hays, W. W.	U.S. Geological Survey	39
Healy, J. H.	U.S. Geological Survey	474
Healy, J. H.	U.S. Geological Survey	477
Henyey, T. L.	Southern California, University of	299
Henyey, T. L.	Southern California, University of	480
Herd, D. G.	U.S. Geological Survey	40
Herd, D. G.	U.S. Geological Survey	42
Herriot, J.	U.S. Geological Survey	370
Hildenbrand, T. G.	U.S. Geological Survey	85
Hoffman, J. P.	U.S. Geological Survey	523
Holmes, M. L.	U.S. Geological Survey	44
Irwin, W. P.	U.S. Geological Survey	133
Isacks, B. L.	Cornell University	303
Iyer, H. M.	U.S. Geological Survey	548
Izett, G. A.	U.S. Geological Survey	135

Jachens, R. C.	U.S. Geological Survey	306
Jacob, K. H.	Lamont-Doherty Geological Observatory	213
Jaksha, L. H.	U.S. Geological Survey	525
Jensen, E. G.	U.S. Geological Survey	308
Johnson, C.	U.S. Geological Survey	309
Johnston, M.	U.S. Geological Survey	372
Julian, B. R.	U.S. Geological Survey	438

Kanamori, H.	California Institute of Technology	312
Kane, M. F.	U.S. Geological Survey	87
Keefer, D. K.	U.S. Geological Survey	253
King, C. -Y	U.S. Geological Survey	375
Kiremidjian, A.	Stanford University	260
Kisslinger, C.	Colorado, University of	316
Kohlstedt, D. L.	Cornell University	439
Kohlstedt, D. L.	Cornell University	484
Kohlstedt, D. L.	Cornell University	487
Kvenvolden, K. A.	U.S. Geological Survey	136

Lachenbruch, A. H.	U.S. Geological Survey	490
Lahr, J. C.	U.S. Geological Survey	46
Lajoie, K. R.	U.S. Geological Survey	138
Lamar, D. L.	Lamar-Merifield, Geologists	140
Lamar, D. L.	Lamar-Merifield, Geologists	377
Langer, C. J.	U.S. Geological Survey	214
Langer, C. J.	U.S. Geological Survey	549
Lanphere, M. A.	U.S. Geological Survey	143
Lee, W. H. K.	U.S. Geological Survey	318
Lee, W. H. K.	U.S. Geological Survey	319
Lee, W. H. K.	U.S. Geological Survey	320
Liddicoat, J. C.	Lamont-Doherty Geological Observatory	144
Lindberg, R. G.	California, University of, Los Angeles	381
Lindh, A.	U.S. Geological Survey	355
Liu, H. -P	U.S. Geological Survey	383
Lockner, D. A.	U.S. Geological Survey	441
Logan, J. M.	Texas A & M University	263

Madden, T. R.	Massachusetts Institute of Technology	385
Malin, P. E.	Southern California, University of	388
Marchand, D. E.	U.S. Geological Survey	147
Martin, G. R.	Ertec Western, Inc.	220
Matthiesen, R. B.	U.S. Geological Survey	22
Matthiesen, R. B.	U.S. Geological Survey	222
Mavko, G. M.	U.S. Geological Survey	391
Mavko, G. M.	U.S. Geological Survey	442
McCann, W. R.	Lamont-Doherty Geological Observatory	321
McCarthy, R. P.	U.S. Geological Survey	534
McDowell, R. C.	U.S. Geological Survey	89
McGarr, A.	U.S. Geological Survey	323
McNally, K. C.	California Institute of Technology	393
McNutt, M.	U.S. Geological Survey	444
Merchant, H. C.	Washington, University of	494
Mooney, W. D.	U.S. Geological Survey	495

Morrissey, S.	Saint Louis University	499
Mortensen, C. E.	U.S. Geological Survey	397
Morton, D. M.	U.S. Geological Survey	49
Nash, D. B.	Cincinnati, University of	151
Newman, W. S.	Queens College, City University, New York	91
O'Neil, J. R.	U.S. Geological Survey	400
Orsini, N. A.	U.S. Geological Survey	526
Orsini, N. A.	U.S. Geological Survey	528
Orsini, N. A.	U.S. Geological Survey	529
Otis, L. S.	SRI International	404
Page, R. A.	U.S. Geological Survey	50
Park, R. B.	U.S. Geological Survey	224
Perkins, J. B.	Association of Bay Area Governments	225
Perman, R. C.	Woodward-Clyde Consultants	550
Peselnick, L.	U.S. Geological Survey	446
Peterson, J.	U.S. Geological Survey	530
Pfluke, J. H.	U.S. Geological Survey	408
Phillips, W. J.	Cornell University	409
Pierce, K. L.	U.S. Geological Survey	154
Plafker, G.	U.S. Geological Survey	51
Pollard, D. D.	U.S. Geological Survey	447
Prescott, W. H.	U.S. Geological Survey	326
Priestley, K. F.	California, University of, San Diego	5
Prowell, D. C.	U.S. Geological Survey	553
Ratcliffe, N. M.	U.S. Geological Survey	93
Reichle, M.	California, University of, San Diego	413
Reimer, G. M.	U.S. Geological Survey	414
Rice, J. R.	Brown University	450
Rice, J. R.	Brown University	454
Rogers, A. M.	U.S. Geological Survey	55
Rojahn, C.	U.S. Geological Survey	157
Rosholt, J. N.	U.S. Geological Survey	158
Ross, D. C.	U.S. Geological Survey	159
Rudnicki, J. W.	Illinois, University of	458
Russ, D. P.	U.S. Geological Survey	95
Ryall, A.	Nevada, University of, Reno	57
Sarna-Wojcicki, A. M.	U.S. Geological Survey	162
Sato, M.	U.S. Geological Survey	416
Sbar, M. L.	Arizona, University of	503
Scholl, R. E.	URS/John A. Blume & Associates	266
Schweickert, R. A.	Lamont-Doherty Geological Observatory	507
Scott, W. E.	U.S. Geological Survey	164
Secor, D. T., Jr.	South Carolina, University of	555
Seeber, L.	Lamont-Doherty Geological Observatory	329
Sexton, J. L.	Purdue University	165
Shah, H. C.	Stanford University	269
Shapiro, M. H.	California Institute of Technology	420
Sharp, R. V.	U.S. Geological Survey	167

Sherburne, R. W.	California Division of Mines and Geology	228
Sieh, K. E.	California Institute of Technology	170
Simpson, D. W.	Lamont-Doherty Geological Observatory	557
Simpson, D. W.	Lamont-Doherty Geological Observatory	560
Simpson, R.	U.S. Geological Survey	99
Sims, J. D.	U.S. Geological Survey	172
Sims, J. D.	U.S. Geological Survey	178
Slater, L. E.	Colorado, University of	508
Smith, A. T.	California, University of, Santa Cruz	461
Smith, R. B.	Utah, University of	59
Sondergeld, C. H.	Colorado, University of	462
Spence, W.	U.S. Geological Survey	544
Sprotte, E. C.	California Division of Mines and Geology	229
Spudich, P.	U.S. Geological Survey	231
Stauder, W.	Saint Louis University	100
Stevenson, P. R.	U.S. Geological Survey	335
Stewart, S. W.	U.S. Geological Survey	337
Stickney, M. C.	Montana Bureau of Mines and Geology	233
Stone, B. D.	U.S. Geological Survey	104
Stover, C. W.	U.S. Geological Survey	535
Stuart-Alexander, D.	U.S. Geological Survey	562
Swan, F. H.	Woodward-Clyde Consultants	106
Sylvester, A. G.	California, University of, Santa Barbara	339
Taggart, J. N.	U.S. Geological Survey	7
Talwani, P.	South Carolina, University of	563
Teng, T.	Southern California, University of	423
Thatcher, W.	U.S. Geological Survey	340
Tinsley, J. C.	U.S. Geological Survey	63
Toksoz, M. N.	Massachusetts Institute of Technology	342
Toppozada, T. R.	California Division of Mines and Geology	9
Trexler, D. T.	Nevada Bureau of Mines and Geology	235
Tullis, J.	Brown University	511
Van Schaack, J.	U.S. Geological Survey	238
Van Schaack, J.	U.S. Geological Survey	345
Van Schaack, J.	U.S. Geological Survey	347
Wallace, R. E.	U.S. Geological Survey	180
Ward, P.	U.S. Geological Survey	348
Ware, R. H.	Colorado, University of	425
Warren, D. H.	U.S. Geological Survey	516
Warrick, R. E.	U.S. Geological Survey	239
Weaver, C. S.	U.S. Geological Survey	65
Weber, F. H., Jr.	California Division of Mines and Geology	182
Weber, G. E.	Weber and Associates	185
Wentworth, C. M.	U.S. Geological Survey	23
Westlake, P. R.	Environmental Dynamics, Inc.	428
Wheeler, R. L.	U.S. Geological Survey	110
Whitcomb, H.	U.S. Geological Survey	531
Wilson, R. C.	U.S. Geological Survey	256
Wong, H. L.	Southern California, University of	240

Wood, S. H.	U.S. Geological Survey	67
Wu, F. T.	New York, State University of, Binghamton	349
Wu, F. T.	New York, State University of, Binghamton	463
Wyatt, F.	California, University of, San Diego	518
Wyss, M.	Colorado, University of	10
Wyss, M.	Colorado, University of	351
Yeats, R. S.	Oregon State University	68
Yeats, R. S.	Oregon State University	187
Yeats, R. S.	Oregon State University	189
Yerkes, R. F.	U.S. Geological Survey	71
Youd, T. L.	U.S. Geological Survey	259
Yount, J. C.	U.S. Geological Survey	74
Ziony, J. I.	U.S. Geological Survey	75
Zoback, M. L.	U.S. Geological Survey	76

INDEX 2

INDEX ALPHABETIZED BY INSTITUTION

		Page
Arizona, University of	Sbar, M. L.	503
Association of Bay Area Governments	Perkins, J. B.	225
Brown University	Rice, J. R.	450
Brown University	Rice, J. R.	454
Brown University	Tullis, J.	511
California Division of Mines and Geology	Barrows, A. G.	123
California Division of Mines and Geology	Sherburne, R. W.	228
California Division of Mines and Geology	Sprotte, E. C.	229
California Division of Mines and Geology	Toppozada, T. R.	9
California Division of Mines and Geology	Weber, F. H., Jr.	182
California Institute of Technology	Allen, C. R.	26
California Institute of Technology	Allen, C. R.	116
California Institute of Technology	Allen, C. R.	357
California Institute of Technology	Allen, C. R.	359
California Institute of Technology	Harkrider, D. G.	368
California Institute of Technology	Kanamori, H.	312
California Institute of Technology	McNally, K. C.	393
California Institute of Technology	Shapiro, M. H.	420
California Institute of Technology	Sieh, K. E.	170
California, University of, Los Angeles	Bird, P.	432
California, University of, Los Angeles	Lindberg, R. G.	381
California, University of, San Diego	Berger, J.	274
California, University of, San Diego	Berger, J.	278
California, University of, San Diego	Berger, J.	279
California, University of, San Diego	Chung, Y.	363
California, University of, San Diego	Goodkind, J. M.	365
California, University of, San Diego	Priestley, K. F.	5
California, University of, San Diego	Reichle, M.	413
California, University of, San Diego	Wyatt, F.	518
California, University of, Santa Barbara	Sylvester, A. G.	339
California, University of, Santa Cruz	Smith, A. T.	461
Cincinnati, University of	Nash, D. B.	151
Colorado, University of	Kisslinger, C.	316
Colorado, University of	Slater, L. E.	508
Colorado, University of	Sondergeld, C. H.	462
Colorado, University of	Ware, R. H.	425
Colorado, University of	Wyss, M.	10
Colorado, University of	Wyss, M.	351

Cornell University	Isacks, B. L.	303
Cornell University	Kohlstedt, D. L.	439
Cornell University	Kohlstedt, D. L.	484
Cornell University	Kohlstedt, D. L.	487
Cornell University	Phillips, W. J.	409
Environmental Dynamics, Inc.	Westlake, P. R.	428
Ertec Western, Inc.	Martin, G. R.	220
Foothill-De Anza Community College	Hall, N. T.	129
Illinois, University of	Rudnicki, J. W.	458
Lamar-Merifield, Geologists	Lamar, D. L.	140
Lamar-Merifield, Geologists	Lamar, D. L.	377
Lamont-Doherty Geological Observatory	Aggarwal, Y. P.	78
Lamont-Doherty Geological Observatory	Bilham, R.	281
Lamont-Doherty Geological Observatory	Bilham, R.	468
Lamont-Doherty Geological Observatory	Broecker, W. S.	362
Lamont-Doherty Geological Observatory	Engelder, T.	472
Lamont-Doherty Geological Observatory	Jacob, K. H.	213
Lamont-Doherty Geological Observatory	Liddicoat, J. C.	144
Lamont-Doherty Geological Observatory	McCann, W. R.	321
Lamont-Doherty Geological Observatory	Schweickert, R. A.	507
Lamont-Doherty Geological Observatory	Seeber, L.	329
Lamont-Doherty Geological Observatory	Simpson, D. W.	557
Lamont-Doherty Geological Observatory	Simpson, D. W.	560
Massachusetts Institute of Technology	Counselman, C. C.	471
Massachusetts Institute of Technology	Madden, T. R.	385
Massachusetts Institute of Technology	Toksoz, M. N.	342
Monash University	Etheridge, M. A.	473
Montana Bureau of Mines and Geology	Stickney, M. C.	233
Nevada Bureau of Mines and Geology	Bell, J. W.	124
Nevada Bureau of Mines and Geology	Trexler, D. T.	235
Nevada, University of, Reno	Ryall, A.	57
New York, State University of, Binghamton	Anderson, J. R.	466
New York, State University of, Binghamton	Wu, F. T.	349
New York, State University of, Binghamton	Wu, F. T.	463
Oregon State University	Yeats, R. S.	68
Oregon State University	Yeats, R. S.	187
Oregon State University	Yeats, R. S.	189
Polytechnic Institute of New York	Felsen, L. B.	201

Purdue University	Sexton, J. L.	165
Queens College, City University, New York	Newman, W. S.	91
Rutgers University	Douglas, L. A.	249
Saint Louis University	Morrissey, S.	499
Saint Louis University	Stauder, W.	100
Sierra Geophysics, Inc.	Hadley, D. M.	209
South Carolina, University of	Secor, D. T., Jr.	555
South Carolina, University of	Talwani, P.	563
Southern California, University of	Henyey, T. L.	299
Southern California, University of	Henyey, T. L.	480
Southern California, University of	Malin, P. E.	388
Southern California, University of	Teng, T.	423
Southern California, University of	Wong, H. L.	240
SRI International	Otis, L. S.	404
Stanford University	Clough, G. W.	244
Stanford University	Kiremidjian, A.	260
Stanford University	Shah, H. C.	269
Texas A & M University	Logan, J. M.	263
U.S. Geological Survey	Ager, T. A.	114
U.S. Geological Survey	Algermissen, S. T.	1
U.S. Geological Survey	Algermissen, S. T.	12
U.S. Geological Survey	Allen, R.	273
U.S. Geological Survey	Anderson, R. E.	119
U.S. Geological Survey	Andrews, D. J.	192
U.S. Geological Survey	Archuleta, R. J.	193
U.S. Geological Survey	Arnold, E. P.	532
U.S. Geological Survey	Baker, L. M.	194
U.S. Geological Survey	Bakun, W. H.	431
U.S. Geological Survey	Behrendt, J. C.	80
U.S. Geological Survey	Boatwright, J.	196
U.S. Geological Survey	Bonilla, M. G.	126
U.S. Geological Survey	Boore, D. M.	198
U.S. Geological Survey	Borcherdt, R. D.	200
U.S. Geological Survey	Brabb, E. E.	30
U.S. Geological Survey	Buchanan-Banks, J. M.	34
U.S. Geological Survey	Bucknam, R. C.	35
U.S. Geological Survey	Buland, R.	537
U.S. Geological Survey	Burford, R. O.	284
U.S. Geological Survey	Burke, D. B.	128
U.S. Geological Survey	Byerlee, J. D.	435
U.S. Geological Survey	Byerlee, J. D.	546
U.S. Geological Survey	Carlson, M. A.	522
U.S. Geological Survey	Castle, R. O.	37

U.S. Geological Survey	Choy, G. L.	286
U.S. Geological Survey	Choy, G. L.	539
U.S. Geological Survey	Clark, H. E., Jr.	541
U.S. Geological Survey	Clark, H. E., Jr.	542
U.S. Geological Survey	Cockerham, R.	287
U.S. Geological Survey	Dewey, J. W.	3
U.S. Geological Survey	Dewey, J. W.	290
U.S. Geological Survey	Diment, W. H.	81
U.S. Geological Survey	Ellsworth, W. L.	291
U.S. Geological Survey	Endo, E. T.	294
U.S. Geological Survey	Espinosa, A. F.	13
U.S. Geological Survey	Ferrians, O. J., Jr.	38
U.S. Geological Survey	Fischer, F. G.	296
U.S. Geological Survey	Fletcher, J. B.	205
U.S. Geological Survey	Gibbs, J. F.	208
U.S. Geological Survey	Hall, W.	297
U.S. Geological Survey	Hamilton, R. M.	83
U.S. Geological Survey	Harding, S. T.	16
U.S. Geological Survey	Harding, S. T.	547
U.S. Geological Survey	Harlow, D.	298
U.S. Geological Survey	Harp, E. L.	252
U.S. Geological Survey	Hays, W. W.	20
U.S. Geological Survey	Hays, W. W.	39
U.S. Geological Survey	Healy, J. H.	474
U.S. Geological Survey	Healy, J. H.	477
U.S. Geological Survey	Herd, D. G.	40
U.S. Geological Survey	Herd, D. G.	42
U.S. Geological Survey	Herriot, J.	370
U.S. Geological Survey	Hildenbrand, T. G.	85
U.S. Geological Survey	Hoffman, J. P.	523
U.S. Geological Survey	Holmes, M. L.	44
U.S. Geological Survey	Irwin, W. P.	133
U.S. Geological Survey	Iyer, H. M.	548
U.S. Geological Survey	Izett, G. A.	135
U.S. Geological Survey	Jachens, R. C.	306
U.S. Geological Survey	Jaksha, L. H.	525
U.S. Geological Survey	Jensen, E. G.	308
U.S. Geological Survey	Johnson, C.	309
U.S. Geological Survey	Johnston, M.	372
U.S. Geological Survey	Julian, B. R.	438
U.S. Geological Survey	Kane, M. F.	87
U.S. Geological Survey	Keefer, D. K.	253
U.S. Geological Survey	King, C. -Y	375
U.S. Geological Survey	Kvenvolden, K. A.	136
U.S. Geological Survey	Lachenbruch, A. H.	490
U.S. Geological Survey	Lahr, J. C.	46
U.S. Geological Survey	Lajoie, K. R.	138
U.S. Geological Survey	Langer, C. J.	214
U.S. Geological Survey	Langer, C. J.	549
U.S. Geological Survey	Lanphere, M. A.	143
U.S. Geological Survey	Lee, W. H. K.	318
U.S. Geological Survey	Lee, W. H. K.	319
U.S. Geological Survey	Lee, W. H. K.	320

U.S. Geological Survey	Lindh, A.	355
U.S. Geological Survey	Liu, H. -P	383
U.S. Geological Survey	Lockner, D. A.	441
U.S. Geological Survey	Marchand, D. E.	147
U.S. Geological Survey	Matthiesen, R. B.	22
U.S. Geological Survey	Matthiesen, R. B.	222
U.S. Geological Survey	Mavko, G. M.	391
U.S. Geological Survey	Mavko, G. M.	442
U.S. Geological Survey	McCarthy, R. P.	534
U.S. Geological Survey	McDowell, R. C.	89
U.S. Geological Survey	McGarr, A.	323
U.S. Geological Survey	McNutt, M.	444
U.S. Geological Survey	Mooney, W. D.	495
U.S. Geological Survey	Mortensen, C. E.	397
U.S. Geological Survey	Morton, D. M.	49
U.S. Geological Survey	O'Neil, J. R.	400
U.S. Geological Survey	Orsini, N. A.	526
U.S. Geological Survey	Orsini, N. A.	528
U.S. Geological Survey	Orsini, N. A.	529
U.S. Geological Survey	Page, R. A.	50
U.S. Geological Survey	Park, R. B.	224
U.S. Geological Survey	Peselnick, L.	446
U.S. Geological Survey	Peterson, J.	530
U.S. Geological Survey	Pfluke, J. H.	408
U.S. Geological Survey	Pierce, K. L.	154
U.S. Geological Survey	Plafker, G.	51
U.S. Geological Survey	Pollard, D. D.	447
U.S. Geological Survey	Prescott, W. H.	326
U.S. Geological Survey	Prowell, D. C.	553
U.S. Geological Survey	Ratcliffe, N. M.	93
U.S. Geological Survey	Reimer, G. M.	414
U.S. Geological Survey	Rogers, A. M.	55
U.S. Geological Survey	Rojahn, C.	157
U.S. Geological Survey	Rosholt, J. N.	158
U.S. Geological Survey	Ross, D. C.	159
U.S. Geological Survey	Russ, D. P.	95
U.S. Geological Survey	Sarna-Wojcicki, A. M.	162
U.S. Geological Survey	Sato, M.	416
U.S. Geological Survey	Scott, W. E.	164
U.S. Geological Survey	Sharp, R. V.	167
U.S. Geological Survey	Simpson, R.	99
U.S. Geological Survey	Sims, J. D.	172
U.S. Geological Survey	Sims, J. D.	178
U.S. Geological Survey	Spence, W.	544
U.S. Geological Survey	Spudich, P.	231
U.S. Geological Survey	Stevenson, P. R.	335
U.S. Geological Survey	Stewart, S. W.	337
U.S. Geological Survey	Stone, B. D.	104
U.S. Geological Survey	Stover, C. W.	535
U.S. Geological Survey	Stuart-Alexander, D.	562
U.S. Geological Survey	Taggart, J. N.	7
U.S. Geological Survey	Thatcher, W.	340
U.S. Geological Survey	Tinsley, J. C.	63

U.S. Geological Survey	Van Schaack, J.	238
U.S. Geological Survey	Van Schaack, J.	345
U.S. Geological Survey	Van Schaack, J.	347
U.S. Geological Survey	Wallace, R. E.	180
U.S. Geological Survey	Ward, P.	348
U.S. Geological Survey	Warren, D. H.	516
U.S. Geological Survey	Warrick, R. E.	239
U.S. Geological Survey	Weaver, C. S.	65
U.S. Geological Survey	Wentworth, C. M.	23
U.S. Geological Survey	Wheeler, R. L.	110
U.S. Geological Survey	Whitcomb, H.	531
U.S. Geological Survey	Wilson, R. C.	256
U.S. Geological Survey	Wood, S. H.	67
U.S. Geological Survey	Yerkes, R. F.	71
U.S. Geological Survey	Youd, T. L.	259
U.S. Geological Survey	Yount, J. C.	74
U.S. Geological Survey	Ziony, J. I.	75
U.S. Geological Survey	Zoback, M. L.	76
URS/John A. Blume & Associates	Scholl, R. E.	266
Utah State University	Anderson, L. R.	242
Utah, University of	Smith, R. B.	59
Washington, University of	Merchant, H. C.	494
Weber and Associates	Weber, G. E.	185
Woodward-Clyde Consultants	Dawson, A. W.	247
Woodward-Clyde Consultants	Perman, R. C.	550
Woodward-Clyde Consultants	Swan, F. H.	106